Durham University

Durham E-Theses

Development of Advanced Technology to Enhance the Growth and Maintenance of Liver Cells and Tissue In Vitro

HENRY WILLIAM HOYLE

How to cite:

HOYLE, HENRY WILLIAM (2021) Development of Advanced Technology to Enhance the Growth and Maintenance of Liver Cells and Tissue In Vitro. Doctoral thesis, Durham University.

Use policy

The full-text may be used and/or reproduced, and given to third parties in any format or medium, without prior permission or charge, for personal research or study, educational, or not-for-profit purposes provided that:

- a full bibliographic reference is made to the original source
- a https://etheses.durham.ac.uk/id/eprint/14191/ is made to the metadata record in Durham E-Theses
- the full-text is not changed in any way

The full-text must not be sold in any format or medium without the formal permission of the copyright holders.

Please consult the full Durham E-Theses policy for further details.

Academic Support Office, The Palatine Centre, Durham University, Stockton Road, Durham, DH1 3LE
e-mail: e-theses.admin@durham.ac.uk Tel: +44 0191 334 6107
https://etheses.durham.ac.uk

Department of Biosciences

Development of Advanced Technology to Enhance the Growth and Maintenance of Liver Cells and Tissue *In Vitro*

Henry William Hoyle

2021

A thesis submitted for the degree of Doctor of Philosophy

Abstract

In vitro cell culture models are widely used for much of the research carried out into human diseases and treatments as well as more basic biological research. Due to animal testing becoming increasingly undesirable, the access to accurate *in vitro* models is of utmost importance. For many applications the models used lack physiological relevance, often consisting merely of a single cell line grown in a plastic dish. Techniques such as three-dimensional cell culture have started to bridge the gap between the *in vitro* and *in vivo* cellular microenvironment. To take this a step further, perfusion bioreactors can be used to provide dynamic fluid flow to cultures and mimic the vasculature *in vivo*. These systems commonly suffer from drawbacks such as high cost and complexity as well as large size.

In this project a novel perfusion bioreactor system was developed for use with three-dimensional cell culture models. The aim was to create a system which could provide the same levels of physiological complexity as other systems currently in use whilst reducing cost and complexity and therefore maximising accessibility. To this end, the liver was chosen as a model organ for testing the efficacy of this system due to its high levels of vascularisation suggesting it would benefit greatly from the addition of medium perfusion, as well as the large amount of literature based around perfusion systems for *in vitro* liver models. The system designed for this purpose utilises magnetic stirrer-based perfusion to keep the apparatus simple whilst allowing ease of use and high levels of scalability. An Alvetex® insert is held within the system, providing a complex three-dimensional microenvironment to support the cells and further enhance their structure and function. Extensive optimisation and characterisation of this system was performed to ensure a detailed understanding of the conditions experienced by cultured cells and tissues.

It was found that the novel bioreactor system could greatly increase the expression of key hepatic genes in the HepG2 cell line whilst improving the localisation of many important structural and function proteins. Further use of this system demonstrated the efficacy of this model for modelling drug toxicity. The Alvetex® support for the cells also allows for co-culture of multiple cell types in different organisations. The use of such a co-culture setup was demonstrated with the HepG2 models by successfully incorporating fibroblasts and endothelial cells.

In a different model, utilising precision-cut liver slices, the system demonstrated potential for maintaining the viability of the liver slices over prolonged periods over up to 2 weeks. Inclusion of an oxygenation system to function alongside the bioreactor has the potential to further promote

the viability of precision-cut liver slices, however more research would be required to accurately measure any improvements due to this system. Such a model, if successful, could be of significant research value for the study of chronic diseases such as liver fibrosis.

The results found herein utilising the novel perfusion bioreactor show that complex tissue equivalents can be created using simple, low cost and user-friendly apparatus. Whilst the system was successful for the culture of liver models, the level of control over the properties of the system also gives it potential for use with other organ models and therefore could become a useful platform for a wide range of *in vitro* and *ex vivo* research in the future.

Declaration

The work described within this text was carried out in the Department of Biosciences, Durham University between October 2016 and April 2021. All the work is my own, except where specifically stated otherwise. No part has previously been submitted for a degree at this or any other university.

Statement of Copyright

The copyright of this thesis rests with the author. No quotations from it should be published without prior written consent and information derived from it should be acknowledged

Publications arising from this work:

Applications of novel bioreactor technology to enhance the viability and function of cultured cells and tissues, Hoyle, H. W., Smith, L. A., Williams, R. J., Przyborski, S. A. (2020) Interface Focus. https://doi.org/10.1098/rsfs.2019.0090

Continuous stirred bioreactor for the culture of complex three-dimensional tissue models, Hoyle, H. W. and Przyborski, S. A. - In Preparation

Design constraints for benchtop flow bioreactors in tissue engineering, Hoyle, H. W. and Przyborski, S. A. – In Preparation

Poster presentations:

Increasing the functionality of hepatic cultures through the development of a tissue-specific microenvironment (2020) Durham University Department of Biosciences Research Away Day, Durham, UK

Improvement of three-dimensional liver tissue models through the development of a novel perfusion culture system (2019) Durham University Department of Biosciences Research Away Day, Durham, UK

Improvement of three-dimensional liver tissue models through the development of a novel perfusion culture system (2018) Durham University Department of Biosciences Postgraduate Conference, Durham, UK

Improvement of three-dimensional liver tissue models through the development of a novel perfusion culture system (2018) Durham University Department of Biosciences Research Away Day, Durham, UK

Improvement of three-dimensional liver tissue models through the development of a novel perfusion culture system (2017) White Rose Biomaterials and Tissue Engineering Group Conference, Leeds, UK

Oral presentations:

Improvement of three-dimensional liver tissue models through the development of a novel perfusion culture system (2019) Tissue Engineering and Regenerative Medicine International Society (TERMIS) EU Chapter Meeting, Rhodes, Greece.

Enhancing the structure and function of liver tissue models using advanced cell technologies (2019) Durham University Department of Biosciences Postgraduate Conference, Durham, UK

Improvement of three-dimensional liver tissue models through the development of a novel perfusion culture system (2018) White Rose Biomaterials and Tissue Engineering Group Conference, Sheffield, UK

Acknowledgements

This work was funded by a Durham University Faculty of Science studentship as well as by an EPSRC IAA grant.

I would like to thank my supervisor, Professor Stefan Przyborski, for granting me the opportunity to carry out the work and for all the support and guidance provided over this time, as well as for keeping me on course when I go off on one tangent too many. Thanks also to Ben, for being there both to discuss ideas within the lab as well as for joining me on many extracurricular activities over this time. Thankyou Lucy for being really supportive in the lab and for putting up with me whilst we played around with the initial ideas with the perfusion system. Thanks, Nicole, for keeping me in line and for your support in the lab. Thanks, Claire, for always being up for a trip to the pub when experiments weren't going to plan. Thanks, Pam, for all of the huge amount of support that you provide to the whole lab and thanks also to the entire rest of the Pryzborski laboratory, past and present, for the endless support that you have provided throughout my PhD.

I would also like to thank the vast number of people within the wider university who have helped me throughout this work. Neil Holmes from the mechanical workshop, Kelvin Appleby from the electronics workshop and Aaron Brown from the glassblowing workshop in the Department of Chemistry and Stephen Lishman and Malcolm Robertshaw from the mechanical workshop in the Department of Physics, for your support developing the various prototypes and for sparing your time to discuss design constraints and alternative ways to bring this system into existence. Thank you to Adele, Stacey and Lynne from the Life Sciences Support Unit for all of your help with some of the trickier aspects of this project. Thanks also to Dr Richard Williams and Dr Lian Gan from the Department of Engineering for your support with the fluid dynamics analysis performed on the system.

Thanks to everyone from the Hatfield College Boat Club who made sure I had plenty to do with my free time outside of the lab, and only complaining a small amount at my insistence on only ever training at 6:30am so I could get to the lab in good time.

Finally, thanks to my parents and sister for your support throughout this project. In particular, thanks, Dad, for your amazing proofreading and constant correcting of my grammar, I couldn't have done this without you!

Contents

Abstract 2

Declaration 4

Statement of Copyright 4

Publications arising from this work: 5

Poster presentations: 5

Oral presentations: 5

Acknowledgements 6

List of Figures 17

List of Tables 22

Abbreviations 23

Chapter 1: Introduction 26

1.1. Overview 27

1.1. Background 30

1.1.1. The limitations of conventional *in vitro* cell culture 30

1.1.2. Techniques for creating a more physiologically relevant tissue equivalent 34

1.1.3. Applications and challenges of liver tissue engineering 39

1.1.4. Applications of liver research 49

1.1.5. Methods for reproducing liver function *in vitro* 56

1.2.6. Technologies to improve the physiological relevance of hepatocyte models 65

1.2.7. Conclusions 78

1.3. Hypothesis, Aims and Objectives 80

1.3.6. Hypothesis 80

1.3.2. Project Aims 80

1.3.3. Project Objectives 82

Chapter 2: Materials and Methods 83

2.1. Introduction 84

2.2. Cell Culture Techniques 85

2.2.1. Propagation and maintenance of cell lines 85

2.2.2. Growth of cells in 6 and 12 well plates 88

2.2.3. Growth of cells on coverslips 88

2.2.4. Preparation of Alvetex® 88

2.2.5. Preparation and reuse of the bioreactor system 89

2.2.6. Growth of HepG2 cells on Alvetex® in well inserts 89

2.2.7. Growth of HepG2 cells in static Alvetex® sandwich culture 89

2.2.8. Growth of HepG2 in dynamic Alvetex® culture using the culture holder 90

2.2.9. Growth of HepG2 cells in dynamic Alvetex® culture using the 6-well insert holder 92

2.2.10. Growth of HDFn cells in Alvetex® Scaffold to form an *in vivo*-like supportive layer 92

2.2.11. Addition of HepG2 cells to HDFn cultures 92

2.2.12. Culture of SK-Hep-1 cells on Alvetex® membranes 93

2.2.13. Addition of SK-Hep-1 to HepG2 Alvetex® cultures 93

2.3. *Ex vivo* culture of precision-cut liver slices 94

2.3.1. Extraction of rat liver 94

2.3.2. Slicing of rat liver 94

2.3.3. Culture of rat precision-cut liver slices 94

2.4. Bioreactor development and analysis 96

2.4.1. Manufacture of custom equipment 96

2.4.2. Measuring the permeability of Alvetex® 96

2.4.3. Dye circulation 98
2.4.4. Particle Image Velocimetry 98
2.4.5. Computation Fluid Dynamics 98
2.4.6. Measurement of magnetic fields 99
2.4.7. Measuring stirrer speed with a stroboscope 99
2.4.8. Measuring stirrer speed with slow-motion video....99
2.5. Sample Processing....100
2.5.1. Fixing Cell cultures 100
2.5.2. Wax Embedding and sectioning....100
2.5.3. OCT Embedding and sectioning 101
2.5.4. PCR analysis: RNA extraction 101
2.5.5. PCR analysis: cDNA synthesis....102
2.5.6. Protein extraction for Bradford Assay 104
2.6. Morphological Analysis 105
2.6.1. Haemotoxylin and Eosin Staining....105
2.6.2. Masson's Trichrome Staining....105
2.6.3. Periodic Acid Schiff (PAS) Staining 105
2.6.4. Immunofluorescent staining of paraffin embedded samples 106
2.6.5. Immunofluorescent staining of OCT embedded samples 108
2.6.6. Immunofluorescent staining of coverslips....108
2.6.7. Nile Red Staining 109
2.6.8. Picrosirius red staining....109
2.6.9. Microscopy....109
2.7. Functional Analysis....110
2.7.1. MTT cell viability assay....110
2.7.2. Cell Counting 110

2.7.3. Terminal deoxynucleotidyl transferase dUTP nick end labeling (TUNEL) Assay 110

2.7.4. Albumin Assay for human models 111

2.7.5. Urea Assay.....112

2.7.6. Lactate Dehydrogenase (LDH) Assay 112

2.7.7. Bradford assay for total protein content 112

2.7.8. Polymerase Chain Reaction (PCR) Analysis.....113

2.8. Statistics.....116

Chapter 3: Development of a 3D bioreactor cell culture system 117

3.1. Introduction.....118

3.1.1. The dynamic liver microenvironment.....118

3.1.2 Translating *in vivo* fluid flow to the *in vitro* environment 119

3.1.3. Recapitulating the dynamic environment of the liver *in vitro*.....121

3.1.4. Supporting three-dimensional growth in bioreactors 133

3.1.5. Conclusion 136

3.2. Aims and Objectives 137

3.2.1. Aims.....137

3.2.2. Objectives.....137

3.3. Results 138

3.3.1. Development Criteria.....138

3.3.2. Design Phase I: Initial Prototype 139

3.3.3. Phase II: Further modifications and finalised design 163

3.3.4. Characterisation of the final design 169

3.3.4.5. Physical effects of stirrer 174

3.4. Discussion 178

3.4.1. Development of a novel, three-dimensional cell culture bioreactor 178

3.4.2. Advantages of the novel bioreactor over other systems.....180

3.5. Conclusion 184

Chapter 4: Optimisation and Characterisation of stirred HepG2 models 185

4.1. Introduction.....186

4.1.1 Hepatocyte function *in vivo* 186

4.1.2. Techniques and challenges associated with in vitro culture of hepatocytes 193

4.1.2.1. Primary hepatocytes.....194

4.1.2.3.1. HepG2 cells as an alternative to primary hepatocytes.....195

4.1.3. Methods to improve physiological relevance of hepatocyte cultures 198

4.1.4. Commercially available hepatocyte models 200

4.1.5. Conclusions 203

4.2. Hypothesis, Aims and Objectives 204

4.2.1. Hypothesis.....204

4.2.2. Aims.....204

4.2.3. Objectives.....204

4.3. Materials and Methods 205

4.3.1. Culture of HepG2 models in static and flow conditions for initial optimisation 205

4.3.2. Generation of HepG2 models for structural and functional analysis 208

4.3.3. Sampling of cell culture media for metabolic assays.....210

4.3.4. Quantification of invasion and cell layer thickness 210

4.4. Results 212

4.4.1. Culture of HepG2 cells on different forms of Alvetex®.....212

4.4.2. Effect of fluid flow on cell morphology and polarisation 216

4.4.3. Gross morphology of HepG2 grown on Alvetex® Strata in static and flow conditions.....218

4.4.4. Immunofluorescent analysis of HepG2 cultures in static and fluid flow conditions....220

4.4.5. Functional analysis of HepG2 in 3D and stirred culture conditions....234

4.4.6. Changes in levels of key drug metabolising enzymes....237

4.5. Discussion....241

4.5.1. Culture of HepG2 cells as stirred, three-dimensional tissue equivalents....241

4.5.2. Structural characterisation of stirred HepG2 cultures....242

4.5.3. Variations in membrane transporter expression in stirred 3D culture....244

4.5.3. Changes to basic metabolic functions of HepG2 cells....245

4.6. Conclusions....248

Chapter 5: Response of stirred HepG2 models to toxicological challenge....250

5.1. Introduction....251

5.1.1. The role of the liver in drug detoxification....251

5.1.2. Drug induced liver injury can be caused in significantly different ways....256

5.1.3. Drug discovery models frequently over- and underestimate drug toxicity 259

5.1.4. Increasing the complexity of models can improve their performance for predicting drug toxicity....261

5.1.5. Fluid flow models for drug toxicity prediction....262

5.1.6. Conclusions....263

5.2. Hypothesis, Aims and Objectives....265

5.2.1. Hypothesis....265

5.2.2. Aims....265

5.2.3. Objectives....265

5.3. Materials and Methods....266

5.3.1. Drugs used for toxicological testing....266

5.3.2. Methods for dosing 2D and 3D static models....266

5.3.3. Methods for dosing bioreactor models 267

5.4. Results 272

5.4.1. Response of bioreactor models to toxicological challenge 272

5.5. Discussion 282

5.5.1. Drug toxicity varies significantly with different *in vitro* models 282

5.5.2. Complex metabolic pathways lead to difficulty in replicating *in vivo* results 284

5.5.3. In-depth analysis of *in vitro* models is required for accurate toxicity predictions for many drugs 285

5.5.4. Limitations of the novel bioreactor system for drug toxicity research 286

5.6. Conclusions 288

Chapter 6: Incorporation of non-parenchymal cells into stirred HepG2 models..... 289

6.1. Introduction 290

6.1.1. The important of extracellular matrix in the liver microenvironment 290

6.1.2. Methods to incorporate ECM into *in vitro* cell models.....291

6.1.3. Improvement of hepatocyte models through the addition of ECM 294

6.1.4. Non-parenchymal cells play a major role in liver homeostasis 296

6.1.5. Multicellular liver models can improve hepatocyte function and predictive capacity 299

6.1.6. Methods to utilise Alvetex® membranes for co-culture of different cell types. 300

6.2. Hypothesis, Aims and objectives 303

6.2.1. Hypothesis.....303

6.2.2. Aims.....303

6.2.3. Objectives.....303

6.3. Materials and Methods 304

6.3.1. Co-culture of HepG2 cells with fibroblasts 304

6.3.2. Co-culture of HepG2 cells with endothelial cells. 306

6.3.3. Co-culture of HepG2 cells with fibroblasts and endothelial cells 308

6.3.4. Image processing.....310

6.4. Results 312

6.4.1. Optimisation of 3D fibroblast growth in DMEM 312

6.4.2. Characterisation of HepG2 – HDFn co-culture models.....316

6.4.3. Inclusion of endothelial cells in HepG2 models 331

6.4.4. Creating a HepG2 bioreactor model containing fibroblasts and endothelial cells 342

6.5. Discussion 350

6.5.1. Fibroblasts can be successful incorporated into cultures of HepG2 350

6.5.2. Co-culture of Sk-Hep-1 with HepG2 leads to a reduction in HepG2 cells in culture 352

6.5.3. Addition of SK-Hep-1 to the HepG2 – fibroblast model can produce cultures with desirable culture morphology.....353

6.5.4. HepG2 in triculture exhibit improved structure and function above and beyond the improvements documented previously 354

6.6. Conclusions.....355

Chapter 7: Maintaining the viability of precision-cut liver slices in the bioreactor system 356

7.1. Introduction.....357

7.1.1. *Ex vivo* culture of precision-cut tissue slices 357

7.1.2. Use of precision-cut liver slices for the modelling of liver fibrosis 358

7.1.3. Systems used for the culture of precision-cut liver slices.....363

7.1.4. The pathology of Liver Fibrosis 364

7.1.5. Methods to study liver fibrosis in PCLS.....371

7.1.6. Conclusion 372

7.2. Hypothesis, Aims and Objectives 373

7.2.1. Hypothesis....373

7.2.2. Aims....373

7.2.3. Objectives....373

7.3. Results....374

7.3.1. Optimising the growth of rat PCLS on Alvetex membranes....374

7.3.2. Supporting thicker tissue slices using through-membrane fluid flow....379

7.3.3. Culture properties of rat PCLS in the bioreactor system....381

7.3.4. Incorporation of oxygenation into the bioreactor cultures....384

7.4. Discussion....392

7.5.1. Liver slices can be maintained for up to a week in the bioreactor system .392

7.5.2. Migration and proliferation of non-parenchymal cells could limit the utility of PCLS over longer time periods....393

7.5.3. Further refinements of the protocol are required for accurate testing of profibrotic agents.....394

7.5.4. Incorporating oxygenation into the biore system further improves the viability of cultured PCLS.....394

7.5. Conclusion....396

Chapter 8: General Discussion, Future Directions and Conclusion 397

8.1. Summary of Key Findings....398

8.2. Discussion....399

8.2.1. Development of a d cell culture system....399

8.2.1. Summary of models developed in this work....402

8.2.3. A more physiological microenvironment enhances cell structure and function 402

8.2.4. Applications of the stirred *in vitro* liver models....403

8.2.5. The limitations of the HepG2 cell line....405

8.2.6. Use of *ex vivo* tissue slices in the bioreactor system for *in vitro* disease modelling....405

8.3. Future Directions 407
8.3.1. Recreating the model with alternative hepatocyte sources 407
8.3.2. Including the full range of liver cell types 408
8.3.3 Utility of the bioreactor system for recreation of other tissues 410
8.4. Conclusion 411
Chapter 9: Bibliography 412
Chapter 10: Appendices 457
10.1 Appendix 1 - Abstracts and Posters 458
10.1.1. Posters 458
10.1.2. Oral Presentation Abstracts 463
10.2. Appendix 2: Schematics of custom apparatus 466
10.2.1. PTFE Components 466
10.2.2. Glass Beakers 470
10.2.3. Magnetic Stirrer units 472
10.3. Appendix 3: Recipes 492
10.3.1. Phosphate Buffered Saline (PBS) 492
10.3.2. Citrate Buffer 492
10.3.3. Krebs – Henseleit Buffer (KHB) 492
10.3.4. Haemotoxyin and Eosin (H&E) stain 492
10.3.5. Periodic Acid Schiff (PAS) stain 493
10.3.6. Picrosirius Red Stain 493
10.4. Appendix 4: Calculation of Alvetex Permeability 494

List of Figures

Figure 1.1: The range of factors influencing cells in vivo.

Figure 1.2: Properties of cells grown in 2D and 3D culture.

Figure 1.3: Variation in levels of media constituents in proximity to cell or tissue layers.

Figure 1.4: Perfusion in vivo and methods for recreating this *in vitro.*

Figure 1.5: Costs of drug development stages over time.

Figure 1.6: Statistics on the rate of incidence and five-year cancer survival rates.

Figure 1.7: The vasculature network between the liver and other organs in the body.

Figure 1.8: The microstructure of the liver.

Figure 1.9: Histology of pig liver stained with Masson's trichrome.

Figure 1.10: Zonular variation in function and protein expression in the hepatocytes.

Figure 1.11: Polarisation and junctional localisation in columnar epithelia and hepatocytes.

Figure 1.12: Stages of the drug development pathway with their associated time and monetary costs.

Figure 1.13: Changes in the hepatic microenvironment due to liver fibrosis.

Figure 1.14: Relative abundance of drug-metabolising genes in hepatic cell lines.

Figure 1.15: Methods to derive multipotent hepatic progenitor cells.

Figure 1.16: Setting up Hepatocytes in a collagen sandwich culture.

Figure 1.17: Different methods for forming aggregates.

Figure 1.18: Techniques used for bioprinting of cells.

Figure 2.1: Phase-contrast images of HepG2 cells grown in 2D.

Figure 2.2: Phase-contrast images of SK-Hep-1 cells grown in 2D.

Figure 2.3: Phase-contrast images of HDFn cells grown in 2D.

Figure 2.4: Protocols for setting up cultures in the different systems.

Figure 2.5: Preparation and culture of precision-cut rat liver slices.

Figure 2.6: Apparatus for measuring the permeability of Alvetex

Figure 3.1: Different sources of fluid flow in the liver.

Figure 3.2: The range of functions that fluid flow can carry out in cells or tissues.

Figure 3.3: Commonly used technologies for cell culture perfusion.

Figure 3.4: Commercially available rotary bioreactors for mammalian cell culture.

Figure 3.5: Pump-based perfusion cell culture systems.

Figure 3.6: Magnetic stirrer-based perfusion methods for mammalian cell culture.

Figure 3.7: Rocked and shaken methods for media perfusion.

Figure 3.8: Microfluidic and ‘organ on a chip’ devices.
Figure 3.9: Structure of the three different forms of Alvetex® membrane.
Figure 3.10: Schematic of a magnetic stirrer based Alvetex® cell culture bioreactor.
Figure 3.11: Glass vessel to contain the bioreactor system.
Figure 3.12: Reversible PTFE Lid for the bioreactor system.
Figure 3.13: Magnetic stir bar used for the prototype perfusion cultures.
Figure 3.14: Device for holding a 6-well Alvetex membrane.
Figure 3.15: CFD modelling of a stirred beaker in the absence of further fluid control.
Figure 3.16: Three initial stands designed to hold the culture device.
Figure 3.17: Fluid flow analysis for the vented table culture stand.
Figure 3.18: Time series of crystal violet dye in the system with the vented table stand.
Figure 3.19: Fluid flow analysis for a conical stand with clockwise venting.
Figure 3.20: Time series of crystal violet dye in the system with the clockwise-vented conical stand.
Figure 3.21: Fluid flow analysis for a conical stand with anticlockwise venting.
Figure 3.22: Time series of crystal violet dye in the system with the anticlockwise-vented conical stand.
Figure 3.23: Effects on the viability of HepG2 cells grown in PTFE conditioned media.
Figure 3.24: Schematic of the finalised clockwise-vented conical stand design.
Figure 3.25: The complete prototype bioreactor design.
Figure 3.26: Velp Multi-point magnetic stirrer.
Figure 3.27: Rotational frequency of the Velp magnetic stirrer at different speed settings.
Figure 3.28: Conical stand with holder for 6-well Alvetex insert.
Figure 3.29: Magnetic Stir bars used for the final perfusion system.
Figure 3.30: The complete final bioreactor design.
Figure 3.31: Custom magnetic stirrer system.
Figure 3.32: Computational Fluid Dynamics of the final bioreactor design.
Figure 3.33: Vertical component of fluid velocity across the Alvetex membrane for the two bioreactor systems.
Figure 3.34: Measurements for the permeability of different forms of Alvetex®.
Figure 3.35: Shear stress and through-membrane velocity in the bioreactor system.
Figure 3.36: Oxygen levels in the bioreactor system compared with static culture.
Figure 3.37: Comparison of cell viability at different stirrer speed settings.
Figure 3.38: Media evaporation and degradation in the bioreactor system.
Figure 3.39: Media temperature in the bioreactor system.

Figure 3.40: Magnetic field measurement and effects on HepG2 cells.
Figure 4.1: Common junctional complexes and proteins in hepatocytes.
Figure 4.2: Transporter proteins and their localisation in hepatocytes.
Figure 4.3: Functional processes carried out by hepatocytes.
Figure 4.4: Commonly used methods for culturing hepatocytes.
Figure 4.5: H&E stain of HepG2 grown in static conditions in a 6-well plate and a bioreactor.
Figure 4.6: Protocol for setting up static models in a 6-well plate alongside bioreactor cultures.
Figure 4.7: Protocol for setting up bioreactor cultures in in static and perfusion.
Figure 4.8: Quantification of growth characteristics of HepG2 cells on Alvetex using ImageJ.
Figure 4.9: Growing HepG2 on different forms of Alvetex in static conditions.
Figure 4.10: Investigating different seeding densities of HepG2 on Alvetex Strata.
Figure 4.11: Growth of HepG2 on the three different forms of Alvetex in perfusion.
Figure 4.12: Properties of HepG2 cells grown on Alvetex Strata in static and perfusion.
Figure 4.13: Immunostaining of the different HepG2 models with viability and cell health markers.
Figure 4.14: Expression of adherens junctional proteins in the different models.
Figure 4.15: Localisation of E-cadherin and N-cadherin in the different culture methods.
Figure 4.16: Immunostaining of the different HepG2 models with tight junctional proteins.
Figure 4.17: Immunostaining of the different HepG2 models for different apical transporter proteins.
Figure 4.18: Co-localisation of MRP2 and Villin in different culture methods.
Figure 4.19: qPCR quantification of apical transporter genes.
Figure 4.20: Immunostaining of the different HepG2 models for different basolateral transporters.
Figure 4.21: qPCR analysis of basolateral transporters genes.
Figure 4.22: Metabolic assays carried out on HepG2 cultures grown in static and perfusion.
Figure 4.23: The urea cycle with qPCR expression of key enzymes in the different HepG2 models.
Figure 4.24: qPCR expression of major CYP enzymes in HepG2 cultures.
Figure 4.25: qPCR expression of phase II enzymes in HepG2 cultures.
Figure 5.1: First pass metabolism of orally dosed drugs in the body.
Figure 5.2: Drug metabolism in the liver.
Figure 5.3: Enzymes involved in the phases of drug metabolism.
Figure 5.4: Different types of drug induced liver injury.
Figure 5.5: The dosing regimens used for static and stirred cultures.
Figure 5.6: Comparison of results between the two perfusion dosing regimens
Figure 5.7: The dosing regimen of acetaminophen used for static and stirred cultures.

Figure 5.8: Results of acetaminophen toxicity on the different HepG2 models.
Figure 5.9: Results of Amiodarone toxicity on the different HepG2 models.
Figure 5.10: Results of Isoniazid toxicity on the different HepG2 models.
Figure 5.11: Results of Gemfibrozil toxicity on the different HepG2 models.
Figure 5.12: Results of Ibuprofen toxicity on the different HepG2 models.
Figure 5.13: Results of Tamoxifen toxicity on the different HepG2 models.
Figure 5.14: Results of Indomethacin toxicity on the different HepG2 models.
Figure 5.15: Results of Flutamide toxicity on the different HepG2 models.
Figure 6.1: Methods to incorporate ECM into cell culture.
Figure 6.2: Different methods to utilise Alvetex® membranes for the growth of cells in vitro
Figure 6.3: Protocol for setting up HepG2 and HDFn co-cultures.
Figure 6.4: Protocol for setting up HepG2 and SK-Hep-1 co-cultures.
Figure 6.5: Protocol for setting up HepG2, HDFn and SK-Hep-1 tri-cultures.
Figure 6.6: Optimisation of the growth of fibroblasts in Alvetex Scaffold.
Figure 6.7: Growth of HepG2 cells on Alvetex Scaffold cultured with fibroblasts for different time periods.
Figure 6.8: H&E staining of HepG2 grown on Alvetex in static and perfusion.
Figure 6.9: Invasion quantification for different HepG2 culture methods.
Figure 6.10: General morphology of the stirred HepG2 model with fibroblasts.
Figure 6.11: Immunostaining of the different HepG2 models for key liver extracellular matrix proteins.
Figure 6.12: Immunostaining of the different HepG2 models with viability and cell health markers.
Figure 6.13: Expression of adherens junctional proteins in the different models.
Figure 6.14: Immunostaining of the different HepG2 models with tight junctional proteins.
Figure 6.15: Immunostaining of the different HepG2 models for different apical transporter proteins.
Figure 6.16: Immunostaining of the different HepG2 models for different sinusoidal transporters.
Figure 6.17: Metabolic assays for HepG2 and HDFn co-culture models.
Figure 6.18: SK-Hep-1 cells grown in Alvetex Scaffold and Strata.
Figure 6.19: Proteins used as markers for the different cell types using immunofluorescence.
Figure 6.20: HepG2 and SK-Hep-1 co-cultures on Alvetex Strata at different seeding densities in static conditions.
Figure 6.21: HepG2 and SK-Hep-1 co-cultures on Alvetex Strata in stirred conditions.
Figure 6.22: SK-Hep-1 and HDFn co-cultures on Alvetex Scaffold in stirred conditions.

Figure 6.23: HepG2, SK-Hep-1 and HDFn tri-cultures on Alvetex Scaffold in stirred conditions.
Figure 6.24: Organisation of different cell types in stirred HepG2, SK-Hep-1 and HDFn tri-cultures.
Figure 6.25: Expression of adherens and tight junctional proteins in stirred tri-culture.
Figure 6.26: Expression of MDR1 in stirred tri-culture.
Figure 6.27: Metabolic assays for HepG2, HDFn and SK-Hep-1 co-culture models.
Figure 7.1: Preparation of precision-cut liver slices.
Figure 7.2: Variation of fibrosis severity with injury timing.
Figure 7.3: Different fibrosis pathologies from the three main insults.
Figure 7.4: Mechanisms of the inflammatory phase of liver fibrosis.
Figure 7.5: Mechanisms of fibrogenesis and resolution phases of liver fibrosis.
Figure 7.6: Properties of precision-cut liver slices produced using the protocol developed.
Figure 7.7: Rat PCLS grown for up to 28 days on Alvetex Scaffold.
Figure 7.8: Rat PCLS grown on Alvetex Scaffold, Strata and HDFn-seeded Scaffold.
Figure 7.9: Histology of rat PCLS cut at different thicknesses.
Figure 7.10: MTT Assay of PCLS cultured on Alvetex® Strata.
Figure 7.11: Histology of rat PCLS cultured for 7 days in the perfusion system.
Figure 7.12: Schematic of the oxygenation system.
Figure 7.13: Photos of the oxygenation chamber.
Figure 7.14: Measurements of dissolved oxygen levels in the oxygenated perfusion system.
Figure 7.15: MTT Assays of rat PCLS culture in the bioreactor system in normal conditions and with oxygenation.
Figure 8.1: Overview of the finalised bioreactor apparatus developed in this thesis.

List of Tables

Table 1.1: Different cell types found in the adult liver.

Table 1.2: Enzymes involved in the different stages of drug metabolism.

Table 1.3: Global incidence and annual mortalities from a range of liver diseases.

Table 1.4: A Summary of different techniques which can be used to model the liver.

Table 1.5: Different hepatic cell lines commonly used in research.

Table 1.6: Commonly used 3D hepatocyte cell culture techniques.

Table 1.7: Different types of Scaffolds which are used in cell and tissue culture.

Table 1.8: Comparison of several different commercially available bioreactor systems.

Table 2.1: Components required for cDNA synthesis.

Table 2.2: Thermocycler program used for cDNA synthesis.

Table 2.3: Primary antibodies used for immunofluorescent analysis.

Table 2.4: Secondary antibodies used for immunofluorescent analysis.

Table 2.5: Primer sequences used for qPCR analysis.

Table 2.5: Primer mixture to create the working solutions.

Table 3.1: Advantages and disadvantages of different bioreactor systems.

Table 4.1: Expression of various common phase I and phase II enzymes in HepG2 relative to primary hepatocytes.

Table 4.2: Basic properties of commercially available hepatocyte models.

Table 5.1: Concentrations and vehicles used for the drug tests

Table 7.1: Factors influencing health of precision-cut liver slices.

Table 7.2: Criteria to be used for the oxygenation system.

Abbreviations

2D	Two dimensional
3D	Three dimensional
APAP	Acetaminophen
Arg1	Arginase 1
BAEC	Bovine aortic endothelial cell
BCRP	Breast cancer resistance protein
BM	Basement membrane
BSEP	Bile salt export pump
Cmax	Peak serum concentration
CO_2	Carbon dioxide
Cx	Connexin
CYP	Cytochrome P450
d	Darcy (unit)
dH_2O	Demineralised water
DILI	Drug induced liver injury
DMEM	Dulbecco's modified eagle medium
ECM	Extracellular matrix
EDTA	Ethylenediaminetetraacetic acid
ELISA	Enzyme-linked immunosorbent assay
EpCam	Epithelial cell adhesion molecule
FBS	Foetal bovine serum
GSH	Glutathione
H&E	Haematoxylin and eosin
HBV	Hepatitis B virus
HCC	Hepatocellular carcinoma
HCV	Hepatitis C virus
HDFn	Human neonatal dermal fibroblasts
HIF-1α	Hypoxia-inducible factor 1α
HUVEC	Human umbilical vein endothelial cell
IL	Interleukin
iPSC	Induced pluripotent stem cell
JAM-A	Junctional adhesion molecule A

KHB	Krebs – Henseleit buffer
LDH	Lactate dehydrogenase
LPS	Lipopolysaccharide
LSECs	Liver sinusoidal endothelial cells
MATE1	Multidrug and toxin extrusion exchanger 1
MDR	Multidrug-resistance protein
MEM	Eagle's minimum essential medium
MPER	Mammalian protein extraction reagent
MRP	Multidrug resistance-associated protein
MTT	Thiazolyl blue tetrazolium bromide
n.s.	Not significant
NAFLD	Non-alcoholic fatty liver disease
NAPQI	N-acetyl p-benzoquinone imine
NC3Rs	National Centre for the Replacement, Refinement and Reduction of animals in research
NGS	Normal goat serum
NIH	National Institute of Health
NTCP	Na+-taurocholate co-transporting polypeptide
O_2	Oxygen
OAT	Organic anion transporter
OATP	Organic anion transporting polypeptide
OCT	Optimum cutting temperature compound
OCT	Organic cation transporter
OTC	Ornithine transcarbamylase
PAS	Periodic acid Schiff
PBS	Phosphate-buffered saline
PCLS	Precision-cut liver slice
PDGF	Platelet-derived growth factor
PDMA	Polyhydroxymethylmethacrylate
PFA	Paraformaldehyde
PIV	Particle image velocimetry
PolyHIPE	Polymerised high internal phase emulsion templating
PTFE	Polytetrafluoroethylene
qPCR	Quantitative polymerase chain reaction

SD	Standard deviation
SEM	Standard error on the mean
TGF-β	Transforming growth factor β
TUNEL	Terminal deoxynucleotidyl transferase dUTP nick end labelling
VEGF	Vascular endothelial growth factor
WME	William's Medium E

Chapter 1: Introduction

1.1. Overview

The development of *in vitro* tissue models is a huge and rapidly advancing field which spans a wide range of disciplines. Whilst effective tissue models have always been researched for development of drugs and modelling of diseases there is increasing pressure to improve these models to achieve results which more accurately represent *in vivo* conditions. More recently there has also been a move away from less ethical practices such as animal testing alongside an increase in high-throughput cell based methods in order to more efficiently utilise modern day large-scale research methods (Elliott and Yuan, 2011).

Cell culture started out with very simple apparatus aimed at keeping cells alive *ex vivo.* An early method used by Ross Granville Harrison, adapted from methods for biological cell culture, involved the culture of frog embryonic tissue in a hanging drop of lymph on the underside of a coverslip (Harrison, 1907). Methods quickly moved on to culture using glass cell culture flasks and increasingly reproducible media with known constituents (Carrel and Burrows, 1911). Cell culture techniques have come on a long way from these basic beginnings with a large number of cell and tissue specific culture consumables and additives available which can be tailored to create a variety of physiological conditions (Taylor, 2014). Meanwhile, the availability of a wide range of human cells allows for more accurate models to be created which have the full set of genes and proteins expected in humans. This is an improvement on using animal cells and tissue which can lack key proteins involved in studied pathways, or in other cases have orthologs which could have different levels of activity to those in humans (Hammer *et al.*, 2021).

Cells *in vivo* exist in a complex microenvironment with a wide range of factors governing their function and health. These factors can range from the levels of nutrients that the cells receive to more complex signalling pathways between cells and the matrix which forms a feedback mechanism between the cells and their environment (Yamada and Cukierman, 2007). To create an improved cell culture microenvironment many great steps have been made to increase the physiological relevance of cultures through the addition of some of these more complex factors. At the most basic level plastic cell culture dishes and flasks are used which can have different adhesive properties and can be coated with extracellular matrix to suit different cell types. Increasing in complexity from here, more modern techniques involve the use of topographical surfaces, three-dimensional (3D) cell culture technologies, co-culture with multiple cell types and at the most complex end of the spectrum there are bioreactor systems which can be used to even maintain entire organs (Ahmed *et al.*, 2019; Mirbagheri *et al.*, 2019). By utilising the broad spectrum of

expertise across a range of scientific fields it is possible to develop more effective methods for the culture of cells and tissues *in vitro*, pushing ever closer to recapitulating the *in vivo* microenvironment and therefore drastically improve the clinical relevance of *in vitro* models.

This thesis will cover the development, characterisation and application of a novel three-dimensional bioreactor system which can be used for a variety of applications in the fields of cell culture and tissue engineering. The liver was chosen as a model organ to test this system due to the high level of blood flow provided to it *in vivo*, leading us to hypothesise that it would benefit greatly from the use of a more complex culture system with fluid flow which can mimic the vasculature. Initially the system will be designed to recreate the liver microenvironment due to its highly dynamic environment. Due to the flexibility of the apparatus, the need for and possible uses of this system in the modelling of several other organs and *in vitro* applications will also be explored.

To detail the requirements for such a system and investigate the technology currently available for this a thorough literature review will initially be carried out. The structure and function of the liver will be investigated from both an anatomical and physiological viewpoint to discover which properties will need to be achieved for successfully reproducing *in vivo* conditions. This will be followed by a detailed analysis of current methods used in cell culture and their applications, successes, and limitations for liver modelling. This will then be followed by a review of the different uses for liver models in research and industrial applications and the potential requirements for these.

Chapter 3 will lead with a critical analysis of current dynamic culture systems being utilised at present and use the advantages and disadvantages of these to create a series of criteria which must be met for the development of a more effective culture system. This will be followed by the technical development of the bioreactor system with both computer modelling, experimental measurements and *in vitro* techniques utilised to validate the properties of the system.

In Chapter 4 the optimisation of this equipment for use with the hepatocellular carcinoma cell line HepG2 is carried out and a thorough analysis of the structural and functional properties of the cultures is presented. This will look at a range of functional hepatocyte markers such as drug transporters, junctional proteins, and expression of metabolic enzymes. These models will then be tested in Chapter 5 for their effectiveness at predicting drug hepatoxicity, a key use for hepatocyte models. A variety of drugs will be tested, covering a broad spectrum of pathways and levels of hepatotoxicity, and the results compared with results seen from other models in literature.

Chapter 6 will further increase the complexity of the HepG2 models by including fibroblasts and endothelial cells, specifically human neonatal dermal fibroblasts (HDFn) and the human liver adenocarcinoma cell line SK-Hep-1. The main objective is to investigate whether it is possible to incorporate these cell lines into HepG2 models, and if so to carry out a structural characterisation to examine any changes to hepatocyte morphology.

Chapter 7 looks at a further use for the system to aid liver modelling, this time through the culture of *ex vivo* rat liver tissue slices. The current state of research in this area will be presented and the bioreactor apparatus herein will be utilised to investigate potential uses for these models. Further development of the experimental apparatus will be carried out to incorporate oxygenation into the culture system to help with maintaining the liver slices, with the impact of this then analysed.

The final discussion will detail the significance of these results and their potential impact and applications to the wider fields of cell culture and tissue engineering. This will be followed with future work which could lead from this and potential directions which the research could take.

1.1. Background

1.1.1. The limitations of conventional *in vitro* cell culture

In vitro cell and tissue models are becoming increasingly important as more complex cellular systems are investigated and animal models are gradually phased out. Routine *in vitro* cell culture models, utilising cells grown on two-dimensional plastic surfaces, bear little resemblance to the environment of cells *in vivo.* As such, the pathways studied using these methods can have significant variations compared with physiological responses which limits their utility for carrying out accurate biological research (Duval *et al.*, 2017).

These issues arise because the *in vivo* cellular microenvironment is a complex, dynamic system with a wide variety of factors impacting the structure and function of cells. While the exact impacts of different conditions are variable between cell and tissue types the major factors can be grouped as shown by Figure 1.1. Including these factors in culture at physiologically relevant levels is one of the main aims for many modern *in vitro* cell culture technologies (Rijal and Li, 2018).

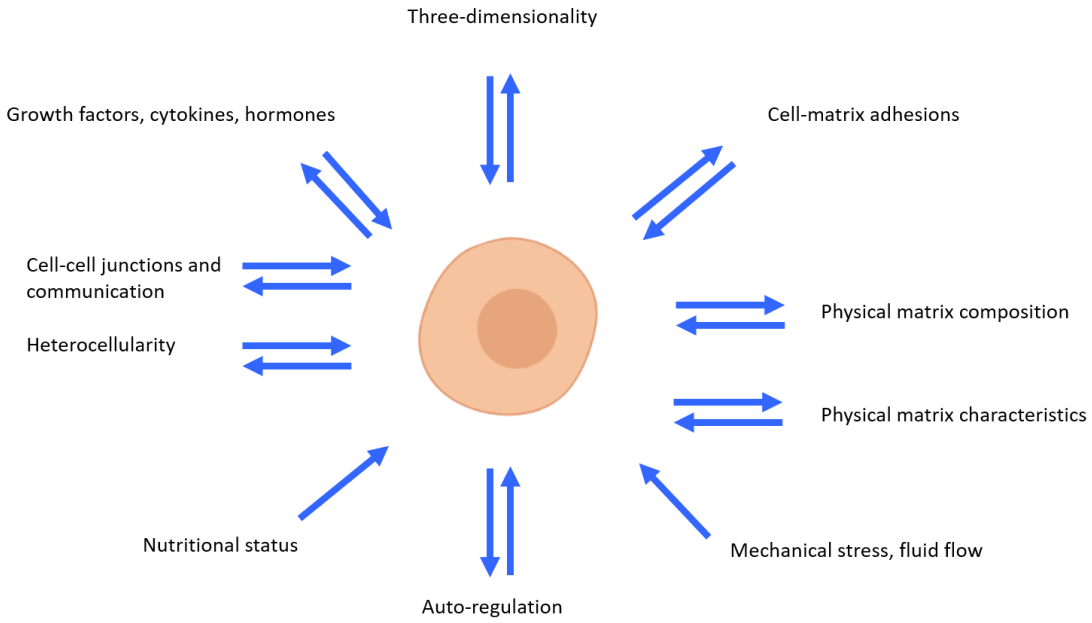

Figure 1.1: The range of factors influencing cells in vivo. In the body a variety of factors affect the structure and function of cells. These can be one-way inputs such as mechanical stress or consist of complex feedback loops such as with cell-cell communication. There is also interplay and regulation between the different input factors which is not shown. Adapted from Cukierman *et al*., 2007.

Cell culture techniques have been developed to recreate some of these properties *in vitro,* however combinations of multiple such methods to push the limits of physiological relevance are utilised

less frequently (Grün, Altmann and Gottwald, 2020). The nature of the cellular microenvironment is incredibly dynamic and the interplay between different mechanisms leads to complex feedback mechanisms. This also means that some apparently simple techniques can have further reaching consequences and provides further evidence for the need to create complex *in vitro* culture systems (Yamada and Cukierman, 2007). A lot of research has been carried out into the different factors presented in Figure 1.1 and their effects on cell culture. By first investigating these then the requirements for an advanced *in vitro* system with a high level of physiological relevance can be elucidated.

1.1.1.1. Three-dimensionality

Three-dimensionality is a property of cells which also has major influences on other factors such as cell-cell junctions and cell-matrix adhesion (Yamada and Cukierman, 2007). Three-dimensionality refers to the complex shapes which cells can possess *in vivo*, in contrast to the flattened morphology typically seen *in vitro* (Kapałczyńska *et al.*, 2018). As shown by Figure 1.2 this has serious impacts on the properties of the cell microenvironment. Cellular flattening seen in 2D culture leads to limited cell-cell junctions at the narrow lateral regions of cells whilst cell-matrix adhesion occurs only underneath the cell. This leads to an enforced polarisation which is unlike many tissues in the body which can migrate and interact in all three dimensions (Baker and Chen, 2012; Duval *et al.*, 2017).

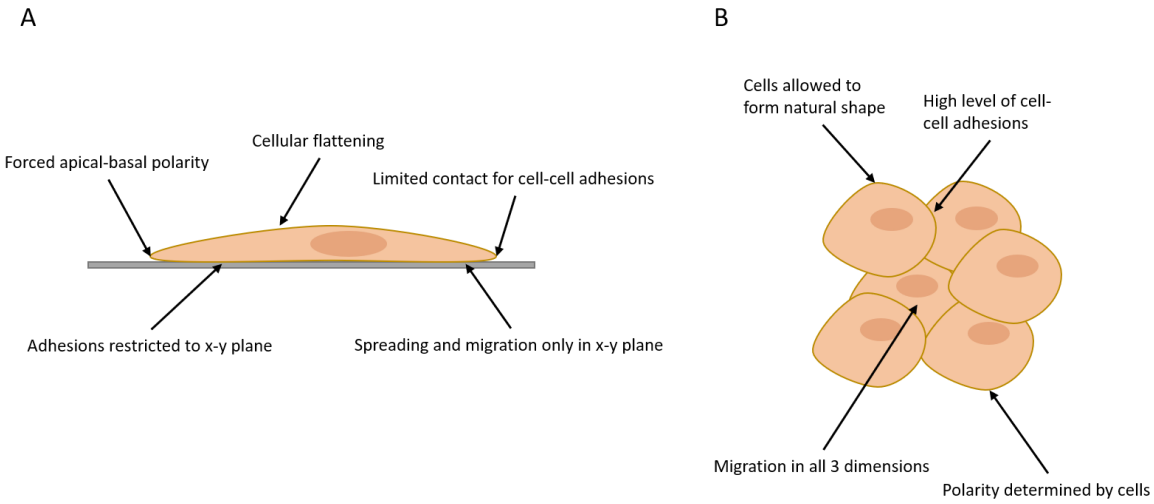

Figure 1.2: Properties of cells grown in 2D and 3D culture. A) Cells in 2D experience cellular flattening and the effects of forced polarity due to the plastic dish acting as a basal membrane. This leads to a change in the proportion and location of different junctional complexes. B) Cells in 3D self-organise and determine their own polarity. This leads to a more *in vivo*-like localisation of cellular junctions.

Incorporating techniques into cell cultures to allow greater three-dimensionality has been shown to have wide ranging effects of cells. Whilst simple visual analysis shows the cell morphology to be significantly altered in 3D (Breslin and O'Driscoll, 2016), further effects have also been reported. The differentiation pathways taken by cells are often different between 2D and 3D culture, for example bone marrow-derived mesenchymal stem cells have been shown to have enhanced adipogenic and osteogenic differentiation potential (Bae *et al.*, 2017; Bicer, Cottrell and Widera, 2021) whilst the ability for pluripotent stem cells to form neuronal networks is improved (Centeno, Cimarosti and Bithell, 2018) with greater neurite outgrowth also found in 3D (Hayman *et al.*, 2004). Drug resistance is another property which is significantly altered with 3D culture. Cells in 3D often show improved responses to known cytotoxic drugs (Sun *et al.*, 2006; Justice, Badr and Felder, 2009) whilst the resistance to anticancer drugs has also been found to increase (Loessner *et al.*, 2010; Breslin and O'Driscoll, 2016). Culture of primary hepatocytes in 3D aggregates has shown that protein expression of key hepatic proteins is maintained over 14 days at higher levels than seen using the typical collagen sandwich culture technique, whilst a rapid deterioration is seen with a simple 2D monolayer(Bell *et al.*, 2018). Similar results can also be seen with commonly used hepatic cell lines such as HepG2 and HepaRG, with enhanced expression of transporter proteins and drug-metabolising enzymes apparent after culture using 3D techniques(Sreenivasa C Ramaiahgari *et al.*, 2014; Ramaiahgari *et al.*, 2017).

1.1.1.2. Matrix composition and structure

Cells *in vivo* reside within the extracellular matrix (ECM) which provides support to the cells, provides mechanical strength to tissues and contains a range of structural proteins and growth factors which influence the behaviour of the cells (Yue, 2014). The exact composition of this matrix has variation both between and within tissues with cells residing in a specific niche which supports their function. For example, the stromal compartments of many tissues, such as the dermis of the skin, are high in proteins such as collagen I, collagen III and fibronectin (Tracy, Minasian and Caterson, 2016). On the other hand, epithelial cells typically reside on a basement membrane consisting of proteins like collagen IV and laminin (Hohenester *et al.*, 2017). These variations influence factors such as cell differentiation, function and viability and can therefore be used to measure tissue health and function, for example with basement membrane components being useful as biomarkers for liver fibrosis (Mak and Mei, 2017). On the plastic surface of a typical 2D cell culture plate these cues are absent and therefore cells often lose their physiological differentiation status over time or possess an abnormal morphology.

1.1.1.3. Chemical and nutritional factors

The supply of nutrients in the body is highly variable between tissues with some receiving highly oxygenated blood, such as the liver and kidneys, while others receive a far more depleted blood supply, with regions of tissues such as stem cell niches typically existing in a very low oxygen environment (Mohyeldin, Garzón-Muvdi and Quiñones-Hinojosa, 2010). Tissues can also derive nutrients from other sources, for example the epidermis of the skin can take up oxygen from the surrounding air (Stücker *et al.*, 2002).

Growth medium used for cell culture can be formulated for specific cells or tissues, particularly those which require specific growth factors to survive. More frequently generic formulations are used for cell culture such as Eagle's minimum essential medium (MEM). This was first developed in 1959 and contains the nutrients required to maintain viability however lacks any tissue specific nutritional factors (Eagle, 1959). This means that cultured cells often have a suboptimal nutritional supply which can lead to variations in functionality whilst variations in media choice between studies is a large source of variability between scientific studies. This variation is exacerbated by the frequent use of serum supplementation, which has undefined components and exhibits high levels of batch variability. Due to this, as well as ethical concerns, the use of serum-free media is becoming increasingly desirable and commonplace (van der Valk *et al.*, 2010).

Medium changes in cell culture also contribute to non-physiological nutritional conditions. Whilst adding factors to media is one way to provide cells with the correct nutrients, the cells themselves also release factors into the media which support their environmental status. This can be particularly important in co-culture experiments where several cell lines are producing different factors to create a physiologically relevant microenvironment. Typically, media changing is carried out by a full removal and replacement of the cell culture media. This removes all these secreted factors and effectively resets the environment back to the beginning of the culture period (Vis, Ito and Hofmann, 2020). Methods have been developed to work around this problem, such as through using conditioned media, larger media volumes, and continuous fluid flow, with the benefits of such techniques being heavily documented (Dowling and Clynes, 2011; Tarng, Huang and Su, 2012; Dixon *et al.*, 2014; Chen *et al.*, 2019; Caneparo *et al.*, 2020).

1.1.1.4. Mechanical forces and fluid flow

Mechanical forces have major impacts on cells in the body and manifest in a range of different ways. Tissues such as the skin, muscles and bones frequently experience mechanical forces due to the movement of the body leading to stretching, shear and compressive forces. These have impacts upon the structure and function of the cells through complex mechanosensory pathways and in some cases are required for correct differentiation of cells (Nomura and Takano-Yamamoto, 2000; Chanet and Martin, 2014; Chen *et al.*, 2018).

Other sources of mechanical stress come from the flow of liquids within the body, in particularly the blood stream. The shear stresses caused by blood flow are typically shielded from the parenchymal cells of tissues by the endothelial cell linings of blood vessels (Ballermann *et al.*, 1998). Other cells can also experience shear stress, such as when hepatocytes extend cytoplasmic processes into the sinusoidal lumen in the liver (Warren *et al.*, 2006), and other fluids in the body such as interstitial fluid also contribute to shear stress on cells, albeit at much lower levels than from the blood (Yao, Li and Ding, 2012; Tarbell and Shi, 2013). The peristaltic flow of the blood also causes expansion and contraction of blood vessels, which in turn is passed on to the surrounding cells such as vascular smooth muscle cells (Owens, 1995).

1.1.2. Techniques for creating a more physiologically relevant tissue equivalent

The wide range of factors involved in the *in vivo* cell microenvironment and their major impacts upon cell structure and function suggest that there is a great need highly complex *in vitro* systems which recapitulate many of these variables. There has been a large amount of research carried out to produce such systems which often trade off ease-of-use for high physiological complexity.

1.1.2.1. Creating an improved cell morphology using 3D culture techniques

The development of 3D culture techniques was carried out to combat the flattening of cells seen in conventional 2D cell culture and these have become increasingly common in literature (Jensen and Teng, 2020). These use growth substrates with complex, three-dimensional structures which can be in the form of Scaffolds and hydrogels which cells can reside within or on the surface of, topographical surfaces which can be used to control the patterning and interactions of cells or matrix-free techniques such as cell aggregates which allow cells to self-assemble into their preferred morphology. All these techniques have their advantages and disadvantages with the choice of method related to the nature of the tissue being modelled.

One of the major advantages of typical 3D culture systems is the ability to long term viable culture of cells. Many cells *in vitro* can take up to several weeks to reach a fully differentiated state with highly functional apical-basolateral polarisation. This time scale can be difficult for some 2D cultures, with loss of viability often seen before this point with primary cells such as hepatocytes or airway epithelia (Wiszniewski *et al.*, 2006). With 3D culture this has been carried out successfully for many cell and tissue types, with the inclusion of ECM often also being used to help support the cells (Kervancioglu *et al.*, 1994; Moghe *et al.*, 1996; Miessen *et al.*, 2011; Schlaermann *et al.*, 2016).

Further issues with simple 2D culture with polarised cells stem from transport of fluids across the membranes. With the Caco-2 cell line, for example, formation of dome-like structures can be seen in 2D monolayer culture (Ramond, Martinot-Peignoux and Erlinger, 1985). This is due to transport of molecules basally, building up between the growth substrate and the cells and therefore disrupting the formation of a homogeneous monolayer. This effect which can be resolved using permeable basal substrates, a property possessed by many 3D culture systems (Ramond, Martinot-Peignoux and Erlinger, 1985; Darling *et al.*, 2020).

3D systems also often allow for co-culture of several cell lines, both in direct contact and spatially separated (Roger *et al.*, 2019; Xin *et al.*, 2019). This allows for investigations into both juxtacrine and paracrine effects, which are not as easily carried out with conventional 2D techniques (Bhardwaj, Singh and Mandal, 2019; Piard *et al.*, 2019). With the high complexity and multicellular nature of tissues *in vivo* this is another significant step towards the recreation of a physiologically relevant cellular microenvironment.

1.1.2.2. Recreating the dynamic in vivo environment

One property that is more difficult to accurately recreate *in vitro* is the vascularised nature of tissues *in vivo*. The impact of vascularisation comes from both the mechanical stimulus provided by the fluid flow as well as the interactions between the endothelial cells lining the blood vessels and the surrounding tissue. This lack of fluid flow also allows the build-up of unstirred layers of media above the cell surface, the effects of which are shown in Figure 1.3. These layers, which can be up to several hundred microns thick, can be a major problem as they can have a significant impact on cell functionality and can reduce the predictability of models (Green and Otori, 1970). The primary effect of unstirred layers is a reduction in diffusion rates, which then leads to reduced levels of nutrients such as oxygen above the cell surface (Tramper, 1995) and a build-up of cellular waste which does not occur in natural tissue (McMurtrey, 2014).

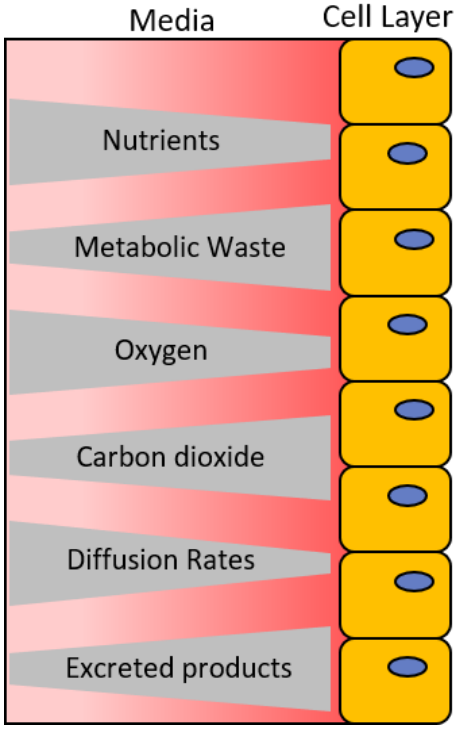

Figure 1.3: Variation in levels of media constituents in proximity to cell or tissue layers. Compounds metabolised by the cells reduce in close proximity due to the rate of transport into the cells being greater than the rate of diffusion through the unstirred layers. Excreted products and metabolic waste build up close to the cell layer as their transport from the cell is at a higher rate than their diffusion into media.

Due to the nutrient levels differing in the layer above the tissue in comparison with the bulk values in the medium, osmotic gradients across the cell membrane differ compared with the expected and *in vivo* gradients. One study found that the unstirred layers were the rate limiting step in diffusion of carbon dioxide across a cell membrane (Missner *et al.*, 2008) whilst the same has been calculated to be true for oxygen (Dotson *et al.*, 2017). Due to the thickness of unstirred layers being several orders of magnitude larger than membrane thickness this can influence the apparent activity of membrane transporters (Barry and Diamond, 1984; Verkman and Dix, 1984). Research into this

phenomenon have found levels of import and export which do not match physiological levels with errors ranging from a few percent to more than an order of magnitude (Spivak *et al.*, 2006). Kinetics experiments can be greatly altered by these effects with the time taken for drug penetration to be increased and mechanisms such as non-specific receptor binding becoming more common.

In the body the cells have a constant supply of nutrients from the blood. In cell culture this is not the case, with the cells typically immersed in static medium. This causes a build-up of waste products near the cell surface as well as nutrient and oxygen gradients which mean that the cells are not receiving consistent levels of these as they would in vivo. This means that osmotic gradients across the cell membrane differ from natural gradients which can lead to a change in the levels of membrane permeability and cellular import and export, altering the functionality of cells (Barry and Diamond, 1984; Bojesen and Hansen, 2006).

In addition, there is an assortment of paracrine signals from neighbouring cells within *in vivo* tissue (LeCluyse *et al.*, 2012) and specific levels of shear stress caused by the flow of blood in different regions (Tilles *et al.*, 2001). All these factors are missing in static 2D and 3D cultures and affect the behaviour of the cells, reducing the physiological relevance of observations. Bioreactors can be used to overcome these limitations by introducing dynamic conditions to the culture (Hansmann *et al.*, 2013; Gelinsky, Bernhardt and Milan, 2015). Such systems can be designed to incorporate fluid motion in a way which best represents the tissue of interest.

1.1.2.3. Types of media motion

There are several different ways in which fluid motion can be introduced to cell cultures and specific methods can be more suited to certain tissue types. Perfusion, the convective flow of fluids through a tissue, can be broken down into two basic categories of flow across a tissue surface and flow through a tissue (Salehi-Nik *et al.*, 2013) as shown by Figure 1.4. Flow across a tissue can be useful to model organs with a tight epithelial barrier which fluids such as blood would not be expected to pass, for example blood flow in the dermis and hypodermis of skin or flow of chyme through the intestinal lumen. This form of fluid flow provides mechanical stimulus to the cells and can provide a better supply of nutrients as well as removal of waste products.

The other form of fluid flow, passing fluid through a tissue, is more relevant for highly vascularised organs and tissues without a tight epithelial barrier. Examples of relevant tissues would be the liver, where blood flows through the tissue between plates of hepatocytes as well as various stromal tissues. Through-tissue flow has the same benefits as flow across a tissue however can be applied

more broadly to all cells in a tissue rather than just the surface layer and therefore gives a closer resemblance to vascularisation *in vivo* (Plunkett and O'Brien, 2011). This has particular use for maintaining larger tissue constructs in which the diffusion limitations typically would prevent creation of tissues more than a couple of hundred microns in thickness (Malda *et al.*, 2008).

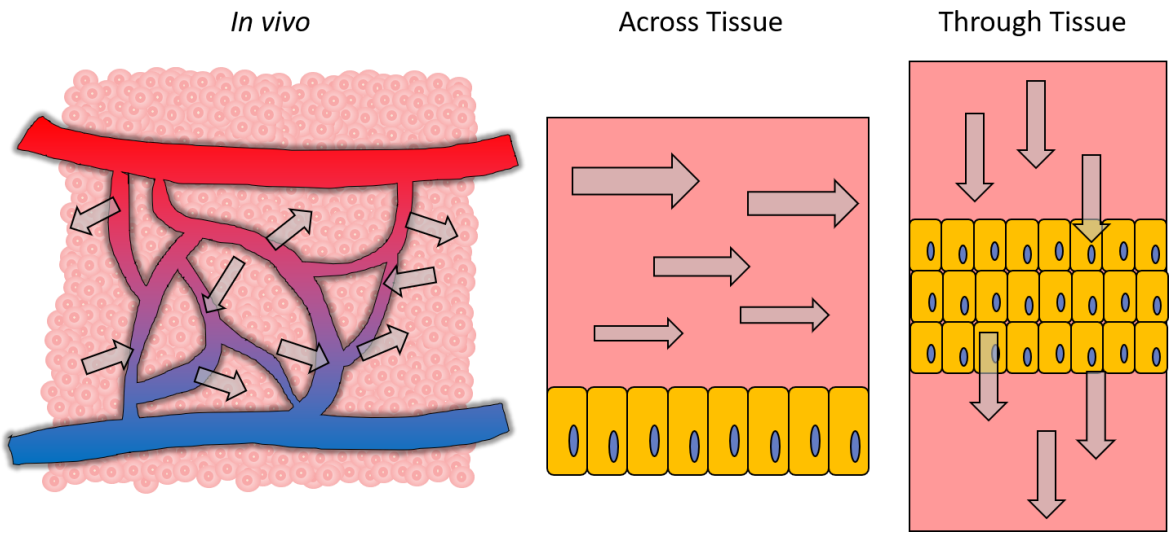

Figure 1.4: Fluid flow in vivo and methods for recreating this in vitro. A) Fluid flow in tissues takes place inside blood vessels. Compounds are transported both into and out of the blood vessels through the permeable walls of capillaries. The composition of the blood changes between the arterial and venous regions of a tissue as cells take up and secrete molecules into the blood flow. B) Passing media over a cell layer helps keep media mixed and increases diffusion close to the cell layer by disrupting unstirred layers. C) Passing media through a cell layer increases media turnover around the cell layers and can help to deliver nutrients deeper into thick tissue constructs.

The bulk flow of this medium as discussed is carried out by convective fluid flow, caused by forces acting on the fluid. Biological examples of this include the pumping motion of the heart driving blood flow, or the active secretion of bile constituents from hepatocytes causing pressure-driven motion (Boyer, 2013). Another form of mass transport which is present is diffusion. This occurs when regions within the medium have varying concentrations of a substance, for example due to nutrient depletion close to cell layers, leading to a flow of such molecules from regions of high concentration towards the regions of low concentration. Whilst diffusion is responsible for movement of soluble factors within static cell culture systems where convective flow is minimal, once convective motion is present this generally becomes the predominant form of fluid motion due to the flow rate typically being considerably larger than the rate of diffusion for typical cell culture medium constituents (Rouwkema *et al.*, 2009).

To investigate the impacts of a novel bioreactor system a model needs to be chosen which should have clear benefits from the addition of fluid flow and a 3D environment. The liver was chosen for this due to its complex structure high levels of blood flow it receives *in vivo*, therefore suggesting that it would benefit greatly from the vascular mimicry provided by a bioreactor.

1.1.3. Applications and challenges of liver tissue engineering

The liver is a large organ found in vertebrates which carries out a variety of important roles such as blood detoxification, protein synthesis and bile production. It is of great interest in the drug development pathway as a large proportion of drug metabolism takes place in the liver and therefore thorough research into the pharmacokinetics of drugs in the liver is a requirement for moving any drug to the market.

Drug-induced liver injury (DILI) in particular is a major issue from drugs which have effects not found during testing and is the cause of most of the drug recalls that occur (Ballet, 1997). This costs large amounts of time and money for pharmaceutical companies and has led to a lot of research into better ways to predict drug hepatotoxicity. One study (DiMasi, 2002) found that a decrease in drug development time of one quarter reduced the total cost to develop a drug by 16%. With the capitalised cost of getting an approved drug on the market being over 2.5 billion US dollars and a timespan of 12-15 years of development, the savings that can be made through more efficient research and development are huge (DiMasi, Grabowski and Hansen, 2016). Figure 1.5 shows various timescales and costs estimated by recent research on drug development and how these have increased significantly over time.

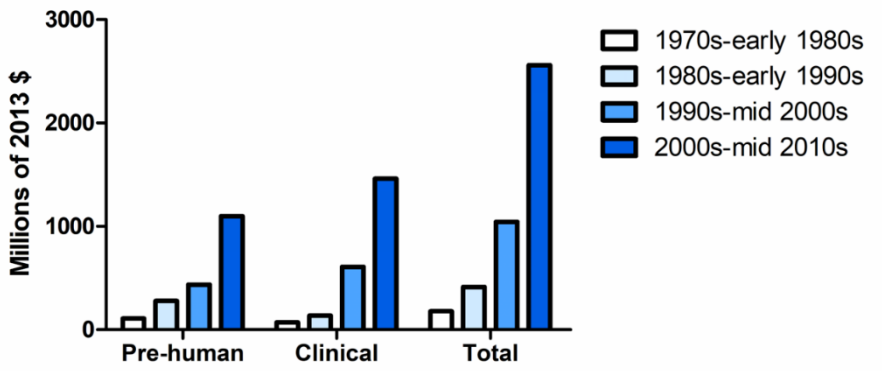

Figure 1.5: Costs of drug development stages over time. The costs for the two major stages of drug development, pre-human and clinical trials, are shown. Costs are normalised to 2013 dollars to account for inflation. Over the past 40 years total drug development costs have increased more than 10-fold. Data adapted from DiMasi *et al*., 2016.

Another important use for liver models is the modelling and treatment of liver cancer. As shown by Figure 1.6 Liver cancer is a very common form of cancer with the second highest mortality rate out of the 20 most common cancers (Jemal *et al.*, 2017). In Europe roughly 12% of those diagnosed with liver cancer survive for more than 5 years and it is the 8th highest cause of cancer death in the United Kingdom. Around 70% of patients with stage 1 liver cancer have surgery to remove the tumour with only 20% at the same stage receiving chemotherapy. This highlights a potential need for improved non-invasive treatments, something which typical liver models are not particularly effective for researching due to their inherent simplicity.

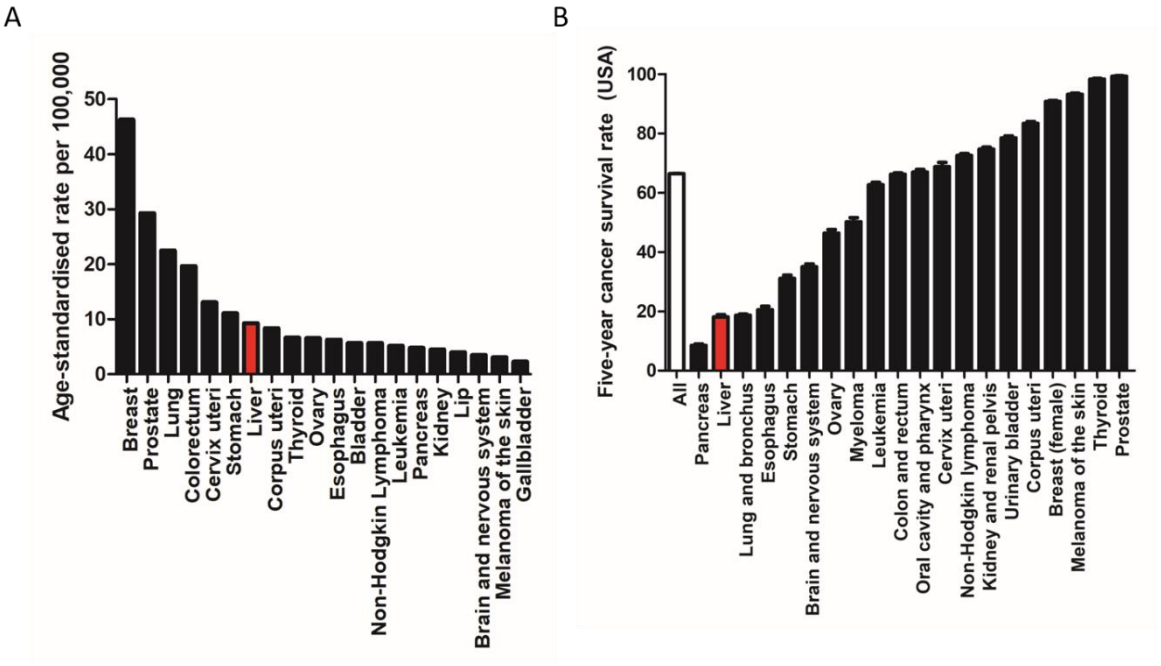

Figure 1.6: Statistics on the rate of incidence and five-year cancer survival rates. A) Age-standardised rate of incidence per 100,000 people for the 20 most common cancers in the world in 2018. According to this data, the liver is the 7th most common cancer worldwide. Data adapted from the International Agency for Research on Cancer B) Five year cancer survival rate in the USA from 2006-2012 with 95% confidence limits. Only pancreatic cancer has a lower survival rate than liver cancer with many of the more common cancers having much higher survival rates. Data adapted from Jemal *et al*., 2017. Values for liver cancer have been shaded in red.

To look at developing more effective models for the liver we first must have a thorough understanding of the structure and function of the liver at both the anatomical and physiological levels.

1.1.3.1. Gross morphology of the liver

The gross morphology of the human liver is a structure consisting of four lobes: the left and right lobes visible from above and the caudate and quadrate lobes which are also visible when viewed from below along with the gall bladder, a small organ used for the storage of bile. The blood supply to the liver is a mixture of roughly 70% venous and 30% arterial blood (Burt and Day, 2002). The detoxification processes are carried out on the venous blood which is fed to the liver from the gastrointestinal tract and spleen via the hepatic portal vein as shown by Figure 1.7. The arterial blood, transporting roughly 60% of the liver's oxygen requirements, is fed directly from the heart via the hepatic artery. The blood is then removed from the liver through the hepatic artery which leads to the inferior vena cava (Abdel-Misih and Bloomston, 2014).

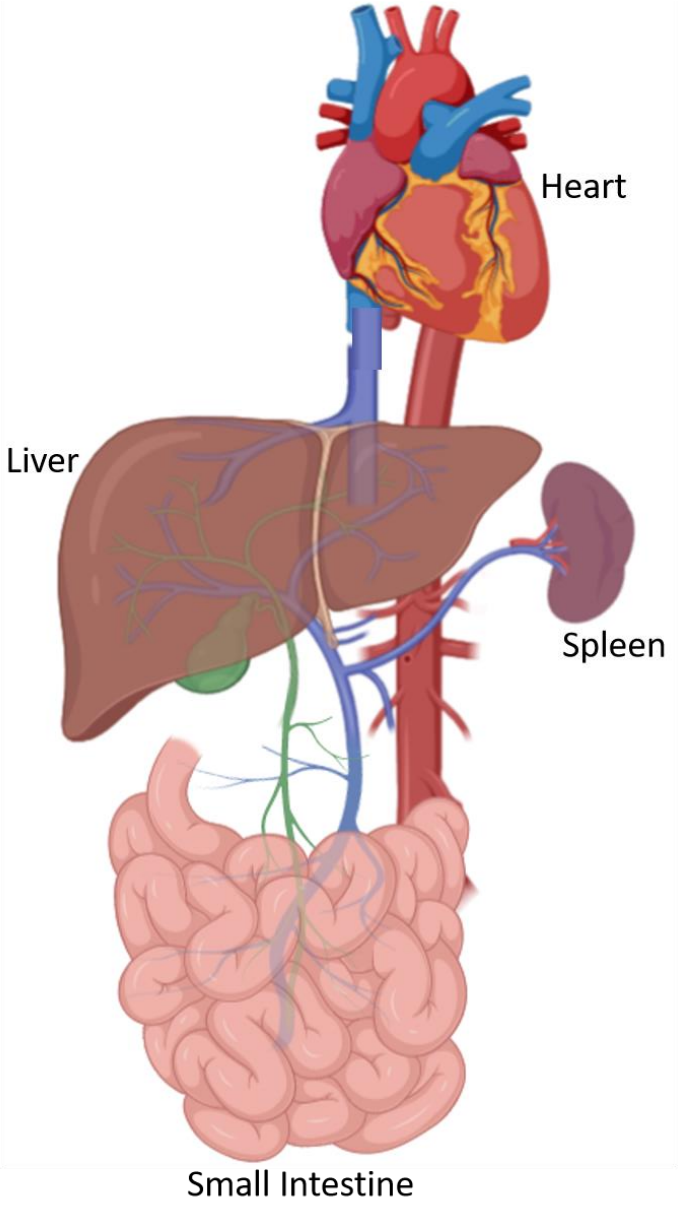

Figure 1.7: The vasculature network between the liver and other organs in the body. The liver has a venous supply of blood from the spleen and small intestine and an arterial supply from the heart. Bile flows from the liver to the gallbladder, where it is stored, and then onwards to the small intestine where it helps with the digestion of lipids. Blood leaves the liver through the hepatic vein to return to the heart. Created using BioRender.com.

Further movement of fluids is carried out by the bile duct network. Bile is produced in the liver and transported to the common bile duct through bile canaliculi where it is then either stored in the gallbladder or drained into the duodenum (Strazzabosco and Fabris, 2008). The liver is also responsible for production of about half of the lymph in the body, and the lymphatic system draining this further adds to the complexity of the fluid transport networks in the liver (Tanaka and Iwakiri, 2016).

1.1.3.2. Cellular Structure of the liver

The microscopic structure of the liver is formed from a series of repeating units called lobules. These lobules are formed from the portal region, containing the portal triad of the portal vein, portal artery and bile duct, and the central vein which removes blood from the liver. There are several different variations of repeating unit which have been used over time to describe the liver, each focusing on different aspects of the functional unit as shown in Figure 1.8A. The earliest unit described is known as the classical lobule and is based around the sinusoidal blood flow, with blood flowing from the edges inwards. This is a hexagonal unit centred around a central vein and has a portal triad, consisting of the portal vein, the portal artery and the bile duct, located roughly at each corner of the structure (Ishibashi *et al.*, 2009). Alternatively the portal lobule is a triangular area centred on the portal triad with a central vein at each corner (Mall, 1906) and is a concept which can be of use when carrying out biliary studies. The acinus is a third method to break down the structure in the form of an elliptical shape with the left and right extremes at the central veins and the top and bottom being on portal triads. This is a more useful model for research into the liver metabolism as the acinus can be split into 'zones' at certain distances from the centre, each containing blood with particular oxygen and nutrient levels and expressing different functional characteristics (Rappaport *et al.*, 1952).

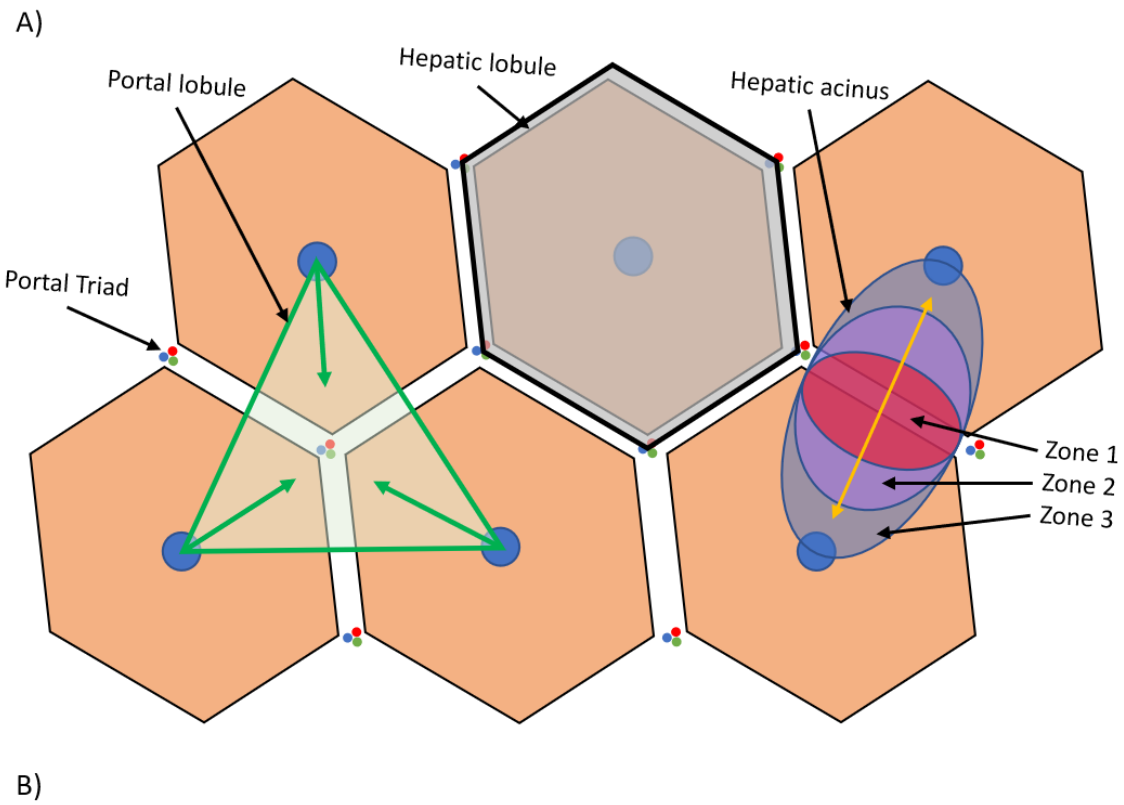

Figure 1.8: The microstructure of the liver. A) Schematic representation of the different lobules that the structure can be divided into. The portal lobule is centred around a portal triad with corners on three central veins. Green arrows represent the direction of bile flow. The hepatic lobule is centred around the central vein and encompasses the hexagonal structure formed by adjacent portal triads. The hepatic acinus is an oval with its long edges centred on portal triads and short edges on central veins. This oval structure can be divided into three zones with different oxygen concentration and functional phenotype. Orange arrows represent the direction of the oxygen gradient from the centre of the acinus. B) Microstructure of liver centred around a sinusoid. Blood flows from the portal vein and hepatic artery on the right towards the central vein on the left. Bile flows in the opposite direction towards the bile duct.

Regardless of the interpretation of the lobule there are several key features that are present which can be seen in Figure 1.8B. The blood enters the tissue from the portal triad which consists of a portal vein, a portal artery, and a bile duct, with multiple of each vessel often present in a single triad. The two blood supplies join in the tissue to form the sinusoids, highly porous capillaries which vascularise the tissue. These then lead to the central vein at the centre of the classical lobule, where the blood flows out of the liver via the hepatic veins and into the inferior vena cava and back to the heart. The bile in the liver flows counter current to the blood supply through bile canaliculi (channels formed between adjacent hepatocytes) to the bile duct where it is then transported away from the liver (R. Burt, A. Portmann, Ferrell, 2017). Figure 1.9 shows the lobular structure in the

liver of a pig when stained with Masson's trichrome. The portal regions can be clearly seen due to the collagen deposition in these regions, outlining the hepatic lobule. The portal regions have a variable morphology due to the isotropic morphology of the liver, with the lumens of the different fluid vessels clearly visible in Figure 1.9B, whilst in figure 1.9C these vessels are less easily distinguished due to the angle of sectioning relative to the vessel morphology in this region.

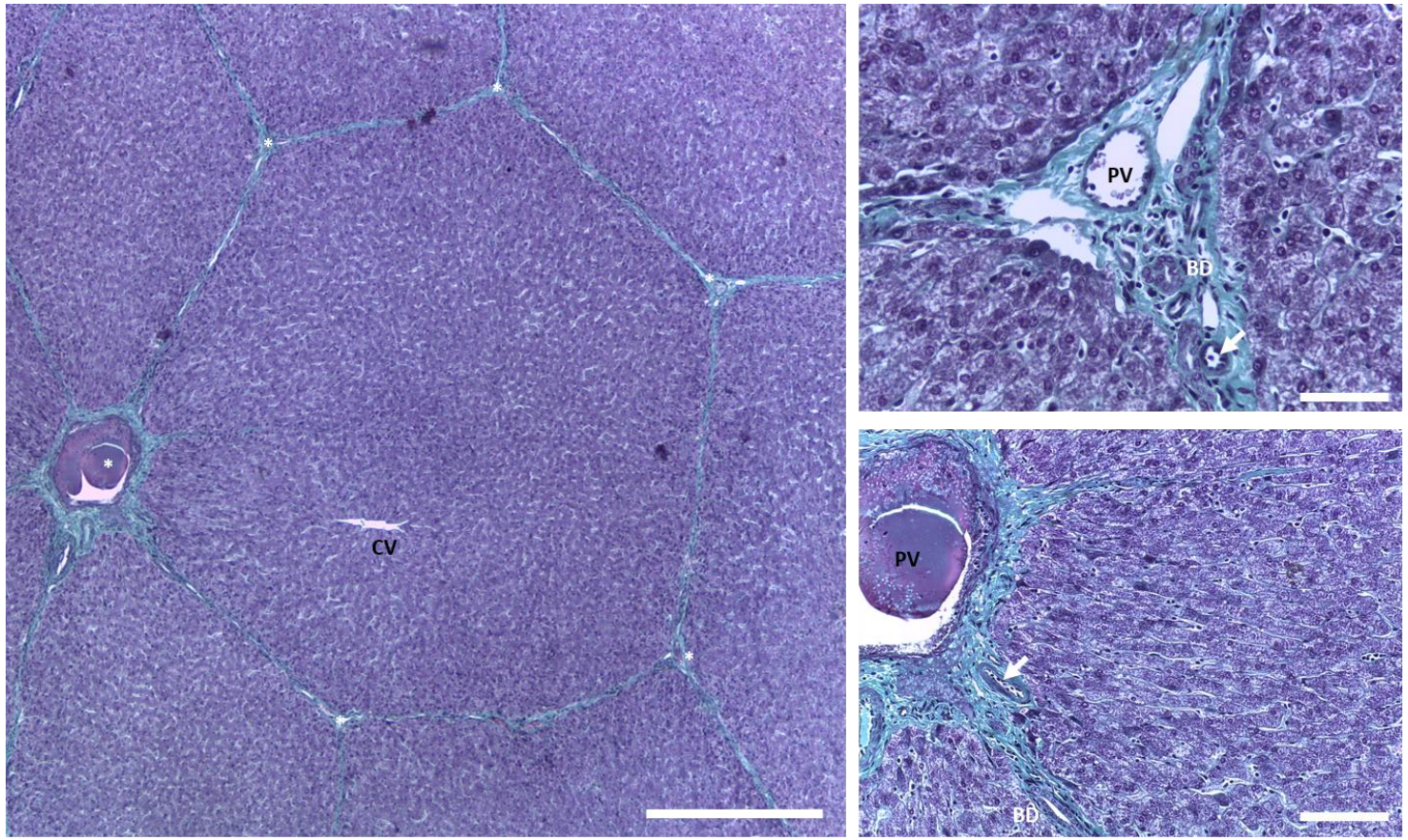

Figure 1.9: Histology of pig liver stained with Masson's trichrome. The hepatic lobule can be clearly visualised when using Masson's trichrome due to the high levels of collagen in the portal regions (blue staining). A) Low magnification image showing a hepatic lobule. A central vein is present towards the centre of this lobule and portal triads are typically located at the intersection between three hepatic lobules. The scale bar is 1 mm. B) A typical portal triad consists of a portal vein, bile duct and hepatic artery, all of which are clearly present in this image. The scale bar is 50 µm. C) Due to the isotropic nature of the liver structure the morphology of the portal triad often looks different from that seen in 1.9B. In this image a large portal vein takes up most of the region with the hepatic artery and bile duct located further away. The scale bar is 100 µm. * = portal triad, CV = central vein, PV = portal vein, BD = bile duct, arrow = hepatic artery.

Structurally the liver is composed of over a dozen different cell types, the most common of which are shown in Table 1.1. Hepatocytes are the most common cell type and form the parenchymal tissue of the liver, consisting of 70-85% of the liver mass (Kmiec, 2001). Another major cell type found in the liver are liver sinusoidal endothelial cells (LSECs) which are highly fenestrated endothelial cells lining the sinusoids to form a discontinuous epithelial wall which allows the passing of substances both into and out of the blood. Present within the sinusoidal lumen, adhered to the endothelial cells, are Kupffer cells. These are resident macrophages which have a role in the degradation of red blood cells and clearance of bacteria from the blood stream (Bilzer, Roggel and Gerbes, 2006). A further important cell type are the hepatic stellate cells. These reside in the space of Disse, between the LSECs and the hepatocytes, and play a major role in the onset of diseases such as fibrosis through their activation into myofibroblasts (Friedman, 2008). Other cells present include portal fibroblasts and bile duct epithelial cells which both reside in the portal regions of the tissue (Crawford, Bioulac-Sage and Hytiroglou, 2018).

1.1.3.3. Functions of the liver in vivo

As the most common cells in the liver and the main parenchymal cells, the hepatocytes are incredibly important for liver function. These cells carry out the metabolic processes of the liver such as protein synthesis, bile formation and secretion and glycogen formation as well as major drug detoxification processes (Schulze *et al.*, 2019). It is this wide range of function that makes the hepatocytes the most heavily studied cell type for use in liver tests *in vitro* (Hewitt *et al.*, 2007).

Looking at the liver in respect to the three zones described by the acinus the hepatocytes in each region can be divided based on their functions in each zone as shown in Figure 1.10. This variation in function with oxygen gradient has developed from the evolutionary advantage it provides by maximising the efficiency of the liver and allowing all hepatocytes to balance the workload of the liver instead of loading those closest to the portal region the heaviest (Kietzmann, 2017).

Table 1.1: Different cell types found in the adult liver. The cells listed can be further divided into numerous subtypes depending on their location within the liver lobule. Further cell types such as various immune cells and bone marrow derived stem cells are also present circulating within the blood and are recruited into the tissue in response to liver damage.

Cell Type	Localisation	Proportion
Parenchymal Cells		
Hepatocyte	Hepatic lobule interior	70% (Zeilinger 2016)
Cholangiocyte	Interlobular bile ducts	3-5%(Zeilinger 2016)
Non-Parenchymal cells		
Stellate Cells	Space of Disse	5-8% (A. Geerts 2001)
Sinusoidal Endothelial Cells	Sinusoids	15-20% (Poisson et al. 2016)
Kupffer cells	Sinusoidal walls	5-7% (T. Zeng 2016)
Oval Cells	Portal region	1-3% (Lotowska et al. 2017)
Portal fibroblasts	Portal region	(Wells 2015)
Dendritic Cells	Sinusoids	(Rahman and Aloman 2013)

The regions with the highest oxygen levels carry out functions such as gluconeogenesis, fatty acid oxidation, sulfation, and a larger proportion of urea synthesis. Those found closer to the portal vein, with the lowest oxygen levels, perform functions such as glycolysis, lipo- and ketogenesis, cytochrome P450-based drug detoxification and a greater proportion of bile acid synthesis (Lindros, 1997). These variations in physiological function are very important to the healthy function of the liver and are something which is incredibly difficult to accurately replicate *in vitro*, though there are methods in development which look to replicate this environment (Ahn *et al.*, 2019; Tomlinson *et al.*, 2019).

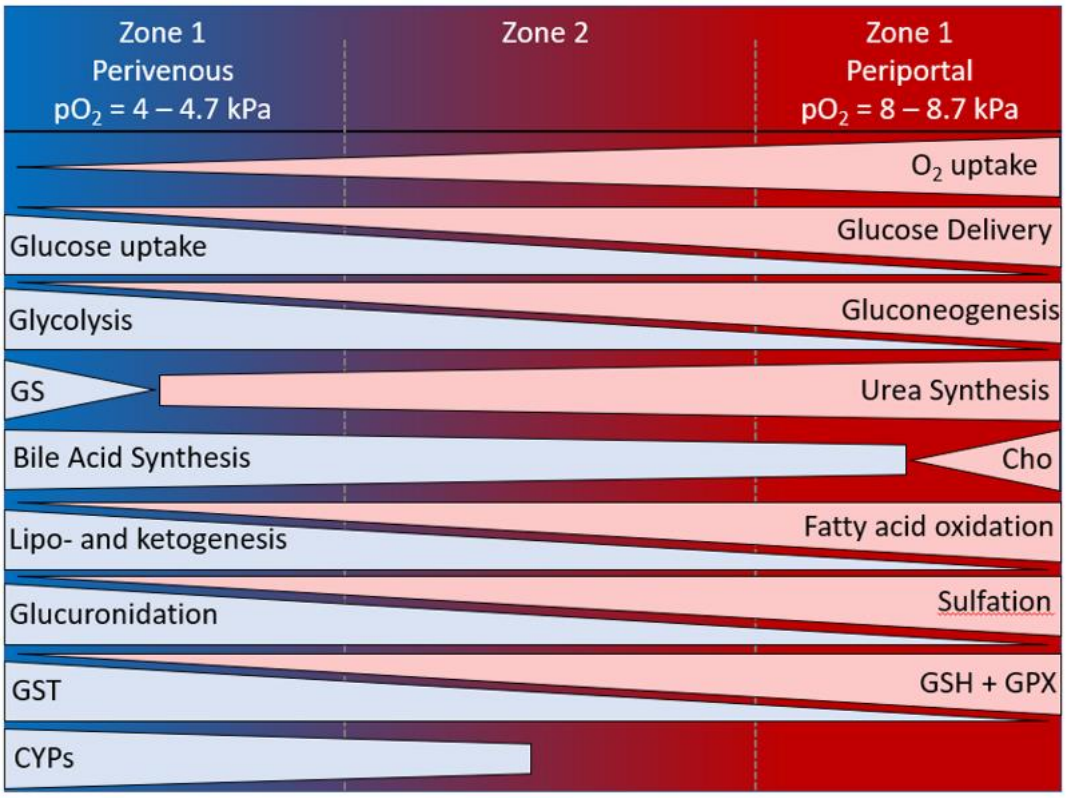

Figure 1.10: Zonular variation in function and protein expression in the hepatocytes. Hepatocyte function varies within the hepatic lobule when divided into zones based on blood oxygen content. This variation shares the functional load across hepatocytes in the entirety of a lobule instead of placing a disproportionately large load on periportal hepatocytes and underutilising perivenous hepatocytes. By distributing the functional processes of the liver in this way, the cells of the liver are able to perform a wide range of functions at a high efficiency. Adapted from Kietzmann, 2017.

Figure 1.11 highlights the unique polarity phenotype of hepatocytes which has been formed to allow them to carry out their wide range of functions. Due to the lack of basement membrane found supporting most epithelial cells, the hepatocytes instead form two polarised domains; an apical domain on faces joining between hepatocytes containing the bile canaliculi and a basolateral domain which faces outwards towards the sinusoidal endothelial cells (Müsch, 2014). This polarity is mediated by a variety of junctional proteins, and is difficult to recapitulate *in vitro* due to the complex interactions and self-organisation between neighbouring cells and ECM (Treyer, Aleksandr; Müsch, 2013).

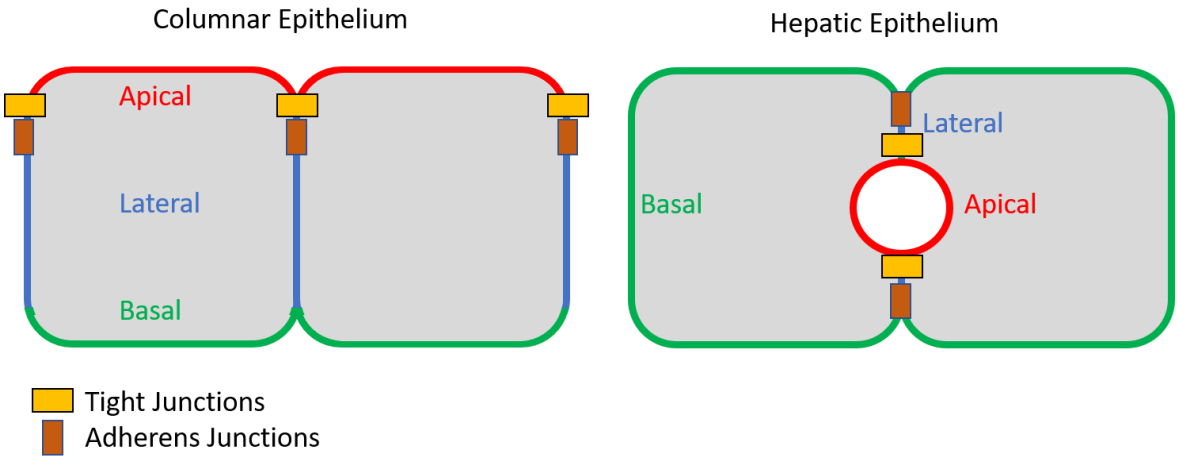

Figure 1.11: Polarisation and junctional localisation in columnar epithelia and hepatocytes. Hepatocytes show a unique polarisation compared to most epithelial cells. The apical surface forms between to adjacent hepatocytes to outline the bile canaliculi. Tight junctions seal this surface to maintain the blood-bile barrier with adherens junctions positions further towards the basal edges, making this part of the membrane equivalent to the lateral membrane in columnar epithelium. The basal membranes form on the edges which are not in contact with hepatocytes which instead face towards the sinusoids. The basal and lateral membranes are usually group together to form the basolateral membrane of a hepatocyte.

Key proteins in the formation of these junctions and a functional hepatocyte phenotype include the Junctional adhesion molecule-1 (JAM-1) (Konopka *et al.*, 2007), connexin 32 (Cx32) (Vinken *et al.*, 2006) and E-Cadherin (Gonzalez-Sanchez *et al.*, 2015), the latter displaying an oxygen-dependent expression in hepatocytes with increased levels in periportal hepatocytes (Doi *et al.*, 2007), which help to traffic proteins such as the claudin and occludin tight junctional proteins to their correct cellular localisation.

1.1.4. Applications of liver research

Due to the large number of functions carried out by the liver it also is of great importance to be able to understand and accurately model liver processes. The main areas of liver research can be grouped broadly into four categories: basic research, drug development, fibrosis modelling and the study of liver disease.

1.1.4.1. Basic research

The liver is responsible for a variety of functions which ensure the key running of the body and contributes to a range of other processes. The synthesis and storage of glycogen from glucose is

one of the main synthetic pathways in the liver however it is also responsible for the production of many proteins including albumin. Non-parenchymal cells also have specialised functions such as stellate cells being a major storage site for vitamin A. On top of this new functions are continually being discovered for specific cells in the liver, such as the active regulatory role hepatic stellate cells play in fibrosis (Fujita and Narumiya, 2016), and some processes have functions which are unconfirmed, such as the production of elastin and microfibrils by portal fibroblasts (Wells, 2015). Detailed research into the pathways of these functions and the influence they have on the normal function of the body would be valuable to feed into many other areas of research including those of other organs which the liver can impact.

1.1.4.2. Drug Development

As mentioned previously the development of drugs is a costly and time-consuming process which would benefit greatly from improved liver models. Being able to more accurately predict hepatotoxic effects earlier in the development pathway would mean less drugs would make it to later stages such as animal tests and human clinical trials as shown in Figure 1.12 (Paul *et al.*, 2010). This would reduce the number of animals which need to be used and allow a vast cost reduction in the most expensive steps of the drug discovery pathway by removing unsuitable compounds earlier in the discovery pathway.

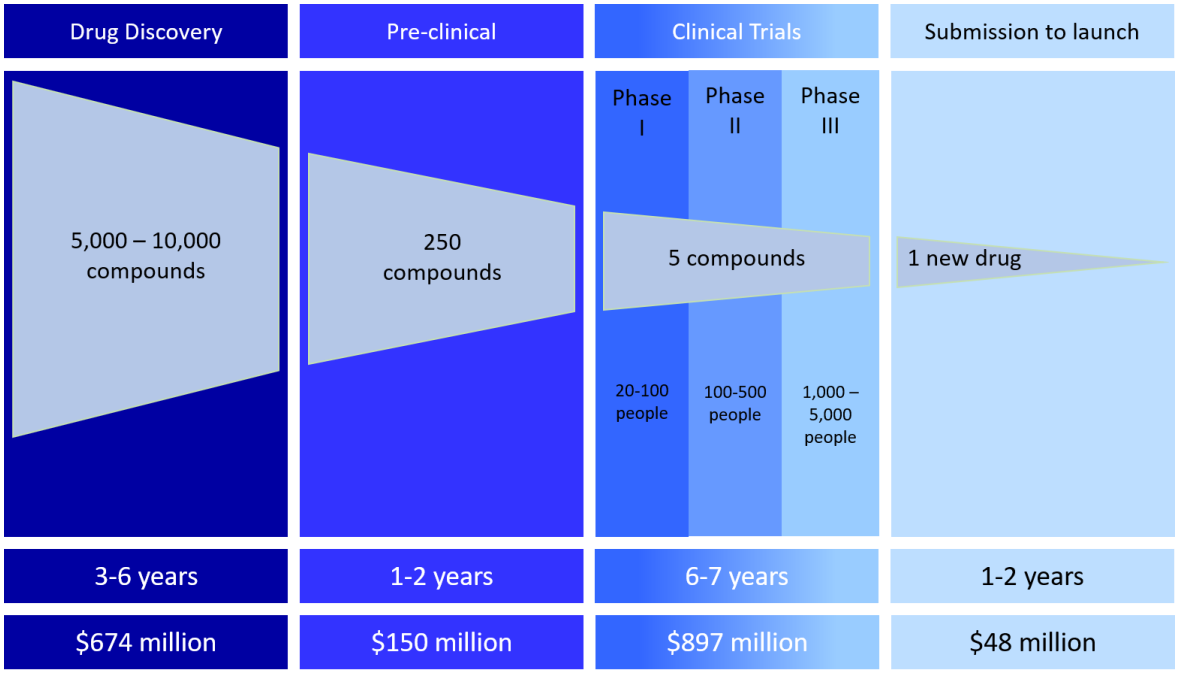

Figure 1.12: Stages of the drug development pathway with their associated time and monetary costs. The pathway starts on the left with screening of compounds and follows the pathway to the right over time. As the development process gets closer to the final stages the cost increases significantly alongside a reduction in the number of compounds tested. The later stages utilise more physiologically relevant models, such as animal models, or clinical trials in humans. The typical time in each stage along with the average capitalised costs in 2008 are displayed at the bottom of each stage. Data is adapted from Paul *et al.*, 2010.

For a liver model to be of use for pharmacological studies it needs to have a robust expression of the major phase I, phase II and phase III drug metabolism enzymes with an overview of the phase I and II enzymes and their functions being shown in Table 1.2. This is usually through oxidization, reduction, or hydrolysis. The cytochrome P450 superfamily of enzymes tend to be the most heavily studied phase I enzymes due to their involvement in the metabolism of around 75% of all drugs and 90% of drug oxidation reactions (Bibi, 2008; Fred Peter, 2008). In some cases phase I metabolism pharmacologically activates prodrugs, such as codeine which is converted to morphine by cytochrome P450 (CYP) 2D6 (Kirchheiner *et al.*, 2007), and induce toxicity in others, such as acetaminophen (APAP) which is metabolised to the toxic intermediate N-acetyl-p-benzoquinone imine (NAPQI) by CYP2E1 (Gonzalez, 2005).

Table 1.2: Enzymes involved in the different stages of drug metabolism. Phase I metabolism carries out processes to increase the reactivity or polarity of substrates, with around 80% of these processes involving the cytochrome P450 superfamily of enzymes. Phase II metabolism involves the conjugation of the substrate with charged molecules to allow for active transport out of the cell.

Enzyme	Process
Phase I	
Cytochrome P450s	Oxidation
Flavin-containing monooxygenases	Oxidation
Alcohol dehydrogenases	Oxidation
Aldehyde dehydrogenases	Oxidation
Monoamine oxidases	Oxidation
NADPH-cytochrome p450 reductases	Reduction
Esterases	Hydrolysis
Amidases	Hydrolysis
Epoxide hydrolases	Hydrolysis
Phase II	
Methytransferases	Methylation
Sulfotransferases	Sulfation
N-acetyltransferases	Acetylation
UDP-glucuronosyltransferases	Glucuronidation
Glutathione s-transferases	Glutathione conjugation
Glycine N-acetyltransferases	Glycine conjugation

Phase II drug metabolism involves conjugation reactions such as sulfation, acetylation, and glutathione conjugation. While these are less studied *in vitro* than phase I metabolism, particularly that of the CYPs, it is still an important step in drug clearance and therefore *in vivo*-like expression of the enzymes involved is required for a model to accurately predict drug response (Jancova, Anzenbacher and Anzenbacherova, 2010). Phase III metabolism is a broader range of processes which lead to excretion of drug metabolites. The multidrug resistance-associated protein (MRP) family of membrane transporters are one of the more heavily studied proteins in this phase of metabolism due to their role in export of glutathione, glucuronate and sulfate conjugates (Homolya, Váradi and Sarkadi, 2003).

1.1.4.3. Fibrosis research

Despite the extensive regenerative capacity of the liver permanent damage can still take place in the form of fibrosis. This typically occurs after the liver tissue is repeatedly damaged and the cells can no longer keep up with the required level of regeneration, instead forming ECM-rich scar tissue as shown in Figure 1.13. Increasing levels of ECM proteins which make up this scar tissue and the crosslinking which occurs between them makes it increasingly difficult for the cells to resolve, leading to irreversible tissue damage (Cordero-Espinoza and Huch, 2018).

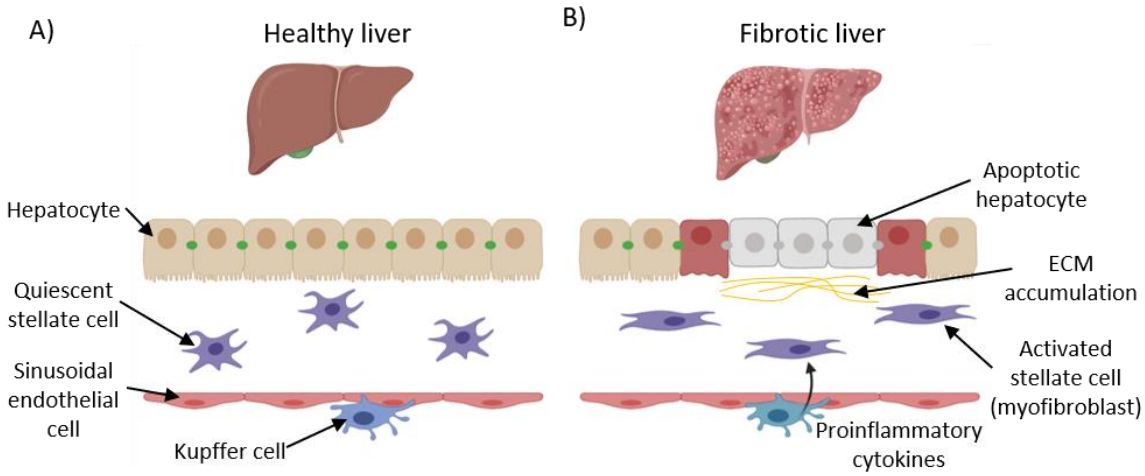

Figure 1.13: Changes in the hepatic microenvironment due to liver fibrosis. A) Healthy liver has populations of quiescent hepatic stellate cells in the space of Disse and Kupffer cells resident in the sinusoids. Regions of hepatocyte-hepatocyte contact form bile canaliculi which transport bile towards the portal regions. Endothelial cells form a highly permeable barrier between the blood flow and the fluid in the space of Disse. B) Fibrotic liver has an accumulation of ECM over apoptotic hepatocytes produced by activated stellate cells. This apoptosis also results in a loss of bile canaliculi, inhibiting effective bile transport. Kupffer cells produce proinflammatory factors to promote stellate cell activation which then deposit the ECM. Created using BioRender.com.

Studying fibrosis *in vitro* is difficult due to the wide range of cells and environmental factors which are involved. The majority of ECM deposition is carried out by the hepatic stellate cells which activate into myofibroblasts as part of the inflammatory response (Manka, Zeller and Syn, 2019). Presence of stellate cells is therefore one of the requirements for an accurate fibrosis model and is one of the reasons that PCLS offer an effective platform for the study of fibrosis due to having an intact native morphology with all types of liver cell present. Even these are limited however due to the chronic nature of fibrosis making it difficult to model over the short functional lifespan of PCLS (Westra *et al.*, 2013). An effective model for fibrosis would need to be a robust recreation of the *in vivo* tissue with potential to be studied over the course of many weeks, something which no platform at present can fulfil (van Grunsven, 2017).

1.1.4.4. Liver disease

Whilst fibrosis is a widely studied aspect of liver injury, other diseases are also of significant research interest. These can often lead to fibrosis and cirrhosis as final endpoints; however, the pathologies are variable. Such major complications in the liver involve diseases such as non-alcoholic fatty liver disease (NAFLD), hepatocellular carcinoma (HCC) and hepatitis B and C infection (HBV, HCV). Incidences of these have been increasing over time and all have a major burden on global healthcare. NAFLD affects almost a third of the US population and the number of cases are expected to hit 100 million by 2030 with the increase linked to the increasing prevalence of obesity and diabetes (Loomba and Sanyal, 2013; Estes *et al.*, 2018). HBV and HCV combined infect more than 500 million people globally (Protzer, Maini and Knolle, 2012) meanwhile HCC is a possible outcome from all of these diseases, being the most common primary livery malignancy, the second highest cause of cancer deaths worldwide and the fastest-rising cause of cancer mortality (Tang *et al.*, 2018). Table 1.3 shows some of the most common liver diseases and their burden on the global population.

Table 1.3: Global incidence and annual mortalities from a range of liver diseases. Many diseases have typically have comorbities both with other liver diseases and diseases in other organs therefore some deaths may be counted under several diseases. Diseases with N/A for annual deaths tend to not cause death directly but instead lead to it through causing other diseases such as cirrhosis, therefore accurate death statistics are not available. NAFLD, Non-alcoholic fatty liver disease; NASH, Non-alcoholic steatohepatitis. *Prevalence values are given for genetic disease instead of incidence.

Disease	Incidence (millions per year)	Annual deaths (thousands)	Treatments	Year
NAFLD	1,900	N/A		Younossi 2018
NASH	114 - 490		Lifestyle & dietary modification, transplantation	
Cirrhosis	122	1320	Lifestyle & dietary modification, transplantation	Sepanlou et al. 2020, Ge et al. 2016
Alcohol-related liver disease	15	493	Reducing alcohol intake	Rehm et al. 2013
Hepatitis B	257	887	Vaccine, antiviral medicine (lifetime)	WHO
Hepatitis C	71	399	Antiviral medicine	WHO
Liver Cancer	0.8 (HCC 80%)	746	Largely untreatable	WCR 2014
Autoimmune hepatitis	0.075 - 0.15	N/A	Immunosuppression, transplantation	Francque et al. 2012
Primary sclerosing cholangitis	0.07	17	Transplantation	Mendes et al. 2008
Primary biliary cholangitis	0.2	18	Ursodeoxycholic acid treatment, transplantation	Mendes et al. 2008
Wilson's disease	1 - 2*	N/A	Low copper diet, copper chelator treatment, transplantation	Liu et al. 2017
Haemochromatosis	38*	N/A	Phlebotomy	Olynyk et al. 1999

At present the only treatments for these diseases are limited, with a highly expensive drug programme needed to cure HCV. HBV requires lifetime drug therapy at present whilst there are no approved drugs for use to treat NAFLD. For HCC the best options for treatment are surgical resection or transplantation. Development of treatments for these diseases is a time consuming process and relies heavily on the use of animal test, in particular rodent models which have their limitations when applied to the case of humans (Underhill and Khetani, 2019).

1.1.5. Methods for reproducing liver function *in vitro*

There are many different methods which can be used to model the liver and the choice of these depends on the specifics of the processes under investigation and the desired throughput. An overview of these techniques is presented in Table 1.4. Simple models subcellular fractions such as microsomes, cytosol and the S9 fraction can be useful for looking at the interactions of a specific proteins and compounds of interest whilst more complex multicellular models are more effective for looking at the interactions between pathways and give a more complete picture of processes which are occurring. These models can be scaled up all the way to whole perfused livers, however with every increase in complexity there is a significant increase in time and cost and a decrease in throughput therefore it is key to find the model which is most applicable to the research aims (Guillouzo, 1998).

Table 1.4: A Summary of different techniques which can be used to model the liver. The first entries in the table are the highest throughput. The throughput decreases going down the table whilst the physiological relevance increases. CYP, cytochrome P450; UGT, glucuronosyltransferase; NAT, N-acetyltransferase; ST, sulfotransferase; GST, glutathione s-transferase.

In vitro technique	Advantages	Disadvantages
Human liver microsomes	Affordable Study of individual, gender-, and species-specific biotransformation	Unsuitable for quantitative measurements Only CYP and UGT enzymes
Human liver cytosol	NAT, ST and GST activity depends on cofactors present Study of individual, gender-, and species-specific biotransformation	Only NAT, ST and GST
Human liver S9 fraction	Both Phase I and Phase II Study of individual, gender-, and species-specific biotransformation	Lower enzyme activity than in microsomes and cytosol
Human liver cell lines	Easy to culture Relatively stable enzyme expression levels CYPs inducible	Low expression levels
Stem cell derived hepatocytes	Improved enzyme levels compared to cell lines Immortalised populations	Presence of unwanted cell types Acquisition of genetic mutations over time Complex culture media required
Primary Hepatocytes	Well established and characterised Study of mediators and enzyme inducers possible Drug transporters still present and operational	Isolation can be complicated and time consuming Only preselected cells can be study Cell damage during isolation
Liver Slices	Intact cellular interactions Morphological studies possible Interindividual variation can be studied	Inadequate penetration Damaged cells on the edges Limited viable period Expensive equipment
Isolated Perfused Liver	Bile formation Three-dimensional architecture	Delicate model Limited viable period Poor reproducibility No human liver available

1.2.5.1. Subcellular fractions

Subcellular fractions present a very simple and easy to use model to investigate mechanisms of drug and chemical induced hepatoxicity. There are several fractions which are commonly used for this, in particular microsomes, cytosol and the S9 fraction, which have their uses for looking into different effects of hepatotoxins (J. Richardson *et al.*, 2016). Isolated organelles can also be used for hepatic studies, for example mitochondria can be used to investigate the effects of chemicals on processes such as ATP synthesis and oxidative phosphorylation. These models are widely used in compound screening due to their high throughput and ease-of-use as well as the ability to carry out population specific screens however they are overly simplistic when studying the complex multistage detoxification pathways and can be greatly affected by exogeneous stresses on the cells prior to translation (Plant, 2004).

1.2.5.2. Primary hepatocytes

Cultured primary hepatocytes are in principle a very good model for testing of drugs and xenobiotics due to being highly representative of the *in vivo* liver as the major parenchymal cells. These can be used very effectively for testing as they initially have an enzyme expression profile matching that *in vivo* (Dambach, Andrews and Moulin, 2005). There are several drawbacks to primary hepatocytes which make them less appealing for high throughput research and for use in chronic studies. Once removed from the body the hepatocytes stop proliferating and therefore the quantity of cells available is very limited, whilst relying on multiple sources brings in the problems of donor variation which can have huge effects on the toxicity of drugs. Due to the difficulty maintaining and expanding primary hepatocyte cultures, with techniques such as fibroblast feeder layers needed to achieve this (Cho *et al.*, 2008), progress is now being made through the culture of hepatocyte progenitor populations which can be found in the liver or taken from other tissues such as the pancreas (Huch *et al.*, 2015; Zeilinger *et al.*, 2016; Garnier *et al.*, 2018).

Another issue with primary hepatocytes is their rapid dedifferentiation *in vitro* which can limit their predictive lifespan to a couple of days. The use of collagen sandwich cultures can maintain the viability for primary hepatocytes along with proper localisation of apical and basolateral transporters for longer periods than on conventional cell culture plasticware this is still limited to up to a couple of weeks, therefore limiting the usefulness of these models for chronic studies (Swift, Pfeifer and Brouwer, 2011; Yang *et al.*, 2016).

1.2.5.3. Hepatic cell lines

An alternative to primary hepatocytes to overcome these drawbacks is the use of cell lines which are typically either derived from hepatic tumours or from lab-immortalised primary hepatocytes. The main advantage with these populations is the ability to maintain proliferative status over extended periods of time and achieve a high level of differentiation, therefore they could potentially offer an effective and low-cost solution to the issues with primary hepatocytes. For this reason cell lines are frequently used both in industry and for academic research (Gomez-Lechon *et al.*, 2008). An overview of commonly used cell lines with their advantages and disadvantages is presented in Table 1.5.

Table 1.5: Different hepatic cell lines commonly used in research. A wide range of cell lines have been used in literature; this table shows a selection of the more commonly used cell lines. Many of the cell lines exhibit similar characteristics overall but have different expression patterns of specific genes within families when looking at the single gene level. The wide availability, unlimited proliferation potential and low costs of cell lines often makes them preferable to primary hepatocytes.

Cell Line	Advantages	Disadvantages
HepG2	Large volume of literature Ease of use Low cost	Low enzyme levels Lack of expression of some enzymes
Huh7	Ease of use Low cost Highly susceptible to hepatitis C virus Good levels of enzyme expression	Point mutation in p53 gene Lack of expression of some enzymes
THLE2	Ease of use Good levels of enzyme expression	Lack of expression of some enzymes Contains SV40 viral DNA Complex media requirements
Hep3B	Ease of use Low cost Good levels of enzyme expression	Contain hepatitis B Null mutation in p53 gene Low enzyme levels Lack of expression of some enzymes
HepaRG	Ease of use Very good levels of enzyme expression	Complex media requirements

The major issue with hepatic cell lines is the limited expression of key metabolic proteins found in many hepatic cell lines. Figure 1.14 shows the expression of a wide range of genes involved in the three phases of drug metabolism in different commonly used hepatocyte cell lines relative to primary hepatocytes (Guo *et al.*, 2011). This shows that cell lines express incomplete or reduced

expression profiles of drug metabolism enzymes which has a significant impact on their ability to predict drug toxicology *in vivo* (Castell *et al.*, 2006).

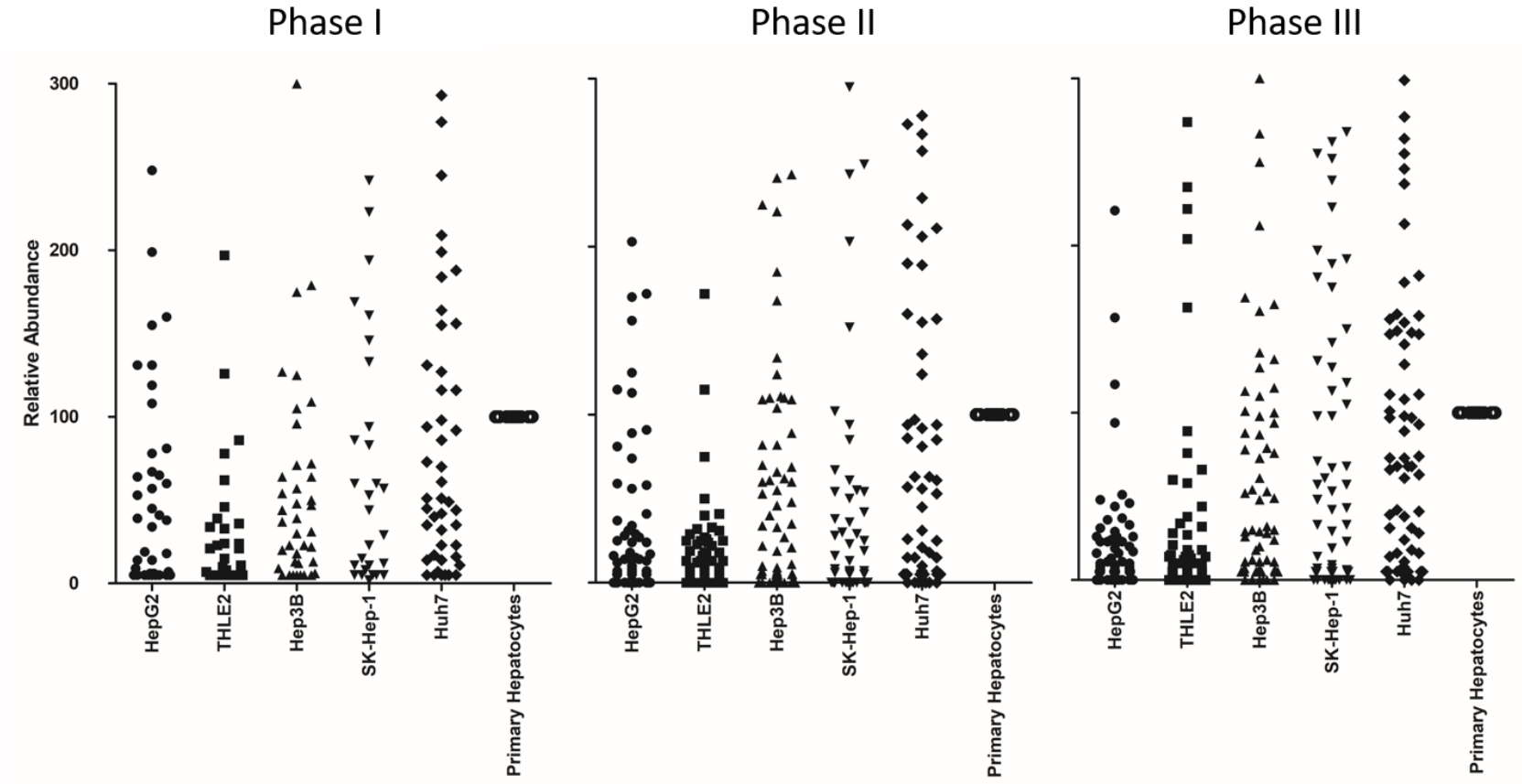

Figure 1.14: Relative abundance of drug-metabolising genes in hepatic cell lines. Expression of all three phases of the drug metabolism enzymes at levels similar to primary hepatocytes is required for an accurate *in vitro* model. Data points for each gene are relative to the corresponding expression level in pooled primary hepatocytes. 69 phase I, 73 phase II and 78 phase III genes are displayed. As seen here, cell lines exhibit gene expression which is widely variable between genes and rarely reflects the levels expected from primary hepatocytes. Adapted from L. Guo *et al*. (2011)

The degree to which this is a problem varies with different cell lines with poorly differentiated lines such as HLE having downregulated expression of metabolic proteins and reduced hepatocyte function (Nwosu *et al.*, 2018) whilst the highly differentiated HepaRG cell line shows one of the closest expression profiles to primary hepatocytes, though its proprietary nature leads to much higher costs (Gerets *et al.*, 2012). Different culture techniques can also be implemented to attempt to improve these properties and induce greater expression levels (Liu *et al.*, 2007; Baudoin *et al.*, 2011; Deng *et al.*, 2015) however a method has yet to be found which can bring them up to the same predictive levels of primary hepatocytes with inducibility varying with different enzyme isoforms (Westerink and Schoonen, 2007b, 2007a).

1.2.5.4. Stem cell derived hepatocytes

There are several possible sources for obtaining stem cell derived hepatocytes as summarised in Figure 1.15. The most recent approach to generating functional hepatocytes in vivo is with stem cell derived hepatocytes. Two main sources of these are induced pluripotent stem cells (iPSCs) shown in Figure 1.15A and hepatic progenitor cells which reside in the liver, shown in Figure 1.15B. While iPSCs seem a good source for the generation of liver cells, with studies finding they can be differentiated to resemble hepatocytes with high levels of phase I and II enzyme expression they do not reach levels seen in primary hepatocytes and have limited polarisation (Corbett and Duncan, 2019). Combined with issues over control of differentiation leading to incorporation of unwanted cell types along with high variability in success rates between research groups the use of iPSCs is still quite far off being feasible for the generation of robust and reproducible models of the adult liver (Palakkan, Nanda and Ross, 2017).

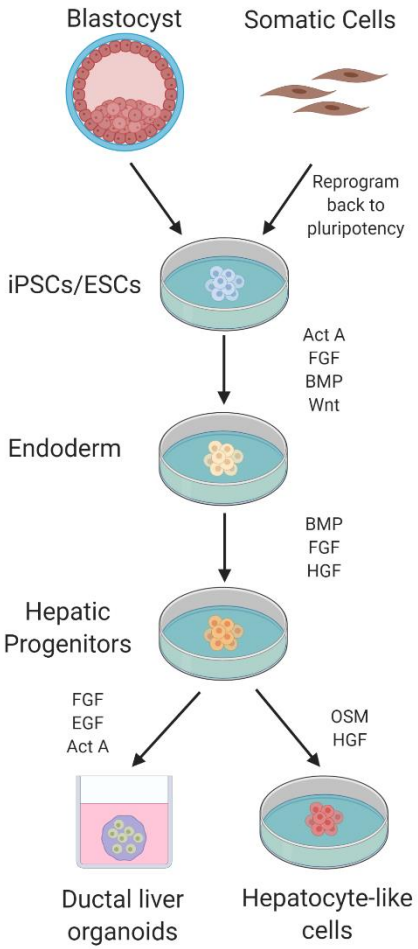

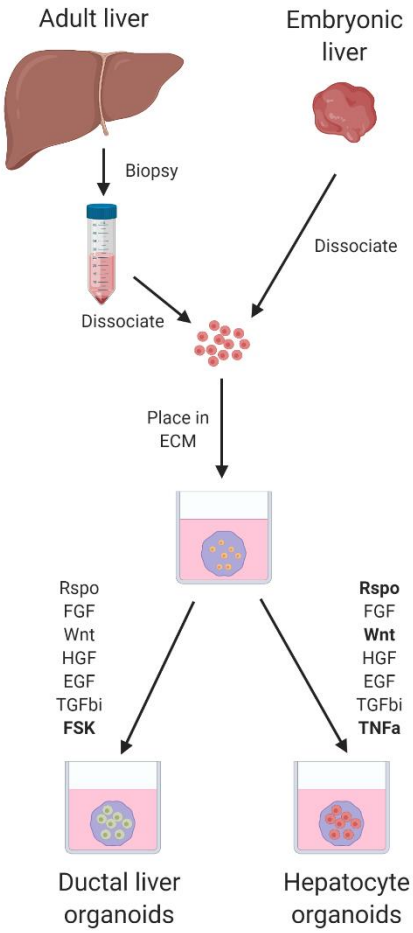

Figure 1.15: Methods to derive multipotent hepatic progenitor cells. A) Hepatic progenitors can be created through the use of induced pluriopotent stem cells reprogrammed from adult somatic cells or embryonic stem cells derived from the inner cell mass of a blastocyst. B) Bipotent hepatic progenitor cells can be derived from adult liver biopsies or dissociated embryonic liver. Act A, Activin A; BMP, Bone morphogenetic protein; ECM, extracellular matrix; EGF, epidermal growth factor; ESCs, embryonic stem cells; FGF, fibroblast growth factor; FSK, forskolin; HGF, hepatocyte growth factor; ICM, inner cell mass; iPSCs, induced pluripotent stemm cells; OSM, Oncostatin M; TGFbi, transforming growth factor beta inhibitor; TNFa, tumour necrosis factor-alpha. Adapted from Prior *et al.* (2019). Created using BioRender.com.

The use of bipotent liver progenitor cells is a more recent technique which shows more promise due to the stricter control over cell fate and the higher functional maturity of the cells. One method utilises Epithelial cell adhesion molecule (EpCam) positive bile duct cells which are generated from human liver by collagenase perfusion. Isolated single cells from these populations were used to generate clonal cell lines with a high level of genetic stability. These cells could be differentiated into hepatocytes with expression of phase I and II enzymes and functions such as ammonia detoxification at equivalent levels to the HepaRG cell line (Huch *et al.*, 2015). An alternative method involves reprogramming hepatocytes back to bipotent progenitors through the use of small molecules with similar outcomes to the previous method (Kim *et al.*, 2019). The major drawback of these methods is the high cost of use, with numerous expensive supplements being required both for expansion and differentiation of the cells.

1.2.5.5. Precision cut tissue slices

If the aim is to study disease pathways in the liver, such as liver fibrosis, then a culture consisting of hepatocytes alone is inadequate. To properly model such disease the entire structure of the liver is required, including the different cell types as well as the extracellular matrix and other molecular components of the tissue. For example, hepatic stellate cells are the major depositors of ECM in liver fibrosis (Bataller and Brenner, 2005) whilst Kupffer cells play a key role in the inflammatory response in liver disease (Bilzer, Roggel and Gerbes, 2006). Precision-cut liver tissue slices (PCLS) are a technique which can be used for this purpose due to the entire structure of the tissue remaining intact through to culture (van de Bovenkamp *et al.*, 2005; Olinga and Schuppan, 2013). Studies have been carried out using PCLS with livers from numerous animal sources and they represent a positive improvement on typical animal tests as many slices can be obtained from one animal, therefore increasing its research usefulness. Human PCLS have been used however the limited availability of viable human liver tissue is a severe limitation (Starokozhko, Vatakuti, *et al.*, 2017).

PCLS suffer from similar drawbacks to primary hepatocytes due to the short lifespan of hepatocytes *ex vivo.* To maintain the tissue for prolonged periods an atmosphere containing 95% oxygen is typically used, leading to complex apparatus requirements, however this still typically limits the tissue to up to one week of functional lifespan. Recent research has managed to increase the functional lifespan of the tissue however even with the latest techniques a culture period of above 2 weeks isn't feasible (Wu *et al.*, 2018; Paish *et al.*, 2019b) and replacement of hepatocytes with

other cells from the liver means that simply monitoring viability is not adequate to ensure proper liver functionality (Verrill *et al.*, 2002).

1.2.5.6. Whole perfused liver

Isolated perfused livers represent the most physiologically relevant of the liver models, with the entire liver being perfused with oxygenated buffer to maintain viability whilst studies are carried out. Typically rat livers are used for this method as they strike a good balance between being large enough to work with comfortably whilst not so large that nutrient and oxygen delivery becomes a challenge. These models can be used for many liver studies including investigating biliary clearance due to still having a functional bile duct network in place from which the bile can be collected and analysed (Pastor, 2018).

The two major limitations of this method are the time constraints and throughput. The isolated perfused liver preparations are typically only maintained for 2-3 hours, though in some cases can be up to 12 hours. This means that they only have applications for the short term study of drug uptake, metabolism and secretion but are not useful when looking at drug toxicology due to the timescales for drug toxicity typically being much longer than the viable time of these cultures (Bessems *et al.*, 2006). The throughput issue means that each rat used can only be used for one experiment, drastically increasing the number of rats needed when compared with methods such as PCLS. It is therefore a technique which is less preferable within modern scientific practice, with organisations such as the National Centre for the Replacement, Refinement and Reduction of animals in research (NC3Rs) promoting a move away from inefficient animal models like this (National Centre for the Replacement, 2020).

1.2.6. Technologies to improve the physiological relevance of hepatocyte models

As outlined in Section 1.2.4., there are a wide variety of models available to study the structure and function of the liver. Whilst more physiological options such as the use of PCLS and whole perfused organs offer the most accurate, relevant, and reliable data, these methods are hampered by severe limitations, namely the inability to maintain tissues for prolonged periods of time and a low throughput. To overcome this problem, studies are now focussing on improving the accuracy and physiological relevance of cell-based models which offer the opportunity for high throughput studies and have the potential to achieve an accurate predictive capacity.

Advances in this area have led to a numerous topographical surfaces and 3D cell culture methods being developed which all have advantages over conventional 2D cell culture however still leave out a lot of other properties which are of interest for fully recreating the *in vivo* microenvironment (Ahmed *et al.*, 2019; Mirbagheri *et al.*, 2019). Table 1.6 shows a summary of a selection of commonly used culture methods to induce more of a 3D cellular phenotype, with a few of their advantages and disadvantages listed.

Table 1.6: Commonly used 3D hepatocyte cell culture techniques. These can be used alone or in conjunction with each other for the culture of hepatocytes and other cells. Methods such as scaffolds and bioprinting can utilise both synthetic and natural scaffolds to tailor the properties to those desired for by the study. Research into these techniques is evolving constantly and novel manufacturing methods are being found to overcome some of the disadvantages for the different techniques.

Technique	Advantages	Disadvantages
2D cell culture	Ease of use Huge volume of literature	Very different to *in vivo* microenvironment
Collagen sandwich culture	Maintains viability and differentiation of primary hepatocytes Ease of use High throughput	Use of exogenous ECM Limited control over patterning
Aggregates	Maintains viability and differentiation of primary hepatocytes Ease of use High throughput	Use of exogenous ECM Limited control over patterning
Scaffolds	Ease of use Greater control over patterning Tailor surfaces to cell type	Lower throughput Higher cost
Bioprinting	Complete control over patterning Tuneable Can be mixed with other methods	Expensive Greater user input required Lower throughput

1.2.6.1. Collagen gels

The key difficulty to overcome for the culture of primary hepatocytes is the rapid dedifferentiation which is seen when hepatocyte suspensions are seeded to a plate in conventional cell culture. To overcome this, hepatocytes can be cultured between two layers of gelled collage known as a sandwich culture, with the technique for carrying this out shown in Figure 1.16. This causes them to better maintain a function differentiated phenotype and show enhanced morphology, metabolism and viability (Dunn *et al.*, 1989).

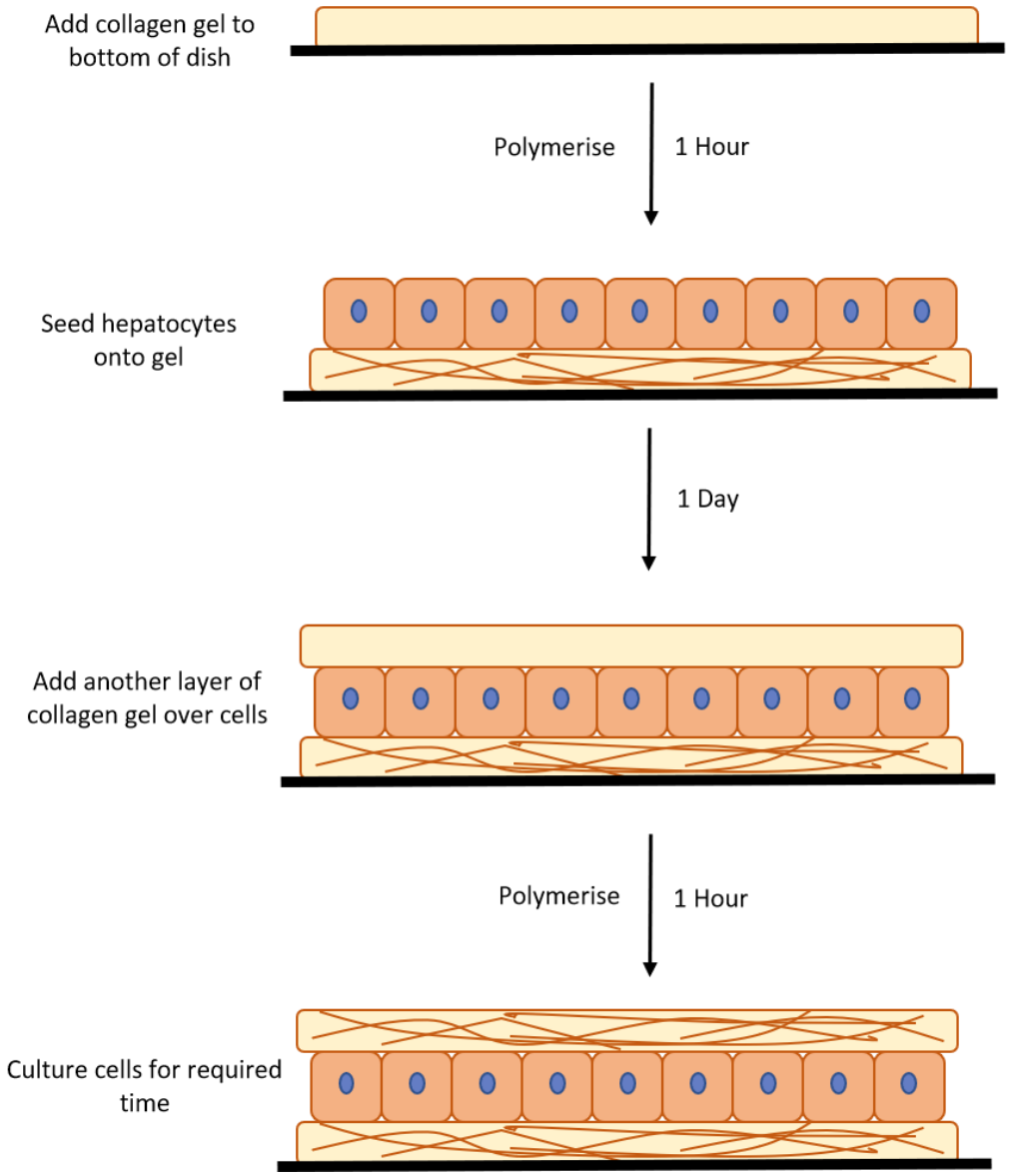

Figure 1.16: Setting up Hepatocytes in a collagen sandwich culture. Collagen is added to the bottom of a culture dish and polymerised for 1 hour at 37°C. Hepatocytes are added and incubated overnight to adhere the cells before adding the collagen overlay. This is polymerised again for 1 hour and the cultures can then be maintained for up to 2 weeks for running experiments. With this technique, primary hepatocytes better maintain their high levels of polarisation and functionality compared to culture on conventional 2D surfaces.

This technique promotes the formation of different cellular junctions as well as a functional bile canalicular network (LeCluyse, Audus and Hochman, 1994; Liu *et al.*, 1998). This leads to the polarisation of transporter proteins, with proteins such as multidrug resistance-associated proteins

2 and 3 (MRP2 and MRP3) showing discrete apical and basolateral localisation respectively (Zhang *et al.*, 2005).

1.2.6.2. Aggregates

Cells have an intrinsic ability to self-assemble and self-organise which can be taken advantage of to form aggregates (Simunovic and Brivanlou, 2017). There are a number of ways to generate aggregates as shown by Figure 1.17, with methods including the hanging drop method where cells are seeded into a hanging drop of medium in which they adhere to each other to form a complex 3D cell mass due to lack of any other adherent structures (Foty, 2011). Similarly vessels can be coated with non-adhesive coatings such as polyhydroxymethylmethacrylate (PDMA) which induces aggregates formation (Lee and Liu, 2007). Constant motion of the culture can also prevent cells from being able to adhere and instead cause them to aggregate together (Sarika *et al.*, 2016).

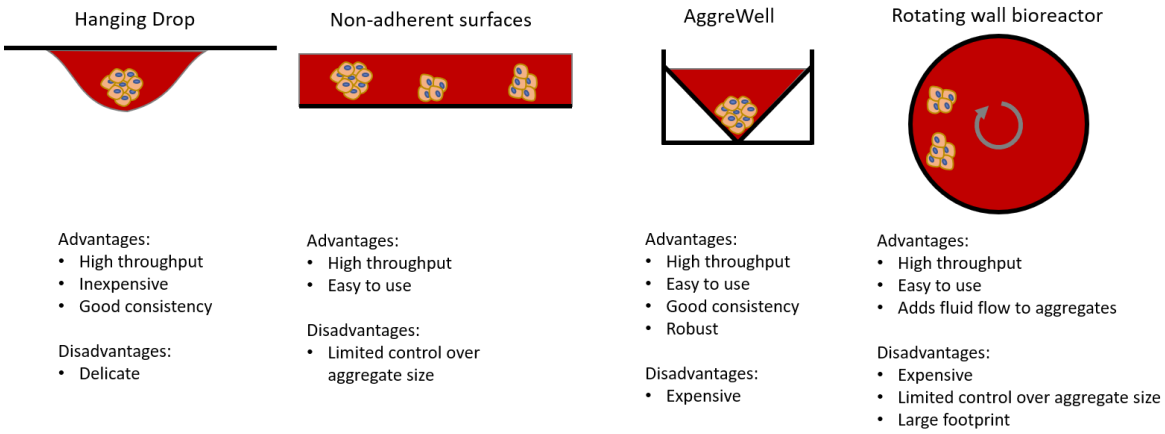

Figure 1.17: Different methods for forming aggregates. Aggregates are a widely used method to create 3D cell cultures due to their ease of use and high throughput. These rely on self-assembly of the cells, allowing the formation of a more natural morphology compared to the forced polarisation induced by conventional 2D surfaces. All techniques rely on providing the cells with an environment lacking adherent surfaces to promote cell to cell adhesion and aggregation and typically aim to create a large quantity of uniformly sized aggregates. Each method has advantages and disadvantages which mean that the method should be chosen which most closely fits experimental requirements.

These cultures offer advantages over 2D cultures in that there is a large amount of cell-cell contact and therefore an increase in signalling between cells. The structure also supports the cells in a more rounded shape instead of flattened as in 2D, leading to a more natural cytoskeleton and protein expression (Berthiaume *et al.*, 1996; Moghe *et al.*, 1996) whilst the ability to self-organise allows

the cells to polarise in an *in vivo*-like manner instead of undergoing forced polarisation due to being grown on adherent surfaces (Rappel and Edelstein-Keshet, 2017). Aggregate cultures of both rat and human primary hepatocytes have found development of bile canaliculi and advanced cell adhesion alongside the increased metabolic profile, one of the aims in creating more physiologically relevant tissues (Wu *et al.*, 1996; Yamada *et al.*, 1998).

More recent advances with liver aggregates have focused on using stem cell derived hepatocytes (Prior, Inacio and Huch, 2019). These can display a very stable morphology and maintain function and viability over several weeks, offering an effective alternative to primary hepatocytes (Huch *et al.*, 2015). These cultures still suffer from limitations regarding control over the patterning of structures formed and issues with diffusion distances limiting the maximum size of constructs.

1.2.6.3. Scaffold based methods

Scaffolds provide a physical support on which cells can grow and are another method for growing 3D cell cultures which have been applied to hepatocytes in a wide range of forms (Patel, Bonde and Srinivasan, 2011). Scaffolds allows cells to adopt a more natural, *in vivo*-like morphology rather than the flattened shape they become in 2D. As shown by Table 1.7, scaffolds can be made from a variety of materials from natural ones such as collagen and chitosan (Dash *et al.*, 2011) to synthetic polymers (Patel, Bonde and Srinivasan, 2011) and ceramics (Wei and Ma, 2004). Another main factor which varies in scaffolds is the architecture of the structure. Fibrous scaffolds can be randomly orientated or in uniform structures whilst synthetic structures can have a very complex architecture using methods such as 3D printing.

Table 1.7: Different types of Scaffolds which are used in cell and tissue culture. This table groups the methods into broad categories however these are not exclusive and some more complex techniques may utilise several of these. Many of the disadvantages can be overcome depending on the scale of the production. For example, injection moulding allows large scale production of highly reproducible porous scaffolds however this would not be suitable for the scale required within a single laboratory.

Method	Advantages	Disadvantages
Hydrogels & Protein Scaffolds		
Collagen gel	Very pure Can match collagen levels to tissue	Limited control over structure Exogeneous substances
Basement membrane extract	Contains a wide range of ECM proteins Can be with or without growth factors	Limited control over structure Exogeneous substances Varied composition
Synthetic protein gels	Highly controllable protein content High level of Control over mechanical properties	Less representative of proteins *in vivo*
Decellularised Tissue	Retains *in vivo* structure Correct ECM content for tissue studied	Time consuming production Potential for cellular contamination
Synthetic Scaffolds		
Porous Scaffolds	Easy to produce Tuneable porosity Can be formed into structures such as tubes Formed from a wide range of materials	Structural variations Specialist equipment needed to produce
Fibrous Scaffolds	Easy to produce Tuneable fibre properties Orientation can be controlled	Not all commonly used materials form fibres at desired scale Structural variations Specialist equipment needed to produce
3D Printed Scaffolds	Precise control over structure Wide range of compatible materials 3D printers widely available	Slower production for large quantities

Hepatocyte cultures have been carried out extensively using scaffolds. The properties of scaffolds for use in culturing hepatocyte tissues has been heavily studied, with effects such as cell-scaffold adhesion (Sarika *et al.*, 2015), matrix conductivity (Rad *et al.*, 2014) and matrix composition (Glicklis *et al.*, 2000; Jiankang *et al.*, 2009; Nishida and Taniguchi, 2016) being found to affect the properties of the resulting tissue. The ability to vary these properties along with its ease of use and reproducibility make scaffolds an effective method for culturing tissues in 3D. Scaffolds have been shown to be effective at maintaining metabolism and functionality in primary hepatocytes (Glicklis *et al.*, 2000; Kim *et al.*, 2010) as well as enhancing expression of key functional proteins in cell lines such as HepG2 (Bokhari, Carnachan, Cameron, *et al.*, 2007a; Lv *et al.*, 2007; Nishida and Taniguchi, 2016).

1.2.6.4. 3D Bioprinting

3D bioprinting is a method which is becoming more commonly used in cell biology due to its ease of use and ability to form complex cellular structures. This utilises a 3D printer to physically pattern cells onto a substrate and therefore can be used to position multiple cell types correctly to replicate complex *in vivo* structures of tissues. Figure 1.18 shows some of the 3D bioprinting methods which have been described in literature which can each be used for the generation of micropatterned cultures.

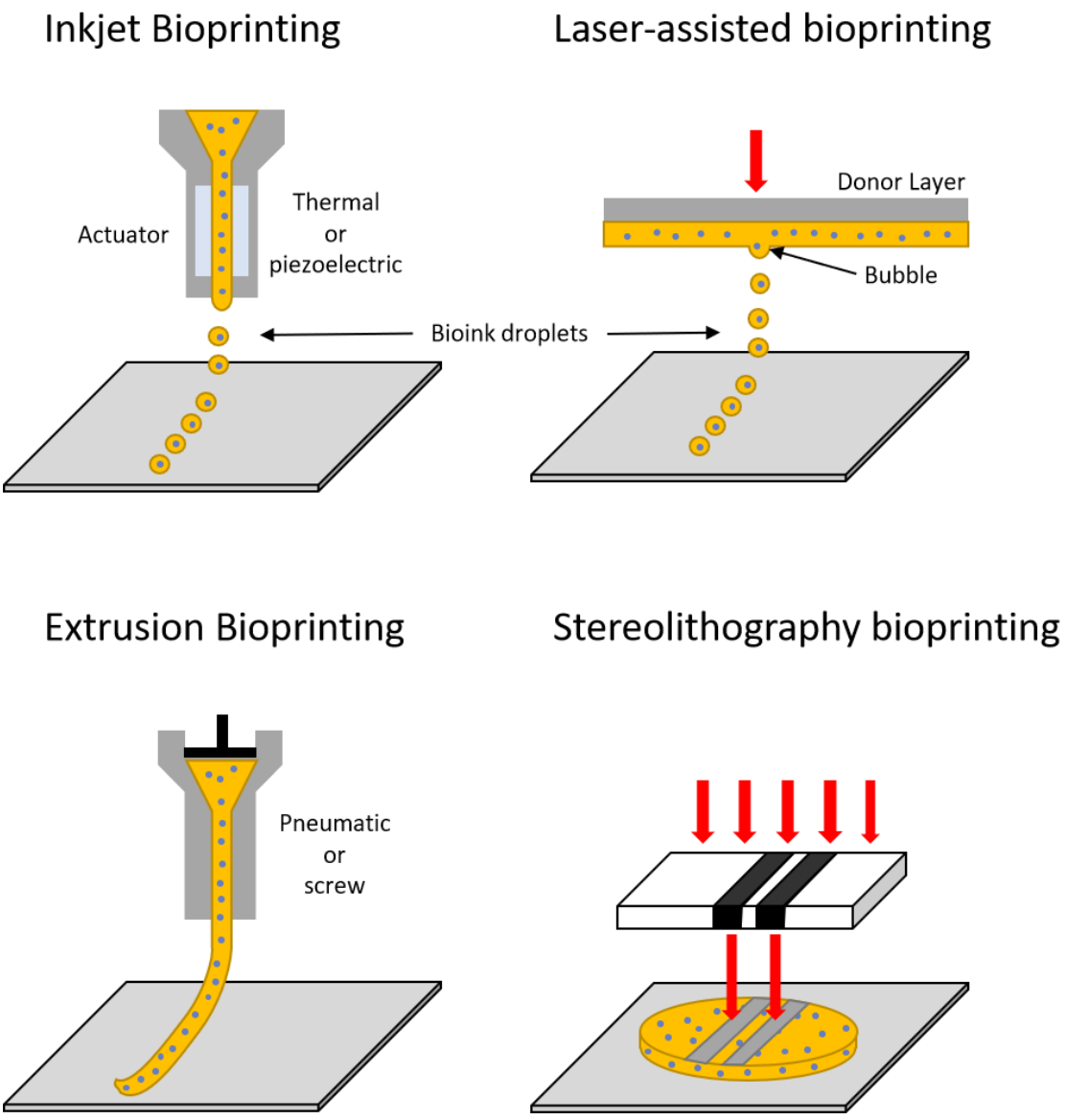

Figure 1.18: Techniques used for bioprinting of cells. Using bioprinting, cells can be spatially arranged with a high level of accuracy to recreate complex tissue structures *in vitro.* A) Inkjet printers can be used to build up tissues through ejection of small droplets of cells and hydrogel. B) Laster bioprinters vaporise a region in the donor layer forming a bubble to propel suspended bioink onto the substrate. C) Extrusion bioprinters extrude a liquid cell-hydrogel solution onto the substrate. D) Stereolithographic printers use a digital light project to selectively crosslink bioinks plane-by-plane. Red arrows in B) and D) represent a laser pulse and projected light respectively. Adapted from Mandrycky *et al*., 2016.

Bioprinting can be of particular use for recreating the liver lobules *in vitro*, with the ability to print multiple cell types into structures which more closely match those seen *in vivo* (Ma *et al.*, 2016).There are also possibilities to create structures which allow media perfusion (Neiman *et al.*,

2015) or have improved biocompatibility (Zhong *et al.*, 2016), leading to potential applications in both research and clinical settings. Work with these models is still in early stages and the ability to form three-dimensional liver constructs with increased functional properties compared with other *in vitro* methods has yet to be shown.

1.2.6.5. Incorporation of non-parenchymal cells

To recreate the liver microenvironment at the cell culture level most cultures focus on the hepatocytes whilst leaving out the other important cells present in the liver. Many studies have shown the beneficial effects of co-culture of both primary hepatocytes and hepatocyte cell lines with non-parenchymal cells such as stellate cells, endothelial cells, and fibroblasts. Primary hepatocytes have been shown to have an improved functional lifespan when co-cultured with stellate cells (Abu-Absi, Hansen and Hu, 2004; Krause *et al.*, 2009), endothelial cells (Kang *et al.*, 2013) and fibroblasts (Evenou *et al.*, 2011), with combinations of several different non-parenchymal cells also possible (Ahmed *et al.*, 2017a).

This method is also highly flexible and can be coupled with other cell culture techniques to push the boundaries of *in vitro* liver recreation, with micropatterning of different cells to form structures being possible (Cho *et al.*, 2010; H. W. Lee *et al.*, 2014) as well as use of co-culture alongside 3D scaffolds (Kook *et al.*, 2017). Incorporation of these different methods has been shown to improve the predictive capacity of hepatocyte cell lines and is a promising method to push the phenotype of cell lines closer towards that of primary hepatocytes.

1.2.6.6. Current research on hepatic bioreactors

Methods used in hepatic bioreactors include the use of both radial and perfused fluid flow. Table 1.8 shows a range of commercially available bioreactor systems which can be used to introduce fluid flow for liver models. These create fluid flow by a variety of methods such as physical motion of the vessel or use of pumps. The size and cost of these systems varies widely however systems with reusable vessels typically have costs in the thousands of pounds. The less expensive systems, under £1,000, tend to use disposable vessels, therefore having increased running costs. The footprint of these systems, a key property due to the often-limited availability of laboratory space, is also highly variable. Systems which require significant addition equipment, such as power supplies or pumps, tend to be larger whilst self-contained systems such as the stirred and shaken

systems typically need less space. These systems and their applications for dynamic culture of liver models will be discussed in greater detail in Section 3.1.3, with a brief summary of methods given here.

Table 1.8: Comparison of several different commercially available bioreactor systems. A variety of methods can be employed to introduce fluid flow not a system. These also vary in terms of number of samples, vessel volume and reusability. Reusable vessels are typically autoclavable to allow effective sterilisation.

Manufacturer	Model	Bioreactor Type	Number of samples	Vessel Volume	Approximate Footprint[a]	Reusable Vessels	Approximate Cost[b]
Synthecon	RCCS-1	Rotary	1	1 – 500 mL	0.07 m^2	Yes	£7,000 - £9,000
Synthecon	RCCS-4H	Rotary	4	1 – 500 mL	0.15 m^2	Yes	£16,000 - £20,000
Kirkstall	QV500	Pumped	6	2 mL	0.05 m^2	No	
Kirkstall	QV900	Pumped	6	4 mL	0.05 m^2	No	
Reprocell	Perfusion Plate	Pumped	4	10 mL	0.047 m^2	No	£800 - £900
Ibidi	Pump System Quad	Pumped	4	10 mL	0.15 m^2	No	
ABLE® Biott®	Magnetic Stirred Bioreactor System	Stirred	6	5 mL	0.052 m^2	Yes	£5,500-£6,000
Athena Technology	Micro-plate Shaker	Shaken	4 Plates	<10 mL (6-well plate)	0.075 m^2	No	£600 - £700

[a] **Approximate footprint was estimated as the space taken by the minimum required components to run the system as according to the manufacturers data.**

[b] **Cost represents the cost to set up the systems from scratch, including purchasing of equipment such as pumps which may be reused for multiple bioreactors. This also includess the cost for consumables for one experiment of the number of samples.**

Where not specified by the manufacturer, a Velp Scientifica™ SP311 peristaltic pump was used for calculations due to its low cost and small size.

Flow across the surface can be useful to maintain the viability of cells and can be relevant for the liver when modelling monolayers, in which the model is effectively a single hepatic plate which would have fluid flow occurring on either side of it through the sinusoids. Such systems are typically pump-based and can be set up with complex media recirculation systems (Powers *et al.*, 2002; Freyer *et al.*, 2018).

For more complex tissue constructs the recreation of fluid flow through the tissue is required to represent the 3D structure of the parenchymal tissue more accurately in the liver. Porous membranes, scaffolds and hollow fibres are frequently used to support a more physiologically relevant microenvironment (Domansky *et al.*, 2010; Dash *et al.*, 2013; Knöspel *et al.*, 2016) whilst multiple methods have been developed to provide fluid flow to liver spheroids, utilising both primary hepatocytes and cell lines (Powers *et al.*, 2002; Annamalai and Matthew, 2019). The incorporation of multiple non-parenchymal cells into hepatic bioreactor cultures has also been carried out with results showing an improved hepatocyte phenotype and more physiologically relevant drug response (Allen and Bhatia, 2003; Nguyen *et al.*, 2016; Kehtari *et al.*, 2018).

For primary hepatocytes the main target is to achieve long term viability and maintenance of a highly differentiated, polarised phenotype. Studies using bioreactors such as these have shown that it is possible to maintain primary hepatocyte expression of detoxification genes at similar levels to those when freshly isolated for several weeks (Gebhardt *et al.*, 2003; Toh *et al.*, 2009), however this effect varies between genes and doesn't apply uniformly to all genes in a family, a possible limitation of such systems (Vinci *et al.*, 2011).

As an alternative to the larger bioreactors, microfluidic systems offer a simple and highly controllable environment for cell-based assays. These utilise microlitre volumes of medium in perfused systems to create more responsive hepatocyte cultures(Goral and Yuen, 2012). The most basic systems use smooth microfluidic channels lined with hepatocytes(Baudoin *et al.*, 2011). More complex systems have also been developed which can incorporate 3D technology through hydrogels or scaffolds (Toh *et al.*, 2007; Yajima *et al.*, 2018; Tan *et al.*, 2019). The co-culture of hepatocytes with other cell types has also successfully been carried out in many studies and distinct micropatterning of these cells can be performed(Kang *et al.*, 2015; Haque, Gheibi, Stybayeva, *et al.*, 2016). The incorporation of these techniques can allow the microfluidic systems to achieve an environment with a high level of physiological relevance. These systems have benefits over the larger bioreactors due to the low spatial requirements as well as the reduced media volume and cell numbers, allowing them to be used with relatively low cost. These scale issues can also be a

drawback, however, with reduced cell-cell contact in smaller systems as well as potential issues caused by media evaporation(Berthier *et al.*, 2008).

1.2.7. Conclusions

Through this literature review the need for physiologically relevant tissue engineered models is highlighted with the numerous drawbacks of conventional 2D culture presented. A variety of techniques can be used to increase the biologically complexity of modelled systems and incorporating multiple of these into one system would allow for the creation of tissue models which recapitulate many *in vivo* functions. This would have uses for modelling a wide range of organs and increasing the predictivity of models during investigations into pathways such as xenobiotic transformation. To investigate the impacts of such a system the liver has been selected as an effective model organ due to its complex tissue structure and high levels of fluid flow through its dual blood supply. This leads to the hypothesis that it would benefit greatly from the use of a 3D bioreactor system.

The importance of the liver to maintaining the body in a healthy state has also been highlighted in this literature review, along with some of the reasons why it is an important organ to thoroughly understand and study. The liver is a highly complex organ with numerous different cell types performing a wide range of functions. The vasculature present allows for a huge amount of blood to flow through the liver, providing oxygen for effective cell function as well as delivering toxins and other substances for the cells to metabolise.

The liver is involved in numerous debilitating diseases such as liver cancer and viral hepatitis for which the treatments are limited. Drug-induced liver injury is another form of damage which the liver can experience which leads to a need for platforms to model the liver *in vitro* as accurately as possible. There are many different methods to model the liver *in vitro* which vary dramatically in both predictive capacity and throughput however the two are usually inversely linked and there is a need for highly predictive liver models which maintain a level of throughput which makes them of important diagnostic value. Cell-based models show a lot of promise to achieve this, and many different methods are being developed utilising cells from a variety of different sources, each with their advantages and drawbacks. Through complex cell culture techniques such as the use of 3D cell culture it is possible to improve the liver-specific functions of these cells and therefore increase their value as *in vitro* liver models. The complex nature of the liver means that there are many factors which need to be accounted for to fully recapitulate native *in vivo* liver. Bioreactors are the next step to achieving this, with the addition of shear stress and media turnover through the addition of fluid flow, mimicking the dynamic liver microenvironment.

The complexity of creating accurate *in vitro* models of the liver has been highlighted by this literature review as well as the need to combine different techniques to fully recreate the structure and function of the liver. By incorporating these methods into one system whilst maintaining a simplicity which allows for routine use in research it will be possible to produce a model of the liver with a high value in applications such as disease modelling and drug development.

1.3. Hypothesis, Aims and Objectives

1.3.6. Hypothesis

From the background presented in this chapter, it is clear that a wide range of techniques can impact the structure and function of cells cultured *in vitro*. Whilst many studies have utilised systems for increasing the complexity of culture methods, these often lead to reduced throughput and ease-of-use alongside increased costs and spatial requirements. We hypothesise that a highly scalable system could be created utilising a 3D Alvetex® insert to allow complex co-culture models to be created with relative ease. We further hypothesise that this system will be of great benefit for models of the liver, due to the high level of fluid flow present in the tissue *in vivo*, and therefore will aim to test the apparatus with hepatic cultures as a model system.

1.3.2. Project Aims

The aim of this thesis is to develop a novel system for increasing the complexity and physiological relevance of tissue engineered cell models. The liver will be used as a target organ for modelling due to its high levels of vasculature suggesting it would benefit from the addition of fluid flow *in vitro*. This will be then used for the culture of a variety of different *in vitro* and *ex vivo* liver models to investigate the change in function with increasing complexity of the models. This process will build on other developments in the field such as 3D cell culture and co-culture models and combine these different advances into one system which can create complex tissue models whilst retaining a level of simplicity to make it feasible for use in a typical research environment.

1.3.2.1. Development of the bioreactor system

The development stage will initially derive a list of criteria which the system will need to achieve in order to effectively serve its purpose and be a useful addition to the field. From this starting point the system will be designed and optimised to maximise both user friendliness and the ability to reproducibly produce and maintain complex tissue constructs. Full characterisation of the various properties of this system will be carried out to ensure that a full understanding of its effects on the culture of cells can be gained.

1.3.2.2. Creation of increasingly complex cell line-based liver models

The apparatus will be utilised to create a series of *in vitro* liver models using the cell line HepG2 to replicate the parenchymal tissue of the liver. These cells are commonly used in drug discovery and

are inexpensive and easy to culture however are lacking in key hepatocyte functions. The aim of these models will be to see if a higher level of functionality can be restored through the application of cellular cues mimicking the *in vivo* microenvironment. As well as using the developed apparatus the addition of non-parenchymal cells will also be carried out to recreate the structure of the liver.

1.3.2.3. Testing the drug response of in vitro models

For the models to truly be improved over current methods, their response to a variety of different drugs will be observed. There are typically large discrepancies between the response of *in vitro* models to toxicological challenge compared with that seen in the liver *in vivo* which creates a tremendous challenge for the drug development pathway. If the models show a more *in vivo*-like response to drugs compared with standard models then their predictive capacity is improved, and the cultures are more useful for research. Different drugs respond in different ways when applied to 2D and 3D models and therefore a broad selection of drugs will be investigated to gain a thorough understanding of changes to the more complex tissue models.

1.3.2.4. Ex vivo maintenance of precision-cut liver slices

Another use for this system is the maintenance of precision-cut liver slices. These are a more physiologically relevant model of the liver compared with i*n vitro* cell models due to the entire tissue microenvironment being present and unchanged since removal from the body. There are limitations on the duration that it is possible to maintain these slices for at present which limits their usefulness to acute studies. The aim for this section of work would be to use the developed system to try and maintain rat PCLS for a longer period, up to several weeks, therefore increasing their usefulness for chronic studies. These slices will also be used to investigate the cellular changes during the onset of fibrosis, a chronic disease which is difficult to model *ex vivo* due to the time constraints with typical culture methods.

1.3.3. Project Objectives

The project objectives are as follows:

- Develop and characterise a dynamic cell culture system which conforms to a series of criteria which ensure its relevance to improving modern cell culture techniques.
- Create *in vitro* liver models based on the HepG2 cell line to demonstrate the effects of a dynamic culture system on the structure and function of these cells.
- Demonstrate changes in the predictability of these models when exposed to toxicological challenge.
- Investigate if the HepG2 models can be further improved through the addition of non-parenchymal cells.
- Utilise the system to maintain the viability of rat precision-cut liver slices over a prolonged period and demonstrate the uses of these models for chronic disease studies.

Chapter 2: Materials and Methods

2.1. Introduction

In this project a wide range of methods have been utilised for data collection and analysis including cell culture, computational analysis, and a range of quantitative and qualitative analytical techniques. In this chapter these techniques will be described in detail with the techniques broken down into the following categories:

- Cell Culture Techniques
- *Ex vivo* culture of precision-cut liver slices
- Bioreactor apparatus development and analysis
- Sample processing
- Morphological analysis
- Functional analysis

Further chapter specific techniques, in particular design of specific experiments, are discussed prior to presentation of results in their respective chapters.

2.2. Cell Culture Techniques

2.2.1. Propagation and maintenance of cell lines

2.2.1.1. HepG2

HepG2, a human hepatocellular carcinoma cell line, was maintained using Minimum Essential Medium (MEM, Gibco, Invitrogen, Paisley, Scotland) supplemented with 10 % Foetal Bovine Serum (FBS, Gibco), 2 mM L-glutamine (Lonza, Basel, Switzerland) and 100 U/mL of Penicillin/Streptomycin (Gibco) in T75 and T175 flasks (Greiner Bio-One, Kremsmunster, Austria). Cells were passaged at 80 % confluency using 0.25 % Trypsin / EDTA (Gibco) and split into new flasks at a ratio of 1:3. Cells were incubated and maintained at 37 °C and 5 % CO_2. In 2D culture these cells typically grow in islands of cells, as seen in Figure 2.1.

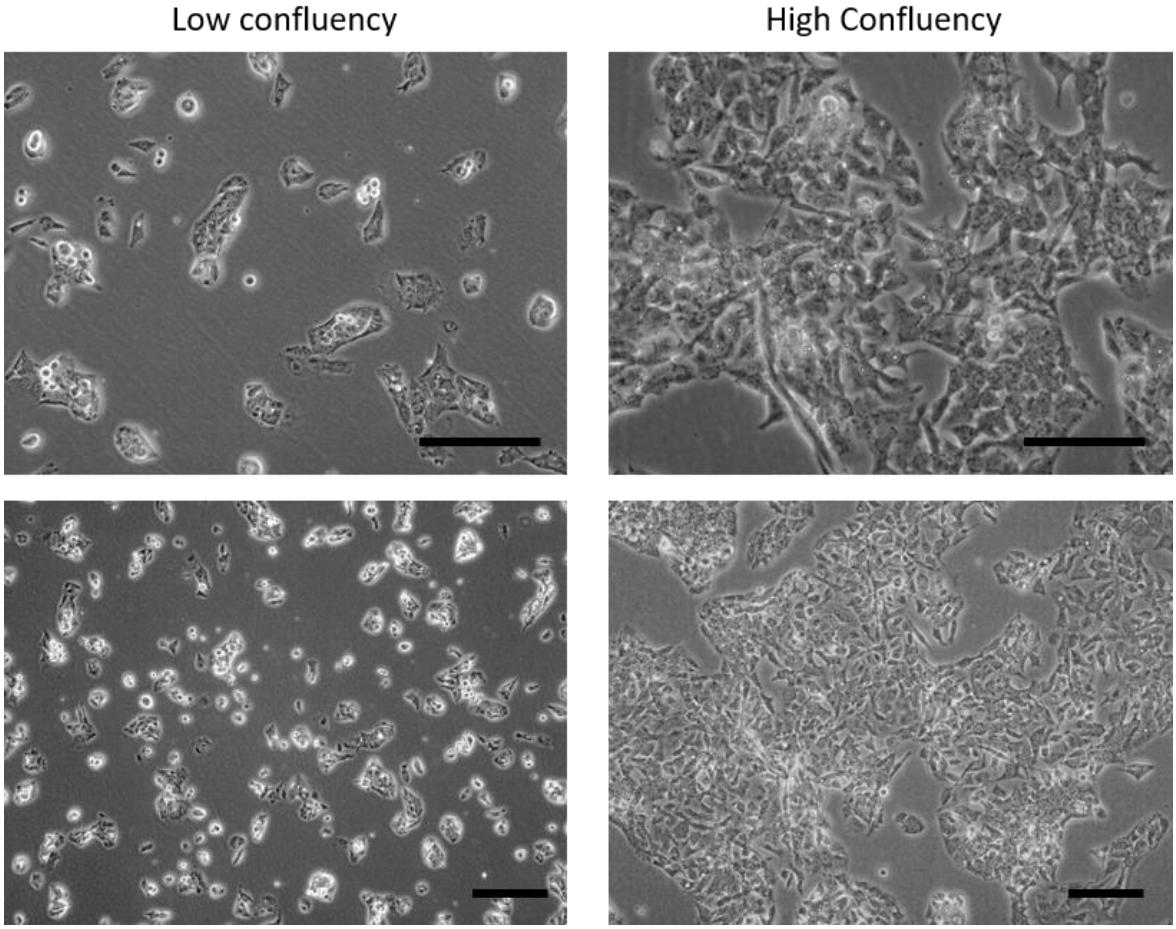

Figure 2.1: Phase-contrast images of HepG2 cells grown in 2D. In 2D, HepG2 cells grow with a clustered morphology. This leads to formation of islands of cells over time, as can be seen between the low confluency (Left) and high confluency (right) images, rather than a uniform monolayer. Due to this, a small degree of multilayering is also often seen. Scale bars are 100 μm.

2.2.1.2. SK-Hep-1

SK-Hep-1, a human hepatic adenocarcinoma cell line, were maintained using MEM supplemented with 10 % FBS, 2mM L-Glutamine and 100 U/mL Penicillin/Streptomycin in T75 and T175 flasks. Cells were passaged at 80-90 % confluency using 0.25 % Trypsin / EDTA and split into new flasks at a ratio of 1:4. Cells were incubated and maintained at 37 °C and 5 % CO_2. When grown in 2D culture these cells show an elongated morphology at low confluency (Figure 2.2A) but start to become compact and closely packed at higher confluency (Figure 2.2B)

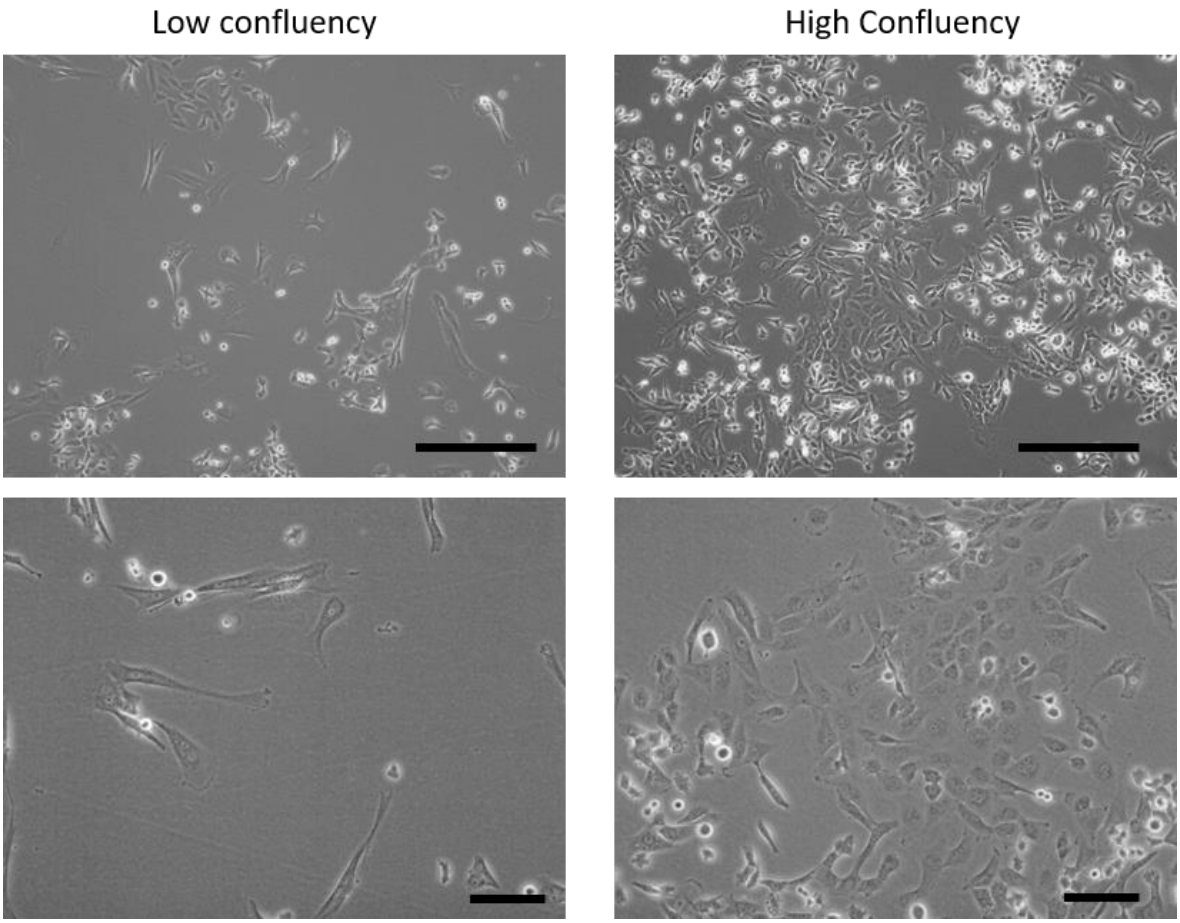

Figure 2.2: Phase-contrast images of SK-Hep-1 cells grown in 2D. In 2D, SK-Hep-1 cells tend to form an elongated morphology at low confluency (Left) and exist as isolated cells and in small clusters. At high confluency the cells become more compacted and some regions with a cobblestone morphology can be seen (right). Scale bars are 100 µm.

2.2.1.3. HDFn

Neonatal human dermal fibroblasts (HDFn, Lot #1366434, Fisher Scientific) were maintained using Dulbecco's modified Eagle Media (DMEM, Gibco) supplemented with 10 % FBS, 2mM L-Glutamine and 100 U/mL Penicillin/Streptomycin in T175 flasks. Cells were passaged at 90 % confluency using 0.25 % Trypsin / EDTA and split into new flasks at a ratio of 1:6. Cells were incubated and maintained at 37 °C and 5 % CO_2. As shown by Figure 2.3, these cells exhibit a typical flattened and elongated fibroblast morphology in 2D culture.

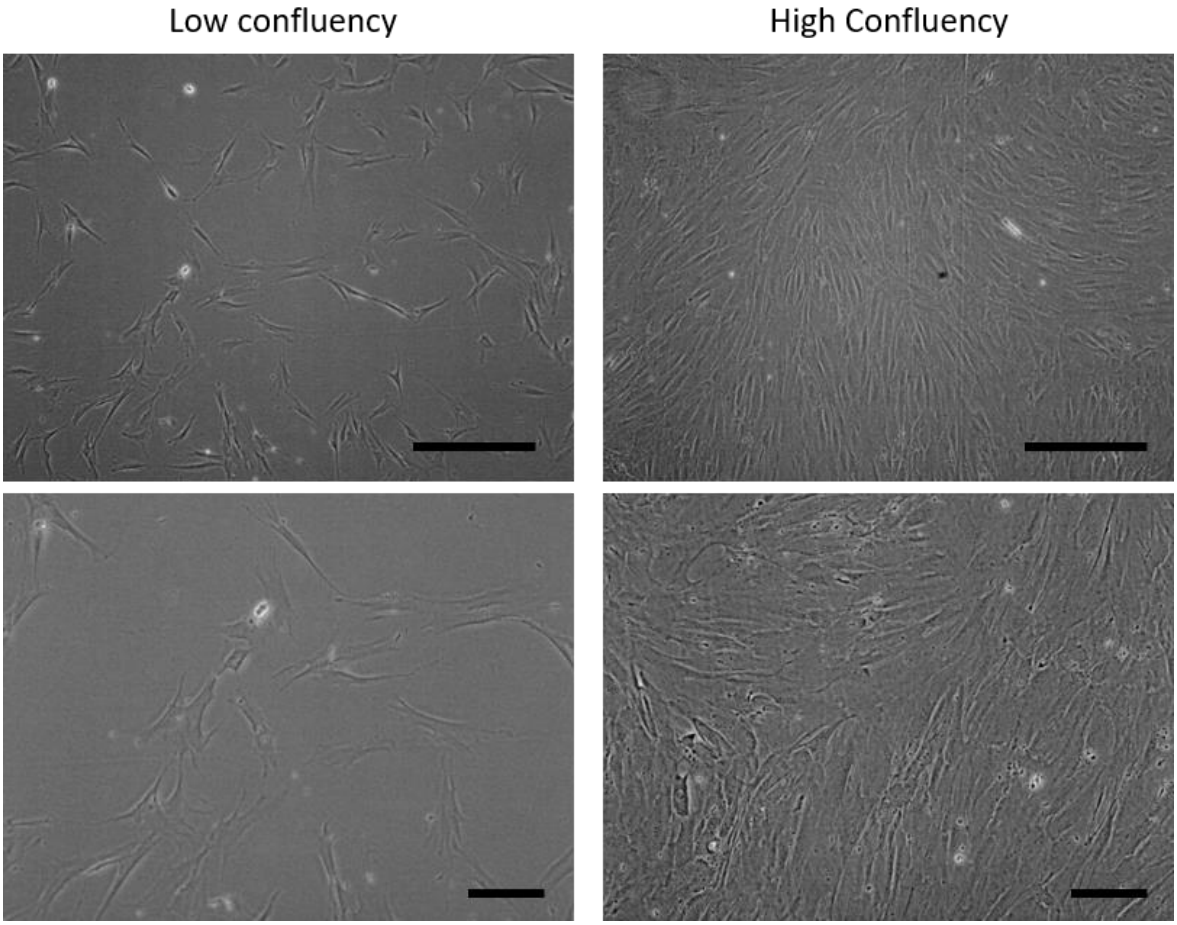

Figure 2.3: Phase-contrast images of HDFn cells grown in 2D. In 2D, HDFb cells flatten and spread across the bottom of the plate, leading to being more difficult to see under phase-contrast microscopy than the other two cell lines. At high confluency the cells start to align with adjacent cells giving a more organised appearance (Right). Scale bars are 100 µm.

2.2.2. Growth of cells in 6 and 12 well plates

Wells were filled with 8 mL and 4 mL of warm media for 6- and 12-well plates (Greiner Bio-One) respectively. Cells were trypsinised using 0.25 % trypsin / EDTA and live cells were counted using the trypan blue exclusion assay on a haemocytometer. For this, a fraction of the resuspended cells was diluted 1:10 in Trypan Blue (Sigma Aldrich, Dorset, UK) and unstained live cells could be counted using a haemocytometer. Cells were diluted accordingly so that 10,000 cells/cm^2 could be seeded in a media volume of 100 µl. The plates were placed in a humidified incubator at 37 °C / 5 % CO_2 and had a full media change every 3 days. Cultures were continued for 7 or 14 days in line with the growth period of the complementary 3D samples.

2.2.3. Growth of cells on coverslips

Coverslips were oxygen plasma treated before use to aid cellular adherence using an Emitech K-1050X plasma asher. An ashing time of 5 minutes at 40 W was used for coverslips. Coverslips were then placed into a 12-well plate and treated with ethanol for 10 minutes followed by two washes in phosphate-buffered saline (PBS). 4 mL of warm media was then added to the wells. Cells were trypsinised using 0.25 % trypsin / EDTA and live cells were counted using the trypan blue exclusion assay on a haemocytometer. The cell suspension was seeded to the coverslips at 10,000 cells/cm^2 in 100 µL of media. Cells were placed in a humidified incubator and maintained at 37 °C and 5 % CO_2 for 5 days.

2.2.4. Preparation of Alvetex®

Alvetex® membranes (Reprocell Europe Ltd, Sedgefield, UK) were used in this work for the culture of cells in a 3D microenvironment. Three forms of Alvetex® were used: Scaffold, Strata and Polaris (Not currently commercially available). These are 200 µm thick, porous membranes made from polystyrene which vary in the size of their pores. Alvetex® Scaffold, the most porous substrate, has an average pore size of 38 µm, compared to 13 µm and 3 µm for Strata and Polaris respectively. Further details of the Alvetex® membranes can be found in Section 3.1.4.1.

Alvetex® was rendered hydrophilic by soaking inserts in 70 % ethanol for 10 minutes for Scaffold and Strata and overnight for Polaris. It was then placed into a 6-well plate and washed twice in PBS. After aspirating the second PBS wash 5 mL of complete cell culture medium was added to the well in preparation for cell seeding. Most of this work was performed using Alvetex® Strata, with the exception of Chapter 6 in which Alvetex® Scaffold was the predominant form used.

2.2.5. Preparation and reuse of the bioreactor system

The components of the bioreactor system were initially washed in warm water with detergent to remove any debris left from the manufacturing process. These were then dried and assembled with the lid placed on top in the vented orientation. The assembled bioreactors were autoclaved at 121 °C for 20 minutes to sterilise them before being stored with the lids inverted in the sealed orientation until required. Prior to use the bioreactors were moved into a sterile cell culture hood and cleaned thoroughly with 70 % ethanol. These were then stored in the cell culture hood to evaporate any excess ethanol before use with cell cultures.

After cultures were completed and the Alvetex® inserts removed, all media was aspirated from the bioreactors. The empty bioreactors were filled with 10 % Distel™ solution (Tristel, UK) and stored overnight to sterilise any remaining cellular debris. After this the Distel™ solution was drained from the cultures and a thorough washing in warm water with detergent was carried out before drying and autoclaving, as carried out previously, to prepare them for the next use.

2.2.6. Growth of HepG2 cells on Alvetex® in well inserts

HepG2 cells were trypsinised for 15 minutes using 0.25 % trypsin / EDTA and live cells were counted using the trypan blue exclusion assay on a haemocytometer. 100 µl of the cell suspension, containing 2 million cells, was seeded onto 6-well Alvetex® inserts in a 6-well plate containing 5 mL of cell culture medium. Seeded plates were placed in a humidified incubator at 37 °C / 5 % CO_2 and maintained for between 7 and 14 days. A media change was performed every 2 days with the 6-well plate being replaced at the first media change to remove cells which had not adhered to the Alvetex® membrane. An overview of the alternative culture techniques for these inserts using the bioreactor systems is shown by Figure 2.4 and described in the next sections.

2.2.7. Growth of HepG2 cells in static Alvetex® sandwich culture

Cells were initially seeded in 100µl of medium to Alvetex® well inserts and incubated at 37 °C and 5 % CO_2 as in standard Alvetex® culture described above. After one day of culture a second Alvetex® membrane was placed over the first to create the sandwich culture. The second piece of Alvetex® was first soaked in 70 % ethanol, PBS and then medium. The seeded inserts were removed from the incubator and dissembled, the second sheet of Alvetex® placed gently on top and then the full sandwich culture was reassembled. The inserts were then placed into a fresh six well plate and

topped up with 5 mL of medium. This was placed back in the incubator for a further 7 days with medium changes every two days.

2.2.8. Growth of HepG2 in dynamic Alvetex® culture using the culture holder

Alvetex® cultures were set up as previously described and incubated at 37 °C / 5 % CO_2 for one day in 5 mL of media. The Alvetex® membrane holder was treated overnight in 10 % Distel™ followed by one hour in 70 % ethanol to sterilise it. This was then washed twice in PBS and stored in PBS until ready to use.

The culture plates containing seeded 6-well Alvetex® inserts were removed from the incubator and the inserts dismantled to remove the Alvetex® membrane. One half of a membrane holder was placed in a 6-well plate containing PBS to maintain humidity and the Alvetex® membrane was placed on top of it. Another prepared Alvetex® membrane was then placed gently over the top of the cells, if required. The second half of the membrane holder was clipped on top, having been soaked beforehand in 70 % ethanol followed by PBS. The bioreactor system was filled with 110 mL of prewarmed culture media. The assembled culture in the membrane holder was placed into the bioreactor with care being taken to avoid formation of bubbles. The culture was then incubated on a magnetic stirrer at 37 °C and 5 % CO_2 for 6 days. Unless stated otherwise the magnetic stirrer was set to 100 rpm for the duration of the culture.

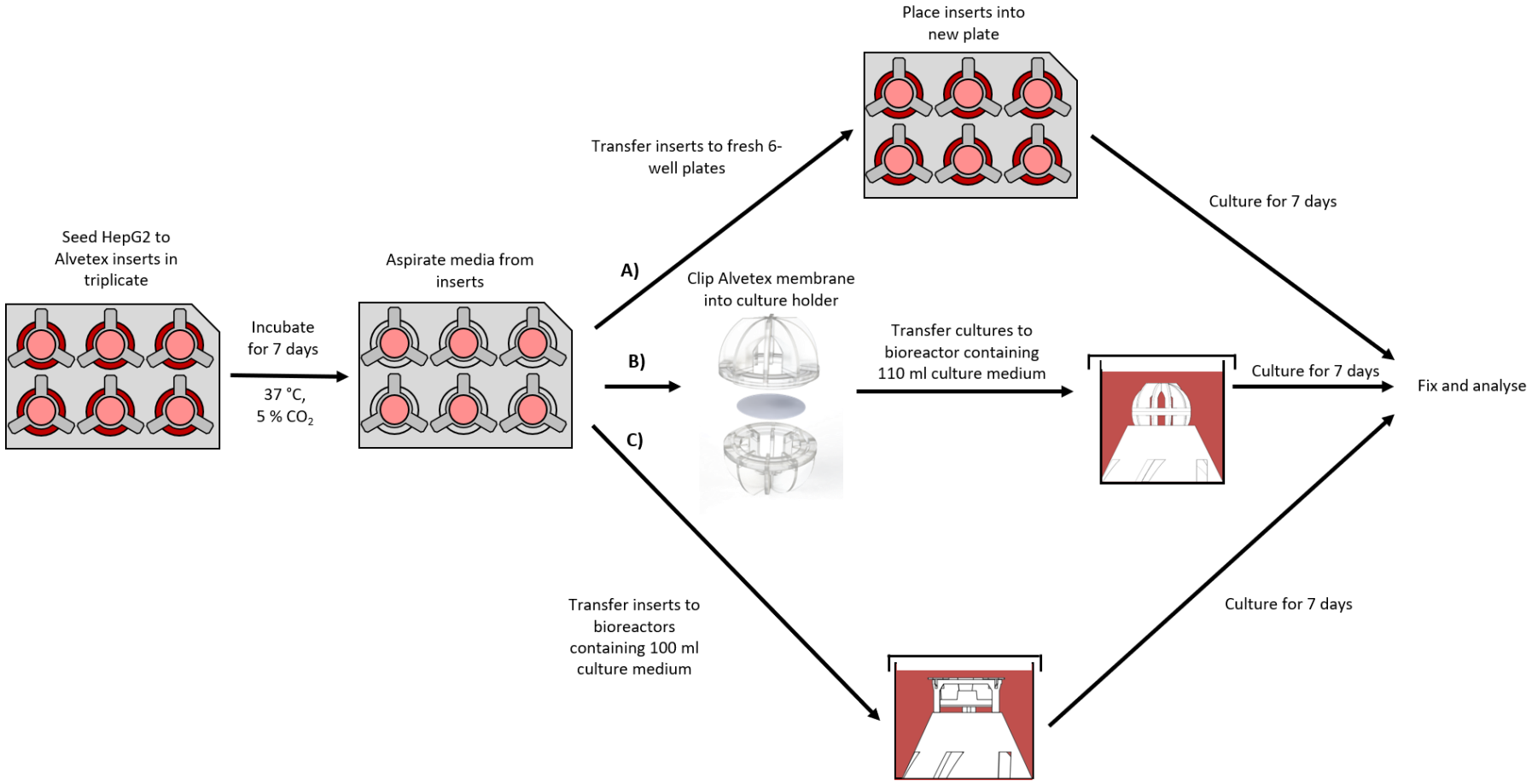

Figure 2.4: Protocols for setting up cultures in the different systems. Cells in 6-well plates simply get transferred to a fresh plate after 7 days whilst for stirred cultures in the prototype bioreactor the Alvetex membrane is unclipped from the insert and placed into the spherical culture holder, before being placed into a bioreactor containing 110 mL of cell culture medium. For the final bioreactor design inserts are simply lifted from the 6-well plate and placed into a bioreactor containing 100 mL of medium. This can then be cultured for a further time, in the case of this study 7 days, prior to analysis.

2.2.9. Growth of HepG2 cells in dynamic Alvetex® culture using the 6-well insert holder

Alvetex® cultures were set up using 6-well inserts as previously described and placed in a humidified incubator at 37 °C / 5 % CO_2 with 5 mL of media. These cultures were maintained out for 7 days with media changes every 2 days. At the end of the 7 days the cultures were moved to bioreactors. The assembled bioreactors were filled with 100 mL of prewarmed cell culture media. The Alvetex® inserts were moved from their 6-well plates into the holder, with the arms of the inserts aligned with the slots in the holder and care being taken to avoid bubble formation. The bioreactor lid was seated in the vented orientation and the culture was placed on a magnetic stirrer in a humidified incubator. The culture was then incubated at 37 °C and 5 % CO_2 for a further 7 days.

2.2.10. Growth of HDFn cells in Alvetex® Scaffold to form an *in vivo*-like supportive layer

Alvetex® Scaffold 6-well inserts were washed in 70 % ethanol followed by PBS before being placed into a 6-well plate and covered with 5 mL of complete DMEM containing 10 % FBS, 2 mM l-glutamine and 100 U/ml penicillin-streptomycin. The media was aspirated from the wells and 1 million HDFn cells were seeded in 100 µl of medium onto the Alvetex® inserts. These were placed in an incubator for an hour to allow the cells to adhere. 8 mL of media was then added as made up previously with the addition of 100 ng/ml of ascorbic acid. The plates were placed back in the incubator and cultured for a further 14 to 28 days. Where the exact culture time is not stated in the experiment the culture period used was 21 days. A media change was performed the day after seeding, including replacing the six well plate to remove cells which had not adhered. Further media changes were carried out twice weekly.

2.2.11. Addition of HepG2 cells to HDFn cultures

For the growth of HepG2 cells on HDFn-seeded Scaffolds the HDFn compartment was first produced as described in the previous section. At the end of the culture period the culture media was aspirated and 5 mL of DMEM containing 10 % FBS, 2mM l-glutamine and 100 U/ml penicillin/streptomycin was added to the cultures. 2 million HepG2 cells were seeded to the surface of the Alvetex® Scaffold in 100 µL of cell culture media. These were placed in a humidified incubator at 37 °C / 5 % CO_2 for 7 to 14 days with media changes every two days.

2.2.12. Culture of SK-Hep-1 cells on Alvetex® membranes

SK-Hep-1 cells were trypsinised from flasks using 0.25 % Trypsin / EDTA and cell counts were performed with a haemocytometer using the trypan blue exclusion assay. Prepared Alvetex® inserts were placed into 6-well plates and 5 mL of DMEM with 10 % FBS, 2 mM l-glutamine and 100 U/ml penicillin/streptomycin was added. SK-Hep-1 cells were seeded to the inserts in 100 µL of media and the cell quantity was 1 million cells, unless stated otherwise. The cultures were placed in a humidified incubator at 37 °C and 5 % CO_2 for 7 days with media changes every 2 days.

2.2.13. Addition of SK-Hep-1 to HepG2 Alvetex® cultures

For co-culture of SK-Hep-1 cells with HepG2, either on Alvetex® Strata or Alvetex® Scaffold seeded with HDFn, the initial seeding of HepG2 was carried out as described previously. Alvetex® Polaris was not used for this combination of cell lines. Following seeding of HepG2 cells, SK-Hep-1 cells were also added in 100 µl of media with 100,000 cells added if not stated otherwise. These cultures were placed in a humidified incubator at 37 °C and 5 % CO_2 and cultured for 7 days with media changes every two days.

2.3. *Ex vivo* culture of precision-cut liver slices

2.3.1. Extraction of rat liver

Rat livers were harvested from Wistar rats killed by cervical dislocation after being anaesthetised with isoflurane. Immediately after removal, livers were washed twice in ice-cold, oxygenated Krebs-Henseleit buffer supplemented with an additional 14 mM d-glucose and 10 mM HEPES before being stored on ice in this buffer in a sterile specimen container. All further processing was carried out in a timely manner with no more than 3 hours between sacrifice of the rat and placing the liver slices into the incubator for culturing. An overview of the steps in the protocol is shown by Figure 2.5.

2.3.2. Slicing of rat liver

Cores were cut from the livers using an 8 mm biopsy punch (Kai Medical, Solingen, Germany). Cores were washed in ice-cold Krebs – Henseleit Buffer (KHB) and excess liquid was removed with filter paper. Washed cores were placed into 3 % low gelling temperature agarose (Sigma Aldrich) in PBS maintained at 37 °C in a specimen container, with a maximum of 6 cores per container, which was subsequently placed on ice to polymerise the agarose. Blocks were removed from the specimen containers and trimmed with a razorblade to remove excess agarose. These blocks were attached to a flat specimen holder using universal super glue (Loctite, Düsseldorf, Germany) and left for 10 minutes to allow the glue to set. The specimen holder was mounted on a Leica VT1000 S vibratome (Leica Biosystems, Milton Keynes, UK) and sectioned with a thickness of 250 µm. A blade amplitude of 1 mm, frequency setting of 10 and forward speed of 0.1 mm/s were found to be optimum for cutting liver slices. Cut slices were stored in a 24-well plate on ice with oxygenated Krebs-Henseleit buffer made up as previously until ready for culture.

2.3.3. Culture of rat precision-cut liver slices

The bioreactor apparatus was filled with 100 mL of William's Medium E (WME) supplemented with 10% FBS, 2 mM l-glutamine, 25mM D-glucose and 100 U/ml penicillin-streptomycin prewarmed to 37 °C. 6-well Alvetex® inserts were washed with 70% ethanol followed by KHB and placed into the holder in the bioreactor apparatus. Sections were gently placed onto the Alvetex®® inserts ensuring an even tissue distribution as centrally as possible. The lids were fitted to the beakers in the vented orientation before being placed into a humidified 37 °C, 5 % CO_2 incubator on a magnetic stirrer set to 100 rpm and cultured for between 1 and 28 days.

For slices cultured in static conditions 6-well Alvetex® inserts were used in a 6-well plate. 8 mL of prewarmed WME with 10 % FBS, 2 mM l-glutamine, 25 mM D-glucose and 100 U/ml penicillin/streptomycin was added to the wells. Sections were gently placed onto the Alvetex® inserts as in the bioreactor. Plates containing the cultures were then placed into a humidified incubator at 37 °C and 5 % CO_2 for up to 7 days.

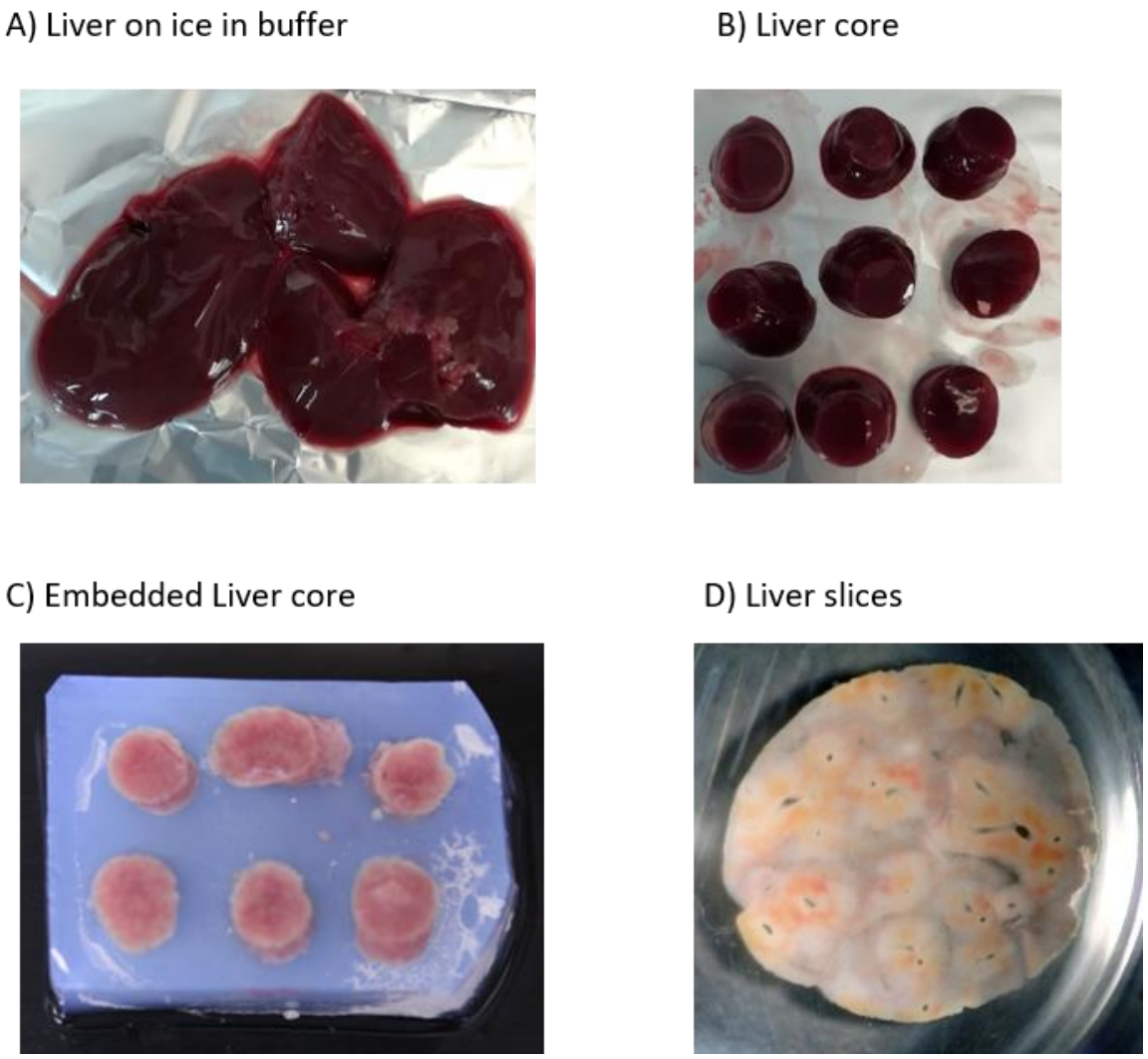

Figure 2.5: Preparation and culture of precision-cut rat liver slices. A) Liver is excised from the rat immediately upon death and washed twice in ice-cold KHB before being stored in KHB on ice. B) 8 mm Liver cores are created using a biopsy punch. Multiple cores can be created from each lobe of the liver. The cores with the best morphology are selected for further processing. C) Liver cores are embedded in low gelling temperature agarose and placed on ice to polymerise. Up to six cores are embedded in an agarose block to maximise throughput. D) 250 µm Liver slices are cut using a Leica VT1000S Microtome. Holes visible in the slice are blood vessels. Slices are stored on ice in KHB until placed into culture.

2.4. Bioreactor development and analysis

2.4.1. Manufacture of custom equipment

Manufacture of prototypes was performed in-house by the University of Durham. Specifically, the PTFE machining was carried out by the mechanical workshops in the Departments of Chemistry, Engineering and Physics. Glassblowing for the prototype beakers was performed by the glassblowing workshop in the Department of Chemistry.

The finalised PTFE parts were produced by Roechling Fibracon Ltd, Derbyshire, UK. Further production of glass beakers was carried out by Scientific Glass Services, Nottinghamshire, UK.

The custom magnetic stirrer units were designed and manufactured by Kelvin Appleby in the electrical workshop, Department of Chemistry at Durham University.

2.4.2. Measuring the permeability of Alvetex®

To measure the permeability of Alvetex®, apparatus was assembled to utilise Darcy's law for laminar flow. The formula

$$\kappa = -\frac{QL\mu}{A\Delta p} \tag{2.1}$$

allows calculation of the permeability coefficient, κ, when the flow rate Q, the thickness of the material L, the viscosity of the liquid μ, the cross-sectional area of the sample A and the pressure difference across the medium Δp are all known. With a vertical head of water, the pressure exerted can be obtained using

$$p = \rho g h \tag{2.2}$$

where p is the pressure exerted by the head, ρ is the density of the liquid, g is the acceleration due to gravity, 9.81 m/s, and h is the height of the head of water above the medium. For the experiments carried out water was used with a viscosity at 25°C of 0.89 mPa s and the thickness of Alvetex® is a known value given as 200 μm. Integration of Darcy's law gives the following equation, in which the h_1 and h_2 are the start and end heights of the head and t is the time taken for the height to move between the two. The derivation of this equation is provided in more detail in Appendix 4.

$$\kappa = -\frac{A_{head}L\mu}{A_{membrane}\rho g t} ln\left(\frac{h_1}{h_2}\right) \tag{2.3}$$

Apparatus was assembled as shown in Figure 2.6. using commercially available 15 mm copper pipe and brass pipe fittings. Alvetex® was secured into the lower compression fitting of the isolation valve by removing the copper olive and using several 15 mm rubber washers. The header tank was filled to a set height measured in 10 mm intervals between 100 mm and 200 mm above the Alvetex® membrane. To measure the permeability the valve was opened and the flow rate through the membrane can be measured. Water flowing through the membrane was collected in a beaker and weighed after a measured time. The water level at the start and endpoint were also recorded to calculate the head pressure.

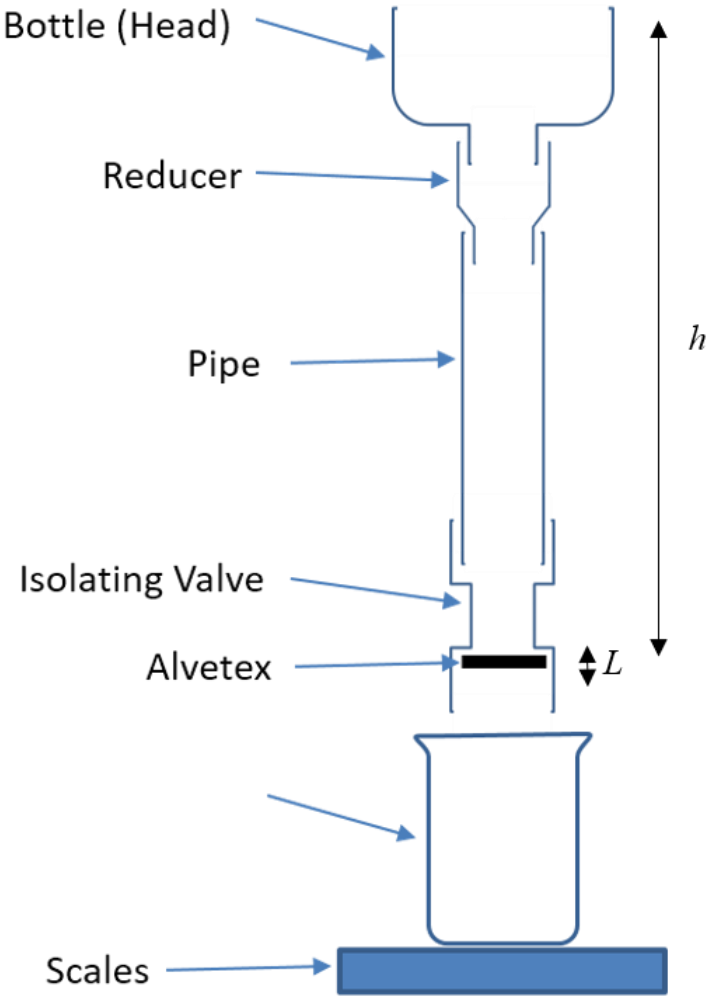

Figure 2.6: Apparatus for measuring the permeability of Alvetex. Alvetex membranes were placed within one end of the isolating value with a head of water above. The height of the head, h, and the thickness of the membrane, L, are both used for the permeability calculation. When the valve is opened water moves through the membrane and the change in mass across a known time period is measured using the scales. The volume flow rate, Q, can then be calculated using the mass change, time period and known density of water.

2.4.3. Dye circulation

To visualise the circulation pattern in the apparatus at a simple level an assembled bioreactor system had 125 mL of water added to it and the magnetic stirrer turned on at the desired frequency. This was left for a minimum of 5 minutes to equilibrate. Following this 200 µL of 0.1 % crystal violet in 70 % ethanol was quickly added using a pipette. A Canon 550D camera was set up to take photos every two seconds using a timer. This was performed over time periods of up to two minutes. Images were then processed using the ImageJ software (National institute of Health, https://imagej.nih.gov/ij/) and organised into chronological order.

2.4.4. Particle Image Velocimetry

To view the turbulent effects in the beaker at the level of the cell culture particle image velocimetry (PIV) was carried out in a horizontal plane across the centre of the beaker by Doctor Lian Gan in the Department of Engineering, Durham University. Due to the nature of the rotating flow generated by the stirrer, the simple two-dimensional PIV measurement in a horizontal plane, which resolves the two-component in-plane velocity distribution, captures most of the energy content as the out-of-plane velocity component was considered to be relatively unimportant. To carry this out with PTFE stands the stand was first coloured black to minimise any interference caused by reflection. The PIV sample rate used was 4 Hz and the spatial resolution was 0.05 mm. The mean velocity magnitude and the root mean square contours were calculated from a time-mean of 400 velocity fields. The samples were taken from a plane 40 mm from the bottom of the vessel, approximately the same height as the Alvetex® membrane would be supported. Analysis of this data was carried out using the MATLAB software (The Mathworks Inc., Natick, MA, USA).

2.4.5. Computation Fluid Dynamics

Computational fluid dynamics modelling of the system was carried out with support from Doctor Richard Williams in the Department of Engineering, Durham University. The bioreactor system was analysed using transient 3D computational fluid dynamic studies based on numerical solution of the Navier-Stokes equations. The geometry of the system was generated using Solidworks 2018 (Dassault Systèmes, Vélizy-Villacoublay, France). The meshing, fluid flow calculations and post processing were carried out using ANSYS Fluent (Ansys, Canonsburg, Pennsylvania, USA). Patch conforming tetrahedral meshing was used to create a mesh for the system with a minimum orthogonal quality greater than 0.1 in all simulations. The fluid flow was simulated as water, with

an incompressible, isothermal fluid with a dynamic viscosity of 1.003 g/m s and a constant density of 998.2 kg/m3. A transient, pressure-based solver was used with the realisable k-epsilon turbulence model and scalable wall functions. The Pressure Implicit with Splitting of Operator algorithm was used for pressure-velocity coupling and second order special discretization was used throughout. The stir bar motion was modelled using a rotating region with a rotational frame motion around the y axis centred on the origin with varying speeds from 50 rpm to 200 rpm. Shear stress and through-membrane velocity were calculated as a mass flow-weighted average across a horizontal plane at the membrane surface and at the midpoint of the membrane respectively with minimum and maximum values as the upper and lower limits respectively.

2.4.6. Measurement of magnetic fields

Magnetic field measurements were taken using the Hall effect sensor in an Honor 9 Lite mobile phone and the My Magnetic Field application. Prior to measurements the sensor was calibrated using the developers' instructions. The phone was mounted on a retort stand with the sensor centred over the magnet to be measured. A steel ruler was used to measure the distance between the probe and the magnet and measurements were taken at a series of distances with the entire process repeated three times.

2.4.7. Measuring stirrer speed with a stroboscope

A stroboscope was used to measure the rotation speed of the stirrer. The stirrer was set up in a dark room with the stroboscope set up to one side. When the stirrer was turned on at a chosen setting the frequency of the stroboscope was adjusted until the stir bar appeared to be stationary. This frequency was then halved from this point to confirm that this was the base frequency whilst a measurement at twice the frequency was also taken to increase the accuracy.

2.4.8. Measuring stirrer speed with slow-motion video

A GoPro Hero 3+ action camera (GoPro, California, USA) was used to record the stir bar rotating. A frame rate of 240 frames per second was used for the recordings. These were subsequently broken down to individual frames and the number of frames required for ten full rotations of the stir bar was recorded. From these data the time taken for one rotation could be calculated, and this could then be further used to calculate the rotation speed of the stirrer.

2.5. Sample Processing

2.5.1. Fixing Cell cultures

For cultures fixed using paraformaldehyde (PFA, Fisher Scientific), medium was aspirated from cell cultures and Alvetex® membranes were unclipped from the inserts and placed into a fresh 12-well plate. Cultures were then washed twice in PBS and soaked either overnight in 4 % PFA in PBS at 4 °C or for one hour at room temperature. Following PFA fixation the samples were washed three times in PBS and stored at 4 °C in the final PBS wash until further processing was performed.

For cultures fixed using methanol-acetone, media was aspirated from cell cultures and Alvetex® membranes were unclipped and placed into a fresh 12-well plate. These were then washed twice in PBS and soaked in a 50:50 mixture of methanol and acetone at -20°C. Alvetex® cultures were fixed for 20 minutes whilst monolayer cultures were fixed for 10 minutes. Following fixation cultures were washed three times in PBS to remove the fixative and stored in PBS at 4 °C until needed.

2.5.2. Wax Embedding and sectioning

The fixed samples were dehydrated through a series of ethanol concentrations, specifically 30 %, 50 %, 70 %, 80 %, 90 % and 95 % for 15 minutes in each before being left in 100 % ethanol for half an hour. After this the samples were moved into tissue embedding cassettes and soaked in Histoclear II (National Diagnostics, Lichfield, UK) for 30 minutes. The Histoclear II was then topped up with paraffin wax (Fisher Scientific) to make a 50:50 mixture and left in an oven for 30 minutes. Finally, the Histoclear:wax mix was drained and replaced with 100 % wax. This was placed in the oven for a minimum of one hour. After being soaked in wax the Alvetex® samples are cut in half. A small amount of wax was added to an embedding mould and samples were placed cut-edge down into this. The mould was then topped up with wax and allowed to set overnight at room temperature.

For sectioning, the wax blocks containing the samples were clamped into a Leica RM2125RT microtome (Leica Biosystems, Wetzlar, Germany). These were sectioned at a thickness of 5 µm. The sections were then floated onto a SuperFrost™ Plus microscope slide (Fisher Scientific) using a water bath at 40 °C with two sections typically mounted on each slide. These were left to dry on a heated slide drying rack for a minimum of one hour.

2.5.3. OCT Embedding and sectioning

Fixed samples for OCT embedding were first treated with sucrose as a cryoprotectant. Samples were soaked in 15 % sucrose in PBS overnight, or until the sample started to sink, at 4 °C. A second soak with 30 % sucrose in PBS was then carried out overnight at 4 °C. Cryomoulds were filled with optimum cutting temperature compound (OCT, Fisher Scientific) and left for 5 minutes to uniformly fill the mould with care being taken to avoid bubble formation. Alvetex® samples were cut in half and trimmed to fit into the moulds before being embedded into the OCT compound with the central cut edge at the bottom. The samples were left for a few minutes to equilibrate with the OCT compound before reorientating them as required and freezing by placing them on a metal rack surrounded by liquid nitrogen. Once completely frozen the samples are stored in the freezer at -80^{o}C until needed.

For sectioning the samples were transferred from the freezer to an OFT5000 cryostat (Bright Instruments, Bedfordshire, UK). Sections were mounted to the specimen holder with a drop of OCT compound and placed on the freezing rack until the OCT compound was completely frozen. The specimen holders were then mounted on the cryostat and sections were cut with a thickness of 7 µm and mounted on positively charged glass slides. Following sectioning slides were placed in demineralised water (dH_2O) for 10 minutes to dissolve the surrounding OCT compound before being placed on a slide dryer for 30 minutes to remove excess water and bake the samples onto the slides. Slides were then stored until ready to be stained.

2.5.4. PCR analysis: RNA extraction

RNA isolation was performed using the Reliaprep RNA Tissue Miniprep system (Promega UK, Southampton, UK) using the manufacturer's protocol for fibrous tissue. Alvetex® membranes were removed from the inserts and placed in the bottom of 12-well plates containing ice cold PBS whilst 2D cells grown in 6-well plates were washed once with ice cold PBS. After aspiration of PBS, 500 µL of lysis buffer was added to the samples and a cell scraper used to aid in the removal of cells. The lysed samples were stored in Eppendorf tubes at -80 °C until further processing was carried out. Upon thawing, the resulting liquid was passed several times through a 21G needle to shear the DNA. 500 µL of RNA dilution buffer was added to these samples before centrifugation at 10,000 g for 3 minutes to pellet insoluble debris. The supernatant was transferred to a new Eppendorf tube to which 340 µL of RNase-free 100% isopropanol was added. The lysate was vortexed briefly and transferred to a minicolumn in a collection tube.

Minicolumns were centrifuged at 13,000 rpm for 1 minute. The column eluate was discarded and 500 µL of RNA wash solution was added prior to another centrifugation at 13,000 rpm for 30 seconds. DNase I incubation mix was made up with 24 µL of yellow core buffer, 3 µL of $MnCl_2$ and 3 µL of DNase I, giving a total volume of 30µl, per sample. DNase I incubation mix was added to the minicolumns and incubated for 15 minutes at room temperature. 200µl of column was solution was added to the minicolumns prior to centrifugation at 13,000 rpm for 15 seconds. A further 500 µL of RNA wash solution was added and minicolumns were centrifuged again at 13,000 rpm for 30 seconds. A new collection tube was placed under the minicolumn, 300 µL of RNA was solution added and centrifugation carried out at 13,000 rpm for 2 minutes. Finally, the minicolumns were placed over a 1.5 mL capped elution tube and 30 µL of RNase-free water added. Minicolumns were centrifuged at 13,000 rpm for 1 minute to collect the RNA and the elution tubes containing purified RNA were stored on ice. The RNA yield and quality were assessed using a Nanodrop spectrophotometer (Fisher Scientific). Samples were stored at -80 °C until cDNA synthesis was performed.

2.5.5. PCR analysis: cDNA synthesis

cDNA synthesis was carried out using the Applied Biosystems High-Capacity cDNA Reverse Transcriptase Kit (Applied Biosystems, Fisher Scientific, UK) following the manufacturer's instructions. Samples were diluted to an RNA concentration of 100 µg/mL with 10 µL, containing 1 µg of RNA, required for each cDNA synthesis reaction. A 2X master mix was made up using the reagent volumes shown in Table 2.1.

Table 2.1: Components required for cDNA synthesis. Volume is made up for the number of reactions required plus an extra 10 % to account for pipetting error. This volume is added 1:1 with the extracted RNA to make the mixture for cDNA synthesis.

Component	Volume per reaction (µl)
10X RT Buffer	2
25X dNTP Mix (100mM)	0.8
10X RT Random Primers	2
MultiScribe™ Reverse Transcriptase	1
Nuclease-free H_2O	4.2

10 µL of both the master mix and diluted RNA were added to a 0.2 mL PCR tube to give a total volume of 20 µL. This mixture was centrifuged briefly to ensure all reagents were at the bottom of the tube before being placed into an Eppendorf Mastercycler gradient thermocycler (Eppendorf) using the program shown in Table 2.2. The cDNA produced was stored at -20 °C until the PCR reaction was performed.

Table 2.2: Thermocycler program used for cDNA synthesis. The program was used to make 1 µg of cDNA using a 20 µL sample size. The final step holds the samples at 4 °C until further processing can take place.

Step	Temperature	Time
1	25 °C	10 minutes
2	37 °C	120 minutes
3	85 °C	5 minutes
4	4 °C	Indefinitely

2.5.6. Protein extraction for Bradford Assay

Samples were washed in PBS and then lysed by placing in Mammalian Protein Extraction Reagent (MPER, Fisher Scientific) with 1 % protease and phosphatase inhibitor cocktail (Fisher Scientific) in a 1.5 mL Eppendorf tube on ice. A pipette tip was used to break down Alvetex® membranes whilst an Eppendorf micropestle (Eppendorf Ltd, Stevenage, UK) was used for homogenising PCLS. Samples were stored on ice and vortexed every 5 minutes over half an hour and then sonicated for 30 minutes. Samples were centrifuged at 12,000 rpm for 20 minutes and the supernatant stored at -80 °C until further use.

2.6. Morphological Analysis

2.6.1. Haemotoxylin and Eosin Staining

Haematoxylin and Eosin (H&E) staining was carried out according to the following protocol. Slides were deparaffinised in Histoclear (National Diagnostics) for 15 minutes, before rehydration through 100 % ethanol for 2 minutes, 95 % ethanol for 1 minute, 70 % ethanol for 1 minute, and dH_2O for 1 minute. Slides were stained in Mayer's Haematoxylin (Sigma Aldrich) for 5 minutes, before washing in dH_2O for 30 seconds, and incubating in alkaline alcohol for 30 seconds to blue the nuclei. Slides were dehydrated in 70 % ethanol and 95 % ethanol for 30 seconds each. Slides were stained in Eosin for 1 minute before 2 washes in 95 % ethanol for 10 seconds. Slides were then dehydrated in 100 % ethanol for 15 seconds, and then again in 100 % ethanol for 30 seconds. Slides were cleared twice in Histoclear for at least 5 minutes in each. To mount, excess Histoclear was carefully removed from the slides, and a small amount of DPX (Fisher Scientific UK) or Omni-mount (National Diagnostics) placed on the slide, before a coverslip was added to the top. Slides were left to dry and set for at least 30 minutes before imaging using a Leica ICC50 HD brightfield Microscope.

2.6.2. Masson's Trichrome Staining

Masson's Trichrome staining was used to visualise collagen in samples. Wax embedded sections were deparaffinisation with Histoclear for 5 minutes in a slide bath followed by rehydration in 100 % ethanol for two minutes 95 % ethanol, 70 % ethanol and finally distilled water for 1 minute each. Staining with Weigherts Iron Haematoxylin was carried out for 10 minutes followed by a rinse in running tap water for 10 minutes and finally a rinse in distilled water. Biebrich Scarlet-Acid Fuschin staining was performed for 10 minutes followed by a rinse in distilled water. The samples were then placed in phosphomolybdic/phosphotungstic acid for 15 minutes and rinsed in distilled water. Aniline blue staining was carried out for 7 minutes and then 1% acetic acid for 3 minutes. Finally, the sample was dehydrated in 70 %, 90 % and 100 % ethanol for 10-15 seconds each and placed in two washes of Histoclear for 3 minutes each. The samples were then mounted on coverslips using omnimount.

2.6.3. Periodic Acid Schiff (PAS) Staining

PAS staining was used to visualise glycogen in rat liver tissues slices. Wax sections were deparaffinised in Histoclear for 20 minutes and rehydrated through 100 %, 95 %, 70 % ethanol for 2 minutes in each before another 2 minutes in distilled water. The samples were laid in a staining

tray and stained with Alcian Blue for 10 minutes. Following this the samples were washed in tap water and soaked in 1 % Periodic Acid solution for 10 minutes. The samples were washed again in tap water and placed in Schiff reagent for 10 minutes. Washes were then carried out for 2 minutes in hot tap water and 10 minutes in cold tap water before staining with Haemalum Mayer for 30 seconds. Finally, the samples were rinsed in running tap water before being dehydrated through 70 %, 90 %, 95 % and 100 % ethanol for 1 minute in each followed by Histoclear for 5 minutes. Coverslips were placed onto slides using Omnimount and the results imaged using a brightfield microscope.

2.6.4. Immunofluorescent staining of paraffin embedded samples

Slides were first deparaffinised in Histoclear for at least 15 minutes, before rehydration for 5 minutes each in 100 % ethanol, 95 % ethanol, 70 % ethanol and dH_2O. Antigen retrieval was performed by incubation in citrate buffer at 95 °C for 20 minutes, and slides were cooled by the addition of dH_2O. Blocking buffer was prepared with 20 % normal goat serum (NGS, Sigma Aldrich) and 0.4 % Triton-X-100 in PBS. The slides were blocked for 1 hour at room temperature. Primary antibodies diluted in blocking buffer were added at the concentrations listed in Table 2.3 and incubated at 4 °C overnight.

Table 2.3: Primary antibodies used for immunofluorescent analysis. Antibodies were typically used at a dilution of 1 in 100 or 1 in 200. A negative control was performed alongside antibody staining to ensure the results were not mistaken with background fluorescence.

Antibody	Dilution	Supplier	Product Code
α Smooth Muscle Actin	1 in 200	Abcam	ab7817
β Catenin	1 in 200	BD Biosciences	610153
BCRP	1 in 100	Santa Cruz Biotechnology	sc-377176
BSEP	1 in 100	Santa Cruz Biotechnology	sc-74500
Cytokeratin 8	1 in 200	Abcam	ab59400
Claudin 1	1 in 100	Abcam	ab15098
Claudin 2	1 in 100	Abcam	ab53032
Cleaved Caspase 3	1 in 100	Cell Signaling Technology	9661S
Collagen 1	1 in 200	Abcam	ab34710
Collagen 3	1 in 200	Abcam	ab7778
Collagen 4	1 in 200	Abcam	ab6586
E-Cadherin	1 in 200	Abcam	ab1416
Fibronectin	1 in 200	Abcam	ab32419
HIF-1A	1 in 100	Abcam	ab51608
Ki67	1 in 200	Abcam	ab16667
MDR1	1 in 200	Santa Cruz Biotechnology	sc-13131
MDR3	1 in 100	Santa Cruz Biotechnology	sc-58221
MRP2	1 in 100	Santa Cruz Biotechnology	sc-71603
MRP3	1 in 50	Abcam	ab204322
N-Cadherin	1 in 200	Abcam	ab18203
NTCP	1 in 100	Santa Cruz Biotechnology	sc-518115
OATP-1A2	1 in 100	Santa Cruz Biotechnology	sc-365007
Villin	1 in 200	Abcam	ab130751
Vimentin	1 in 200	Santa Cruz Biotechnology	sc-6260

The next day, slides were washed 3 times in PBS before addition of appropriate fluorescently conjugated secondary antibodies and the nuclear stain Hoechst 33342 diluted in blocking buffer at the concentrations listed in Table 2.4. Slides were incubated at room temperature for one hour before washing 3 times in PBS with 0.1 % Tween 20. Slides were mounted in Vectashield™ (Vector Labs, Peterborough, UK) and a cover slip placed on top, which was sealed around the edges using nail varnish. Slides were stored at 4 °C in the dark until imaging. Negative controls were performed for each batch of staining using extra samples with a one-hour incubation in blocking buffer instead of the primary staining step.

Table 2.4: Secondary antibodies used for immunofluorescent analysis. Typically, Anti-mouse 488 and Anti-rabbit 594 were used for staining, unless co-staining with a fluorescent dye was performed. Hoescht-33342 was used to stain nuclei in all fluorescent stains unless a mountant containing DAPI was used.

Antibody	Dilution	Supplier	Product Code
Goat Anti-Mouse 488	1 in 1000	Invitrogen	A11001
Goat Anti-Mouse 594	1 in 1000	Invitrogen	A11005
Goat Anti-Rabbit 488	1 in 1000	Invitrogen	A11034
Goat Anti-Rabbit 594	1 in 1000	Invitrogen	A11012
Hoescht-33342	1 in 5000		

2.6.5. Immunofluorescent staining of OCT embedded samples

For OCT embedded, methanol-acetone fixed samples the slides were first rehydrated in dH_2O. The rest of the protocol was carried out as for wax sections except with the antigen retrieval step omitted.

2.6.6. Immunofluorescent staining of coverslips

For all coverslips the same protocol was used as for OCT embedded samples however all washes were carried out in a 12-well plate. For all staining steps the coverslips were placed with the cells facing down onto a 15 µL drop of antibody solution on parafilm.

2.6.7. Nile Red Staining

Slides were deparaffinised in Histoclear for at least 15 minutes before being rehydrated for 5 minutes each in 100 % ethanol, 95 % ethanol, 70 % ethanol and dH_2O. Samples were incubated at room temperature with 10 µg/mL nile red (Sigma Aldrich) in PBS along with a 1 in 5000 dilution of Hoechst 33342 for 15 minutes. Samples were then washed three times in PBS, coverslip was mounted using Vectashield mounting medium with nail varnish used to seal the edges of the coverslip.

2.6.8. Picrosirius red staining

Collagen deposition was investigated in wax sections using the picrosirius red stain. Slides were deparaffinised in Histoclear for 5 minutes before being rehydrated for 2 minutes in 100 % ethanol followed by 1 minutes each in 95 %, 70 % and distilled water. Nuclei were stained for 8 minutes in Weigert's haematoxylin followed by washing for 10 minutes in running tap water. Staining in picrosirius red was carried out for 1 hour followed by two washes in acidified water for 2 minutes each. Slides were dehydrated in three changes of 100 % ethanol for 30 seconds each followed by Histoclear for 5 minutes. Coverslips were mounted using Omnimount mounting medium.

2.6.9. Microscopy

Phase-contrast imaging for live cells was carried out using an EVOS™ XL Core phase contrast microscope (Fisher Scientific).

Histological staining and other brightfield analyses were imaged using a Leica DM500 (Leica Microsystems, Wetzlar, Germany) with an ICC50 HD camera module (Leica).

Immunostained samples were imaged using the ZEISS LSM 880 confocal microscope with Airyscan or ZEISS LSM 800 confocal microscope (Carl Zeiss AG, Oberkochen, Germany). Negative controls were performed for each experiment to determine background levels of fluorescence for each sample.

2.7. Functional Analysis

2.7.1. MTT cell viability assay

Alvetex® membranes were unclipped from inserts and transferred to 12 well plates before washing in sterile PBS. PBS was then aspirated, and 1 mL of Thiazolyl Blue Tetrazolium Bromide powder (MTT, Sigma Aldrich) dissolved in phenol free DMEM (Fisher Scientific) at a concentration of 1 mg/ml was added to each well. Cells were incubated at 37 °C and 5 % CO_2 for 60 minutes. MTT solution was then aspirated, and 1 mL of acidified isopropanol was added to each well to lyse cells. These were placed on a shaker set at 120 rpm for 20 minutes. Sample solution was then diluted appropriately in isopropanol and placed in a flat bottomed 96-well plate to a final volume of 200 µl. Absorbance of samples was read at 570 nm on a microplate spectrophotometer.

For drug toxicity samples where relative viability was used, the equation

$$\%\, Viability = \frac{Treated\ MTT\ value - Negative\ Control\ MTT\ value}{Positive\ Contro\ MTT\ Value - Negative\ Control\ MTT\ Value} \quad (2.4)$$

was used to calculate the relative viability for each sample.

2.7.2. Cell Counting

Medium was aspirated from samples which were then washed with PBS. 0.25 % Trypsin was then added to the wells and they were placed in the incubator for 10 minutes. A phase contrast microscope was used to ensure full detachment of cells. The cells were then washed out with the addition of a small volume of medium and moved to a 15 mL Falcon tube. 20 µl of cells was mixed with 20 µl of Trypan blue in an Eppendorf tube and this mixture was pipetted into a haemocytometer. A phase contrast microscope was used to count the unstained cells in one square. This count was repeated three times and the mean value was used to predict the number of cells present in the sample.

2.7.3. Terminal deoxynucleotidyl transferase dUTP nick end labeling (TUNEL) Assay

Apoptotic cell death was assessed in PFA fixed, wax embedded sections using the DeadEnd™ Fluorimetric TUNEL assay system (Promega) performed according to the manufacturer's instructions.

Slides were deparaffinised in Histoclear for 15 minutes and washed in 100 % ethanol for 5 minutes. Slides were then rehydrated through 100 %, 95 %, 80 %, 70 % and 50 % ethanol for 3 minutes each. Slides were washed in 0.85 % NaCl in dH_2O for 5 minutes followed by PBS for 5 minutes. Fixation

was performed with 4 % PFA in PBS for 15 minutes at room temperature then samples were washed twice in PBS for 5 minutes each. 100 µL of the 20 µg/ml Proteinase K solution was added to slides and incubated for 10 minutes at room temperature. Slides were washed in PBS and fixed again with 4 % PFA for 5 minutes. 100 µL of Equilibration Buffer was added to slides and incubated for 10 minutes. 50 µL of TdT reaction mix was then added and a plastic coverslip place on top to distribute evenly. Slides were incubated for one hour in the dark in a 37 °C, humidified incubator. Coverslips were removed and 2X SSC added to slides for 15 minutes. Finally, slides were washed three times for 5 minutes each in PBS before being mounted with VectaShield® HardSet™ mounting medium containing DAPI (Vector Labs). After the mountant had set the slides were visualised using a Zeiss 880 confocal microscope.

Treatment of positive controls was carried out as an extra process prior to addition of the Equilibration Buffer. 100 µL of DNase I buffer was added to samples and incubated at room temperature for 5 minutes. 100 µL of DNase I buffer containing 5.5-10 units/ml of DNase I and slides were incubated for 10 minutes at room temperature. Excess liquid was removed, and the slides washed four times in dH_2O. The positive controls then had the equilibration buffer added and the rest of the protocol carried out as described previously.

2.7.4. Albumin Assay for human models

Albumin secretion was measured using the AssayMax™ Human Albumin Enzyme-Linked Immunosorbent Assay (ELISA) Kit (AssayPro, St Charles, MO, USA). 50 µl of sample media, diluted 1 in 20 in PBS, or standard was added to wells in the provided plate and tapped gently to cover the entire lower surface. Wells were covered with an adhesive plate cover and incubated for 1 hour at room temperature. Wells were washed thoroughly with 5 washes using 200 µL of wash buffer. 50 µl of Biotinylated antibody was added to each well followed by a 30-minute incubation at room temperature. The microplate was washed again 5 times with 200 µL of washer buffer and 50 µl of SP conjugate was added to each well before resealing and incubating for a further 30 minutes. The wells were washed again with wash buffer as previously and 50 µl of Chromogen substrate added to each well. The plate was incubated for 30 minutes before adding 50 µl of stop solution to each well. The plate was tapped gently to mix the contents and then the absorbance at 450 nm read immediately using a BioTek ELx400 plate reader.

2.7.5. Urea Assay

Urea secretion was quantified using the QuantiChrom™ Urea assay kit (BioAssay Systems, Haywood, California, USA) according to the manufacturer's instructions for cell culture media with low urea levels. Briefly, 5 µL of sample was placed in the wells of a flat bottomed 96-well plate. The working reagent was made up from a 1:1 mix of reagent a and reagent B and 200 µL of this was added per well. Samples were incubated at room temperature for 40 minutes and the absorbance at 430 nm was then read using a BioTek ELx400 plate reader. The resulting values were normalised to the total protein in the samples as measured with the Bradford Assay.

2.7.6. Lactate Dehydrogenase (LDH) Assay

An alternative measure of cell viability used was the release of lactate dehydrogenase into the cell culture media. The LDH activity was measured using the CyQuant™ LDH cytotoxicity assay (Invitrogen) following the manufacturer's instructions. Briefly, 50 µL of sample was added to the wells of a flat bottomed 96-well plate. 50 µL of reaction mixture was then added and the plates were incubated in the dark at room temperature for 30 minutes. 50 µL of stop solution was then added to each well and the absorbance values were read at 490 nm and 680 nm. For the data analysis the absorbance at 680 nm was taken from the value at 490 nm to remove background.

Media from untreated samples was used as the spontaneous LDH activity and for the maximum LDH activity three untreated samples were placed in a 12-well plate with 1ml of growth media containing 10X lysis buffer diluted to a 1X final concentration. These were incubated for 1 hour and the resulting media was mixed with the initial media to achieve the correct dilutions and maximum LDH media samples were taken from this.

To calculate the percentage cytotoxicity, the equation

$$\%\ Cytotoxicity = \frac{Treated\ LDH\ activity - Spontaneous\ LDH\ activity}{Maximum\ LDH\ Activity - Spontaneous\ LDH\ Activity} \quad (2.5)$$

was used.

2.7.7. Bradford assay for total protein content

The total protein in the samples was measured using a Bradford assay. Sample protein lysate was produced as described in Section 2.4.5, then 5 µL of lysate was placed in a well of a flat-bottomed 96-well plate with 250 µl of Bradford reagent (Bio-Rad, Oxford, UK) and incubated at room

temperature for 20 minutes. The absorbance at 570 nm was then measured using a BioTek ELx400 plate reader and values were quantified using a standard curve produced from serial dilutions of bovine serum albumin (Sigma Aldrich).

2.7.8. Polymerase Chain Reaction (PCR) Analysis

PCR was carried out using the SYBR Green reporter system. KicqStart primers (Thermo Fisher) were used with sequences as listed in Table 2.5. Primers were reconstituted to a concentration of 100 mM using RNase-free Tris-EDTA Buffer (Sigma Aldrich). A stock solution of each gene was made as shown in Table 2.6. These were diluted 1 in 4 in RNase-free dH_2O to make a working concentration for the PCR reaction.

Table 2.5: Primer sequences used for qPCR analysis. All the primers used were KicqStart primers produced by Sigma Aldrich. The product codes for each primer are given along with the forward and reverse sequences.

Gene	Forward Sequence	Reverse sequence	Product Code
CYP1A1	CATTAACATCGTCTTGGACC	TCTTGGATCTTTCTCTGTACC	H_CYP1C1_1
CYP1A2	CACTATCAGGACTTTGACAAG	AGGTTGACAATCTTCTCCTG	H_CYP1A2_1
CYP2A6	TAGAGGGAAGAGAAGAAACAG	TTTGCTCAGGAAATAAGAGC	H_CYP2A6_1
CYP2B6	AGGTTCCGAGAGAAATATGG	TTTCCATTGGCAAAGATCAC	H_CYP2B6_1
CYP2C19	CATGGATATGAAGTGGTGAAG	TCCATTGCTGAAAACGATTC	H_CYP2C19_1
CYP2C8	CCAAATATCTTTGACCCTGG	AAATTCGTTTTCCTGCTGAG	H_CYP2C8_1
CYP2C9	ATCTCTCAAAGGTCTATGGC	CAAATCCTCTGTTAGCTCTTTC	H_CYP2C9_1
CYP2D6	CCTATGAGCTTTGTGCTG	TTTGGAACTACCACATTGC	H_CYP2D6_1
CYP2E1	GACACCATTTTCAGAGGATAC	TTCATTCAGGAAGTGTTCTG	H_CYP2E1_1
CYP3A4	AGTCTTTCCATTCCTCATCC	TGCTTTTGTGTATCTTCGAG	H_CYP3A4_1
NAT1	TAAGAAAGGGGATCATGGAC	GGATGTTAAGGTTCTCAAAGG	H_NAT1_1
NAT2	CAAAGGGATCATGGACATTG	GATCAAAAATAGCCTCTAAGCC	H_NAT2_1
ABCC2	AAATTGCTGATCTCCTTTGC	GATAGCTGTCCGTACTTTTAC	H_ABCC2_1
ABCB1	AGTGAAAAGGTTGTCCAAG	AGTCTGCATTCTGGATGG	H_ABCB1_1
ABCB4	GAGGTCAAAAACAGAGGATTG	CCTTTTCACTTTCAGTATCCAG	H_ABCB4_1
SLCO1A2	CATGCTCACACAAATAGAGAG	TTTCCAATCTCAAAGCTTCC	H_SLCO1A2_1
ABCB11	CAGATTACAAATGAAGCCCTC	TCCATATCTGTAGGAAGCAG	H_ABCB11_1
ABCC3	TTTTCTGGTGGTTCACAAAG	GGATCTGTCCTCTTCCTTTAG	H_ABCC3_1
ABCG2	AAAGCCACAGAGATCATAGAG	GATCTTCTTCTTCTTCTCACC	H_ABCG2_1
ARG1	ACTAGGAAGAAAGAAAAGGC	TCTTCTGTGATGTAGAGACC	H_ARG1_1
GSTA1	AGGTATAGCAGATTTGGGTG	AAGACTTTTTCAAAGGCAGG	H_GSTA1_1
GAPDH	TCGGAGTCAACGGATTTG	CAACAATATCCACTTTACCAGAG	H_GAPDH_1
OTC	AAATGATCCATTGGAAGCAG	AGCAGTGTAAAAATGTCCAG	H_OTC_1
SULT1A1	CTTCTATGAAGACATGAAGGAG	TGTAGTTGGTCATAGGGTTC	H_SULT1A1_1
UGT2B7	ACGTATGGCTTATTCGAAAC	CATGTTACTGACCATTGACC	H_UGT2B7_1
UGT1A6	TCACCTTATATCAGAAGGTCTC	TTCCTGAGACAAGTCTTTCC	H_UGT1A6_1
UGT1A1	GTGACTTTGTGAAGGATTACC	TCCTGGGATAGTGGATTTTG	H_UGT1A1_1
UGT1A3	TGCTTTTTCTGCTCCTTATG	CAAATTCCTGAGATAGTGGC	H_UGT1A3_1

Table 2.6: Primer mixture to create the working solutions. Both the forward and reverse primers were added together along with RNase-free dH_2O to a final volume of 100 µL. This was stored at -80 °C when not in use.

Component	Volume per sample (µl)
Forward Primer	10
Reverse Primer	10
RNase Free dH_2O	80

cDNA samples were diluted to a concentration of 1.25 µg/ml in RNase-free dH_2O. A 10 µL PCR reaction was set up using the SsoAdvanced™ Universal SYBR Green Supermix (Bio-Rad). A master mix for each primer as first made up with 5 µL of 2X SYBR dye and 1 µL of gene working solution for each sample. 6 µL of primer master mix was added to each well of a low-profile hard-shell skirted 96-well PCR plate (Bio-Rad) along with 4 µL of sample cDNA. Plates were then sealed with an adhesive plate seal (Bio-Rad) and centrifuged at 1000 rpm for 3 minutes to ensure the reaction components were at the bottom of the wells. Plates were stored at 4 °C prior to running in the qPCR machine. A fast 2-step reaction was run using a Bio-Rad CFX Connect qPCR machine (Bio-Rad) with the settings as shown in Table 2.7.

Table 2.7: Settings used for the qPCR cycles. For all PCR analysis a 10 µL sample size was used. All the primers were run using a 55 °C annealing temperature and 40 cycles were performed. A melt curve analysis after the amplification ensured no co-amplification of off-target DNA had taken place.

Step	Details	Settings
1	Initial Denaturation	95 °C for 2 minutes
2	Denaturation	95 °C for 15 seconds
3	Annealing, extension and fluorescence read	55 °C for 15 seconds. 40 cycles of step 2 and 3.
4	Melt Curve analysis	Up to 95°C

For normalisation of all PCR data, GAPDH was used as the housekeeping gene due to its relative stability in hepatocytes between 2D and 3D culture, compared with the large fluctuations seen in genes such as β-actin (Fox *et al.*, 2010).

2.8. Statistics

Statistical analysis was performed using GraphPad Prism version 5.01 for Windows (GraphPad Software, San Diego, California, USA). A two-way analysis of variance (ANOVA) was used for calculating significance of grouped data with a Bonferroni post-test to give significance within groups. The significance is depicted graphically on data sets with n.s = $p > 0.05$, * = $p \leq 0.05$, ** = $p \leq 0.01$, *** = $p \leq 0.001$.

Chapter 3: Development of a 3D bioreactor cell culture system

3.1. Introduction

The liver is a highly complex organ with a vast number of processes and pathways contributing to its homeostasis. As mentioned in Chapter 1 there have been many methods used to try and recapitulate the liver microenvironment *in* vitro with varying levels of success. Most techniques used at present add extra properties such as a 3D microenvironment, multiple cell types or flow of fluid over the cells however few studies look at combining all these techniques to push the boundaries of the physiological relevance of *in vitro* models. In this chapter the development of a cell culture system which allows for more complex, physiologically relevant culture to be performed is presented.

3.1.1. The dynamic liver microenvironment

One major aspect of the complexity of the liver microenvironment is the large amount of fluid flow from a variety of sources as shown in Figure 3.1. The blood flow in the liver is the greatest in any organ with the liver receiving 25% of the cardiac output whilst constituting 2.5% of the total body weight. Blood enters the liver from two sources as shown towards the left of Figure 3.1: 25% of the supply is arterial blood through the hepatic artery which provides oxygenation and the remaining 75% is venous blood from the gastrointestinal tract which contains nutrients and toxins acquired through digestion (R. Burt, A. Portmann, Ferrell, 2017).

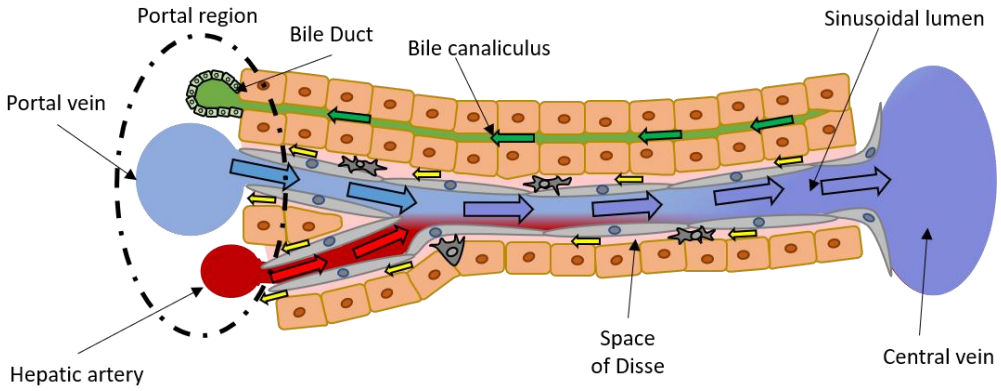

Figure 3.1: Different sources of fluid flow in the liver. At the portal region, blood flows into the liver from both the portal vein (blue arrows) and hepatic artery (red arrows) and leaves the liver through the central vein. Bile flows counter-current to this (green arrows), running through the bile canaliculi and leaving the liver at the bile ducts, located in the portal region. The combination of the bile duct, portal vein and hepatic artery in the portal region is collectively known as the portal triad. Lymph (yellow arrows) is formed by filtration of blood components through the fenestrated sinusoidal endothelial cells and flows towards the portal region through the space of Disse.

Bile is another fluid present in the liver which contributes to the highly dynamic environment experienced by cells, with approximately 750 mL produced per day in the average adult (Boyer, 2013). Bile is transported through the bile canaliculi, channels formed on the apical region between adjacent hepatocytes and isolated from the blood flow by tight junctions (Arias *et al.*, 1993). The bile is excreted into the bile canaliculi by the hepatocytes and is transported in the opposite direction to the flow of blood, entering the bile ducts located in the portal region where it is transported away from the liver.

A third contributor to the movement of nutrients and waste in the liver is lymph. In the liver lymph is thought to accumulate in the space of Disse between the sinusoidal endothelial cells and the hepatocytes from plasma components which are filtered through the fenestrae of the sinusoidal LSECs. From here it can generally flows towards the portal tract and out of the liver through lymphatic vessels however it can also leave through the interstitium around the central vein (Tanaka and Iwakiri, 2016). The liver is a major source of lymph with roughly 25% of the thoracic duct supply originating from the liver (Chung and Iwakiri, 2013).

With this highly dynamic environment it is hypothesised that introduction of fluid flow to bring culture conditions closer to those *in vivo* should have a profound effect on the structure and function of the resulting tissues formed. These more physiologically relevant cultures could be used to bridge the gap between *in vitro* testing and clinical trials, therefore reducing the need for animal testing, a practice which is deemed unethical and modern techniques aim to move away from.

3.1.2 Translating *in vivo* fluid flow to the *in vitro* environment

The presence of fluid motion in tissues and cell culture has several key effects on the microenvironment of the cells as illustrated by Figure 3.2. The most prominent effects are the turnover of nutrients and removal of waste products, the mechanical shear stress at the cell surface and the enhanced mixing and consequent reduction in unstirred layer thickness.

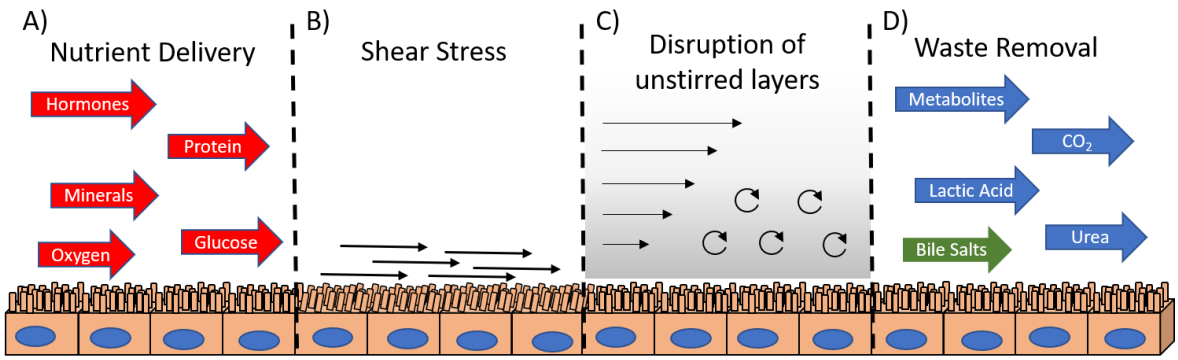

Figure 3.2: The range of functions that fluid flow can carry out in cells or tissues. A) Nutrients and signalling molecules such as hormones are delivered to the cells through the bloodstream. B) Shear stress provides a mechanical stimulus to cells which can induce specific functionality or polarisation. C) Flow disrupts unstirred layers which build up close to the cell surface, increasing turnover of nutrients and waste products in this region through a reduction in the diffusion distance of the unstirred layer. D) Waste products and metabolites from the cells are removed, preventing a build-up of toxic molecules, and maintaining osmotic balance. In hepatocytes, products such as bile salts are also secreted.

Fluid motion facilitates the transport of nutrients and waste products both to and from the tissue. Blood provides the cells with a continuous supply of oxygen and other nutrients such as proteins and mineral ions. It also removes metabolic waste products to prevent a potentially toxic build up at the cell surface (Malda *et al.*, 2008; Lovett *et al.*, 2009). Transport of bile away from the cells also prevents it from accumulating close to the cells as happens in static cell culture with potentially detrimental effects on the cells and provides another excretory pathway for metabolites such as bilirubin (Memon *et al.*, 2016).

The shear stress experienced by cells in contact with these fluids has been shown to have a great effect on their metabolism and differentiation state. Endothelial cells are the typically the cells in a tissue which are the most exposed to shear stress, particularly arterial endothelial cells due to the high pressure of arterial blood with a shear stress on average of around 15 dynes/cm^2 (Ballermann *et al.*, 1998). Sinusoidal endothelial cells have been estimated to receive shear stress of around 0.05 - 0.1 dynes/cm^2 which is a low level compared with most vasculature (Lalor and Adams, 1999). The endothelial cells shield the other cells in the tissue such as the hepatocytes from the majority of the effects of the shear stress however they still experience lower levels of shear stress from fluid movement in the space of Disse and from the bile flow. Due to this it is difficult to acquire accurate measurements for the levels of shear stress experienced by hepatocytes (LeCluyse *et al.*, 2012) however they have been found to have upregulated metabolic functions such as albumin

production (Tanaka *et al.*, 2006), urea secretion (Ortega-Ribera *et al.*, 2018) and CYP enzyme levels (Rashidi *et al.*, 2016) when exposed to microdyne/cm^2 levels of shear stress. Levels close to and above one dyne/cm^2 on the other hand have shown negative impacts on the viability of hepatocytes (Tilles *et al.*, 2001).

One of the lesser studied properties of biological fluids is the formation of unstirred layers. This is a phenomenon which is present *in vivo* however is considerably increased in static cell culture. In static culture unstirred layers build up close to the cell surface which can be up to several hundred microns in thickness depending on the diffusivity of the compound. These unstirred layers limit diffusion of molecules which has several knock-on effects. The first problem is the potential for waste build up due to inadequate diffusion away from the cells as well as lack of nutrients from inadequate diffusion towards the cells (Tramper, 1995; McMurtrey, 2014). The second problem this poses is the inaccuracy it can add to experiments such as those looking at the effects of drugs on hepatocytes. The limited diffusion can mean that the effective dose received by the cells is markedly different from the dose added to the sample, leading to inaccurate results which are incomparable to *in vivo* experiments (Barry and Diamond, 1984; Verkman and Dix, 1984; Spivak *et al.*, 2006). Outside of the liver, studies looking at transport across intestinal epithelia *in vitro* have found that the presence of unstirred layers can significantly reduce the apparent permeability of molecules (Korjamo, Heikkinen and Monkkonen, 2009).

With the combined impacts of these effects of fluid flow the requirement for addition of media flow to accurately recapitulate the dynamic *in vitro* microenvironment becomes apparent to create organotypic cultures which have a high predictive capacity for *in vivo* processes.

3.1.3. Recapitulating the dynamic environment of the liver *in vitro*

Mimicking the dynamic environment of the liver *in vitro* is an important task if cell cultures are to be created which accurately represent the physiological microenvironment. *A* variety of different methods have been developed to overcome the lack of fluid flow *in vitro*. Figure 3.3 shows a selection of commonly used methods for introducing fluid flow into cell culture. These typically involve a trade-off between complexity and control versus size and throughput with more complex systems such as pumped bioreactors and microfluidics requiring external equipment such as pumps and media reservoirs, increasing their physical size and complexity (Kaarj and Yoon, 2019). To create effective fluid flow in a higher throughput and more flexible way large pieces of equipment such as

these need to be removed or simplified so many experiments can be run in parallel on a physiologically relevant multicellular scale.

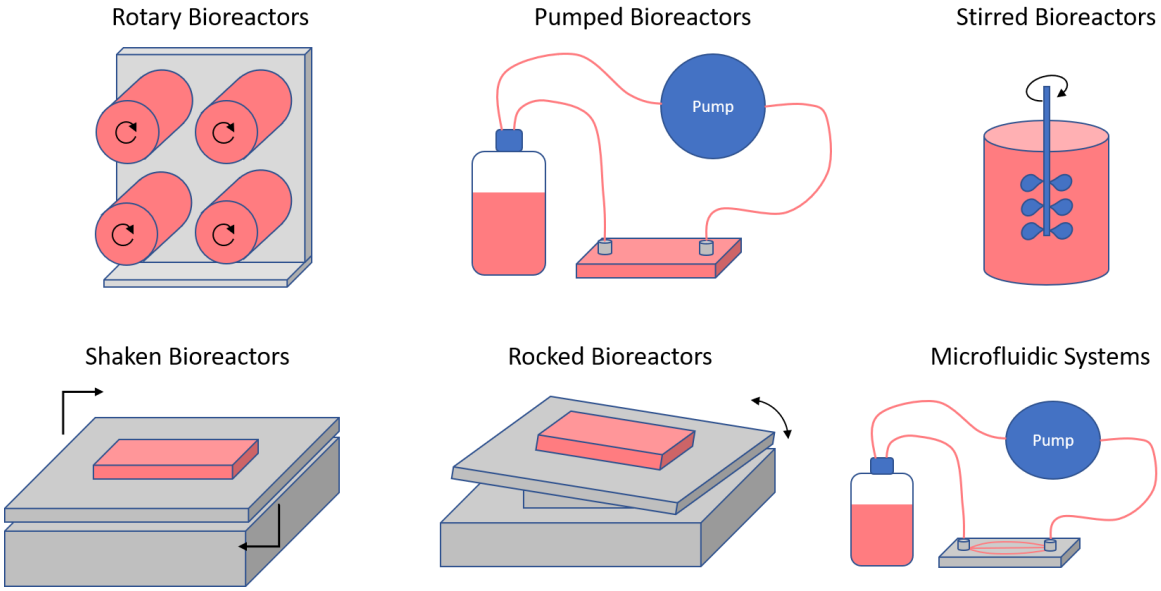

Figure 3.3: Commonly used technologies for introducing fluid flow to cell cultures. Designs shown are simple methods for creating a bioreactor of each however variations exist for each design. Far more complex systems have also been developed which utilise a wide range of additional methods as well as through combinations of several of these technologies. These methods are generally driven by electrical power which is not shown. Techniques such as shaken and rocked bioreactors typically use equipment which is commonly found in a laboratory and basic cell culture ware whereas rotary, stirred and pumped bioreactors typically require additional equipment such as bespoke culture vessels.

Categorising the different bioreactors by their method of introducing fluid flow is a simple way to split them into groups of similar scales and with similar properties. The major methods used are rotary bioreactors, pump-based systems, stirrer-based systems, and shaken/rocked systems. Microfluidic systems can also be separated into a category of their own as these can utilise a variety of methods to generate fluid flow but operate on a much smaller scale to most other bioreactor systems and trade off the ability to form large, complex organoids in favour of more flexible systems with greater scalability (Coluccio *et al.*, 2019). Some of the advantages and disadvantages often associated with these different systems are shown in Table 3.1. These lead to the choice of fluid flow method being driven largely by the desired properties of the tissue cultures, though minimising complexity is also often a key aim. This list of advantages and disadvantages is not exhaustive, and methods can be utilised to overcome some disadvantages. To fully recreate the conditions *in vivo,*

these bioreactors need to be coupled with other technologies such as 3D cell culture to aid in the formation of physiologically relevant tissue structures.

Table 3.1: Advantages and disadvantages of different bioreactor systems. Due to the wide variation in the levels of complexity and control over cultures between different bioreactor systems, the choice is typically specific for the desired properties of the culture. Whilst methods such as shaken and rocked bioreactors offer a simple platform for introducing fluid flow, using equipment which is readily available in most laboratories, these are less tuneable compared to more complex methods such as pump-based systems.

Bioreactor Type	Advantages	Disadvantages	Examples
Rotary	• Simple • Effective for 3D culture using spheroids • Further technology such as media pumps can be easily incorporated	• Limited control over patterning • Systems tend to be small with limited scalability	• Synthecon Rotary Cell Culture System • Zhang et al. (2013) • Costantini et al. (2019)
Pumped	• Allows significant control over fluid flow properties • Complex, interconnected systems can be created • Compatible with many 3D culture techniques	• Can become overly complex when scaled up • Spatial requirements can be large	• 3D Biotek Perfusion Bioreactor System • Mueller et al. (2013) • Tan et al. (2013) • Hosoya et al. (2014)
Stirred	• Simple • Effective for 3D culture using spheroids • Minimal spatial requirements	• Limited compatibility with some 3D technologies	• ABLE Bioreactor Magnetic Stir System • Tostões et al. (2012) • Khodabakhshaghdam et al. (2021)
Shaken	• Simple • Allows effective convective mixing over monolayers or 3D scaffolds	• Minimal control over fluid flow • Only capable of producing flow across a surface	• Adam et al. (2018) • Gilglioni et al. (2018)
Rocked	• Simple • Allows effective convective mixing over monolayers or 3D scaffolds • Can be used to allow direct contact of cells with air	• Minimal control over fluid flow • Only capable of producing flow across a surface	• Cytiva WAVE™ Bioreactor System • Brophy et al. (2009)
Microfluidic	• Allows significant control over fluid flow properties • Complex, interconnected systems can be created • 3D technologies can be readily incorporated • Small medium volumes ideal for testing compounds which are expensive or have limited availability	• Can become overly complex when scaled up • Spatial requirements can be large • Reduced levels of cell-cell contact compared with larger methods	• Baudoin et al. (2011) • Bhushan et al. (2013) • Tan et al. (2019)

3.1.3.1. Rotary bioreactors

Rotary bioreactors are one of the simplest methods for creating fluid motion in cell culture. These utilise a rotating cylinder containing cell culture medium which keeps the medium mixed and supports the cells in suspension to form aggregates. These allow the generation of cell constructs both with and without scaffolds which can incorporate multiple cell types to create complex, dynamic spheroids. In the context of hepatocyte models, for the cell line HepG2 it was found that growth in a rotating wall bioreactor promoted an increase in albumin production and CYP enzyme levels compared with 2D monolayers (Chang and Hughes-Fulford, 2009) whilst primary hepatocytes have been shown to have maintained long-term albumin expression and form liver tissue-like structures in the simulated microgravity of rotary bioreactors (Khaoustov *et al.*, 1999). Figure 3.4 shows several of the rotary bioreactors produced by Synthecon which allow the culture of cell aggregates in a moving fluid through simulated microgravity (Ingram *et al.*, 1997). Whilst simple systems incorporate fluid flow through the rotary motion (Figure 3.4A, B) others can include further fluid control using pumps and external media reservoirs (Figure 3.4C) to allow greater control over media turnover.

Figure 3.4: Commercially available rotary bioreactors for mammalian cell culture. Such rotary bioreactors maintain the cells in suspension within the medium, facilitating the formation of aggregates. Three bioreactors produced by Synthecon based on the rotary wall bioreactor design originally developed by NASA are shown here. Each unit consists of the bioreactor unit, single use or autoclavable culture vessels and a power supply unit. A) RCCS-4D with disposable culture vessels allowing the culture of 4 samples simultaneously. B) RCCS-D with disposable culture vessel for the culture of a single sample. C) RCCMAX with peristaltic pump, media bottle, media oxygenator, autoclavable culture vessel and power supply for the culture of a single sample in a highly controlled environment.

An advantage of these systems is the typically modular design with removable vessels which can be disposable or autoclavable for multiple uses (Kaiser *et al.*, 2014). These designs are also easily scalable, with vessels from the millilitre to the litre scales available, and with the bioreactor being entirely self-contained this allows for low-cost fluid flow cultures to be created. ECM scaffolds (Li

et al., 2019) and microcarriers (Mitteregger *et al.*, 1999; Lei *et al.*, 2011) have been used to provide limited control over tissue structures however the microtissues formed have far less similarity to *in vivo* tissue than current static tissue culture systems (Ghorbel *et al.*, 2019; Roger *et al.*, 2019). This is in part due to the very limited control over the spatial distribution of cells within these systems, limiting the potential applications for complex hepatic co-cultures with physiologically relevant patterning.

For growth of hepatocytes these have been found to have several potential applications. One study found that the growth of liver stem cells seeded onto a polysulphone membrane in a rotary bioreactor showed enhanced differentiation into mature hepatocytes. These secreted high levels of albumin and urea as well as possessing enhanced CYP function (Fonsato *et al.*, 2009). Other studies have also shown the ability to derive hepatocytes from other stem cell sources using rotary bioreactors (Wang *et al.*, 2012; S. Zhang *et al.*, 2013).

The ability to create highly polarised hepatocyte cultures using immortal cell lines has also been shown, with improvements to metabolic function and increased CYP expression (Sainz, Tencate and Uprichard, 2009; Sarika *et al.*, 2016; Costantini *et al.*, 2019). Despite these achievements very little work has been carried out with more complex hepatocyte cultures, such as co-cultures with non-parenchymal cells. This could be due to the simplicity of the system and limited control over cellular patterning making effective co-cultures difficult to produce, though examples can be found from other tissues (McConkey *et al.*, 2016; Weiss *et al.*, 2017).

3.1.3.2. Pump-based systems

Another simple method to achieve a fluid flow in cell culture is to use pumps to move fresh media into the cell culture and remove the old media from the other side (Domansky *et al.*, 2010). This allows the media to be kept nutrient-rich as well as creating a fluid flow across the culture, mimicking *in vivo* conditions (Freyria *et al.*, 2004). This is one of the most heavily studied fluid flow methods due to its relatively low cost and ease of use and pumped systems have been developed in a variety of forms and sizes, a few examples of which are shown in Figure 3.5. Systems can incorporate the use of 3D scaffolds to support the cells (Figure 3.5A, B) however others use the pumps to control fluid through specially designed slides or plates (Figure 3.5C).

Figure 3.5: Pump-based fluid flow culture systems. These systems utilise external pumps to drive the perfusion, not shown in A and B. Pump-based systems allow for significant control over the properties of the fluid flow, including the direction and flow rate. Other optional components of these systems include fresh and waste media bottles, oxygenators and heated water jackets for systems not contained within an incubator. A) Reinnervate perfusion plate holding 12-well Alvetex inserts. Pumps are connected by pipes to the luer lock connectors on the right of the image. B) Ebers seeding circuit and rack for P3D chambers. Single use P3D containers are connected to the perfusion circuit with luer lock connectors. C) Ibidi Pump System Quad with a computer-controlled pump.

The pump-based bioreactors have several benefits when compared with other types of bioreactor. The medium flow generated by the pumps provides a constant flow of nutrients at controlled and consistent levels leading to highly reproducible tissue formation and increased viability over longer culture times (Freyberg and Friedl, 1998; Yeatts and Fisher, 2011). Whilst some systems circulate the same medium instead of a constant supply of fresh medium, the larger volumes typically available for these systems mean that the consistency does not vary much during a culture (Martin and Vermette, 2005).

These systems also have a major advantage in their scalability. Whilst some studies have simply used one pumped circuit to provide medium to a tissue, others have connected numerous wells together, both in series and parallel, to allow for larger scale experiments (Domansky *et al.*, 2010; Balakrishnan *et al.*, 2015). This also has uses for studying paracrine signalling, as different cell types can be placed in successive wells, causing paracrine factors released by the first cell type to be carried in the medium through to the next, which allows for studies into cell-cell signalling (Lichtenberg *et al.*, 2005). Peristaltic pumps with multiple channels are also available which can drive numerous independent fluidic systems simultaneously allowing for an increase in throughput without a linear increase in physical size.

Pumped perfusion systems have long been known to be beneficial for 2D culture of hepatocyte monolayers (Gebhardt and Mecke, 1979; Dich and Grunnet, 1992). They are also commonly used for 3D liver models, likely due to their ease of incorporation with other culture methods. One of the

earlier uses incorporated pumped perfusion in hollow-fibre bioreactors to create bioartificial liver devices to support liver function (Nyberg *et al.*, 1993; Rozga *et al.*, 1993). Further development of these devices demonstrated their potential for use in drug toxicity studies with enhanced transporter localisation and improved drug clearance with primary hepatocytes (Jauregui *et al.*, 1994; Zeilinger *et al.*, 2011). Similar results have since also been reported for cell lines such as HepaRG (Darnell *et al.*, 2011) and HepG2/C3A (Storm *et al.*, 2016).

One issue with pump-based systems is that they take up quite a large amount of space due to the need for pumps, media reservoirs and other equipment. Whilst some aspects of these can be scaled, such as the pumps as mentioned previously, others such as media reservoirs typically need to be unique to one sample. Another issue with these systems is that the shape of the wells can create areas in which the medium pools and is less affected by the fluid flow. These create sections of the tissue which are still under conditions that do not vary much from static conditions, leading to only partial perfusion over a whole tissue and therefore greater variability in results (Zhang *et al.*, 2011). Careful design can usually work around this problem and for some applications this heterogeneity can be beneficial for creating localised areas with lower shear stress (Vogel *et al.*, 2007; Xia *et al.*, 2009).

3.1.3.3. Stirrer-based systems

Stirrer-based systems such as stirred tank bioreactors are another method which have been developed to attempt to overcome the issues of media heterogeneity and the build-up of metabolites. They consist of a main tank in which the culture medium and the cells are contained with a rotating stirrer to keep the media moving and mixed, with this having been shown to prolong the lifespan of cells in culture (Zandstra, Eaves and Piret, 1994; Collins, Miller and Papoutsakis, 1998). The large volumes typically associated with these bioreactors means that the medium content does not vary too much over the culture period whilst the stirring keeps the medium content homogeneous.

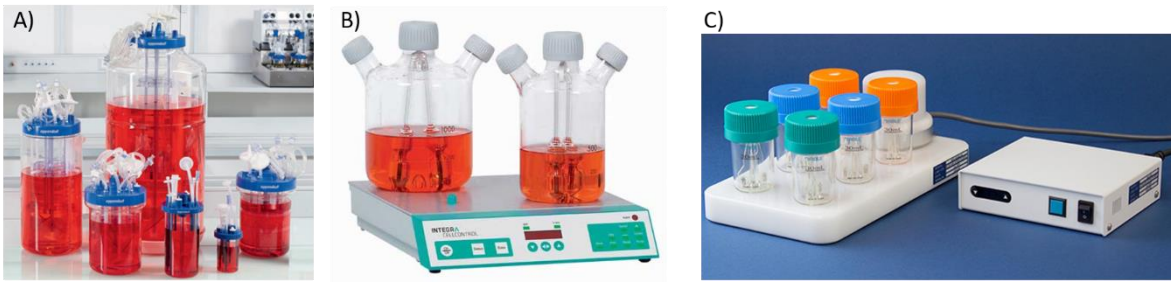

Figure 3.6: Magnetic stirrer-based bioreactors for mammalian cell culture. These systems use magnetic stirrers to maintain cells in suspension within the medium. Typically, a generic magnetic stirrer unit is used to provide motion however some units exist specifically for cell culture. The number of stir points varies, ranging from one to over 15. Flasks have an array of fittings for media turnover, addition of compounds and sampling. A) Eppendorf BioBlu single-use vessels ranging from 3 mL to 500 ml. B) Integra CELLSPIN magnetic stirrer unit with 1000 mL (left) and 500 mL (right) spinner flasks C) Reprocell ABLE Bioreactor Magnetic stir System with 30 mL disposable vessels.

The most common forms of these systems, as shown in Figure 3.6, are to maintain single cell or aggregate suspensions. These systems can be set up so that the stirrer simply keeps the media mixed or so that the cell culture is also perfused by the media flowing through it using permeable membranes. This bioreactor design can also be connected to pumps for further control over media turnover as found in the pumped systems mentioned previously.

The stir speed can be easily adjusted to alter the level of shear stress that the cells undergo which allows for targeted differentiation for cells which respond to different levels of shear stress such as in the differentiation of bone cells (García Cruz, Salmerón-Sánchez and Gómez-Ribelles, 2012). However this is also a limiting factor with some cells as the shear stress generated by a higher stir speed may cause a decrease in viability, and so lower speeds which mix the medium less effectively may have to be used (Liu, Li and Yang, 2014).

As with the rotary bioreactors these systems typically allow for low levels of control over the cell constructs created though some research has looked at coupling stirred tanks with hydrogels and scaffolds to support three-dimensional cell growth (García Cruz, Salmerón-Sánchez and Gómez-Ribelles, 2012; Liu, Li and Yang, 2014). Due to this limited literature has been carried out with hepatic cells in stirred bioreactors, though the formation of aggregates of primary hepatocytes with enhanced metabolic function, including maintained CYP expression, has been documented (Tostões *et al.*, 2012; Rebelo *et al.*, 2015). The limitations of these simple stirred tank designs means that the majority of their use in mammalian cell culture is focused on the expansion of stem cells (Zandstra, Eaves and Piret, 1994; Liu, Li and Yang, 2014).

3.1.3.4. Shaken or rocked systems

Another simple method to introduce media flow into cell culture is the use of a benchtop rocker or shaker. These require minimal apparatus to run and are inexpensive due to the use of standard laboratory and cell culture equipment whilst retaining a lot of flexibility over the culture conditions. Basic culture methods such as cells grown in the bottom of a multi-well plate are compatible with these systems as shown in Figure 3.7 and they can also be scaled up to containers such as flasks and can be used with many routine 3D cell culture techniques such as culture inserts. These also provide a high level of scalability as well as a small level of control over the fluid flow properties.

Figure 3.7: Rocked and shaken methods for introducing fluid flow. Rocked and shaken techniques incorporate convective mixing into culture systems by mechanically moving the medium over the cell cultures. Generic lab shakers and rockers are often used however some systems utilise custom cell-culture specific hardware. Shakers can accommodate vessels such as T-flasks, multi-well plates and cell culture bags. A) Stuart 3D Gyrating Rocker with two cell culture flasks and two multi-well plates. B) Athena Micro-Plate shaker with four 96-well plates. C) GE Life Sciences Wave 25 Rocking bioreactor system with peristaltic pump, gas mixer and 25 l Cellbag for use with suspension or microcarrier cell cultures.

These systems have been used to push mesenchymal stem cells from a variety of sources towards osteogenesis with potential applications in bone tissue engineering (Delaine-Smith, MacNeil and Reilly, 2012). In general, rocked and shaken systems are infrequently used for liver research, though there are some examples of successful applications. The use of rockers has been applied to precision-cut liver slices by rocking the media over the slices using specially design plates. These allow the slice to be alternately exposed to the air and the media, therefore increasing the oxygen uptake of the tissue to maintain viability over prolonged periods (Paish *et al.*, 2019b). Aggregate cultures of primary hepatocytes have also been successfully culture in rocked systems with increases reported in metabolic function and expression of phase I and II drug metabolism enzymes (Brophy *et al.*, 2009).

There are also potential applications for co-culture experiments where media can be washed between wells of a plate or separate microfluidic chambers each containing different cell types to represent different organs connected via the circulatory system (Sung, Kam and Shuler, 2010; Oleaga *et al.*, 2016). One of the main limitations with this method is the lack of control over the direction of the fluid flow which is usually tangential across the surface of the culture and limited to follow either a rotary or reciprocating motion. When culturing aggregates these systems also have limited control over the size of the aggregates, leading to limited reproducibility as well as undesirable effects such as necrosis caused by oversized aggregates.

3.1.3.5. Microfluidic 'organ on a chip' bioreactors

Recently, a large amount of research has been carried out into the use of microfluidic devices to generate high throughput perfused cultures (Baudoin *et al.*, 2012). These are very small scale systems in which complex flow patterns can be created by techniques such as soft lithography for studying vasculature on a small, more manageable scale (Baudoin *et al.*, 2007). Microfluidic systems utilise very small culture areas, typically created from plastics such as PDMS, to allow complex cultures utilising factors such as fluid flow to be created whilst retaining high scalability and minimal media use. A few examples of commercially available microfluidic chips with varying complexities are shown in Figure 3.8.

Figure 3.8: Microfluidic and 'organ on a chip' devices. Such systems provide a platform for studies on a much smaller scale, therefore maximising throughput. There is a large range of different commercially available microfluidic chip designs. These are typically designed for specific functions or cell types and can range from simple single chamber chips to having multiple chambers in series or parallel with other additions such as sampling ports. A) BEOnChip BE-Transflow microfluidic chip with a porous membrane at the bottom of the chambers for 3D microfluidic culture. B) Cellix Vena8™ Biochip for flow assays or microscopy. C) ChipShop Fluidic 221 Rhombic chamber chip with 100 µL reaction chamber.

These systems have been used to investigate the effects of compounds on cells due to their ability to screen multiple compounds simultaneously. The culture of cells from several different organs in interconnected compartments in larger, multi-chip experiments has also been widely studied as these platforms are a very simple method to research processes which take place across many organs *in vivo* (Zhao *et al.*, 2019).

Microfluidic systems have been heavily studied for use with hepatocytes. One major advantage of these systems is the typically small media volumes involved, which can be beneficial when working with expensive novel drug candidates. Many simple microfluidic devices used for hepatocytes grow the cells in a 2D environment or with collagen sandwich cultures. These methods can enhance key hepatic functions whilst maintaining high viability and makes them a useful tool for disease modelling and drug toxicity investigations (Goral and Yuen, 2012; Haque, Gheibi, Gao, *et al.*, 2016; Tan *et al.*, 2019). More advanced systems incorporate 3D techniques such as using confined spheroids or 3D substrates. These have shown further enhancements of hepatic function above those induced by the more simple microfluidic systems with enhanced albumin and urea secretion alongside high expression of CYP enzymes (Toh *et al.*, 2009; Goral and Yuen, 2012; Choi *et al.*, 2020). Co-culture of different cell types is also possible in microfluidic systems. Work investigating the growth of hepatocytes with endothelial cells is often performed as these, coupled with the fluid flow of the system, can recapitulate the vasculature of the liver *in vivo* (Yajima *et al.*, 2018; Busche *et al.*, 2020).

One drawback with these systems which is often overlooked is that the footprint is typically still relatively large due to the need for pumps, media bottles and temperature control, so the initially small 'organ on a chip' designs such as those in Figure 3.7 can still take up a lot of valuable lab space. The small size of microfluidic devices also scales up other problems seen in cell culture such as media evaporation and edge effects leading to a requirement for more complex designs than are needed at the conventional cell culture scale to overcome this (Halldorsson *et al.*, 2015).

The different methods discussed can introduce fluid flow to cell culture, each with their own advantages and disadvantages. A key limitation for many is the lack of tight spatial control over the structures formed, therefore limiting the studies that can be performed. It is therefore important to link multiple technologies to create more physiologically relevant and experimentally valuable *in vitro* structures. While there has been progress made towards this goal current techniques still suffer from various drawbacks which have limited their preferential use over static cell culture techniques.

3.1.4. Supporting three-dimensional growth in bioreactors

Many of the techniques for introducing fluid flow that have been covered are limited by the level of control over the structures formed by the cells. To allow higher complexity and patterning of cultures under the influence of fluid flow, there is a requirement to introduce substrates which can contain the cells and push them towards desired conformations. In Chapter 1 a series of 3D techniques were discussed which can be used to create more physiologically relevant cultures and recent research has looked at incorporating these into bioreactors.

Aggregates are the simplest method of 3D growth which is used in bioreactors due to their inherent simplicity and the large quantity of literature behind aggregate cultures. These are routinely used in methods such as stirred tank and rotating wall bioreactors however more recently systems utilising suspension aggregates in rocked (Davis *et al.*, 2018) and pumped (Massai *et al.*, 2016) systems have been developed. These can suffer from a lack of control over the structural organisation, even when using gel based microcarriers, and there is a high risk of damage if using too high levels of fluid flow.

Hydrogels and scaffolds are technologies which allow for more complex control over the structure of the cultures as well as allowing for components such as ECM to be included in a spatially controlled manner (Eniwumide, Lee and Bader, 2009; Warren *et al.*, 2009). The use of scaffolds has been studied in great depth for the culture of both primary hepatocytes and hepatocyte cell lines with results showing an increase in the maintenance of viability and differentiation in the case of primary hepatocytes (Baze *et al.*, 2018; Bell *et al.*, 2018) and functional metabolism and polarity in the case of cell lines (Mueller *et al.*, 2014; Sreenivasa C Ramaiahgari *et al.*, 2014; Hurrell *et al.*, 2018). Permeable membranes such as these allow fluid to be passed over or through a culture whilst providing anchorage to minimise the risk of washing away the cells. These can be made from a wide range of materials to maximise compatibility with the cells or tissues of interest. Systems such as hollow fibre bioreactors have been further designed to allow 3D cell culture whilst protecting the cells from high levels of shear stress induced by fluid flow (Bartolo, 2015). The utilise semi-permeable capillaries which can support the growth on both the intra- and extra-luminal surfaces as well as surrounding matrices. This allows them to support a range of cell types and have potential applications for modelling a wide range of tissues (De Bartolo *et al.*, 2009; Wung *et al.*, 2014).

Another useful property of 3D cell culture is the ability to create co-cultures with a higher level of control over spatial patterning than is possible with conventional 2D cell culture. Co-culture of

hepatocytes with non-parenchymal cells has been shown to further improve the functional profile of the hepatocytes and leads to enhanced predictive capacity for models for cell types including stellate cells (Abu-Absi, Hansen and Hu, 2004; Thomas *et al.*, 2006), endothelial cells (Kang *et al.*, 2013; Yang *et al.*, 2017) and fibroblasts (Bhandari *et al.*, 2001; Novik *et al.*, 2017) as well as combinations with several of these (Kostadinova *et al.*, 2013; Ahmed *et al.*, 2017a). Experiments with co-cultures of primary hepatocytes and fibroblasts or stellate cells have shown that the beneficial effects of co-culture are due to cell-cell contact and cannot simply be replicated with methods such as conditioning media (Bhandari *et al.*, 2001; Krause *et al.*, 2009). Use of a scaffold which can allow greater possibilities for the creation of physiologically relevant co-cultures will provide the platform on which entire tissue structures can be created to recapitulate the *in vivo* microenvironment.

For the technology we are developing we will be utilising a specific synthetic scaffold in the form of Alvetex®. The inert, synthetic nature of this scaffold minimises potential impacts on the cells and eliminates the possibility of other endogenous substances being present, as can be the case with some naturally derived scaffolds (Spicer, 2020).

3.1.4.1. Alvetex®

Alvetex® is a scaffold made from high internal phase emulsion-templated polystyrene (Knight *et al.*, 2011). This gives it a variety of properties which make it ideal for tissue culture experiments. The production method creates a highly porous structure with a large amount of control over the pore size through variation of properties such as temperature and stir speed (Barbetta *et al.*, 2005; Carnachan *et al.*, 2006). This porosity allows some cells to migrate into the scaffold and attain a fully 3D morphology. Medium can also travel through the scaffold allowing cells inside to get a good supply of nutrients. At 200µm thick, all cells within the scaffold are within 100µm of the medium, mimicking the proximity of cells to the vasculature in vivo (Carmeliet and Jain, 2000).

Being based on a synthetic polymer, Alvetex® has a highly consistent structure and lacks unknown materials such as animal proteins present in some natural scaffolds (Dash *et al.*, 2011). This allows for tight control over experimental conditions and a high level of reproducibility. As 2D culture normally takes place on polystyrene the results from Alvetex®® are very comparable. At present there are three Alvetex® substrates which are readily available; Scaffold, Strata and Polaris, as shown in Figure 3.9. These each have a significantly different pore size, leading to different properties in cell culture and therefore covering a wide range of potential applications. Scaffold has

very large pores of around 38µm in diameter. This allows for rapid diffusion of nutrients through the membrane and most cells are able to invade completely into the membrane in a short space of time. Strata has smaller pores of 13µm. This still allows for nutrients to diffuse easily through the membrane however limits cell invasion, with a lot of cell types only invading a short way into the membrane with many cells staying on the surface in typical cultures. Polaris utilises considerably smaller 3µm pores, completely limiting cell invasion and causing cells to form a layer on the surface.

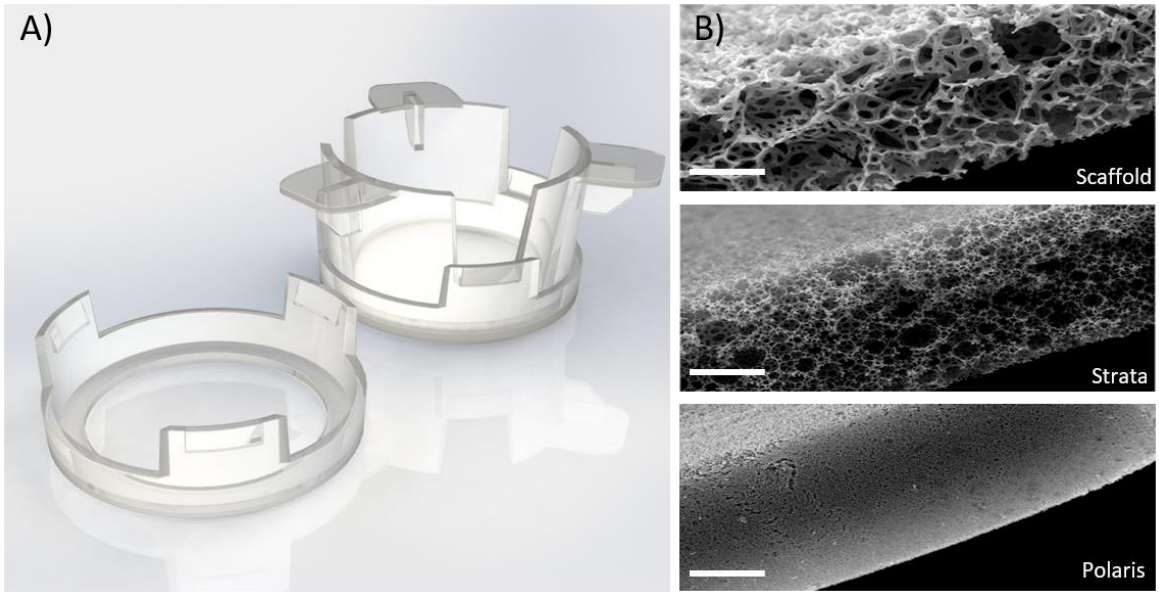

Figure 3.9: Structure of the three different forms of Alvetex® membrane. A) Alvetex is available in a series of multi-well plate formats from 6-well down to 96-well. A 6-well Alvetex insert is pictured here, with a complete insert to the back and in the foreground is the base of an Alvetex insert. The base can unclip to release the membrane for further analysis such as embedding and sectioning. B). Three forms of Alvetex exist with different pore sizes: Scaffold, Strata and Polaris. Alvetex Scaffold and Strata, with the larger pore sizes, are currently commercially available however Polaris, with a much smaller pore size, is not. Scale bars are 100 µm.

Alvetex® has previously been shown to have a positive impact on the culture of hepatocytes and the ability to use the different properties to create complex co-cultures makes it a good candidate for use in a bioreactor (Bokhari, Carnachan, Cameron, *et al.*, 2007b). Studies carried out using HepG2 cells and primary rat hepatocytes grown on Alvetex® Scaffold have shown that this environment leads to an improved drug response (Bokhari, Carnachan, Cameron, *et al.*, 2007a; Fox *et al.*, 2010). Another study found that expression of CYP2B6 and CYP3A4 were increased in Upcyte hepatocytes when cultured in Alvetex® Scaffold compared with 2D culture but reported mixed results for CYP1A2 (Burkard *et al.*, 2012). Alvetex® Scaffold has also been used to create models of

other tissues such as skin (Roger *et al.*, 2019) and intestine (Darling *et al.*, 2020), demonstrating its capacity for creating spatially patterned 3D co-cultures.

3.1.5. Conclusion

The liver has a complex, dynamic microenvironment with a large amount of fluid flow from several sources. This has a significant impact on the structure and function of liver at the cellular and tissue level due to effects such as nutrient and waste turnover, shear stress and the reduction of unstirred layers. By introducing these properties into cell culture, we can improve the physiological relevance of cell and tissue models and a large quantity of literature has demonstrated the potential of bioreactor systems.

Fluid flow alone is insufficient to create the complex microenvironment which permits the formation of such tissues. Additional cues such as three-dimensionality and co-culture are required to fully recapitulate *in vivo* conditions. Solid scaffolds allow for this and have been used previously with success. Alvetex® is a solid scaffold which has been used previously with hepatocytes and could be used to develop a simple medium throughput bioreactor system, with the opportunity to add further complexity or alter to suit the experimental needs.

One of the limitations of tissue bioreactor systems is the trade-off between cost, ease of use and spatial size against complexity and physiological relevance of generated tissues. There is therefore a need for the creation of a culture system which can recapitulate the complex, dynamic tissue microenvironment whilst retaining simplicity and minimising required technical expertise. The applications of such a system for the culture of liver tissue equivalents could allow for improvements in the drug discovery pathway and disease modelling as well as providing an effective platform for basic research.

3.2. Aims and Objectives

3.2.1. Aims

The numerous factors which impact the structure and function of cells makes the creation of accurate *in vitro* models a major challenge. Whilst technologies exist to recapitulate some of these factors there are few which combine several techniques to create a highly complex, physiologically accurate recreation of the cellular microenvironment. Therefore, there is a need to develop a system which can be used to incorporate these different technologies whilst avoiding some of the drawbacks which are often seen with such techniques.

In this chapter development of an advanced cell culture bioreactor system for tissue engineering is carried out. This draws upon different technologies, incorporating 3D culture and fluid flow alongside the potential to be used with complex co-cultures. This can therefore maximise the physiological relevance of the tissue equivalents created, supplying cells with high levels of nutrition whilst providing mechanical cues such as shear stress and structural support. Refinements are made to the system to maximise reproducibility and ease-of-use, two key properties which many bioreactor systems perform poorly on. The system is assessed for both its direct impact on cells as well as the formation and control over the fluid flow within the system. The fluid flow properties are quantified to allow comparisons to conditions *in vivo* and therefore tailor the system for use with a variety of tissues and cells.

3.2.2. Objectives

1. Develop a bioreactor system for dynamic, three-dimensional cell culture which meets a set of criteria designed to ensure it fits the current gap in tissue engineering technology.
2. Optimise this system for both culture properties and ease of use.
3. Fully characterise the mechanical properties of the fluid flow within the system
4. Test the cytocompatibility of the system and monitor potentially undesirable effects.

3.3. Results

3.3.1. Development Criteria

There are a number of criteria which need to be met for the bioreactor system to be successful and fulfil its intended purpose. These are based upon the current gaps in the tissue engineering field and the required properties for effective tissue recreation.

1. Introduce fluid flow into the culture system in a controlled and tuneable way.
2. Be reusable and therefore autoclavable or otherwise easily sterilisable.
3. Comprise of materials which are inert and non-cytotoxic or otherwise non-effective on cells.
4. Be inexpensive, easy to set up and require minimal technical knowledge.
5. Have a small footprint with minimal parts to allow ease of use and high levels of scalability.

3.3.2. Design Phase I: Initial Prototype

The decision was made to base the bioreactor around a magnetic stirrer. This is due to the simplicity and ease of use associated with a stirred system as well as the availability of high-density multi-point magnetic stirrers to allow for suitable throughput for the system at minimal cost.

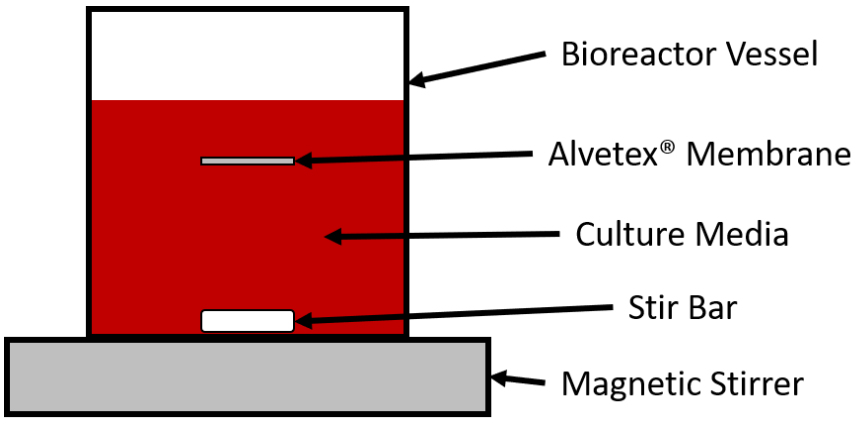

Figure 3.10: Schematic of a magnetic stirrer based Alvetex® cell culture bioreactor. A vessel is selected to hold the culture, the culture medium, and a magnetic stir bar. This sits on a magnetic stirrer to drive the stir bar at the desired speed. Further components required and not pictured include some sort of holder for the Alvetex® membrane and a method for accessing the culture whilst also keeping it sterile such as a removable lid.

There are several components which are needed for such a system, as shown in Figure 3.10. The initial component to design is the vessel which will hold the culture as this determines the scale and properties of the further components. A method to seal this whilst still allowing access, such as a removeable lid, is also needed as part of this. A stir bar can then be selected, and a holder can be created to contain the culture as desired. Finally, a stirrer unit needs to be chosen to complement the system and ensure it has the desired fluid flow properties.

To hold the media a vessel was needed which could hold a large volume of media and was suitable to contain a 6-well Alvetex® membrane. A custom beaker, shown in Figure 3.11, was produced by the glassblowing workshop in the department of Chemistry, Durham University. This can hold up to 120 mL of media without risk of spilling and with a diameter of 70 mm has plenty of space to generate effective media recirculation. The use of glass for this design means that it is easy to make and is autoclavable, adding to the reproducibility of the system. Full schematics of the system can be found in Appendix 3.

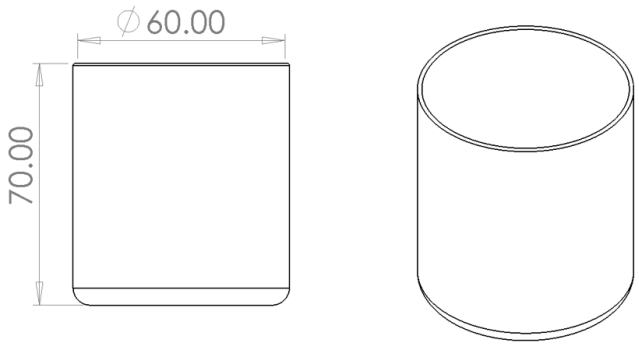

Material	Glass
Dimensions (Diameter x height)	60 mm x 70 mm
Wall Thickness	2.2 mm
Fabricator	Scientific Glass Services

Figure 3.11: Glass vessel to contain the bioreactor system. The glass beakers are created from a standard size of glass tube to maximise reproducibility. This set the internal diameter to 60 mm and the wall thickness is approximately 2.2 mm. The total volume held by the beaker is 195 ml. All dimensions are in millimetres. Complete schematics can be found in Appendix 2. Fabricated by the glassblowing workshop, Department of Chemistry, Durham University.

A lid was designed which could be used for the sterilisation, storage of the system and in culture to maximise ease of use and reusability. This was done through the creation of a double-sided PTFE lid which sealed the beaker when placed one way up and allowed adequate air transfer for cell culture when the other way up, as shown in Figure 3.12. To allow air transfer, the cell culture side was designed similarly to a petri dish lid with three 2 mm high flanges which held the surface of the lid from the top of the beaker, permitting airflow into the vessel. On the other side a thin ring was inset into the plastic which fits tightly around the rim of the beaker, severely limiting the air flow. This design allows the apparatus to be autoclaved as an entire unit without the need for any extra preparation.

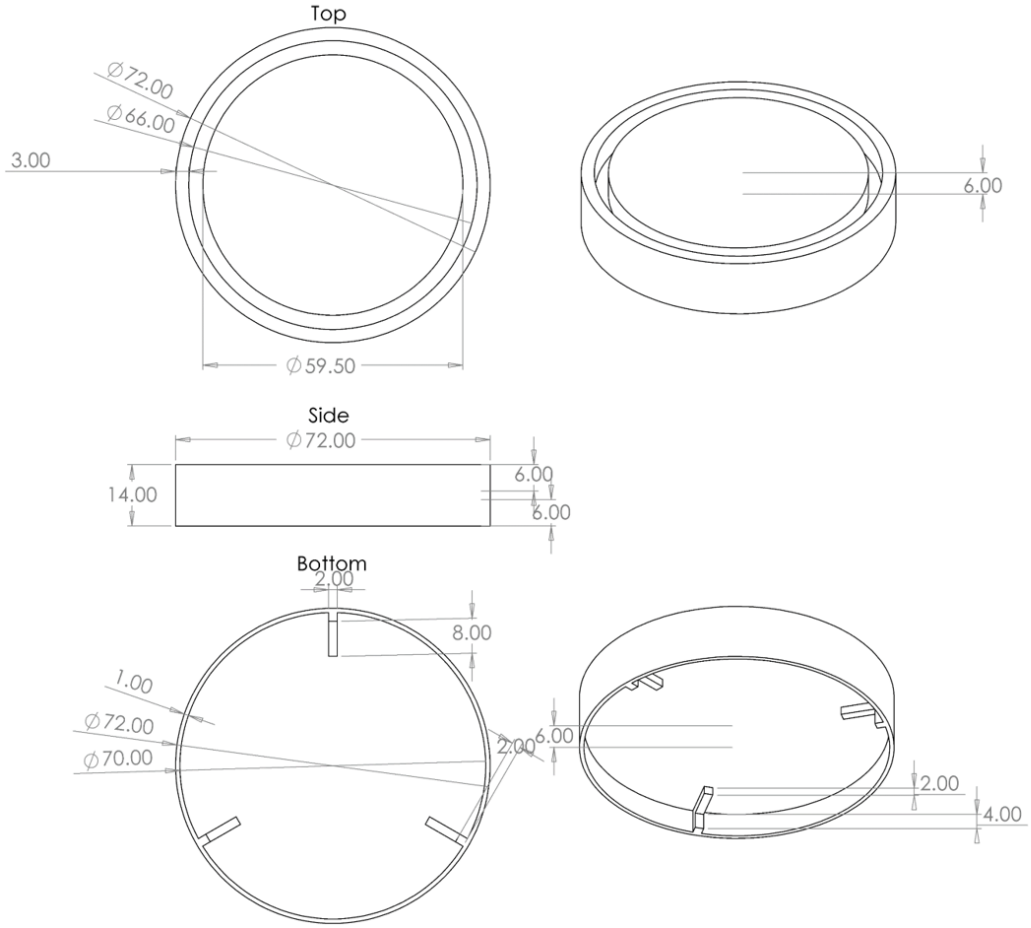

Material	PTFE
Dimensions (diameter x height)	72 mm x 14 mm
Upper recess dimensions (outer diameter x inner diameter x depth)	66 mm x 59.5 mm x 6 mm
Lower recess dimensions (diameter x depth)	70 mm x 6 mm
Fabricator	Roechling-Fibracon

Figure 3.12: Reversible PTFE Lid for the bioreactor system. The double-sided design allows the lid to be used to both seal the system after autoclaving as well as to allow ventilation during cell culture when turned over. The lid is composed entirely of PTFE and fabrication was carried out by Roechling-Fibracon. Complete schematics can be found in Appendix 2. All dimensions are in millimetres.

To stir the media a magnetic stir bar was needed which was large enough to produce a significant amount of recirculation given the large volume of media used in the system. A large crosshead stir bar was chosen, as shown in Figure 3.13. This has a diameter of 25 mm which allows it to stir the fluid at a substantial distance from the centre of the vessel, maximising mixing. This stir bar is coated in PTFE which maximises cytocompatibility and allows for autoclave sterilisation.

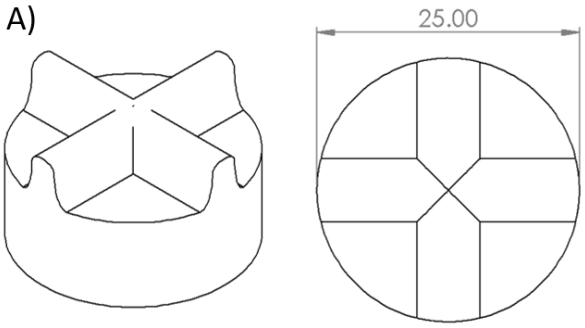

Material	PTFE
Dimensions (diameter x height)	25 mm x 15 mm
Supplier	Fisher Scientific UK

Figure 3.13: Magnetic stir bar used for the prototype bioreactor cultures. This stir bar consists of a magnetic metal core coated in PTFE and has a cylindrical body with a raised, cross-shaped surface for stirring. All dimensions listed are in mm. The stir bar has a diameter of 25 mm and a height of 15 mm. The stir bar is commercially available from Fisher Scientific UK.

3.3.2.1. Membrane holder

To hold the Alvetex® membrane in place above the stirrer a device was needed which could contain the membrane whilst enabling flexibility over the exact orientation of the membrane. For this a spherical device was designed by Stefan Przyborski to hold a 6-well Alvetex® membrane, shown in Figure 3.14. The device is produced in two identical halves have the Alvetex® placed in between and then hold together with a friction fit to form the complete device.

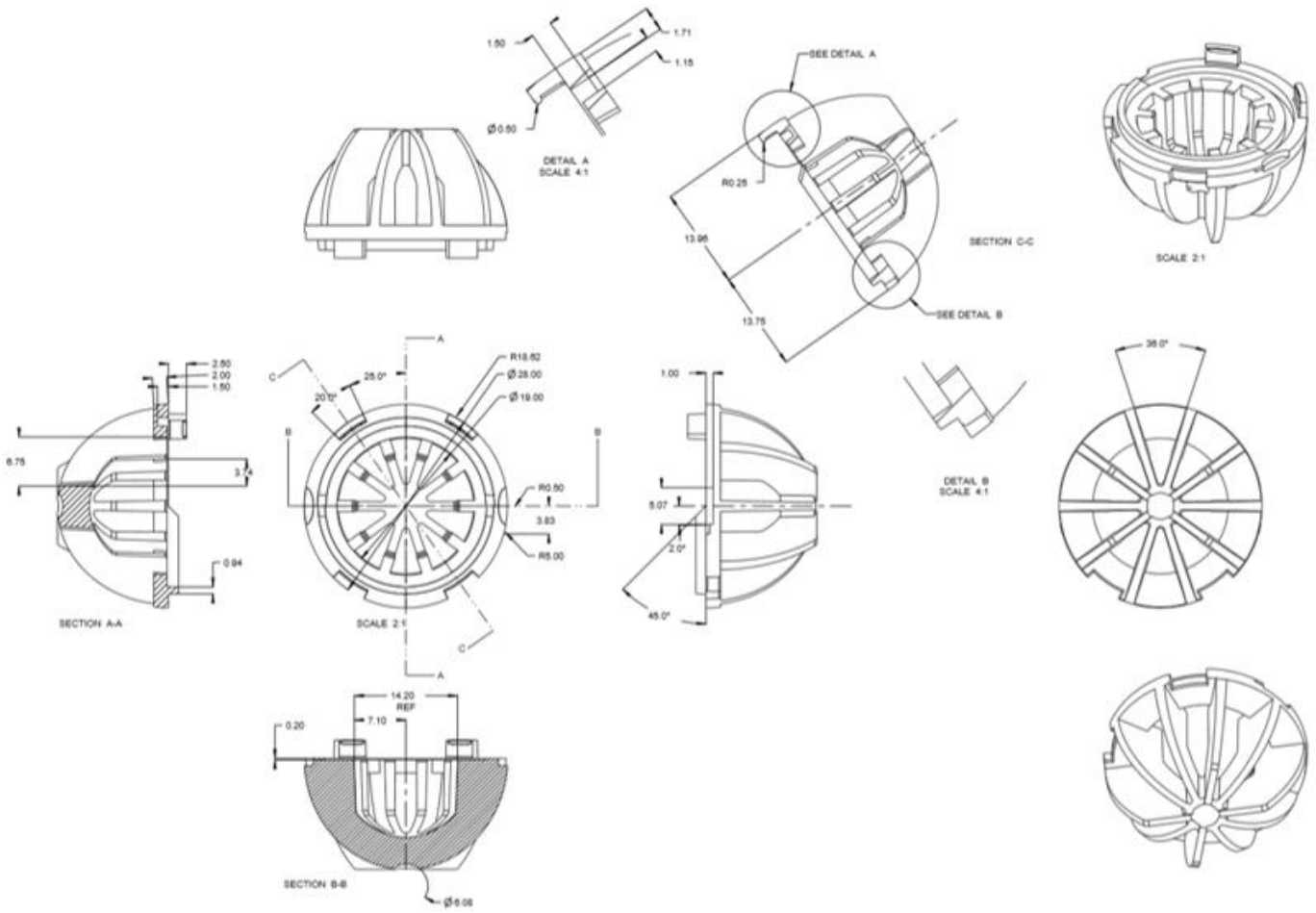

Figure 3.14: Device for holding a 6-well Alvetex membrane. The spherical shape of the device allows a range of orientations to be utilised for the culture.The two halves of the device clip together with friction-fit tabs once Alvetex has been placed between them. Indentations on the sides allow for decoupling of the halves using forceps. The device was designed by Stefan Przyborski and manufactured from polystyrene. All dimensions are in millimetres.

Each half has a radius of 28 mm at the widest point, where the Alvetex® is placed in which it forms a 5 mm wide ring with a height of 2 mm. Ten 1 mm thick radially symmetric arches protrude upwards from this to join in the middle, giving the assembled device it's spherical shape.

3.3.2.2. Controlling fluid flow

Using a magnetic stirrer for cell culture is an effective method for creating medium recirculation however the properties of the fluid flow need adjustment to optimise them for cell culture applications. A stirrer alone in a vessel produces medium recirculation as required by drawing medium down the middle of the vessel and recirculating it upwards towards the outside of the vessel as shown in Figure 3.15. This flow is mainly laminar flow which is not conducive to properly mixing the constituents of the medium. By placing a baffle over the stir bar, the flow can be contained to force it to be more turbulent around the stirrer, therefore allowing better mixing, whilst also concentrating the downwards flow centrally in the region of the cell surface with minimised turbulence at this area.

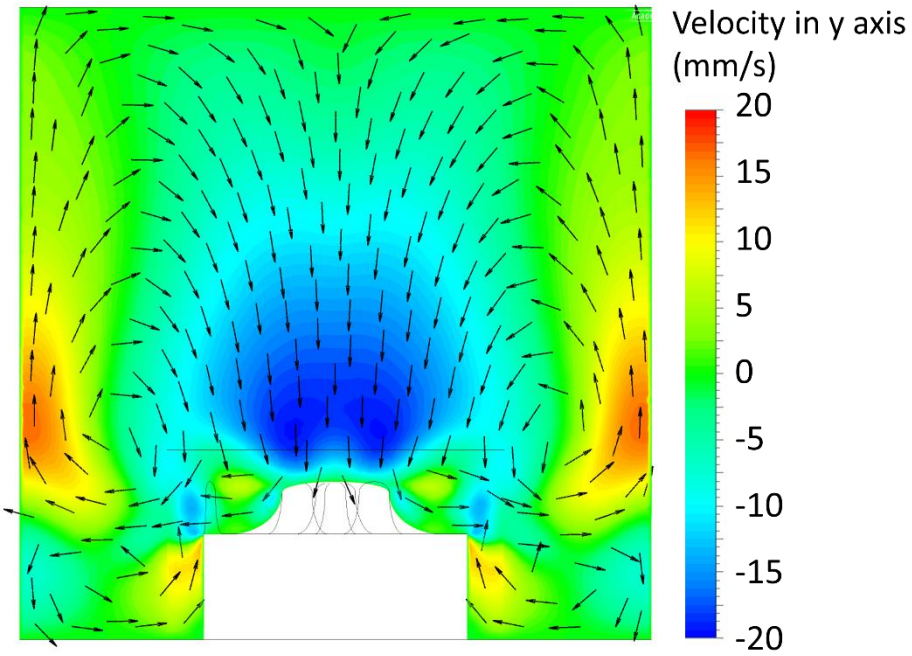

Figure 3.15: CFD modelling of a stirred beaker in the absence of further fluid control. With no further control over the flow a recirculation pattern is formed with fluid flowing upwards towards the edges of the vessel and downwards in the centre. The heatmap shows the y-velocity of the fluid across the liquid region whilst the vectors to show the direction of fluid in the x-y plane across the liquid region.

3.3.2.3. Different designs for stirred flow

One of the variables that needs to be controlled in bioreactor culture when striving for *in vivo*-like conditions is the level of shear stress experienced by the cells. In the body different cells experience different levels of shear stress induced by factors such as blood, bile or other fluid flow or movement such as cellular contractions. The highly vascularised structure of the liver means that a lot of shear stress can potentially be experienced by cells however it is difficult to quantify exactly how much is experienced by particular cell types such as hepatocytes.

Shear stress against the lining of blood vessels can be calculated from the blood flow rate, giving a value of 0.1 - 0.5 dyne/cm^2 in liver sinusoids (Lalor and Adams, 1999). Due to the structure of the blood vessels most of this shear stress is felt by the sinusoidal endothelial cells lining the sinusoids and so the hepatocytes are protected from it. Some level is experienced by hepatocytes due to fluid movement in the space of Disse caused by the high rates of diffusion through the lobular structure. Calculating the exact value of this is difficult and models for it must incorporate many variables, making precise values for the shear stress experienced by hepatocytes difficult to find.

To minimise undue shear stress in the bioreactor system the design would need to draw fluid through the plane perpendicular to the cell culture whilst reducing tangential elements. Several stand designs, as shown in Figure 3.16, were tested which each had different effects on the fluid flow.

A)

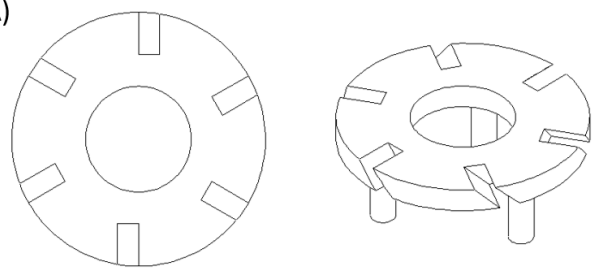

Material	PTFE
Dimensions (Diameter x height)	59 mm x 32mm
Vent dimensions (width x height)	5 mm x 10 mm Angled 45° from normal

B)

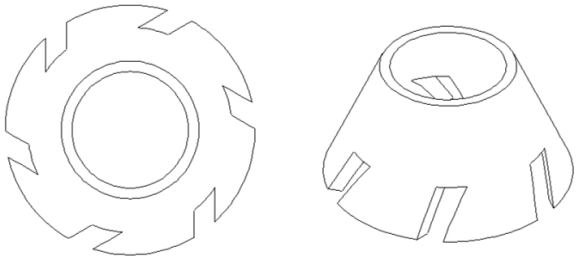

Material	PTFE
Dimensions (Diameter x height)	59 mm x 32mm
Vent dimensions (width x height)	5 mm x 10 mm Angled 315° from normal

C)

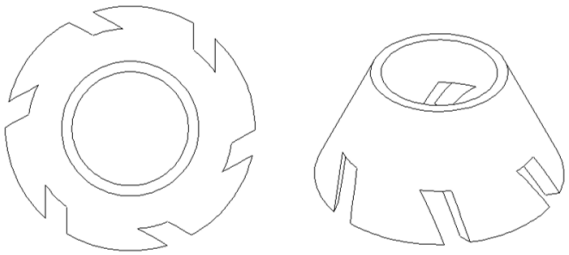

Material	PTFE
Dimensions (Diameter x height)	59 mm x 32mm
Vent dimensions (width x height)	5 mm x 10 mm Angled 315° from normal

Figure 3.16: Three initial stands designed to hold the culture device. Each design holds the culture device at a height of 32 mm above the base of the vessel and has venting around the outer edges to coincide with regions of fluid with high y-velocity. All three designs are made from PTFE and are optimised for production by milling PTFE rods. A) Raised platform with clockwise venting B) Conical stand with clockwise venting C) Conical stand with anti-clockwise venting. Complete schematics for these designs can be found in Appendix 2.

Two conical designs were tested with venting up the sides in clockwise or anti-clockwise orientation, directing flow with the direction of the stirrer and against it respectively. The third design was a simpler table-based stand with vents to direct media upwards around the outside of the beaker. This design was advantageous in that it was simple to produce and could easily be created in a variety of materials

3.3.2.3.1. Design 1: Vented Table

The most basic design tested, the vented table is easy to produce and promotes the recirculation of the medium whilst shielding the culture from a considerable proportion of shear stress created by the stirrer.

Initial analysis of the designs was carried out using Particle Image Velocimetry (PIV) with the results shown in Figure 3.17. PIV is an established non-invasive flow measurement technique which is ideal for the purpose of the current study. The turbulence level and hence the mixing efficiency can be inferred by the root mean squared contours. Particle image velocimetry shows that the turbulence at the cell surface is very low with this design, resulting in most of the shear stress being formed by the vertical component of the velocity. This suggests that the media mixing is being inhibited by this design, which is slowing the fluid rotation. This design also shields the fluid flow quite effectively, resulting in quite low velocity above the cell membrane.

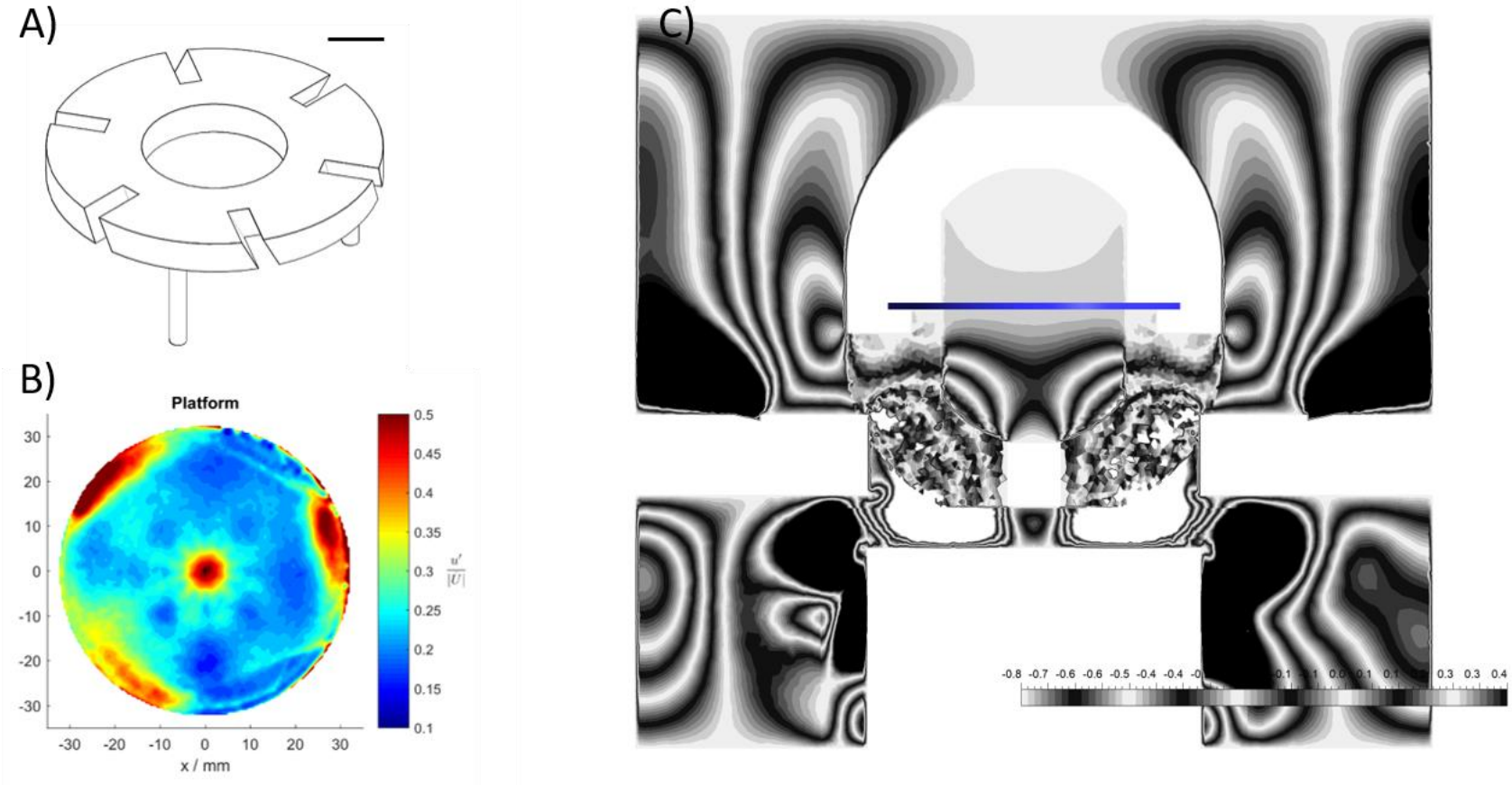

Figure 3.17: Fluid flow analysis for the vented table culture stand. Fluid flow was analysed both computationally and experimentally to compare the different baffle designs. This stand design utilised a flat , table-like surface to support the culture holder with angled venting around the outer edges to promote medium recirculation. A) Schematic of the table stand. The scale bar is 10 mm. B) PIV analysis of the system with the table stand in a plane at a height corresponding with the upper surface of the Alvetex membrane. C) CFD analysis of the y-velocity in the fluid region of the bioreactor using the table stand. The blue line represents the Alvetex membrane.

Alongside the PIV analysis a simple dye circulation experiment was also carried out to evaluate the mixing capacity of each stand (Figure 3.18). In this experiment an effective stand should form a strong flow through the central column of the beaker, where the cell culture is placed, as well as providing recirculation and mixing around the sides of the beaker. Results from the dye recirculation experiment match the PIV findings with a strong vortex being formed at the centre of the system but minimal mixing further towards the edges with the baffle containing a lot of the mixed fluid. Whilst this suggests that this design would produce a strong flow of media through the cell culture, therefore creating the shear stress and fluid movement at the required, the lack of mixing of the rest of the media could lead to poor nutrient distribution.

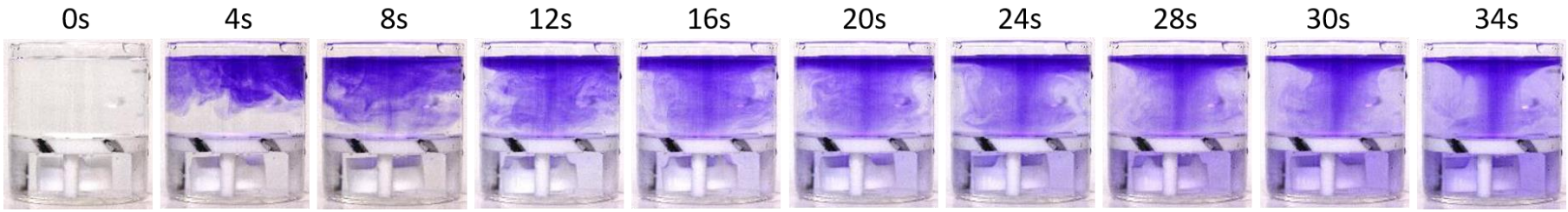

Figure 3.18: Time series of crystal violet dye in the system with the vented table stand. Crystal violet is added to the bioreactor and the distribution over time can be visualised. Over time the dye is distributed throughout the liquid whilst forming a high-concentration vortex between the surface and the top of the stir bar. The vessel was filled with 130 mL of distilled water and placed on a magnetic stirrer at 100 rpm and allow to equilibrate. Crystal violet was added to the surface of the water at the 0s time point and photos were taken every four seconds using a remote trigger.

3.3.2.3.2. Design 2: Conical Stand, Clockwise Venting

A more complex stand design uses a conical shape to act as a baffle to control shear stress. The culture device can be held at the top of this cone and venting around the bottom edges allows media to travel outwards and recirculate within the vessel therefore performing adequate mixing and inducing shear stress on the cells.

PIV analysis of this stand shows higher turbulence around the cell layer compared with the previous design however the overall flow rate is also increased, therefore allowing lower stir speeds to be used for equivalent levels of mixing (Figure 3.19). The improved downwards flow through the cultures suggests that this design would lead to greater levels of fluid flow around the culture and therefore have a greater effect on nutrient delivery to the cells. Dye recirculation with this design shows a similar result with a dense core of dye forming down the centre of the stand demonstrating effective downwards fluid flow at this position and recirculation outwards from the bottom of the vessel occurring, allowing effective mixing to take place (Figure 3.20).

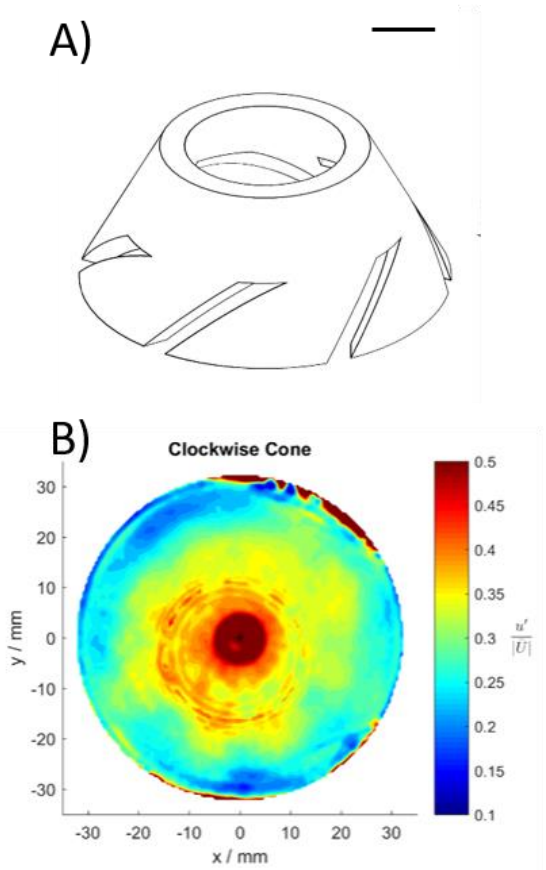

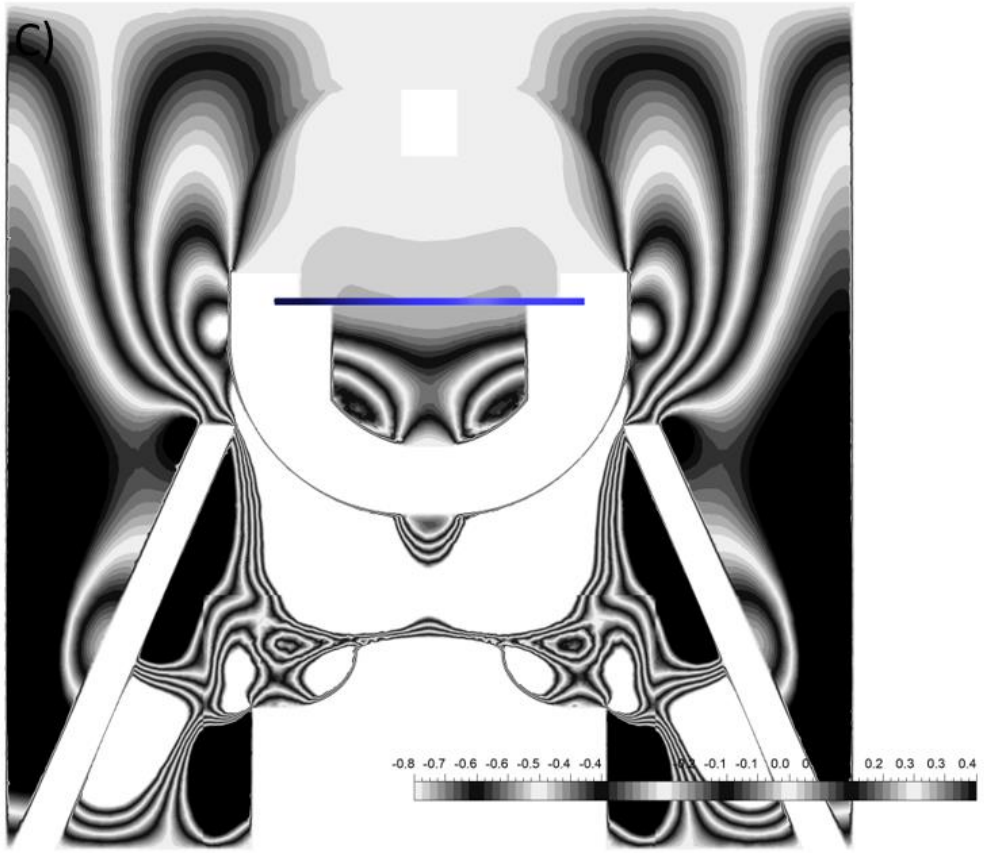

Figure 3.19: Fluid flow analysis for a conical stand with clockwise venting. This design uses a conical support with venting around the lower, outer edges to facilitate fluid recirculation. Fluid flow was analysed both computationally and experimentally to compare the different baffle designs. A) Schematic of the clockwise-vented conical stand. The scale bar is 10 mm. B) PIV analysis of the system with the clockwise-vented conical stand in a plane at a height corresponding with the upper surface of the Alvetex membrane. C) CFD analysis of the y-velocity in the fluid region of the bioreactor using the clockwise-vented conical stand. The blue line represents the Alvetex

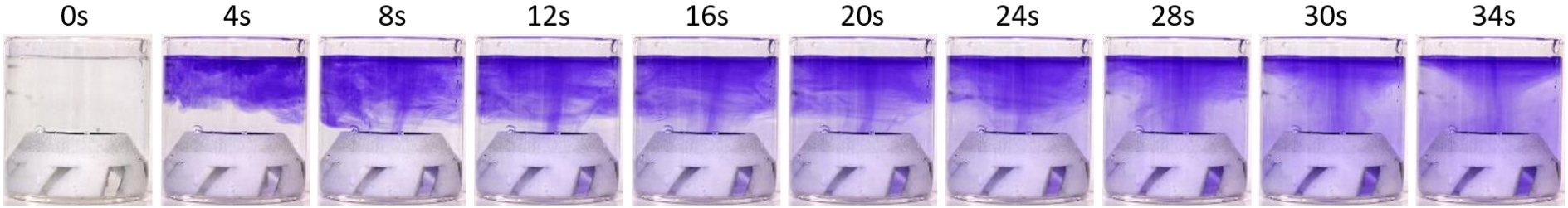

Figure 3.20: Time series of crystal violet dye in the system with the clockwise-vented conical stand. Crystal violet is added to the bioreactor and the distribution over time can be visualised. Over time the dye is distributed throughout the liquid whilst forming a high-concentration vortex between the surface and the top of the stir bar. The vessel was filled with 130 mL of distilled water and placed on a magnetic stirrer at 100 rpm and allow to equilibrate. Crystal violet was added to the surface of the water at the 0s time point and photos were taken every four seconds using a remote trigger.

3.3.2.3.3. Design 3: Conical Stand, Anticlockwise Venting

With the vents directing flow against the rotation of the stirrer in the second design a large amount of turbulence is created as expected (Figure 3.21). Whilst this method is effective for mixing the media the fluid velocity recirculating in the vessel is noticeably reduced, therefore leading to increased stirrer speeds being required to create the desired levels of fluid flow through the culture. This in turn would lead to unwanted high levels of shear stress which could have negative impacts on cell health and viability.

Dye recirculation patterns mirror this finding with a broad central core of downwards flow which demonstrates the lower downwards velocity in the centre, whilst the effective mixing around the sides of the vessel is apparent (Figure 3.22).

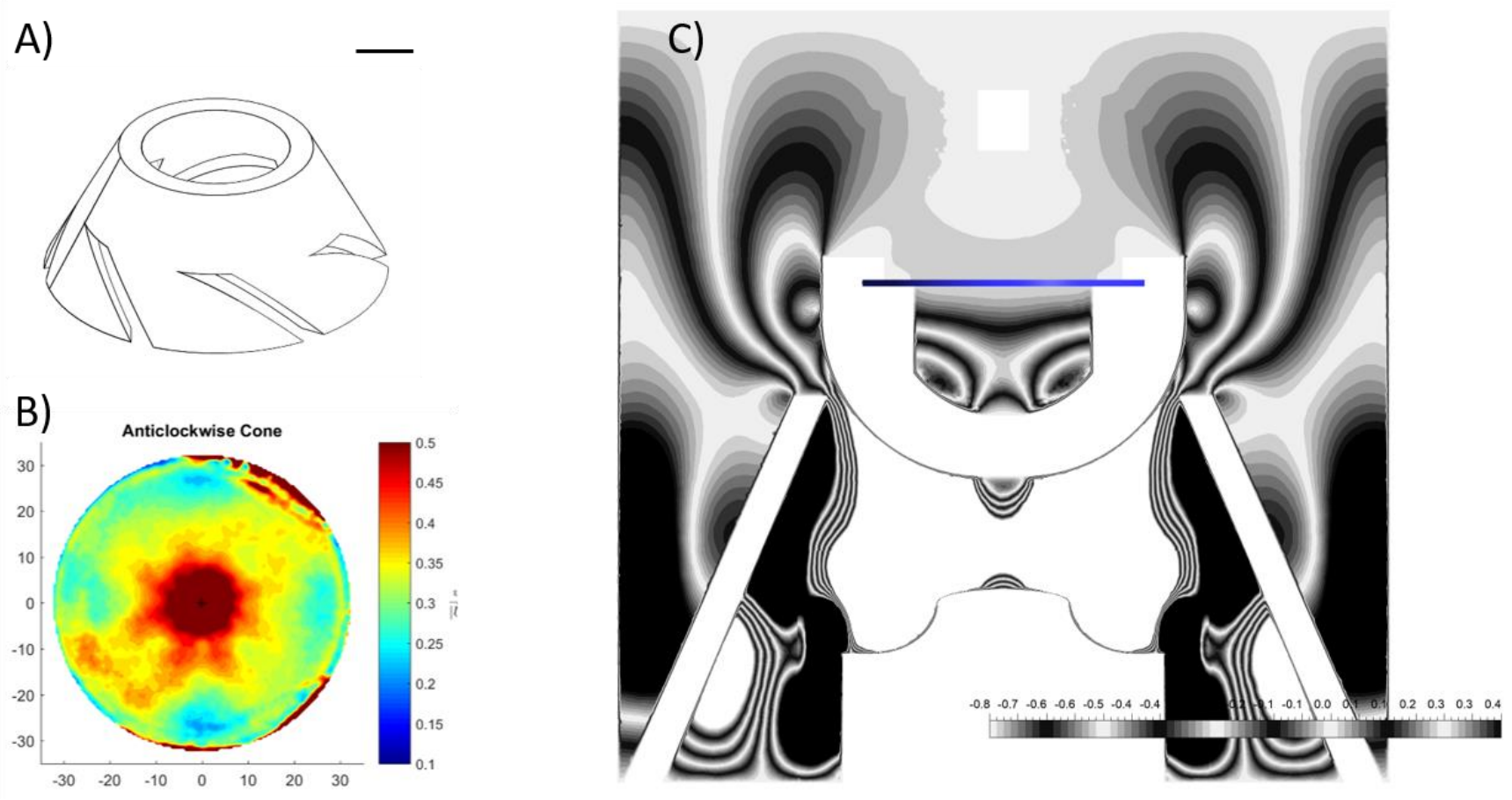

Figure 3.21: Fluid flow analysis for a conical stand with anticlockwise venting. This design utilises a conical support with venting at the lower, outer edges in a direction opposite to the fluid flow to facilitate convective mixing. Fluid flow was analysed both computationally and experimentally to compare the different baffle designs. A) Schematic of the anticlockwise-vented conical stand. The scale bar is 10 mm. B) PIV analysis of the system with the anticlockwise-vented conical stand in a plane at a height corresponding with the upper surface of the Alvetex membrane. C) CFD analysis of the y-velocity in the fluid region of the bioreactor using the anticlockwise-vented

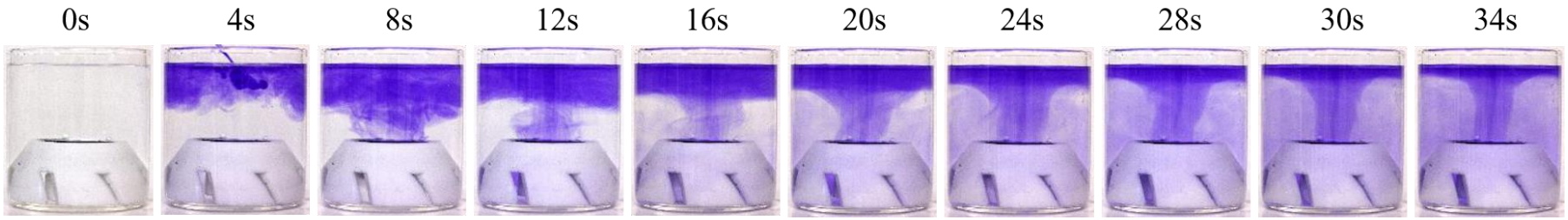

Figure 3.22: Time series of crystal violet dye in the system with the anticlockwise-vented conical stand. Crystal violet is added to the bioreactor and the distribution over time can be visualised. Over time the dye is distributed throughout the liquid whilst forming a high-concentration vortex between the surface and the top of the stir bar. The vessel was filled with 130 mL of distilled water and placed on a magnetic stirrer at 100 rpm and allow to equilibrate. Crystal violet was added to the surface of the water at the 0s time point and photos were taken every four seconds using a remote trigger.

From these results the first design for the conical stand with clockwise oriented vents appears to create the most desirable circulation pattern in the media for this culture method and so it was decided that this would be the design to be used going forwards.

3.3.2.4. Cellular compatibility of materials

Where possible components of the bioreactor system were made from materials with high cytocompatibility however another property taken into consideration was the ease of machining. Due to this, parts of the apparatus were made from glass and polystyrene where possible, both routinely used for cell culture. In some cases, this was not achievable due to fabrication limitations so other materials had to be used. Polytetrafluoroethylene (PTFE) was used for creation of stands for the culture holders. PTFE is known to be very inert and have a high level of cytocompatibility. Some plastics can display cytotoxicity when treated in certain ways such as via autoclaving. Brief tests were carried out to ensure that the PTFE, both new and autoclaved, had no negative effects on the cell cultures (Figure 3.23)

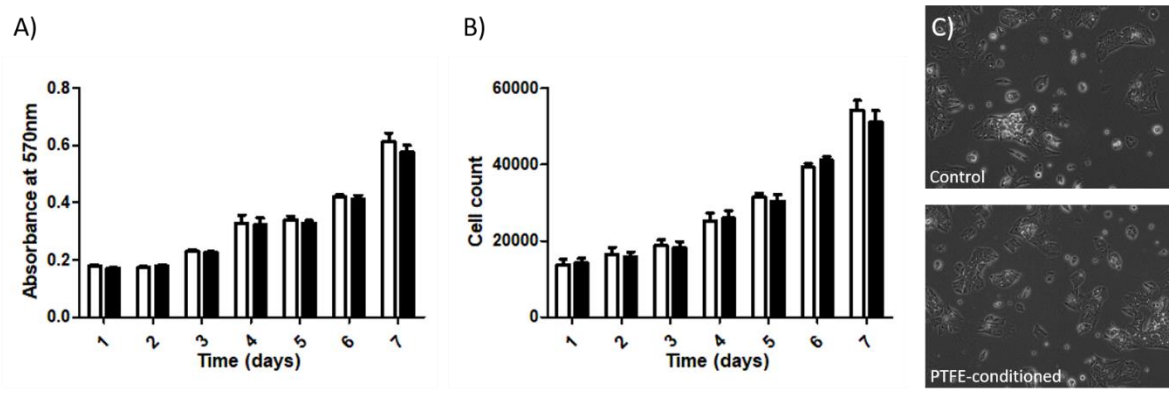

Figure 3.23: Effects on the viability of HepG2 cells grown in PTFE conditioned media. Medium Conditioning was carried out by incubating 500 mL of media with a 1 cm^3 block of PTFE at 37°C for 7 days prior to culture. This was then used to grow HepG2 cells in 2D plates and compared to a control of media incubated in the absence of PTFE. A) Results of an MTT assay at for cells grown for 7 days in conditioned media compared to control. B) Cell count for cells grown for 7 days in conditioned media compared to control. C) Phase-Contrast images of cells grown in conditioned media for 7 days compared to control. Values show mean ± SEM. N = 3, n = 3.

The results of the MTT assay show that there is no significant change in cellular viability when cultured in media conditioned with either type of PTFE. The H&E staining shows the same morphology for the cells I each condition, suggesting that the cell behaviour has not been affected by the PTFE.

From these results the design for the stand was finalised, as shown in Figure 3.24. This was designed to take on board the results of the previous experiments to maximise flow control and cellular compatibility as well as being easy to manufacture.

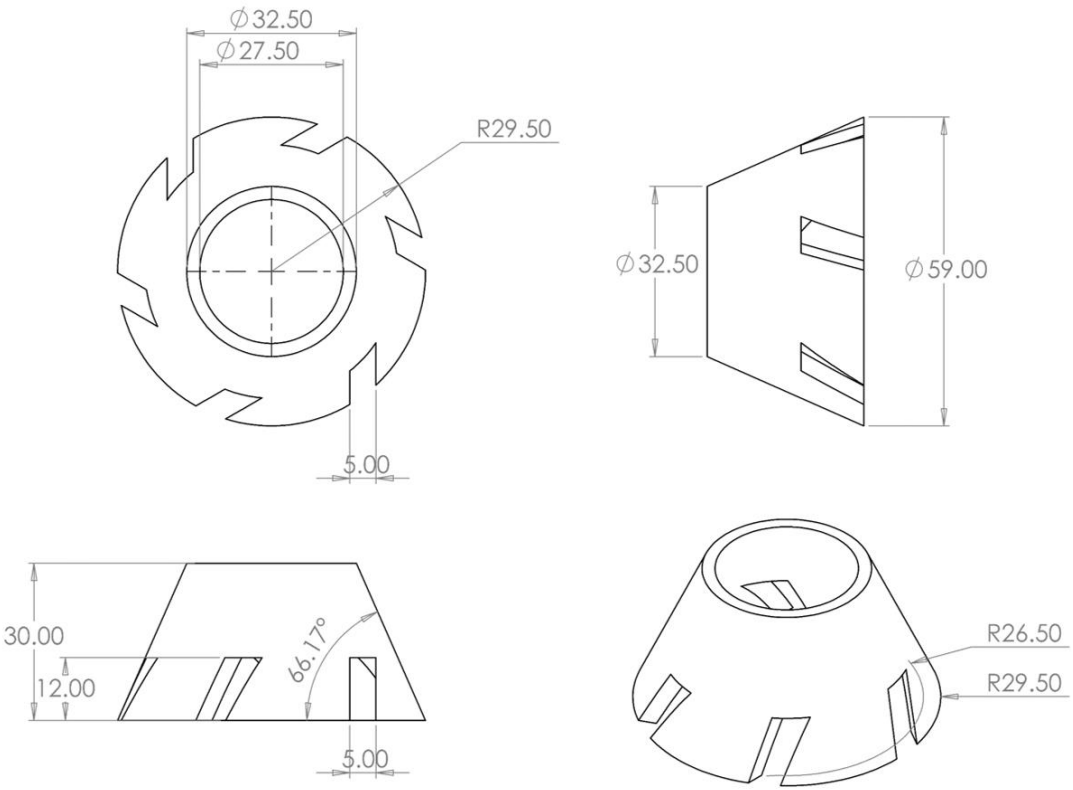

Figure 3.24: Schematic of the finalised clockwise-vented conical stand design. This design has clockwise-facing vents at the bottom to enhance medium recirculation. The culture holder is supported in the circulation opening at the upper end of the support. The design can be readily milled from 60 mm diameter PTFE rod. Fabrication was carried out by the mechanical workshop in the Department of Chemistry, Durham University. All dimensions are in millimetres. The full schematics can be found in Appendix 2.

3.3.2.5. Complete prototype system

Following the data collected previously a design was finalised which meant that the criteria laid out at the start of the chapter could be met (Figure 3.25). The use of a magnetic stirrer allows for precise control over the fluid flow through alteration in stir speed. The flow caused by this is then controlled by the baffled stand to create the desired flow pattern. This system allows 3D culture of cells to be carried within a recirculating fluid medium, therefore closely resembling the microenvironment experienced by cells *in vivo.*

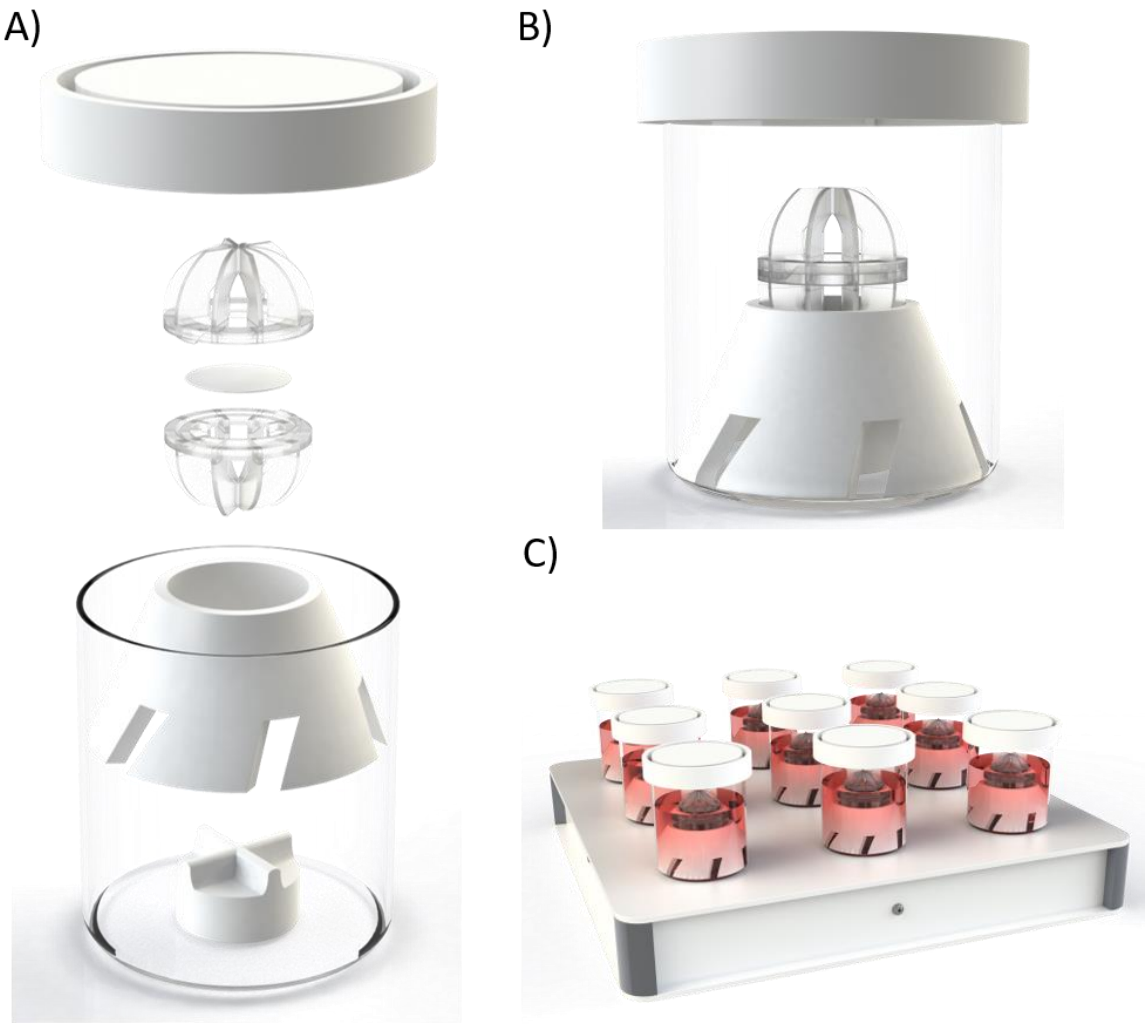

Figure 3.25: The complete prototype bioreactor design. The design incorporates all the components detailed previously. The conical support holds the culture device which in turn contains the Alvetex® membrane used as a growth surface. A) Exploded diagram of the complete bioreactor system with an Alvetex insert. B) Render of the assembled bioreactor system with no medium. C) Render of the bioreactors on a magnetic stirrer with 110 mL of cell culture medium.

3.3.2.6. Magnetic Stirrer unit

To run the system initially a Velp 6-point magnetic stirrer, as shown in Figure 3.26, was used. This allows the cultures to be easily accessible due to only having a depth of three cultures on either side whilst also tying in with running experiments in triplicate. This stirrer is low cost and therefore suitable to be used in most laboratories without a major financial commitment as well as being able to function normally in a humidified 37 °C incubator.

Dimensions (WxHxD)	230 x 51.5 x 370 mm
Stir Speed	80 – 1500 rpm
Number of stir points	6
Distance between stir points	100 mm
Manufacturer	Velp

Figure 3.26: Velp Multi-point magnetic stirrer. The 6-point magnetic stirrer manufactured by Velp which has been used for preliminary experiments. This stirrer can reach a minimum speed of 80 rpm which makes it suitable for use with cell culture in the designed system, whilst the operating parameters are flexible enough to allow for use in the heated and humidified environment of an incubator.

This stirrer unit also features a wide range of stir speeds, going as low as 80 rpm, a feature which many commercially available units cannot manage. This can allow the fluid properties to be controlled over a very wide range and cells which may be highly sensitive to shear stress can also be incorporated when using lower stir speeds. Due to the arbitrary units for the speed settings on this stirrer it was necessary to quantify the stirrer speed at different settings. This allows the exact speed of the stirrer to be set, therefore matching results to quantification from fluid dynamics models. As shown by Figure 3.27 the stirrer showed a linear correlation between the speed setting and the measured speed with all the measured values within the manufacturer's specifications. The lowest achievable value was with a speed setting of 0.8, below which the stirrer would cease to function.

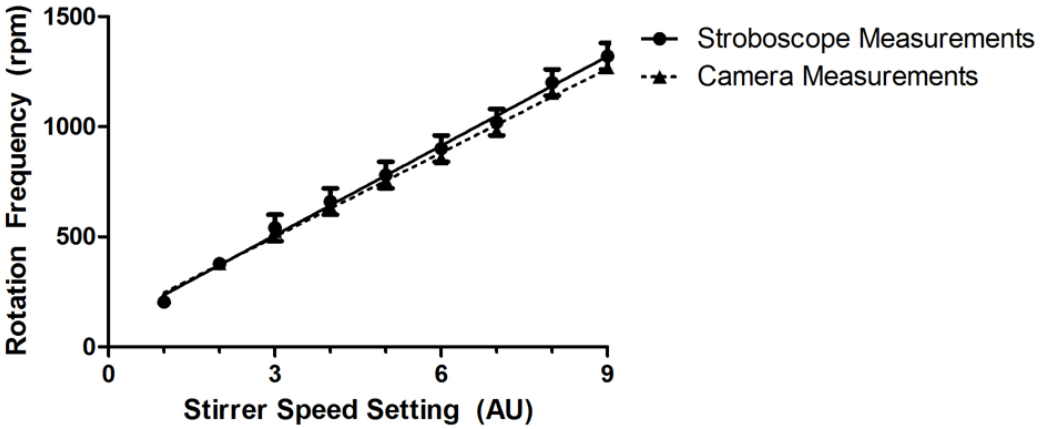

Figure 3.27: Rotational frequency of the Velp magnetic stirrer at different speed settings. The results measured using both a stroboscope and a slow-motion camera match closely and demonstrate a strict linear correlation between the speed setting and the rotational frequency. These results agree with the specification for the speed limits provided by the manufacturer. All values are mean ± SEM.

3.3.3. Phase II: Further modifications and finalised design

3.3.3.1. Improved bioreactor system

Through use of the prototype system over time some further refinements which could be made were identified and implemented to aid with reproducibility and ease of use. The amount of handling required to fit Alvetex® into the spherical device whilst seeded with cells introduced a significant contamination risk as well as potential disruption to the cell membrane. On top of this the shape of the culture holder leads to an uneven level of shear stress across the membrane leading to heterogeneous conditions experienced by the cells and tissues.

To improve the apparatus a new stand was designed which built the previous baffle design into a holder which could accept 6- and 12-well Alvetex® inserts (Figure 3.28). This allows cultures to be transferred directly into the equipment from at 6-well plate without any further disruption required, or in the case of sandwich cultures simply the transfer of an unseeded Alvetex® membrane. Whilst this reduces the flexibility of the system to allow for different membrane orientations, the improved robustness of the created models leads to greater reproducibility of results, an important aspect for any cell culture system.

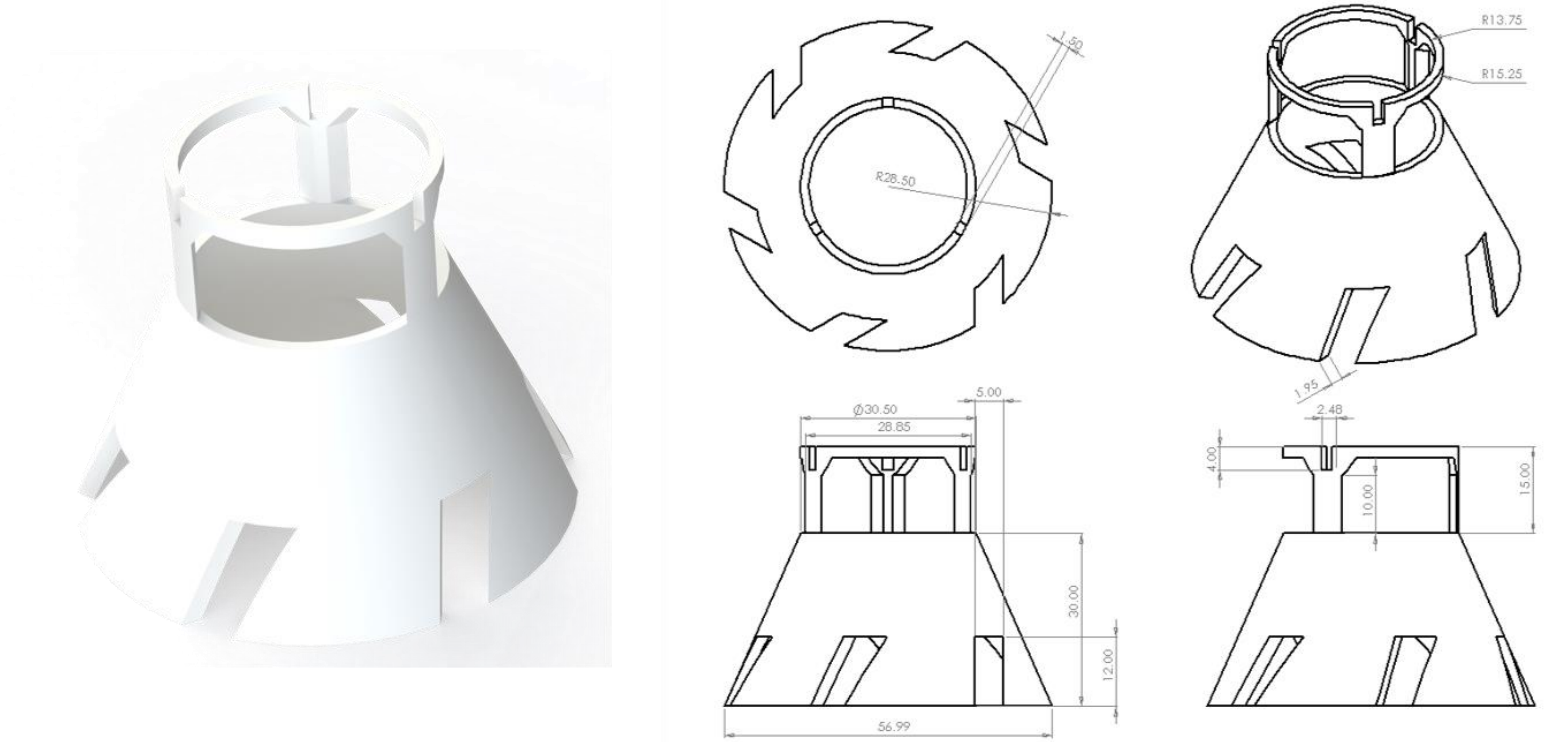

Figure 3.28: Conical stand with holder for 6-well Alvetex insert. The new design allows complete Alvetex inserts to be placed into the bioreactor with minimal additional handling. The dimensions are based on the original conical design with minor dimension changes. This also removes the need for the addition culture holder which was used in conjunction with the previous stand. The PTFE part was fabricated by Roechling-Fibracon. All dimensions are in millimetres. Full schematics can be found in Appendix 2.

To coincide with these changes the stir bar was replaced with a cylindrical one as described in Figure 3.29. A smaller cylindrical stir bar with a central ring was preferable with the new stands due to the lower position of the culture within the vessel leading to higher levels of shear stress on the cultures. The cylindrical nature of this stir bar also led to a smoother stirring motion than with the previous stir bar due to a reduction I friction with the bottom of the bioreactor vessel.

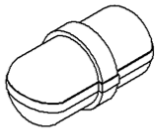

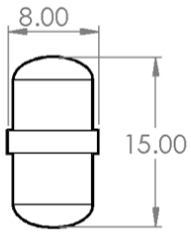

Material	PTFE
Dimensions (length x diameter)	15 mm x 8 mm
Supplier	Fisher Scientific UK

Figure 3.29: Magnetic Stir bars used for the final bioreactor system. Due to its smaller size this stirrer allows higher stir speeds to be used without causing deleteriously high levels of shear stress. This stir bar is available bulk packaged from Fisher Scientific UK. It is 15 mm in length with an 8 mm diameter and consists of a PTFE coated metal magnet. In contrast to the previous stir bar, this stir bar has a cylindrical profile from the front and has a central ring to ensure smooth rotation.

A further advantage of this design is the reduction in parts as shown in Figure 3.30 with just four parts being required, as well as the Alvetex® insert, all of which are autoclavable and indefinitely reusable. The removal of the disposable culture holder significantly simplifies the system to one which can easily be carried out by anyone working in cell culture with minimal experience required.

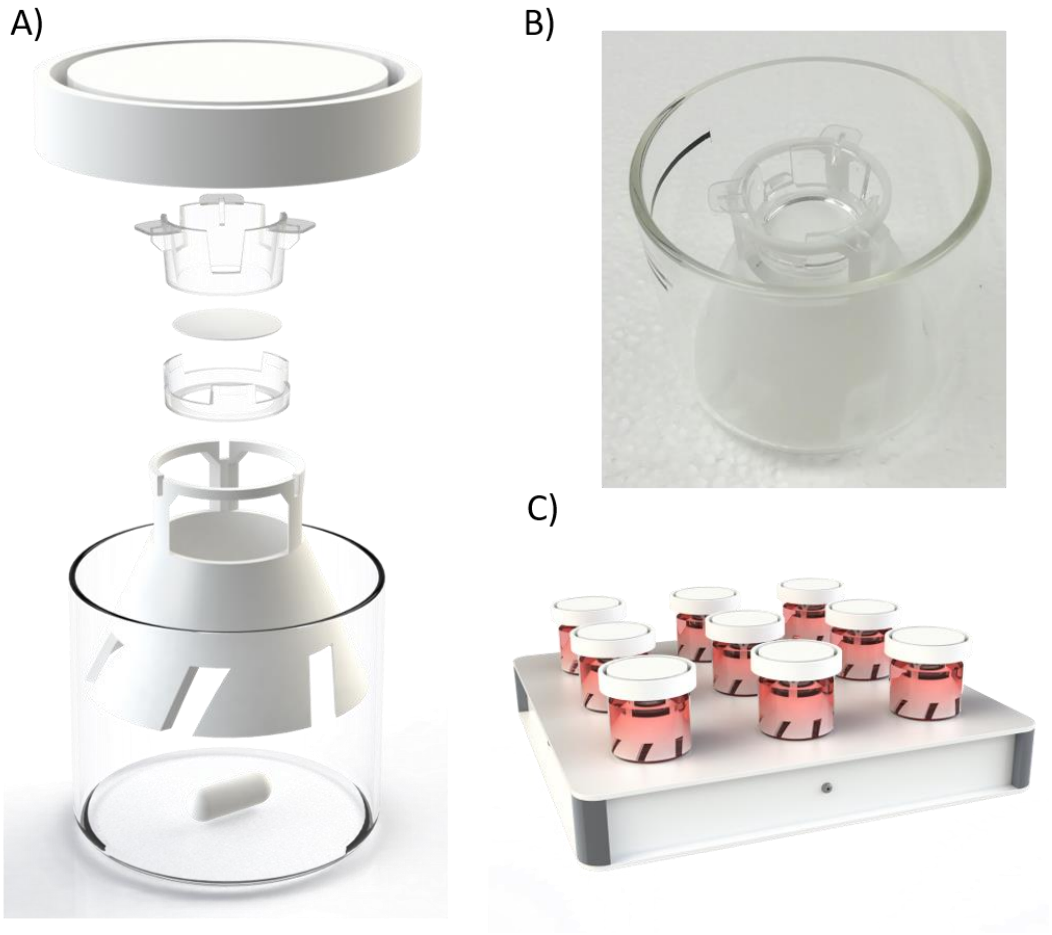

Figure 3.30: The complete final bioreactor design. This design incorporates includes the conical stand to hold a 6-well Alvetex insert and no longer uses the spherical culture holder. A smaller stir bar is also incorporated to compensate for the reduced disruption between the stir bar and the culture. A) Exploded diagram of the final bioreactor system with a 6-well Alvetex insert. B) Photo of the assembled system with a 6-well Alvetex insert but no lid or no culture medium. C) Render of the bioreactors on a magnetic stirrer with 100 mL of cell culture medium.

3.3.3.2. Custom magnetic stirrer system

To further increase the throughput of the system and increase user control a custom stirring system was produced as shown in Figure 3.31. This incorporates several additional design features to increase the reproducibility and fine tuning of cultures. Three stirrer units are driven by a control unit which can sit externally to the incubator. By moving all the power circuitry to the outside of the incubator the temperatures of the equipment can be reduced leading to a decrease in possible unwanted effects of improper culture temperatures.

Each stirrer unit has its own speed control to drive its nine stirrer points, which can be powered off and on in groups of three. The rotary motion is driven by a signal generator which causes the stepper motors to rotate at a finely controllable speed which is then displayed on the LCD screens. This accuracy ensures that the conditions in the culture system match the optimum conditions chosen through computer modelling.

All the units are sealed and have anodised aluminium top plates and waterproof electronic connections to improve durability for use in a humidified 37 °C incubator. Overall, the cost to produce this system was in the same range significantly as buying multiple commercially available stirrer units, therefore making it fairly accessible for use in academic laboratories.

Stirrer Dimensions (WxHxD)	230 x 51.5 x 370 mm
Stir Speed	80 – 288 rpm
Number of stir points	9
Distance between stir points	100 mmm

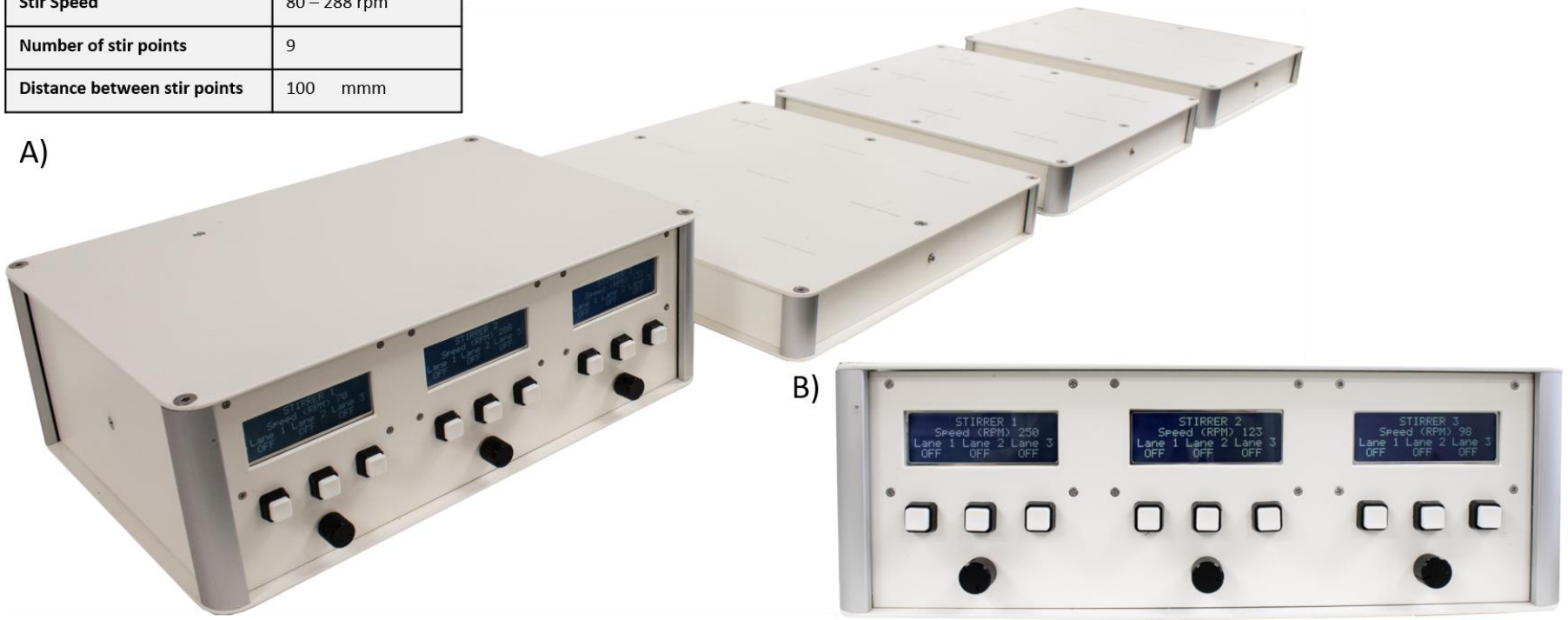

Figure 3.31: Custom magnetic stirrer system. The stirrer system was designed and fabricated by the electrical workshop, Department of Chemistry, Durham University. All the stirrers are environmentally sealed to ensure smooth operation in the heated and humidified atmosphere of an incubator. A) One control unit with three 9-point stirrer units. B) Front panel of control unit when powered on showing individual speed and channel controls for three stirrer units. Full schematics, including circuit diagrams, can be found in Appendix 2.

3.3.4. Characterisation of the final design

3.3.4.1. Computational fluid dynamics modelling on the macro scale

The final design was simulated at a variety of stir speeds using ANSYS Fluent. This allowed visualisation of the fluid flow direction at different points in the apparatus as well as giving meaningful values for properties such as the flow rate, turbulence, and shear stress.

Figure 3.32 shows the y-velocity in the x-y plane as a heatmap as well as the projected velocity in this plane as vectors. With this design there is a concentrated downwards flow in the centre of the beaker which draws the media through the cell culture as desired. Towards the bottom the outward pressure can be seen leading the media towards the walls of the vessel and then upwards with the help of the angled vents. Turbulence around the stir bar is effectively contained under the stand so that it reduces any effect it will have on the culture as shown by the earlier PIV results.

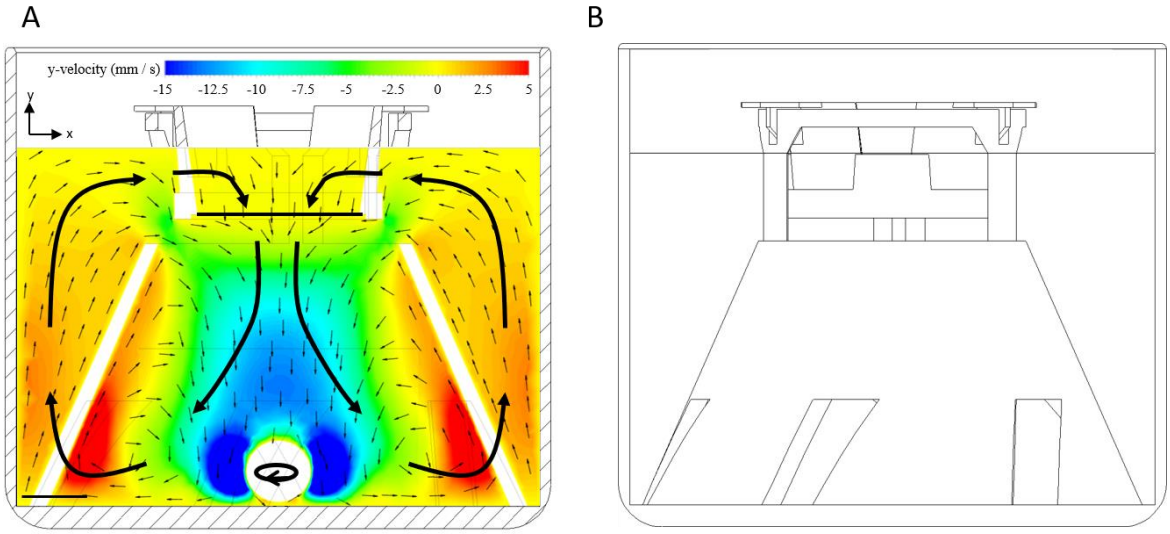

Figure 3.32: Computational Fluid Dynamics of the final bioreactor design. The system was modelled using ANSYS Fluent to examine the fluid recirculation through the system. A) Heatmap of the y-velocity of media within the system with evenly spaces vectors showing the direction of fluid at points in the system. Larger arrows have been added to show the overall fluid recirculation. B) A diagram of the bioreactor from the side to show how the fluid flow relates to the system. The level of fluid shown is when the bioreactor is filled with 100 mL of media.

Another advantage of this design is the greater uniformity of flow through the Alvetex® membrane (Figure 3.33). With the membrane holder used previously the fluid was diverted around the lower joint shielding the centre of the membrane and leading to radial variations in shear stress across the membrane. With the insert being used to hold the membrane there is no disruption to the flow

and therefore the cells will receive a more consistent shear stress directly from the stir bar with reduced spatial variability.

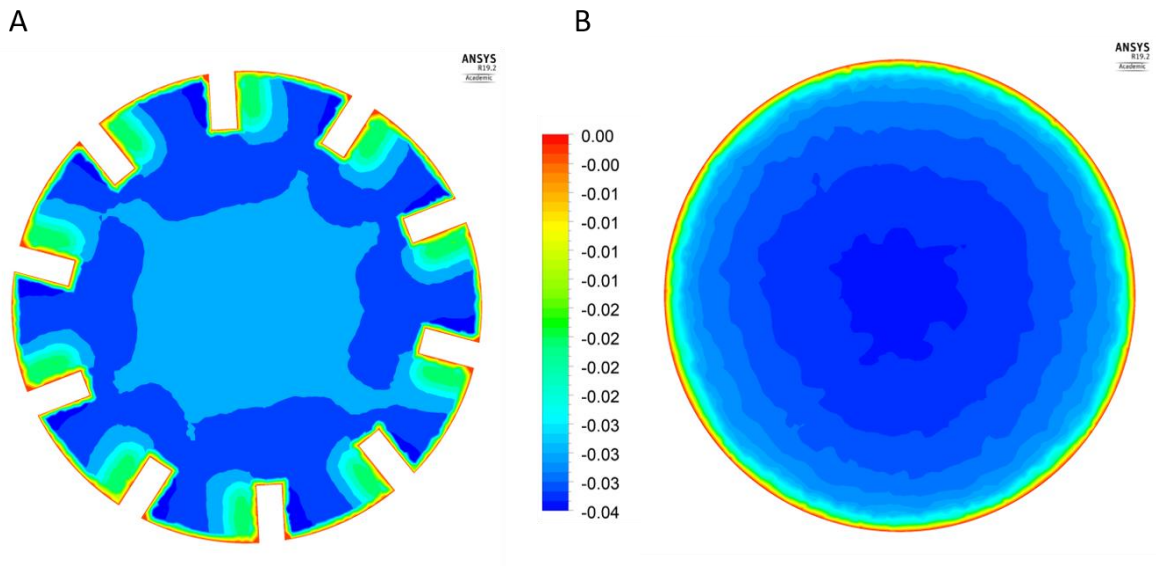

Figure 3.33: Vertical component of fluid velocity across the Alvetex® membrane for the two bioreactor systems. The velocity through the membrane is highly sensitive to changes in holder topography in the region surrounding the membrane. A) The velocity with the initial design incorporating the spherical membrane holder. The notches in the sides of the membrane are due to the regions where the holder clamps the membrane to secure it. B) The velocity in the final design utilising the Alvetex® insert as the holder. The simpler geometry of this design leads more consistent flow across the entire membrane.

3.3.4.2. Computational fluid dynamics modelling on the micro scale

To accurately model the flow in the stirrer to produce values for properties such as the shear stress on the culture the permeability of the Alvetex® membrane is needed. Utilising Darcy's law the permeability at a range of pressures was measured, shown in Figure 3.34. These results show the linear correlation for the membrane permeability with respect to pressure, verifying that the use of Darcy's law was valid. The resultant values are presented with the darcy unit, with a permeability of 1 darcy allowing a flow of 1 $cm^3 \cdot s^{-1}$ of fluid with a viscosity of 1 mPa·s across an area of 1 cm^2 under a pressure gradient of 1 $atm \cdot cm^{-1}$.

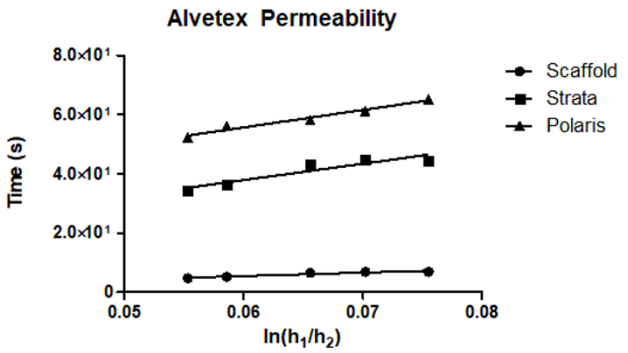

Alvetex	Darcy Permeability
Scaffold	5.5 ± 0.1
Strata	0.81 ± 0.02
Polaris	0.57 ± 0.01

Figure 3.34: Measurements for the permeability of different forms of Alvetex®. The permeability of the three forms of Alvetex® was measured using the Darcy method. The height of the head of water was set to a known level and the time taken to drop by 20 mm was measured. The permeability values can be calculated from the inverse of the gradient of this graph. From these results a decreasing permeability can be seen as the pore size of the Alvetex® decreases. A) Graph of time against the natural log of the starting height divided by the final height for the three forms of Alvetex®. Values are mean ± SEM. N = 3, n = 3. B) Permeability values calculated for each form of Alvetex® using the results of the graphs shown in Figure 3.34A.

The results show a value for the permeability of 5.5 ± 0.1 d for Alvetex® Scaffold, 0.81 ± 0.02 d for Alvetex® Strata and 0.57 ± 0.01 d for Alvetex® Polaris. These values are within the ranges of values calculated for other porous membranes produced by the polymerised high internal phase emulsion (PolyHIPE) method (Malakian *et al.*, 2019; Mravljak *et al.*, 2021). An attempt was made to calculate the permeability of a membrane with cells seeded to it, however this was unsuccessful due to the low permeability in such a situation leading to no measurable levels of fluid flow. For modelling purposes the culture was therefore treated as an Alvetex® membrane alone in the absence of cells.

Utilising the permeability values the Alvetex® can be modelled in the CFD model. This allows a value to be calculated for the transverse shear stress on the surface of the membrane. Figure 3.35 shows the change in shear stress at different stirrer speeds for Alvetex® Scaffold, Strata and Polaris.

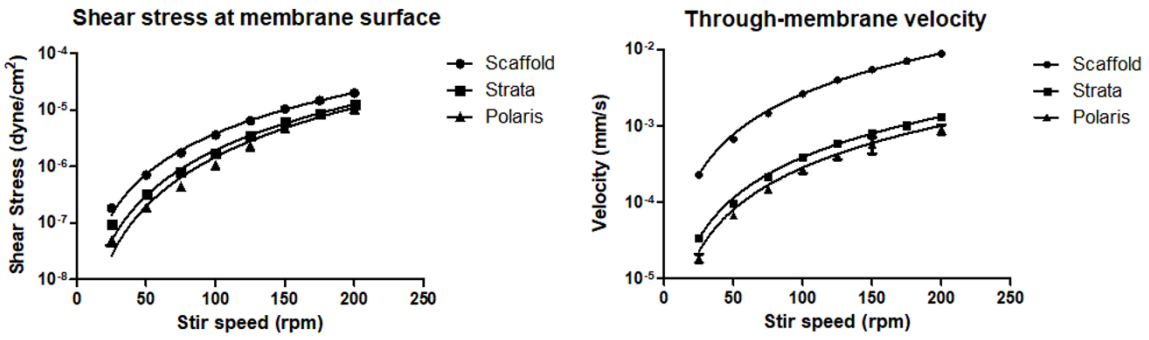

Figure 3.35: Shear stress and through-membrane velocity in the bioreactor system. Values are calculated at the upper surface of the Alvetex® membrane utilising the CFD analysis carried out previously. The decrease in permeability with decreasing pore size leads to a reduction in shear stress and through-membrane velocity. A) The value of the shear stress at varying stir speeds for the three different Alvetex® membranes in the system. B) The velocity in the y-axis at the membrane surface for the three forms of Alvetex® at different stir speeds. Both graphs show mass flow average ± SD.

From these data it is was decided that a stir speed of 100 rpm is adequate for the fluid flow requirements, giving a flow rate through the Alvetex® membrane of 3.6 x 10^{-6}, 1.7 x 10^{-6}, and 1.1 x 10^{-6} dynes/cm^2 respectively for Scaffold, Strata and Polaris. The shear stress on the membrane surface is in the same range as that typically found to be beneficial for the culture of hepatocytes (Leo *et al.*, 2009; Vinci *et al.*, 2011; Rashidi *et al.*, 2016), however the values at higher speeds also represent the shear stress endothelial cells receive in arteries (Ballermann *et al.*, 1998), showing the flexibility of this system for the culture of a variety of tissues.

3.3.4.3. Dissolved Oxygen levels in the bioreactor

One of the possible effects of fluid flow in culture is to the dissolved oxygen content. Disturbance of the air-liquid interface of the media can lead to a greater uptake of gas into the liquid, which could cause a higher level of media oxygenation. The stirrer could also be responsible for changes to oxygenation levels throughout the culture due to mixing of media reducing the lower oxygen conditions typically found towards the bottom of cell culture vessels.

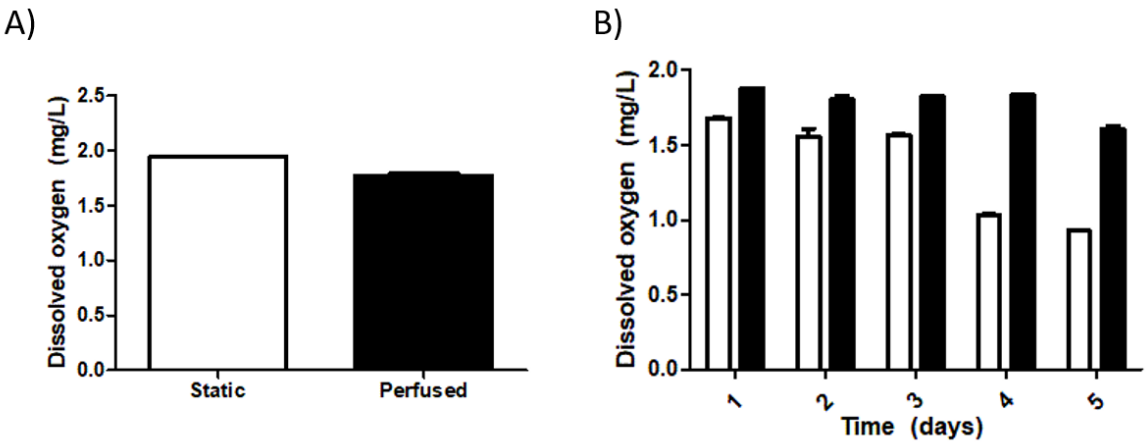

Figure 3.36: Oxygen levels in the bioreactor system compared to static culture. As oxygen is a key parameter in cell culture, accurate measurements of the dissolved oxygen levels in the system allow for a more accurate interpretation of the effects of the system. Oxygen measurements were taken using a PyroScience FireStingO2 oxygen meter with the probe clamped 2 mm above the membrane surface. A) Oxygen levels in the bioreactor with the stirrer off compared to when the stirrer is switched on at 100 rpm in the absence of cells. B) Measurements of oxygen concentration in the bioreactor over 7 days of HepG2 cell culture with and without fluid flow. Unfilled columns are static conditions, filled columns are stirred conditions. Both graphs show mean ± SD. N = 3, n = 1.

From the dissolved oxygen measurements (Figure 3.36) it is apparent that the levels within the cell culture media vary very little due to fluid flow. The stirred media shows a reduction in dissolved oxygen compared with static, however this is likely due to the change in temperature when the stirrer is switched on. Upon use, the stirrer raises the media temperature by roughly one degree Celsius, which would cause the reduction in dissolved oxygen seen. The lack in greater dissolved oxygen is likely due to the stirrer not rotating at a high enough speed to cause any noticeable disruption to the surface of the liquid.

When comparing between samples with cells in culture it is obvious that the stirred media maintains a higher level of dissolved oxygen through the media compared with static. This provides the cell surface with a greater turnover of oxygen, reducing potential hypoxic effects. The same result is seen in comparison with cells in a 6-well plate as well. This suggests that whilst the fluid flow has limited effects on the oxygen uptake of the media, the transfer to the cells can be increased therefore leading to the same effect as increased oxygen tension in static media would deliver.

3.3.4.4. Effects of stirrer speed

To ensure that the stir speed chosen was suitable for the culture of these cells the growth was tested at a variety of different speeds to compare the effects of each. A low speed of 50 rpm was used as the lowest value, 100 rpm as the standard value and 150 rpm as an upper value. As seen in Figure 3.37 the different flow conditions had a limited effect on the cultures however it appeared that the middle value, as selected previously, was the most successful at producing a thick hepatocyte tissue layer and this also demonstrated the highest metabolic values as seen in the MTT assay.

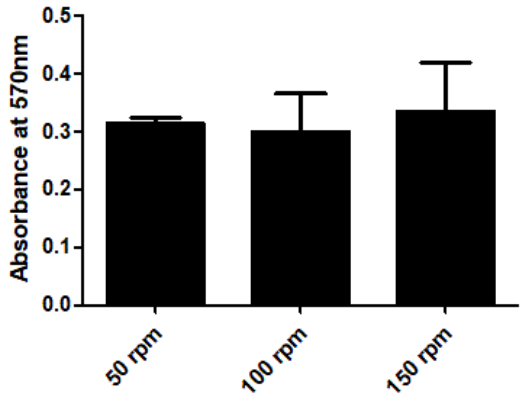

Figure 3.37: Comparison of cell viability at different stirrer speed settings. The stirrer was tested to ensure the speed settings with desired levels of shear stress as modelled can maintain cells. MTT assay of HepG2 cells grown in the bioreactor at varying stir speeds shows limited difference between the different stir speeds. This demonstrates that the system can support cells across a broad range of stir speeds and consequent shear stress levels. Values are mean ± SEM. n = 3.

These data back up the previously calculated stir speed value of 100 rpm for use with these hepatocyte cultures however also highlights the ability for the system to be useful at a range of stir speeds, which allows for matching of conditions *in vitro* to physiological conditions *in vivo*.

3.3.4.5. Physical effects of stirrer

Due to the potential use for long term cultures over several weeks with minimal or no media changes it is important to ensure that there is not a significant level of media evaporation which could lead to altered metabolism. For this media levels were measured over one month to investigate the rate of evaporation and whether this could be problematic for long term culture.

Figure 3.38 shows that the vessel does experience a low level of evaporation of approximately 5 mL per week, or 5 % of the total media volume of 100 ml. This is low enough that it is within tolerances for the successful culture of cells, as shown by the evaporation values for 6-well and 96-well plates in comparison with this system, whilst having the added benefit of reducing the sudden changes in conditions caused by media changes.

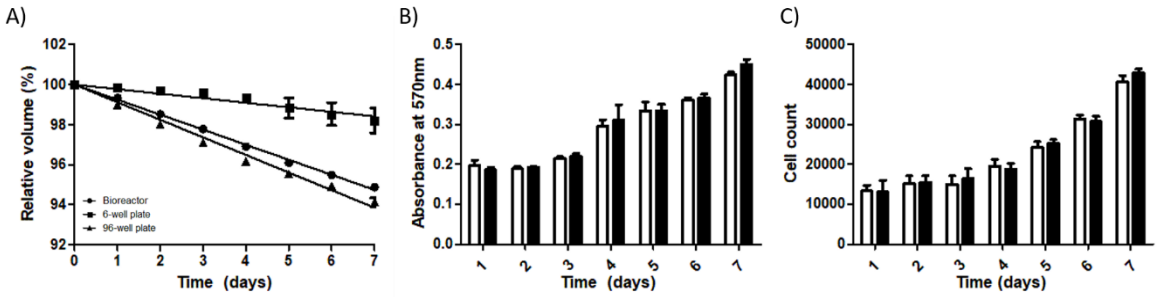

Figure 3.38: Media evaporation and degradation in the bioreactor system. Measurements show the impact of two major effects of long-term culture without media changing: media evaporation and degradation. A) Change in volume of media over 7 days as a percentage of the total mass in the bioreactor compared to 6-well and 96-well plates. Values are mean ± SEM. n = 3. B&C) Results of MTT assay and cell counts of HepG2 and HDFn cells grown in media conditioned over 7 days at 37°C compared to controls. Values are mean ± SEM. N = 3, n = 3.

Another factor which could affect cells grown using this method is the degradation of media components due to the use of a long culture period of 7 days with no media changes. In particular l-glutamine is known to have limited thermostability and a decomposition of this could lead to decreasing cell metabolism and proliferation (Khan and Elia, 1991). An MTT assay was run to assess the difference in growth using fresh media compared with media conditioned at 37 °C for 7 days, shown in Figure 3.38B and 3.38C. The degradation over one week does not appear to have a significant effect on metabolic activity of HepG2 cells. The scale of this impact is cell line dependant (Jagušić *et al.*, 2016) so for other cells, particularly primary cells, there may be a need for partial media changes or supplementation with thermostable versions of l-glutamine such as GlutaMAX to overcome this.

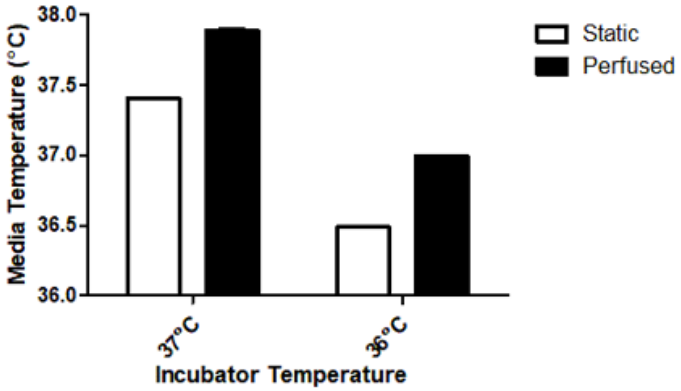

Figure 3.39: Media temperature in the bioreactor system. Different conditions were tested to investigate the changes in temperature. Temperature of media was investigated using incubators set to 36 °C and 37 °C. The bioreactor was placed on the stirrer which was either set to 100 rpm for stirred conditions or 0 rpm for static conditions. Temperature values are an average of 17,280 data points evenly spaced over 24 hours taken using an automated datalogger.

Further potential impacts from using a magnetic stirrer for cell culture are the heat generated and the dynamic magnetic field which it creates. Tests showed that the heat generated from the stirrer was enough to cause the cultures to sit roughly one degree higher than their optimum temperature as seen in Figure 3.39. This can be overcome by reducing the temperature of the incubator to compensate for this change. It was found that a reduction of 1 degree Celsius for the incubator led to a correct media temperature of around 37 degrees Celsius for cell culture.

An MTT assay shows that the effect of the magnetic field created by the magnetic stirrer has a negligible effect on the viability of the cells whilst visual analysis of the cells also shows no obvious changes to morphology induced by the magnetic field (Figure 3.40A). Direct measurement of the magnetic field using a gaussmeter shows the field at the level of the cell cultures to be less than 1 mT (Figure 3.40B), significantly lower than the levels commonly used for observing magnetic field-induced changes to cells (Miyakoshi, 2005; Kim *et al.*, 2016; Izzo *et al.*, 2019).

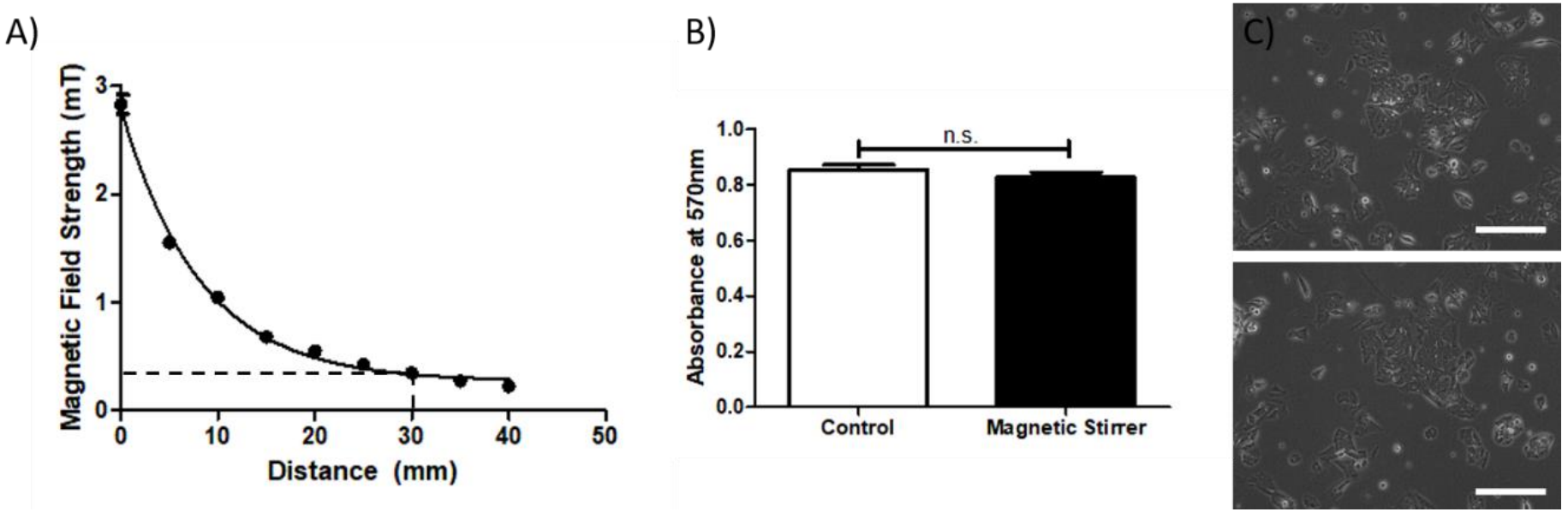

Figure 3.40: Magnetic field measurement and effects on HepG2 cells. Due to the potentially harmful effects of magnetic fields in cell culture the levels were tested, and cells grown in the magnetic fields to examine this. A) Direct readings of the magnetic field strength at distances from the stirrer. Dashed line indicates the level of the cell culture. Values are mean ± SEM. N = 3, n = 3. B) MTT assay of cells grown over 7 days in the magnetic field compared to control cells. Values are mean ± SEM, n = 3. C) Phase contrast images of cells grown in normal cell culture conditions (top) compared to those cultured in a static magnetic field (bottom). Scale bars are 100 µm.

3.4. Discussion

3.4.1. Development of a novel, three-dimensional cell culture bioreactor

Through this chapter the development and characterisation of a novel bioreactor for dynamic 3D cell culture has been presented with the aim of accurately recapitulating the *in vivo* microenvironment whilst maintaining ease of use.

Several designs for a baffle to control the fluid flow within the system were tested and a design finalised for using with the system. CFD, PIV and dye recirculation were used to examine the properties of the different stands to select one which had adequate recirculation as well as controlled turbulence away from the cell surface.

Cytocompatibility can be a big obstacle for reusable tissue engineering technology with commonly used materials. Many materials used *in vitro* have limited lifespans and cannot withstand routine sterilisation such as autoclaving. Some reusable polymers have other problems for example polycarbonate has been shown to release the estrogenic compound bisphenol-A when exposed to commonly used sterilisation methods such as autoclaving (Krishnan, Permuth and Alto, 1993) and ethanol treatment (Biles *et al.*, 1997). PTFE was selected due to its excellent chemical stability and high melting point allowing it to be repeatedly autoclaved. The experiments carried out showed that this is accompanied by high levels of cytocompatibility with no different between cells grown in PTFE conditioned media and control media, backing up the results from previous use of the polymer in cell culture (Ammar, Lagenaur and Jannetta, 1990). The use of PTFE for all the complex parts of the system coupled with glass for the external beaker allows the system to be repeatedly reusable whilst also retaining the required high levels of cytocompatibility.

Other effects of this cell culture method have been quantified and controlled to keep them within tolerances for cell culture. The strength of the magnetic field experienced by the cells is below 1 mT, significantly less than the levels which have been shown to impact cells in literature (Dini and Abbro, 2005; Miyakoshi, 2005). No other bioreactor stirred bioreactor system has reported the magnetic field levels, with many stirred system often having the cells in much closer contact to the magnets, therefore increasing the need for such measurements (García Cruz, Salmerón-Sánchez and Gómez-Ribelles, 2012; Liu, Li and Yang, 2014). Media temperature has been controlled to avoid the reduction in viability observed when temperatures rise above 37 °C and tests with the media have shown negligible effects from the use of media over prolonged periods for the cell lines tested, suggested issues such as the thermal degradation of L-Glutamine are not having a major impact on

cell growth. This is in line with literature suggesting that negative effects from l-glutamine degradation are cell line dependent (Jagušić *et al.*, 2016). This suggests that for the cell lines used herein, l-glutamine is suitable for long term studies however, for other cell lines which may be more sensitive, the replacement of l-glutamine with thermostable forms such as GlutaMAX would overcome this issue.

Through the process of testing the system further refinements were made and the design was updated to maximise ease of use and minimise handling, therefore increasing reproducibility of experiments. CFD analysis of the finalised design also showed it had improved fluid recirculation properties compared with the previous design due to lack of disruption in the space between the Alvetex® membrane and the stir bar, further improving reproducibility. Computationally modelling the system in this way is a powerful tool to investigate the fluid properties of a system and is becoming increasingly common in bioreactor research (Vogel *et al.*, 2007; Werner *et al.*, 2014).

Full analysis of the fluid mechanical properties of this system has been carried out to allow the bioreactor to be tailored for the conditions experienced in different tissues. Achieving the correct, tissue and cell specific, levels of shear stress *in vitro* is an important factor when creating a system incorporating fluid flow. Hepatocytes are an excellent example of this, with high levels of shear stress leading to a loss in viability and function (Tanaka *et al.*, 2006; Park *et al.*, 2007) whilst lower, microdyne/cm^2, levels lead to improved functionality and maintenance of viability and differentiation compared with static cultures (Leo *et al.*, 2009; Rashidi *et al.*, 2016). Using computational fluid dynamics, the levels of shear stress in the system has been calculated at different stir speeds. This method is frequently used in literature due to difficulties directly measuring shear stress in small, enclosed volumes used in cell culture. The large range of shear stress values that are achievable in this system not only cover those required for effective hepatocyte culture but also give the system flexibility for use with other cell and tissue types which require higher shear stress levels such as endothelial cells or bone (Leo *et al.*, 2009; Wittkowske *et al.*, 2016).

Oxygen transport can be a major problem in cell and tissue cultures, both with thick tissue slices or constructs which require high levels of oxygen to maintain viability (Drobner, Glöckner and Müller, 2000) and also for cells such as hepatocytes which use large amounts of oxygen to fuel metabolic processes (Brauer, 1963). The results from measurements of dissolved oxygen in the system show that whilst there is no change in the steady state levels of dissolved oxygen in the system due to fluid motion, the transport of oxygen throughout the media is significantly improved therefore

allowing the cells to receive a consistent supply of high levels of oxygen and minimising the deleterious effects of consumptive oxygen depletion (Place, Domann and Case, 2017). These results are comparable to the changes seen in literature for similar bioreactor systems and are therefore in-line with the expected levels (Bergemann *et al.*, 2015; Schmid *et al.*, 2018; Shoemaker *et al.*, 2020). This has the potential to improve culture viability and reduce the need for external oxygenation apparatus that is currently used in many cultures with high oxygen demands such as *ex vivo* tissue slices (Jeffries *et al.*, 2013; Pham *et al.*, 2015).

With larger volumes of medium often being desirable to ensure an adequate supply of nutrients, these often lead to an increased height of medium above the culture. This is a key factor which effects the levels of dissolved oxygen at the cell layer as an increase in the height of medium above the cells also leads to an increased diffusive barrier for oxygen (Pettersen *et al.*, 2005). This can lead to a reduction in dissolved oxygen over time, as oxygen is diffusing through the medium at a slower rate than cellular consumption, resulting in unintentional hypoxia of the cells (Metzen *et al.*, 1995). From the results with this bioreactor it is apparent that the convective mixing produced by the stirrer is able to overcome the limitations of oxygen delivery by diffusion alone, as has been reported elsewhere (Fleischaker and Sinskey, 1981). The system can therefore be useful in applications where a larger volume of medium is desired without sacrificing the oxygen delivery to the cells. A further benefit could be seen when culturing cells in controlled oxygen environments, such as for studies of hypoxia, as the levels of oxygen at the cell surface are more responsive and more closely follow the input levels (Allen, Schneider and White, 2001; Pavlacky and Polak, 2020).

The scale of the development process highlights the large number of variables involved in the creation of cell culture bioreactor systems. Often these factors are not reported in literature, or not accounted for at all, which can lead to potentially undesirable effects. It is therefore key that a thorough characterisation of the system has been carried out to make accurate comparisons with systems in literature and increase the understanding of the processes occurring within the cultured tissues (Salehi-Nik *et al.*, 2013; Mattei, Giusti and Ahluwalia, 2014).

3.4.2. Advantages of the novel bioreactor over other systems

This system has a series of advantages over many other bioreactor systems currently used for *in vitro* models. The use of a multi-position stirrer allows the system to maintain a small footprint, particularly when running at full capacity, along with being easily scalable. Many systems currently used in literature take up large amounts of bench space, even supposedly small microfluidic

systems. A recent paper found sizes in a range of 0.1 – 0.8 m^3 for the bioreactors reported (de Bournonville *et al.*, 2019). By contrast the system developed herein has a square volume of less than 0.02 m^3 for one stirrer with all 9 bioreactors running. Even with the control unit, designed to fit in otherwise unusable space such as above incubators, included, the system takes up roughly 0.03 m^3. While still two orders of magnitude larger than a typical microplate used for conventional cell culture this is significantly smaller than many systems described in literature.

The use of Alvetex® membranes in this system means that accurate comparisons can be made to equivalent experiments carried out in static conditions, therefore allowing the impacts of fluid flow alone to be elucidated. This also provides an environment which allows co-culture of multiple cell types within the Alvetex® membrane with distinct spatial patterning (Roger *et al.*, 2019; Darling *et al.*, 2020), something which is often difficult with some 3D techniques such as spheroids without the use of more complex techniques such as bioprinting (Otsuka *et al.*, 2013).

A further advantage with this system is due to the large media volume used within the bioreactor. This allows long-term culture to be carried out without the need for media changes. Regular media changes with lower media volumes can be problematic in cell cultures due to the temporal variation in nutritional status caused by media depletion as well as the sudden change in media composition that occurs when media changing. This can lead to variable growth profiles with cells most proliferative immediately after a media change (Griffiths, 1971).

Whilst many dynamic systems in literature also use large media volumes these typically have medium reservoirs external to the culture to support this, contributing to the increased physical size of the system (Tehranirokh *et al.*, 2013; Gilbert *et al.*, 2014; Paim *et al.*, 2018). By having the cells in a large vessel with this media it reduces the complexity and scale of the system. It is worth noting, however, that large volumes can be problematic for applications such as investigating the metabolism of novel drugs. Due to the large costs associated with producing drug candidates alongside often small quantities being produced it is often preferable to use small volumes in this situation.

The high level of complexity involved with bioreactor systems means that often many properties are left out during the characterisation stages. This can lead to unexplained variation in cultures alongside potential reproducibility issues and therefore it is preferable to investigate these parameters (Salehi-Nik *et al.*, 2013). In this chapter the characterisation has been carried out to incorporate as many different variables as possible. Most of this characterisation is precautionary

for properties that shouldn't be problematic levels for cell culture, such as the strength of magnetic fields. However, by having a thorough knowledge of the exact culture conditions within the system, the causes of any problems which occur down the line, for example if using highly sensitive cell types, can be more easily elucidated.

A final benefit of this system is the low-cost relative to other commercially available systems. The autoclavability of the entire system allows it to be full reusable, therefore eliminating ongoing costs for the system. The simple manufacturing processes required for production lead to fabrication costing very little, with each complete bioreactor costing less than £50 to produce for this project whilst the complete magnetic stirrer unit cost approximately £2500. In comparison with commercially available bioreactors this is significantly lower cost. The Synthecon RCCS-4H costs a similar amount for a system which runs 4 bioreactors simultaneously, compared with the 27 run by the system developed herein. Pump-based alternatives such as the 3D Biotek Bioreactor system costs over £10,000 each for a system to run 6 samples simultaneously (*3D Biotek Bioreactor System*, 2021), whilst the 3DKUBE system costs around £10 per disposable bioreactor chamber with an extra larger cost required for the peristaltic pump (*3DKUBE by Kiyatec*, 2021). For research use in academia, where this system is most suited due to the culture size and the system throughput, low costs are important and therefore this system become a very effective alternative to the other available systems.

Despite these advantages of the system, there are also some disadvantages. The use of stirrer provides limited control over the flow properties, despite use of a baffle to direct the flow. The overall recirculation pattern is difficult to change, therefore limiting this system to through-membrane flow only. The levels of shear stress are also closely correlated with the flow rate in the system. Therefore, it is difficult to increase convective mixing within the bulk medium without also increasing the shear stress experienced by the cells. The use of different forms of Alvetex® membrane gives a low level of control, however the morphology of these different forms also has an influence on the growth and behaviour of the cells.

Finally, the use of large volumes of media, whilst being beneficial due to reduced media changes and therefore more consistent conditions, can be problematic in some instances. The use of supplements with short half-lives, such as ascorbic acid, requires consistent addition to maintain correct levels (Golubitskii *et al.*, 2007). This leads to a requirement for frequent media changes, resulting in high media usage which can be problematic with expensive formulations. Alternatively, spiking the media periodically with the supplement is an option. This can also have issues such as

leading to a build-up of potentially harmful degradation products within the medium. The other limitation of high media requirements is that this also means large quantities of compounds are required in applications such as drug testing. Whilst not a problem for inexpensive and readily available drugs, higher cost drugs or those which are only available in small quantities would be difficult to test in this system.

3.5. Conclusion

In this chapter the development of a novel bioreactor which incorporates simplicity and ease of use, low cost and space demands and tuneable levels of fluid flow has been shown. The results of the CFD analysis show that the model can be used with physiologically relevant application to liver cell cultures with shear stresses matched to those found *in vivo* and a fluid flow rate that allows sufficient turnover of nutrients with a minimised unstirred layer at the cell-media interface.

The optimisation and development herein have led to an efficiently designed and user-friendly bioreactor system which meets all the criteria set out at the start of the chapter. The system allows finely tuneable fluid flow through the system which can be tailored for a variety of microenvironments. This bioreactor is novel as it uses the simplicity and scalability of magnetic stirrer-based systems and combines this with the capability to be used alongside commercially available 3D culture inserts to allow effective comparisons between static and dynamic conditions. The system is fully reusable and is fully compatible with autoclaving, disinfectant, and ethanol. On top of this the materials all display excellent cytocompatibility with no cytotoxic effects measured in experiments utilising conditioned media. The system is low cost due to the absence of complex equipment and the reusability further reduces ongoing costs.

Finally, the footprint of the system is reasonably small in comparison with the size of cultures achievable, with all the media contained within the beaker and therefore no external equipment except for a magnetic stirrer, the size of which can be chosen for the desired throughput and spatial constraints. Relative to other commercially available 3D bioreactor systems, the system developed in this chapter allows for greater throughput, reduced complexity, and consequently reduced cost.

With the design of the system finalised and many of the properties characterised, it is now possible to use this system for investigating the growth of cells under fluid flow conditions. This will initially start with the optimisation of growth of hepatocytes as a simplistic liver model and the capabilities can be expanded to include multiple cell types to look at the impact on the clinical relevance of the cultures.

Chapter 4: Optimisation and Characterisation of stirred HepG2 models

4.1. Introduction

A vast number of processes, such as drug metabolism and protein synthesis, are carried out by hepatocytes. It is therefore key that this is recreated in *in vitro* models of the liver, to provide optimal scientific and industrial value. As discussed in Chapter 1 there are a variety of properties which need to be introduced to fully recapitulate the liver microenvironment. The system developed in Chapter 3 aims to implement many of these in a controllable and physiologically relevant manner.

Many studies using bioreactors for hepatocyte culture suffer limitations due to the focus on bioreactor design parameters instead of the biological impact of the chosen variables on the cells. For example, measures such as albumin and urea secretion are often used as the sole outputs of improved hepatocyte phenotype, occasionally alongside specific metabolic enzymes (Park *et al.*, 2007; Baudoin *et al.*, 2011; Tan *et al.*, 2013). Meanwhile, factors such as cell structure and protein localisation are disregarded, despite their major effects on intra- and extra-cellular processes.

A complete characterisation of the generated tissue-equivalents is necessary to fully investigate the impact of bioreactors on cell function and a thorough understanding of the biology of the hepatocyte is required from both the structural and functional perspectives. In this chapter the structure and function of hepatocytes will be explored in depth followed by coverage of the *in vitro* methods used for their culture, building on the information presented in Chapter 1 and Chapter 3. Extensive characterisation of HepG2 cultures produced using our bioreactor system will then be performed to ensure the impact of this technique on the cells can be fully understood.

4.1.1 Hepatocyte function *in vivo*

As the primary parenchymal cell in the liver, hepatocytes account for roughly 80% of the cells in the liver by mass (Burt, Ferrell and Hubscher, 2017). Therefore, when creating *in vitro* platforms for studying the liver, the ability to maintain hepatocytes in an *in vivo*-like state is critical. Rapid dedifferentiation of primary hepatocytes *in vitro* is one of the main issues facing researchers looking to model the liver, therefore maintenance of the correct cellular conformation is a highly studied aspect of hepatocyte cell culture (Arterburn *et al.*, 1995; Bhandari *et al.*, 2001).

Hepatocytes exist in the liver lobules as hexagonal shaped cells. They have an apical domain facing other hepatocytes within the hepatic plate and a sinusoidal domain facing the sinusoids via the space of Disse and the sinusoidal endothelial cells (Kietzmann, 2017). The patterning of the cells in this manner is not identical for each cell and there can be multiple apical domains on a single hepatocyte depending on the exact placement of surrounding hepatocytes and sinusoids (Gissen and Arias, 2015).

The sinusoidal domain is coated with a variety of both export and import transporter proteins, such as the organic anion transporter polypeptides (OATPs), and is covered with microvilli to increase surface area (Kock and Brouwer, 2012; Schulze *et al.*, 2019). These microvilli can also contact the sinusoidal blood by extending through the space of Disse and through the fenestrations present in the sinusoidal endothelial cells, therefore preventing them from being constrained to the fluid in the space of Disse and allowing maximal mass transfer (Martinez-Hernandez and Peter S Amenta, 1993).

The contact region between hepatocytes forms two distinct domains; the lateral domain and the apical domain (Müsch, 2014). The lateral domain contains many junctional proteins to facilitate adhesion of cells and intracellular transport. It is typically grouped with the sinusoidal, or basal domain using the blanket term 'basolateral'. There are, however, significant differences between these to warrant keeping the two distinct for the purposes of discussing the specific structure and function of these regions (Bender, Büschlen and Cassio, 1998; Treyer, Aleksandr; Müsch, 2013).

The apical domain forms the bile canaliculi structure between two neighbouring hepatocytes bounded by tight junctions to maintain the integrity of the blood-bile barrier. The bile canaliculi form a channel between adjoined hepatocytes to transport bile out of the lobule and into the bile duct. Hepatocytes excrete a range of bile acids into these channels as well as some metabolites and other waste products (Strazzabosco and Fabris, 2008). The apical domain of the hepatocyte, like the sinusoidal domain, is covered with microvilli which can help to increase surface area and allow efficient secretion of molecules into the bile canaliculi (Arias *et al.*, 1993).

Effective recapitulation of liver function *in vitro* requires recreation of these structures and their associated cellular domains. By investigating junctional complexes, transporter localisation and the functional processes of hepatocytes, the parameters for a successful hepatic cell culture model can be generated.

4.1.1.1. Junction formation and development

Within the liver the majority of junctional complexes exist in hepatocytes (Vinken *et al.*, 2006). Non-parenchymal cells in the liver express few junctional complexes despite expressing some of the component proteins, for example Kupffer cells express β-catenin and connexin (Cx) 43 though have neither adherens junctions nor gap junctions (Monga *et al.*, 2001; González *et al.*, 2002). The quantity of junctions in hepatocytes highlights their need to function cooperatively and as such are highly important for maintaining hepatocyte polarisation.

Studies have shown that adherens junctions and gap junctions are required for various hepatic functions such as albumin secretion (Yang, Ichikawa and Tsuchiya, 2003), glycogenolysis (Stümpel *et al.*, 1998) and bile secretion (Nathanson *et al.*, 1999; Gonzalez-Sanchez *et al.*, 2015). Meanwhile the presence of Cx32 containing gap junctions and E-cadherin based adherens junctions has been shown to modulate some cytochrome P450 isoforms (Nicholson, Babcock and Pitot, 1994). This further demonstrates how an accurate recreation of *in vivo* structure with properly expressed and localised junctional proteins is a requirement for a successful *in vitro* model (Vinken *et al.*, 2006).

Gap junctions in hepatocytes are abundant, taking up around 3% of the total area of the cell membrane, and are key to the maintenance of function (Treyer, Aleksandr; Müsch, 2013). These allow for the passage of signalling molecules between adjacent hepatocytes and mediate the expression of many other hepatocyte proteins. In hepatocytes the key gap junction proteins are the connexins, of which Cx32 and Cx23 are the two typically found with roughly 90% of gap junctions containing Cx32 and 5% containing Cx23 (Neveu *et al.*, 1995). A loss of these proteins, particularly Cx32, is a result of many diseases such as fibrosis, cirrhosis, and hepatocellular carcinoma; meanwhile Cx43 is often upregulated in liver disease (Vinken, 2012).

Adherens junctions are typically formed from either E-cadherin or N-cadherin in hepatocytes (Hartsock and Nelson, 2008). These bind to the actin cytoskeleton within the cell via the catenin proteins as shown in Figure 4.1. E-Cadherin is typically found towards the periportal region of the liver acinus whilst N-cadherin has increased expression towards the perivenous regions suggesting a potential role for cadherins in organising the differential functions of hepatocytes in the different zones of the hepatic acinus (Doi *et al.*, 2007). Expression of the two cadherins is also tied to carcinoma cells malignancy, with a reduction in E-cadherin particularly correlating with poor prognosis. When working with cells derived from tissue such as hepatocellular carcinoma, as in this work, high levels of heterogeneous expression of the two cadherin proteins is hypothesised to be

a positive marker for improved cell function and reduction of the carcinoma phenotype (Liu *et al.*, 2015; Long *et al.*, 2015).

Tight junctions form between adjoining hepatocytes and maintain the blood-bile barrier in the liver tissue. These junctions are found at the sides of the bile canaliculi and separate this domain from the sinusoidal domain (Turksen and Troy, 2011; Pradhan-sundd and Monga, 2019). Key proteins involved in these junctions are occludin, claudin-1 and -2, and junctional adhesion molecule-1 (JAM-1) (Vinken *et al.*, 2006). As well as their role in maintaining the blood-bile barrier, tight junctions have many other functions in hepatocytes. For example, absence of JAM-1 has been shown to cause a complete loss of bile canaliculi alongside an increase in the expression levels of E-cadherin suggesting a feedback mechanism for maintenance of cell adhesion (Konopka *et al.*, 2007).

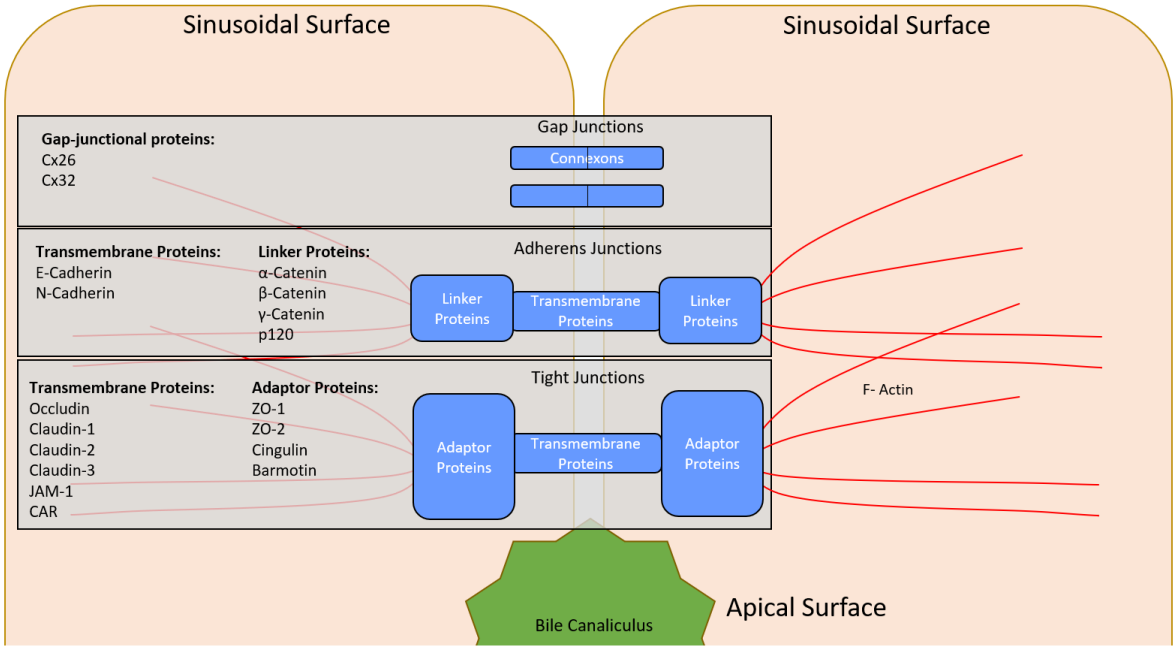

Figure 4.1: Common junctional complexes and proteins in hepatocytes. Gap Junctions are formed by connexin proteins forming structures called connexons. These facilitate exchange of molecules between cells. Adherens junctions consist of a transmembrane domain and linker proteins within the cytoplasm which connect the adherens junctions to the actin cytoskeleton. Tight junctions form a barrier between the sinusoidal blood and the canalicular bile. These consist of transmembrane proteins and adaptor proteins which link the junctions to the actin cytoskeleton.

Tight junctions are also important in a variety of disease mechanisms. Disruption of tight junctions leading to a loss of blood-bile barrier function has long been known to result from cholestasis (Kojima *et al.*, 2003; Pradhan-sundd and Monga, 2019), whilst claudin-1 and occludin have both been found to act as an entry point into the cells for viral hepatitis (Lee and Luk, 2010). Meanwhile

loss of tight junctions is seen in hepatocellular carcinoma and biliary tract cancer which could be involved in the loss of cell-cell adhesion and onset of epithelial to mesenchymal transition seen in these conditions (Németh *et al.*, 2009; Bouchagier *et al.*, 2014).

4.1.1.2. Transport

To facilitate the transport of compounds into and out of the hepatocytes, a wide range of transporter proteins can be found bound to the cell membranes. The distribution of these varies and is typically split between the apical and sinusoidal domains as shown by Figure 4.2 with most transporters facilitating transport only in one direction.

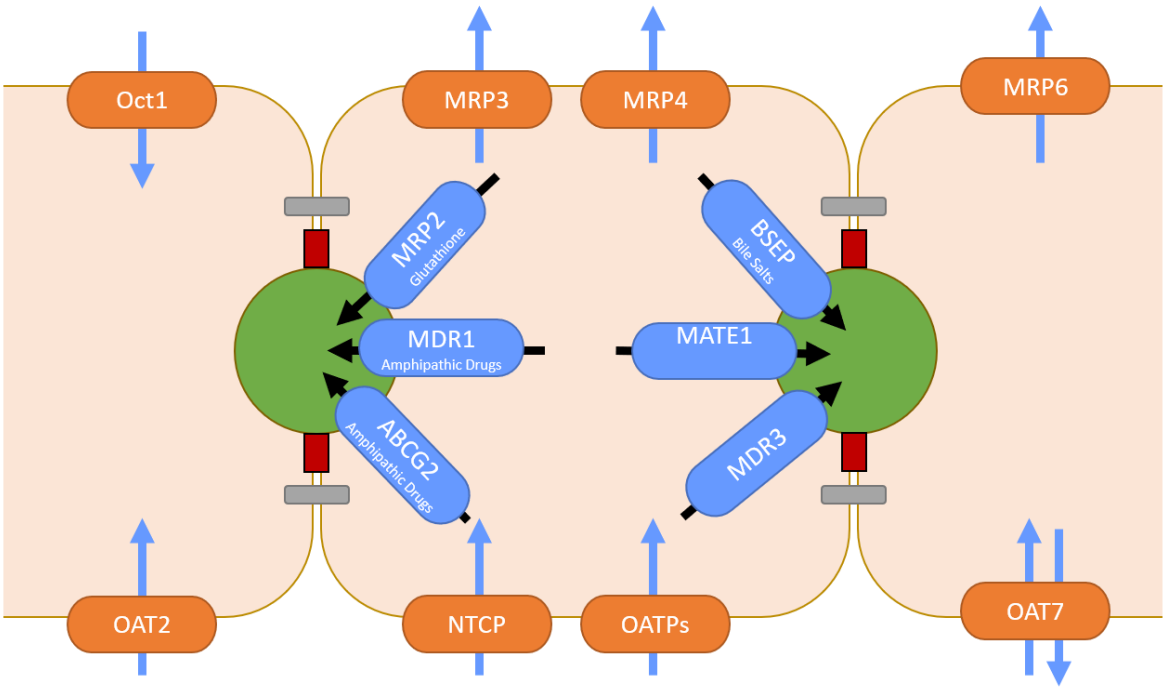

Figure 4.2: Transporter proteins and their localisation in hepatocytes. Hepatocytes express a wide range of transporters proteins with specific localisation based on the apical and sinusoidal domains. The apical domain has expression of many efflux proteins which transfer compounds such as bile salts and drug metabolites into the bile. On the sinusoidal domains there are transporters for both influx and efflux, allowing efficient nutrient exchange between the cell and the blood.

The cell membrane of apical domain contains a range of transporters to move metabolites into the bile as well as transporting bile acids. Some of the transporter proteins have specialised functions

such as bile salt export pump (BSEP) which carries out the task of transporting organic anions, including bile salts, into the bile canaliculi (Kubitz *et al.*, 2012), and multidrug-resistance-associated protein 2 (MRP2) which maintains high levels of glutathione (GSH) in the bile relative to the cell to facilitate osmosis of water into the bile canaliculi (Jedlitschky, Hoffmann and Kroemer, 2006). Other transporters in the apical membrane such as multidrug-resistance protein 1 (MDR1), breast cancer resistance protein (BCRP) and multidrug and toxin extrusion exchanger 1 (MATE1) have a much broader specificity and play a role in the biliary excretion of drugs and other compounds (Kock and Brouwer, 2012).

The sinusoidal membranes contain transporters from numerous families which facilitate both influx and efflux of substrates. The efflux transporters facilitate the removal of endogenous and xenobiotic compounds from the hepatocyte into the bloodstream. Sinusoidal multidrug resistance-associated proteins (MRPs) are involved in the transport of organic anions and of many conjugated drug metabolites for urinary clearance (Borst *et al.*, 2000). MRP3, MRP4 and MRP6 are commonly studied examples which can be found in hepatocytes, though other transporters from this family are also present (M Kool *et al.*, 1999; Marcel Kool *et al.*, 1999; Rius *et al.*, 2003; Bakos and Homolya, 2007). It is also worth noting that the expression of these transporters is not always limited to a single domain with MRP6, for example, having also been found in low levels in the apical domain in rat hepatocytes despite being predominantly expressed sinusoidally (Madon *et al.*, 2000).

Hepatocyte sinusoidal influx transporters are a broad group of proteins which have substrate specificities for a variety of different compounds. Bile salts are removed from the blood primarily through Na^+ dependent uptake, the proportions of which being approximately 80% for taurocholate and 50% for cholate (Stanca *et al.*, 2001). The Na^+-taurocholate co-transporting polypeptide (NTCP) is the major transporter for this pathway. The organic anion transporting polypeptide family (OATP) is responsible for the Na^+ independent uptake of amphipathic substrates whilst the organic ion transporter family (OAT/OCT) are responsible for Na^+ independent uptake of hydrophilic organic anions and organic cations(Geier *et al.*, 2007). Primarily OAT2 and OAT7 are responsible for the transport of hydrophilic organic anions and OCT1 for organic cations in the human liver (L. Chen *et al.*, 2014; Vildhede *et al.*, 2018).

4.1.1.3. Functional processes

The large amount of transport, both efflux and influx, of hepatocytes allows them to maintain a wide range of functional processes including glycogen storage, protein synthesis, and xenobiotic

metabolism (Figure 4.3). Many of these functions are not carried out solely in hepatocytes, however the high level of mass transfer in the surrounding vasculature supports high efficiency of these processes and consequent importance in homeostasis.

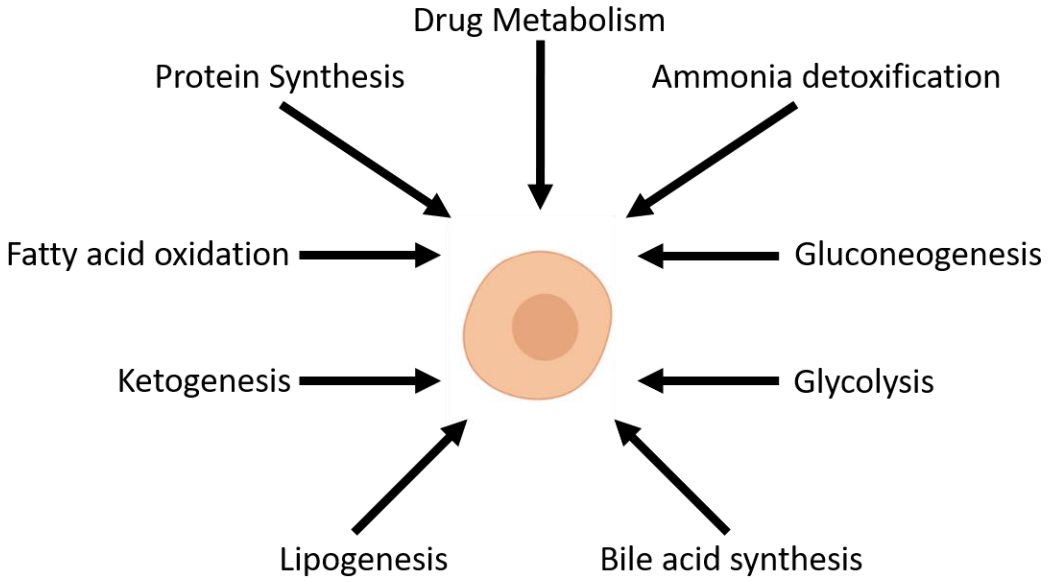

Figure 4.3: Functional processes carried out by hepatocytes. Hepatocytes are a major cell type involved in homeostasis due to the wide range of functions that they perform. This functionality varies depending on the specific location of the hepatocyte within the liver lobule, spreading the wide range of functional processes across hepatocytes in the entire lobule to allow them to function at a high efficiency.

The large scale production of proteins within hepatocytes leads to them having a high cytoplasmic content of excretory vesicles and mitochondria as well as an extensive endoplasmic reticulum and Golgi network (Malarkey *et al.*, 2005; Schulze *et al.*, 2019). Major proteins synthesised and secreted by hepatocytes include transferrin, plasminogen and fibrinogen (Tavill, 1972). These proteins are important not only in the liver but also for homeostasis of the entire body due to their wide-ranging functions. Another major protein synthesised by hepatocytes is serum albumin. This is produced in huge quantities and constitutes over half of the circulating blood plasma content; an average of around 10.5 g is produced per day by the adult liver (Levitt and Levitt, 2016). Due to these large quantities, albumin is often used as a simple measure of the functionality of hepatocytes under different conditions *in vitro*.

Hepatocytes have another major synthetic role in production of the components of bile (Zsembery, Thalhammer and Graf, 2000) including cholesterol, phospholipids, electrolytes, conjugated bilirubin and bile acids (Reshetnyak, 2013). Hepatocytes secrete bile into the bile canaliculi which transport

it to the gall bladder for storage and finally into the gastrointestinal tract (Boyer, 2013), where it enables the emulsification, digestion, and adsorption of fats in the intestinal lumen.

The xenobiotic metabolism in hepatocytes is carried out through the phase I and phase II enzymes, as discussed in Chapter 1. The major phase I enzymes are the Cytochrome P450 (CYP) superfamily, therefore these tend to be the most studied when looking at induction of the native hepatocyte phenotype *in vitro* (Ogu and Maxa, 2000; Bibi, 2008). Levels of CYP enzymes can be measured directly for both RNA and protein expression, however other common methods include luminescent activity assays (Westerink and Schoonen, 2007a) and measurement of metabolites in media for compounds which are a substrate of specific CYP enzymes (Pelkonen *et al.*, 1998). Despite other phase I enzymes being present in hepatocytes most of the research focuses on the CYPs due to their broad substrate specificity and involvement in the initial stages of biotransformation for a large number of drugs.

Phase II metabolism involves a range of conjugation reactions to make the substrates more polar prior to excretion. Activity of these is important for the completion of detoxification pathways and many thorough analyses of levels of phase II enzymes in different hepatocyte cell lines have been carried out (Hewitt and Hewitt, 2004; Westerink and Schoonen, 2007b).

Urea is another product excreted from hepatocytes which is a highly soluble metabolite of ammonia. Ammonia is formed in the body through the breakdown of amino acids and is a highly toxic compound in the body. In the liver, it is mainly converted to urea through the urea cycle (Häussinger, Sies and Gerok, 1985) and therefore urea cycle activity *in vitro* is often used as a marker for hepatocyte functionality due to the ease of measuring urea secretion with colorimetric assays (Donato *et al.*, 2008; Kim *et al.*, 2018).

4.1.2. Techniques and challenges associated with in vitro culture of hepatocytes

Culturing hepatocytes alone in vitro would appear to be a straightforward method to model a substantial proportion of the liver functionality. This would be particularly useful for studying hepatocyte specific functions such as drug metabolism and toxicity. The major drawback to this is the difficulty presented with culturing primary hepatocytes and the limitations of alternative hepatocyte cell sources. Development of novel cell culture techniques is therefore rapidly ongoing to allow for the culture of physiologically relevant hepatocytes with functionality maintained over the long periods required for many chronic toxicological studies.

4.1.2.1. Primary hepatocytes

Hepatocytes derived directly from liver are readily available from humans and other animal sources. These can be either fresh cells or cryopreserved, a process which has been shown to have minor effects on cell function however significantly improves the ease of use and reproducibility of experiments (McGinnity et al., 2004).

The major advantage of primary hepatocytes is the expression of all proteins which would be present in vivo, a property which no current hepatocyte cell line possesses (Guo et al., 2011). This is counteracted by the limited viability and proliferation in vitro which leads to a major challenge in creating an environment which can support the cells over prolonged periods of time. Methods such as collagen sandwich cultures (Swift, Pfeifer and Brouwer, 2011) and spheroids (Tong et al., 2016) have been utilised to improve the value of hepatocytes for in vitro studies however these still fall short of producing a model which is functionally stable over time. For the purposes of this work the cell line HepG2 will be utilised as an alternative to primary cells due to the ease of culture and ability to proliferate in vitro. This allows for the creation of high throughput, centimetre-scale cell constructs, something which is not possible with primary hepatocytes due to the limitations of cell yields.

4.1.2.2. Stem cell-derived hepatocytes

An alternative source of hepatocytes for cell culture comes from stem cells. These can be generated both from stem cells derived from the liver as well as stem cells from other tissues such as embryonic stem cells or induced pluripotent stem cells (Huch *et al.*, 2015; Garnier *et al.*, 2018; Dao Thi *et al.*, 2020; Messina *et al.*, 2020). The function of these cells is highly variable depending on the culture techniques used. Some studies show the cells to have limited polarisation and CYP expression (Corbett and Duncan, 2019) whilst others achieve high levels of expression for a range of drug transporters whilst also achieving high levels of polarisation and consequent directional transport (Dao Thi *et al.*, 2020). This variability between studies is a major limitation of stem cell-derived hepatocytes, caused by the wide range of techniques utilised for deriving these cells. The relative expression of CYP enzymes in embryonic stem cell-derived hepatocytes, for example, varies from 0 % to 90 % of that in primary hepatocytes between studies (Kia *et al.*, 2013). Meanwhile, many reprogramming techniques which use viral vectors can lead to unwanted genetic mutations which can affect the function of the resultant cells (Miyoshi *et al.*, 2011).

Use of hepatic progenitor cells to produce hepatocytes is a preferable alternative due to the minimal processing required to achieve differentiated hepatocytes. These can be created with high levels of phase I and II enzyme expression and therefore offer a valuable alternative to embryonic or induced pluripotent stem cells (Huch *et al.*, 2015). Though less work has been carried out using this technique, one of the key focuses for this at present is the ability to dedifferentiate mature hepatocytes into progenitor cells for the purposes of cell expansion (Garnier *et al.*, 2018). This therefore has potential to overcome the limited availability of primary hepatocytes, though the requirement for many expensive reagents to direct the differentiation processes means it will not be attempted in this work, where the aim is to produce a simple and low-cost alternative to primary hepatocyte cultures.

4.1.2.3. Hepatic cell lines

Hepatic cell lines are a commonly used alternative to primary hepatocytes. These are immortal cells typically derived from liver tumours and therefore proliferate indefinitely in culture. Due to their ease-of-use, high availability, and low cost these are frequently used in academic research. As discussed in Chapter 1, cell lines such as Huh7, HepG2, Hep3B and HepaRG are examples of frequently investigated cell lines for this purpose. Despite their high availability, these suffer from a significant reduction in expression of hepatocyte-specific genes, with a complete loss for some genes (Guo *et al.*, 2011; Gerets *et al.*, 2012; Yun *et al.*, 2019). The exact levels of expression are variable between cell lines, however HepaRG appears to be the most hepatocyte-like cell line in use at present (Jennen *et al.*, 2010; Gerets *et al.*, 2012).

When plated at low confluency the HepaRG acquire an undifferentiated morphology which can proliferate, providing constant supply of cells. When confluency is reached the cells differentiate into either hepatocyte-like or biliary epithelial cell-like (Guillouzo *et al.*, 2007). Upon differentiation the hepatocyte-like cells express high levels of hepatocyte-specific genes and perform key hepatocyte functions such as albumin secretion and drug detoxification (Parent *et al.*, 2004; Ramaiahgari *et al.*, 2017). Though an effective alternative to primary hepatocytes, these cells utilise expensive media supplements for propagation and culturing. Due to this the HepG2 cell line was instead chosen for the work carried out in this thesis.

4.1.2.3.1. HepG2 cells as an alternative to primary hepatocytes

The cell line HepG2 has been selected as a useful alternative to primary hepatocytes due to its ease of use and large quantity of background literature. This is an immortal hepatocellular carcinoma-

derived cell line which exhibits a hepatocyte-like phenotype and is widely used in industry and research (Aden *et al.*, 1979). Whilst these cells are not the most robust cell line for modelling hepatocyte function, they benefit from being highly proliferative and growing in very basic media formulations such as MEM and DMEM, a trait which is particularly useful when looking at co-culture with other cell lines (Donato, Tolosa, Laia and Gomez-Lechon, 2015). The use of immortal cell lines is also beneficial over primary cells due to the removal of inter-doner variability.

Table 4.1: Expression of various common phase I and phase II enzymes in HepG2 relative to primary hepatocytes. The lack of drug detoxification enzymes is a major issue for a lot of hepatocyte cell lines due to the impacts this has on predicting drug toxicity. Inducing these enzymes *in vitro* has become a target for a lot of literature aiming to increase the research value of hepatocyte cell lines.

Enzyme	Function	Expression in HepG2 relative to Primary Hepatocytes	References
Cytochrome P450s	Oxidation	Expression at least 10-fold lower in HepG2	Westerink & Schoonen, 2007 (A)
Methytransferases	Methylation	No Data	
Sulfotransferases	Sulfation	Generally similar levels in HepG2 and primary hepatocytes	Westerink & Schoonen, 2007 (B)
N-acetyltransferases	Acetylation	Generally similar levels in HepG2 and primary hepatocytes	Westerink & Schoonen, 2007 (B)
UDP-glucuronosyltransferases	Glucuronidation	Expression 10- to 100- fold lower in HepG2	Westerink & Schoonen, 2007 (B)
Glutathione s-transferases	Glutathione conjugation	Generally similar levels in HepG2 and primary hepatocytes	Westerink & Schoonen, 2007 (B)
Glycine N-acetyltransferases	Glycine conjugation	Lost in HCC	Matsuo et al., 2012

Like all immortal hepatocyte cell lines, HepG2 have a limited expression of key genes in the drug metabolism pathway as shown by Table 1. This can lead to results for drug toxicity which do not match the *in vivo* conditions due to under- or over-estimating the toxicity of compounds (Gerets *et al.*, 2012). Addition of CYP inducers to cell culture media has shown induction levels similar to those in primary hepatocytes, suggesting that expression of some of these proteins is not irretrievably lost (Choi *et al.*, 2015). Several studies have suggested that many of these genes can be upregulated with more physiologically relevant culture conditions such as 3D cell culture (Sreenivasa C. Ramaiahgari *et al.*, 2014; Luckert *et al.*, 2016). Another study has suggested that 3D culture has a limited impact on the levels of CYP enzymes in HepG2 with the variability coming instead from the longer time periods used for 3D culture (Luckert *et al.*, 2016). They found that when HepG2 were cultured in 2D for three weeks the CYP expression levels were often comparable to those in 3D cultures utilising collagen, Matrigel and Alvetex®, therefore counteracting some of the proposed benefits of 3D culture techniques (Luckert *et al.*, 2016). Further studies have also shown beneficial impacts on HepG2 from co-culture with non-parenchymal cells (Kostadinova *et al.*, 2013; Novik *et al.*, 2017) and perfused media (Allen, Khetani and Bhatia, 2005; Tostões *et al.*, 2012), both of which are factors which we are looking to incorporate with our system.

4.1.3. Methods to improve physiological relevance of hepatocyte cultures

Due to the difficulty with culturing hepatocytes *in vitro* a variety of methods discussed in Chapter 1 have been utilised, including those which change the structure of the tissues formed, incorporate extracellular matrix components such as collagen, and bring physiological properties such as fluid flow into the cultures.

4.1.3.1. Advanced Hepatocyte culture techniques

The enforced polarisation of 2D cell culture plasticware causes rapid dedifferentiation, loss of function, and reduced viability in primary hepatocytes. Figure 4.4 shows a selection of the most widely used methods found in literature, of which one of the first to be developed is the collagen sandwich culture. When grown on a single layer of collagen hepatocytes dedifferentiate and suffer from loss of function after about one week. The use of a second layer of collagen over the cells, creating a sandwich culture which simulates the space of Disse found to the sides of hepatocytes *in vivo*, has been used since to overcome these issues (Berthiaume *et al.*, 1996). When cultured in this way the cells express enhanced polarisation with the formation of sinusoidal and apical domains (Dunn *et al.*, 1989; De Bruyn *et al.*, 2013).

The use of ECM in hepatocyte culture has since expanded with a wide range of gels and scaffolds being created (Zhang *et al.*, 2018). Alternative proteins such as chitosan and alginate have been used to make scaffolds for hepatocytes either alone or in combination with other proteins (Chung *et al.*, 2002; Jiankang *et al.*, 2009). These have shown comparable results to collagen however include a wider range of physiological proteins therefore bringing them closer to the *in vivo* microenvironment. Alternatively, decellularized ECM scaffolds have also been widely used (Croce *et al.*, 2019). These create a complex 3D environment with a full complement of ECM proteins as seen *in vivo* as well as retaining the structural organisation of native liver tissue (Mazza *et al.*, 2015). Many studies have shown the benefits of hepatocyte cultures grown in decellularized scaffolds through improvements in long-term function and structural differentiation (Coronado *et al.*, 2017; Bual and Ijima, 2019); however the introduction of exogenous factors which cannot easily be quantified is a drawback of this method, particularly when using non-human tissue sources.

Synthetic scaffolds can also be used as an alternative to protein-based scaffolds. These can be produced with complex structures and benefit from the lack of exogenous material and batch variability therefore giving improved reproducibility with minimal risk of adverse biological reactions (Kazemnejad, 2009). These typically take the form of synthetic protein gels or polymer scaffolds and can be produced via a wide range of techniques such as electrospinning, emulsion templating and 3D printing. Similar beneficial results have been found with these as with ECM scaffolds with increased polarisation and expression of CYP enzymes often reported (Bokhari, Carnachan, Cameron, *et al.*, 2007a; Wang *et al.*, 2008) whilst the greater control offered by method such as 3D printing allows for the creation of more physiologically relevant structures such as liver lobule analogues.

For a much simpler and higher throughput method, the use of aggregates is common for hepatocytes. These are particularly useful for applications such as drug screening where large numbers of compounds need to be tested and therefore the scales offered by many scaffold-based techniques would be impractical. Hepatocytes have been shown to form bile canaliculi-like networks in aggregates (Abu-Absi *et al.*, 2002) whilst functional improvements also include increase in albumin and urea secretion and upregulated CYP expression (Chang and Hughes-Fulford, 2009; Mueller, Koetemann and Noor, 2011; Mueller *et al.*, 2014). Whilst factors such as ECM proteins can be incorporated into these, the major limitation of aggregate cultures comes from the limited control over structural formation (Sarika *et al.*, 2016). Further tissue engineering technologies such as bioreactors can also be more difficult to develop for aggregates due to their lack of anchorage

to a surface. This leads them to be easily damaged or washed away by the fluid flow (Tong *et al.*, 2016).

4.1.3.2. Introducing shear stress to hepatocyte culture

The impact of shear stress on hepatocytes and HepG2 cells varies depending on its magnitude. Many studies have demonstrated that shear stress detrimentally affects hepatocytes at levels greater than approximately 1 dyne/cm^2 through loss of viability, reduction in albumin and urea synthesis and decreased CYP activity (Tilles *et al.*, 2001; Tanaka *et al.*, 2006; Park *et al.*, 2007). One study has shown that 3D culture can protect from the detrimental effects of shear stress seen in 2D whilst also improving hepatocyte-like properties such as CYP activity (Rashidi *et al.*, 2016).

Due to this many bioreactors commonly used with hepatocytes utilise shear stress values in the microdyne/cm^2 range. To grow the cells in 3D a method of anchoring the cells is required and therefore scaffold-based methods are often used, with medium being perfused either across or through the membranes. Pump-based systems utilising scaffolds created from a range of materials have shown improved albumin and urea metabolism. These also maintain this function over multiple weeks, compared with the gradual reduction seen in 2D static cultures (Shvartsman *et al.*, 2009; Neiman *et al.*, 2015). Other studies have shown increased phase I and phase II expression using similar systems (Allen, Khetani and Bhatia, 2005; Altmann *et al.*, 2008; Vinci *et al.*, 2011), suggesting a significant beneficial impact from the inclusion of a perfused, 3D environment for HepG2 cell culture.

4.1.4. Commercially available hepatocyte models

A variety of commercially available hepatocyte models currently exist, incorporating a mixture of culture techniques and cell types. As can be seen in Table 2, the majority of these utilise primary hepatocytes, with only the Visikol OpenLiver™ model using the immortal HepaRG cell line (Visikol, 2021). The systems all incorporate non-parenchymal cells to varying degrees, with the Visikol model at the more complex end of the scale, being able to contain five different liver-specific cell types, whilst the BioIVT model more simply contains unspecified stromal cells (BioIVT, 2021). These all support the need for an effective liver model to ultimately be able to contain a variety of liver-specific cells for proper physiological function.

These models cover a significant range of scales with the spheroid-based systems being available in 384-well plates (Messner *et al.*, 2013; Visikol, 2021), meanwhile the HemoShear model uses large

75 mm Transwell. Only three of the systems incorporate fluid flow, two of which being in the form of microfluidics. Both microfluidic systems have demonstrated enhanced hepatocyte function and potential for disease modelling (Feaver *et al.*, 2016; Jang *et al.*, 2019). The Emulate Liver-Chip suffers from the limitation of limited cell-cell contact due to the very small growth surfaces used, whilst small media volumes can also lead to issues from factors such as media buffering, with higher concentrations of secreted factors from cells (Hughes, Kostrzewski and Sceats, 2017). Both systems also suffer from the scale limitation of microfluidic systems through the need for an external pump.

The HemoShear system bears the most similarity to the system developed in this work, utilising an insert-based culture in a large format. This model has been shown to improve hepatocyte function, with increased albumin and urea secretion and enhanced CYP gene expression (Chapman *et al.*, 2016). The utility of this system for modelling diseases has also been demonstrated, however there are limited publications available using this system (Dash *et al.*, 2013; Feaver *et al.*, 2016). This may be due to the large number of primary hepatocytes required, almost 10 million per model, being prohibitively expensive for many researchers.

Whilst this demonstrates that commercially available hepatocyte models can be created, the typically small size of the tissue constructs can limit the level of control over their structure and patterning. Therefore, the creation of centimetre-scale hepatocyte models incorporating properties such as fluid flow could be beneficial to many aspects of hepatic research.

Table 4.2: Basic properties of commercially available hepatocyte models. Most models utilise primary hepatocytes in combination with other non-parenchymal cells. A mixture of static and perfused technologies are available at varying scales. These systems often also incorporate non-parenchymal cells such as endothelial cells, Kupffer cells an d stellate cells.

Manufacturer	Model	Cells used	Culture Techniques	Static / Perfused	Scale	References
InSphero	InSight™ Human liver Microtissues	Primary Human Hepatocytes, Kupffer cells and endothelial cells	Spheroids	Static	96- or 384- well format	Messner et al., 2013
Organovo	ExVive™ Human Liver	Primary or iPS human hepatocytes, stellate cells and endothelial cells	3D Bioprinting, Transwell inserts	Static	24-well insert	Nguyen et al., 2016
BioIVT	HEPATOPAC® Technology	Primary hepatocytes and stromal cells	Micropatterned plates	Static	Up to 96-well format	Ramsden et al., 2014
Visikol	OpenLiver™ HepaRG™ NP 3D Model	HepaRG cells, hepatic biliary cells, liver endothelial cells, Kupffer cells and stellate cells	Spheroids	Static	96- or 384- well format	Visikol, 2021
HemoShear	Liver disease model	Primary human hepatocytes, stellate cells and macrophages	Collagen sandwich culture, Transwell inserts	Perfused	75 mm Transwell	Feaver et al., 2016
CN Bio	PhysioMimix ™ Liver-on a chip	Primary human hepatocytes and non-parenchymal cells	Collagen-coated scaffold, microfluidic chip	Perfused	12-well plate	Kostrzewski et al., 2017
Emulate	Liver-Chip	Hepatocytes, endothelial cells, Kupffer cells and stellate cells	Microfluidic chip with ECM coated channels and porous membranes	Perfused	N/A	Jang et al., 2019

4.1.5. Conclusions

Hepatocyte culture *in vitro* suffers from issues such as poor viability, limited proliferation, and loss of cell function. Through the introduction of the bioreactor system developed in the previous chapter, it could be possible to create a new platform for *in vitro* hepatocyte research. This would utilise the hepatocellular carcinoma cell line to minimise cost and maximise throughput with the bioreactor providing a microenvironment to enhance the hepatocyte-like function of these cells.

Creating a centimetre-scale hepatocyte model allows a range of interactions between cells to induce polarisation and increase metabolic function. This paves the way for less time consuming and more cost-effective *in vitro* liver models for applications such as drug development, where the improved predictive capacity could significantly reduce the investment required to create new drugs.

In this chapter a HepG2 model will be optimised using the bioreactor equipment discussed in Chapter 3. The optimisation will start at the basic levels looking at cell number and gross morphology and before moving on to an in-depth characterisation through techniques such as immunofluorescent staining, biochemical assays, and quantitative polymerase chain reaction (qPCR).

4.2. Hypothesis, Aims and Objectives

4.2.1. Hypothesis

From the work carried out in literature and the background on the liver microenvironment, we hypothesise that the application of fluid flow to *in vitro* liver models will have a beneficial impact on the cell structure and function. We further hypothesise that these beneficial effects will transfer across to hepatic cell lines such as HepG2, which are often used as a low-cost alternative to primary hepatocytes. Therefore, with the culture of HepG2 cells in a dynamic three-dimensional environment we would expect to see an improvement in function of key hepatic proteins and therefore improved utility of these cells as an alternative to primary hepatocytes.

4.2.2. Aims

The aim for this chapter is to develop and characterise a three-dimensional, stirred, hepatocyte model using the HepG2 cell line. The limited hepatocyte-specific function of HepG2 cells allows for analysis of a range of properties such as transporter protein expression and drug metabolism. The impact of a more physiologically relevant environment on HepG2 cells and whether this can be used to bring them functionally closer to primary hepatocytes will be investigated, whilst taking advantage of the cost and availability benefits of using an immortal cell line.

4.2.3. Objectives

1. Develop and optimise a protocol to incorporate the HepG2 hepatocellular carcinoma cell line into the bioreactor system developed in Chapter 3.

2. Investigate the structural characteristics of the HepG2 cells in this model with a focus on the induction and localisation of domain-specific proteins such as membrane transporters.

3. Investigate changes in expression of key hepatocyte-specific genes to assess impact of fluid flow on the functionality of HepG2 cells.

4.3. Materials and Methods

Most of the methods utilised in this chapter are as described in Chapter 2. However, some chapter specific protocols which have not been mentioned previously are described here. These include the methods used for generation of models for structural analysis and collection of media samples for metabolic assays. HepG2 cells are used for all cell culture in this chapter and are maintained as described in Chapter 2.

4.3.1. Culture of HepG2 models in static and flow conditions for initial optimisation

4.3.1.1. Static culture in the bioreactor and in a 6-well plate

Due to throughput limitations, it is preferable to run non-stirred samples in a multi-well plate rather than the bioreactor where possible for large optimisation experiments. This was carried out for the generation of models for gross morphological analysis, such as with the H&E staining during optimisation. More sensitive structural analysis, metabolic assays and PCR analysis was carried out using static culture in bioreactors due to their highly sensitive nature and to minimise the variables between conditions.

To confirm that models generated in the bioreactor without fluid flow and those generated in a multi-well plate are comparable side-by-side cultures of both were set up and analysed histologically. As can be seen in Figure 4.5 the gross morphology of the cultures under H&E analysis is comparable with no major deviations seen. Therefore, it was assumed that these could be used interchangeably for gross morphological analysis in the early stages of optimisation.

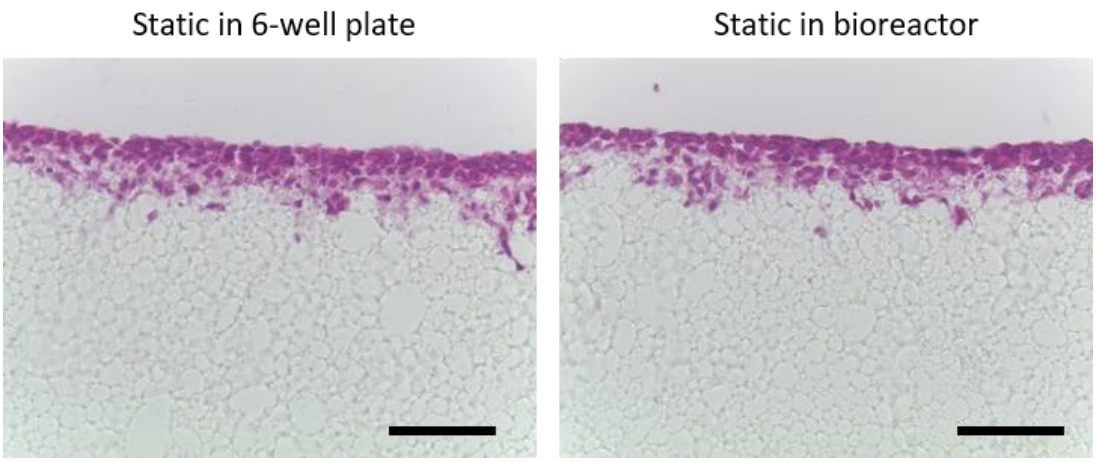

Figure 4.5: H&E stain of HepG2 grown in static conditions in a 6-well plate and a bioreactor. The two different methods show minimal difference in histological staining with comparable numbers of cells and levels of invasion into the substrate. Culture of HepG2 in static conditions in a 6-well plate dramatically reduces the media usage and allows greater throughput. This is therefore a beneficial alternative for initial optimisation experiments in which many different conditions are tested simultaneously. Scale bars are 50 µm.

4.3.1.2. Generation of HepG2 models for initial optimisation of conditions

The optimisation of culture conditions was carried out using a 6-well plate culture for static conditions and the bioreactor system for stirred conditions. HepG2 models were set up on 6-well Alvetex® as discussed in Chapter 2. Briefly, the models were cultured in MEM with 10 % FBS, 2 mM L-glutamine and 100 U/ml penicillin / streptomycin at 37 °C and 5 % CO_2. Media changes were carried out every 2 days. The samples were set up in triplicate with each condition occupying one row of a 6-well plate (Figure 4.6).

After 7 days of culture the media was aspirated from the wells. For static samples, the Alvetex® inserts were placed into a fresh 6-well plate and a further 5 mL of media added. These were then incubated for a further 7 days with media changes every 2 days as previously. For stirred samples, the Alvetex® inserts were placed into a sterilised bioreactor system containing 100 mL of prewarmed media. The lid was replaced in the vented orientation and the cultures were placed onto a magnetic stirrer in the incubator with each set of conditions occupying one 3-point lane on the stirrer. These were incubated for 7 days with no further media changes. At the end of the culture period the Alvetex® membranes were removed from the inserts and placed into a fresh 12-well plate. These were washed twice with PBS and processed for wax embedding or the MTT assay as discussed in Chapter 2.

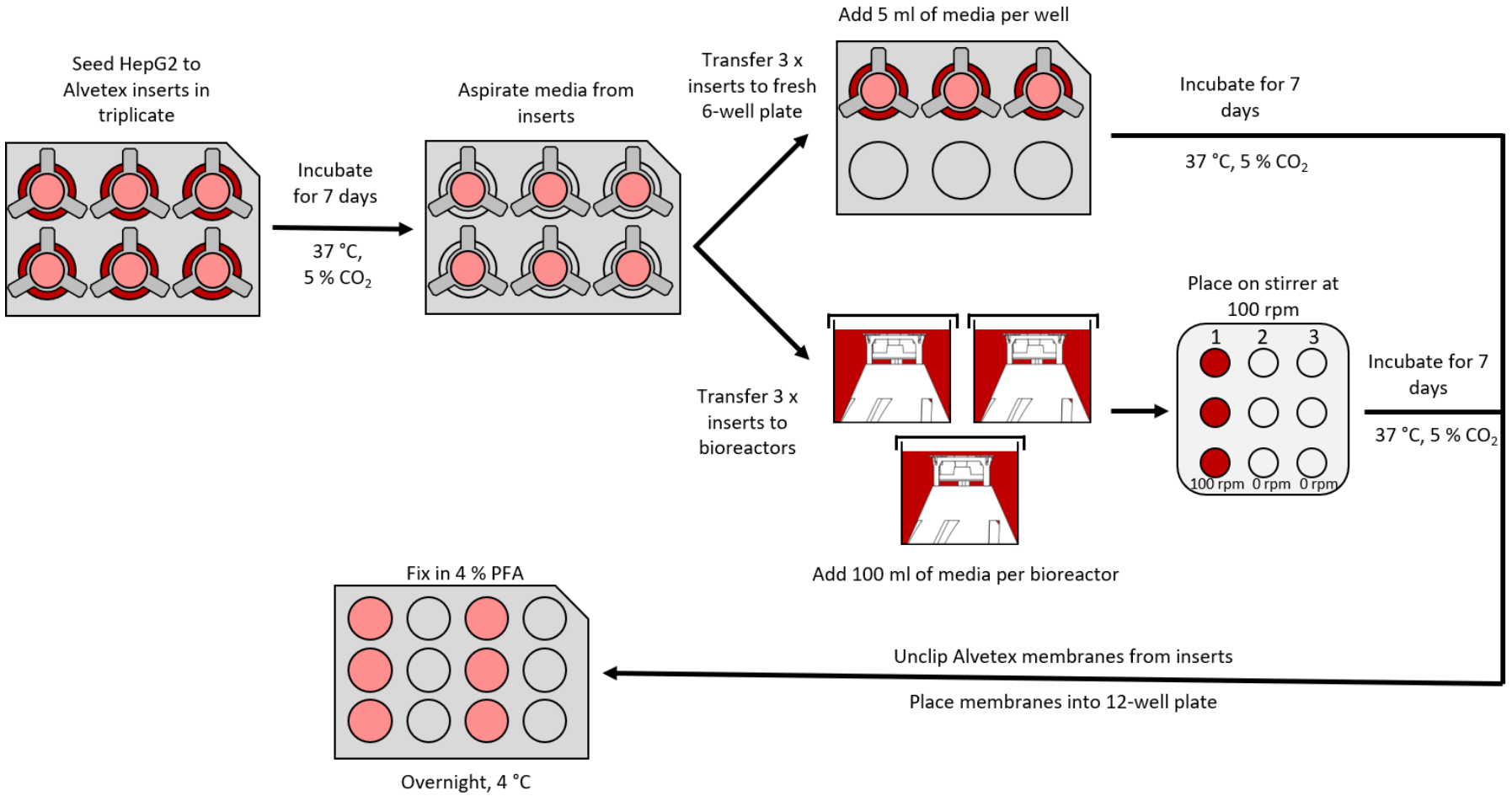

Figure 4.6: Protocol for setting up static models in a 6-well plate alongside bioreactor cultures. HepG2 cells are initially seeded into Alvetex inserts in a 6-well plate and cultured for a week to allow the cells to adhere and migrate across the membrane. After this period half of the samples are placed in a fresh 6-well plate whilst the other half are moved into the bioreactors containing 100 mL of cell culture medium. The bioreactors are placed on a magnetic stirrer at 100 rpm and both conditions are then cultured for a further 7 days before fixation.

4.3.2. Generation of HepG2 models for structural and functional analysis

For more complex analysis the cultures were all set up in the bioreactor system at the 7-day time point. Before the 7-day time point the culture conditions and initial setup were the same as for the optimisation cultures. These were set up in triplicate for each condition with comparable samples set up in the same 6-well plate where possible (Figure 4.7).

After 7 days of static culture the models were moved to their respective conditions. The samples upon being placed in the bioreactor were cultured on the magnetic stirrer in a 37 °C, 5 % CO_2 incubator with each condition utilise a lane of three stir points. The individual lane control of the custom stirrer discussed in Chapter 3 could then be used to have stirred lanes turned on and static lanes turned off whilst maintaining all other culture parameters.

The cultures were left to incubate for 7 days with no further media changes. At the end of the culture period media was aspirated from the bioreactors and the Alvetex® membranes were unclipped from the inserts and placed in a fresh 12-well plate. The samples were washed twice in PBS and processed for further analysis as discussed in Chapter 2.

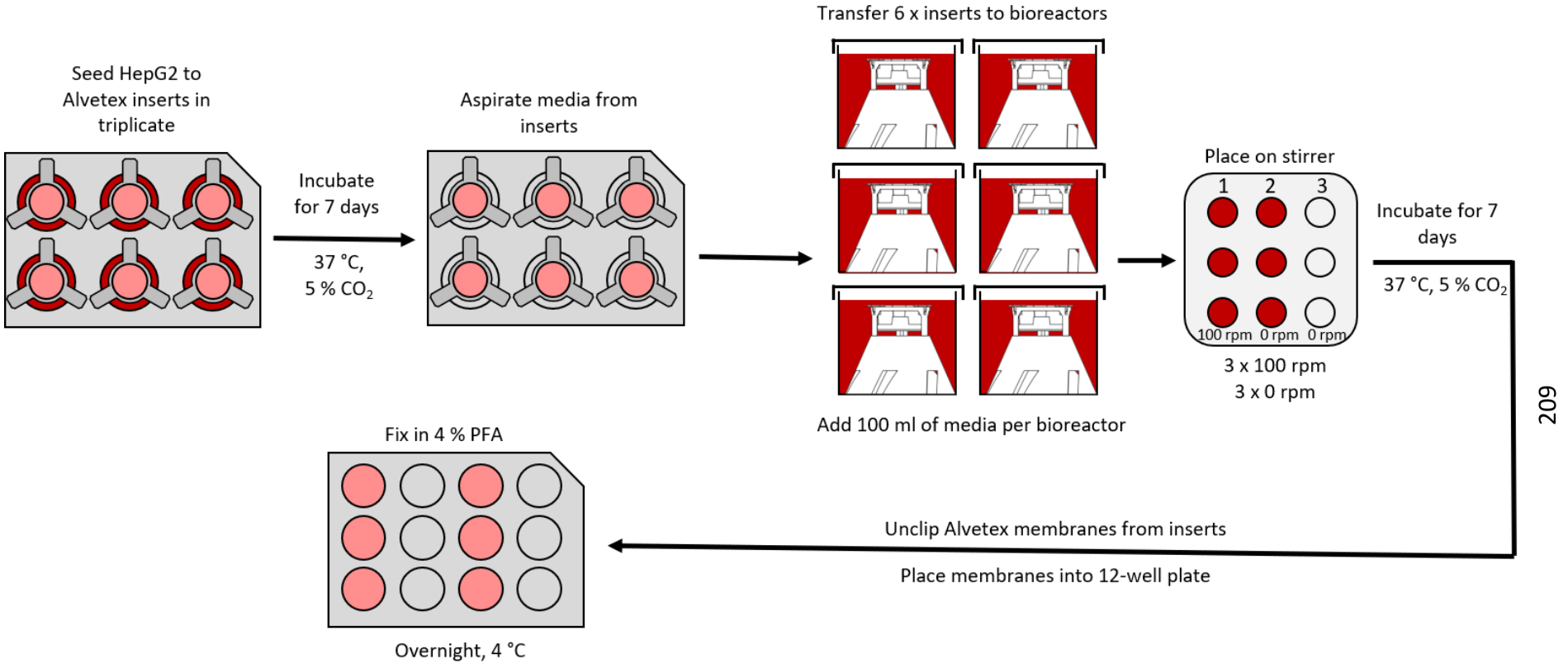

Figure 4.7: Protocol for setting up bioreactor cultures in in static and dynamic conditions. HepG2 cells are initially seeded into Alvetex inserts in a 6-well plate and cultured for a week to allow the cells to adhere and migrate across the membrane. The samples are then moved into bioreactors containing 100 mL of cell culture medium and placed on the stirrer unit. The stirred samples are placed on a lane set to 100 rpm and the static samples placed on a lane which is turned off. The samples are then cultured for a further 7 days before fixation.

4.3.3. Sampling of cell culture media for metabolic assays

Samples used for the albumin and urea assays were set up in the same way as for the structural and functional analysis cultures mentioned previously. Once these cultures were in the bioreactors after 7 days a 200 µL sample of media was taken from the media bottle and placed into a 500 µL Eppendorf tube. This was frozen at -20 °C until the assays were carried out.

After one day in culture the bioreactors were removed from the incubator and 200 µL of media was removed using a pipette with the sample taken from directly above the Alvetex® membrane. The samples were placed in a labelled 500 µL Eppendorf tube and frozen at -20 °C until needed. This process was repeated every two days until the final day of culture, resulting in 1-, 3-, 5- and 7-day time points. After the media for the final time point was collected the models were unclipped from the membrane and placed in a fresh 12-well plate. Models were washed twice with PBS and placed into a 1.5 mL Eppendorf tube containing MPER for lysis and protein quantification using the Bradford assay as described in Chapter 2.

4.3.4. Quantification of invasion and cell layer thickness

For quantification of invasion and cell layer thickness analysis the images produced from the H&E stains were quantified using the ImageJ image analysis software (National institute of Health, https://imagej.nih.gov/ij/). Nine representative images were used from each model with three models used per condition to a total of 27 images. The Analysis was carried out using ImageJ with generation of a grid with 9 evenly spaced points across the width of each image (Figure 4.8).

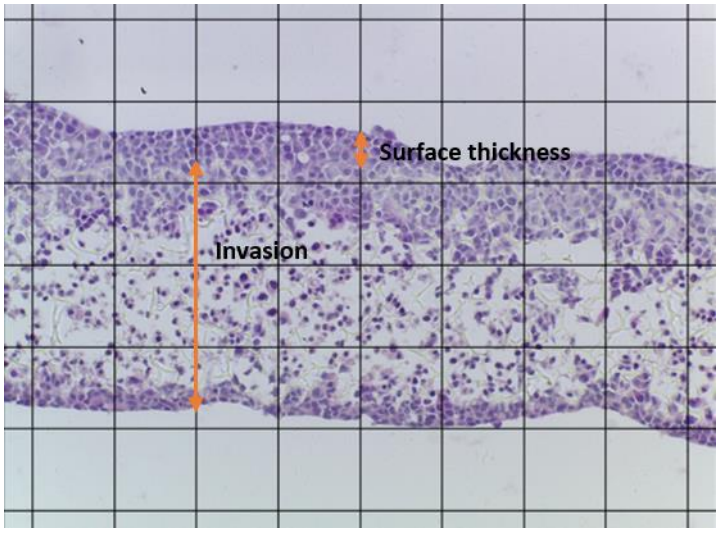

Figure 4.8: Quantification of growth characteristics of HepG2 cells on Alvetex using ImageJ. An equally spaced vertical grid was placed across the images. Using this as a guide a line was drawn vertically from the upper surface of the Alvetex to the top of the cell layer or the lowest cell in the Alvetex from that point respectively for cell layer thickness and invasion. Using the measure function the length of this line was calculated and recorded, and the process repeated at subsequent gridlines. An average and standard deviation of these results across nine images was calculated from these results.

For each point measurements were taken manually using the line tool to measure from the Alvetex® surface to the top of the cell layer or to the lowest cell vertically from that point for the cell layer thickness and cell invasion into the Alvetex® respectively. The results, a total of 540 data points per condition, were analysed in Microsoft Excel with the average and standard deviation for each condition calculated. The results were then exported into GraphPad Prism 5.0 for Windows (GraphPad Software, San Diego, California, USA) where visualisation into a bar graph was carried out.

4.4. Results

Initial growth and characterisation of HepG2 in static Alvetex® culture was first carried out to generate control cultures and investigate some properties in higher throughput multi-well plates. This was followed by the optimisation of the bioreactor protocol to generate robust and reproducible models. Once the optimisation was complete further characterisation of the liver-specific properties was carried out.

4.4.1. Culture of HepG2 cells on different forms of Alvetex®

To understand the growth properties of HepG2 on porous scaffolds the cells were initially cultured on the three different forms of Alvetex®: Scaffold, Strata and Polaris. From this it is possible to see the morphology of the cells on the different substrates as well as to investigate which substrate best supports healthy cell growth using histology and the MTT assay.

As shown by Figure 4.9, the cells had formed very different structures on the different membranes, with the porosity directly impacting their invasion into the substrate as well as their viability. Over one-week, HepG2 cells on Alvetex® Scaffold invaded around halfway into the scaffold and formed a loosely packed structure towards the surface. By contrast on Alvetex® Strata a small amount of invasion is seen with a thicker and more densely packed surface layer forming. With Polaris, no invasion is seen and instead a highly uniform, densely packed surface layer is produced. Viability on Polaris is significantly reduced, as can be seen by the pink cytoplasmic staining and dense nuclei in the H&E-stained samples as well as the significantly reduced absorbance value from the MTT assay (Figure 4.9B).

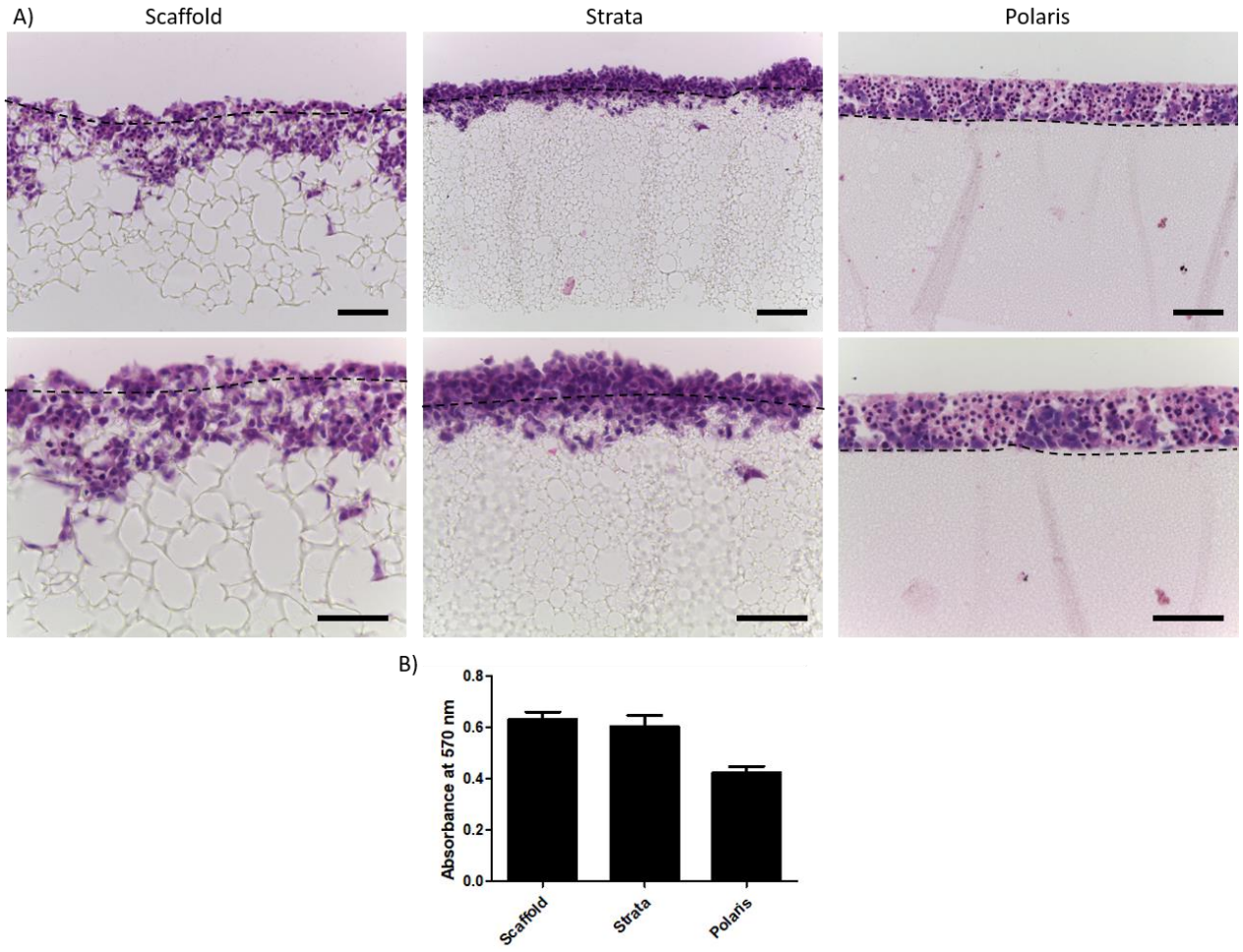

Figure 4.9: Growing HepG2 on different forms of Alvetex in static conditions. A) HepG2 cells display a different morphology on the different Alvetex forms with regard to the size of the surface layer and the level of invasion into the membrane. Scaffold, with the largest pores, displays high levels of invasion which is significantly reduced on Strata. Polaris exhibits virtually no invasion due to the pore size being smaller than the cells. Dashed lines indicate the surface of the Alvetex membrane®. Scale bars are 50 µm. B) MTT assay shows the similar levels of viability between Alvetex Scaffold and Strata with a reduction when grown on Polaris. Values are mean ± SEM, n = 3.

From these results Alvetex® Strata was selected as the most promising support for the HepG2 cultures, with an appropriate balance between forming a thick and uniform surface tissue layer to maintaining a high level of viability. Whilst the layer of HepG2 cells appears to be quite dense, the thickness is considerably lower than 200 µm, which is considered the diffusion depth of oxygen in avascular tissue (Carmeliet and Jain, 2000). It is therefore assumed that the cells are still able to receive adequate nutrients at the centre of this layer and remain in a healthy state. Further optimisation was carried out to look at how the seeding density of the cells affects the resulting tissue. As can be seen in Figure 4.10 the changes in seeding density have a noticeable effect on the thickness of the tissue layer formed at the end of the culture period with the lower two densities forming discontinuous cell layers. In the MTT assay the doubling of cell seeding density leads to a small increase in absorbance value suggesting that the relationship between seeding density and final cell density is not linear. The value of 2×10^6 cells per 6-well insert was chosen as the optimum seeding density, balancing the formation of a substantial tissue disc alongside using a practical quantity of cells.

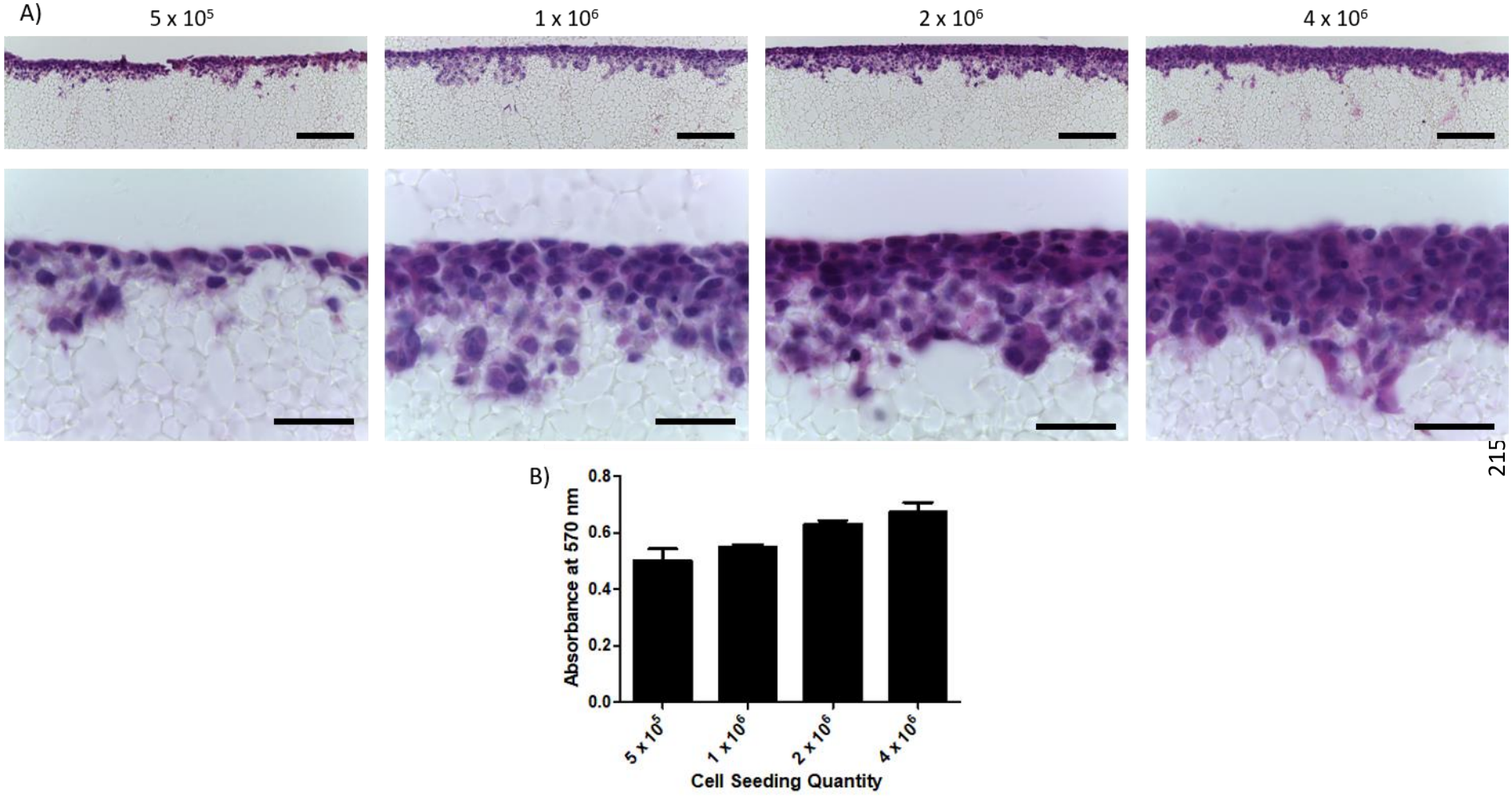

Figure 4.10: Investigating different seeding densities of HepG2 on Alvetex Strata. A) H&E Staining of HepG2 grown on Alvetex Strata at the four seeding densities investigated. All densities form a uniform cell layer however high densities lead to increased thickness of this layer. Scale bars are 100 µm and 25 µm respectively for low (top) and high (bottom) magnification. B) MTT Assay shows a small increase in absorbance with increased seeding density. Values are mean ±SEM, n = 3.

4.4.2. Effect of fluid flow on cell morphology and polarisation

To investigate the changes in morphology when cultured in flow conditions, HepG2 were cultured again on the three different forms of Alvetex® but this time in the bioreactor system. As shown by Figure 4.11 the predominant effect of this is on the quantity of cells present in the culture, which is noticeably increased under fluid flow, a result backed up by the MTT assay. The level of invasion into the substrate is also increased noticeably under fluid flow. With Alvetex® Scaffold complete invasion through the membrane is apparent, leading to loss of cells through the bottom of the membrane which is an undesirable effect. With Strata this is overcome with invasion significantly reduced whilst invasion is almost eliminated using Alvetex® Polaris. The surface layer thickness is similar in size between Strata and Polaris however the cells appear to be forming a more viable culture on Strata with cell morphology appearing healthier with less cell death, a finding supported by the results of the MTT assay.

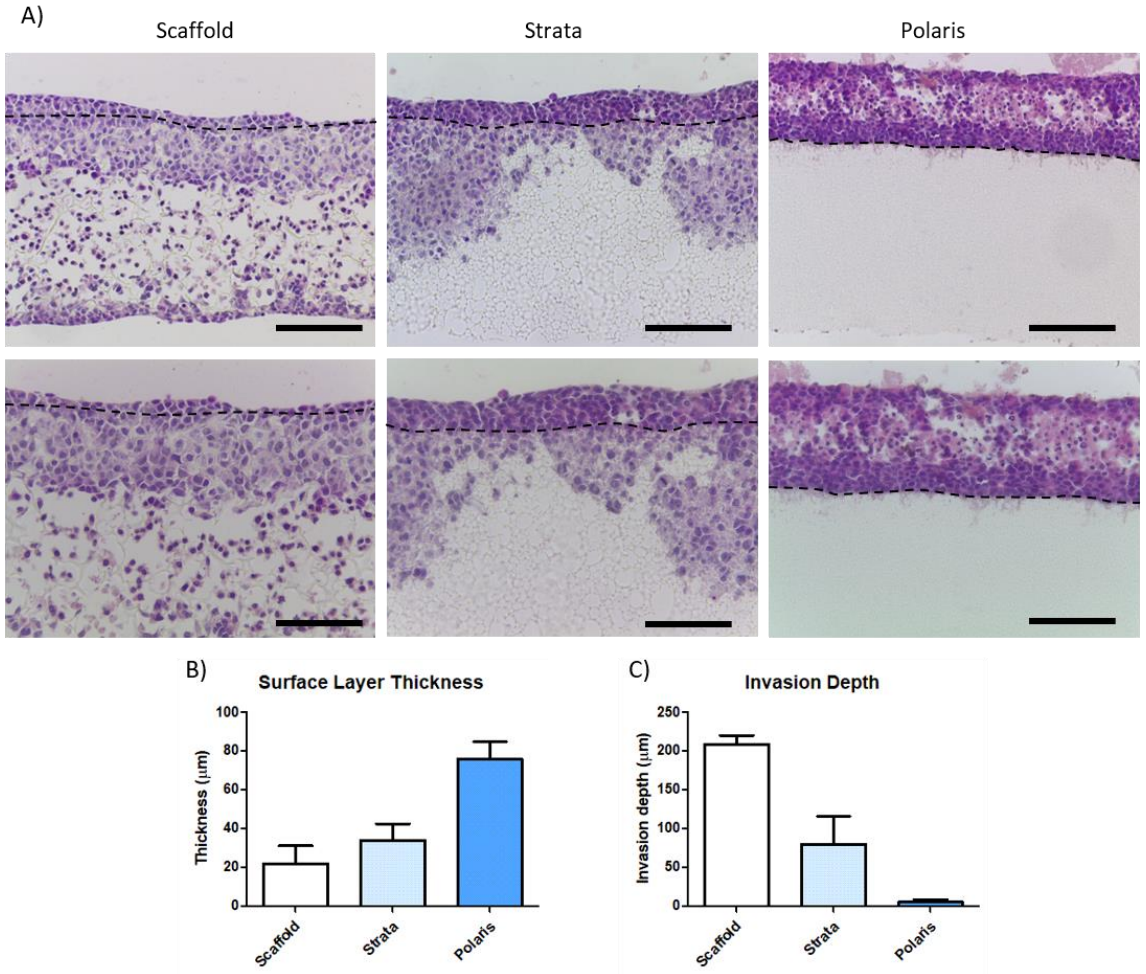

Figure 4.11: Growth of HepG2 on the three different forms of Alvetex in dynamic culture. A) H&E Staining of HepG2 grown on the different forms on Alvetex at high and low magnification. Major differences in cell layer thickness and invasion can be seen between conditions. Dashed lines indicate the surface of the Alvetex® membranes. Scale bars are 100 µm (top) and 50 µm bottom). B) Quantification of HepG2 cell invasion into the Alvetex membrane. C) Quantification of the thickness of the surface cell layer on the different Alvetex membranes. Both graphs show mean ±SD, n = 3.

4.4.3. Gross morphology of HepG2 grown on Alvetex® Strata in static and flow conditions

With the optimisation of the culture techniques completed the difference between a dynamic and static culture is shown in Figure 4.12. H&E staining shows the thicker cell layer and greater invasion present in the stirred models. The uniformity of the two models is confirmed by the H&E stain over the full length of the Alvetex® membranes displaying a uniform distribution of cells with minimal variation across the membrane (Figure 4.12B). This is further confirmed by the dark staining of the MTT assay which covers the entire membrane, with a few areas of low density visible in static and complete dark cover in dynamic conditions (Figure 4.12C). The absorbance values of the MTT assay are higher for the stirred sample despite the uniform coverage in both samples. The thicker cell layer present in the stirred samples (Figure 4.12A,B) explains this variation in MTT value, with the stirred samples appearing to have enhanced proliferation.

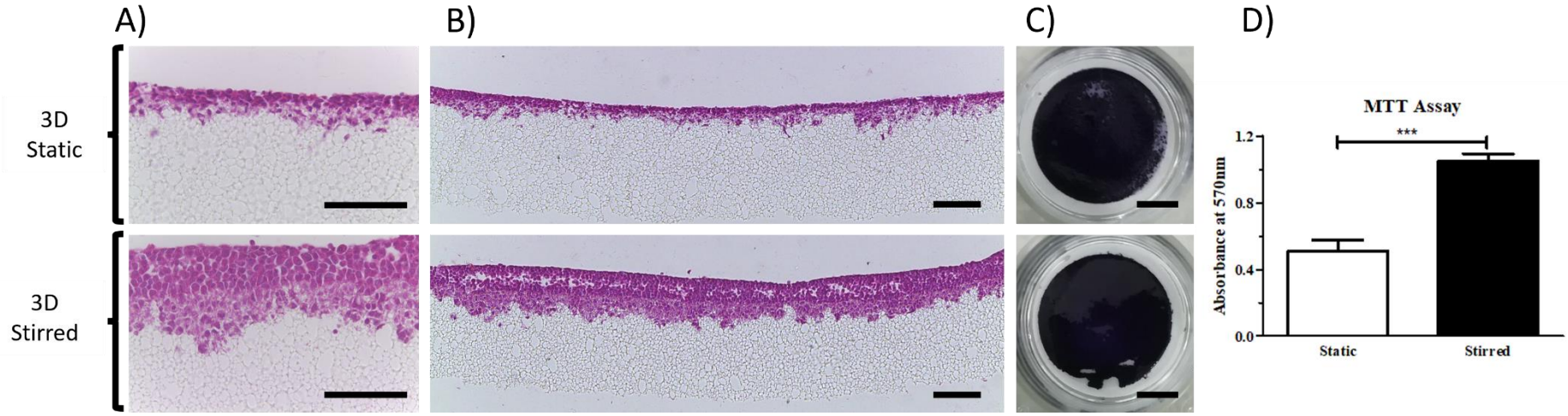

Figure 4.12: Properties of HepG2 cells grown on Alvetex Strata in static and dynamic conditions A) H&E stain of HepG2 cells grown on Alvetex Strata in static and dynamic conditions. The formation of a thicker cell layer and greater invasion can be seen in dynamic culture. Scale bars are 100 µm B) Lower magnification images of the H&E-stained models show even coverage of cells across the Alvetex membranes. Scale bars are 100 µm. C) Photos of the membranes after carrying out an MTT assay to show the even distribution of cells across the membrane. Gaps seen in the staining are likely due to disruption when removing the membranes from the inserts. Scale bars are 5 mm. D) Results of the MTT assay for HepG2 on Alvetex Strata in static and stirred conditions. Values are mean ± SEM with N =2, n = 3. Significance values calculated with an unpaired t test: *** = $p \leq 0.001$.

4.4.4. Immunofluorescent analysis of HepG2 cultures in static and fluid flow conditions

Immunofluorescent staining is a valuable tool to investigate the expression and localisation of proteins within a cell or tissue. This can be used to look at the changes in expression of proteins of interest when making the change from 2D culture to 3D culture as well as any further changes induced by media flow. The proteins investigated here reflect the wide range of hepatocyte functions, from health and proliferation to molecular transport and the formation of polarised structures.

4.4.4.1. Cell death, proliferation, and oxidative stress

The initial staining of the cultures investigated the health of the HepG2 cells using markers of apoptosis and proliferation as well as oxygen stress (Figure 4.13).

Cell death was examined using the TUNEL assay (Figure 4.13A) and the cleaved form of the caspase 3 protein, found in apoptotic cells (Figure 4.13B). Both these markers show an absence of expression in static cultures whilst a low level is present in the centre of the stirred cultures likely due to a lack of nutrient diffusion to the centre of the thick cell layers. A representative image of a region with this cell death present has been displayed however this expression is not uniform across the entire cell layer, suggesting the regions of cell death are localised. Ki67, a protein used as marker of cell proliferation, shows uniform expression across all culture types with minimal variation between them suggesting no inhibitory processes such as contact inhibition are taking place in the different culture methods (Figure 4.13C).

Hypoxia-inducible factor 1α (HIF-1α), expressed when a cell is suffering from hypoxia, is visible across all HepG2 cells in static 2D and 3D culture (Figure 4.13D). In contrast to this the stirred 3D culture of HepG2 cells has an absence of HIF-1α expression.

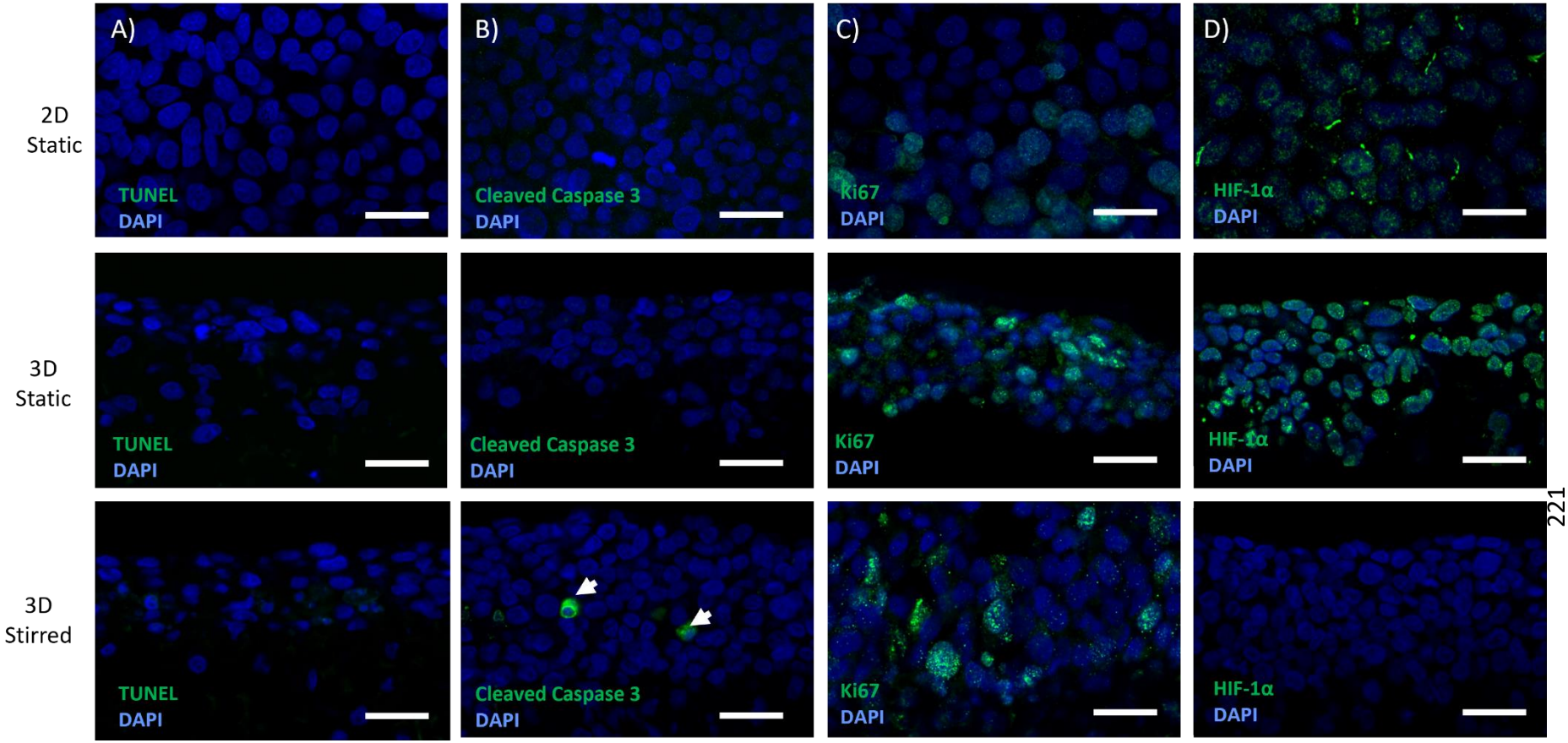

Figure 4.13: Immunostaining of the different HepG2 models with viability and cell health markers. A & B) The TUNEL stain and cleaved caspase 3 show minimal cell death in all of the models suggesting a high level of viability and absence of necrotic core. A small number of apoptotic cells can be seen in stirred conditions, indicated by the white arrows. C) Ki67 shows high proliferation with all models suggesting that the proliferation does not slow down in 3D culture or under fluid flow. D) Expression of HIF-1α is absent in perfused culture compared to fairly high, uniform expression in 2D and 3D static cultures suggesting a greater oxygen availability in stirred culture. Scale bars are 50 μm.

4.4.4.2. Adherens Junctions

Adherens junctions are found in all hepatocytes in the region between the tight junctions surrounding the bile canaliculi and the sinusoidal domain of the cells. β-catenin, a common linker protein between the transmembrane domain and the actin cytoskeleton, is uniformly expressed in all cells across all three conditions (Figure 4.14A). The expression is typically focused on the cell membranes however a large amount of staining can also be seen in the cytoplasm in all conditions. Two major transmembrane proteins are found in adherens junctions in hepatocytes: E-cadherin and N-cadherin. Both proteins exhibit heterogeneous expression *in vivo* with E-cadherin typically found in periportal hepatocytes whilst N-cadherin tends to have greater expression in perivenous hepatocytes. Between neighbouring HepG2 a heterogenous expression of both E- and N-cadherin can be seen in 2D culture (Figure 4.14B,C). Whilst it could be hypothesised that the oxygen levels in the cultures drive the varied expression of the cadherins, as seen in hepatocytes *in vivo* (Doi *et al.*, 2007), further investigation into this mechanism would need to be performed to determine if this was the case. An alternative explanation could be simply due to the relative expression of the individual cells which initially derive the populations across the culture, with this expression retained after cell division.

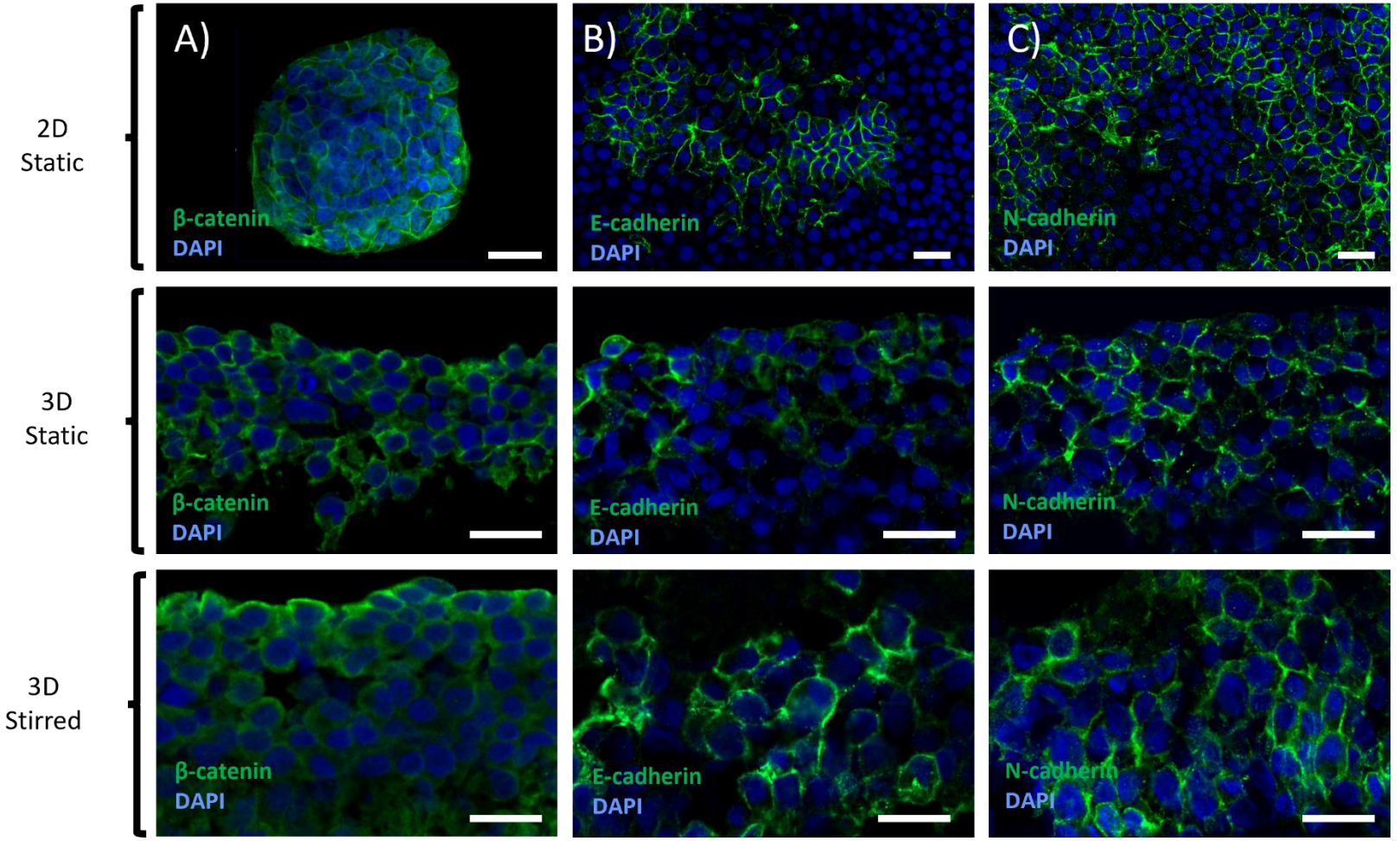

Figure 4.14: Expression of adherens junctional proteins in the different models. A) β-catenin is expressed at high levels in all three culture conditions with both membrane and cytoplasmic staining visible. B) E-cadherin staining shows varied distributions of expression across the cultures with a very strong localisation to cell membranes in all conditions. C) N-cadherin expression matches E-cadherin expression displaying strong membrane staining with heterogeneous expression across the culture. Scale bars are 50 μm.

The expression of the two proteins typically occurs in different regions of cells with limited overlap suggesting differential expression across the culture, like the variation seen in the liver lobule (Figure 4.15). These patterns are also seen in both static and stirred 3D cultures however expression of E-cadherin tends to occur in smaller regions of cells that those seen in 2D.

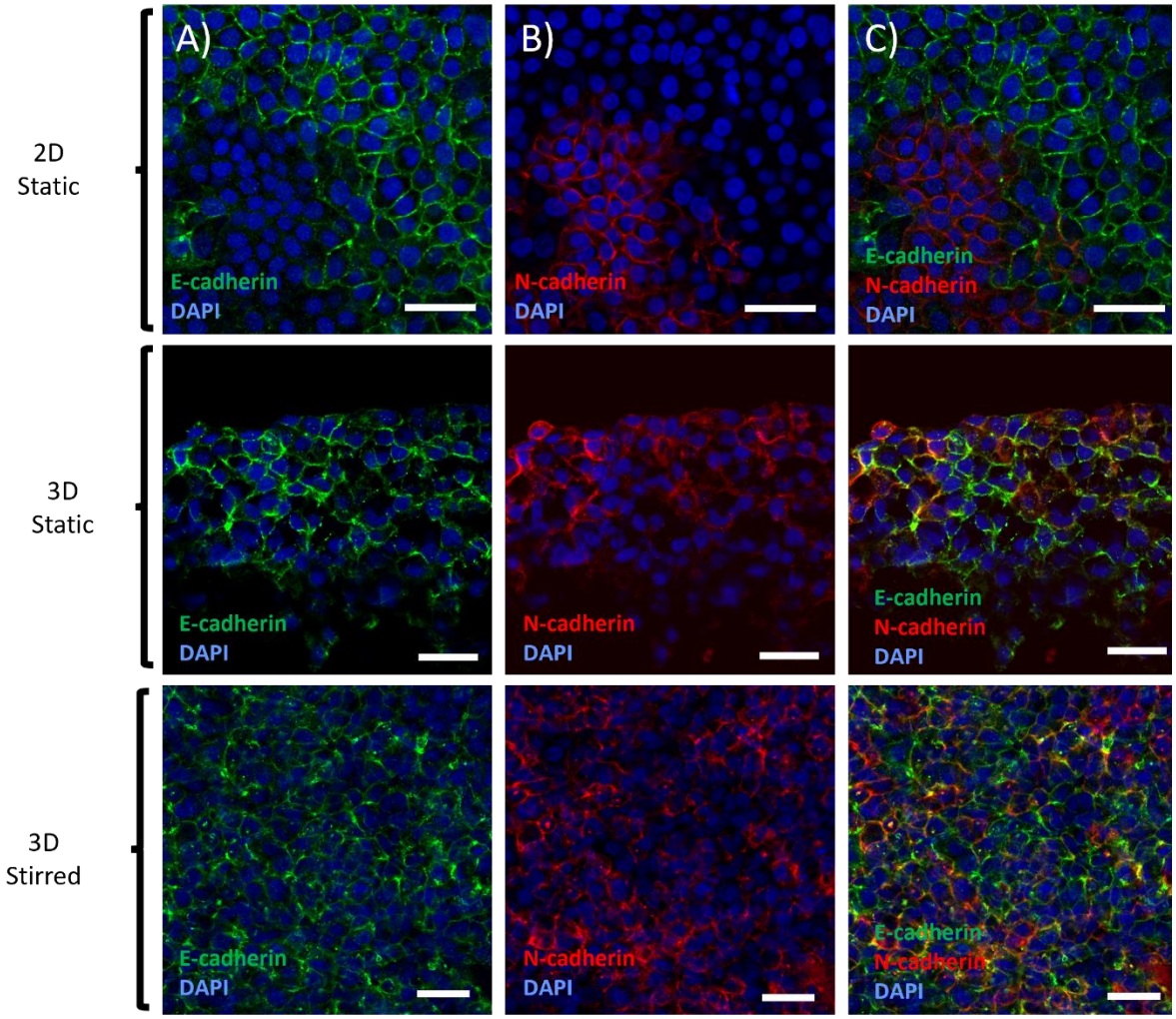

Figure 4.15: Localisation of E-cadherin and N-cadherin in the different culture methods. A & B) Both E-cadherin and N-cadherin are expressed at cell membranes in high levels in all culture methods. Stirred cultures see a more uniform expression of N-cadherin compared to static however E-cadherin levels show similar levels of variability across all culture methods. C) In all conditions, cells typically express either E-cadherin or N-cadherin exclusively with minimal co-expression. Scale bars are 50 µm.

4.4.4.3. Tight Junctions

A wide range of tight junction proteins are expressed in hepatocytes. For the analysis of tight junctions in these models the expressions of the two transmembrane proteins claudin-1, claudin-2

were investigated. In 2D culture uniform expression of the proteins is seen across most cell membranes forming a honeycomb pattern for both proteins investigated (Figure 4.16). This is likely due to the enforced polarisation caused by growth on a 2D substrate leading to apical domains on all sides of hepatocytes when viewed from above. In contrast these markers are more variable in 3D in both static and dynamic conditions as would be expected from liver tissue *in vitro*.

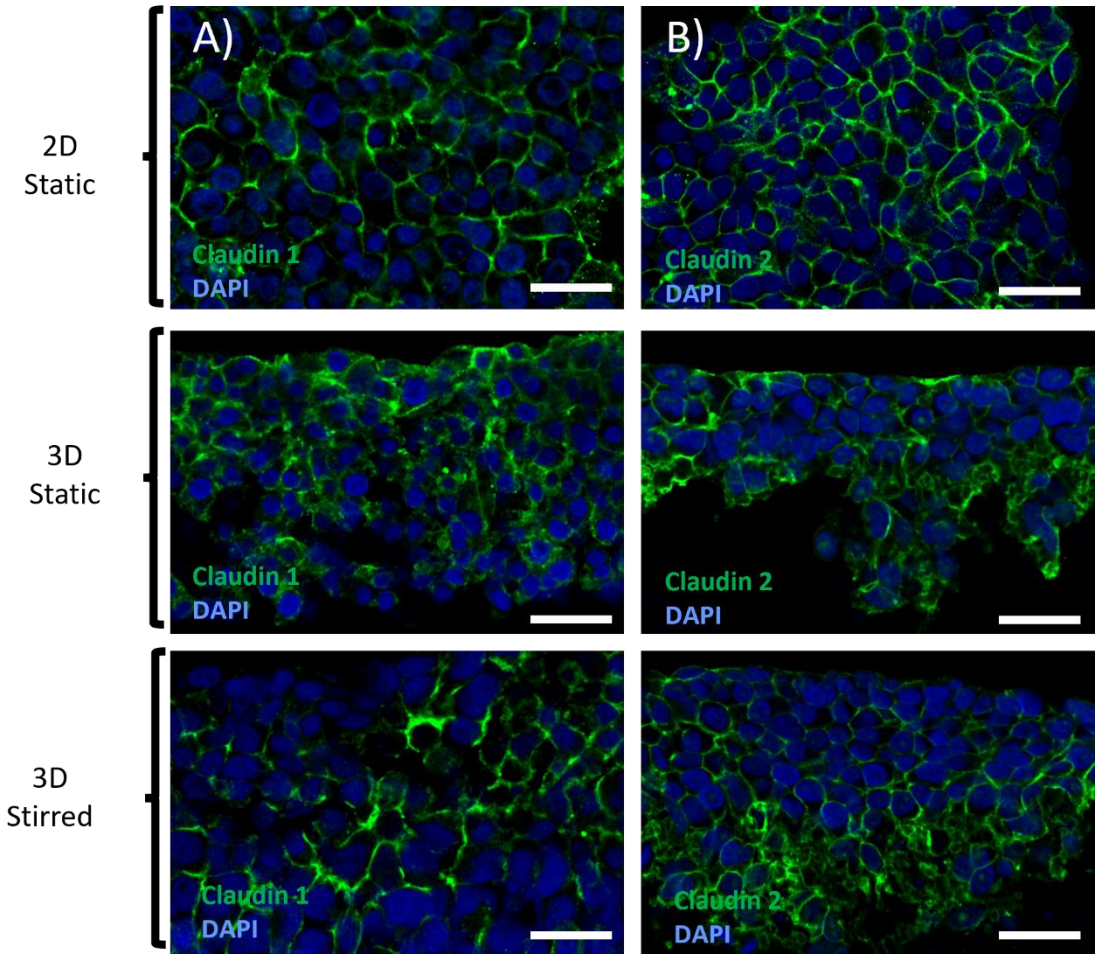

Figure 4.16: Immunostaining of the different HepG2 models with tight junctional proteins. Transmembrane tight junction proteins claudin 1 (A) and claudin 2 (B) show maintained expression in 3D and stirred models compared to levels in static 2D culture. High levels of staining localised to the cell membranes can be seen with very minimal staining elsewhere in the models. Scale bars are 50 µm.

4.4.4.4. Apical proteins

With the apical domain containing a variety of important transporter proteins to excrete molecules into the bile canaliculi the expression of these proteins is key to creating functional hepatocyte

cultures. For this the proteins Multidrug resistance protein (MDR) 1 and 3 were used along with bile salt export pump (BSEP) and multidrug-associated resistance protein (MRP) 2 (Figure 4.17).

Both MDR1 and MDR3 are weakly expressed in 2D culture whilst in 3D static and dynamic conditions enhanced expression is seen throughout the cell layer as well as a low degree of membrane localisation (Figure 4.17A, B). BSEP is absent in 2D culture as expected due to the incomplete set of hepatocyte proteins expressed by HepG2 (Figure 4.17C). In 3D static and stirred cultures this protein remains absent, suggesting that 3D culture and fluid flow are not able to fully restore aspects of HepG2 cells hepatic functionality that are completely absent in 2D.

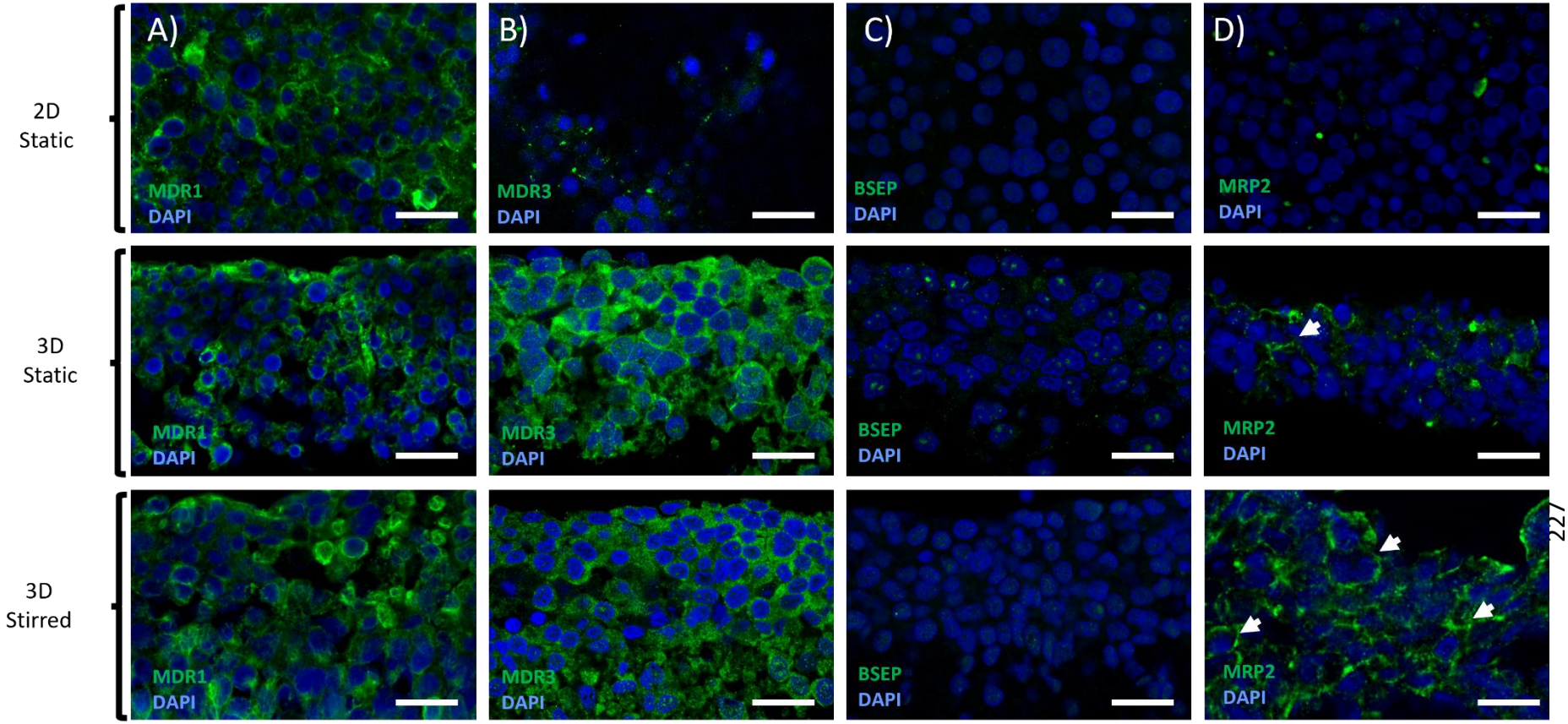

Figure 4.17: Immunostaining of the different HepG2 models for different apical transporter proteins. Expression of MDR1, MDR3, BSEP and MRP2 were investigated. The four proteins examined are efflux transporters which are important parts of the drug detoxification pathway. A) MDR1 staining can be seen in all conditions distributed throughout the cytoplasm across most cells. B) MDR3 expression is increased in 3D culture with high levels of cytoplasmic staining. Minimal localisation to the cell membranes is present. C) No BSEP expression can be determined from background fluorescence in any conditions. D) MRP2 expression appears to be increased in 3D and dynamic cultures with greater membrane-bound staining. Formation of network-like structures are present in 3D culture and are abundant in dynamic conditions (white arrows). Scale bars are 50 µm.

MRP2 has a discontinuous expression in 2D in small areas whilst in 3D this becomes more uniform, and expression can be seen at many areas across the cell layer (Figure 4.17D). In 3D with fluid flow the protein appears to be localising to cell membranes and forming a network, as would be expected from an apical-expressed protein. As can be seen in Figure 4.18 the expression of MRP2 is always in regions with expression of the microvillus protein villin, though not all regions that are villin-positive also stain positive for MRP2. All regions with very high localised expression of MRP2 also have a high expression of villin. This further supports the idea that MRP2 is forming in regions with a canaliculi-like structure.

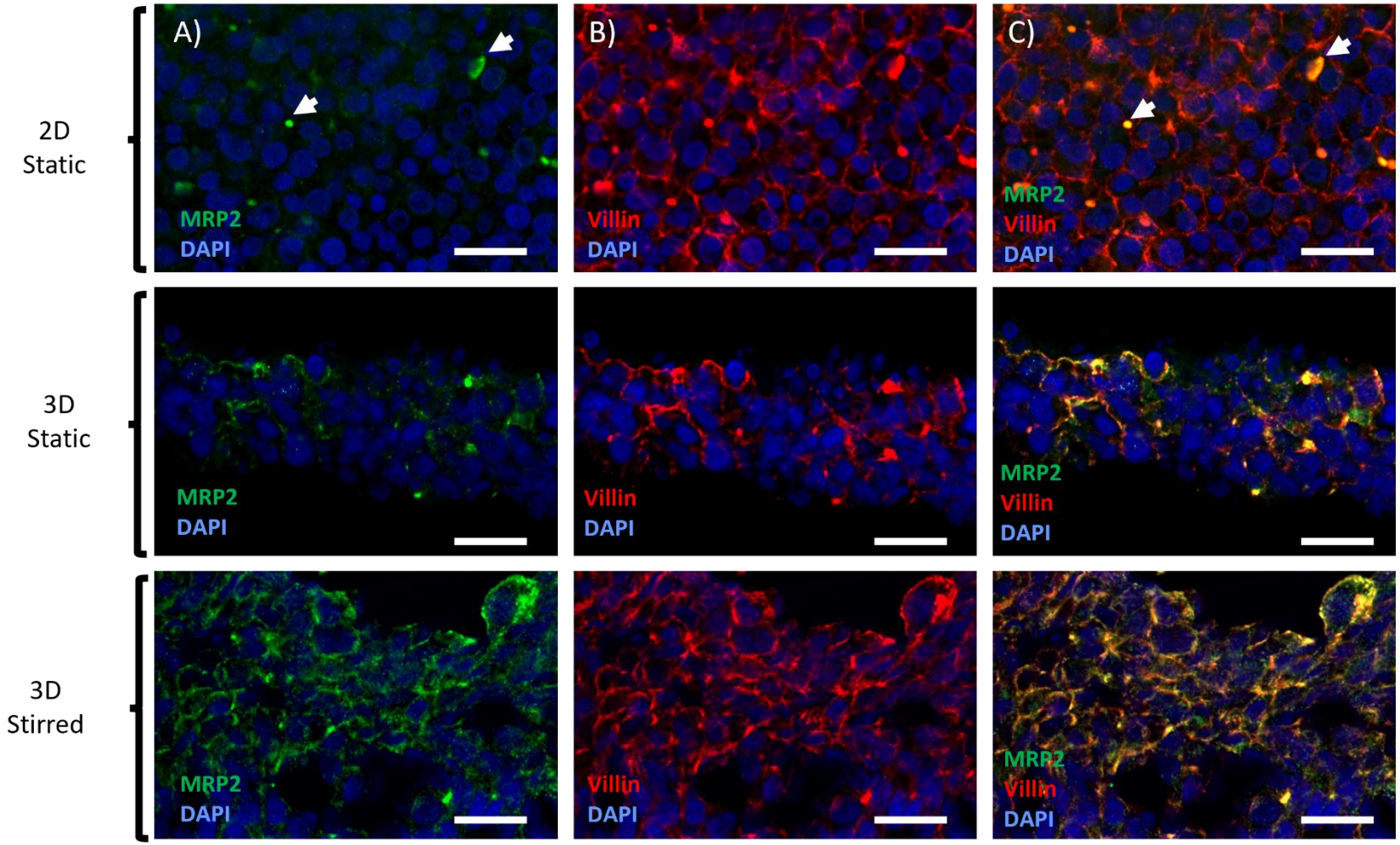

Figure 4.18: Co-localisation of MRP2 and Villin in different culture methods. A) MRP2 expression is only in isolated pockets in 2D culture however in 3D static and stirred a larger network formation is seen with higher overall expression. B) Villin expression, a marker for microvilli, is distributed throughout cell membranes. C) MRP2 colocalises around the cell membranes with villin, suggesting potential bile canaliculus formation. Scale bars are 50 µm.

The results from the PCR for apical transporters show a similar pattern to that seen with the immunofluorescent staining. *ABCB1*, the gene encoding MDR1, shows a similar level of expression between 2D and 3D with a small upregulation in flow conditions (Figure 4.19A). Meanwhile *ABCC2* (MRP2) shows a similar small upregulation in 3D followed by a larger upregulation of around 500 % in flow conditions (Figure 4.19B), supporting the results seen in the immunofluorescence analysis. The genes *ABCG2* (BCRP) and *ABCB11* (BSEP) show no expression in all conditions (Figure 4.19C, D).

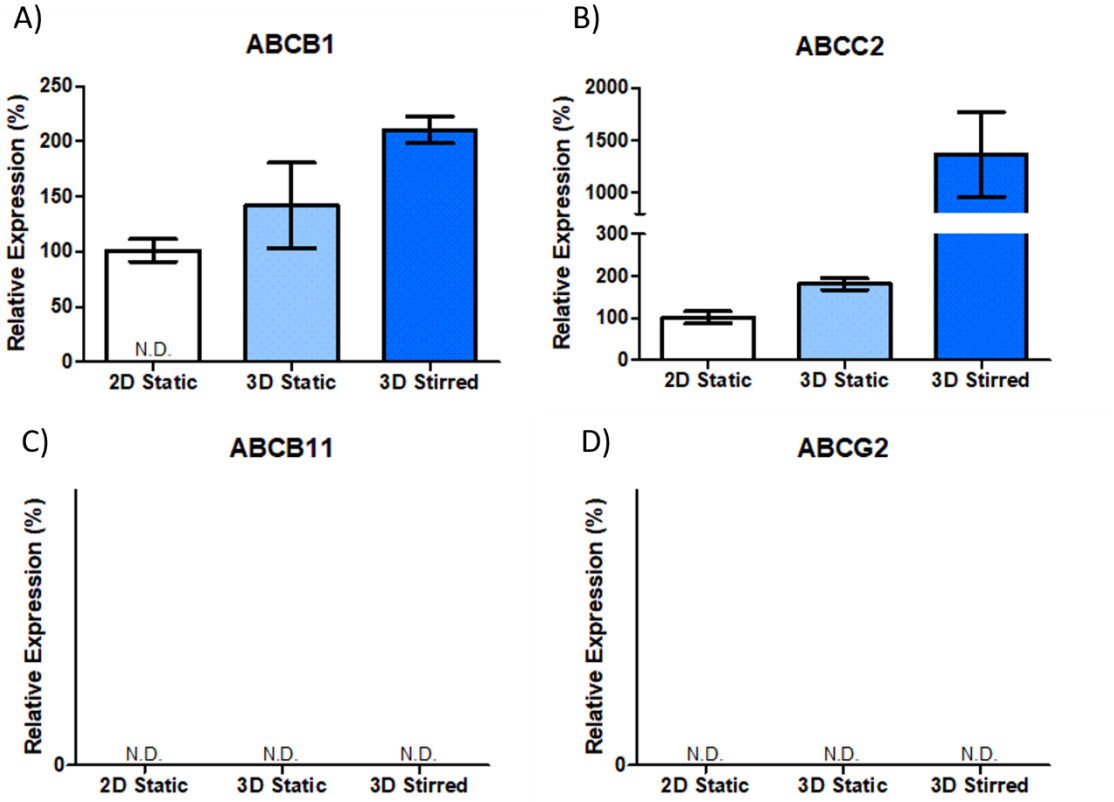

Figure 4.19: qPCR quantification of apical transporter genes. A) ABCB1, the gene for MDR1, has a slight upregulation in dynamic conditions and is highly variable in static 3D culture. B) ABCC2, the gene for MRP2, has minor upregulation in 3D static and significant upregulation in 3D stirred culture. C&D) ABCB11 and ABCG2, the genes for BSEP and BCRP respectively, are not detected in any conditions. Error bars are ±SEM, n = 3.

4.4.4.5. Basolateral proteins

Basolateral transporters in hepatocytes are important for the import and export of compounds from the blood and are therefore crucial exploring the metabolism of drugs in cells. MRP3, sodium taurocholate cotransporting polypeptide (NTCP) and OATP1A2 were investigated to analyse the effects of fluid flow on the basolateral domain of HepG2 cells.

As seen in Figure 4.20 the expression of sinusoidal transporters in HepG2 cultures was very variable between different markers and conditions. In 2D, MRP3 expression was localised to the cell membranes whilst NTCP and OATP-A were both absent across the entire cell culture. The expression of MRP3 appeared to be relatively unchanged in 3D static and dynamic conditions, though did appear to be more widely expressed in dynamic conditions with a slightly more diffuse localisation (Figure 4.20A). NTCP remained absent in both 3D static and dynamic cultures (Figure 4.20B, C). OATP-1A2 appeared to be present at very low levels in 3D static and stirred cultures. Despite the small increase in expression this seemed there is no membrane localisation apparent, unlike what would be expected for this protein.

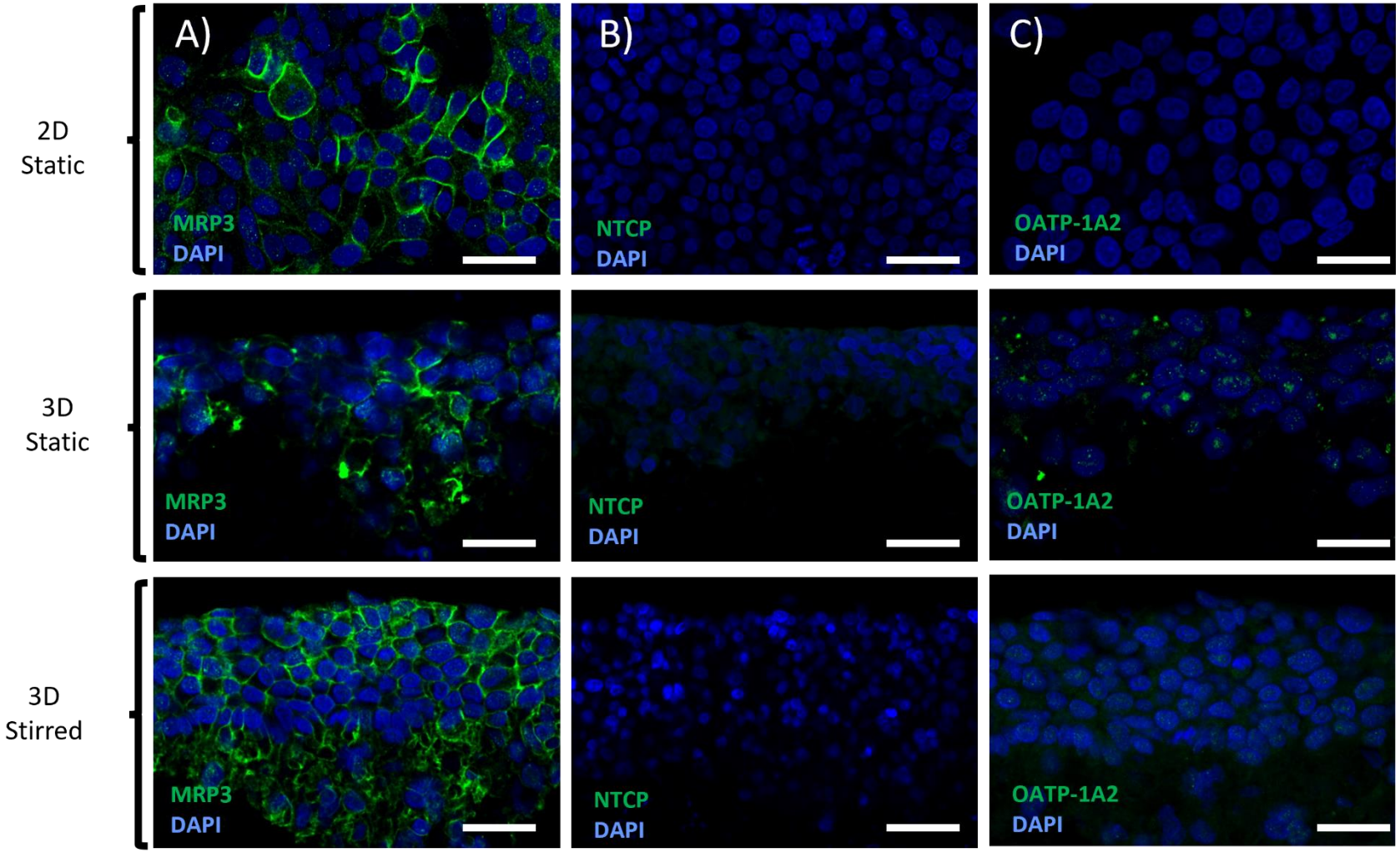

Figure 4.20: Immunostaining of the different HepG2 models for different basolateral transporters. A) MRP3, a transporter which is present in the basolateral membrane of hepatocytes, has expression around the membrane of cells with minimal expression in the cytoplasm and can be seen similar levels in all conditions. B&C) Expression of NTCP and OATP-1A2 cannot be determined above background levels in any of the conditions. Scale bars are 50 µm.

The gene expression of the two sinusoidal transporters investigated, *ABCC3* (MRP3) and *SLCO1A2* (OATP1A2), showed a large increase in fluid flow conditions compared with 2D (Figure 4.21). For ABCC3 the expression was the same in 2D and 3D static culture however was increased to around 500 % in dynamic culture. SLCO1A2 had approximately 1,000 % relative expression in 3D static and almost 10,000 % in dynamic culture. The results from the immunofluorescence show that whilst the gene may be expressed at higher levels this does not appear to lead to higher levels of protein transcribed, therefore being of limited experimental value. This highlights the requirement to investigate quantitative changes in expression levels alongside spatial localisation of proteins to achieve a full picture of changes induced, with one technique alone having the potential to lead to inaccurate conclusions.

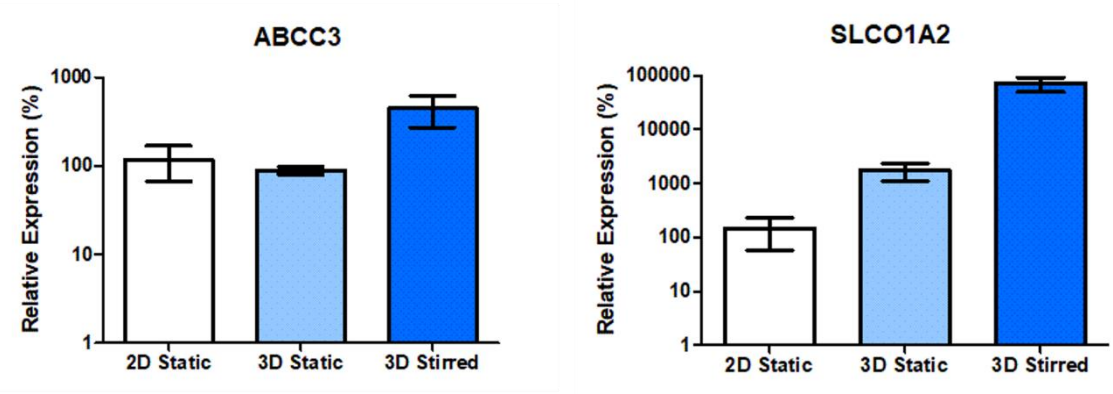

Figure 4.21: qPCR analysis of basolateral transporters genes. ABCC3 and SLCO1A2, the genes for MRP3 and OATP-1A2 respectively, both show increased expression in dynamic conditions with SLCO1A2 showing a similar fold increase between 3D static and 3D stirred as is seen between 2D and 3D static. Values are mean ± SEM, n = 3.

4.4.5. Functional analysis of HepG2 in 3D and stirred culture conditions

Albumin production in 3D dynamic culture is significantly increased compared with static 3D culture. Over the seven days which measurements were taken both cultures produce albumin at a roughly linear rate with the production from stirred cultures being around three times greater than from static culture (Figure 4.22A).

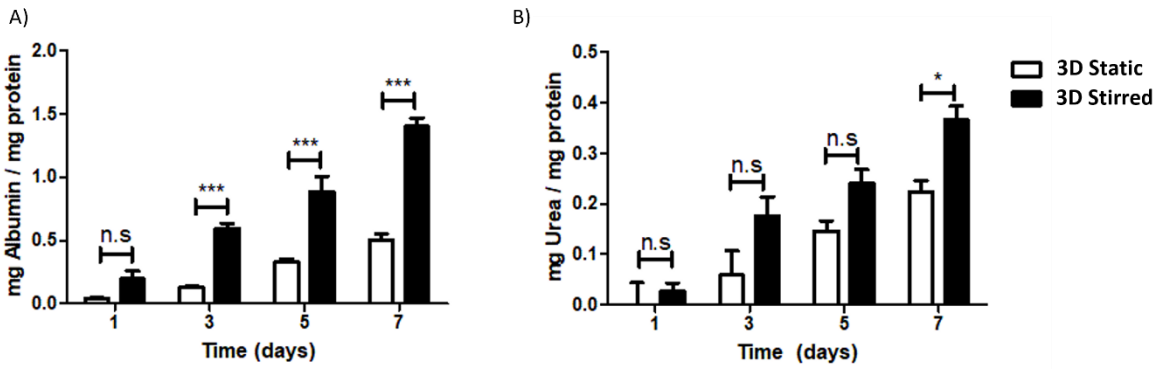

Figure 4.22: Metabolic assays carried out on HepG2 cultures grown in static and dynamic conditions. A) Albumin assay carried out over 7 days with a media sample taken every two days after the initial 1-day time point. N = 2, n = 3. B) Urea assay carried out over 7 days with media taken as per the albumin assay. N = 1, n = 3. Values are mean ± SEM. Significance values calculated with two-way ANOVA: n.s = $p > 0.05$, * = $p \leq 0.05$, ** = $p \leq 0.01$, *** = $p \leq 0.001$.

Urea production sees a similar change in stirred 3D culture compared with static 3D culture with an increase across all time points (Figure 4.22B). This change is not as significant as that seen in albumin and has a greater variation between individual cultures. Overall, the quantity of urea produced after seven days is roughly 1.5 times higher in stirred culture than in static.

By investigating some of the enzymes in the urea cycle which are known to be under expressed in HepG2 an interpretation of these results becomes clearer (Figure 4.23). Arginase I (ARG1), the final enzyme in the cycle leading to urea production, has no noticeable change in expression between 2D, 3D and stirred conditions. Ornithine transcarbamylase (OTC), an enzyme involved earlier in the pathway, is important in the detoxification of ammonia and is not detected in 2D. In 3D the gene can be detected and in dynamic culture the levels are over 1,000 % the levels of static.

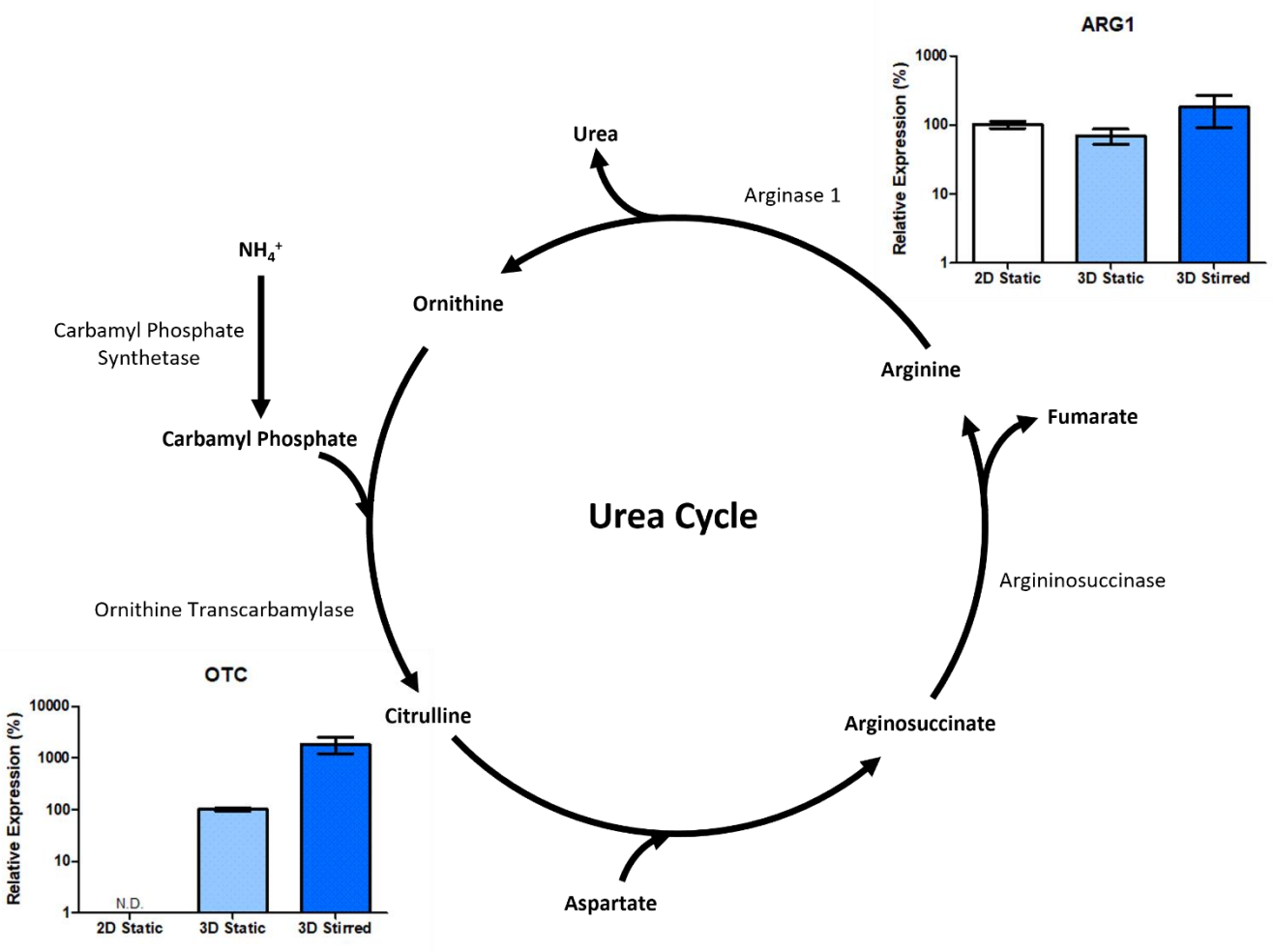

Figure 4.23: The urea cycle with qPCR expression of key enzymes in the different HepG2 models. The urea cycle detoxifies and removes ammonia from cells through the production of urea and is a key functional pathway in hepatocytes. The expression of two key genes OTC and ARG1, which have been suggested to have low expression or be absent in HepG2, are displayed. OTC shows significant upregulation in dynamic culture compared to static and is not detected in 2D culture. ARG1 has similar expression across all culture conditions. Values are mean ±SEM, N = 3.

4.4.6. Changes in levels of key drug metabolising enzymes

To study drug metabolism the phase I metabolism was first explored. The expression of genes for ten of the main CYP enzymes was examined with qPCR. The results from this show that the effects of fluid flow vary between the different CYP isoforms (Figure 4.24). For most isoforms, the change between 2D and 3D is negligible whilst a high change in expression is seen when moving to stirred culture. The biggest changes are seen in CYP2A6, CYP2C8 and CYP2C9 which see a change in expression from 2D of around 3500 %, 4500 % and 6500 % respectively.

CYP2E1 and CYP1A1 both show a small upregulation from 2D to 3D static with a minimal further change when cultured under fluid flow conditions. CYP1A2 is the only one of the CYP isoforms investigated which has no change in expression between the different conditions.

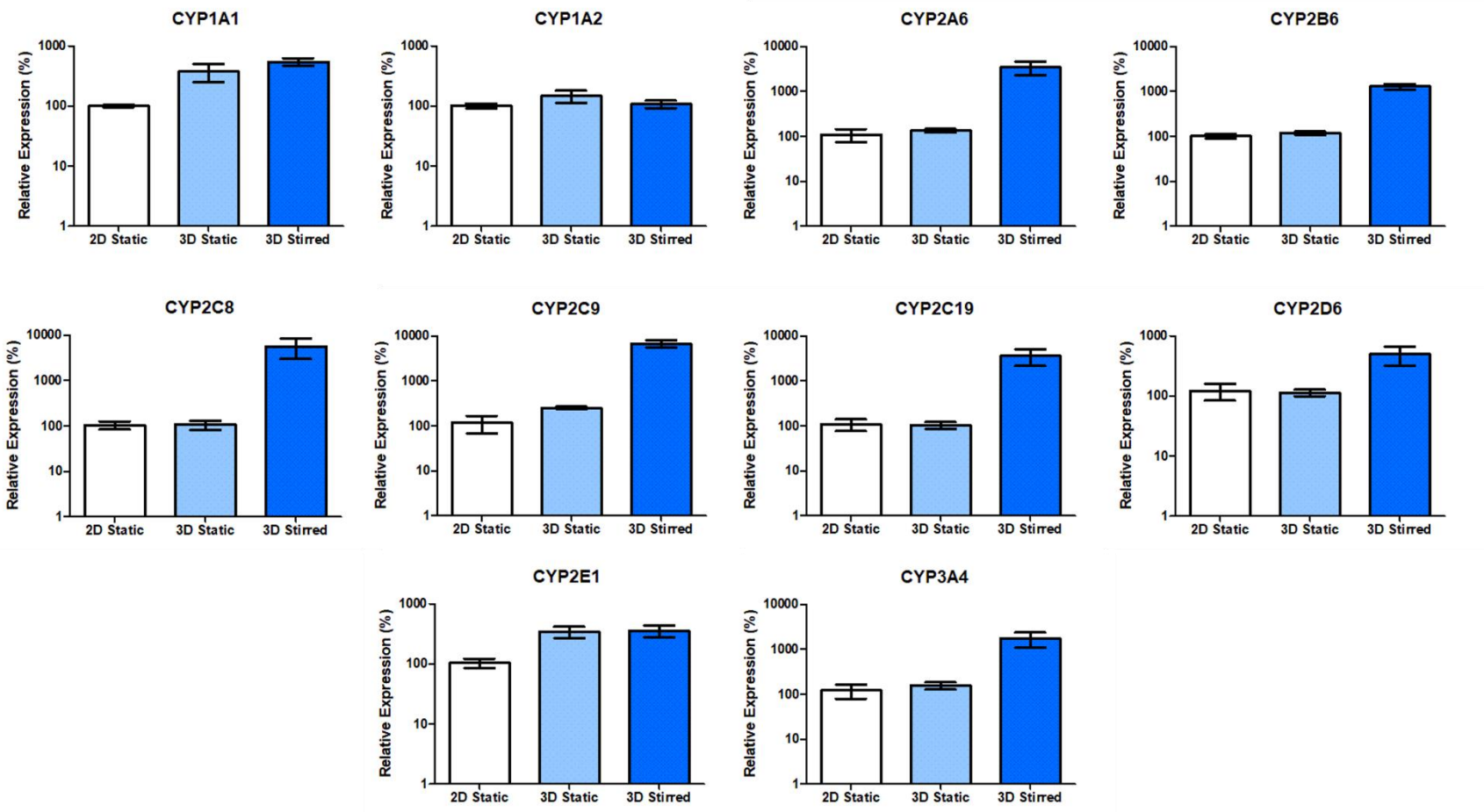

Figure 4.24: qPCR expression of major CYP enzymes in HepG2 cultures. A range of different results can be seen for the gene expression of different CYP enzymes between 2D, 3D and stirred conditions. The general trend shows a major upregulation in dynamic conditions with some also seeing upregulation from 3D conditions. CYP1A2 is the exception with no change seen between conditions whilst genes such as CYP2C8 and CYP2C9 show over 50-fold increase in expression between 2D and 3D stirred culture. Values are mean ±SEM, n = 3.

For the investigation of phase II drug metabolism, a set of genes was chosen which encompassed the important UGT, GST, NAT and SULT enzyme families (Figure 4.25). For the four UGT enzymes investigated the results were quite variable between genes. For UGT1A3 and UGT1A6 no variation was seen between 2D and 3D culture however the addition of fluid flow significantly upregulated these by around 1,800 % and 3,500 % respectively. UGT2B7 has the same pattern of expression however the change in fluid flow conditions is much smaller at around 250 %. For UGT1A1 an initial change of 240 % is seen from the incorporation of 3D culture however this does not change further when fluid flow is added.

GSTA1 shows a small increase to 290 % from the move to 3D culture however this then greatly increases to 6,850 % when fluid flow is added. The same pattern is seen for NAT1 with an increase to 170 % in 3D culture and a further change to 1,170 % when fluid flow is added. NAT2 on the other hand shows no change between 2D and 3D culture systems however does have an increase to 550 % once fluid flow is incorporated. This expression pattern is also seen for SULT1A1 however a smaller 330 % change is seen from the addition of fluid flow to the cultures.

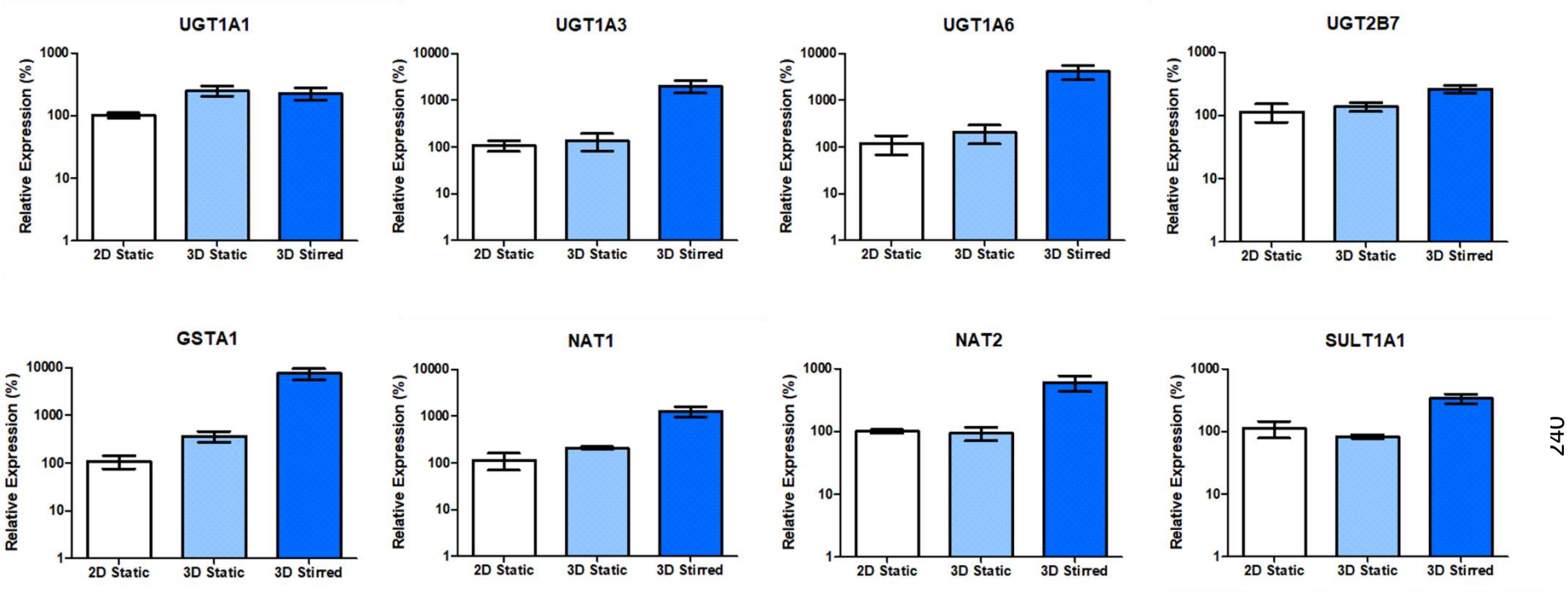

Figure 4.25: qPCR expression of phase II enzymes in HepG2 cultures. A selection of the phase II enzymes are shown covering the drug metabolism pathways for some of the more common drugs tested on hepatocytes. A general trend of upregulation under fluid flow conditions compared to static 2D and 3D can be seen. UGT1A1 shows the smallest difference between conditions with slight upregulation in the 3D conditions compared to 2D culture. GSTA1 shows the highest different in dynamic culture with over 70-fold upregulation in dynamic conditions compared to 2D culture. Values are mean ±SEM, n = 3.

4.5. Discussion

In this chapter a liver model composed of HepG2 hepatocellular carcinoma cells and incorporating the bioreactor system developed in the previous chapter was optimised and characterised. With the highly perfused environment of the liver being something missing from the majority of cell culture models the recapitulation of this was hypothesised to improve the structure and function of the cells. Before thorough characterisation could be carried out a range of culture parameters were explored and optimised to promote the formation of reproducible, healthy liver tissue equivalents. Initial characterisation investigated the cell structure to see if a more physiologically relevant hepatocyte phenotype could be produced. This was followed with an exploration into the changes in cell function with genes for key enzymes in the drug metabolism pathway of particular interest for the effective use of these models for drug hepatotoxicity testing, one of the important uses of such models.

4.5.1. Culture of HepG2 cells as stirred, three-dimensional tissue equivalents

The addition of 3D and stirred conditions to tissue equivalents has a major impact on their structure and function and these properties need to be controlled to optimise the viability and function of their component cells. HepG2 cells can be grown with ease on all three of the different forms of Alvetex®, as has previously been shown for Alvetex® Scaffold and Strata (Bokhari, Carnachan, Cameron, *et al.*, 2007a; Reprocell Europe, 2021). The different Alvetex® substrates led to drastically different cell morphologies with the highly porous Alvetex® Scaffold allowing a high level of invasion into the membrane whilst Alvetex® Strata reduces this to form a thicker tissue disc on the Alvetex® surface. The smaller pores present in Alvetex® Polaris prevent any invasion and instead lead to a thick, uniform tissue disc on the surface. Whilst these cultures have the highest level of homogeneity, they also appear to reduce nutrient transport such that a noticeable reduction in cell viability can be detected.

Under fluid flow conditions, the differences between the substrates are even more pronounced. Alvetex® Scaffold displays two regions with distinct morphologies. Towards the surface a densely packed layer of cells is formed however within the Scaffold the cells become increasingly dispersed and the cells exhibit a more rounded morphology. This suggests a reduction in cell-cell contacts in this region which is detrimental to the functional polarisation of HepG2 cells due to a reduction in cell-cell junctions (Theard *et al.*, 2007). Similar results are also seen with Alvetex® Strata however a thicker surface layer is present and invading cells do not penetrate as far through the substrate.

The invading cells are grouped much more closely together in Alvetex® Strata compared with the dispersed positioning seen in Alvetex® Scaffold which should be beneficial for maintenance of function. Whilst Alvetex® Polaris formed a thick, homogeneous cell layer on the surface with no invasion, the levels of viability were significantly reduced, seen by the dense nuclei and pink cytoplasmic staining of the H&E stain. This is likely due to the severely reduced fluid flow, as quantified in Chapter 2, leading to reduced nutrient supply. Therefore, this membrane was not beneficial for the culture of HepG2 in dynamic culture over the two-week total culture period tested. From these results, it was decided to continue using Alvetex® Strata for all experiments going after this point due to the high viability and high homogeneity of the dense cell structures.

4.5.2. Structural characterisation of stirred HepG2 cultures

The initial characterisation of the tissue structures was carried out using fluorescent staining. The TUNEL assay and immunofluorescent staining for cleaved caspase 3 were used to asses levels of apoptosis in the tissue models, detecting cells in late- and early-stage apoptosis respectively (Nagata, 2000). These both show low level or absent staining in all the models suggesting a low level of cell death and therefore that the entire tissue is getting an adequate nutrient supply. The few apoptotic cells that are present reside in the central portion of the surface cell layer, as might be expected due to limitations in the diffusion through the construct, for example oxygen which can diffuse up to between 100 µm and 200 µm through avascular tissue (Carmeliet and Jain, 2000). Similar effects are commonly seen in other tissue constructs with dense 3D tissue cultures such as spheroids (Gaskell *et al.*, 2016; Štampar *et al.*, 2020). Ki67 staining shows similar levels of proliferation across all the models showing that proliferation was maintained until the endpoint of the cultures. This result matches previous findings in literature which suggest that the levels of ki67 expression are similar between 2D and 3D culture techniques (Sreenivasa C. Ramaiahgari *et al.*, 2014; Luckert *et al.*, 2016).

The hypoxia marker HIF-1α was investigated to look for changes in hypoxic stress between cell models. HIF-1α is not usually present in hepatocytes *in vivo* whilst HepG2 cells, like most cancerous cells, are known to have an overexpression of this gene in static culture (Yoo *et al.*, 2014; Feng *et al.*, 2018). In both 2D and 3D static conditions, positive staining for HIF-1α can be seen in all cells, as expected from literature. In flow conditions the staining is completely absent suggesting that the bioreactor system aids in transporting oxygen to the cells. This result supports the oxygen measurements taken in Chapter 3 which show that the convective mixing in the bioreactor system maintains high oxygen levels without the reduction over time seen in static. In hepatocellular

carcinoma HIF-1α is associated with cell invasion, metastasis and therapy resistance with high levels typically associated with poor prognosis (Luo *et al.*, 2014). HIF-1α also has a regulatory effect on many genes including glucose transporters and glycolytic enzymes (Semenza, 2000). The reduction in expression seen in stirred cultures could therefore be beneficial for enhancing the hepatic processes of the HepG2 cells whilst reducing the unwanted HCC phenotype.

When investigating the expression and localisation of tight junction proteins minimal change is seen in 2D static, 3D static and dynamic culture conditions. In 2D culture the cells form junctions with their neighbouring cells within the monolayer, therefore leading to an unnatural phenotype with a polarisation enforced by the plastic substrate (Yamada and Cukierman, 2007). The 3D scaffolds allow cells to make contacts in all directions, therefore allowing more complex junctional networks and a more natural cell polarisation. As the natural liver parenchymal morphology typically looks the same when viewed from any orientation, the formation of junctions in all directions is a preferable result to simply the lateral junctions and cell-cell contact seen in 2D culture (Matsumoto and Kawakami, 1982; Malarkey *et al.*, 2005).

For adherens junctions the change is more complex with the distribution of E-cadherin and N-cadherin changing between 2D and 3D. In 2D the distribution of E-cadherin and N-cadherin appears to be in discrete, exclusive clusters. This could be due to the cells from which these populations arose having expression of different types at the start of culture. Alternatively, the local levels of oxygen may be variable, due to factors such as cell density, leading to expression similar to that seen *in vivo* with the expression of N-cadherin in the lower oxygen region around the central vein, whilst E-cadherin tends to be in cells nearer the higher-oxygen portal region (Sekine *et al.*, 2009). In 3D this pattern is not observed. Instead, the distinct expression of E- or N-cadherin varies between adjacent cells. Expression of the proteins also appears to be less exclusive, particularly in dynamic culture, than in 2D with cells maintaining low levels of the alternative cadherin alongside the higher expressed form. The specific impact this has on the cultures is unclear however E-cadherin plays an important role in cell signalling and maintenance of differentiation (Gonzalez-Sanchez *et al.*, 2015) whilst a downregulation is implicated with progressing of epithelial-to-mesenchymal transition (Loh *et al.*, 2019), therefore it is highly possible that these changes could prove beneficial for the overall cell function.

β-catenin, an important cytoplasmic linker protein in adherens junctions, has aberrant localisation to the cytoplasm in HepG2 with significant levels of cytoplasmic and nuclear expression (Yamashita *et al.*, 2007). One possible reason for this is a deletion of amino acids 25-140 in the β-catenin

protein, caused by a large deletion in the CTNNB1 gene, in HepG2 cells(De La Coste *et al.*, 1998; Zhou *et al.*, 2019). This could potentially lead to poor binding with α-catenin and therefore the consequent reduction in membrane localisation. The lack of change in this expression through addition of 3D culture and fluid flow shows one of the limitations of these techniques. Whilst the induction of some proteins, which are normally downregulated in cells such as HepG2, is possible using these advanced culture methods, expression issues due to limitations of the cell line used, such as genetic mutations, cannot be rescued.

4.5.3. Variations in membrane transporter expression in stirred 3D culture

The expression of membrane transporters is highly important for hepatocytes to carry out many of their functions. Both apical and sinusoidal transporters play a role in molecular turnover and therefore the full complement of transporters as seen in hepatocytes *in vivo* is a requirement for effective *in vitro* models for drug metabolism and toxicology, particularly when using cell lines such as HepG2 which have limited expression of many key transporters (Faber, Müller and Jansen, 2003; Jigorel *et al.*, 2006; Louisa *et al.*, 2016).

Significant differences in protein expression were seen between 2D, 3D static and 3D stirred samples for some apical transporters. MDR1 gene expression sees a minor upregulation however the immunofluorescence suggests a lack of membrane localisation, instead forming networks through the cytoplasm as has been reported elsewhere (Colombo *et al.*, 2014). Similarly, immunofluorescence for MDR3 suggests much higher levels in both 3D static and stirred compared with 2D, however this is also highly localised to the cytoplasm. In 3D static some regions of membrane localisation can be seen, which seem to be lost under fluid flow. In 2D, MRP2 is localised to small regions between cells as has been found previously (Kubitz *et al.*, 2001). A minor upregulation in gene expression is seen in 3D static culture whilst a significant upregulation is induced with the addition of fluid flow. Alongside these upregulations enhanced network formation and colocalisation to villin can be seen between adjacent cells in 3D models, most noticeably in dynamic conditions, which suggests there may be improved bile canaliculi formation. This canalicular network formation in 3D culture is similar to those reported previously with HepG2 spheroid cultures (Hiemstra *et al.*, 2019).

No expression of BSEP, an important protein for hepatocytes *in vivo*, can be seen in 2D HepG2 culture, as reported in literature (Donato, Tolosa, Laia and Gomez-Lechon, 2015). The addition of 3D culture and fluid flow does not have any measurable impact on the expression with it being

absent in both qPCR and immunofluorescence analyses for both 3D static and stirred conditions. Whether this has much effect on the predictivity of models for drug toxicity experiments in unclear, with some papers suggesting using BSEP inhibition as a marker for DILI (Garzel *et al.*, 2014; Woodhead *et al.*, 2014) whilst a more recent article has reviewed studies linking BSEP-inhibition and DILI to find no useful predictive capacity from this method (Chan and Benet, 2018b). Therefore, while not matching the expression of primary hepatocytes, the lack of BSEP expression may be of limited consequence in a hepatocyte monoculture system.

Of the three sinusoidal transporters investigated via immunofluorescence only MRP3 showed expression patterns like those in primary hepatocytes, as is often the case for HCC cells (Zollner *et al.*, 2005). The formation of networks around cell membranes shows that these are being correctly transported to the membranes and therefore the formation of a function sinusoidal domain may be taking place. In 3D culture limited changes are seen to the localisation of MRP3 with strong membrane staining in both static and dynamic conditions, however expression of the ABCC3 (MRP3) gene is upregulated noticeably in the bioreactor to a level which should be similar to primary hepatocytes (Wiśniewski *et al.*, 2016). Unlike MRP3, NTCP and OATP-1A2 show absent or aberrant expression respectively and this is not improved through the addition of 3D culture or fluid flow. NTCP is known to be absent in HepG2 cells and, as with BSEP, is not induced through 3D culture or fluid flow in these results (Donato, Tolosa, Laia and Gomez-Lechon, 2015). OATP-1A2 gene expression is seen to increase hugely in fluid flow conditions however the expression appears to be cytoplasmic and nuclear rather than at the cell membranes as would be expected. The increases to MRP3 and OATP-1A2 expression with the addition of fluid flow are in-line with expectation due to their expression in close proximity to the sinusoidal blood flow *in vivo.*

Overall, the results for transporter expression levels and localisation show a positive improvement for markers which are already expressed and properly localised in HepG2 cells however those which are absent or have aberrant localisation in 2D culture appear to benefit little from the addition of 3D culture and fluid flow.

4.5.3. Changes to basic metabolic functions of HepG2 cells

The levels of albumin and urea produced by hepatocytes are often used as a basic measure for the health and functionality of the cells. These are both key functions of hepatocyte *in vivo* as discussed previously. These functions are enhanced in stirred 3D culture compared with static 3D culture, building on previous literature which shows that 3D culture techniques lead to an improvement

over conventional 2D culture (Bokhari, Carnachan, Cameron, *et al.*, 2007a). The levels of albumin production in the bioreactor were consistently around 3 times higher at each time point than those found in static. This is consistent with previous studies using different forms of bioreactors for the culture of HepG2 (Coward *et al.*, 2005; Shvartsman *et al.*, 2009; Sassi *et al.*, 2021). Sharifi et al. showed that albumin production is proportional to shear stress and oxygen delivery (Sharifi, Firoozabadi and Firoozbakhsh, 2019), therefore it could further be hypothesised that changes to the Alvetex® porosity, through the use of Alvetex® Scaffold or Alvetex® Polaris, as well as changes to the stir speed of the bioreactor could be used to modulate hepatocyte metabolism.

For the secretion of urea the results also showed a significant increase in dynamic culture over static culture however it has been found that HepG2 cells have limited ammonia detoxification capacity despite production of urea therefore making this measure of limited functional importance if ammonia detoxification is to be studied (Wang *et al.*, 1998). One study has previously found that HepG2 lack ARG1 and OTC, two of the enzymes involved in the urea pathway for the detoxification of ammonia, and therefore the production of urea does not convey the full picture of the HepG2 cultures functionality in this process (Mavri-Damelin *et al.*, 2007). Another paper has since shown the expression of these enzymes can be detected in HepG2 by western blotting however it is in very low levels (Tang *et al.*, 2012). In the gene expression analysis of these two genes the expression of OTC was not detected in 2D culture while ARG1 was detected. The incorporation of 3D culture and fluid flow with HepG2 had no measurable effect on the expression of ARG1 however OTC expression could be detected in 3D culture and was at least a further 10-fold higher in flow conditions. This suggests that although urea production is not vastly upregulated in the bioreactor, the ability of the stirred HepG2 cells to detoxify ammonia may be significantly improved. Further experiments to directly test this would be required to conclude this definitively however experiments investigating ammonia toxicity in HepG2 cell lines stably transfected with OTC and ARG1 overexpression showed a reduction in toxicity, supporting this hypothesis (Tang *et al.*, 2012; F. Y. Zhang *et al.*, 2013).

4.5.4. Expression of key drug metabolism enzymes is significantly enhanced in stirred culture

One of the major goals of any *in vitro* liver tissue model for drug toxicology is to achieve phase I and II enzyme levels like those found *in vivo*. With HepG2 cells known to have very low CYP expression, an improvement in these is key for accurate modelling of drug metabolism. From the gene expression data presented here, 3D culture alone has limited impact on the expression of most CYP genes. This has been found elsewhere with factors such as time in culture instead being the major

influence (Luckert *et al.*, 2016; Štampar *et al.*, 2020) with research comparing showing increased expression in 3D typically using significantly shorter 2D experiments alongside longer-term 3D cultures (Sreenivasa C. Ramaiahgari *et al.*, 2014; Bell *et al.*, 2018).

In contrast to this the incorporation of fluid flow into the 3D culture has a dramatic impact on many of the CYP genes and increases of between 1,000 % and 10,000% were found for many of the key CYPs. This result shows that fluid flow can play an important role in the creation of highly functional hepatocyte models with greatly improved function than found with 3D culture techniques alone. Not all CYP enzymes benefit as much from fluid flow, however, as can be seen for CYP2E1 and CYP1A2 in particular. CYP2E1 has a very minor improvement for stirred culture over 2D culture with no further induction beyond that caused by 3D culture alone. For CYP1A2 no change can be seen between the different conditions tested. Other studies have found levels of CYP1A2 to be very low or undetectable in HepG2 with minimal change in 3D stirred culture (Deng *et al.*, 2019; Ruoß *et al.*, 2019). One recent study found that the addition of 3D culture and fluid flow was able to induce CYP1A2 expression, contrary to the results found here, however a more complex model was used incorporating further physiological factors such as an extracellular matrix (Sassi *et al.*, 2021).

For the phase II metabolism, fluid flow was able to increase the expression for all the enzymes investigated, in many cases to a level over 10-fold that seen with static 3D culture. This agrees with other research which has shown the same induction with fluid flow conditions for phase II enzymes compared with phase I (Altmann *et al.*, 2008; Deng *et al.*, 2019; Sassi *et al.*, 2021). These results are very important for the accurate study of drug metabolism due to the wide range of metabolic pathways involved in drug biotransformation, for example with acetaminophen being primarily metabolised by phase II enzymes with minimal phase I metabolism at therapeutic doses (Mazaleuskaya *et al.*, 2015). Overall, the results of the phase I and II expression in HepG2 using this bioreactor model suggest significant improvements over 2D culture which should dramatically increase the research value of the cells. A comparison of these enzyme levels to those in primary human hepatocytes would be required to fully investigate the physiological relevance of these models.

4.6. Conclusions

In this chapter the major aim was to demonstrate the application and performance of the cell culture bioreactor created in the previous chapter. This was carried out by creating an *in vitro* hepatocyte model utilising a 3D scaffold and hepatocellular carcinoma cell line HepG2. With the limited hepatocyte function of HepG2 cells under standard culture conditions, it was hypothesised that the use of a 3D bioreactor could enhance the structure and function of these cells to better resemble primary hepatocytes.

Initial results found that HepG2 could be grown successfully on all three Alvetex® membranes, and further optimisation was carried out using Alvetex® Strata to create a homogeneous cell layer in fluid flow conditions whilst minimising properties such as cell quantity where possible. Characterisation carried out to look at markers of cell health and viability suggested that the cultures were performing acceptably in these conditions with the stirrer speed set at 100 rpm, based off the work in the previous chapter.

Following this initial optimisation an in-depth characterisation of proteins key for the formation of viable and physiologically relevant hepatocyte culture was performed. Both tight junctions and adherens junctions showed strong expression at cell membranes in this model with little difference compared with 2D culture. Apical and basolateral transporters were generally expressed at higher levels in fluid flow than in static 2D and 3D culture however those which were not expressed or aberrantly expressed were not improved by the addition of fluid flow.

The next stage was to look at functional improvements in HepG2, focusing on the phase I and II drug metabolism. Nearly all studied genes saw a major increase in dynamic conditions whilst often the move from 2D to 3D culture alone would have limited effect. These upregulations were often 10-fold higher with some closer to 100-fold, bringing the expression far closer towards that seen in primary hepatocytes and suggesting significant improvements in the drug biotransformation properties of the cells.

In summary, the data presented in this chapter suggests that HepG2 cells grown in a 3D microenvironment in the presence of fluid flow exhibit favourable changes to their structure and function. These changes include a reduction in hypoxic stress, increased expression and localisation of key drug transporter proteins and an upregulation in some of the drug metabolising enzymes such as members of the cytochrome P450 family. It is notable, however, that genes and proteins

found in hepatocytes which are typically absent in HepG2 in static 2D conditions do not appear to be induced by such culture methods. From these data the model developed shows many enhancements over typical 2D culture and in many cases also outperforms the comparable 3D cultures. Due to this, the models show a lot of potential for accurate prediction of drug toxicology and the following chapter will investigate this predictive capacity over a range of commonly used drugs.

Chapter 5: Response of stirred HepG2 models to toxicological challenge

5.1. Introduction

To test if a bioengineered tissue model can function effectively as a viable alternative to methods such as animal testing, the correct expression and localisation of proteins along metabolic pathways is a promising start. However, the liver, like all organs, is a complex system with a wide range of metabolic processes which can often interact with each other. Therefore, to see if a tissue engineered model can lead to improvements over simple 2D cultures it is best to analyse the metabolism and toxicity of drugs directly. By choosing drugs which are metabolised by known pathways it is possible to correlate the changes seen in drug response to what is known from previous experiments looking at protein and gene expression. From this a more accurate picture of changes that are taking place can be made.

To investigate this, the role of the liver in drug detoxification will first be investigated, followed by an analysis of limitations of drug discovery models. Finally, the different types of injury which can occur in drug toxicity. The models which have been developed will then be tested with a series of drugs and the changes in viability in these experiments will be compared with what is known about the metabolic pathways as well as the data about the models collected in Chapter 4.

5.1.1. The role of the liver in drug detoxification

The liver plays a hugely important role in the body for removal of toxins and xenobiotic substances. As shown in Figure 5.1, the main source of venous blood to the liver through the portal vein comes directly from the gut (Burt, Ferrell and Hubscher, 2017). Toxins absorbed through the intestine get transported in this blood to the liver before passing on to other organs. The liver can then effectively remove any unwanted substances before the blood is transported elsewhere in the body (Ohtani and Kawada, 2019). These unwanted substances do not merely include xenobiotics such as drugs but also molecules in the blood produced by the body, such as hormones. These can build up to toxic levels if not controlled though some also rely on the liver to further activate hormones to their more active metabolites (Langer and Chiandussi, 1987; Charni-Natan *et al.*, 2019).

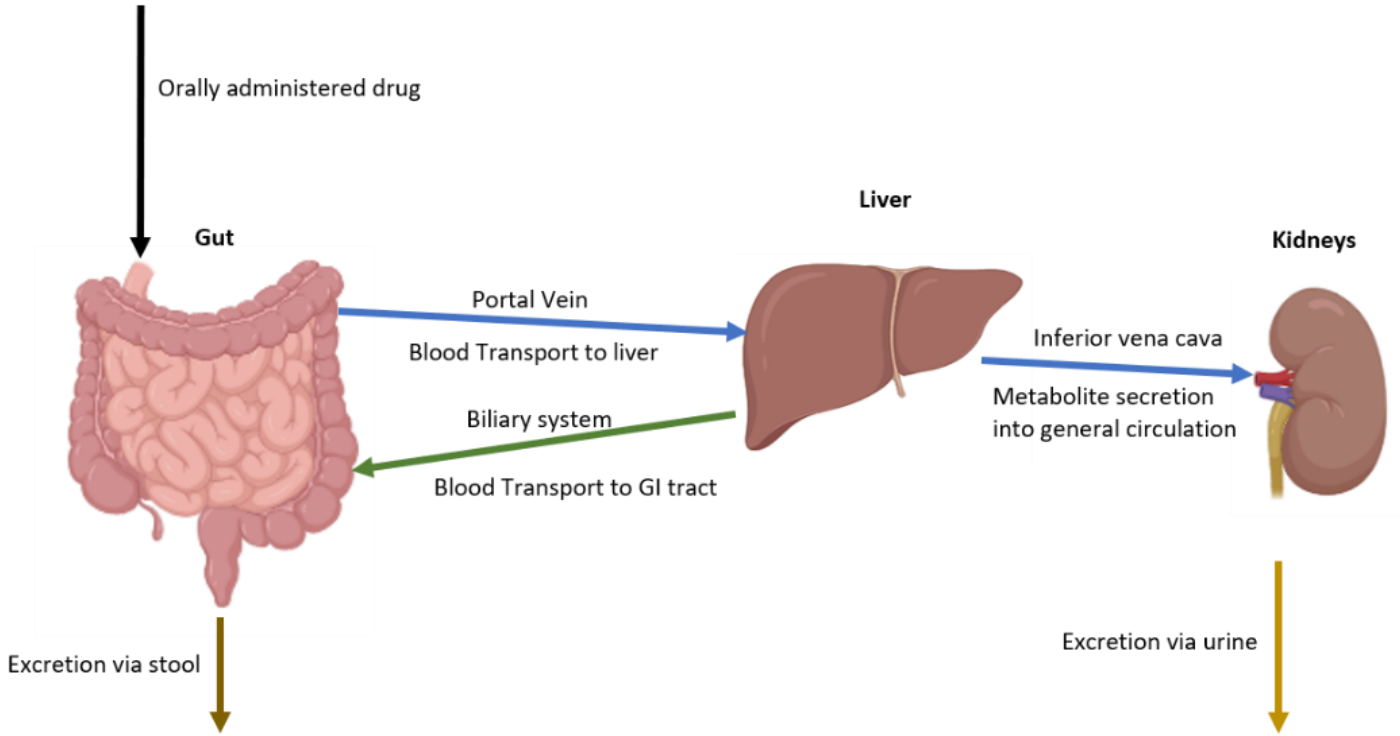

Figure 5.1: First pass metabolism of orally dosed drugs in the body.. Drugs taken orally are transported into the bloodstream in the intestines. This blood then enters the liver through the portal vein. Hepatocytes detoxify the drugs, and the metabolites are transported into either the bile or the bloodstream. Metabolites in bile are transported back into the gut for excretion via stool. Metabolites in blood are removed by the kidneys and excreted in urine.

Once blood reaches the liver it passes through the sinusoids, maximising the surface area and effectively causing the liver to act as a biological filter for the blood. Kupffer cells in the sinusoidal lumen remove bacteria and foreign debris from the blood whilst compounds such as drugs can pass through the fenestrated endothelial lining of the sinusoids and reach the sinusoidal-facing surface of the hepatocytes (Figure 5.2) (Bilzer, Roggel and Gerbes, 2006; Sörensen *et al.*, 2015; Shetty, Lalor and Adams, 2018). Upon reaching the hepatocyte surface a range of transporter proteins import the larger molecules such as drugs into the hepatocyte as discussed in Chapter 4, whilst smaller molecules can diffuse through the membrane (Schulze *et al.*, 2019).

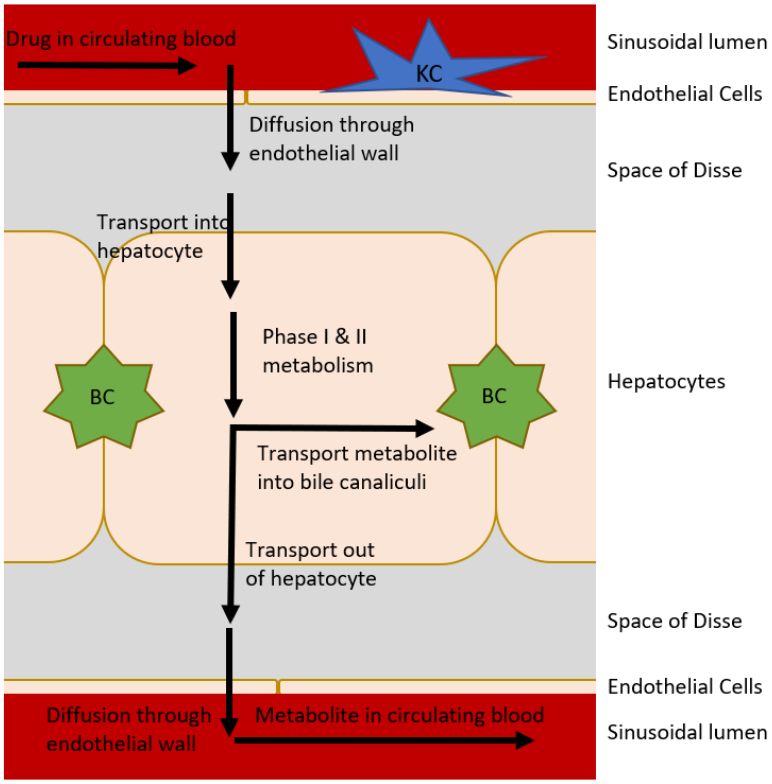

Figure 5.2: Drug metabolism in the liver. Drugs in the blood diffuse through the sinusoidal fenestrae into the space of Disse. Transporters in the sinusoidal membrane of the hepatocytes bring the drugs into the cytoplasm of the hepatocyte where they can be metabolised. The metabolites are then either transported via apical transporters into the bile canaliculi or transported by sinusoidal transporters back into the blood stream. KC, Kupffer cell; BC, Bile canaliculus.

Inside the hepatocyte drugs undergo transformation via the phase I and phase II metabolic pathways. The initial phase I metabolism typically involves oxidation of the compounds, metabolised mostly by the cytochrome P450 enzymes, however other enzymes can also carry out this function, as shown in Figure 5.3 (Gibson and Skett, 1994; Zhang and Surapaneni, 2012). This often creates a highly reactive intermediate which is often more cytotoxic than the original

compound and therefore needs to be transformed again efficiently (Dekant, 2009). A good example of this is the drug codeine, which is metabolised into its reactive metabolite, morphine, by CYP2D6 as part of phase I metabolism. This can be problematic for people who have significantly higher or lower CYP2D6 expression. Low CYP2D6 expression leads to limited pain relief from codeine whilst high expression can lead to symptoms of morphine overdose at normal doses (Kirchheiner *et al.*, 2007; Laura, 2018).This also highlights the potential for problems with patient variability which makes accurate drug toxicity prediction very difficult, as will be discussed later in this chapter.

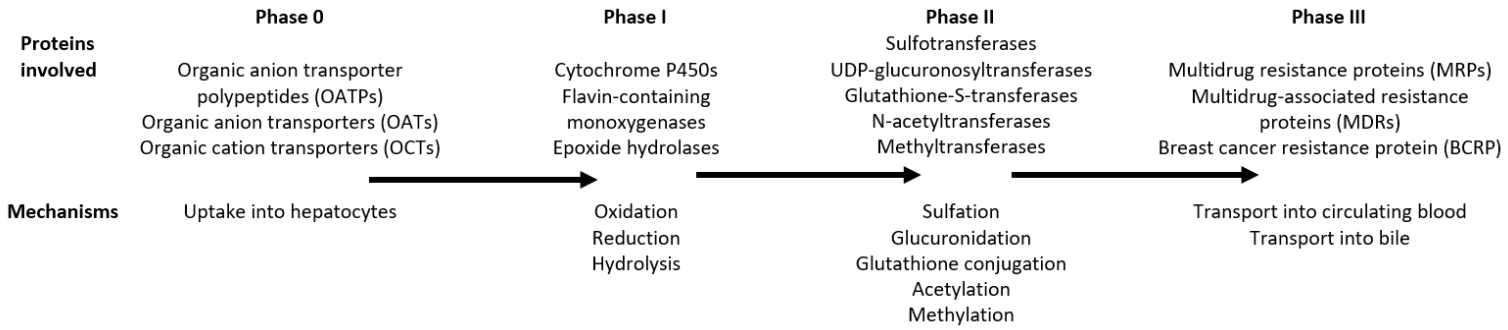

Figure 5.3: Enzymes involved in the phases of drug metabolism. Phase 0 consists of sinusoidal transporter proteins which import drugs into the cells. Phase I metabolism increases the reactivity of the drugs, usually through oxidation, reduction, or hydrolysis. Phase II metabolism adds charged conjugates to the compound. Phase III metabolism consists of secretion into either the blood stream or bile canaliculi. Intact function of all of these phases of the drug metabolism pathway is required for an *in vitro* model to accurately recapitulate the *in vivo* drug response.

Phase II metabolism conjugates polar groups to the metabolites to aid with active transport across cell membranes and increase water solubility (Jančová and Šiller, 2012). This can inactivate the reactive metabolites created by phase I metabolism or further increase the reactivity of a compound (Ionescu and Caira, 2005). The most common phase II biotransformation pathway is glucuronidation, carried out by the UGT enzymes however other pathways also exist such as glutathione-s-conjugation and acetylation. Expression levels of these enzymes in *in vitro* models are typically less regularly reported than phase I enzymes such as the CYPs, and the expression of them in liver cell lines tends to be closer to the levels of primary hepatocytes than CYP expression (Westerink and Schoonen, 2007b). Enhanced expression is nonetheless still a requirement for accurate predictivity of *in vitro* models due to the involvement in many drug metabolic pathways (Sevior, Pelkonen and Ahokas, 2012).

Following the phase II conjugation, the final stage in the pathway is the phase III secretion of the transformed molecule from the hepatocyte. Further reactions can take place during this phase such as processing the conjugated groups to other more readily secreted species (Cooper and Hanigan, 2018). The conjugations can then direct the compounds towards specific excretory transport proteins such as those of the MRP and MDR families (Stanca *et al.*, 2001; Döring and Petzinger, 2014). Excretion can take place on both the sinusoidal and apical surfaces of hepatocytes (Figure 5.2).

Compounds trafficked through the sinusoidal membranes are transferred back into the bloodstream. These are then typically removed through renal elimination into the urine however less frequently can occur via fluids such as sweat, milk and saliva (Stowe, 1968; Johnson and Maibach, 1971; Idkaidek, 2017). Otherwise, compounds are transported into the bile. Flow through the biliary system leads these compounds back towards the gastrointestinal tract where they are then secreted, though some may be reabsorbed into the blood or conjugates can be hydrolysed by gut bacteria to reform the original drug (Rollins and Klaassen, 1979; Ghibellini, Leslie and Brouwer, 2006).

5.1.2. Drug induced liver injury can be caused in significantly different ways

The complexity of the drug metabolism pathway means that there is a great range of aspects which can lead to drug induced liver injury (DILI) *in vivo.* While the exact mechanism behind the DILI varies between different drugs the nature of the injury is typically grouped into the two categories of

intrinsic or idiosyncratic DILI, as shown by Figure 5.4. These refer to whether the injury is caused by a drug in a dose-related manner, for intrinsic DILI, or where the relationship between toxicity and dose is more complex, as in idiosyncratic DILI (Funk and Roth, 2017). Idiosyncratic can be further divided into metabolic and immunologic DILI, which have different modes of onset and symptoms (Teschke and Danan, 2018).

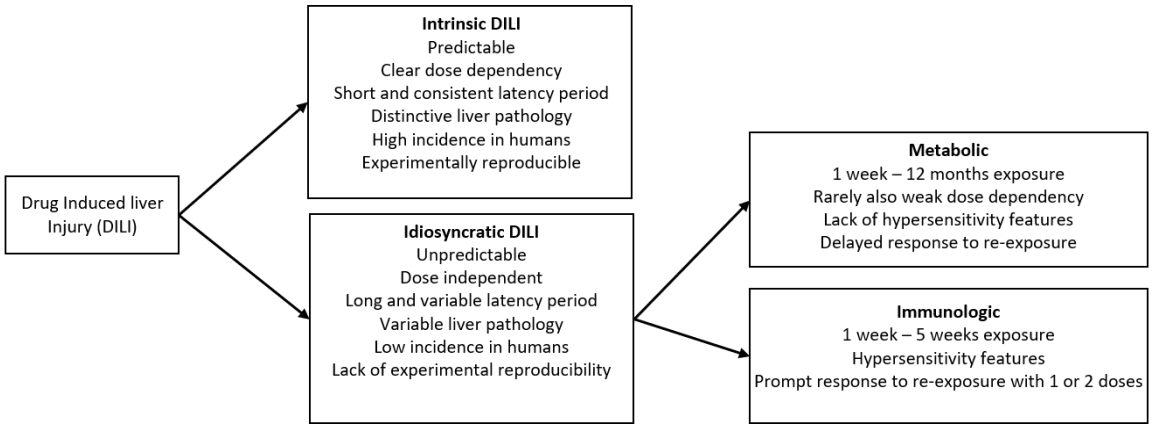

Figure 5.4: Different types of drug induced liver injury. Intrinsic DILI is the easier of the two types for predicting with *in vitro* models due to the clear dose response and common pathology. Idiosyncratic DILI is more unpredictable with no dose dependency and variable presentation in different patients. This can be further divided into metabolic and immunologic DILI which both have different presentations. Reproduced from Teschke & Danan (2018)

5.1.2.1. Intrinsic DILI

Intrinsic DILI is regarded as the simpler of the two forms of DILI to model *in vitro*. These injuries display a simple dose-dependent response, can be impacted by environmental and genetic factors and are typically reproducible in animals (Mosedale and Watkins, 2017). Despite the apparent simplicity of the pathology for this form of DILI, *in vitro* models still regularly miss potential hepatotoxic compounds which then make it through to animal or clinical trials where the adverse effects are discovered (LeCluyse *et al.*, 2012; Bale *et al.*, 2014).

The reasons for intrinsic DILI being undetected through *in vitro* testing can be varied but some main factors have been suggested. The most prominent is the unstable expression of the CYP enzymes in cultured hepatocytes (Miranda *et al.*, 2009). Whilst some drugs may be of limited toxicity in their dosed form, the impact of the phase I metabolism adding reactive groups to the drug can have a major effect on their toxicity (Kalgutkar and Soglia, 2005). Low expression of the various CYP

enzymes can lead to reduced formation of reactive metabolites than found *in vivo*, therefore underpredicting the hepatotoxic impacts of a drug (Bale *et al.*, 2014).

Another potential hindrance to accurate hepatotoxicity prediction is the absence of recirculating bile within many *in vitro* systems. Most of the bile acids present in the liver *in vivo* come from the extrahepatic pool via enterohepatic recirculation (Chiang, 2013). The intracellular levels of bile acids *in vitro* never reach these levels with media changes removing produced bile acids and absent or unstable levels of bile acid importers preventing uptake of secreted bile acids for recirculation (Schupp *et al.*, 2016). This leads to reduced levels of intracellular bile acids than found *in vivo.* This has a consequent effect on the metabolic function of hepatocytes due to the transcriptional control exerted by bile acids through activation of the farnesoid X receptor (Chiang, 2002; Lefebvre *et al.*, 2009).

Despite this, advances in cell culture techniques have led to improved predictability of *in vitro* models for intrinsic DILI and therefore has increased their research value relative to animal models, which often lack analogues of human metabolic enzymes or have limitations due to differences in binding kinetics of transporters (M Chen *et al.*, 2014; Kuna *et al.*, 2018).

5.1.2.2. Idiosyncratic DILI

Idiosyncratic DILI is a more complex form of DILI to study and model. For drugs known to cause this, the mechanisms are often unknown. Alternatively, they can be caused by immune responses, interactions with factors such as other molecules or previous injury meaning that the dose-dependent response can be indeterminate (Fontana, 2014; Uetrecht, 2019). The nature of the response itself also is highly variable. Both the onset period and the pathology can be significantly different between individuals making accurate identification of the cause difficult (Roth and Lee, 2017).

Methods to predict idiosyncratic DILI have been rapidly developing with some success. Identification of measurable factors involved in the injury process allows for limited predictivity. Factors such as BSEP inhibition, reactive metabolite formation and inhibition of the mitochondrial electron transport chain have been suggested to increase the capacity to improve the predictive capacity of *in vitro* models (Nakayama *et al.*, 2009; Thompson *et al.*, 2012; Kenna *et al.*, 2015, 2018). The efficacy of these different techniques is widely disputed. Mitochondrial electron chain inhibition has been suggested to lack relevance to most drug pathways unless specifically targeted (Kenna and Uetrecht, 2018) whilst BSEP inhibition has only been suggested to be effective for

classes of drug which are already thought to be the most likely to induce DILI (Chan and Benet, 2018b).

A lot of the work on predictive models for idiosyncratic DILI focused towards the addition of Kupffer cells to the culture models in an attempt to replicate the immune response pathways seen *in vivo* (Atienzar *et al.*, 2016; Kenna and Uetrecht, 2018; Uetrecht, 2019). For the purposes of this study the focus will therefore be on intrinsic DILI, due to the use of a single cell type in these models. Further development of the models down the line could investigate incorporating Kupffer cells, thus increasing the utility for predicting idiosyncratic DILI.

5.1.3. Drug discovery models frequently over- and underestimate drug toxicity

Whilst many different models exist for evaluating drug toxicity these all act as limited approximations of the pharmacological processes which take place in the body and frequently misrepresent the biocompatibility of drugs. This is a problem for all models from simple 2D culture to animal models (Kuna *et al.*, 2018).

The throughput of the model is typically inversely proportional to its predictive capacity. With the simple but high-throughput 2D cultures the cell culture conditions are far from physiologic conditions with typically just hepatocytes present, enforced polarisation and minimal cell-cell contact, among other limitations (Cukierman *et al.*, 2001; Duval *et al.*, 2017; Kenna and Uetrecht, 2018). This leads them to exhibit drug responses which often do not correlate with results seen in animal models or clinical trials. This issue is further exacerbated by toxicity studies utilising cells such as HepG2. These allow for simple, high-throughput assays at low costs however their limited hepatic functionality, detailed in the previous chapters and in literature, makes them less able to accurately predict the impacts of drugs (Xu, Diaz and O'Brien, 2004; O'Brien *et al.*, 2006). This issue is coupled with lack of an accurate assay which can predict DILI across a range of drugs.

Cell viability is often used as a measure for predicting DILI in *in vitro* models. This is a simple measure but typically requires a few assays to be multiplexed. This ensures that aberrant results due to the mechanism of the assay are not caused, as can be the case for metabolic assays. For example cells can have their reductive potential altered by some drugs, therefore giving misleading results for viability with reductive assays such as the MTT assay (Riss *et al.*, 2013; Van Tonder, Joubert and Cromarty, 2015). A commonly used technique is to multiplex viability assays and cytotoxicity assays. Membrane integrity assays are often used for measuring cytotoxicity, with leakage of compounds

such as lactate dehydrogenase (LDH) typically assayed for this purpose (Fotakis and Timbrell, 2006; Niles, Moravec and Riss, 2009).

Alternative endpoint assays can be used such as BSEP inhibition, reactive metabolite quantification and mitochondrial injury, as has been discussed previously for idiosyncratic DILI, with varying success (Chan and Benet, 2018b; Kenna and Uetrecht, 2018; Kenna *et al.*, 2018). One issue with these methods are that some assays measure effects which may not be involved in the toxicity pathway of a drug, for example not all drugs cause mitochondrial damage or BSEP inhibition and therefore a hepatotoxic drug may appear to be non-toxic from these assays in this case (Uetrecht, 2006; Chen, Borlak and Tong, 2016; Kenna and Uetrecht, 2018). To counter this, combinations of assays can be used to screen compounds with improved accuracy over a wider range of drugs than simple single-assay methods (Persson *et al.*, 2013; Chen, Borlak and Tong, 2016; Watkins, 2019).

One final issue with predictivity of *in vitro* DILI models is the disagreement in literature of the *in vivo* DILI potential of drugs from which *in vitro* models compare their results. For example, for two compounds investigated in this chapter, ibuprofen and flutamide, Schadt et al. found the former to be DILI negative whilst the latter was DILI positive (Schadt *et al.*, 2015). Conversely Porceddu et al. used ibuprofen as DILI positive and flutamide as DILI negative (Porceddu *et al.*, 2012). Other studies such as Williams et al. (Williams *et al.*, 2020) and O'Brien et al. (O'Brien *et al.*, 2006) stated both compounds to be DILI positive. This variation in the literature makes defining it difficult to find a commonly agreed measure for DILI positivity for use in *in vitro* studies. This issue is further compounded by the fact that stated peak serum concentration (Cmax) values, often used to calculate the dose ranges, could vary by over an order of magnitude for some drugs between studies (Walker *et al.*, 2020).

At the lower throughput end of the scale animal models allow for more physiologically relevant conditions for drug metabolism to be investigated (Deng *et al.*, 2009). Ethical issues of these models make them increasingly undesirable however the issues with animal models are greater than simply ethics. Many model organisms used for drug testing express key enzymes, such as the CYPs, in different levels to humans (McGill and Jaeschke, 2019). Others express similar enzymes which can carry out many of the same functions but are not the same as those found in humans, whilst other enzymes are lacking altogether with CYP2E1 being shown to be the only CYP which is conserved across all species (Turpeinen *et al.*, 2007). This lack of specific detoxification genes can lead to toxicity in animals not seen in humans. This has been seen in the case of dogs due to lack of N-acetyltransferase (Trepanier, 2004) or cats due to lack of UTG1A6 (Court and Greenblatt, 2000).

Despite these drawbacks, animal models remain a widely used technique for predicting DILI due to the full physiological complexity of the liver being present, therefore providing a higher degree of relevance than standard *in vitro* models (Roth and Ganey, 2011; M Chen *et al.*, 2014).

5.1.4. Increasing the complexity of models can improve their performance for predicting drug toxicity

With the limitations seen in many conventional drug toxicity models studies have frequently investigated improving these using more complex systems. Such systems include co-culture with other cell types as well as use of 3D and micropatterned substrates (Dash *et al.*, 2009; Elliott and Yuan, 2011; Rimann and Graf-hausner, 2012; Sreenivasa C Ramaiahgari *et al.*, 2014; K. A. Rose *et al.*, 2016).

Three-dimensional culture systems are one of the simpler techniques to increase physiological complexity and these have had a lot of attention for drug toxicity studies. The use of 3D cultures can maintain the expression of key metabolic enzymes and transports over prolonged periods and can increase the levels of these in immortal hepatic cell lines, as shown in this work and in literature (Gomez-Lechon *et al.*, 2014; Vorrink *et al.*, 2018). This should then lead to enhanced performance for predicting drug toxicity and DILI (Fey and Wrzesinski, 2012; Proctor *et al.*, 2017). Despite the improvements seen with 3D cultures, they are still a long way from accurately modelling the wide range of drugs available due the other factors of the physiological microenvironment which are still absent (Jian *et al.*, 2015; Cox *et al.*, 2020). It is also of note that most of the drug metabolism assays carried out with 3D models use spheroid models, likely due to the lower volumes of media and drug required as discussed previously.

When using 3D cultures for DILI prediction a range of results are seen with different techniques. With the commonly used spheroid models, primary human hepatocytes regularly show increased sensitivity to hepatotoxic substances, though some substances which are of severe DILI concern still show no sensitivity in these models (Proctor *et al.*, 2017; Li *et al.*, 2020). Interestingly, for 3D models using HepG2 cells instead of primary hepatocytes a decreased sensitivity is often seen with some drugs such as acetaminophen and tamoxifen (Bokhari, Carnachan, Cameron, *et al.*, 2007a; Mueller, Koetemann and Noor, 2011; Sreenivasa C Ramaiahgari *et al.*, 2014). The exact cause for this is unknown and whether this is thought to be an advantage or disadvantage varies between publications. One possible explanation is due to the reduced drug bioavailability in the centre of spheroids compared with 2D monolayers, where every cell is in direct contact with the medium.

However, as mentioned previously for primary human hepatocytes, models with different cells do not exhibit this decrease in sensitivity with the same drugs. For example, the HepaRG cell line shows increased sensitivity to acetaminophen in 3D, more closely matching the response of primary human hepatocytes (Gunness *et al.*, 2013).

To further increase the complexity and physiological relevance, co-culture models have been created which incorporate non-parenchymal cells and can be used for drug toxicity assays. Models with Kupffer cells are the most found co-culture models in literature for DILI prediction due to incorporating the immune response component of DILI. These allow the inflammatory responses to drugs to be modelled, hypothetically improving their performance for prediction of DILI (Kelly A. Rose *et al.*, 2016; Li *et al.*, 2020). Models incorporating other non-parenchymal cells that have been tested for DILI prediction are less common, with the majority of research into these currently focused on CYP expression and basic metabolic function, as discussed in the previous chapter, rather than direct measurements of drug hepatotoxicity (Abu-Absi, Hansen and Hu, 2004; Thomas *et al.*, 2006). However, one recent article highlighted success with co-culturing hepatocytes with stellate cells, LSECs and Kupffer cells in a 3D spheroid model. This model could accurately predict cytotoxicity of the drugs tested and allowed both short term and long term exposure studies, though no comparison with a hepatocyte-only control was presented (Nudischer *et al.*, 2020).

5.1.5. Fluid flow models for drug toxicity prediction

The models mentioned previously contribute to increased physiological relevance of models however lack the dynamic nature of the liver, caused by the turnover of fluids. Further increasing the complexity of *in vitro* DILI models through the incorporation of fluid flow has been widely studied with many studies focusing predominantly on the use of microfluidic systems. These have been shown to allow effective perfusion of drug-spiked media through hepatocyte cultures and often outperform comparable static cultures (Rowe *et al.*, 2018; Bircsak *et al.*, 2021).

A major advantage of these systems comes from their small size which allows drug trials to be carried out with small quantities of drugs, particularly useful with expensive drug candidates. A limitation with these systems comes from their frequent use with 2D cell substrates, limiting the cell-cell contact and enforcing a specific polarisation on cells (Goral and Yuen, 2012). Some microfluidic systems have been developed which utilise hydrogels and scaffolds to recreate the 3D culture systems, overcoming this shortfall (Powers *et al.*, 2002; Kim, Yeon and Park, 2007; Toh *et*

al., 2009). Further advances with microfluidic systems come from the incorporation of NPCs, as seen with 3D static systems. The benefits of these systems, for both longevity of culture and predictive capacity, are well documented with many new systems being developed for DILI prediction (Long *et al.*, 2016; Busche *et al.*, 2020; Bircsak *et al.*, 2021).

Larger bioreactor systems allow for the creation of more complex tissue equivalents which contain a variety of cell types and can exhibit patterning like that found *in vivo.* Basic forms of these systems utilise hepatocyte spheroids in suspension in a mixed fluid. The rotary bioreactor design is infrequently used for this due to cost and throughput limitations however spinner flasks have often been used as a low-cost alternative (Sakai *et al.*, 1996; Hammond, Allen and Birdsall, 2016). Such systems have shown similar responses to microfluidic systems with improvements over 3D cultures such as maintenance of CYP function over long periods (Miranda *et al.*, 2010; Leite *et al.*, 2012).

Alternative systems include hollow fibre bioreactors, as discussed in previous chapters. For applications with drug toxicity these have successfully been miniaturised to allow small volumes of media to be used, overcoming the cost issues associated with large media volumes for drug testing (Zeilinger *et al.*, 2011; Hoffmann *et al.*, 2012). These have been successfully used for DILI prediction, exhibiting a stable phenotype over a week whilst showing dose-dependent responses to drugs (Knöspel *et al.*, 2016; Freyer *et al.*, 2018, 2019).

5.1.6. Conclusions

It is clear from previous research that improved methods for predicting drug toxicity *in vitro* are required. Whilst major advances have been made using advanced cell culture techniques such as 3D scaffolds and co-cultures with NPCs, the aim of accurately predicting the wide range of toxic pathways from various drugs is still incomplete.

Bioreactors have helped to further increase the physiological relevance of cultures used in DILI investigations. These still tend to suffer from limitations due to throughput, cost, and complexity, however it is a rapidly expanding field and new systems to overcome these problems are continually under research.

From this background, it seems highly likely that the novel bioreactor system developed in this work will be beneficial for the predictive capacity of *in vitro* drug toxicity models. In this chapter the use of the system to explore the toxicity of a range of drugs between static 2D, 3D and stirred culture.

5.2. Hypothesis, Aims and Objectives

5.2.1. Hypothesis

Previous work in literature and the results of the previous chapter showing improved protein and gene expression suggest that the bioreactor system should lead to better representation of the toxic effects of drugs compared with static culture. Therefore, in this chapter we hypothesis that the HepG2 models should better predict the toxicity of a range of drugs which are not always accurately predicted in typical *in vitro* models and therefore present this system as a useful alternative to some models which are used at present for this purpose.

5.2.2. Aims

In this chapter we will test the 3D stirred HepG2 cultures characterised in the previous chapter against a range of drugs with different levels of toxicity and metabolic pathways. The improvements seen in the dynamic cultures leads to a hypothesis that an improved response to drugs should be seen. Drugs which are found to be toxic *in vitro* but not *in vivo* should start to shift towards the *in vivo* response whilst drugs with underrepresentation of toxicity *in vitro* should be more heavily impacted. For this purpose, the models will be treated with a supraphysiological dose over a one-day period at the end of their initial culture time to investigate acute drug toxicity.

5.2.3. Objectives

- Demonstrate the application of the 3D stirred HepG2 model for testing the cytotoxicity of drugs.
- Apply a range of drugs to models and determine the toxicological response and compare this to the response seen in 2D and 3D static models.
- Investigate the changes seen in relation to the known metabolic pathways of the drugs and with reference to the expression of key metabolic proteins as determined in Chapter 4.

5.3. Materials and Methods

5.3.1. Drugs used for toxicological testing

A range of drugs were selected for the testing as set out in Table 5.1. These were selected based on their different metabolic pathways in hepatocytes, different outcomes *in vitro* compared with those seen *in vivo* and previous experience of these drugs within our laboratory. The concentration range was typically chosen to reach 100x the Cmax value, as is often the case in literature. For some drugs, such as gemfibrozil, a lower dose range was chosen due to previous work with this drug on HepG2 cells within the group. For indomethacin a lower dosage range was also used due to solubility issues with this drug at higher concentrations.

Table 5.1: Concentrations and vehicles used for the drug tests. Cmax values were taken from literature and used as a basis for the concentrations used. Typically, the concentration range was chosen to cover 100x the Cmax value, with exceptions due to limitations such as solubility.

Compound	*Drug Class*	*Cmax (µM)*	*Concentration Range (µM)*	Vehicle	References
Acetaminophen	Analgesic	139	2,500 – 40,000	Media	Ramaiahgari et al., 2014
Amiodarone	Arrhythmia	0.85	18.75 – 300	DMSO	Shah et al., 2015
Isoniazid	Anti-tuberculosis	76.6	1,250 – 20,000	Media	Xu et al., 2008
Gemfibrozil	Antilipemic	185	500 – 8,000	Ethanol	Knauf et al., 1990 Previous group work (unpublished)
Ibuprofen	NSAID	36.7	312.5 – 5,000	Ethanol	Kleinbloesem et al., 1995 Previous group work (unpublished)
Tamoxifen	Oestrogen Antagonist	0.16	9.375 – 150	DMSO	Mueller et al., 2011 Fuchs et al., 1996
Indomethacin	NSAID	5.6	31.25 - 500	DMSO	Xu et al., 2008
Flutamide	NSAA	0.36	31.25 - 500	DMSO	Ball et al., 2016

Typically, either DMSO or ethanol was used as a vehicle for the drug. In this case a 200x solution of the highest concentration was produced, with serial dilutions leading to 200x solutions for each concentration in the range. In all cases a vehicle concentration of 0.5 % was used for both ethanol and DMSO.

5.3.2. Methods for dosing 2D and 3D static models

For the static 2D and 3D models a simple dosing regimen was used in which the drug of interest was diluted to the correct concentration in cell culture medium and then the toxicological challenge was initiated through a complete media change for these samples. The exception to this was for acetaminophen which has low solubility and therefore the highest concentration of 40 µM used in

the experiment was used as the master mix, diluted in complete cell culture medium. For all other drugs the stock solution was serially diluted to create a dilution series for use in the experiments with each dilution being 200x the desired final concentration. This means that for those diluted in DMSO and ethanol the concentration of ethanol in cell culture never exceeded 0.5 %. These serial dilutions were added to fresh, prewarmed cell culture medium made up as described in Chapter 2.

Models were removed from the incubator at the end of the 14-day culture period and medium was removed with an aspirator. The medium containing the drug concentrations was then added to the respective wells labelled for each concentration. And the plates were placed back in the incubator for a further 24 hours. At the end of this time period the cultures were removed, media samples taken and stored on ice for the LDH assay and an MTT assay was carried out on the cultures as described in Chapter 2.

5.3.3. Methods for dosing bioreactor models

For the bioreactor cultures a different method of dosing the samples was used. Due to the large volume of media involved in a cell culture a complete media change to add a drug would be an inefficient use of consumables. Due to this it was instead decided to dose the bioreactor models by adding a shot of the 200x concentrated solution to the media, as shown in Figure 5.5. The turbulent motion of the fluid flow evenly distributes this throughout the fluid and avoids areas of localised high concentrations.

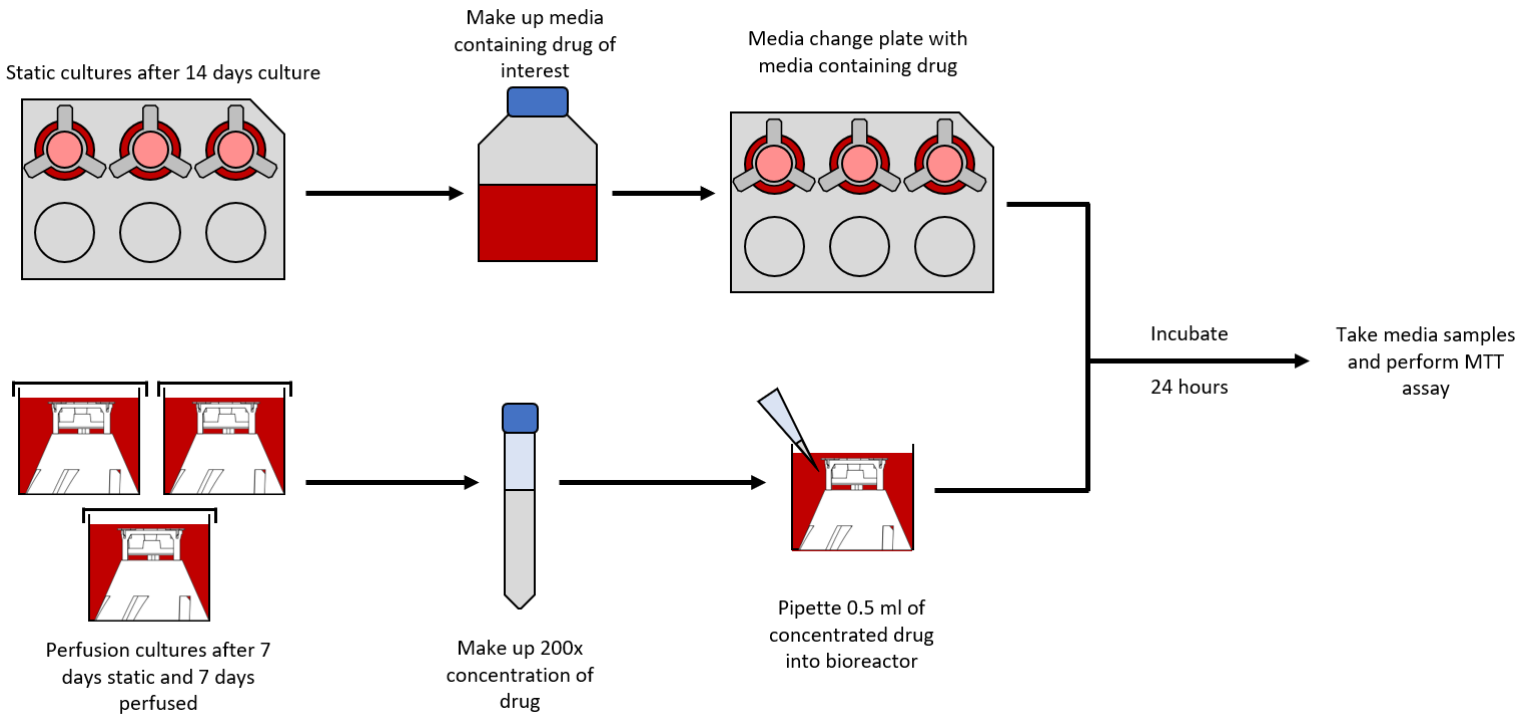

Figure 5.5: The dosing regimens used for static and stirred cultures. For static cultures the drug was added to cell culture medium to the desired concentrations before being added to the cultures in a complete media change. For bioreactor cultures a 200x concentrated solution was made up in the vehicle and added to the bioreactors, with the convective mixing of the fluid flow distributing the drug evenly. Endpoint analysis was then performed with both the MTT assay and LDH assay.

After the 14-day culture period of 7 days in static and 7 days in dynamic conditions, as optimised in Chapter 4, the bioreactors were removed from the incubator. A volume of 0.5 mL of the 200x concentration of the drug dilutions, made up as described in the previous section, was then pipetted into the side of the bioreactor, leading to a final concentration in the 100 mL of media of 1x drug in 0.5 % vehicle for that respective sample. The cultures were then placed back into the incubators on the stirrer units and incubated for a further 24 hours. At the end of this period a sample of media was taken for use in the LDH assay as described previously and the Alvetex® membranes were moved into a 12-well plate for an MTT assay to be carried out as described in Chapter 2.

To ensure this method was suitable and produced the same results as the standard media change dosing method the two techniques were run in parallel using the drug gemfibrozil. Previous research by the lab has shown that this drug has similar dose response in 2D as in 3D and therefore it was chosen as a loss of viability was likely in dynamic culture, therefore allowing any changes to be easily seen unlike some drugs which have stable viability in 3D methods. As shown by Figure 5.6 the results showed no measurable change in dose response between the two methods and therefore the addition of 200x drug solution directly to the bioreactors was chosen as the preferred technique for subsequent experiments.

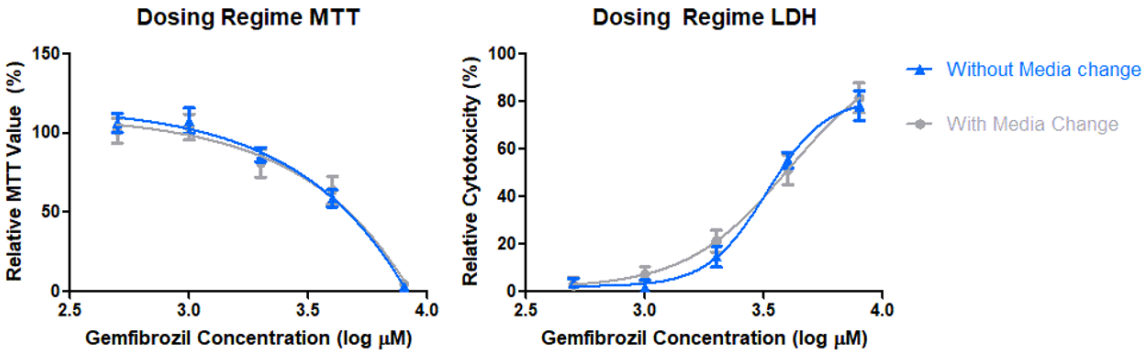

Figure 5.6: Comparison of results between the two bioreactor dosing regimens. All samples were HepG2 on Alvetex Strata cultured in the bioreactor system. One set of models received a complete media change containing gemfibrozil whilst the other had the drug added through a 200x concentrated 0.5 mL dose. Values are mean ± SEM, n = 3.

5.3.3.1. Variation to the protocol for Acetaminophen dosing

Due to the low solubility of acetaminophen at the doses required the dosing procedure for this drug matched that for the 2D and 3D static samples with a full media change taking place, as shown in Figure 5.7. For this purpose, the drug was made up to highest concentration required in cell culture medium and serially diluted into subsequent fresh cell culture medium to create the required dilution series. The cultures were removed from the incubator at the end of the culture period and the media was aspirated off. The drug-spiked media was then added to each bioreactor to a final volume of 100 mL and the cultures were placed back into the incubator for a further 24 hours. The subsequent analysis was carried out as described in the previous section.

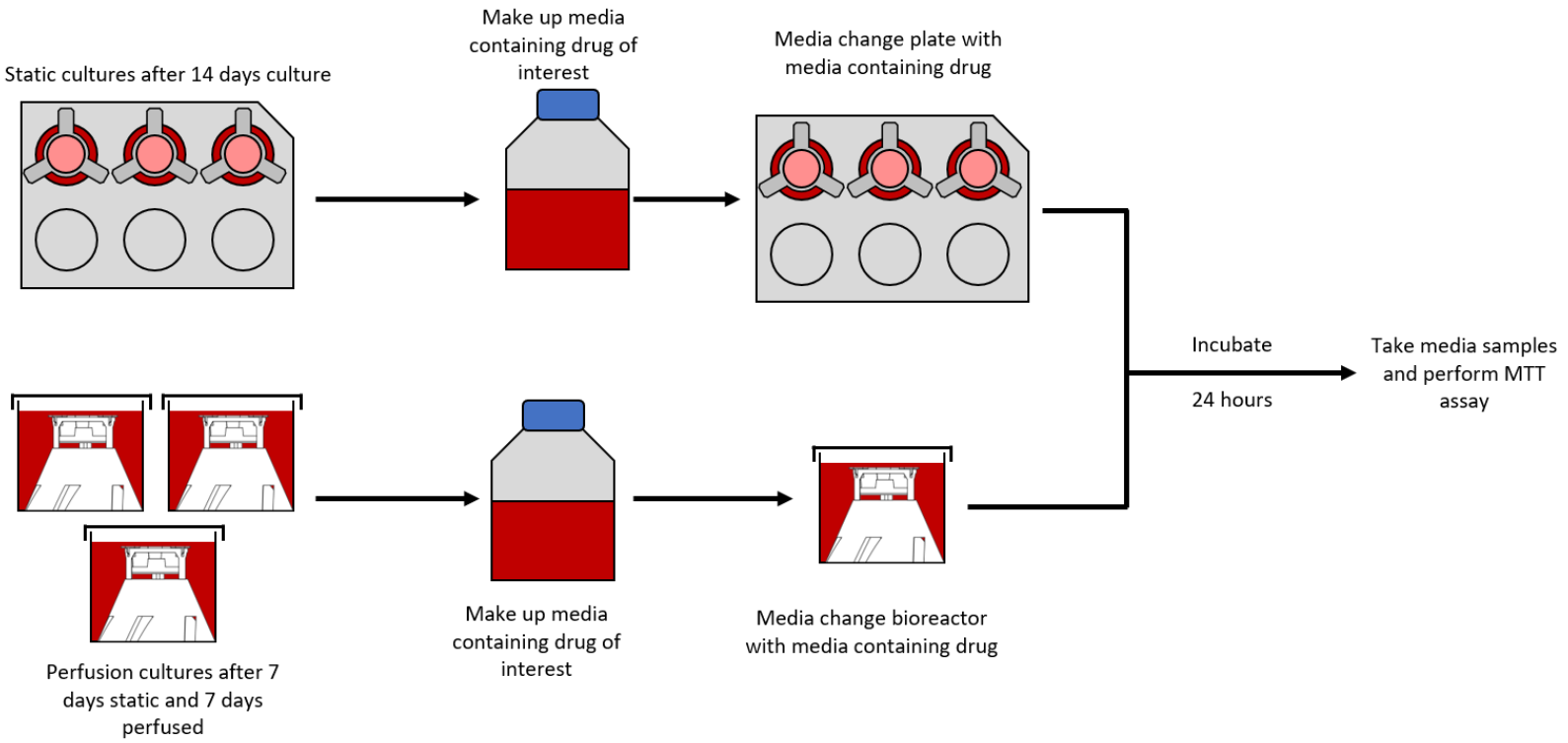

Figure 5.7: The dosing regimen of acetaminophen used for static and stirred cultures. For both static and stirred cultures, the prewarmed media is made up with the final concentrations of acetaminophen. This was then added to the cultures through a complete media change. Models were incubated for 24 hours and before endpoint analysis was carried out. Endpoint analysis was performed with both the MTT assay and LDH assay.

5.4. Results

5.4.1. Response of bioreactor models to toxicological challenge

The response to different xenobiotic substances is one of the key measures of the research value of *in vitro* models. This was investigated by adding different concentrations of drugs to the models and measuring the changes in viability caused by these compounds. The known metabolic pathways of the drugs and the changes in expression of key metabolic enzymes as discovered in Chapter 4 can then be used to elucidate possible reasons for the observed responses.

Both the MTT assay and the LDH assay were used in parallel to produce an accurate picture of the toxic effects. MTT assays are often used as measures of cell viability however their true measure is of metabolic activity, specifically reductive. Whilst this is a good proxy for viability in many circumstances the changes in metabolic rates caused by many drugs can cause the MTT assay to give a reading which is not necessarily directly correlated with cell viability. To overcome this the LDH assay is also used. This measures the level of LDH released, caused by plasma membrane damage, and is therefore an alternative method to measure cytotoxicity which is often used in literature.

5.4.1.1. Acetaminophen drug response

Acetaminophen, a medication used to treat fever and pain, is one of the most used drugs around the world and is widely studied in hepatotoxicity investigations. As can be seen in Figure 5.8 the response in 2D shows a dose-dependent reduction in viability through both a decrease in MTT value and increase in LDH release in line with previous studies with a reduction in viability of around 60 % at the highest concentration tested of 40 µM. This result is not matched in 3D which instead shows no measurable response to the drug at any concentration. When tested in dynamic conditions the response is seen to be the same as in 3D static with no measurable change in viability.

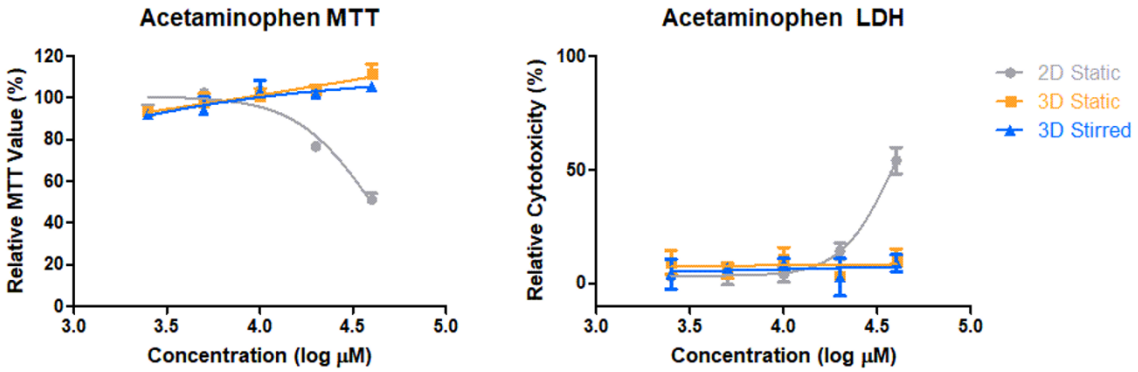

Figure 5.8: Results of acetaminophen toxicity on the different HepG2 models. Graphs show the results of MTT and LDH assays carried out after 24 hours of drug treatment on HepG2. 2D samples were performed in a 6-well plate, 3D static were on an Alvetex® Strata 6-well insert whilst 3D stirred were on an Alvetex® Strata 6-well insert in the bioreactor system. Acetaminophen was added to prepared culture medium and added to the models through a complete medium change. The MTT assay was carried out on the tissue models whilst the LDH assay was performed on the media. Values are mean ± SEM, n = 3.

APAP is metabolised to several different metabolites *in vivo* and the pathway used has a major impact on its toxicity. Whilst the common pathways at therapeutic doses are glucuronidation to APAP glucuronide or sulfation to APAP sulfate, metabolised by UGT and SULT enzymes respectively. Under toxic doses a higher proportion of APAP is metabolised to the toxic metabolite N-acetyl-p-benzoquinone imine (NAPQI), predominantly by CYP2E1. With the findings in Chapter 4 showing that the relevant UGT and SULT enzymes are upregulated significantly in 3D and dynamic culture conditions, compared with a more modest increase in the CYP2E1 levels, it is possible that this reduction in toxicity is caused by the improved ability of the cells to process APAP to the non-cytotoxic metabolites.

5.4.1.2. Amiodarone drug response

Amiodarone is an antiarrhythmic medication which has previously been pulled from the market due to side effects, but subsequently reintroduced when its uses as an antiarrhythmic was discovered (Sneader, 1996). It has been shown to have a rare but serious side effect in the liver, causing hepatotoxicity and cirrhosis (Buggey *et al.*, 2015). In the 2D experiments toxicity can be seen across the whole range of doses tested in the MTT assay, whilst the LDH assay displays toxicity occurring from a concentration of around 75 µM (Figure 5.9). For the 3D static and stirred models,

a similar pattern can be seen to that with acetaminophen, with a much-reduced sensitivity to cytotoxicity. Only at the highest dose of 300 µM can a minor toxic effect start to be seen.

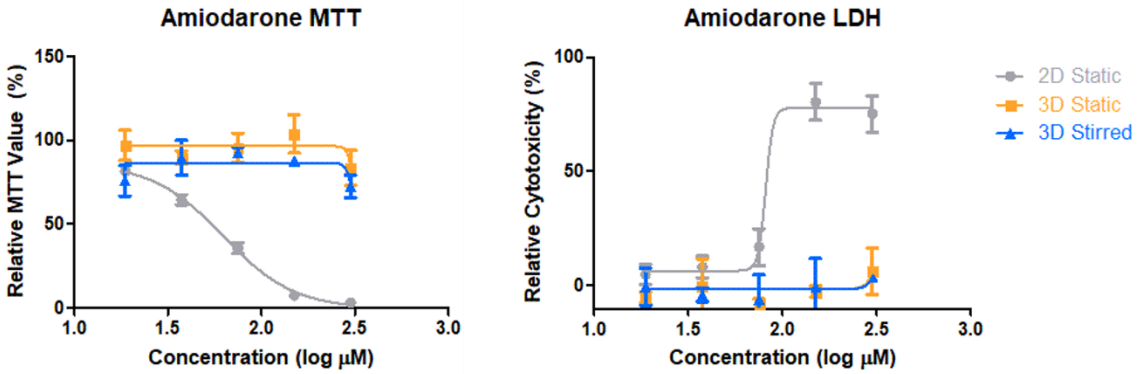

Figure 5.9: Results of Amiodarone toxicity on the different HepG2 models. Graphs show the results of MTT and LDH assays carried out after 24 hours of drug treatment on HepG2. 2D samples were performed in a 6-well plate, 3D static were on an Alvetex® Strata 6-well insert whilst 3D stirred were on an Alvetex® Strata 6-well insert in the bioreactor system. Amiodarone was dissolved in DMSO prior to addition to the cultures. The values are relative to the respective vehicle controls. No difference was seen between the vehicle control and untreated controls. The MTT assay was carried out on the tissue models whilst the LDH assay was performed on the media. Values are mean ±SEM, n = 3.

Amiodarone is primarily metabolised to desmethylamiodarone by CYP3A4 and CYP2C8. As the toxicity is primarily caused by the drug itself, rather than by the metabolites, it would be expected that an increased phase I metabolism would lead to a reduction in hepatotoxicity of this drug. The data in Chapter 4 suggested that both CYP3A4 and CYP2C8 were upregulated in dynamic conditions, therefore suggesting that the metabolism of this drug would be higher in these models and supporting the hypothesis that this is the cause for the reduced sensitivity.

5.4.1.3. Isoniazid drug response

Isoniazid is an antibiotic typically used alone or in combination with other antibiotics for the treatment of tuberculosis. This drug is known to be capable of causing increased serum levels of liver enzymes as well as acute liver injury. As seen for the two drugs previously, a decrease in viability is seen in 2D for isoniazid which is not replicated in 3D static or dynamic conditions (Figure 5.10). This sees a drop to around 50% viability at the highest concentration in both the MTT and LDH assays for 2D whilst for the other two conditions viability remaining stable.

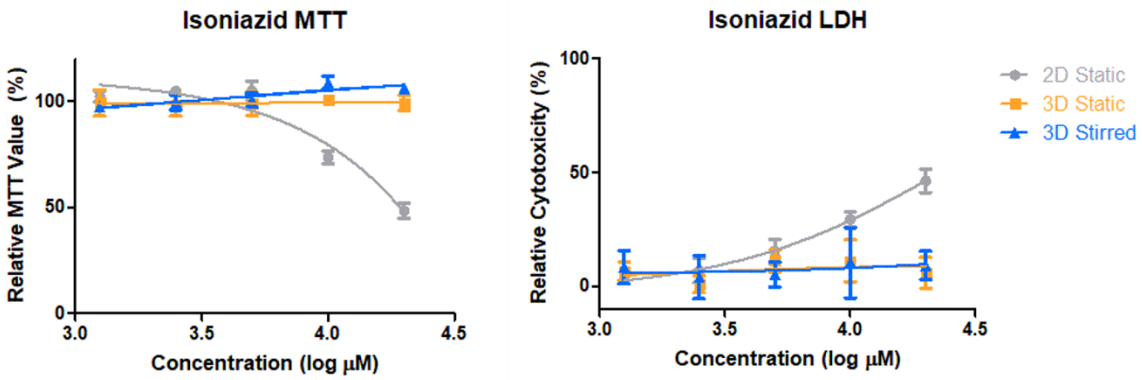

Figure 5.10: Results of Isoniazid toxicity on the different HepG2 models. Graphs show the results of MTT and LDH assays carried out after 24 hours of drug treatment on HepG2. 2D samples were performed in a 6-well plate, 3D static were on an Alvetex® Strata 6-well insert whilst 3D stirred were on an Alvetex® Strata 6-well insert in the bioreactor system. Isoniazid was dissolved in cell culture medium prior to addition to the cultures. The values are relative to the respective untreated controls. The MTT assay was carried out on the tissue models whilst the LDH assay was performed on the media. Values are mean

The metabolism and modes of toxicity for isoniazid are less well-studied than APAP however it is thought that the primary metabolite is N-acetylisoniazid, metabolised by the NAT enzymes. This is then further metabolised to isonicotinic acid and monoacetylhydrazine, the latter of which leads to hepatotoxicity when further metabolised by the CYP enzymes but is not toxic when metabolised by amidase. *In vivo* the levels of NAT enzymes appear to have a correlation with the chance of hepatotoxicity, with individuals expressing low levels of NATs typically experiencing worse hepatotoxic effects (Wattanapokayakit *et al.*, 2016). The gene expression analysis in Chapter 4 the levels of the NAT enzymes were seen to be increased in both 3D static and 3D bioreactor models compared with the levels in 2D, therefore this reduction in sensitivity to isoniazid in these conditions seen here could be due to the increased NAT expression.

5.4.1.4. Gemfibrozil drug response

Gemfibrozil is a drug which can be taken orally to reduce the levels of lipids in the blood with hepatoxicity reported as a rare side effect. A similar response is seen for all three conditions with this drug, in contrast to the variations seen in the previous two drugs (Figure 5.11). A reduction in viability became apparent at a concentration of 2 mM which then continues to decrease through subsequent dose increases and an almost complete loss of viability is seen at the highest

concentration tested of 8 mM. While a large amount of variability is seen between doses and samples for this drug the overall trend seems to show no change between the three culture types.

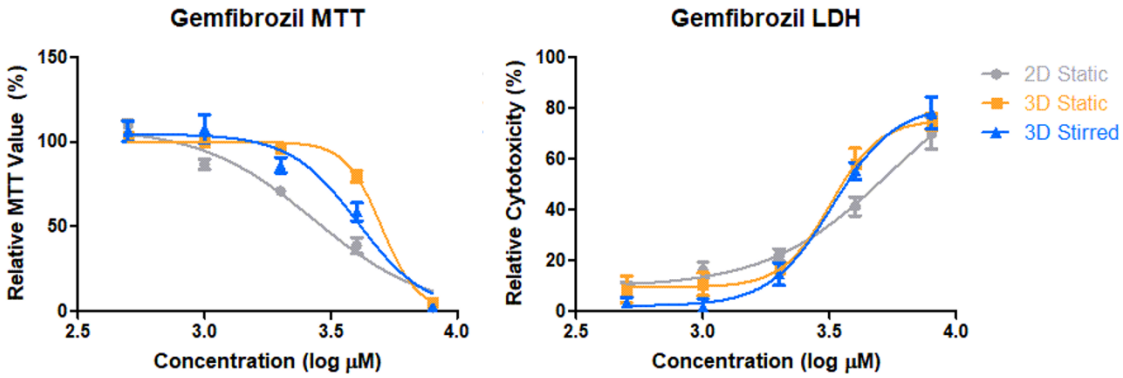

Figure 5.11: Results of Gemfibrozil toxicity on the different HepG2 models. Graphs show the results of MTT and LDH assays carried out after 24 hours of drug treatment on HepG2. 2D samples were performed in a 6-well plate, 3D static were on an Alvetex® Strata 6-well insert whilst 3D stirred were on an Alvetex® Strata 6-well insert in the bioreactor system. Gemfibrozil was dissolved in ethanol prior to addition to the cultures. The values are relative to the respective vehicle controls. No difference was seen between the vehicle control and untreated controls. The MTT assay was carried out on the tissue models whilst the LDH assay was performed on the media. Values are mean ±SEM, n = 3.

Studies have suggested that the toxicity of gemfibrozil stems from an immunologic response to an intermediate in its metabolism. Whilst gemfibrozil 1-O-β-glucuronide, an inhibitor of CYP 2C8 and formed by the UGT enzymes, is a known metabolite of gemfibrozil, several other metabolites exist via unknown pathways. It is typically expected that the increases in the phase I and II enzymes in 3D static and dynamic conditions cause an enhanced drug metabolism, either forming more toxic metabolites or allowing greater clearance and reduced toxicity. The lack of a clear change in viability between the different conditions seen here further confuses an already unclear pathway of toxicity. A potential hypothesis for this effect could be that the levels of metabolite formation and clearance are both similarly boosted, therefore leaving viability unchanged.

5.4.1.5. Ibuprofen drug response

Ibuprofen is a common pain and fever medication and is classed as a nonsteroidal anti-inflammatory drug. The potential side effects of ibuprofen are well documented and liver dysfunction of failure has been found to be a rare side effect. In 2D a reduction in MTT value is seen

at a concentration of 1.25 mM (Figure 5.12). This reduction continues up to the maximum concentration tested of 5 mM where the viability is roughly 60 % of the initial value. For 3D static and dynamic conditions this pattern is not seen with both instead maintaining stable viability over all concentrations. The LDH assay shows a similar result with a reduction of around 50 % seen at the highest concentration, though less effect seen at earlier concentrations.

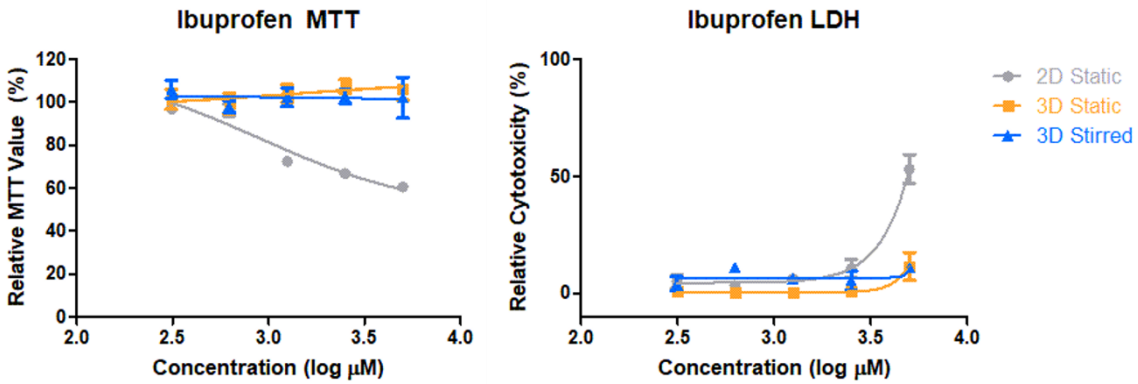

Figure 5.12: Results of Ibuprofen toxicity on the different HepG2 models. Graphs show the results of MTT and LDH assays carried out after 24 hours of drug treatment on HepG2. 2D samples were performed in a 6-well plate, 3D static were on an Alvetex® Strata 6-well insert whilst 3D stirred were on an Alvetex® Strata 6-well insert in the bioreactor system. Ibuprofen was dissolved in ethanol prior to addition to the cultures. The values are relative to the respective vehicle controls. No difference was seen between the vehicle control and untreated controls. The MTT assay was carried out on the tissue models whilst the LDH assay was performed on the media. Values are mean ±SEM, n = 3.

The majority of ibuprofen is transformed to 2-hydroxy ibuprofen *in vivo*, metabolised predominantly by CYP2C8 and CYP2C9. Low levels of ibuprofen are also glucuronidated by the UGTs to form ibuprofen glucuronide, a potential cause of toxicity. The reduction in toxicity seen in 3D static and dynamic conditions suggest that the improved expression of CYP2C9 in 3D static and both CYP2C8 and CYP2C9 in dynamic culture, as reported in Chapter 4, leads to cells being more able to remove ibuprofen by the predominant, unreactive metabolite 2-hydroxy ibuprofen.

5.4.1.6. Tamoxifen drug response

Tamoxifen is an antiestrogenic drug commonly used for the treatment of breast cancer. Tamoxifen has been reported to cause idiosyncratic DILI in rare cases with a variety of different presentations as well as leading to non-alcoholic fatty liver disease in high-BMI women over a timespan of up to

several years (Bethesda (MD): National Institute of Diabetes and Digestive and Kidney Diseases, 2021b). This drug shows a different pattern of toxicity to the other drugs tested prior to this with similar patterns seen in both the MTT assay and the LDH assay (Figure 5.13).

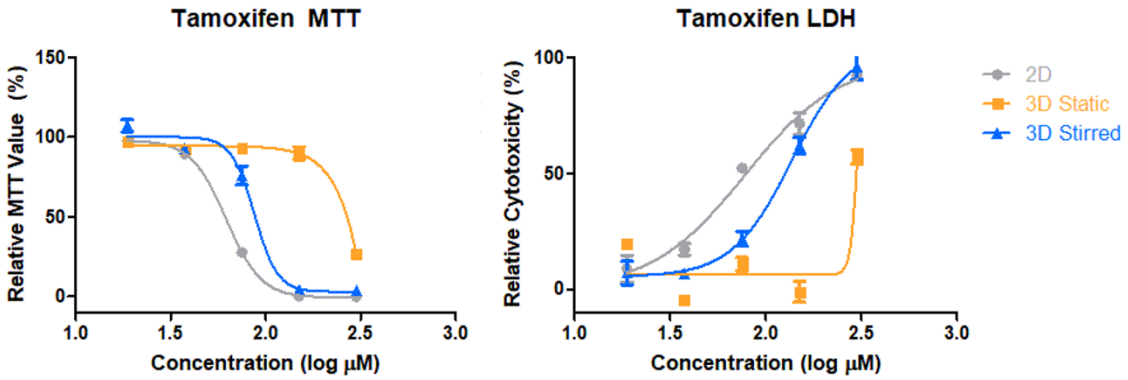

Figure 5.13: Results of Tamoxifen toxicity on the different HepG2 models. Graphs show the results of MTT and LDH assays carried out after 24 hours of drug treatment on HepG2. 2D samples were performed in a 6-well plate, 3D static were on an Alvetex® Strata 6-well insert whilst 3D stirred were on an Alvetex® Strata 6-well insert in the bioreactor system. Tamoxifen was dissolved in DMSO prior to addition to the cultures. The values are relative to the respective vehicle controls. No difference was seen between the vehicle control and untreated controls. The MTT assay was carried out on the tissue models whilst the LDH assay was performed on the media. Values are mean ±SEM, n = 3.

In 3D static culture the models show decreased sensitivity to the compound as has been the trend with these models previously. These models do not start to show a cytotoxic response until around 75 µM compared with the much earlier response seen after 18.75 µM in 2D culture. For stirred 3D culture this effect is reverse with a very similar pattern of cytotoxicity between the 2D static and 3D stirred samples.

Whilst tamoxifen itself has antiestrogenic activity some of the intermediate compounds in its metabolism are far more potent and it is likely that these are the cause of toxicity seen in 2D culture. The initial metabolism is carried out by the phase I enzymes to form the reactive metabolites such as n-desmethyl tamoxifen and 4-hydroxy tamoxifen. These are then further metabolised to other intermediates before finally being glucuronidated or sulphated, inactivating them. One explanation for the results seen here is that the higher ratio of increase for phase II enzymes compared with phase I in the 3D static cultures leads to a greater level of inactivation of the reactive intermediates. Contrary to this, for 3D dynamic culture, in which a much higher increase in gene expression of phase I enzymes was found, it is possible the increase in both metabolisms is balancing out resulting

in similar levels of toxicity as seen for 2D cultures. Further work to decipher these mechanisms could involve an investigation into the metabolites present in the media, as although toxicity would be similar the overall clearance rate would be expected to be higher for 3D stirred cultures in this instance. Once the different pathways can be observed, the results can be linked to the changes in protein and gene expression seen in Chapter 4 to give a broad understanding of the biological processes taking place.

5.4.1.7. Indomethacin drug response

Indomethacin is a non-steroidal anti-inflammatory drug commonly used to treat fever and inflammation. Whilst mild increases in serum aminotransferase levels are seen in up to 15 % of patients taking indomethacin chronically, hepatotoxicity due to indomethacin is rare (Bethesda (MD): National Institute of Diabetes and Digestive and Kidney Diseases, 2021a). For all doses of indomethacin there is little measurable cytotoxicity apparent for all 2D, 3D static and 3D stirred models in both the MTT and LDH assays (Figure 5.14). Whilst this appears to be a result of limited value it is worth testing the system with known *in vitro* true negative drugs to ensure there are no adverse changes which might affect the false positive rate of *in vitro* models.

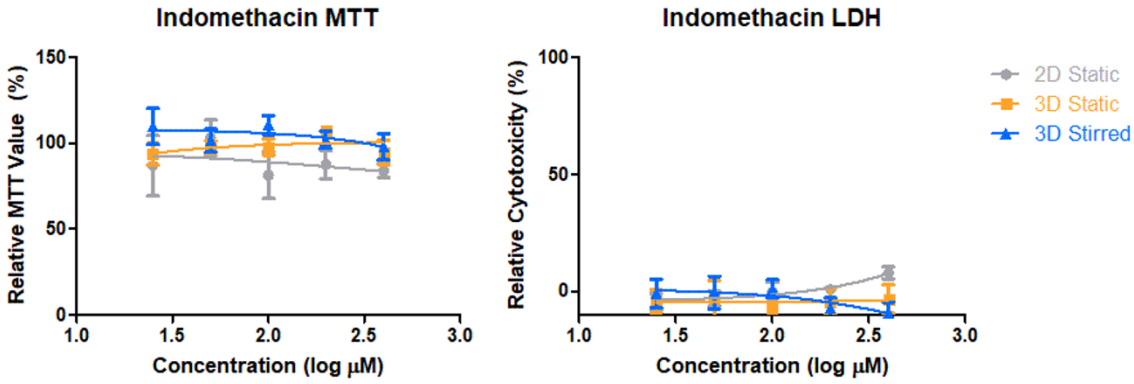

Figure 5.14: Results of Indomethacin toxicity on the different HepG2 models. Graphs show the results of MTT and LDH assays carried out after 24 hours of drug treatment on HepG2. 2D samples were performed in a 6-well plate, 3D static were on an Alvetex® Strata 6-well insert whilst 3D stirred were on an Alvetex® Strata 6-well insert in the bioreactor system. Indomethacin was dissolved in DMSO prior to addition to the cultures. The values are relative to the respective vehicle controls. No difference was seen between the vehicle control and untreated controls. The MTT assay was carried out on the tissue models whilst the LDH assay was performed on the media. Values are mean ±SEM, n = 3.

Indomethacin undergoes transformation to several different metabolites by the CYP and UGT enzymes in hepatocytes. These metabolites are thought to have very limited pharmacological activity, therefore explaining the lack of hepatotoxicity of indomethacin. It would be expected that although no change in viability can be seen in these different culture methods a higher rate of metabolism would be carried out in the 3D static and stirred cultures and this would be something to investigate for future experiments.

5.4.1.8. Flutamide drug response

The final drug tested in this chapter, flutamide, is a non-steroidal antiandrogen used as a treatment for prostate cancer. Flutamide has been found to cause acute liver injury in up to 1 % of patients which can be severe and, in some cases, lead to death. For HepG2 in 2D culture a clear dose response for this drug can be seen with a very high loss of viability by 250 µM in the MTT assay, whilst a slightly slower response is seen for the LDH assay, though still reaching almost complete cell death by 500 µM (Figure 5.15). This response appears to be similar for the 3D static cultures. A slightly less sensitive response can be seen for the MTT assay whilst the LDH assay is more comparable between the two suggesting there is limited difference between these two methods. For the stirred culture, on the other hand, increased sensitivity is apparent in both the MTT assay and the LDH assay with measurable loss in viability almost immediately at the lowest concentration tested of 31.25 µM.

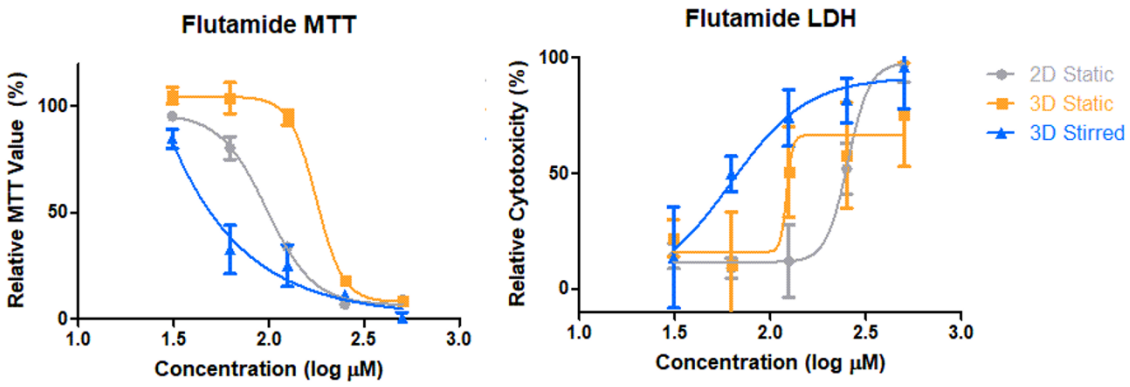

Figure 5.15: Results of Flutamide toxicity on the different HepG2 models. Graphs show the results of MTT and LDH assays carried out after 24 hours of drug treatment on HepG2. 2D samples were performed in a 6-well plate, 3D static were on an Alvetex® Strata 6-well insert whilst 3D stirred were on an Alvetex® Strata 6-well insert in the bioreactor system. Flutamide was dissolved in DMSO prior to addition to the cultures. The values are relative to the respective vehicle controls. No difference was seen between the vehicle control and untreated controls The MTT assay was carried out on the tissue models whilst the LDH assay was performed on the media. Values are mean ±SEM, n = 3.

The exact pathway of flutamide toxicity is not well understood. Flutamide is extensively metabolised by the CYP enzymes, in particular CYP3A4, and it is thought that one of these metabolites is the cause of hepatotoxicity (Goda *et al.*, 2006). With the finding in Chapter 4 that CYP3A4 gene expression was over tenfold higher under fluid flow than in 2D or 3D static culture, the higher toxicity of flutamide in dynamic culture seen here would seem to be as expected.

5.5. Discussion

5.5.1. Drug toxicity varies significantly with different *in vitro* models

From the data in this chapter, the method used for culturing cells can be seen to have a significant impact on their toxicological response. Most of the drugs tested herein showed a different response between at least 2 of the conditions investigated, with the exact nature of the difference's variable between drugs.

In nearly all cases the 3D static culture models displayed decreased sensitivity to the drugs tested. In some cases, this may be as expected, for example in the case of acetaminophen, in which the increased expression of phase II enzymes relative to phase I enzymes would be expected to cause less of the reactive metabolite NAPQI to be formed. This hypothesis is supported by data which shows higher levels of APAP sulfation, forming non-toxic metabolites, in 3D models (Sreenivasa C. Ramaiahgari *et al.*, 2014). Many other papers have similarly found that the use of 3D culture, usually in the form of spheroids, leads to reduced sensitivity to APAP both with HepG2 cells (Bokhari, Carnachan, Cameron, *et al.*, 2007a; Mueller, Koetemann and Noor, 2011; Sreenivasa C Ramaiahgari *et al.*, 2014; Lee *et al.*, 2020) and HepaRG (Gunness *et al.*, 2013; Ramaiahgari *et al.*, 2017).

Some papers, contrary to this, have reported increased sensitivity to APAP toxicity for 3D cultures of both primary hepatocytes and cell lines such as HepG2 and HepaRG (Jang *et al.*, 2015; Gaskell *et al.*, 2016; Liu *et al.*, 2018; Li *et al.*, 2020). These papers all use significantly shorter time periods for 2D culture than 3D, in some cases as many as 3 to 4 weeks less (Gaskell *et al.*, 2016; Liu *et al.*, 2018). This could explain this discrepancy due to the time required for hepatocytes to fully polarise in culture regardless of culture method (Luckert *et al.*, 2016). It is also notable that many studies in literature do not make direct comparisons between their 3D models and comparable 2D models, instead comparing to values from other 2D experiments in literature (Vorrink *et al.*, 2018). Therefore, it is possible that some reported results which seem to differ from these could be due to the variability between experiments when carried out by different laboratories at different times.

In some cases, the reduced toxicity for 3D static models is not as expected. Amiodarone is a good example of this, with increased levels of CYP3A4 associated with enhanced drug detoxification. Given that the gene expression levels of CYP3A4 appeared to be unchanged between 2D and 3D cultures, from the data in Chapter 4, a minimal change would be expected. The dramatic difference seen here suggests that the toxicity can be caused by other mechanisms as well as simply direct

toxicity of a metabolite. Similar results have been reported elsewhere for this drug, suggesting that this mechanism is also the case for other 3D models (Sirenko *et al.*, 2016; Lee *et al.*, 2020). From mass spectrometric analysis a second-generation metabolite has been identified with a higher predicted toxicity than amiodarone itself. While the exact metabolic pathway is unknown, it is possible metabolites further through the pathway such as this could be the cause of the reduced sensitivity (Varkhede *et al.*, 2014).

One possible explanation for the decreases in sensitivity seen in 3D static models is due to the increased cell number found in these models. It has been suggested that this could be leading to reduced toxicological responses due to the greater number of cells being able to tackle the same concentration of a drug more effectively (Fey and Wrzesinski, 2012; Fey, Korzeniowska and Wrzesinski, 2020). One way around this issue has been the idea of using a dose of a drug for cultures, normalised to a metric of cell number such as total DNA or protein, rather than a concentration as is typically used. Equivalent to how drug toxicity is studies in animal experiments, in which animals are dosed per kg of body mass, this would give the cells a comparable level of drug to metabolise between culture methods (Fey and Wrzesinski, 2012).

This method is not without its drawbacks. Due to the immediate availability of the drug within the media, compared with the gradual absorption and consequent dynamic concentration in orally dosed drugs (Li *et al.*, 2011), the cells would have a much higher instantaneous level of drugs than found *in vivo* (Eastman, 2017). A further issue is caused by the reduction in bioavailability of drugs in 3D models, with many of the cells surrounded by other cells rather than in contact with the medium. This could be beneficial when using dosage-based models however it represents another variable which further complicates attempts to compare the results in 2D and 3D culture. While the dosage-based DILI assessment technique is used infrequently in literatures, it could suggest one way to achieve more accurate results for drug toxicity in 3D cultures and improve reproducibility of results between laboratories (Wojdyla *et al.*, 2016; Fey, Korzeniowska and Wrzesinski, 2020; Gouws *et al.*, 2021).

For the bioreactor cultures the results were very similar in general to those seen in 3D culture. However, both tamoxifen and flutamide showed a significant difference between 3D static and 3D stirred cultures. For tamoxifen, a potent antioestrogen used in the treatment of breast cancer, a reversion back to the sensitivity of 2D culture was seen. Whilst the reduction in sensitivity seen in 3D is routinely reported and suggested to be due to increased expression of MRP2 (Mueller, Koetemann and Noor, 2011; Godoy *et al.*, 2013), little study has investigated the effects of

tamoxifen in dynamic conditions. It is possible that this is due to the higher induction of phase I enzymes seen in the stirred cultures compared with 3D static. Tamoxifen biotransformation to a reactive metabolite is mediated by CYP3A4 and cells overexpressing CYP3A4 have shown increased sensitivity to this drug (Holownia and Braszko, 2004), therefore this would seem a likely pathway due to the over 10-fold higher expression of CYP3A4 in bioreactor cultures reported in Chapter 4.

For flutamide, an antiandrogen used to treat prostate cancer, a similar response is seen however in this case the sensitivity appears to be higher than in both 2D and 3D static cultures. This brings it to levels seen in other cell lines *in vitro*, such as HepaRG, with HepG2 typically regarded as underpredicting the toxicity of flutamide (Ball *et al.*, 2016; Yun *et al.*, 2019; Mizoi *et al.*, 2020). Similarly to tamoxifen, studies have demonstrated increased hepatotoxicity of flutamide in cells overexpressing CYP enzymes, in this case both CYP3A4 and CYP2C19 (Tolosa *et al.*, 2018, 2019), which could again suggest the increase in phase I expression in stirred cultures is the cause of the increased toxicity seen here.

Overall, these data show that a combination of changes to cell phenotype contribute to the resultant drug sensitivity. Therefore, a broad, physiologically relevant expression of proteins in the drug metabolism pathways is required to accurately recapitulate the *in vivo* response (Kuna *et al.*, 2018).

5.5.2. Complex metabolic pathways lead to difficulty in replicating *in vivo* results

One of the key issues with these results presented in this work is that the drugs tested have complex metabolic pathways which in some cases contain multiple reactive intermediates and several metabolic steps before clearance (Kuna *et al.*, 2018; Albrecht *et al.*, 2019). For many drugs, the exact metabolites formed and the enzymes which metabolise these are also unknown, further confusing any estimations about physiological relevance of toxicity *in vitro* and making accurate interpretation of data difficult (Atienzar *et al.*, 2016).

This uncertainty about the pathways is further confused by using different measures for enzyme function, such as gene expression used in this work. While this gives a good idea of changes to the cells, downstream events could be leading to a reduced change in expression of protein compared with that seen in gene expression. This could lead to incorrect conclusions based on measurements which do not directly correlate to the final cell phenotype. A more effective measure of CYP metabolism such as an activity assay would give a more accurate representation of the levels of CYP enzymes present in the cytoplasm to compare results in this case, however this can be difficult with

cells such as HepG2 which have low basal expression of CYP enzymes due to the sensitivity limitations of the assays (Gerets *et al.*, 2012).

For these studies the metabolic pathway of drugs is just one of several unknowns which hamper understanding of DILI. For many drugs the levels of a drug within the liver at therapeutic doses remains unclear. Cmax is commonly used as a basis for concentrations used *in vitro*, with values from 20x to 100x Cmax typically used. This can be problematic for two reasons. Firstly, Cmax values can vary significantly between studies, with factors such as age and sex impacting these. Secondly, at levels significantly higher than Cmax, there is no way to know that the metabolic pathways being utilised are the same as those *in vivo*, or whether other pathways are dominant, leading to false positives for hepatotoxicity (Albrecht *et al.*, 2019).

The hepatotoxicity of different drugs is also widely disputed in literature, in some cases with some estimations putting a drug at the highest level of toxicity with some investigations whilst others put it towards the safer end. A review by Walker et al. found that, of 422 compounds classified as DILI positive or negative according to one database, only 189 of these were consistently classified across the publications examined (Walker *et al.*, 2020). Comparisons between the predictive capacity of models is therefore of limited value if each study uses different classifications for their drugs.

There have been attempts to form a single source for drug toxicity data to solve this issue. The Liver Toxicity Knowledge Base project set up by the United States Food and Drug Administration contains DILI ranking for over 1,000 drugs, drawn from other data sources such as the National Institutes of Health LiverTox® database (US Food & Drug Administration, 2019). This has potential to provide uniform DILI rankings for use in research to fix some of the discrepancies between studies (Thakkar *et al.*, 2018). However, it has been pointed out that even here, some of the DILI rankings are consistently in disagreement with studies utilising the drugs (Walker *et al.*, 2020).

5.5.3. In-depth analysis of *in vitro* models is required for accurate toxicity predictions for many drugs

In this work the only measure used for drug toxicity is the endpoint viability, measured with both an MTT assay and an LDH assay. The two assays are used in tandem to ensure results are due to loss of viability, and not due to metabolic impacts of a drug which can lead to variations in MTT Value (Astashkina, Mann and Grainger, 2012). This impact on metabolism could explain why for

some drugs, for example acetaminophen, when no toxicity is seen the MTT value appears to be increasing.

Endpoint viability such as this is widely used for *in vitro* drug toxicity studies, however, is quite a limited approach. The complex pathways of drugs *in vivo* mean that often toxicity is not caused directly by the drug, with many other factors contributing. On top of this for some with low toxicity seen, some other measures of cell health can still detect detrimental impacts. A few papers have investigated the use of visual properties for detecting DILI in HepG2 as an alternative measure of DILI. These included nuclei count, nuclear area and mitochondrial area (Xu *et al.*, 2008; Persson *et al.*, 2013). Alone these were not very accurate measures of toxicity, with nuclear counts found to have a sensitivity of between 20 % and 40 % for example. By screening for a series of these properties, a more accurate prediction of DILI can be formed, with the sensitivity reaching 45 % whilst detecting no false positives. This presents a relatively simple method which can be used to screen large numbers of drugs.

In general, for accurate hepatotoxicity prediction a screen of properties such as this must be carried out, however often these use more complex sets of properties (Minjun Chen *et al.*, 2014). Many studies have developed such screens and successfully used them for detection of DILI-positive drugs. Whilst these are effective the utility with larger-scale systems such as the bioreactor system developed in this work is minimal due to throughput limitations. The need for many assays leads to a requirement for multiple samples to be used to cover the range of assays, drastically scaling up the experiments used here in which both analyses were carried out on the same samples. This is one region where imaging analyses such as that used by Persson et al. could be beneficial, due to being able to perform multiple quantitative counts from the same samples (Persson *et al.*, 2013). Despite the limitation from the number of assays used for this work, the detection of differences in toxicity between static and stirred models does however indicate metabolic differences between the models. That these changes are supported by the differences to gene expression seen in Chapter 4 points towards a potential positive impact of the bioreactor system.

5.5.4. Limitations of the novel bioreactor system for drug toxicity research

The system developed here presents a method for predicting drug toxicity with potential to be more accurate than simplistic models often used at present. It is not, however, without its limitations. One limitation of the system developed in this work is that it does not scale

appropriately for many of these high-throughput assays. Whilst assays looking at media content of metabolites or secreted molecules can be readily carried out, albeit at lower sensitivity due to the large volume of media diluting them more, other assays are not so easy. With assays which require destructive use of the cells themselves, such as the MTT assay, only one assay can be carried out on a sample. Therefore, running multiple such assays would require significant scaling up of the system to cover the wide range of parameters desired. This could be overcome through the use of non-invasive assays, however these are typically always multiplexed along with invasive assays for a sensitive prediction of DILI (Persson *et al.*, 2013).

To gain an accurate insight into the predictive capacity of a system a large screen of drugs needs to be performed, in some cases with several hundred drugs being probed (Xu *et al.*, 2008). Alongside this is the fact that for research into new drug candidates there can often be many thousands of compounds to be screened, something which is not feasible with this system. This ties into a second limitation with this system which again comes from the large size of the system. This means that a large amount of a drug is required per sample, twenty times more than is required for the comparable static samples used in this experiment and significantly more still compared with some literature investigations using microfluidic systems. For readily available, low-cost drugs this is not a problem however when using drugs which have been synthesised in lower quantities this is more difficult. This supports the use for the system for small scale trials pre-animal testing, rather than for high throughput experiments earlier in the drug discovery process.

Whilst a simple method to improve the predictivity of these cultures would be to use a more physiologically relevant cell type, such as primary hepatocytes, this may not be feasible with this system in its current form. The change in physiological relevance from making this switch is enormous, with HepG2 exhibiting low or absent expression of many key proteins, even in complex fluid flow culture systems such as this (Sison-Young *et al.*, 2017). However, the limited viability of primary hepatocytes couple with the limited proliferation *in vitro* means that high quantities of these cells are not readily available, with a single vial of cells only able to make one or two models in this system. One of the potential future modifications with this system, if drug toxicity testing were to become effectively used with it, would be to scale down to smaller Alvetex® formats such as 12- or 24-well, rather than the 6-well inserts used here. This would the allow for use with more costly and less readily available cells such as primary hepatocytes. A consequent reduction in media volume to coincide with this would also be beneficial for reducing costs, as discussed previously.

5.6. Conclusions

From the findings in this chapter the utility for the bioreactor system in drug discovery can be seen. The move from 2D to 3D culture coincides with a significant decrease in drug sensitivity, even with drugs which would be expected to lead to greater cytotoxicity. This could be due to a variety of reasons, such as greater phase II enzyme expression leading to improve clearance of reactive metabolites or greater quantity of cells being able to metabolise the drugs more effectively. It is likely that the exact mechanism of this decrease in sensitivity is variable between drugs and from the data presented here a firm conclusion on the cause is not possible.

The responses seen in 3D culture are generally the same when fluid flow is incorporated into the culture. Tamoxifen and flutamide both exhibit a markedly different response in stirred conditions than in 3D static conditions, having increased sensitivity which leads them to have a response which more closely resembles that seen in 2D cells. A possible cause for this could be the increased CYP activity in dynamic conditions leading to greater formation of reactive metabolites, or the fluid turnover leading to increased drug concentrations at the cell surface. This suggests possible advantages for these cultures over static 3D cultures, which appear to have inadequate sensitivity.

The system is not without limitations, however, with the major problem being the large volume of medium required. Whilst this is useful for culture of the model due to maintaining homogeneous conditions over time, the large amounts of drugs required to be added to this system can be problematic when investigating more expensive drugs. Further addition of alternative liver cell lines such as Kupffer cells and stellate cells would also be beneficial to elucidate a more physiologically relevant DILI response and give the system greater potential for simulating idiosyncratic DILI.

Future work with these drugs could include measurements of the different metabolites present in the cultures after exposure to the drugs. This would then give a broader understanding of the observed changes in viability and allow the results seen to be linked to the gene and protein expression changes measured in Chapter 4, something which is not possible without a detailed knowledge of the metabolic pathways present.

Chapter 6: Incorporation of non-parenchymal cells into stirred HepG2 models

6.1. Introduction

Whilst the culture of hepatocytes on a synthetic scaffold in a bioreactor is a useful technique for improving the phenotype of the cells and providing a more natural organisation there are still limitations to the physiological relevance of such models which reduce their utility when modelling complex processes such as diseases.

The liver *in vivo* has a large amount of ECM throughout the lobule which helps to support the cells. The homeostasis of ECM in the liver also plays a role in disease progression with fibrosis leading to large amounts of deposited collagen. This ECM homeostasis is maintained by a range of non-parenchymal cells which are also absent in the models developed so far in this work. Cells such as stellate cells and Kupffer cells react to stimuli to produce or break down the ECM and therefore have a key role in disease progression. As well as the roles in diseases the presence of these factors have also been shown to improve the physiological function of hepatocytes *in vitro*.

Adding these factors into the models produced in Chapter 4 could lead to the production of an even more effective liver model with a wide range of physiologically relevant responses. In this chapter the addition of fibroblasts to the HepG2 model, which produce an endogenous ECM component for the models, as well as sinusoidal endothelial cells, will be explored. The changes to cultures under the addition of these cells will be investigated using immunofluorescence for structural analysis as well as metabolic assays to determine cell health.

6.1.1. The important of extracellular matrix in the liver microenvironment

The extracellular matrix surrounding hepatocytes in the liver is strikingly different from many organs due to the absence of basement membranes (BM) and only an attenuated ECM between the hepatocytes and the sinusoidal endothelial cells (Martinez-Hernandez and Peter S Amenta, 1993). Most of the ECM consists of fibronectin, collagen I and collagen III with smaller quantities of collagen types IV, V and VI also present (Rojkind, Giambrone and Biempica, 1979). In the liver collagen I forms cables which run through the space of Disse alongside in sinusoids with discrete bundles of the other ECM components including the BM component collagen IV deposited in the remaining space (Hahn *et al.*, 1980). Fibronectin in the space of Disse can be found along the entire length of the sinusoids, coating the hepatocyte microvilli facilitating the attachment of hepatocytes and endothelial cells to collagen (Clement *et al.*, 1986). Basement membranes can be found in the liver in the portal region supporting the bile duct epithelial cells as well as the portal vein and

hepatic artery however the BM surrounding blood vessels does not continue onto the sinusoids (Martinez-Hernandez and Peter S Amenta, 1993; Mak and Mei, 2017). This property supports their high permeability which is also exaggerated by their fenestrated appearance. Typical BM components such as laminin and entactin are only found in these BM regions within the liver lobule and are absent in regions such as the space of Disse, in contrast to the broader expression of collagen IV in the liver.

The liver ECM is highly dynamic and undergoes significant remodelling in disease, particularly when undergoing fibrosis. The activation of stellate cells to myofibroblasts induces them to produce vast quantities of collagen and elastin within the sinusoids. When the injury ceases the liver can then break down this ECM, providing the damage is not too severe, returning to the original composition (Martinez-Hernandez and Peter S. Amenta, 1993). This dynamic remodelling of ECM is one of the factors that allows the liver to support its impressive regenerative capacity *in vivo* (Cordero-Espinoza and Huch, 2018).

6.1.2. Methods to incorporate ECM into *in vitro* cell models

Incorporating ECM into cell culture is a widely used technique and can be carried out in many ways to tune conditions to the tissue of interest. As mentioned in Chapter 4 many methods have already been used for hepatocytes, such as the use of collagen in sandwich cultures. The success of these techniques has led to many methods being developed and the relationship between the hepatocytes and the ECM can be varied, as shown by Figure 6.1.

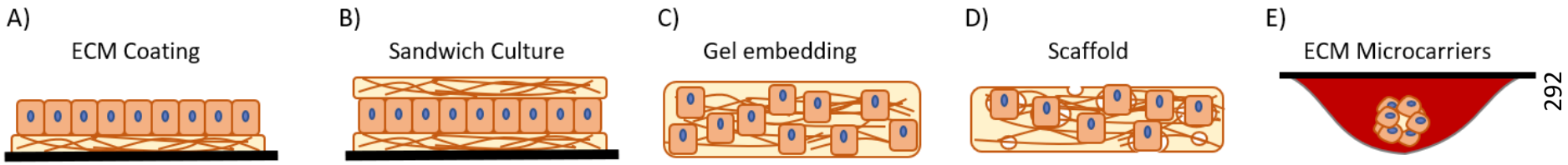

Figure 6.1: Methods to incorporate ECM into cell culture. A) ECM coating a standard cell culture surface is a simple method to get cells into contact with ECM. B) Sandwich culture can aid with the maintenance of viability and polarisation of cells such as primary hepatocytes. C) Gel embedding supports cells in a 3D environment. D) ECM Scaffolds, often made from decellularized tissue, function similarly to gel embedding by maintaining cells in a 3D microenvironment. E) ECM microcarriers can be used to support aggregate cultures, often performed through coating polymer beads with ECM.

ECM coating is a simple technique and can be carried out on most cell culture surfaces. By placing a thin layer of ECM onto a growth surface such as a well plate a more physiologically relevant, biologically active adherence site for cells is created. The ability to specify the protein composition of the gel allows further control to these cultures with single-protein extracts such as collagen I common in studies using hepatocytes (Hansen and Albrecht, 1999; Theos *et al.*, 2005; Godoy *et al.*, 2009). More complex matrix extracts such as the basement membrane extract Matrigel®, containing a mixture of ECM proteins and growth factors, have been used successfully for creating skin epidermal equivalents containing keratinocytes (Gorelik *et al.*, 2000; Sobral *et al.*, 2007) and for the expansion and differentiation of stem cells (Lee *et al.*, 2015). Sandwich cultures are also an extension of this technique more frequently used for primary hepatocytes in which a second layer of ECM is added after the cells have adhered to the initial ECM surface. As discussed in Chapter 1 these have been very successful for maintaining the differentiation and long-term viability of primary hepatocytes by mimicking the space of Disse found on to either side of hepatocytes *in vivo* (Dunn *et al.*, 1989; LeCluyse, Audus and Hochman, 1994; Liu *et al.*, 1999).

An alternative method to seeding cells onto an ECM gel-coated surface is to mix the cells into the unpolymerized gel and seed this mixture onto the growth surface, entrapping the cells within the gel as it polymerises (Wang *et al.*, 2004). This creates a 3D environment for the cells to grow and the gel can contain a variety of ECM proteins as well as growth factors. This method has often been used for the growth of fibroblasts to create dermal tissue equivalents (Tuan *et al.*, 1994; Kanta, 2015). One of the advantages of this method is that the stiffness and density of the gel can be controlled through alterations to the ECM composition (Saddiq, Barbenel and Grant, 2009). Control over cell motility and migration can also be enforced through the use of non-degradable materials such as alginate within which the cells cannot move as they do in ECM proteins such as collagen (Caliari and Burdick, 2016). Combinations of these techniques allows tailored gels for investigations into the mechanotransduction pathways of cells (Cambria *et al.*, 2020).

Scaffolds are another method which has been discussed previously which typically have greater control over the patterning of structures created from ECM. For hepatocytes a common technique is the decellularization of liver tissue, leaving the ECM scaffold which can then be reseeded with cells (Mazza *et al.*, 2015). This not only maintains a physiologically relevant protein composition but also retains the structural patterning found *in vivo* (Croce *et al.*, 2019). An alternative method to create ECM scaffolds is the use of electrospinning. This process uses and electric field to deposit randomly oriented fibres onto a surface (Garg and Bowlin, 2011). The exact morphology of these

fibres can be controlled through changing the solvent properties whilst use of equipment such as a rotating collector allows the creation of fibres which are in oriented parallel to each other (Haider, Haider and Kang, 2018; Lasprilla-Botero, Álvarez-Láinez and Lagaron, 2018). These scaffolds have an advantage of having a large surface area, therefore maximising cell-matrix adhesions and the associated changes in morphology caused by this (Law *et al.*, 2017).

A more recent technique for creation of ECM scaffolds is 3D bioprinting. This allows materials such as ECM to be printed in a predefined structure using a 3D printer (Nakamura *et al.*, 2010). This can be used to make similar structures to those from decellularized tissue however allows more control over the spatial distribution of different components (Lee *et al.*, 2019). These also benefit from a reduction in exogeneous material compared with Scaffolds produced through decellularization. Further complexity can be added by including cells in the printer fluid, allowing the cells to be seeded in specific patterns as well as the ECM (Murphy and Atala, 2014). For liver tissue engineering this technique has been successful used mimicking the structure of the liver lobule *in vitro* (Ma *et al.*, 2016; Wu *et al.*, 2020) as well as to pattern hepatocytes alongside non-parenchymal cells for co-culture liver models (Norona *et al.*, 2016).

Purified proteins are typically used for many of these techniques due to their well-defined content and the ability to mix these together to create matrices with desirable properties. Recently a lot of work has investigated the generation of tissue-specific ECM extracts (Zhang *et al.*, 2009; DeQuach *et al.*, 2010; Lam *et al.*, 2019). These consist of a full complement of matrix proteins at the correct proportions for the tissue of interest and these have been demonstrated to cause improved hepatocyte function when cultured together (Bual and Ijima, 2019). Another alternative ECM source is from the decellularization of *in vitro* cell cultures (Parmaksiz, Elçin and Elçin, 2020). These are straightforward to produce and the choice of cells can lead to control over the proportions of ECM proteins present (Assunção *et al.*, 2020). This benefits from not needing an animal source for the protein, as is often the case for many used *in vitro*, however can suffer from having less well-defined composition and greater batch variation than bespoke ECM solutions (Harris, Raitman and Schwarzbauer, 2018).

6.1.3. Improvement of hepatocyte models through the addition of ECM

The use of the methods mentioned previously for hepatocyte culture has been heavily studied and shown to have great potential for both improved viability and functionality. The benefit from the

techniques can come from the ECM composition, the structural form of the ECM and from the patterning of the hepatocytes within the tissue models.

A huge range of different ECM compositions have been tested, both as individual proteins and as heterogenous mixtures. As the most heavily studied, collagen has been shown to have impacts on hepatocytes in many ways. Collagen I causes hepatocytes to migrate and proliferate (Hansen and Albrecht, 1999) whilst minimising the loss of viability seen when grown on an uncoated surface (Wang *et al.*, 2004). The use of collagen culture methods for hepatocytes have been covered in detail previously in this work so in this section the focus will be on the alternative ECM formulations. Some work has looked at the use of other single-protein matrices for the culture of hepatocytes however a lot of the work which is not collagen based typically looks at matrix mixtures. A few examples of single-protein matrices for hepatocytes include laminin-rich gels which have been shown to maintain viability and albumin production for 3 weeks of culture (Bissell, D. M. Arenson, *et al.*, 1987) and fibronectin matrices which have also been shown to support foetal hepatocytes and play a role in their organisation and gene expression (Sánchez *et al.*, 2000).

For more complex ECM mixtures, the exact composition has variable effects on the structure and function of hepatocytes. Matrigel, an ECM matrix derived from Engelbreth Holm Swarm mouse sarcoma, has been frequently used as an alternative to collagen for the culture of hepatocytes (Lindblad *et al.*, 1991). In this mixture, containing collagens, laminin, heparin sulphate proteoglycan and entactin, among other proteins, hepatocytes have been shown to maintain their polarity for prolonged periods with albumin secretion and CYP activity also retained for several weeks (Bissell, D M Arenson, *et al.*, 1987; Gross-Steinmeyer *et al.*, 2005). The hepatocytes group together to form three dimensional clusters within this matrix, which supports their functional polarisation whilst also maintaining viability and proliferation (Chen *et al.*, 1998). The greater efficacy of either collagen or Matrigel for the culture of hepatocytes is disputed between papers with some finding Matrigel to have a greater beneficial impact than collagen sandwich culture (Moghe *et al.*, 1996) whilst others have suggested that the beneficial impacts are due to increased cell-cell contacts rather than the composition or morphology of the matrix (Hamilton *et al.*, 2001).

To create a more physiologically relevant matrix the use of liver-specific extracellular matrix has also been studied in-depth for the culture of hepatocytes (Reid *et al.*, 1980; Brill *et al.*, 2002; Sellaro *et al.*, 2010; Bual and Ijima, 2019). One study found beneficial effects from growing primary rat hepatocytes on plates containing adult hepatocyte-derived ECM with albumin and the activity of several liver-specific enzymes being upregulated. By contrast they found that fibroblast-derived

ECM had an inhibitory effect on cell proliferation and on the activities of all the enzymes examined (Brill *et al.*, 2002). Reduction in the levels of heparin sulfate in the adult hepatocyte matrix also reduced the levels of several liver-specific proteins. This supports previous work which has suggested the heparin sulfate is involved in the regeneration of hepatocytes (Kimura *et al.*, 2008) and adds weight to the argument that composition of the matrix is an important factor for hepatocyte health *in vitro* (Zeisberg *et al.*, 2006).

Whilst a lot of the work carried out for these models utilises primary hepatocytes there has also been a significant amount of research on the impacts of ECM on cell lines such as HepG2. Collagen I has been shown to promote proliferation and albumin secretion in HepG2 and other hepatocellular carcinoma cell lines (Kono and Roberts, 1996; Zhao *et al.*, 2010; Zheng *et al.*, 2017). Other models have successfully incorporated collagen into HepG2 culture for comparative analysis with other cells (Gerets *et al.*, 2012) and more complex culture techniques such as perfusion and oxygenation (Oshikata-Miyazaki and Takezawa, 2015).

Work has also investigated the use of Matrigel and liver-derived matrices for HepG2 growth with similar findings to those using collagen (DiPersio, Jackson and Zaret, 1991; Luckert *et al.*, 2016). One article found that the improvements to liver-specific function was only the case for ECM which promoted a differentiated, cuboidal morphology of the cell lines, of which both collagen I and Matrigel are able (DiPersio, Jackson and Zaret, 1991). Research with HepG2 on liver-derived matrices has often focused on the use in bioreactors. This takes advantage of the native liver structure including vasculature which is present in these constructs to allow the addition of fluid flow in a physiologically relevant manner. These models have been shown to have beneficial effects similar to those found with Matrigel, supporting HepG2 function at a higher level than found in standard 2D culture (Hussein *et al.*, 2016; Sassi *et al.*, 2021).

6.1.4. Non-parenchymal cells play a major role in liver homeostasis

Another important aspect of liver tissue *in vivo* is the presence of non-parenchymal cell. There are numerous non-parenchymal cells in the liver which, though often not being the direct mediators of liver function like hepatocytes, are incredibly important for the normal function of the liver. These cells carry out wide ranging functions to support and protect the hepatocytes whilst fighting tissue damage and disease (Bouwens *et al.*, 1992). Stellate cells, Kupffer cells and liver sinusoidal endothelial cells (LSECs) are typically the most heavily studied non-parenchymal cells for use in

hepatocyte models and as such have a lot of literature regarding their properties and interactions with hepatocytes (Yin and Evason, 2013; Dixon *et al.*, 2016; Shetty, Lalor and Adams, 2018).

6.1.4.1. Liver Sinusoidal Endothelial Cells

LSECs are a unique type of endothelial cell found only in the liver which have highly fenestrated walls (Poisson *et al.*, 2017). These allow maximum nutrient transfer from the sinusoids to the space of Disse to support the large metabolic capacity of the hepatocytes and maintain the efficient functioning of the liver. Similarly to primary hepatocytes, primary LSECs rapidly lose fenestrations and viability in culture making them difficult to work with for prolonged periods (March *et al.*, 2009). Immortalised cell lines have been developed to try and overcome this issue with maintained viability and proliferation whilst still possessing some LSEC-specific function such as the presence of fenestrations (Heffelfinger *et al.*, 1992; Huebert *et al.*, 2010; Zhu *et al.*, 2018).

Culture techniques which incorporate LSECs vary from simple addition of the two cells to a surface or gel (Sundhar Bale *et al.*, 2015) to more complex techniques such as *in vivo*-like patterning of cells using compartmentalisation (Ahmed *et al.*, 2017a; Mi *et al.*, 2018) or 3D bioprinting (Ware *et al.*, 2018). These studies have investigated the impacts of the relationship between the two cell types in both directions, with endothelial cells also benefitting from the co-culture. When cultured alongside primary hepatocytes LSECs exhibit enhanced viability and functional stability without the need for additional media factors such as vascular endothelial growth factor (VEGF) (Hwa *et al.*, 2007; Sundhar Bale *et al.*, 2015).

When cultured with LSECs primary hepatocytes also experience an increased viability and functionality. Albumin levels are maintained at higher levels than found in monoculture whilst CYP activity is also upregulated and maintained over prolonged periods (Kim and Rajagopalan, 2010; Sundhar Bale *et al.*, 2015). The difficulty isolating and culturing LSECs has also led to many researchers using alternative endothelial cell sources for hepatocyte co-culture. Human umbilical vein endothelial cells (HUVECs) and bovine aortic endothelial cells (BAECs) are often used in hepatocyte studies with comparable results such as increases in albumin and urea secretion and maintained CYP expression over multiple weeks (Guzzardi, Vozzi and Ahluwalia, 2009; Inamori, Mizumoto and Kajiwara, 2009; Kang *et al.*, 2013).

6.1.4.2. Stellate Cells

Stellate cells are another major liver NPC, residing in the space of Disse between the hepatocytes and the LSECs (Friedman, 2008). These play an important role as a mediator of the inflammatory response in many diseases through their activation into myofibroblasts. They typically exist in a quiescent state adjacent to hepatocytes where they extend dendritic processes around the sinusoids to facilitate the detection of chemotactic signals (Melton and Yee, 2007). When activated via various inflammatory stimuli they transdifferentiate into myofibroblasts which produce further inflammatory molecules and signals to create a feedback loop for the inflammation (Gupta, Khadem and Uzonna, 2019). In this state they also produce large quantities of ECM, contributing heavily to the fibrotic phenotype seen in many liver diseases, and recruit other cells such as macrophages to the injury site (Fujita and Narumiya, 2016).

Like co-cultures with LSECs, the culture of primary hepatocytes with stellate cells has been shown to have beneficial effects for the hepatocyte's viability and functionality. Albumin, urea and CYP expression have been shown to be maintained at higher levels when co-cultured in spheroids with stellate cells than is seen in monoculture (Abu-Absi, Hansen and Hu, 2004; Thomas *et al.*, 2005). The beneficial impact of stellate cells can also be achieved using conditioned media, however this requires much larger quantities of stellate cells to achieve the same impacts as seen by direct cell-cell contact (Krause *et al.*, 2009). When cultured with hepatocellular carcinoma cell lines such as HepG2 stellate cells have led to increased viability and migration of the HepG2 coupled with a greater chemoresistance (Song *et al.*, 2016; Iwahasi *et al.*, 2020). Whilst this is less beneficial for the use of HCC cells as a hepatocyte analogue it does create a useful platform for investigations into HCC progression (Amann *et al.*, 2009).

6.1.4.3. Kupffer Cells

As the third major NPC in the liver Kupffer cells function in tandem with stellate cells in many disease conditions. Residing withing the liver sinusoids the Kupffer cells are the predominant macrophage population in the liver whilst constituting 80-90 % of the tissue macrophages present in the body (Bilzer, Roggel and Gerbes, 2006). Their location in the sinusoids leads to them being the first macrophage population to meet bacteria and toxins arriving from the GI tract and they play a hugely important role in the immune response. During liver injury they are a major producer of factors such as transforming growth factor β (TGF-β) which cause the activation of stellate cells and subsequent progression of the inflammatory response (Kolios, Valatas and Kouroumalis, 2006).

The role of Kupffer cells in the immune response has led to a lot of the research combining them with hepatocytes focusing on this aspect of liver function. Treatment of co-cultures with stimulants such as lipopolysaccharide (LPS) and interleukin-6 (IL-6) have been successful used for modelling the impacts of immune response on hepatocytes (Billiar *et al.*, 1989; Nguyen *et al.*, 2015). Recently one study found that the immune-mediated hepatoxicity of APAP and trovafloxacin, not detected in hepatocyte monoculture, can be successfully detected in a co-culture model of hepatocytes and Kupffer cells (K. A. Rose *et al.*, 2016).

6.1.5. Multicellular liver models can improve hepatocyte function and predictive capacity

The inclusion of the different cell types found in the liver into *in vitro* hepatocyte models a broader range of physiological interactions can be modelled. This increase in physiological relevance can enhance the properties of both the hepatocytes and the included NPCs and increase their worth in culture as discussed in the previous section. With complex culture systems becoming more commonly used the culture of hepatocytes with several different types of NPC is also becoming more frequent.

Studies utilising HSCs and LSECs alongside hepatocytes have been able to recapitulate the spatial localisation and cell-cell contacts between the three cell types as seen *in vivo.* The production of albumin as well as the expression of CYP enzymes and drug transformation capacity have been shown to be prolonged in these co-culture models mirroring the results seen for co-culture with NPCs individually (Ahmed *et al.*, 2017a). These platforms are very useful for the study of the interaction between the cells with one study using such a system to demonstrate the function of stellate cells to mediate the communication between hepatocytes and LSECs (Kasuya *et al.*, 2010).

Integration of KCs to these cultures can further improve the hepatocyte phenotype. One study found that adding an NPC fraction containing all the three major NPCs to hepatocyte culture had beneficial effects on albumin production and CYP expression (Baze *et al.*, 2018). Meanwhile one study used primary hepatocytes alongside LSECs, HSCs and KCs to test the immune response to LPS. This incorporated paracrine and juxtacrine signalling with LSECS and KCs grown on a Transwell insert and hepatocytes and HSCs grown in the bottom of the well with a collagen gel overlay (Bale *et al.*, 2016). They found that an immune response could be observed in all models containing KCs however inclusion of hepatocytes could attenuate this response. This demonstrates the value of such systems for examining the complex interplay between the different cell types for modelling

liver tissue responses at a more physiologically relevant level than is achievable with cultures containing hepatocytes alone or with just one other type of NPC.

As well as the inclusion of NPCs in these cultures, other cells with an origin from organs other than the liver have also been shown to be beneficial to hepatocyte growth. Fibroblasts have been used as feeder layers for primary hepatocytes to maintain their viability over time as well as promoting proliferation and increasing hepatocyte function (Cho *et al.*, 2008, 2010). These have also been shown to promote formation of gap junctions between hepatocytes therefore enhancing intercellular communication (Kim, Seo and Kwon, 2015). For cell lines such as HepG2 a similar response can be seen to that found in primary hepatocytes with increased albumin secretion found in several studies co-culturing HepG2 with 3T3 mouse fibroblasts (Ito *et al.*, 2007; H. W. H. J. Lee *et al.*, 2014; He *et al.*, 2018).

6.1.6. Methods to utilise Alvetex® membranes for co-culture of different cell types.

Alvetex® can be utilised in several ways depending on the desired culture properties and the types of cells used. As shown by Figure 6.2 these methods allow for growth of cells both within and on the surface of the scaffold as well as compartmentalisation of different cell types in co-culture with different conditions for the different cells.

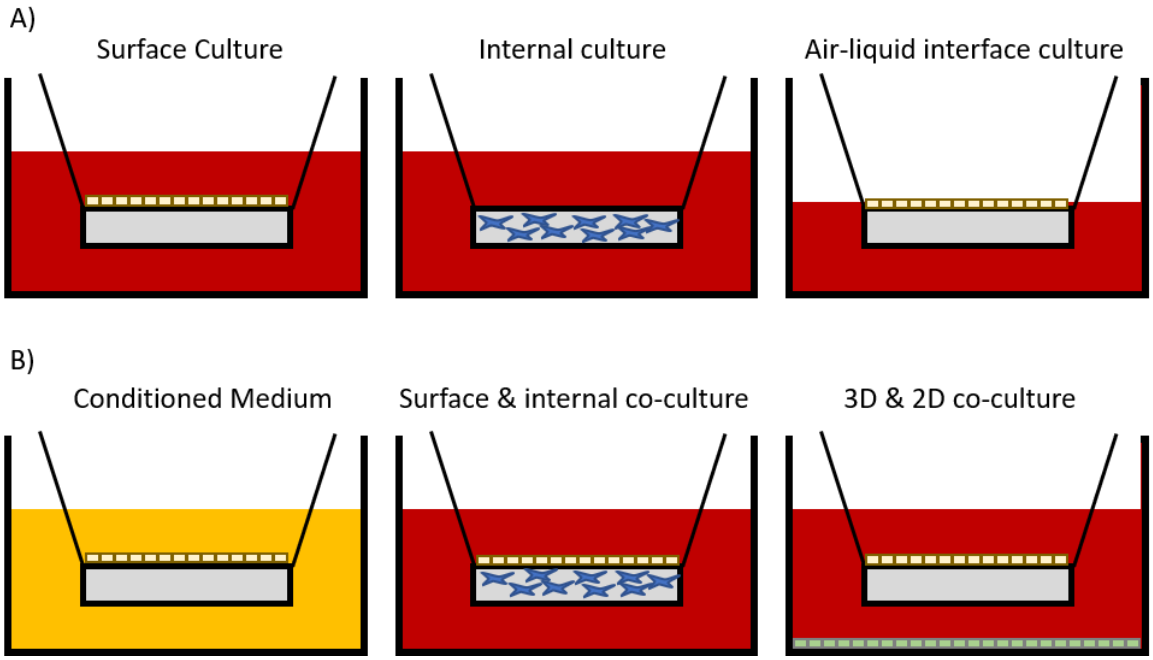

Figure 6.2: Different methods to utilise Alvetex® membranes for the growth of cells *in vitro*. A) When culturing a single cell type there are several techniques which can be used. Surface culture allows growth of epithelial cells to form polarised monolayers. Internal culture uses the Alvetex® as a scaffold to support cells such as fibroblasts in 3D. Air-liquid interface culture is useful for cells such as keratinocytes to recapitulate the microenvironment of the skin epidermis. B) Co-culture can be carried out in several ways. A simple method is the use of conditioned medium from one cell line to use as growth medium for a second. Growth of cells such as fibroblasts inside the Alvetex® membrane can create a supporting surface cells to then be seeded onto the surface of. Cells can also be seeded to the bottom of the culture well in 2D to examine the paracrine effects of the cells in co-culture.

The growth of cells such as fibroblasts within the Alvetex® allows for production of an endogenous ECM as well as providing cell-cell contact between the fibroblasts and any other cell types included. These stromal compartments produce a wide range of ECM proteins and growth factors and have been shown to support robust, highly differentiated epithelial layers in models of both skin and intestine (Roger *et al.*, 2019; Darling *et al.*, 2020).

Co-culture of cell types in the bottom of the well alongside those on the Alvetex® can be useful for the modelling of paracrine interactions (Martín-Saavedra *et al.*, 2017; Saldaña *et al.*, 2017), similarly to the Transwell-based study mentioned in the previous section (Bale *et al.*, 2016). Paracrine factors play an important role in the function of hepatocytes and the different NPCs have been found to have different impacts on hepatocytes (Peterson and Renton, 1986; Stangar and Greenbaum,

2012). This method will not be explored in this work due to the absence of alternative growth surfaces in the bioreactor system apart from the Alvetex® membrane.

Conditioned media is an alternative method to present paracrine signals to cultured hepatocytes with similar results to direct paracrine signalling (Casteleijn *et al.*, 1988). Media from liver NPCs as well as alternative cell sources such as embryonic fibroblasts and mesenchymal stem cells has also been shown to be beneficial for hepatocyte culture with enhancements to albumin and urea secretion, prolonged viability and improved response to toxicological challenge (Hu *et al.*, 2014; Jeong *et al.*, 2016; Temnov *et al.*, 2019).

In this chapter the capability to grow HepG2 in the bioreactor system alongside other cells will be investigated. Initially fibroblasts will be used within the Alvetex® Scaffold to create a supportive layer for the HepG2 to grow on, building on previous literature which has shown the beneficial impacts of fibroblasts in hepatocyte cultures (Kim, Seo and Kwon, 2015; Novik *et al.*, 2017; Sakai *et al.*, 2018). This will be followed by the incorporation of endothelial cells alongside HepG2 alone and in tandem with fibroblasts to add further complexity and physiological relevance to the models.

6.2. Hypothesis, Aims and objectives

6.2.1. Hypothesis

Whilst the addition of three-dimensionality and fluid flow can be beneficial for enhancing the properties of hepatocytes, many experiments in literature have also shown the utility of co-culture with other cell types for this purpose. We hypothesise that the incorporation of further cell types into the system, possible in various ways using different seeding methods with the Alvetex® membrane, will lead to further improvements to structure and function above those seen in previous chapters. We also further hypothesise that by drawing several different cell types into one culture will enhance the performance of HepG2 cells above that seen when co-cultured alongside just one other cell type.

6.2.2. Aims

In this chapter the previous work creating stirred, three-dimensional *in vitro* models with the HepG2 cell lines will be expanded through the addition of other cell types to recapitulate the native liver environment. This will be carried out using dermal fibroblasts as a readily available and well-studied cell line to mimic some of the functions of stellate cells whilst the liver adenocarcinoma cell line SK-Hep-1 will also be utilised to mimic the endothelial cell wall which surrounds the sinusoids *in vivo*. Initial experiments will investigate the feasibility of producing models using these cell lines. Upon successful formation of tissue-equivalent models the impact of adding these two cell lines will be investigated using immunofluorescent microscopy and metabolic assays.

6.2.3. Objectives

- Develop and optimise a protocol for the addition of fibroblasts to 3D HepG2 cell cultures
- Investigate any structural changes to the HepG2 in the co-cultures with fibroblasts.
- Develop and optimise a protocol for the addition of SK-Hep-1 cells either to HepG2 alone or in tandem with fibroblasts.
- Carry out structural and functional analysis of the developed cultures.

6.3. Materials and Methods

6.3.1. Co-culture of HepG2 cells with fibroblasts

To co-culture HepG2 with fibroblasts the first step is to create a mature fibroblast compartment for the HepG2 cells to be seeded upon. Neonatal human dermal fibroblasts were used for this purpose due to the ease of use and experience creating fibroblast compartments with these cells within our lab. Maintenance of the cells was carried out as described in Chapter 2.

The experimental setup for these cultures can be seen in Figure 6.3. One million HDFn cells were initially seeded onto Alvetex® Scaffold 6-well inserts in triplicate, prepared as per the manufacturer's instructions. Medium was added after one hour and subsequent media changes were performed twice weekly. After three weeks in culture the medium was aspirated, 5 mL of fresh medium added 2 million HepG2 cells were seeded to the surface of the Alvetex®. Static and stirred HepG2-only controls were set up simultaneously on Alvetex® Strata membranes as described previously. These cultures were cultured for one week in static conditions with a media change every two days.

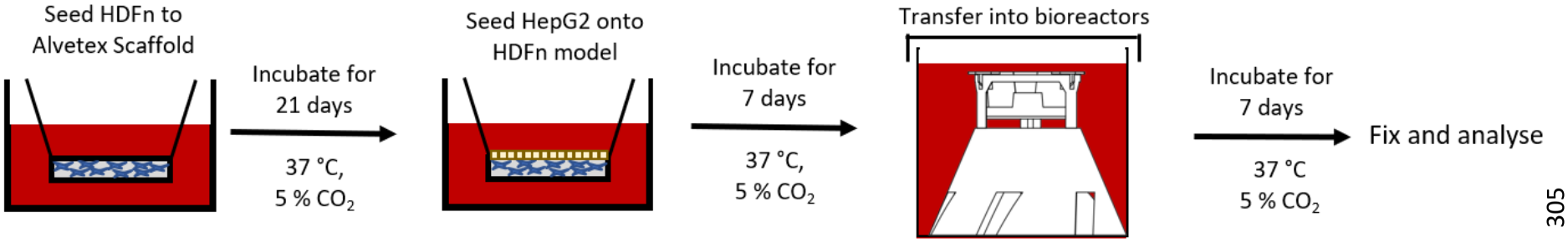

Figure 6.3: Protocol for setting up HepG2 and HDFn co-cultures. HDFn cells were seeded onto an Alvetex® Scaffold insert in a 6-well plate and cultured for 21 days. HepG2 cells were then seeded onto these and cultured for a week to allow the cells to adhere and migrate across the membrane. After this period half of the samples were placed in a fresh 6-well plate whilst the other half were moved into the bioreactors containing 100 mL of cell culture medium. All samples were then cultured for a further 7 days before fixation and analysis.

One week after addition of HepG2 the cultures were transferred to the bioreactor system containing 100 mL of cell culture medium and cultured for a further week with the stirrer set to 100 rpm. Fixation was carried out using 4 % PFA at room temperature for 1 hour before dehydrating and embedding samples in paraffin wax for further analysis. For metabolic assays the static controls were also cultured in the bioreactor system with the stirrer set to 0 rpm as discussed in Chapter 4.

6.3.2. Co-culture of HepG2 cells with endothelial cells.

For the culture of HepG2 with SK-Hep-1 cells both cell lines were seeded at the same point as shown in Figure 6.4. Alvetex® Strata 6-well inserts were prepared as per the manufacturer's instructions and place into a 6-well plate containing 5 mL of cell culture media. Initially 2 million HepG2 cells were added to surface of the Alvetex® membranes. Once all the inserts had been seeded with HepG2 the SK-Hep-1 cells were added in a quantity ranging from 50,000 to 1 million depending on the exact conditions of the experiment. Cultures were incubated for one week with media changes every 2 days.

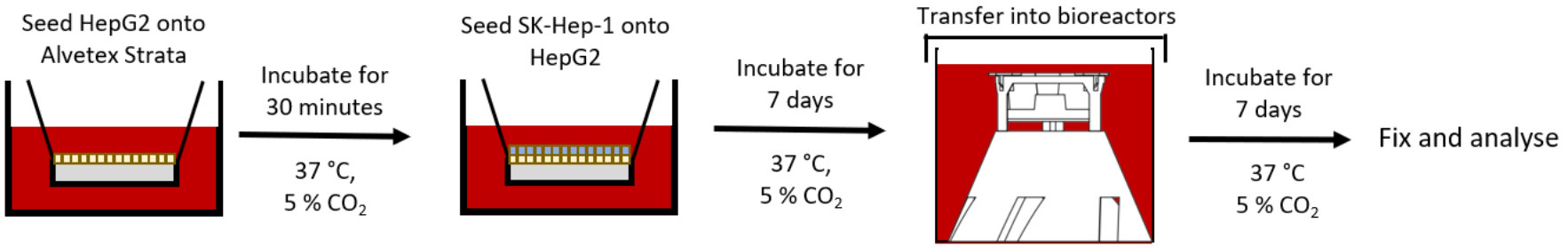

Figure 6.4: Protocol for setting up HepG2 and SK-Hep-1 co-cultures. HepG2 were initially seeded onto an Alvetex® Strata insert in a 6-well plate and incubated for 30 minutes to allow cells to settle. SK-Hep-1 were then also seeded onto the insert and the culture was incubated for 7 days. After this period half of the samples were placed in a fresh 6-well plate whilst the other half were moved into the bioreactors containing 100 mL of cell culture medium. All samples were then cultured for a further 7 days before fixation and analysis.

After 7 days for bioreactor experiments the inserts were removed from the 6-well plates and placed into the bioreactor with 100 mL of cell culture medium before being incubated for a further 7 days with the stirrer set to 100 rpm. For static cultures the inserts were placed into a fresh 6-well plate and incubated for a further 7 days with media changes every 2 days. For metabolic assays the samples were instead maintained in the bioreactor system with the stirrer set to 0 rpm for this period to maximise the comparability between results as discussed in Chapter 4.

6.3.3. Co-culture of HepG2 cells with fibroblasts and endothelial cells

When cultures were set up with all three cell types a combination of the two seeding methods was used as shown in Figure 6.5. Fibroblast cultures were set up in the same way as for cultures with HepG2 alone. After 3 weeks of culture medium was aspirated and inserts were moved to a fresh 6-well plate with 5 mL of media. 2 million HepG2 were added followed by 50,000 to 200,000 SK-Hep-1 depending on the experimental conditions. These were incubated for 7 days with media changes every 2 days.

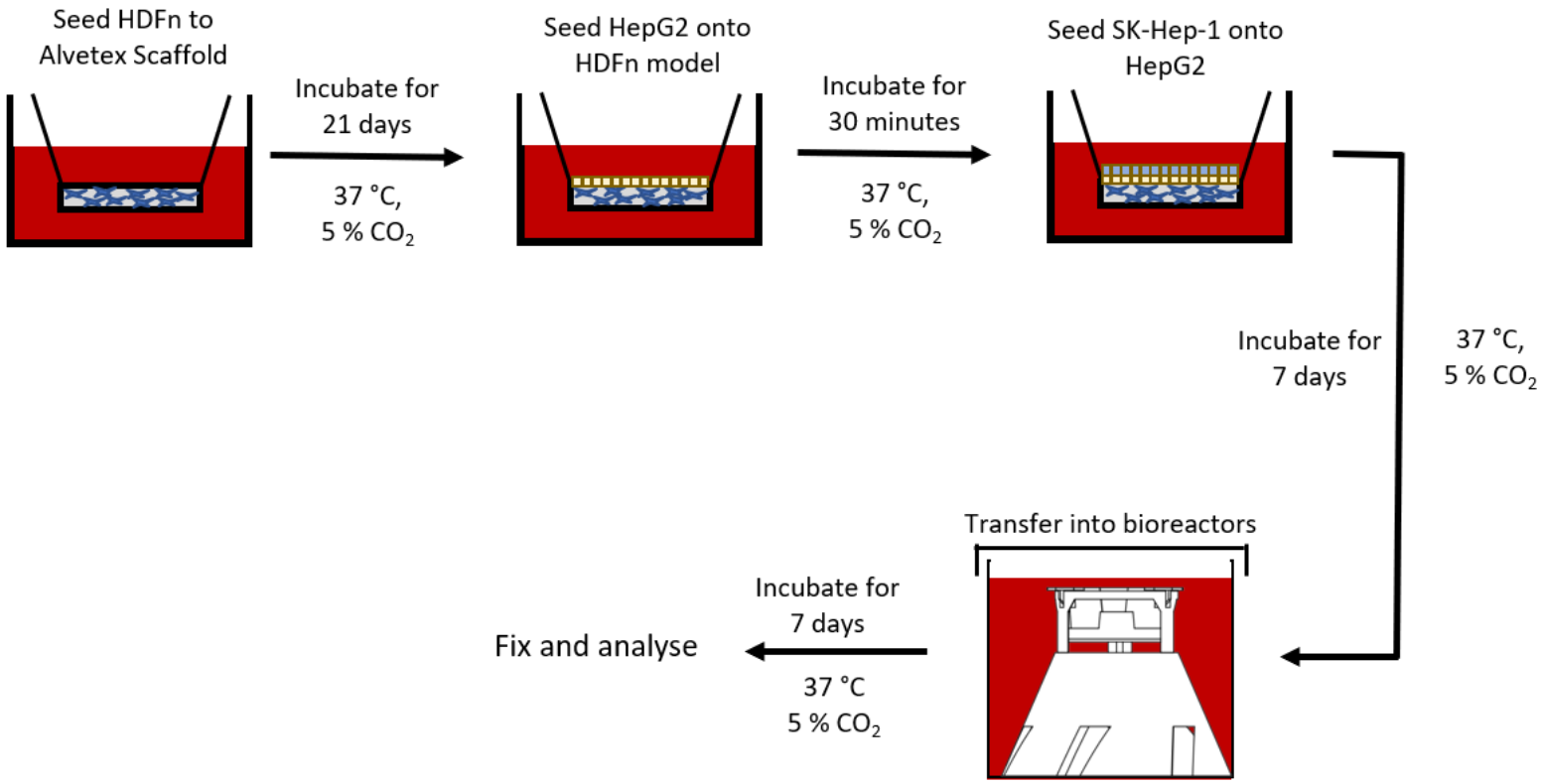

Figure 6.5: Protocol for setting up HepG2, HDFn and SK-Hep-1 tri-cultures. HDFn cells were seeded onto an Alvetex® Scaffold insert in a 6-well plate and cultured for 21 days. HepG2 cells were then seeded onto these and cultured for 30 minutes to allow the cells to settle. SK-Hep-1 cells were then also seeded onto the membrane and cultures for 7 days. After this period half of the samples were placed in a fresh 6-well plate whilst the other half are moved into the bioreactors containing 100 mL of cell culture medium. All samples were then cultured for a further 7 days before fixation and analysis.

After 7 days in culture the medium was aspirated from the inserts and they were moved into the bioreactor system containing 100 mL of cell culture medium. Bioreactors were placed onto the stirrers set to 100 rpm and cultured for a further 7 days. Fixation was then carried out using 4 % PFA for one hour at room temperature followed by dehydration and wax embedding for further analysis.

Static controls for metabolic assays were set up in the bioreactors in the same way as for the stirred samples however these were placed onto stir points set to 0 rpm. For all metabolic assays, media samples were taken after one day and every 2 days subsequently until the final time point at 7 days.

6.3.4. Image processing

6.3.4.1. Measuring invasion and cell layer thickness from fluorescent images

Two different stains were used to quantify invasion of HepG2 into the Alvetex®. For monocultures a simple nile red stain was used alongside DAPI to highlight the Alvetex® membrane and the locations of cell nuclei relative to this. For co-culture with fibroblasts immunofluorescent staining for vimentin and cytokeratin 8 was used to determine invasion of HepG2 into the Alvetex® compartment. Vimentin was used instead of nile red for these cultures due to the broad emission spectrum of nile red across both green and red wavelengths which would make co-staining for HepG2 difficult to carry out.

Quantification of the invasion and cell layer thickness was carried out using the ImageJ image analysis software (NIH) using the same protocol as in Chapter 4. Briefly, an evenly spaced 9-point grid was placed across the images. The line tool was used to measure upwards from each grid point to the highest nucleus or cytokeratin 8 staining respectively for monocultures and co-cultures to gain values for cell layer thickness. For invasion into the Alvetex® compartment the measurement was taken downwards to the lowest nucleus or cytokeratin 8 staining. A total of three models were used for each condition with nine representative images for each, totalling 27 images per condition.

The measured results were analysed in Microsoft Excel with the average and standard deviation for each condition calculated. Visualisation into a bar graph was then carried out using GraphPad Prism 5.0 for Windows (GraphPad Software, San Diego, California, USA).

6.3.4.2. Merging images to show the full width of Alvetex® membranes

Creation of full-width Alvetex® images the Adobe Photoshop CC software (Adobe, San Jose, California, USA) was used. A series of images were taken of H&E-stained samples along the width of the culture with roughly a third of an image overlap between each. Images were imported into Photoshop CC using the photomerge function with the layout set to automatic. Once a merged imaged was imported the individual images were manually moved to ensure overlaps were aligned accurately. Background removal was subsequently carried out to the final images using the magic wand tool with the tolerance set to not include any cells or interior regions of the Alvetex® membrane.

6.4. Results

6.4.1. Optimisation of 3D fibroblast growth in DMEM

Creating a fibroblast embedded Alvetex® Scaffold requires optimisation of culture conditions to produce high levels of ECM and ensure that the Scaffold is filled. Neonatal human dermal fibroblasts were chosen due to their ease of culture and high level of use within our research group. Whilst non-parenchymal cells from the liver would be preferable the isolation and purification of these is difficult and there are few liver-based sources of fibroblasts available.

Initially the use of supplements with these fibroblasts was tested to look for adequate ECM deposition whilst maintaining a healthy phenotype. Culturing the fibroblasts in DMEM results in deposition of minimal collagen 1 into the Alvetex® whilst the addition of both ascorbic acid and transforming growth factor beta (TGF-β) lead to much higher, homogenous levels of collagen 1 deposition (Figure 6.6A). The use of both supplements also results in upregulated alpha smooth muscle actin expression suggesting that the fibroblasts are pushed towards a myofibroblast phenotype. From this experiment it was decided to use ascorbic acid on its own for the culture of the fibroblasts due to the high level of collagen 1 deposition with reduced α-SMA expression compared with cultures including TGF-β. It has been suggested that expression of α-SMA in tumour-associated fibroblasts leads to poor clinical outcomes in HCC and promotes the cancerous phenotype, therefore using a model with minimal α-SMA expression is preferable (Lau *et al.*, 2016; Nii *et al.*, 2020).

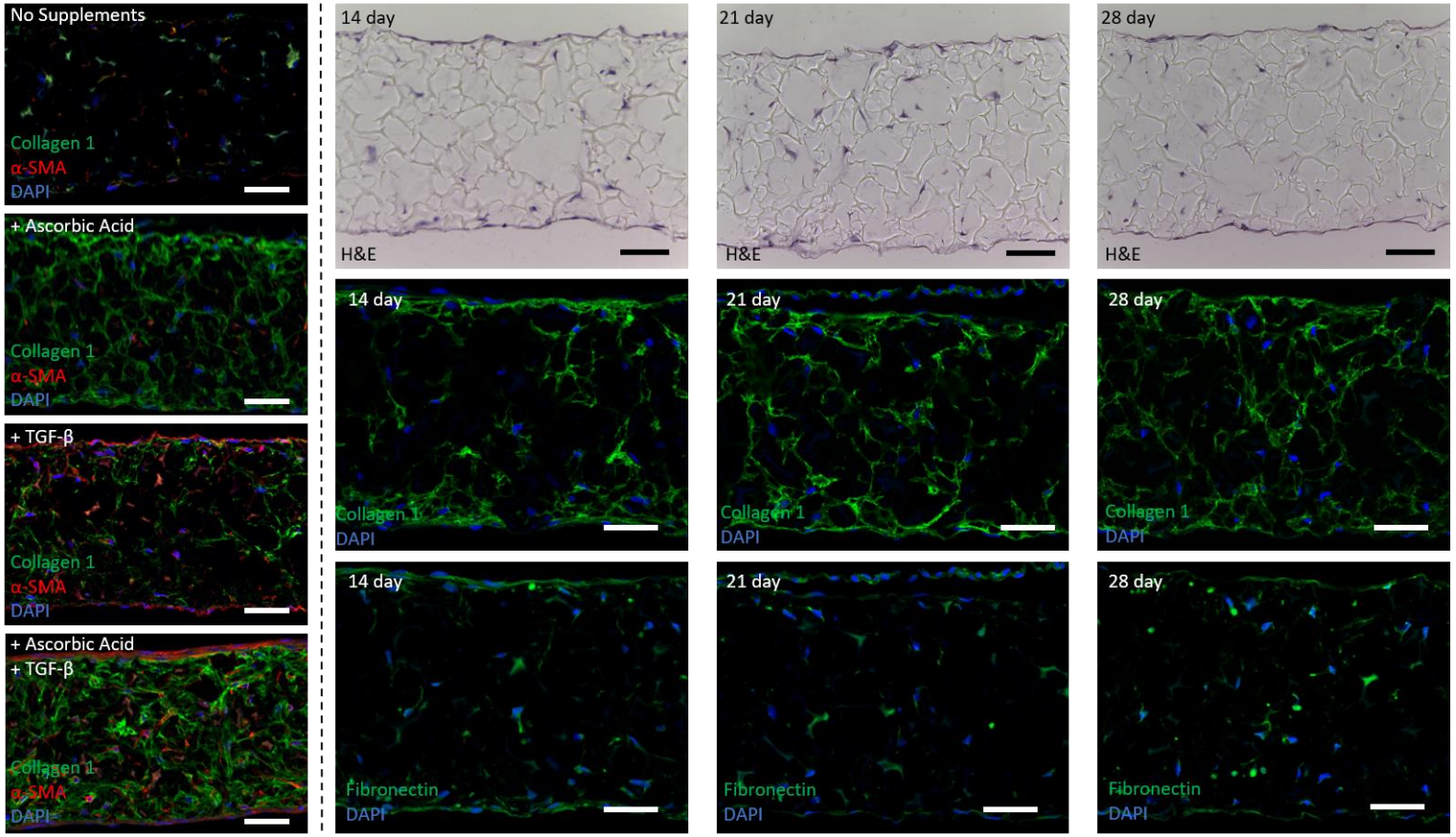

Figure 6.6: Optimisation of the growth of fibroblasts in Alvetex Scaffold. A) Fibroblasts grown in Alvetex Scaffold for 4 weeks with different supplements. Green: Collagen 1. Red: α-SMA, Blue: DAPI. Ascorbic acid leads to increased collagen deposition whilst TGF-β leads to both increased collagen deposition and upregulation of α-SMA. B) H&E stain of fibroblasts grown in Alvetex Scaffold for 2, 3 and 4 weeks. Fibroblasts can be seen distributed throughout the scaffold at all time points. C) Collagen 1 stain of fibroblasts grown in Alvetex Scaffold for 2, 3 and 4 weeks. Collagen 1 can be seen distributed throughout the scaffold at all time points with the coverage increasing with time. D) Fibronectin stain of fibroblasts grown in Alvetex Scaffold for 2, 3 and 4 weeks. Low levels of fibronectin can be seen at all time points. Scale bars are 50 µm.

After the supplement choice had been made the next property to optimise is the culture period. Shorter culture periods are desirable in general however it is essential to leave enough time for adequate ECM deposition and to make sure the Scaffold is filled with fibroblasts to prevent hepatocyte invasion. Figure 6.6B shows that the level of collagen 1 appears to steadily increase up to at least 21 days whilst fibronectin levels are consistent across the three culture periods from 2 weeks to 4 weeks. To fully determine the optimal culture time, it was decided to investigate the effects of the HepG2 cultures grown on fibroblast models with different culture lengths.

Figure 6.7 shows the variation in phenotype of HepG2 and HDFn co-cultures with fibroblast compartments of different maturity. All the culture periods show a thick HepG2 layer forming on the surface whilst the culture using 2-week fibroblasts has an obvious amount of invasion compared with the later time points. HepG2 cells grown on 4-week fibroblast cultures exhibit a necrotic core through the centre of the HepG2 layer, seen by the dense nuclei and increased pink cytoplasmic staining, suggesting the density of these fibroblasts is having a negative impact on nutrient diffusion. From the results of these experiments, it was decided to use fibroblasts grown in Alvetex® Scaffold for 3 weeks as the basis for the co-culture model.

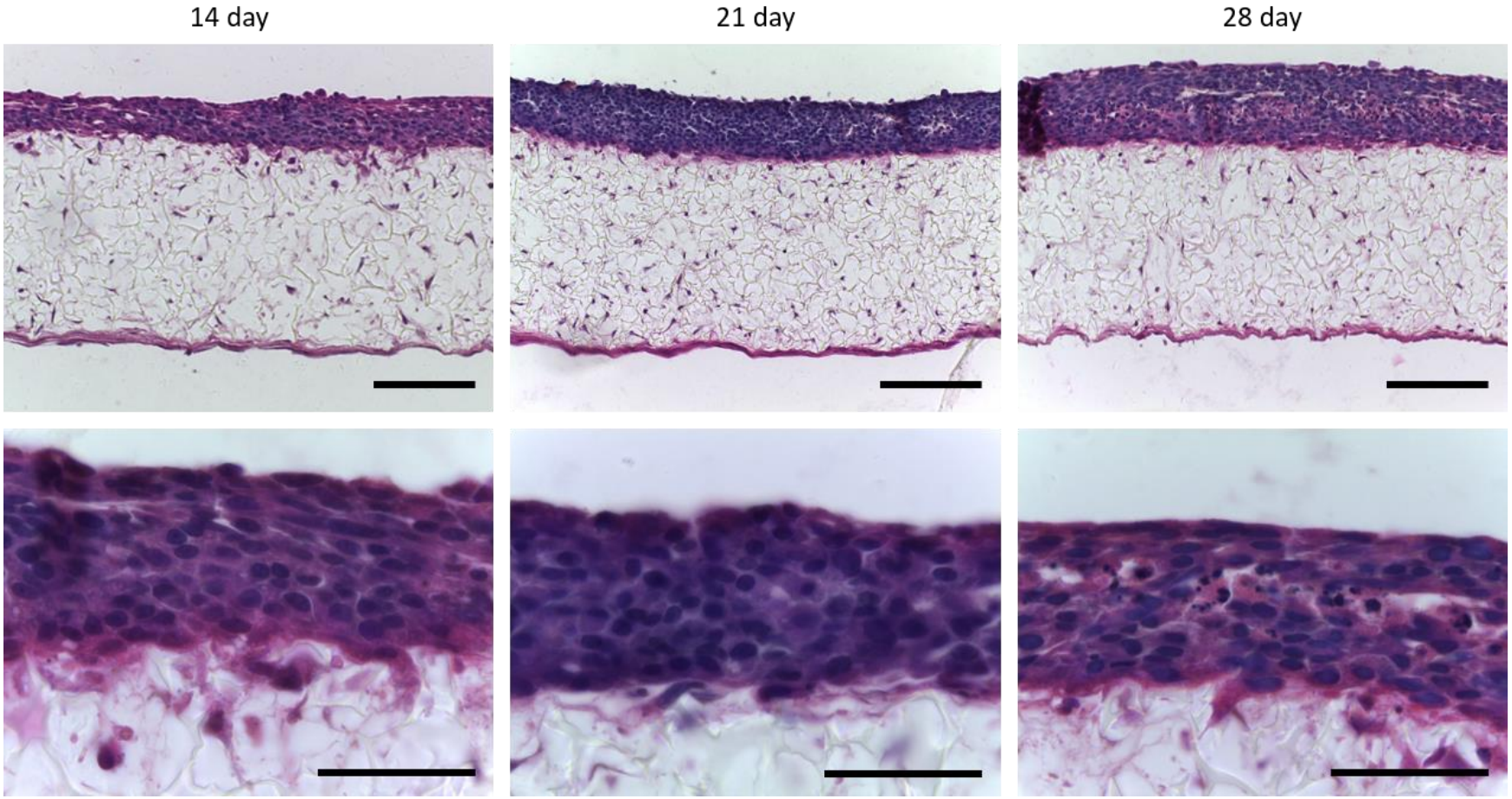

Figure 6.7: Growth of HepG2 cells on Alvetex® Scaffold cultured with fibroblasts for different time periods. The shortest time period of 2 weeks displays a thick cell layer with minor invasion into the substrate. At 3 weeks the invasion is almost eliminated whilst the cell layer is histologically unchanged. At 4 weeks invasion is completely eliminated however necrosis is started to occur in the centre of the HepG2 cell layer. Scale bars are 100 µm (top and 25 µm (bottom).

6.4.2. Characterisation of HepG2 – HDFn co-culture models

6.4.2.1. Gross morphology

The different structures of the HepG2 – HDFn co-culture models compared monoculture of HepG2 on Alvetex® Strata can be seen in Figure 6.8. Use of fibroblasts in the bioreactor creates a dense, constrained layer of HepG2 compared with the heterogeneous cultures of HepG2 on Strata which possess both a surface layer with vast cell-cell contacts as well as regions of invasion with a greater proportion of cell-membrane adhesion and reduced cell-cell contact.

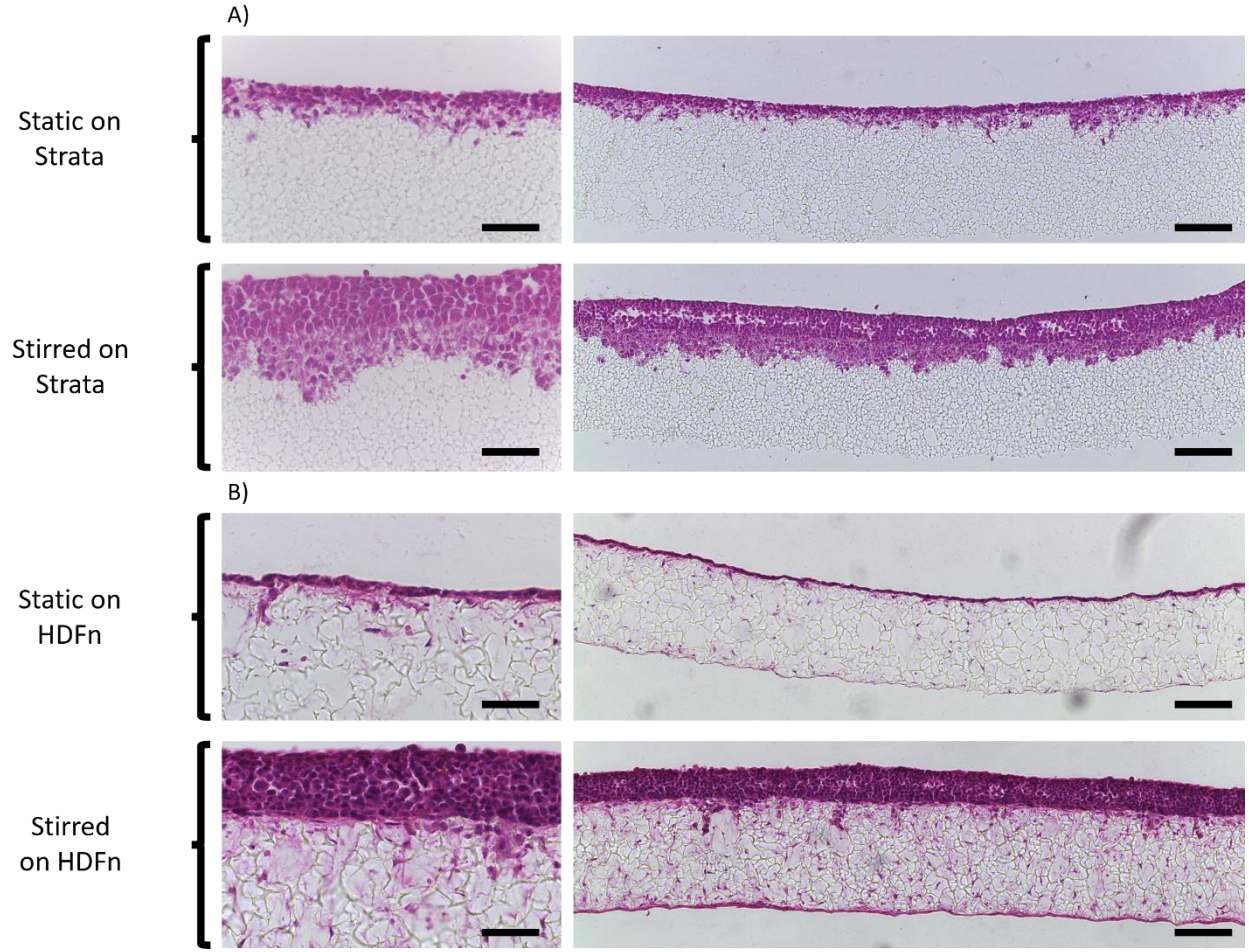

Figure 6.8: H&E staining of HepG2 grown on Alvetex in static and dynamic conditions. A) HepG2 cells were grown on Alvetex Strata in static and dynamic conditions with the formation of a thicker cell layer and greater invasion in dynamic conditions. B) HepG2 cells were grown on Alvetex Scaffold containing fibroblasts in static and dynamic conditions. In static the HepG2 form a monolayer along the surface of the Alvetex whilst in dynamic conditions a thick layer of HepG2 is formed on the surface of the Scaffold. In all conditions the cells are evenly distributed across the entire membrane. Scale bars are 25 µm (left) and 100 µm (right).

A notable result is the formation of a HepG2 monolayer when cultured on HDFn in static. This result matches previous results reported where hepatocytes form monolayers in collagen gels. The large deviation of this model compared with all the other models alongside the difficulty imaging cell-cell structures in cross-section means that it will be removed from subsequent immunofluorescent analysis.

Figure 6.9 provides quantification of the results discussed above. The thickness of the HepG2 layer in dynamic models containing HepG2 is slightly greater than in models of HepG2 alone whilst the variation in thickness is greatly reduced, as shown by the smaller error bar representing a decrease in standard deviation. The thickness of the layer for static co-cultures displays the result discussed previously with a uniform HepG2 layer of one to two cells thick. Results of the invasion quantification also demonstrate the reduction in HepG2 in co-culture models compared with when grown in Strata.

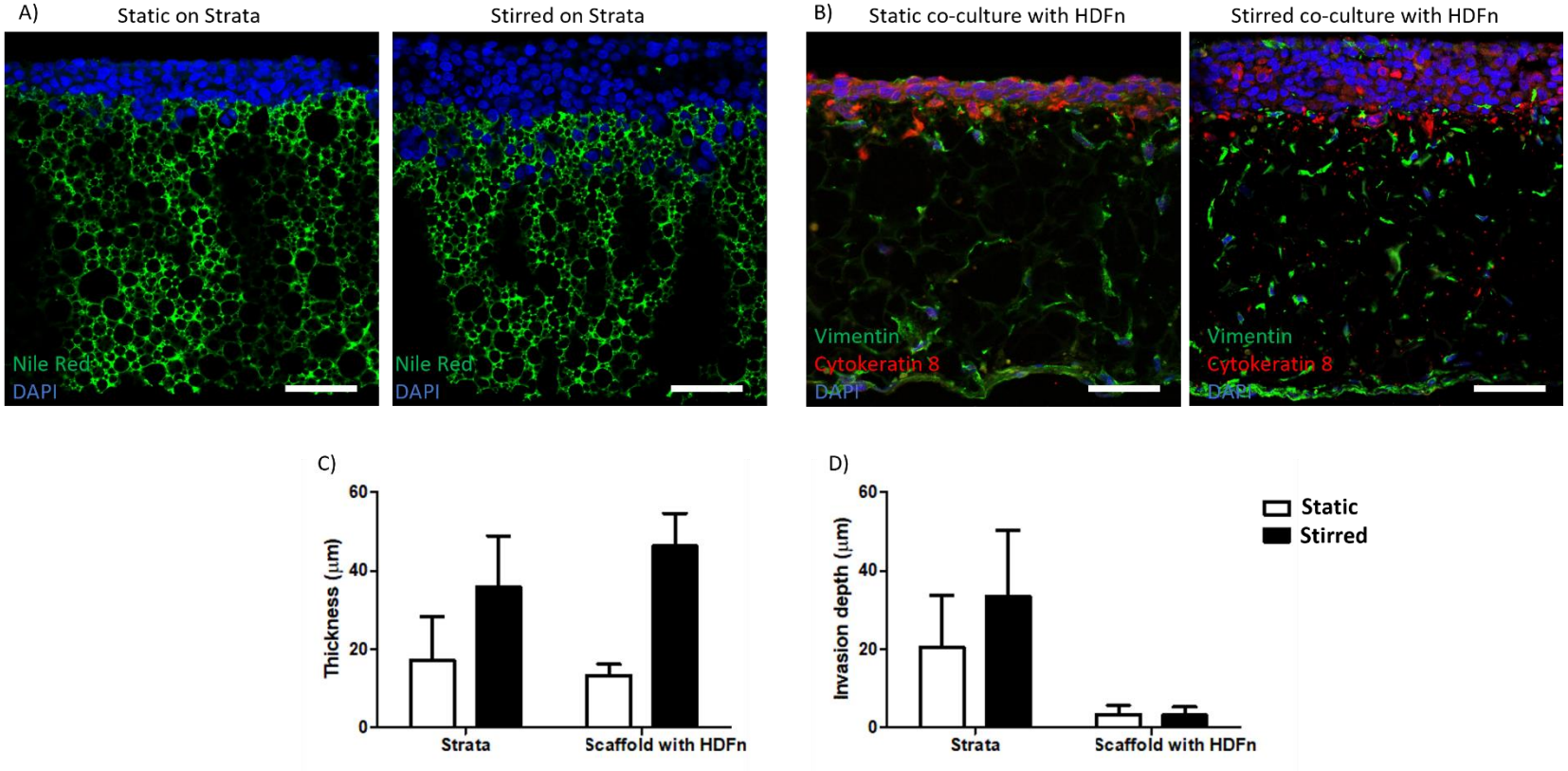

Figure 6.9: Invasion quantification for different HepG2 culture methods. A) HepG2 cells grown on Alvetex® Strata in static and stirred conditions stained with nile red to visualise the Alvetex® and DAPI to visualise the cell nuclei. A greater number of nuclei can be seen inside the Alvetex® structure in dynamic conditions compared with static. Scale bars are 50 µm. B) HepG2 cells grown on Alvetex® Scaffold seeded with fibroblasts. HepG2 cells are stained red for cytokeratin 8 expression whilst fibroblasts are stained green for vimentin expression. under fluid flow, a thicker HepG2 cell layer can be seen on the surface of the Alvetex® whilst invasion into the Scaffold is minimal. C) Quantification of the thickness of the cell layer with the different culture techniques. D) Quantification of the invasion into the membrane with the different techniques. Fluid flow causes an increase in invasion whilst the use of fibroblasts in the Alvetex® almost entirely eliminates invasion. All values are mean ± SD.

The overall morphology of the optimised HepG2 – HDFn culture model can be seen in Figure 6.10. This model has a fibroblast compartment within the Alvetex® Scaffold and a separate HepG2 compartment on the surface of this with a well-defined boundary between the two. This leads to a homogeneous population of HepG2 cells, and this layer is uniform across the whole width of the Alvetex® membrane.

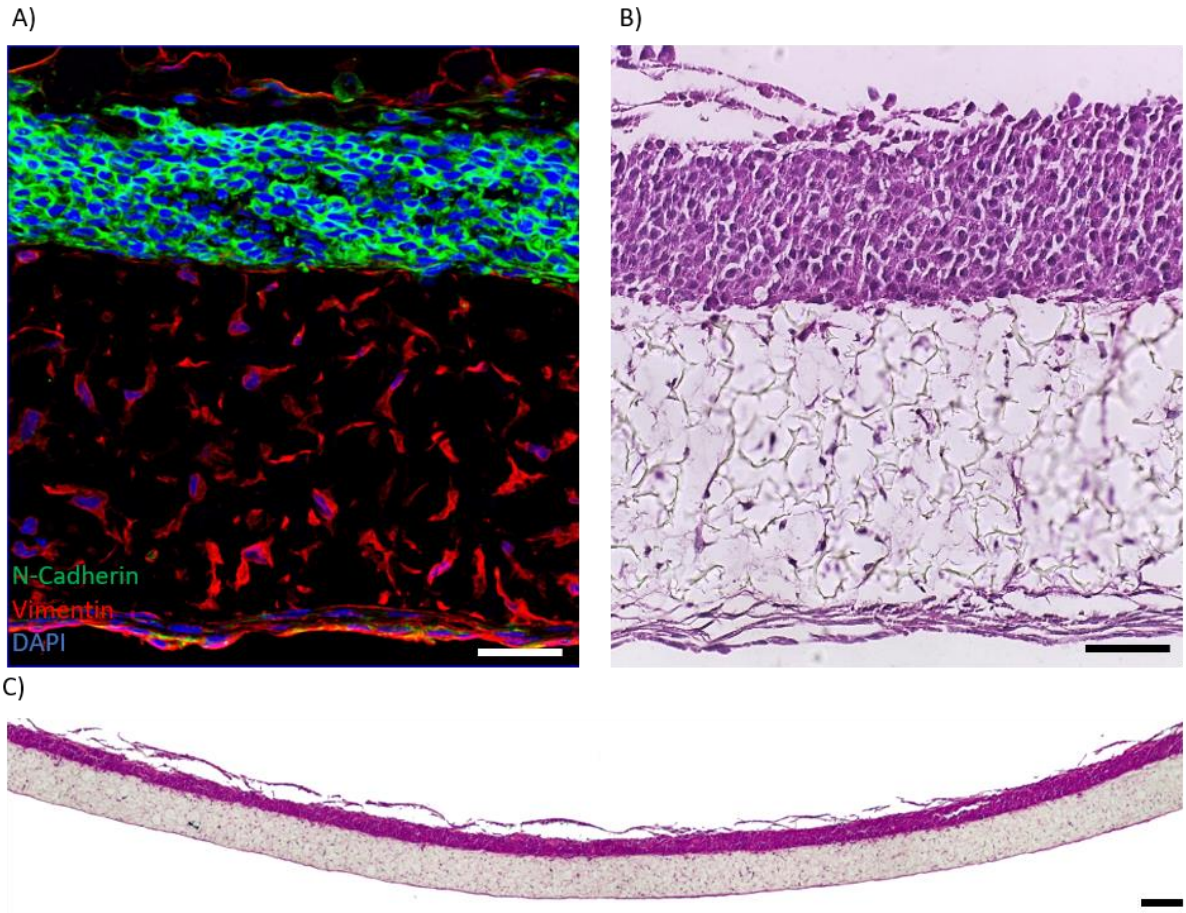

Figure 6.10: General morphology of the stirred HepG2 model with fibroblasts. A) Immunofluorescent stain of the model using N-cadherin in green to show the HepG2 and vimentin in red to show the fibroblasts. The homogeneous HepG2 compartment can be seen on top of the Alvetex® membrane. B) H&E stain of the HepG2 and fibroblast model showing the general morphology of the culture. Scale bars are 50 µm. C) A composite image showing the H&E stain across the entire width of an Alvetex® Scaffold. The thickness is uniform across the entire membrane with minimal variation. Scale bar is 200 µm.

The presence of large quantities of ECM in this model compared with the absence of ECM in the HepG2 monocultures can be seen in Figure 6.11. Both collagen 1 and 3 display high levels of staining across the full thickness of the Alvetex® membrane. With these proteins both being present in high quantities in the space of Disse adjacent to the hepatocytes *in vivo* their presence in these cultures is an important step towards recapitulation of the liver microenvironment. Collagen 4 is also present in the co-cultured though to a lesser extent than collagens 1 and 3. Due to the limited quantities of collagen 4 in the liver and its localisation around endothelial cells and the portal region rather than hepatocytes this result would appear to be beneficial for a physiologically relevant hepatocyte culture. Fibronectin, a protein which is present in large quantities around hepatocytes in the liver, is expressed through the Alvetex® though to a lesser extent than collagen 1 and 3.

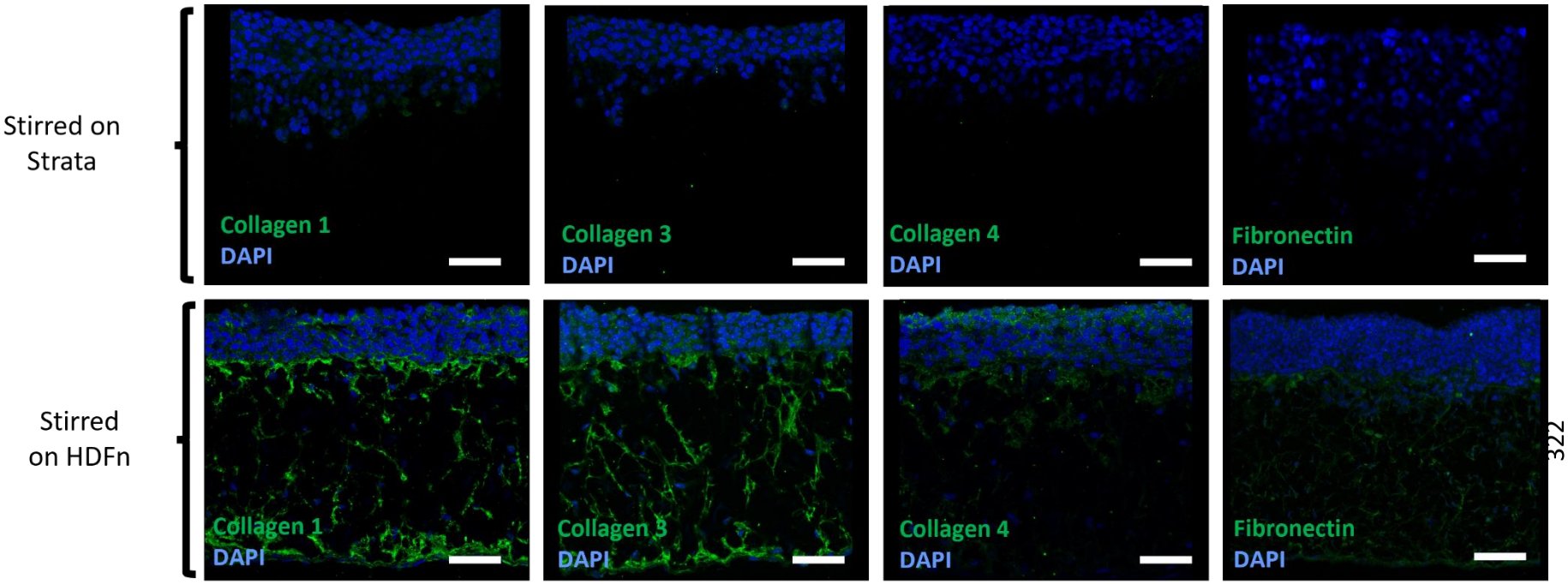

Figure 6.11: Immunostaining of the different HepG2 models for key liver extracellular matrix proteins. Collagen 1, collagen 3 and fibronectin are typically found around the sinusoidal region and in the space of Disse whilst collagen 4 tends to reside in the portal region. All these proteins show low levels of expression in HepG2-only models however with the addition of fibroblasts much greater ECM deposition is observed in the fibroblast compartment due to the production of ECM by the fibroblasts. The high levels of collagen 1 and 3 and lower levels of collagen 4 seen in the cultures with fibroblasts (bottom row) suggest that an *in vivo*-like ECM is being created. Scale bars are 50 µm.

For a more in-depth analysis of the co-culture models a series of important proteins will be examined through immunofluorescent staining. Initially markers of cell health will be examined followed by more hepatocyte-specific markers such as drug transporter proteins.

6.4.2.2. Markers of culture health

Several different methods can be used to analyse cell health as shown in Chapter 4. This analysis will be repeated with stains to look for cell death, proliferation, and hypoxic stress as shown by Figure 6.12.

Two methods were used to look at cell death from different time points in the apoptotic pathway. The TUNEL stain was used to investigate late-stage apoptotic cells (Figure 6.12A) whilst cleaved caspase 3 was used to identify cells in the early stages of apoptosis (Figure 6.12B). These stains both show very low levels of cell death in both cultures. Whilst a few apoptotic cells are identified by cleaved caspase 3 for stirred HepG2 monocultures no cells expressing this marker can be found in the stirred co-culture models suggesting a possible improved viability over long term culture.

For proliferation similar results are seen between cultures however the fibroblast co-cultures appear to express ki67 across a greater number of cells which suggests they are more proliferative. This would coincide with the increased cell layer thickness and improved viability seen for these models.

HIF-1α expression is absent in both bioreactor models which shows that the dynamic co-culture models have the same improvement in oxygen delivery as seen in stirred HepG2 monoculture compared with the static cultures shown in Chapter 4 which had HIF-1α expression in all cells. This data all shows that the HepG2 – HDFn co-cultures are highly viable and healthy with possible improvements over the stirred cultures of HepG2 alone.

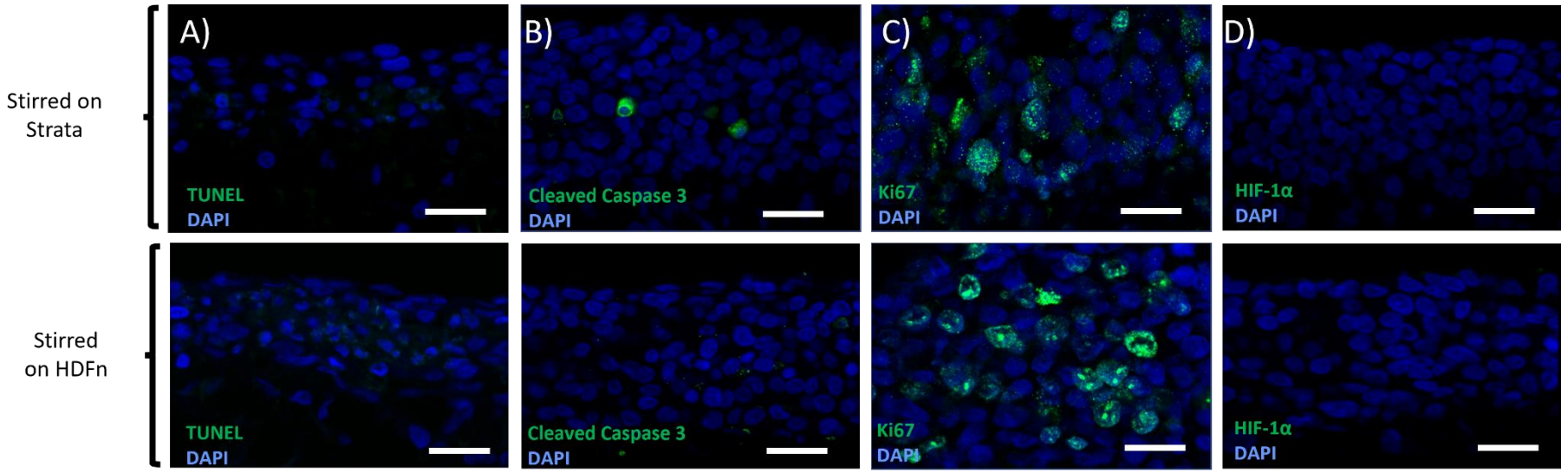

Figure 6.12: Immunostaining of the different HepG2 models with viability and cell health markers. The TUNEL stain and cleaved caspase 3 show minimal cell death in all the models suggesting a high level of viability and absence of necrotic core. Ki67 shows high proliferation with all models suggesting that the proliferation does not slow down in 3D culture or under fluid flow. D) Expression of HIF-1α is absent in stirred culture compared to fairly high, uniform expression in 2D and 3D static cultures suggesting a greater oxygen availability in stirred culture. Scale bars are 50 µm.

6.4.2.3. Markers for hepatocyte function

The expression of a series of proteins will be investigated to analyse any changes seen between HepG2 stirred monoculture and co-culture with fibroblasts in fluid flow. These will include junctional proteins and transporter proteins, as performed in Chapter 4 for the monocultures in static and dynamic conditions.

The first region to be investigated is the adherens junction. The levels of different adherens junctional proteins can lead to further changes to other aspects of cell structure and function. The adherens junction linker protein β-catenin shows similar expression in dynamic HepG2 monocultures and co-cultures with HDFn. Localisation to the cell membranes can be seen at all sides however there is still a large amount of cytoplasmic staining present. For the two transmembrane adherens junctions, E-cadherin and N-cadherin, the expression remains at high levels with strong localisation to the cell membranes and varied expression between adjacent cells.

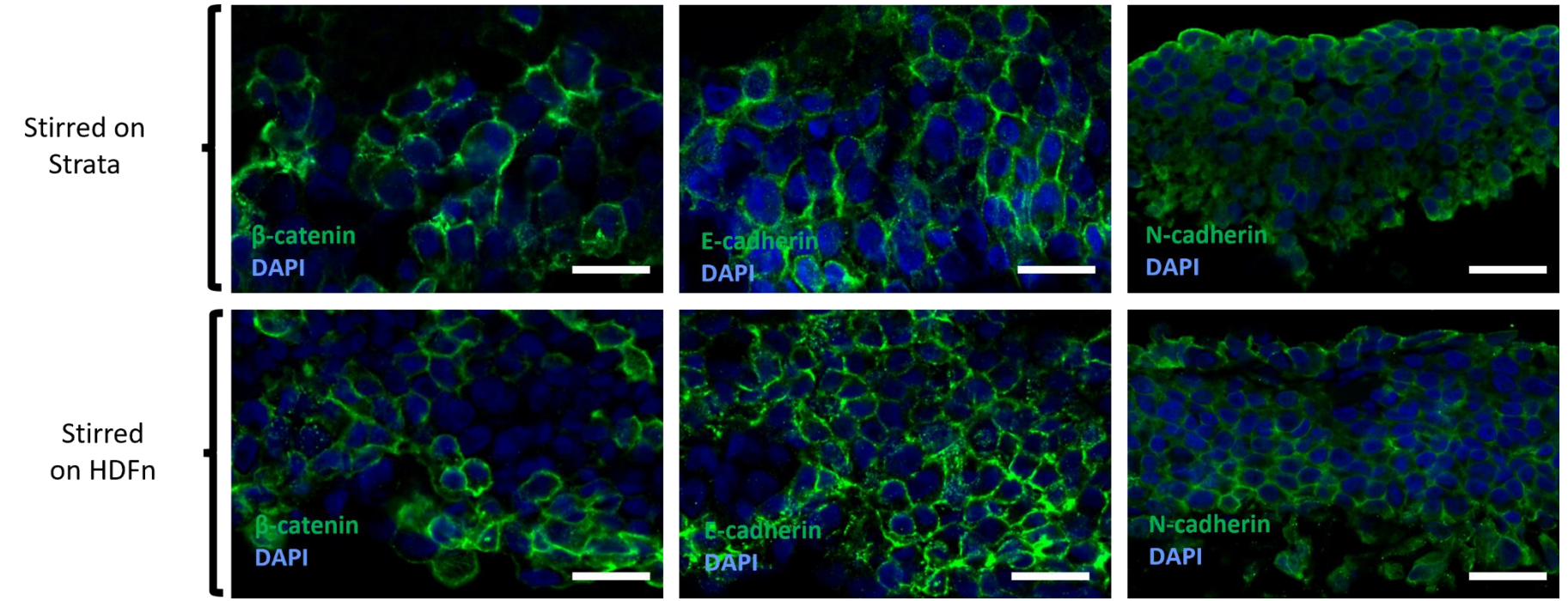

Figure 6.13: Expression of adherens junctional proteins in the different models. Both E-cadherin and N-cadherin are expressed in high levels in all culture methods. Stirred cultures see a more uniform expression of N-cadherin compared to static however E-cadherin levels show similar levels of variability across all culture methods. Expression of E-cadherin *in vivo* tends to be distributed towards the higher oxygen, periportal, region of the hepatic lobule. β-catenin staining is uniform in all cultures with a high level of staining around the membrane areas as well as significant cytoplasmic staining. Scale bars are 50 µm.

Tight junctions similarly show minimal difference between the two culture techniques with high expression of both claudin 1 and claudin 2 in both culture techniques. Expression can be found at all regions around the cell membrane as in static culture which suggests that specific localisation to apical domains is minimal.

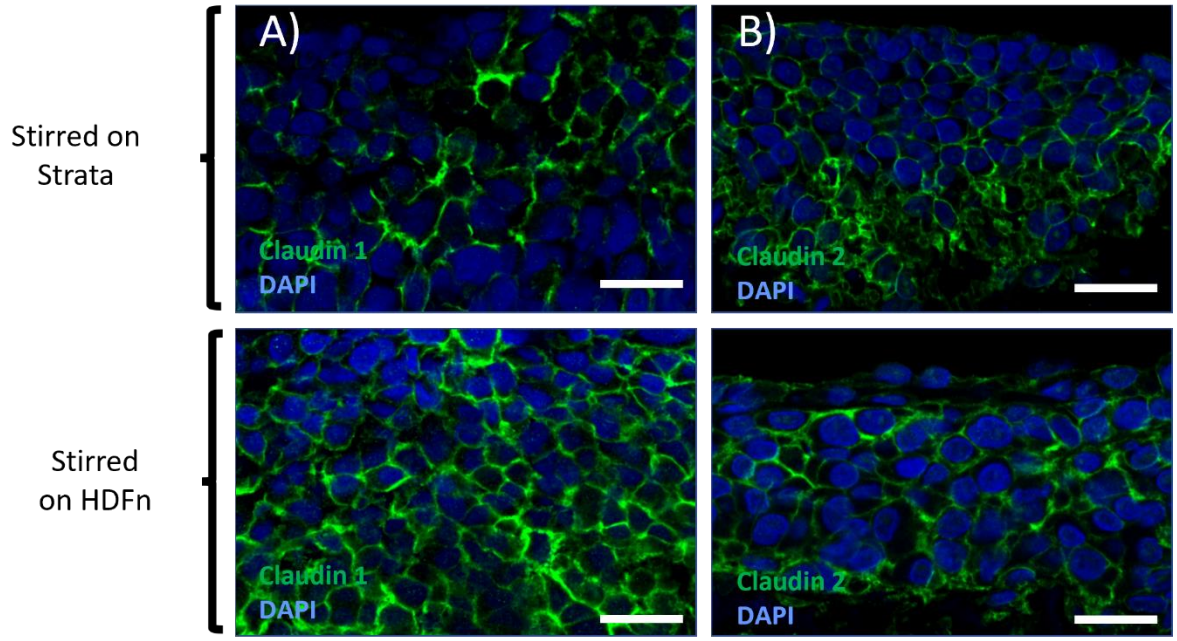

Figure 6.14: Immunostaining of the different HepG2 models with tight junctional proteins. Transmembrane tight junction proteins claudin 1 and claudin 2 show a maintained expression in HepG2 between stirred models on Strata and on fibroblasts in Scaffold. Expression is strongly localised to regions of cell membranes with minimal cytoplasmic staining visible. No expression localised to distinct apical regions of the cells, as found *in vivo,* can be distinguished in these stains. Scale bars are 50 µm.

Results for transporter proteins follow the same trend with no discernible difference between monoculture and co-culture. Improvements seen in dynamic monoculture, such as the increases in MRP2 expression with better network formation, are seen in co-culture as well as monoculture suggesting that enhanced functional localisation induced by fluid flow is not lost with the addition of fibroblasts.

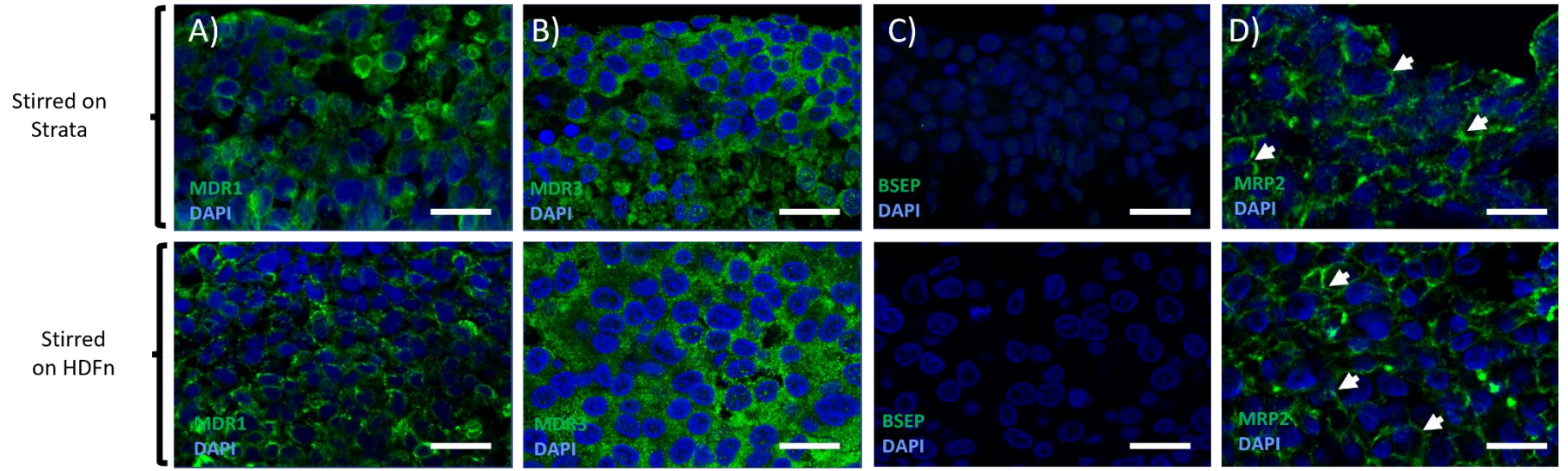

Figure 6.15: Immunostaining of the different HepG2 models for different apical transporter proteins. The four proteins examined are efflux transporters which are important parts of the drug detoxification pathway in hepatocytes. A) MDR1 staining can be seen in both conditions distributed throughout the cytoplasm. B) MDR3 expression is the same in both conditions with high levels of cytoplasmic staining. C) No BSEP expression can be determined from background fluorescence in either conditions. D) MRP2 expression is comparable between the two conditions with localisation towards membranes apparent. Interconnected networks of expression are clearly visible in both conditions (white arrows). Scale bars are 50 µm.

Sinusoidal transporters again mirror these results with maintained expression of MRP3 around the cell membranes as seen in stirred monoculture. Proteins which are not expressed in the other conditions such as NTCP do not appear to be induced through the addition with fibroblasts, repeating the negative staining seen for the previous HepG2-only methods.

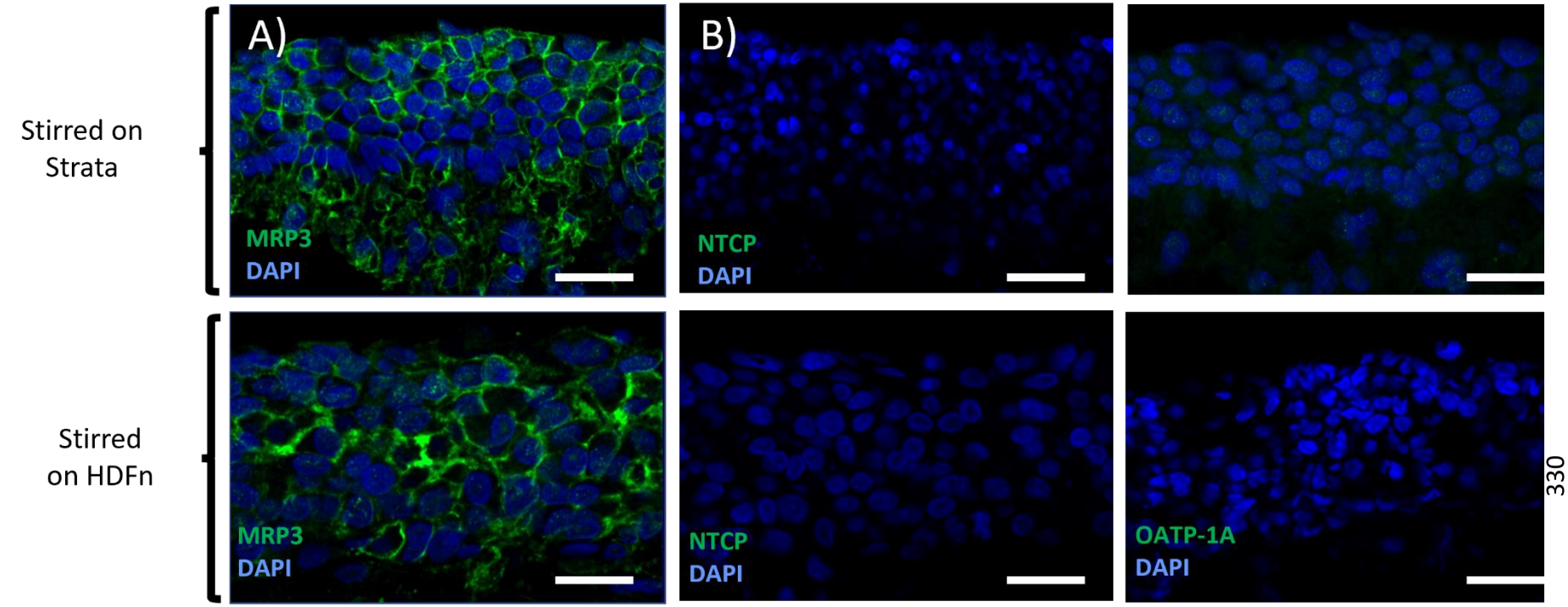

Figure 6.16: Immunostaining of the different HepG2 models for different sinusoidal transporters. MRP3, a transporter which is present in the basolateral membrane of cells, is the only one of the three transporters investigated that is detected in either of the models. Similar expression patterns of strong localisation to cell membranes are apparent in both models. NTCP and OATP-1A are absent in both stirred models. Scale bars are 50 µm.

6.4.2.4. Metabolic profile

The metabolic activity of HepG2 cells grown in stirred co-cultures can be analysed using albumin and urea secretion as shown in Figure 6.17. These are normalised to total protein with a further normalisation to the initial seeding ratio of the cells to give a rough value per the number of HepG2 cells. A thorough literature search for alternative quantification methods to use for normalising these assays to the hepatocyte population, accounting for the presence of the fibroblast population, was carried out. However, no accurate method could be determined for performing this due to limitations identifying the different cells using stable markers therefore the initial seeding ratio was used, as has been performed elsewhere (Cho *et al.*, 2006; Baze *et al.*, 2018).

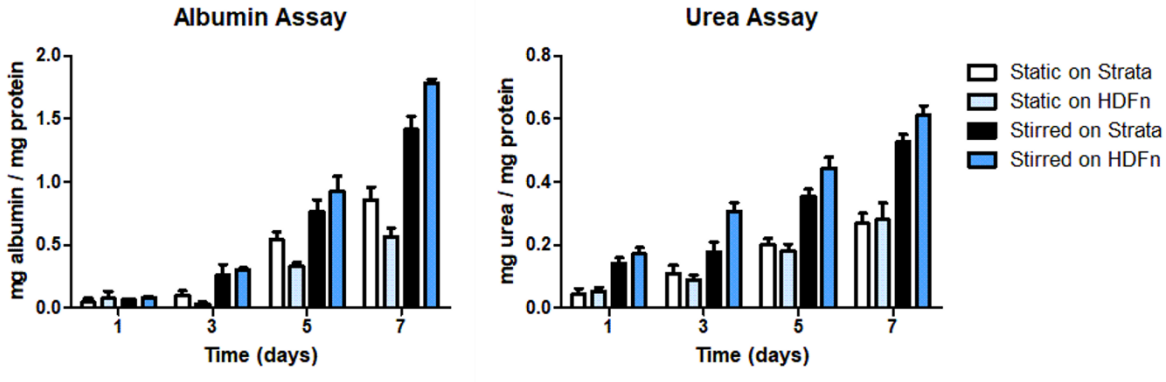

Figure 6.17: Metabolic assays for HepG2 and HDFn co-culture models. The albumin assay and urea assay demonstrate the changes in metabolic function of the HepG2 cells when cultured with fibroblasts. Stirred models containing fibroblasts show comparable levels of secretion to the equivalent models on Alvetex® Strata. Assays were carried out over 7 days with media samples taken every 2 days after the first day. n = 3, values are mean ± SEM.

Compared with monoculture a significant increase is seen in dynamic conditions with HDFn at similar levels to or higher than HepG2 monoculture. This shows that fibroblasts can further enhance the metabolic function of HepG2 cells above the levels induced through fluid flow alone.

6.4.3. Inclusion of endothelial cells in HepG2 models

With endothelial cells accounting for the majority of the non-parenchymal cells in the liver the next cultures to be created will look at including these with the HepG2 as well as in the HepG2 – HDFn co-cultures. The adenocarcinoma cell line SK-Hep-1 will be used for the endothelial cells in this model. These cells have been shown to express an endothelial phenotype and possess LSEC specific properties such as the presence of fenestrations (Heffelfinger *et al.*, 1992; Tai *et al.*, 2018). As work

with these in Alvetex® has not been carried out previously the first steps will look at the growth of these cells in Alvetex® followed by the impacts of different quantities of these cells alongside the other cell types used in this chapter

6.4.3.1. Characterisation of SK-Hep-1 cells

Prior to incorporating SK-Hep-1 into co-cultures the morphology of these cells grown in 3D in the different forms of Alvetex® will be explored. As can be seen in Figure 6.18 the morphology of this cell line in Alvetex® Scaffold and Strata is strikingly different from that of HepG2 or HDFn. In both substrates the cells demonstrate a very high level of migration with invasion through the entire membrane achieved in both Scaffold and Strata after 7 days.

In Scaffold the population of cells appears to have a mixed morphology with cells within the Scaffold exhibiting and elongated, fibroblast-like shape. Cells towards the surface of the Scaffold, where the cell density is greater, have formed into a more compact and rounded conformation. In Alvetex® Strata this compact, rounded morphology is seen more frequently with most cells in this conformation whilst very few elongated cells present.

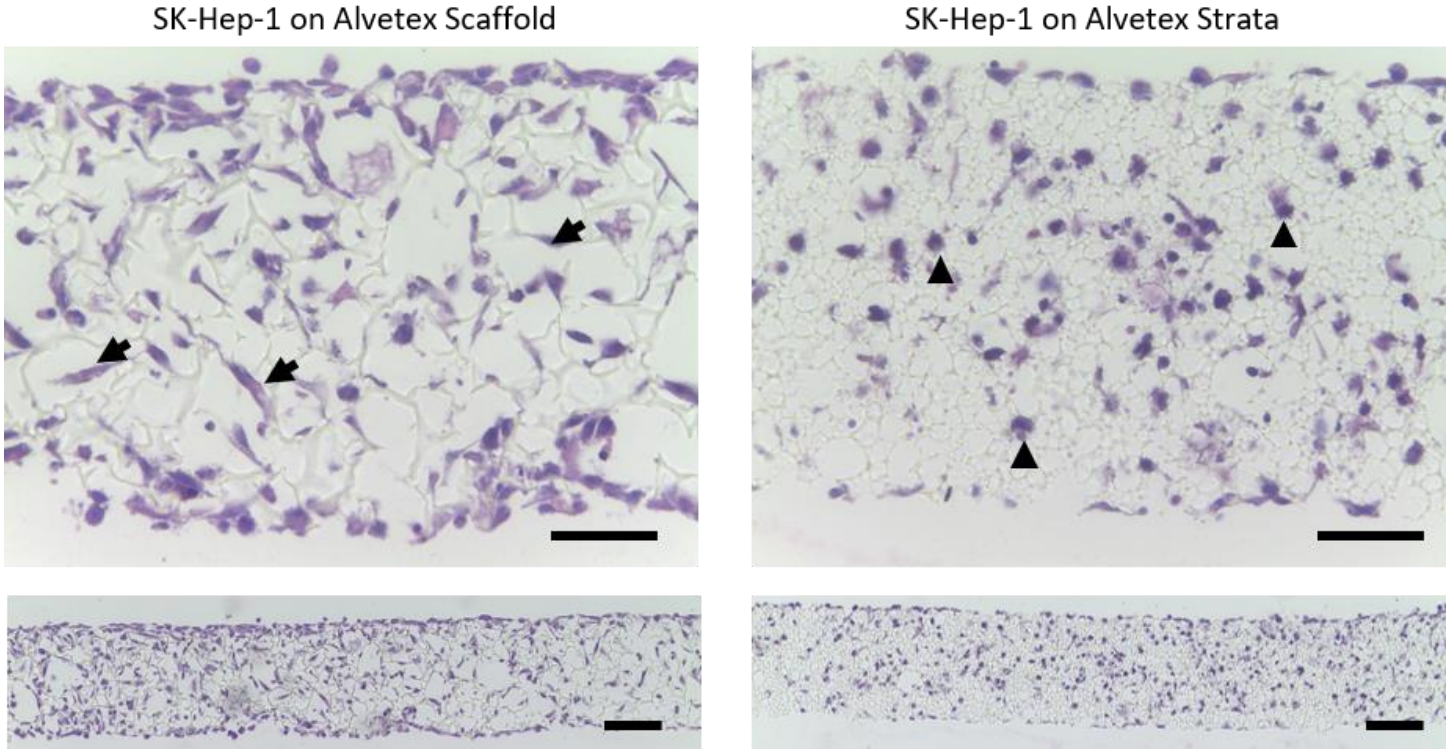

Figure 6.18: SK-Hep-1 cells grown in Alvetex® Scaffold and Strata. SK-Hep-1 cells were seeded onto Alvetex® Scaffold and Strata and cultured for seven days. In Alvetex® Scaffold a higher proportion of cells adopt an elongated and spread out morphology with distribution through the membrane (black arrows). On Alvetex® Strata the cells typically form a much more compact and circular morphology (black triangles) however are still distributed across the entire membrane. No significant formation of a surface cell layer can be seen in either form of Alvetex®. Scale bars are 50 µm (top) and 100 µm (bottom).

For use of the three different cell types together in co-culture a method of identifying the different populations is required. For this a series of proteins were investigated with the combination of vimentin and cytokeratin 8, as used previously for the HepG2 – HDFn co-cultures, was chosen due to the strong staining of both markers in positive cells. Different combinations of these two proteins are expressed in the different cell types, as shown by Figure 6.19, allowing the identities of the cells to be discerned.

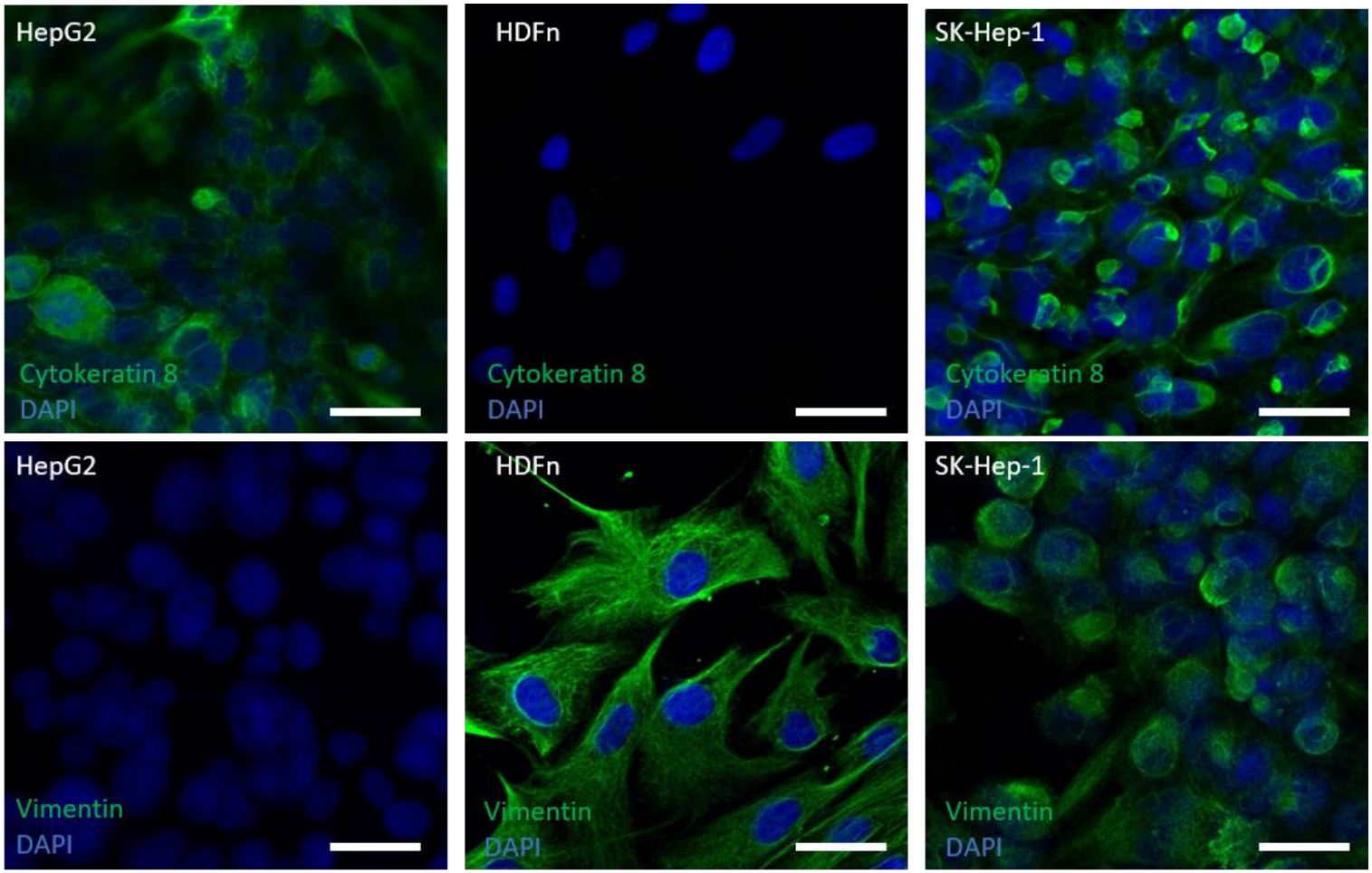

Figure 6.19: Proteins used as markers for the different cell types using immunofluorescence. HepG2 cells stained strongly for cytokeratin 8 whilst had no expression of vimentin. HDFn expressed high levels of vimentin and no cytokeratin 8. SK-Hep-1 expressed both cytokeratin 8 and vimentin at high levels. The different expression of these proteins in the cells can be used to identify the different cell types in co-culture. All stains were performed on cells grown on coverslips in 2D. Scale bars are 25 μm.

HepG2 and SK-Hep-1 cells both express cytokeratin 8 whilst HDFn does not. As this is a protein which is expressed in a lot of liver cells this expression pattern is as expected. Vimentin is not expressed in HepG2 however is expressed in both HDFn and SK-Hep-1. These variations in expression allow the three cell lines to be identified through a simple two antibody stain. HepG2 are therefore identified as cytokeratin 8-positive and vimentin-negative, HDFn are cytokeratin 8-negative and vimentin-positive and SK-HEP-1 are cytokeratin-8 positive and vimentin-positive.

6.4.3.2. Growth of SK-Hep-1 with HepG2

The first investigation into growth of SK-Hep-1 with other cell lines was the growth in static culture with HepG2. Alvetex® Strata was used for this as it has been the preferred form of Alvetex® for the HepG2 culture in previous monoculture experiments. As seen in Figure 6.20 an increase in the seeding density of SK-Hep-1 alongside the standard 2 million HepG2 has significant changes to the morphology. When cultured alone on Alvetex® Strata HepG2 tend to form a layer of cells on the surface with some regions of invasion into the substrate. With SK-Hep-1 included at the lowest amount tested of 100,000 cells the gross morphology appears to be relatively unchanged with the SK-Hep-1 typically being located further into the Alvetex® than the HepG2.

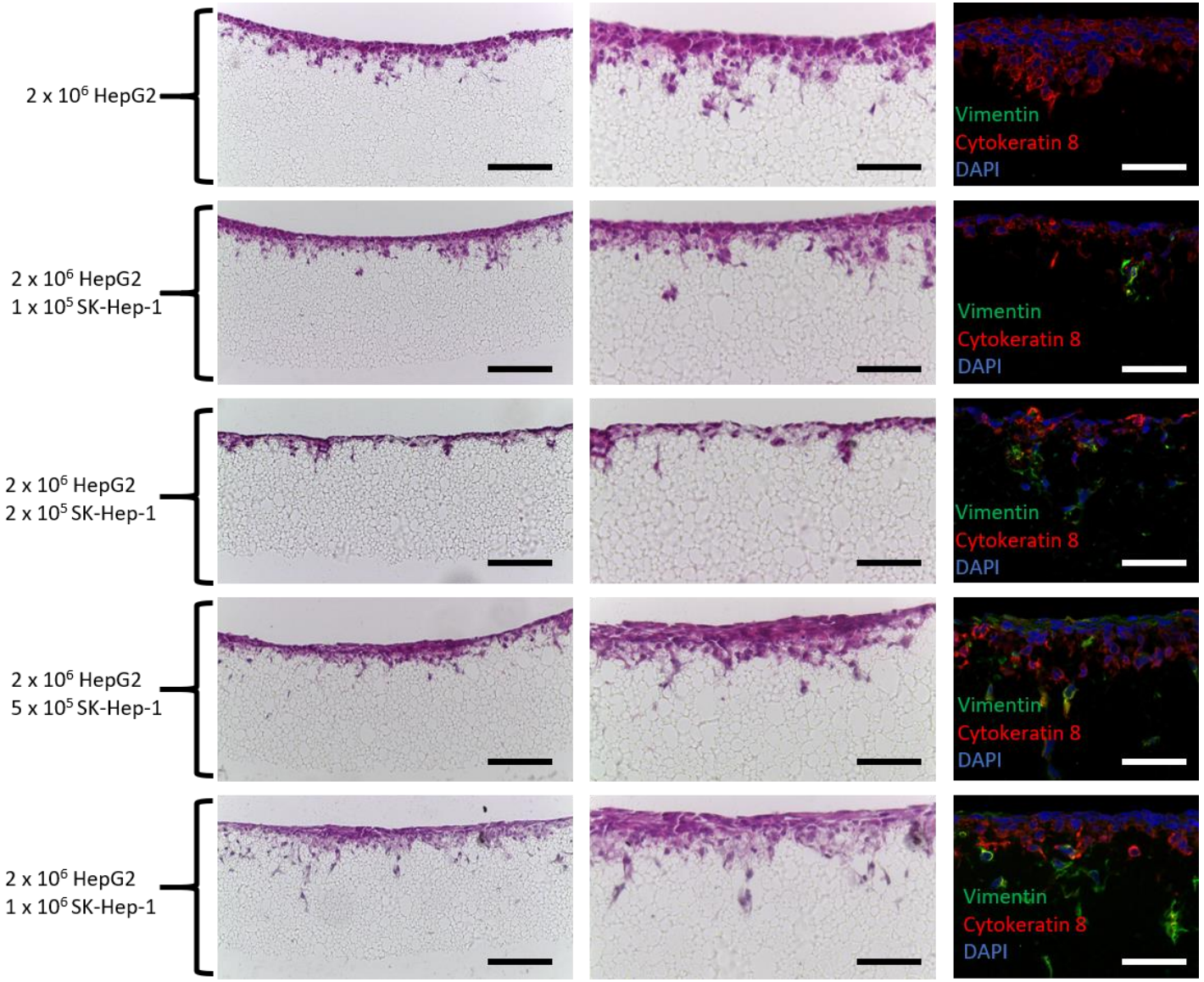

Figure 6.20: HepG2 and SK-Hep-1 co-cultures on Alvetex® Strata at different seeding densities in static conditions. The number of HepG2 cells seeded remained the same across all conditions at 2 x 10^6 however the number of SK-Hep-1 cells was varied from 0 to 1 x 10^6. The analysis was carried out with a H&E stain (left and centre) and immunofluorescence staining for vimentin and cytokeratin 8 (right). Increasing levels of SK-Hep-1 corresponds with increasing levels of invasion into the substrate. Scale bars are 100 µm.

At higher densities of SK-Hep-1 the number of HepG2 in the cultures appears to decrease. This is likely due to the faster doubling time of the SK-Hep-1 allowing them to outcompete the HepG2 in the cultures whilst the increased total number of cells is likely also slowing growth due to nutrients in the cell culture medium being used up at a faster rate. The morphology of the surface layer also changes significantly at high quantities of SK-Hep-1 with a much denser surface layer forming with fewer visible cell-cell junctions than is seen with HepG2 alone.

When these cultures are repeated in the bioreactor a similar effect is seen (Figure 6.21). At low levels of SK-Hep-1 the two cell populations are abundant with HepG2 forming a surface layer on top of the membrane and SK-Hep-1 invading further into the membrane. At higher quantities of SK-Hep-1 the HepG2 cells again seem to be outcompeted as seen in static, with few HepG2 visible at the highest two levels of Sk-Hep-1 cells. As the medium is in excess in these cultures this makes it less likely that this effect is due to reduced nutrient levels and instead there is a mechanism by which the endothelial cells are inhibiting HepG2 growth. This suggests that successful co-cultures of the two cell types require only small numbers of endothelial cells to be added to the cultures.

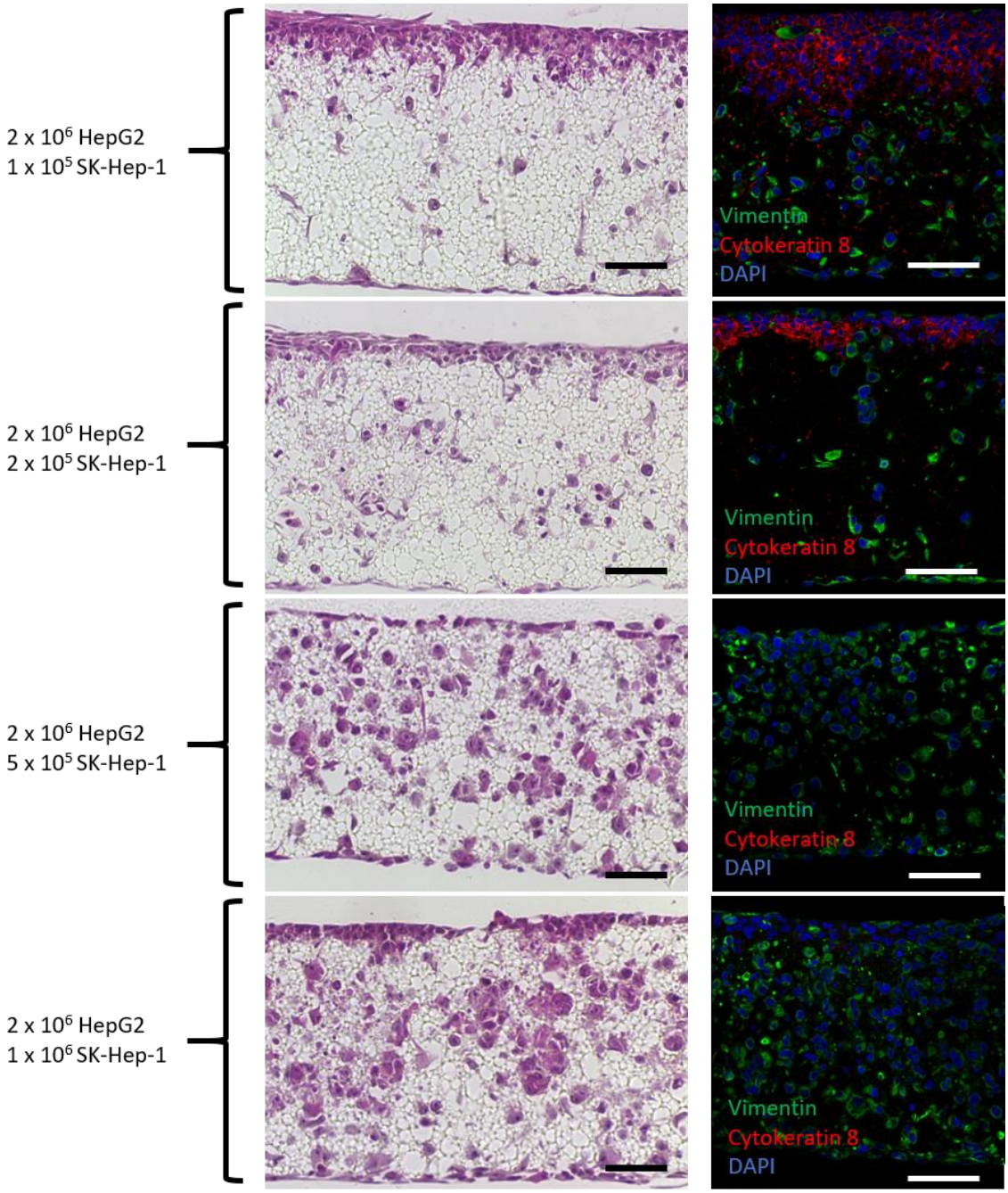

Figure 6.21: HepG2 and SK-Hep-1 co-cultures on Alvetex® Strata in Stirred conditions. The number of HepG2 cells seeded remained the same across all conditions at 2 x 10^6 however the number of SK-Hep-1 cells was varied from 1 x 10^5 to 1 x 10^6. The analysis was carried out with a H&E stain (left) and immunofluorescence staining for vimentin and cytokeratin 8 (right). With low levels of SK-Hep-1, a thick surface layer of HepG2 can be seen (red), as is the case for culture of HepG2 alone. At the higher levels of SK-Hep-1 the HepG2 cells seem to be absent, with no surface cell layer forming and no staining for cytokeratin 8. Scale bars are 50 µm.

6.4.3.3. Growth of SK-Hep-1 with HDFn

When looking instead at the growth of SK-Hep-1 on fibroblasts the cells adopt a morphology like that seen with HepG2 and fibroblasts, as seen in Figure 6.22. Despite the increased invasiveness of SK-Hep-1 relative to HepG2 the fibroblasts are still able to almost prevent invasion into the Alvetex® completely and instead maintain a thick surface layer of endothelial cells. As can be seen with the H&E stain of the SK-Hep-1 at the highest quantity of cells the morphology of the surface layer is structured differently to that seen in HepG2 – HDFn cultures with the endothelial cells forming a flatter morphology on the surface than the more rounded morphology of HepG2 seen previously. These results suggest that the culture of both HepG2 and SK-Hep-1 together on an Alvetex® Scaffold fibroblast compartment may allow for the formation of a multi-layered co-culture system.

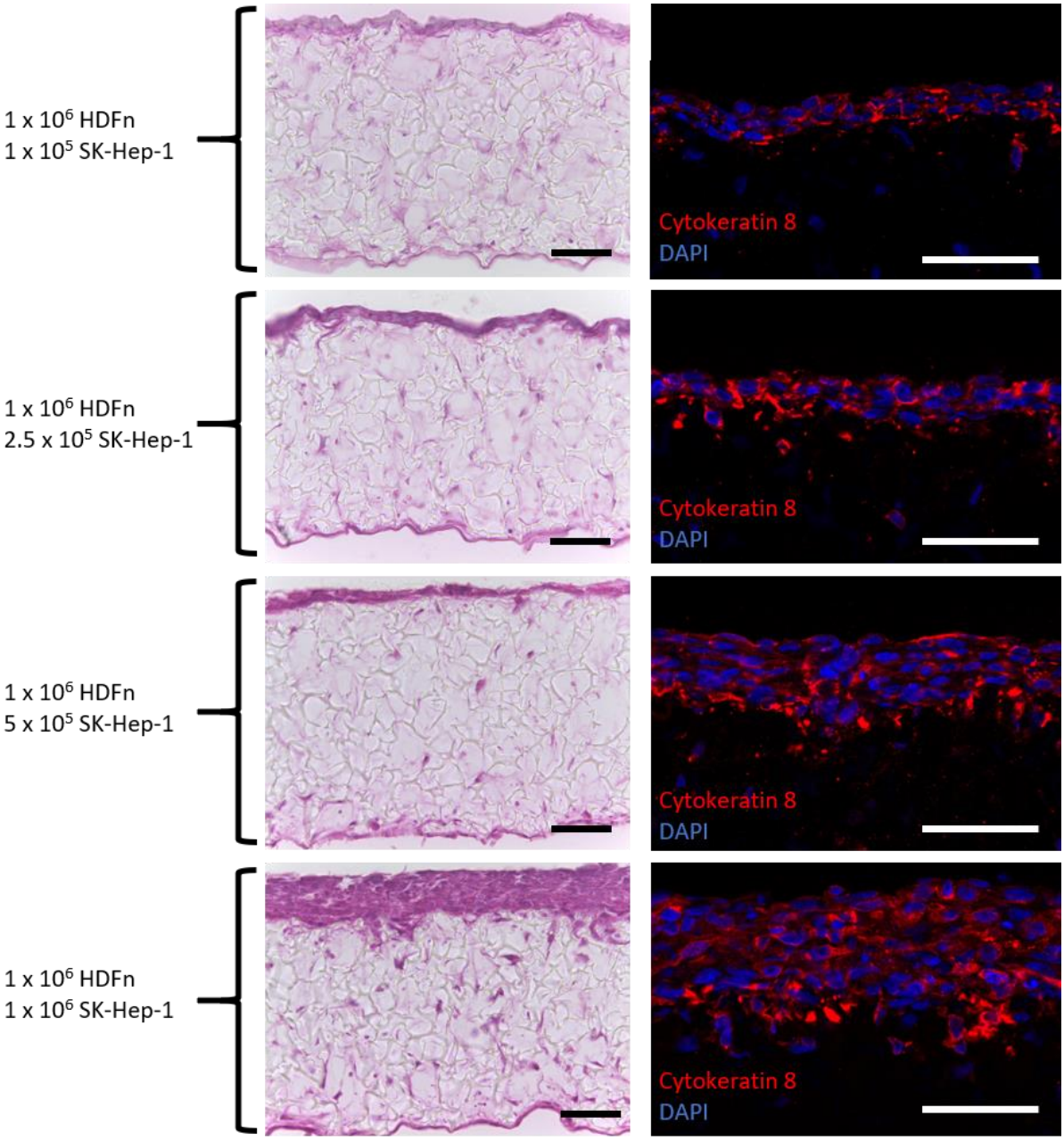

Figure 6.22: SK-Hep-1 and HDFn co-cultures on Alvetex® Scaffold in stirred conditions. The number of HDFn cells seeded remained the same across all conditions at 1 x 10^6 however the number of SK-Hep-1 cells was varied from 1 x 10^5 to 1 x 10^6. The analysis was carried out with a H&E stain (left) and immunofluorescence staining for cytokeratin 8 (right). Alvetex® Scaffold with fibroblasts embedded in it can effectively prevent most SK-Hep-1 cells from invading, as seen by the cytokeratin 8 staining and the formation of a thick surface layer in the H&E stain. This prevention of invasion starts to break down at the higher levels of SKHep-1 but still supports a thick surface layer of cells. Scale bars are 50 µm.

6.4.4. Creating a HepG2 bioreactor model containing fibroblasts and endothelial cells

The culture of the three cell types together was carried out by combining the methods used in the previous section with the fibroblast compartment generated in the Alvetex® Scaffold first followed by seeding with SK-Hep-1. This was carried out using very low numbers of SK-Hep-1 relative to the HepG2 to try and minimise the outcompeting of the HepG2 as seen in previous results. As shown by Figure 6.23 a viable culture is created when seeding 50,000 and 100,000 SK-Hep-1 to the cultures. By contrast when seeding 200,000 SK-Hep-1 to these co-culture models the formation of the HepG2 surface layer is significantly disrupted and a thinner, discontinuous layer instead forms.

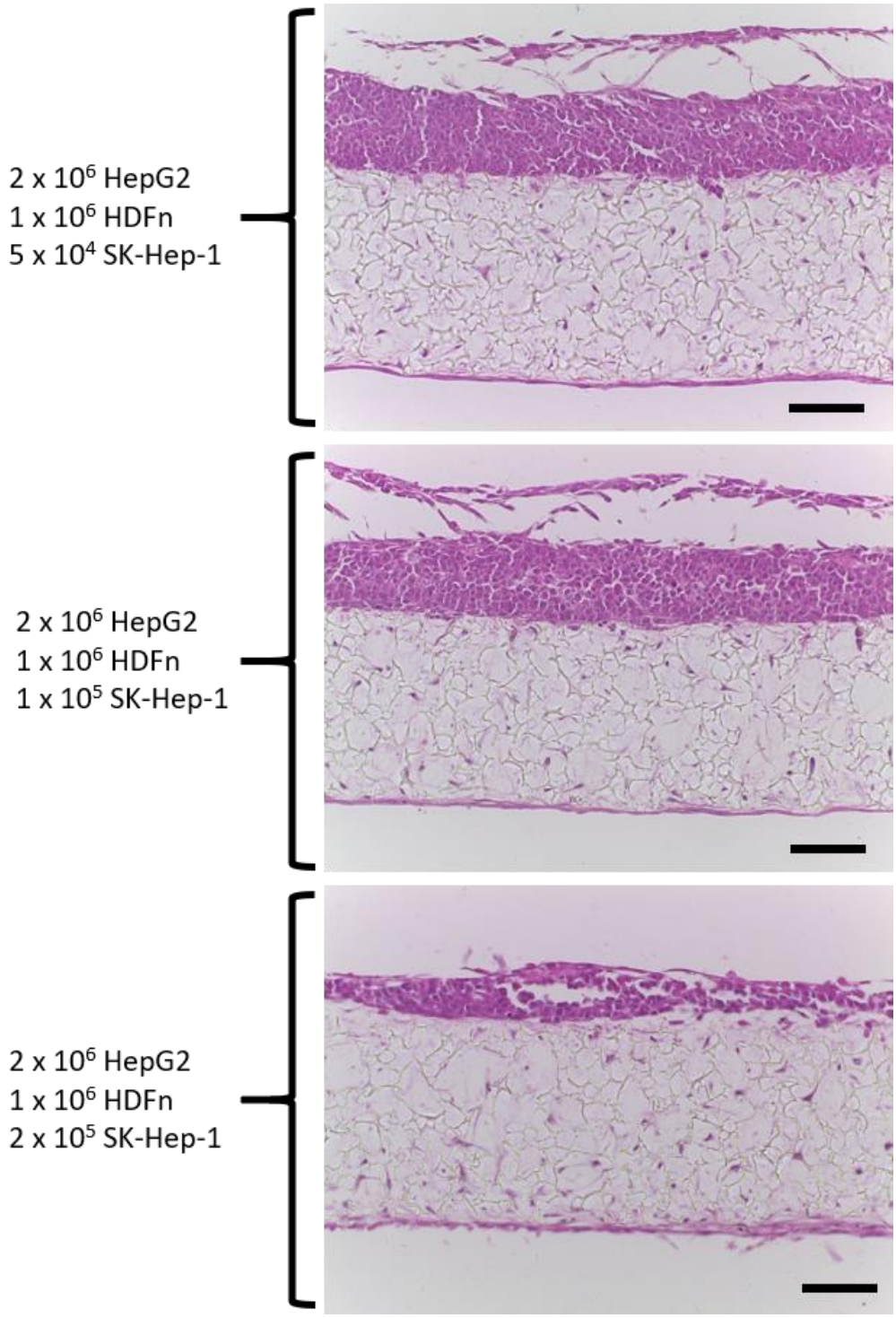

Figure 6.23: HepG2, SK-Hep-1 and HDFn tri-cultures on Alvetex® Scaffold in stirred conditions. The number of HepG2 and HDFn cells seeded remained the same across all conditions at 2 x 10^6 and 1 x 10^6 respectively. The number of SK-Hep-1 cells seeded was varied from 5 x 10^4 to 2 x 10^5. At the highest concentration of SK-Hep-1 the surface layer appears to be significantly reduced, suggesting deleterious effects on the HepG2 from high levels of SK-Hep-1 in the models. Scale bars are 50 µm.

For the culture with 100,000 SK-Hep-1 some immunofluorescent staining for the proteins cytokeratin 8 and vimentin was carried out to identify the populations of the different cell types. A high level of vimentin staining is seen within the Alvetex®, in line with previous results and representing the fibroblast population grown within it. A large population of vimentin positive cells are also present on the surface of the HepG2 layer, possibly representing the SK-Hep-1 cells. The staining of cytokeratin 8 shows strong staining throughout the expected HepG2 cell layer and all the way to the cells at the top of the culture, backing up the assumption that these cells which also stained for vimentin are the SK-Hep-1 cells.

It is possible to false colour this stain for the three different cell types (Figure 24B). In this way the cells which were exclusively expressing vimentin or cytokeratin 8 remained green and red respectively whilst cells expressing both proteins were false coloured in white, representing the endothelial cell population. Through this the endothelial cells can be seen to have migrated to the surface of the HepG2 layer when unable to invade down into the Alvetex® Scaffold. This leads to a final culture morphology not unlike the liver *in vivo*, with the endothelial cells lying between the HepG2 and the fluid flow. However, this lacks the space of Disse which would be present *in vivo* as well as the hepatic stellate cells present in this space.

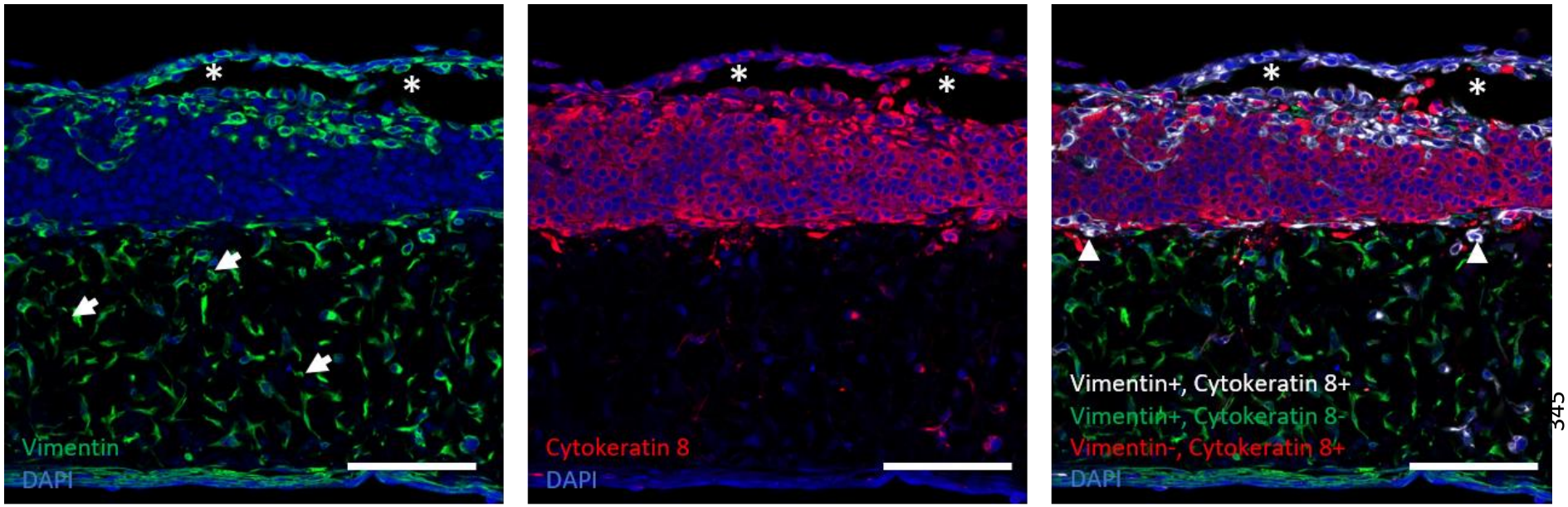

Figure 6.24: Organisation of different cell types in stirred HepG2, SK-Hep-1 and HDFn tri-cultures. Immunofluorescent staining was carried out for vimentin (left) and cytokeratin 8 (centre). Vimentin positive cells can be seen within the Alvetex membrane (white arrows) as well as on top of the HepG2 layer (white stars). With cytokeratin staining the layer of cells at the top of the culture can also be seen to stain positive, suggesting their identity as SK-Hep-1 cells. By masking the image and false-colouring cells expressing both vimentin and cytokeratin 8, the populations of SK-Hep-1 can be identified (right, white stars). These cells tend to form a thin layer on the surface of the HepG2 cells, however small numbers of cells also exist on the boundary between the HepG2 cells and the fibroblasts (white triangles). The models were formed with initial seeding quantities of 1 x 10^6 HDFn, 2 x 10^6 HepG2 and 1 x 10^5 SK-Hep-1. Scale bars are 100 µm.

Further analysis of these cultures was be carried out to see if there are any further improvements seen due to this culture method. Junctional proteins were the first area to be investigated (Figure 6.25). For adherens junctions N-cadherin was investigated and displays a similar morphology to that seen in previous monoculture and co-culture experiments. The SK-Hep-1 cells on the top of the HepG2 layer do not express N-cadherin, as expected for an endothelial cell.

Looking at tight junctions there is minimal difference between these tri-cultures and the co-cultures of HepG2 and HDFn investigated earlier in this chapter. Both claudin 1 and claudin 2 are expressed in high levels in this culture technique, as found with the previous models suggesting no detrimental effects to these tight junctions due to the co-culture method.

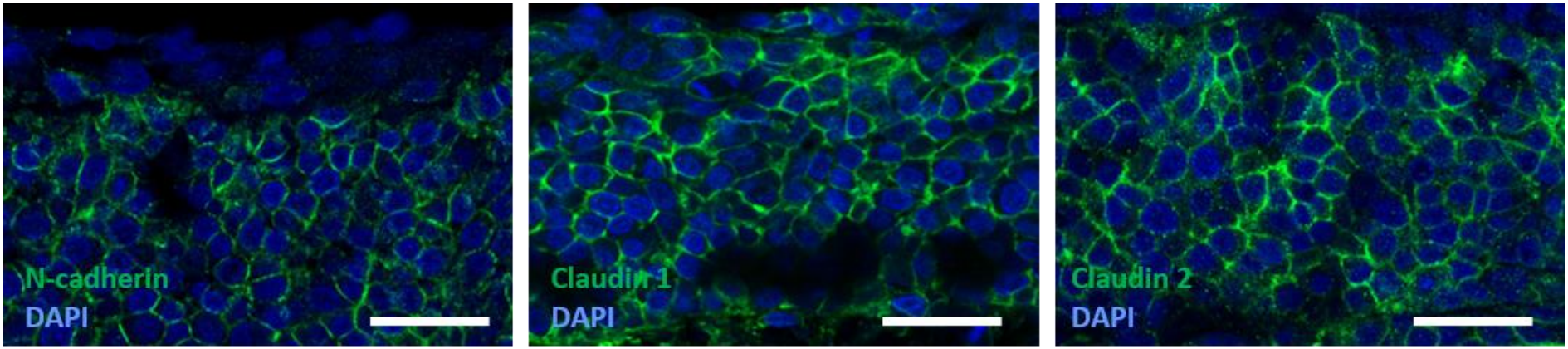

Figure 6.25: Expression of adherens and tight junctional proteins in stirred tri-culture. Immunofluorescent staining for N-Cadherin was used to investigate adherens junctions (left) whilst claudin 1 and claudin 2 were used to visualise tight junctions (centre and right). All the stains show high levels of membrane staining with minimal cytoplasmic staining, as has been seen for the HepG2 models in previous chapters. No expression around particular domains can be discerned, with almost complete staining of membranes instead visible. Scale bars are 50 µm.

MDR1 was used to investigate potential changes to transporter function in this model (Figure 6.26). This showed high levels of cytoplasmic staining in previous models with no apparent membrane localisation. In the tri-culture models MDR1 expression, while high, still appears to be distributed throughout the cytoplasm and not localised to any specific regions of the membranes as would be expected.

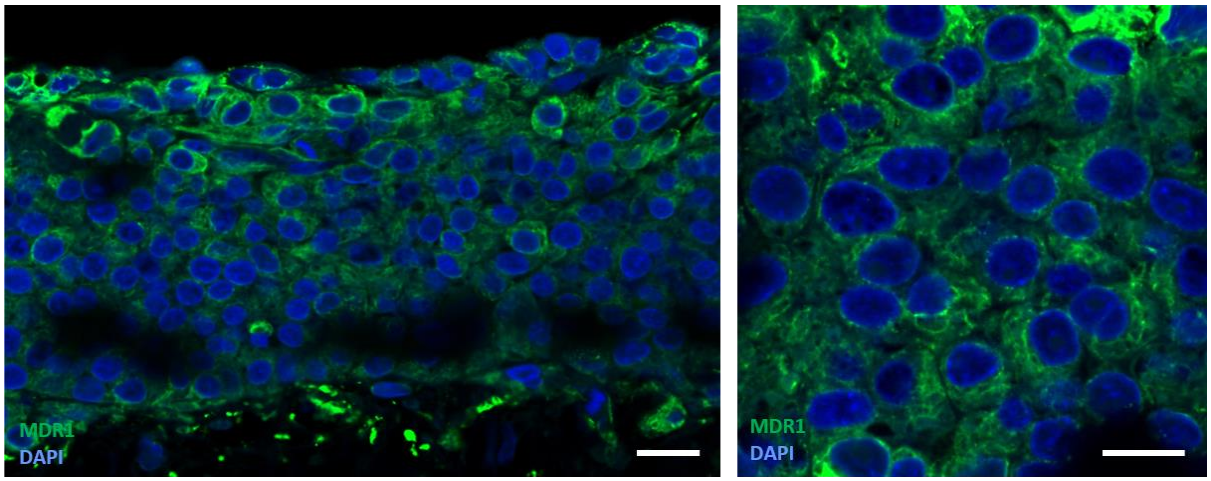

Figure 6.26: Expression of MDR1 in stirred tri-culture. MDR1 is an important apical efflux protein in hepatocytes. Immunofluorescent staining shows high levels of MDR1 through the HepG2 region of the models. High magnification images show that this staining is not localised to membranes, as would be expected for an apical transporter, instead being distributed throughout the cytoplasm with membrane staining almost absent. Scale bars are 50 µm (left) and 20 µm (right).

As a final measure of hepatocyte function the secretion of albumin and urea was quantified (Figure 6.27). Normalisation of these assays was carried out with the initial seeding ratio used to normalise this to hepatocytes, rather than to the total quantity of cells, as carried out for the HepG2 and HDFn models. Interestingly the level of secretion for both markers drops with the addition of SK-Hep-1 only in dynamic conditions, likely due to this outcompeting the HepG2 and reducing the proportion of these cells in the cultures. For the tri-culture with all three cell types present an increase is again seen, making both albumin and urea secretion comparable with or slightly higher than the stirred model with just HepG2 on HDFn. This suggests that further functional improvements to the hepatocytes metabolic function can be induced using endothelial cells, though a balance needs to be found to prevent the HepG2 being lost in culture.

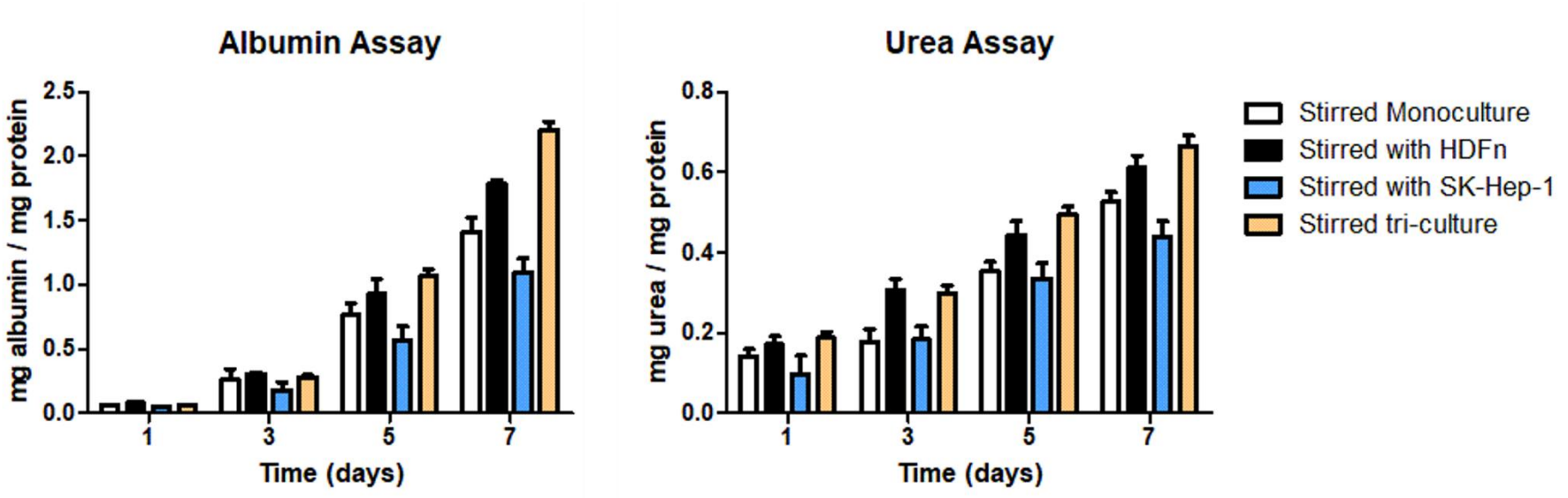

Figure 6.27: Metabolic assays for HepG2, HDFn and SK-Hep-1 co-culture models. The albumin assay and urea assay demonstrate the changes in metabolic function of the HepG2 cells when cultured with other cell types. Models with all three cell types secrete the highest levels of both albumin and urea, whilst cultures with simple HepG2 and SK-Hep-1 display a much-reduced secretion compared to other stirred conditions. For both models using SK-Hep-1 cells 1 x 10^5 SK-Hep-1 cells were seeded per model. Assays were carried out over 7 days with media samples taken every 2 days after the first day. n = 3, values are mean ± SEM.

6.5. Discussion

The ability to co-culture multiple cell types alongside HepG2 cells was explored in this chapter. A model consisting of both HepG2 and HDFn cells was initially created to explore the impacts of culturing fibroblasts with HepG2 in dynamic conditions. A second model was developed to incorporate SK-Hep-1 cells, mimicking the endothelial cell networks found in the liver *in vivo*. The overall aim of this chapter was to demonstrate that the basic fluid flow culture model developed and characterised in previous chapters possesses the potential to have further complexity added to push the boundaries of physiological relevance *in vitro*.

6.5.1. Fibroblasts can be successful incorporated into cultures of HepG2

The initial co-culture work investigated the use of a fibroblast embedded Alvetex® Scaffold. The use of this technique is routinely used in our research group for other tissue types and has demonstrated its ability to support a range of epithelial cell types (Roger *et al.*, 2019; Darling *et al.*, 2020). This also draws upon the large amount of literature which has demonstrated the effectiveness of fibroblast feeder layers to support viability, metabolic function and drug metabolizing enzyme expression of both primary hepatocytes (Bhatia *et al.*, 1999; Bhandari *et al.*, 2001; Cho *et al.*, 2008, 2010; Kim, Seo and Kwon, 2015; Mittal *et al.*, 2018) and cell lines such as HepG2 (Sakai *et al.*, 2013; H. W. H. J. Lee *et al.*, 2014; He *et al.*, 2018; Ware *et al.*, 2021). Human neonatal dermal fibroblasts (HDFn) were used for this project due to the success within the lab for using these in tissue models of other organs, as well as their known properties within Alvetex® (Roger *et al.*, 2019; Darling *et al.*, 2020). Whilst these are not liver-specific fibroblasts, of which only small populations exist, the typical fibroblasts used in literature are 3T3 embryonic fibroblasts, of mouse origin (Todaro and Green, 1963). It was therefore chosen to use cells of human origin to maximise physiological relevance of the model.

In our system an optimised fibroblast compartment was formed which prevented invasion into the Alvetex®, therefore producing a homogeneous surface cell layer, whilst minimising cell death due to hypoxia. With the maximum diffusion distance of oxygen in cell culture being around 200 µm there is a possibility that some cells would suffer from hypoxia and nutrient starvation if the fibroblast layers were too dense. This is demonstrated by the cell death which starts to become present in cultures utilising fibroblast compartments that are matured for 4 weeks.

Using fibroblast compartments which are matured for 3 weeks a dense and uniform HepG2 layer can be created. This layer is thicker than those seen in cultures of HepG2 on Strata in the bioreactor, likely in part to the reduced invasion. The layer is also more uniform than those seen in previous culture methods which improves the reproducibility of the model, a factor which is of high importance for 3D *in vitro* models (Hirsch and Schildknecht, 2019).

When cultured with fibroblasts HepG2 cells see minimal changes in protein expression for many of the proteins investigated. Beneficial effects seen from the addition of 3D culture techniques and fluid flow are maintained however no further changes can be readily identified. Cell health is maintained with high viability and low cell death, whilst hypoxic stress is also at the same low levels seen from bioreactor cultures of HepG2 on Alvetex® Strata. One study found increased levels of HIF-1α gene expression in hepatocyte-fibroblast co-cultures, however the absence seen here suggests that fluid flow is able to overcome this limitation due to the increased oxygen delivery (Sakai *et al.*, 2018).

Junctional proteins between HepG2 exhibit the same expression in co-culture with fibroblasts as they do when HepG2 are cultured alone with a high level of localisation to the cell membranes, though no detectable variations can be attributed to apical and basolateral polarisation. Transporter proteins see similar impacts with no change in expression to those already caused by fluid flow. Transporters which are not present in the previous culture techniques are still not induced through the addition of fibroblasts to the cultures. From literature it is difficult to ascertain whether any further changes would be expected above those found in 3D culture as many fibroblast-HepG2 cultures have optimisation of growth conditions reported with very limited evaluation of the HepG2 performance, often amounting simply to an albumin secretion assay (Ito *et al.*, 2007; Sakai *et al.*, 2013; H. W. Lee *et al.*, 2014; Kook *et al.*, 2017). One paper reported improved formation of bile canaliculi in rat primary hepatocytes when co-cultured with fibroblasts, however this was in comparison with 2D culture on a collagen coated dish, compared with the 3D control here which already displays improved bile canaliculi formation above that seen in 2D (Sakai *et al.*, 2018). Similarly, some benefits of co-culture with fibroblasts, such as increased MRP2 expression, have been seen to be reduced over a prolonged culture period of 10 days (Sakai *et al.*, 2018). Due to the 14 days in culture total for these hepatocytes it seems likely that this could be the case here.

Metabolic assays on the other hand show a more noticeable improvement from the addition of fibroblasts. Both albumin and urea see an upregulation compared with HepG2 in monoculture, a

result which has also been shown elsewhere when culturing primary hepatocytes with fibroblasts. This suggests that while it may be difficult to locate any major changes from protein localisation there are some functional changes being induced by the presence of the fibroblast compartment. No investigation was carried out in this work into the levels of CYP activity in the co-culture models. Several studies have found increases to CYP activity when cultured with fibroblasts, suggesting that this could be another beneficial effect of these cultures, however further investigation would be needed to confirm this in these models (Liu, Zhang, *et al.*, 2014).

6.5.2. Co-culture of Sk-Hep-1 with HepG2 leads to a reduction in HepG2 cells in culture

Addition of endothelial cells to the cultures would add further complexity to the models whilst also incorporating the second most common cell type in the liver after the hepatocytes. For this purpose, the SK-Hep-1 cell line was chosen due to its ease of culture, high proliferation, and ability to be continually passaged. This cell line also expresses properties seen in LSECs such as membrane fenestrations, making it desirable over endothelial cells from other tissue sources (Heffelfinger *et al.*, 1992; Tai *et al.*, 2018).

When cultured in static with HepG2, the endothelial cells appear to cause a reduction in the number of HepG2 present. This could be explained by the doubling time of SK-Hep-1 being roughly half that of HepG2, leading to it outcompeting HepG2 by the end of the culture period when similar quantities are seeded. Whilst this does not appear to have been reported elsewhere there are few studies into co-culture with HepG2 and SK-Hep-1 with most utilising cell lines such as human umbilical vein endothelial cells (HUVECs). One study reported reduced glucose consumption in a HepG2-HUVEC co-culture system, alongside increased albumin and urea secretion, suggesting that the HepG2 actually performed in a more energetically-efficient manner when co-cultured in this way, going against the hypothesis of the endothelial cells outcompeting the HepG2 (Guzzardi, Vozzi and Ahluwalia, 2009). However, HUVECs have a significantly longer doubling time of about 5 days, compared with around a day for SK-HEP-1, which could explain the differences in results seen between these two cell lines.

This issue is exacerbated in dynamic culture where SK-Hep-1 cells undergo huge proliferation to the detriment of the HepG2 which appear to be completely absent when using quantities of the two cells of the same order of magnitude. These results show that for successful culture of SK-Hep-1 cells with HepG2 the number of SK-Hep-1 to be seeded must be carefully selected and typically kept significantly lower than the quantity of HepG2. In literature relative seeding densities of around 1:5

or 1:10 are used when co-culturing HUVECs with HepG2 (Lasli *et al.*, 2019), whereas for SK-Hep-1 we found that 1:20 or 1:40 was more preferable, again suggesting that the impact may be due to the differences in growth rate of the two cell lines.

In both dynamic and static conditions there appears to be very limited mixing of the two cell types in a heterogeneous population, despite being seeded to the Alvetex® at the same time. Both cells display a morphology matching that seen when culture in Alvetex® individually, with HepG2 forming a surface layer and SK-Hep-1 invading far into the membrane. Whilst this limits the heterocellular interactions between the two cell types it allows for the formation of distinct regions of cells like the linings of sinusoids and the hepatic plate *in vivo.*

6.5.3. Addition of SK-Hep-1 to the HepG2 – fibroblast model can produce cultures with desirable culture morphology

Culture of SK-Hep-1 on Alvetex® showed the ability to almost eliminate the invasion of the endothelial cells completely into the membrane, despite their high invasiveness when seeded to Alvetex® on their own. This result matches those seen with HepG2 grown on fibroblasts showing the ability of the fibroblast compartment to support hepatic carcinoma cells. By utilising a fibroblast-seeded membrane to support the co-culture of HepG2 and SK-Hep-1 it is then possible to create a distinct hepatic region containing both hepatocytes and endothelial cells in a physiologically relevant manner.

When cultured in this way the SK-Hep-1 cells display a very different morphology when seeded at low levels relative to the HepG2. The two cell types separate out as shown previously however without the ability to enter the membrane below they instead form a layer on the upper surface of the HepG2 cells. This forms an environment for the hepatocytes which has similarities with the situation *in vivo* with the hepatocytes protected from the direct impacts of the fluid flow by the endothelial cell layer. This variability in migration was observed regardless of the order in which the cells were seeded, including if a period of several days was left between seedings. This result could be explained by previous research showing that endothelial cells migrate towards and align themselves with fluid flow (Simmers, Pryor and Blackman, 2007; Ostrowski *et al.*, 2014), with the fluid flow over the upper surface of the membrane providing the necessary mechanical cues in the case of this system.

6.5.4. HepG2 in triculture exhibit improved structure and function above and beyond the improvements documented previously

With a culture formed that has endothelial cells and hepatocytes growing in a physiologically relevant morphology it was hypothesised that this would significantly benefit their structure and function, with previous studies reporting enhanced hepatic-specific function and drug biotransformation capacity when using similar culture conditions (Ahmed *et al.*, 2017b; Wang *et al.*, 2018). For the proteins investigated a range of results could be seen with some proteins such as the adherens junction protein N-cadherin and the drug transporter proteins such as MDR1 displaying no change in morphology compared with the previously investigated culture techniques.

On the other hand, tight junction proteins such as claudin 1 and claudin 2 exhibit regions of parallel expression, suggesting the formation of tight junctions to the sides of bile canaliculi, as expected in mature hepatocyte cultures (Herrema *et al.*, 2006). This result suggests that bile canaliculi are becoming increasingly functionalised, something which is a requirement for studies to accurately model drug metabolism for drugs secreted in bile. Metabolic improvements can also be seen in the results from the albumin and urea assays carried out for these cultures. Similar experiments utilising tri-cultures of hepatocytes, LSECs and fibroblasts have reported similar results with increased liver specific function in this configuration (Liu, Li, *et al.*, 2014; Ware *et al.*, 2018).

6.6. Conclusions

Overall, the results in this chapter show the potential for this stirred liver model to be brought closer to physiological conditions through the addition of other cell types. Both the fibroblast cell line HDFn and the endothelial cell line SK-Hep-1 showed significant research value for use in co-cultures with HepG2.

The first objective of this chapter was to create a protocol to culture HepG2 cells on a 3D fibroblast support, like feeder layers used in many hepatocyte cultures. This was carried out through the optimisation of a protocol used previously in our group for the creation of fibroblast compartments for models of other tissues. Optimisation included minimising culture time whilst maximising cell viability and reproducibility and the ability for fibroblasts to support a healthy culture of HepG2 cells was demonstrated.

Following this a thorough characterisation of the protein expression in these cultures was performed with a range of proteins explored including those found in adherens junctions and tight junctions as well as domain-specific drug transporter proteins. Although the gross morphology of these models seemed promising no changes in the protein expression could be readily determined for any of the proteins investigated, though any beneficial changes induced previously using 3D culture and fluid flow were maintained in the co-culture model. Modest increases to albumin and urea secretion can be seen suggesting some areas of hepatocyte function benefit from this technique, which further analysis to look at a broader range of proteins may be able to elucidate.

Another objective of this chapter was to attempt to incorporate endothelial cells into the HepG2 model. With the endothelial cell line SK-Hep-1 chosen as a viable candidate for carrying this out analysis of the growth profile of these cells in Alvetex® was performed as well as looking at the impacts of coculturing these cells both with HepG2 and HDFn. In co-culture experiments with HepG2 the impact of SK-Hep-1 appeared to be detrimental to the HepG2 with reduced cell numbers seen in static conditions whilst in dynamic conditions the HepG2 cells were found to be virtually absent when SK-Hep-1 were also seeded in quantities of a similar order of magnitude. This highlights the issues of co-culturing cells with markedly different growth rates and is an area in which future work could look to instead use cell lines which have more closely matching doubling times.

Chapter 7: Maintaining the viability of precision-cut liver slices in the bioreactor system

Chapter 7: Maintaining the viability of precision-cut liver slices in the bioreactor system

7.1. Introduction

In vitro models are becoming increasingly effective at modelling the liver microenvironment but there are some applications that are still a long way from being accurately modelled. Diseases in the body are highly complex and involve interactions between numerous cell types as well as soluble factors, ECM and mechanical cues which make them more difficult to fully recreate.

Liver fibrosis is one such disease which is highly prevalent, as discussed in chapter 1. To accurately model liver fibrosis precision-cut liver tissue slices (PCLS) are becoming increasingly common as technology is developed to improve their viability *ex vivo* and therefore enhance their usefulness for the study of chronic conditions.

In this chapter the use of precision-cut tissue slices will be discussed with a specific focus on precision-cut liver slices. Methods to culture precision-cut liver slices and previous attempts to model fibrosis using this method will then be discussed alongside the pathology of liver fibrosis. Work will then be carried out to investigate the potential for culture of rat PCLS in the bioreactor developed in this work. Different parameters of slices will be explored as well as the properties of the slices cultured in this system. Further development will also be carried out to create an oxygenation system to work alongside the bioreactor.

7.1.1. *Ex vivo* culture of precision-cut tissue slices

Precision-cut tissue slices have been useful for a wide range of research and have been utilised to model organs such as brain (Mewes, Franke and Singer, 2012; Dionne and Tyler, 2013; Croft *et al.*, 2019; Schwarz *et al.*, 2019), lung (Akram *et al.*, 2019; Liu *et al.*, 2019; Bailey *et al.*, 2020; Bryson *et al.*, 2020), intestine (Groothuis and de Graaf, 2013; Punyadarsaniya *et al.*, 2015; Li, De Graaf and Groothuis, 2016), liver (R. J. Price *et al.*, 1998; Lerche-langrand and Toutain, 2000; Olinga and Schuppan, 2013; Inge M Westra *et al.*, 2014) and kidney (Poosti *et al.*, 2015; Genovese *et al.*, 2016; Stribos *et al.*, 2017). One of the key features of these slices is the intact cellular microenvironment, with no disruption due to trypsinisation or culture of cells in 2D flasks prior to creating models. This makes them immensely useful as a system for the modelling of disease as a much wider range of responses can be investigated than are possible with a typical *in vitro* model. These are also preferable to animal models due to the ability to harvest multiple slices from the same animal, in some cases several hundred depending on the species and the organ (Olinga and Schuppan, 2013), therefore leading to a far more efficient use of animals.

One of the most widely studied aspects of precision-cut tissue slices is for modelling of fibrosis, something which can be difficult using *in vitro* models due to the large numbers of different cells which are often involved. This can be carried out for a variety of organs with reasonable success.

Another use for tissue slices is the study of immune responses. The presence of many of the *in vivo* immune cells in these slices leads to a more physiologically relevant response than seen *in vitro.* Studies of precision-cut lung slices have shown a high level of cytokine induction when stimulated with lipopolysaccharide as well as being permissive to viruses (Rosales Gerpe *et al.*, 2018; Bryson *et al.*, 2020), with one study creating a model to investigate coinfection of bacteria and viruses (Meng *et al.*, 2015).

Precision-cut brain slices are a good example of an *ex vivo* platform for modelling biological and developmental pathways. These have been used to investigate properties such as neural signalling, alongside the impacts of drugs and viruses on these processes (Dionne and Tyler, 2013; Loryan, Fridén and Hammarlund-Udenaes, 2013; Schwarz *et al.*, 2019). Modelling of neurodegenerative diseases such as Alzheimer's disease has also been shown to be possible using brain slices (Cho, Wood and Bowlby, 2007; Croft *et al.*, 2019).

In this work precision-cut liver slices will be focused on due to the promising results using *in vitro* liver models in the bioreactor in previous sections. As PCLS have high oxygen and nutrient requirements it is hypothesised that they may benefit greatly from the addition of fluid flow.

7.1.2. Use of precision-cut liver slices for the modelling of liver fibrosis

The culture of liver slices for *in vitro* studies was first published by Otto Warburg in 1923 as part of research work with carcinoma tissue (Warburg and Minami, 1923). Whilst these have been widely used for biochemical studies the difficulty in cutting consistent slices within a suitable time period for maintaining viability has typically limited them to short term studies of less than 6 hours due to loss of CYP function over longer timescales (Lerche-langrand and Toutain, 2000). The development of the Krumdieck slicer in 1980 allowed for the generation of highly consistent tissue slices ranging in thickness from 100 um to 1 mm, termed precision-cut tissue slices (Krumdieck, dos Santos and Ho, 1980). This has seen the use of liver slices increase with further developments such as oxygenation systems and more effective culture media allowing tissue slices to be cultured for longer time periods. With these developments the use of precision-cut liver slices for modelling fibrosis has become more feasible and can be a valuable tool for the study of liver disease (van de Bovenkamp *et al.*, 2005, 2006).

Tissue slices have several advantages over other *in vitro* techniques due to their relatively undisturbed microenvironment. The absence of proteases such as trypsin or collagenase in the generation of the tissue slices ensures that the ECM is present in the same conformation as found *in vivo* and extracellular proteins such as signal receptors are present and have not been cleaved off leaving the cells much more responsive to microenvironment cues (Sewald and Braun, 2013). A great number of different cell types are present in these tissue slices from the parenchymal hepatocytes and cholangiocytes to endothelial cells, stellate cells and macrophages such as Kupffer cells (van de Bovenkamp *et al.*, 2008). This heterocellularity is greater and more structured than is currently achievable with *in vitro* techniques which makes tissue slices an invaluable tool for studying pathways on the entire liver microenvironment rather than simply on individual cells.

Figure 7.1 shows two of the main methods used to generate PCLS. These share many aspects in common with the key difference being the cutting method used. Cutting with a Krumdieck slicer is simple and quick due to the high sectioning speed and limited processing required before cutting (de Graaf *et al.*, 2010). Meanwhile vibratome sectioning is more labour and time intensive, with the tissue being embedded into low gelling temperature agarose prior to cutting and the generally lower cut speed utilised by vibratomes (Iulianella, 2017). Vibratome sectioning has been shown to lead to more reproducible slice thicknesses compared with the Krumdieck slicer (Zimmermann *et al.*, 2009) so each method has its own advantages and the choice tends to depend on to which one a particular lab has access. A third option is the use of a Brendel-Vitron tissue slicer which functions in a similar manner to a Krumdieck slicer but has a higher level of complexity, with a rotating cutting blade and continuous oxygenation (Parrish, Gandolfi and Brendel, 1995). This apparatus tends to be less commonly found in literature compared with the Krumdieck slicer however it has been found that there is minimal difference between slices produced with these two systems (R J Price *et al.*, 1998; R. J. Price *et al.*, 1998; Lerche-langrand and Toutain, 2000).

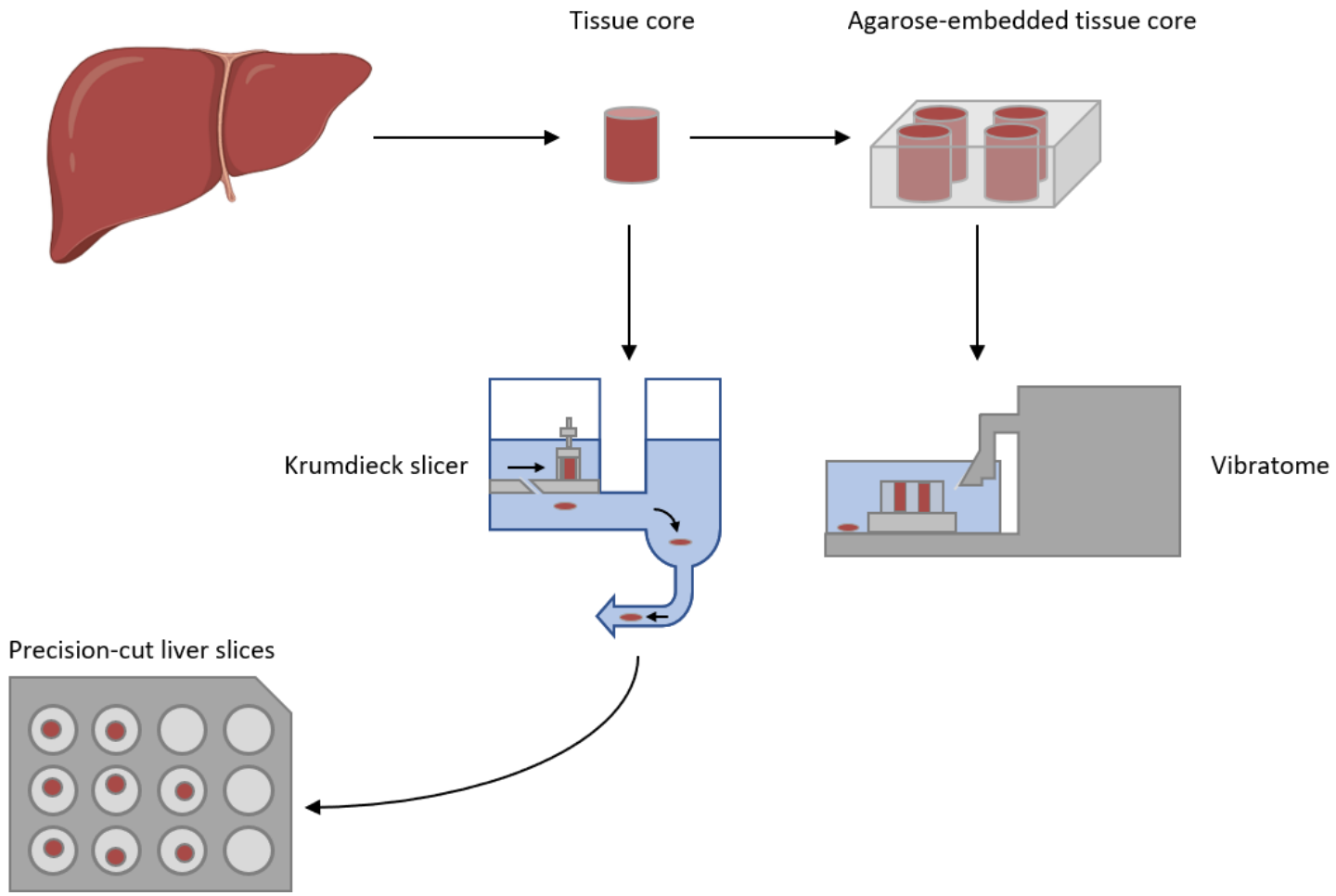

Figure 7.1: Preparation of precision-cut liver slices. The two main methods for preparation of PCLS are shown: using a Krumdieck slicer and a vibratome. Vibratome sectioning involves the extra step of embedding the tissue core in agarose prior to sectioning to secure the tissue whilst the Krumdieck slicer utilises a mechanical holder for the tissue core. The Krumdieck slicer offers a faster slicing process however the embedding of multiple cores in a block of agarose can increase the throughput of the vibratome method.

7.1.2.1. Factors influencing long-term viability of PCLS

Numerous methods have been developed to prolong the function lifespan of PCLS in culture and a large number of variables need to be controlled to achieve successful culture, as summarised in Table 1. These initially used a hyperoxic environment, typically from 70-95%, to meet the high oxygen needs of the tissue and overcome the limited oxygen transfer in cell culture medium (Drobner, Glöckner and Müller, 2000). This typically involves the use of oxygenated incubators (Peter Olinga *et al.*, 1997) or incubator subchambers (de Graaf *et al.*, 2010; Palma, Doornebal and Chokshi, 2019) leading to large volumes of oxygen required to maintain hyperoxia over prolonged culture periods. Other techniques have used individual oxygenation for each sample which reduces the oxygen turnover required due to the reduced volume of gas present however this adds a further level of complexity to such systems (P. Olinga *et al.*, 1997; Hadi *et al.*, 2012).

Table 7.1: Factors influencing health of precision-cut liver slices. A series of values can have impacts on the growth and viability of PCLS, often through limiting nutrient transfer or leading to a high ratio of damaged cells compared to healthy cells. Many of these values have previously been investigated and values found from literature are presented here.

Parameter	Typical Values	References
Slice thickness	200-300 µm	Price et al., 1998
Slice diameter	6-8 mm	Fisher et al., 1995
Ischemia time	<30 minutes warm, up to 18 hours cold	He et al., 2004 Olinga et a., 1998
Storage medium	Oxygenated Krebs buffer	Fisher et al., 1995
Oxygen levels	95% Oxygen or air-liquid interface	Drober, Glöckner and Müller, 1999

More recent systems have attempted to move away from using an oxygenated environment, instead using alternative methods to provide the necessary oxygen supply to the tissue. Addition of artificial oxygen carriers to the culture medium is one method which has been used to increase the oxygen availability in many cell culture environments (Lowe, 2002). Specifically to the liver, acellular haemoglobin-based oxygen carriers have previously been shown to be useful as a blood substitute for the perfusion of whole isolated livers (Laing *et al.*, 2017) while Koch et al. found that the addition of perfluorodecalin to cell culture media improved the ATP levels in the liver tissue slices up to 72 hours (Koch *et al.*, 2014).

A study which cultured the slices at the air-liquid interface found genes related to the immune response remained stable over 15 days however these tissues also had high levels of spontaneous apoptosis and fibrogenesis (Wu *et al.*, 2018). Another method using a mechanical rocker to induce media flow in a modified well plate containing Transwell inserts showed that tissue health could be maintained for up to 6 days and these tissues displayed an appropriate response to both profibrotic and antifibrotic molecules (Paish *et al.*, 2019a). These results suggest that there is potential to culture PCLS in a standard cell culture incubator without the need for additional oxygenation, significantly reducing the complexity of the system, though direct contact with air does not resemble the *in vivo* conditions of the liver cells.

As well as achieving high levels of oxygen delivery to the PCLS there are many other factors which influence the outcome of the culture. Many of these are introduced during the processing of the slices. Upon death the liver must be removed from the body and put on ice as fast as possible to minimise damage due to warm ischaemia. This has been found to have a detrimental impact on tissue health during transplantation if the warm ischaemia time is greater than 30 mins (He *et al.*, 2004). Once on ice the tissue can be stored for longer periods of up to a few days, with one study finding no significant difference in metabolic rates between fresh tissue and after 18 hours of cold ischaemia (Olinga *et al.*, 1998). Pre-incubation of slices for one hour before use is also a common technique to increase the metabolism and ATP levels of the tissue prior to long term culture. The use of relevant buffer and media formulations, typically Krebs-Henseleit buffer and William's Medium E, are required for viable tissue slices over more than one day (Fisher, Hasal, *et al.*, 1995; Starokozhko *et al.*, 2015), though more complex buffers such as University of Wisconsin organ preservation solution can also be used successfully (de Graaf *et al.*, 2010; Palma, Doornebal and Chokshi, 2019).

Factors such as slice thickness have a major effect on the culture outcomes with slices around 200 – 250 µm frequently used, though slices as thin as 100 µm have been used successfully (De Graaf *et al.*, 2006). This is due to thinner slices suffering more from the effects of damaged cells around the edges whilst thicker slices experience necrotic cores due to lack of diffusion through the thick tissue (Fisher *et al.*, 2001). Slice diameter has also been suggested to affect the viability of PCLS with one paper suggesting 8 mm slices have greater viability than 6 mm slices for rat and mouse liver tissue, likely also due to the greater proportion of intact cells to damaged exterior cells (Fisher, Hasal, *et al.*, 1995).

7.1.3. Systems used for the culture of precision-cut liver slices

There are several methods for long-term culture of PCLS which have been used routinely as well as some recently developed methods to look at overcoming the need for oxygenation, as mentioned in the previous section. The simplest and most widely used methods involve culturing the slices in a standard multi-well plate (Lagaye *et al.*, 2012). Many systems utilising PCLS place them into culture for only an hour to stabilise the slice before carrying out experiments lasting only 24 to 48 hours (van de Bovenkamp *et al.*, 2008). Due to this a very simple system is required, allowing this use of multi-well plates alongside oxygenation with a 95 % oxygen supply, though values as low as 40 % have shown some success (Drobner, Glöckner and Müller, 2000). Simple forms of media flow are utilised alongside this, typically using an orbital shaker which can allow culture of viable slices for up to one week (Inge M Westra *et al.*, 2014; Starokozhko, Vatakuti, *et al.*, 2017; Ximénez *et al.*, 2017; Bigaeva *et al.*, 2019; Palma, Doornebal and Chokshi, 2019).

Alternatively, shaken flasks have been used for culture of PCLS, though these have become less common over time (de Kanter and Koster, 1995; Toutain *et al.*, 1998). These use oxygenated flasks which can be shaken in a water bath, keeping tissue slices in suspension within the media to provide high levels of nutrients. Such systems have been shown to maintain viability over 24 hours of culture, though limited research has looked at longer culture periods (Peter Olinga *et al.*, 1997; Neupert, Glockner and Muller, 1998; Lerche-langrand and Toutain, 2000; Granitzny *et al.*, 2017).

Alternative techniques have tried to remove the need for external oxygenation systems. This has been carried out through culturing the slice at, or close to, the air-liquid interface, therefore allowing maximum oxygen to transfer directly from the air, as mentioned in the previous section. Rocker systems for this purpose use a rocking motion to pass media over the slice, maintaining the nutrient transfer and preventing the slice from drying out, whilst also allowing direct contact with the air (Lerche-langrand and Toutain, 2000; Wu *et al.*, 2018). A tissue holder, such as a Netwell insert, is used to elevate the slice so nutrient transfer from the medium on the lower surface of the slice can be achieved (Leeman, van de Gevel and Rutten, 1995; Peter Olinga *et al.*, 1997). A more recent form of this system has used a modified 12-well plate with pairs of interconnected wells, showing this to maintain slice viability for up to 14 days (Paish *et al.*, 2019b; Barcena-Varela *et al.*, 2020).

The roller system is another technique for maintaining close contact between the slice and the air (Smith *et al.*, 1985, 1987; Peter Olinga *et al.*, 1997; Vickers, Ulyanov and Fisher, 2018). These use

tissue rollers, which are placed inside a roller flask and rotated with the slice supported at the air-liquid interface by the tissue roller and with access by medium to the underside of the slice (Fisher, Shaughnessy, *et al.*, 1995; R. J. Price *et al.*, 1998). With these systems enhanced viability was seen compared with control slices cultured in a multi-well plate with an oxygenated atmosphere. Oxygenation of the roller systems also proved to improve viability above the levels reached with the roller system alone in a standard air environment (Fisher, Shaughnessy, *et al.*, 1995).

These systems have all shown potential for culturing PCLS *ex vivo* however long term cultures of over one week are rare, with those that do often still exhibiting loss of function (Wu *et al.*, 2018; Paish *et al.*, 2019b). There is therefore still a need for an effective system which can maintain slice viability and function over prolonged periods.

7.1.4. The pathology of Liver Fibrosis

To create an effective model of liver fibrosis the various pathways of fibrosis must first be explored to gain an understanding of the complexity of this disease. The most basic description of liver fibrosis is the excessive build-up of extracellular matrix proteins, in particular collagen 4 during the early stages and collagens 1 and 3 at later stages (Villesen *et al.*, 2020), mediated by cells such as activated hepatic stellate cells and Kupffer cells, as discussed in chapter 1.

This perspective of fibrosis is overly simplified as a vast array of processes contribute to the onset and development of liver fibrosis leading to a range of potential outcomes (Roehlen, Crouchet and Baumen, 2020). To further add to this complexity fibrosis is a dynamic process which can be reversed before reaching cirrhotic levels (Zhou, Zhang and Qiao, 2014; Cordero-Espinoza and Huch, 2018). Figure 7.2 shows how the severity of fibrosis changes depending on the timing of the liver insults with multiple insults over a short space of time causing a greater degree of damage than the same number spread out, allowing the liver to undergo regeneration between insults. This can make predicting of the impact of liver challenges difficult due to the history of liver being so variable between individuals.

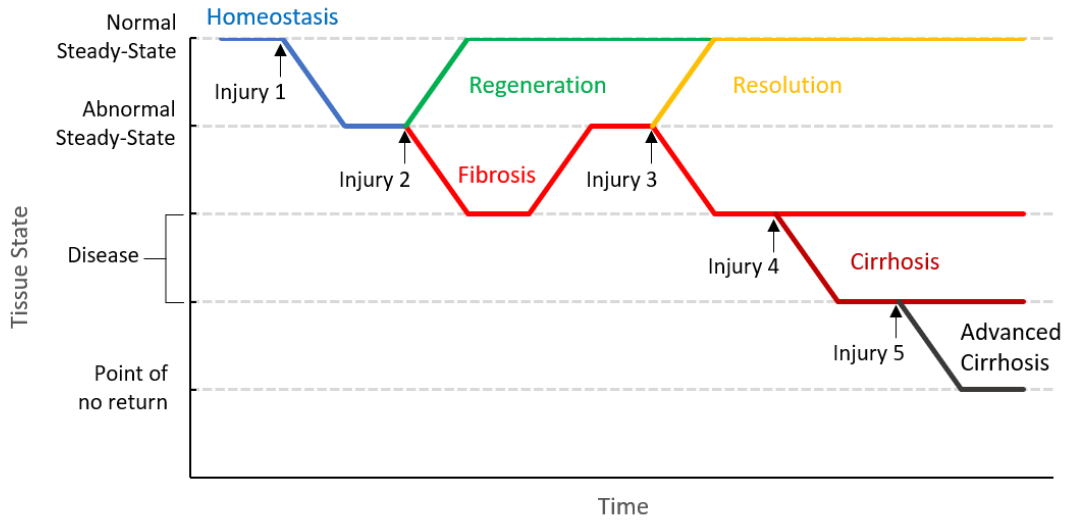

Figure 7.2: Variation of fibrosis severity with injury timing. The regenerative potential of the liver allows it to recover from injury. Repeated injuries can push it further from the normal state until a disease state is reached. If injury continues without time for the liver to recover, then eventually the point of no return is reached with advanced cirrhosis. Adapted from Cordero-Espinoza and Huch, 2018.

The pathology of fibrosis also varies depending on the cause, with different areas of the liver lobule affected as shown by Figure 7.3 (Villesen *et al.*, 2020). Cholestatic fibrosis, as caused by blockages in the bile ducts, leads to activation of fibroblasts located around the portal region leading to deposition of fibrillar collagen through the portal region (Penz-Österreicher, Österreicher and Trauner, 2011). Metabolic fibrosis such as that caused by alcoholic liver disease leads to the formation of collagen networks in pericentral and perisinusoidal regions whilst viral fibrosis exhibits collagen networks around periportal hepatocytes couple with fibrillar collagen deposition in the portal region (Villesen *et al.*, 2020).

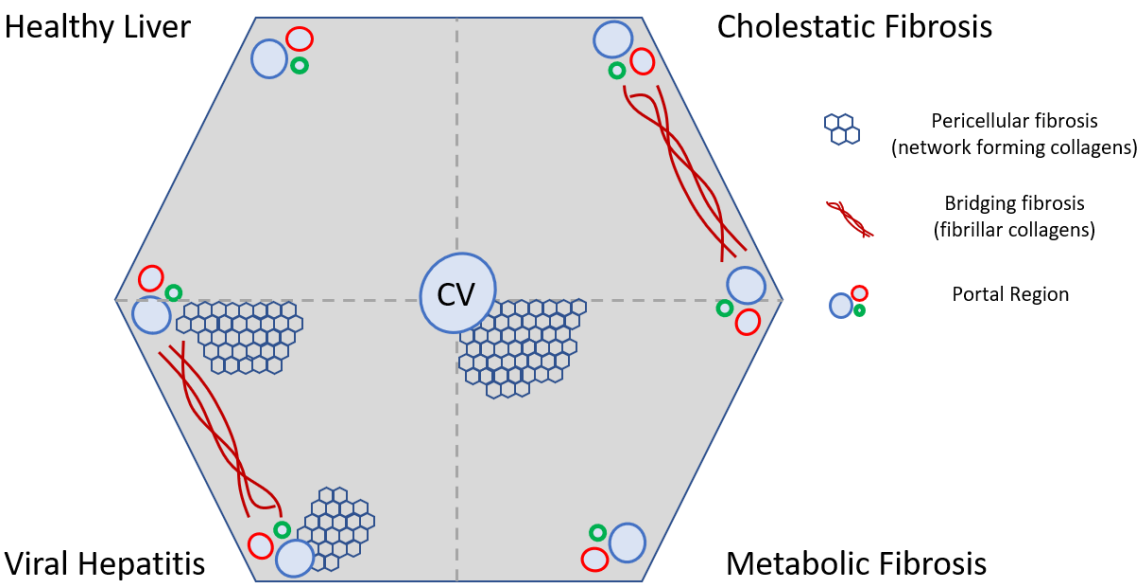

Figure 7.3: Different fibrosis pathologies from the three main insults. Fibrosis pathology varies depending on the cause. Cholestatic fibrosis, based around the bile ducts, leads to a build-up of fibrillar collagen in the portal region whilst metabolic fibrosis leads to pericellular fibrosis within the hepatic plates. Viral hepatitis leads to a combination of both. This deposition is typically mediated by the stellate cell or fibroblast populations in the damaged region. Adapted from Villesen *et al.*, 2020.

Despite the different pathologies seen with different causes of fibrosis the underlying mechanisms are very similar. During liver injury, the quiescent hepatic stellate cells in the space of Disse are activated and become myofibroblast-like. These then migrate towards the site of injury and deposit ECM. As Figure 7.3 shows this activation can be induced by a range of molecules depending on the cause of the inflammation. The trigger for induction of fibrosis comes from different cell types depending on the injury. Viral infection such as hepatitis B or C causes the hepatocytes to release inflammatory factors whilst LPS from bacterial infection activates Kupffer cells and a build-up of bile acids such as in cholestasis causes induction through biliary cells (Bataller and Brenner, 2005). Activation of HSCs causes them to produce factors such as TGF-β1 and endothelin-1 which create a feedback loop, maintaining their activated phenotype.

Hepatic stellate cells are not the only source of activated myofibroblasts in liver fibrosis as myofibroblasts can also be generated from other cell sources. During cholestatic liver injury the fibroblasts located around the bile ducts in the portal region activate to produce ECM leading to the periportal ECM deposition characteristic of this form of liver fibrosis (Dranoff and Wells, 2010; Karin *et al.*, 2016). Circulating hematopoietic stem cells of bone marrow origin have also been shown to respond to growth factors and migrate into the liver tissue in fibrosis.

Figure 7.4 shows what happens in the fibrogenesis and resolution phases of fibrosis (Bataller and Brenner, 2005)b. With repeated injuries the regenerative process eventually fails leading to overproduction of ECM, blocking the fenestrations in sinusoidal endothelial cells and therefore limiting bidirectional metabolic exchange between portal blood and hepatocytes (Hernandez-gea and Friedman, 2011). Over time the injured hepatocytes undergo apoptosis and are replaced with ECM, further promoting the fibrotic phenotype. While collagens are the most studied there is an increase in a wide range of ECM proteins in liver fibrosis such as fibronectin, elastin, laminin, undulin and hyaluronan (dos Santos *et al.*, 2005; Matsuda and Seki, 2020). This is caused by both upregulation of ECM production in the cells as well as increased levels of TIMPs, the inhibitors of the ECM-degrading MMPs (Hemmann *et al.*, 2007).

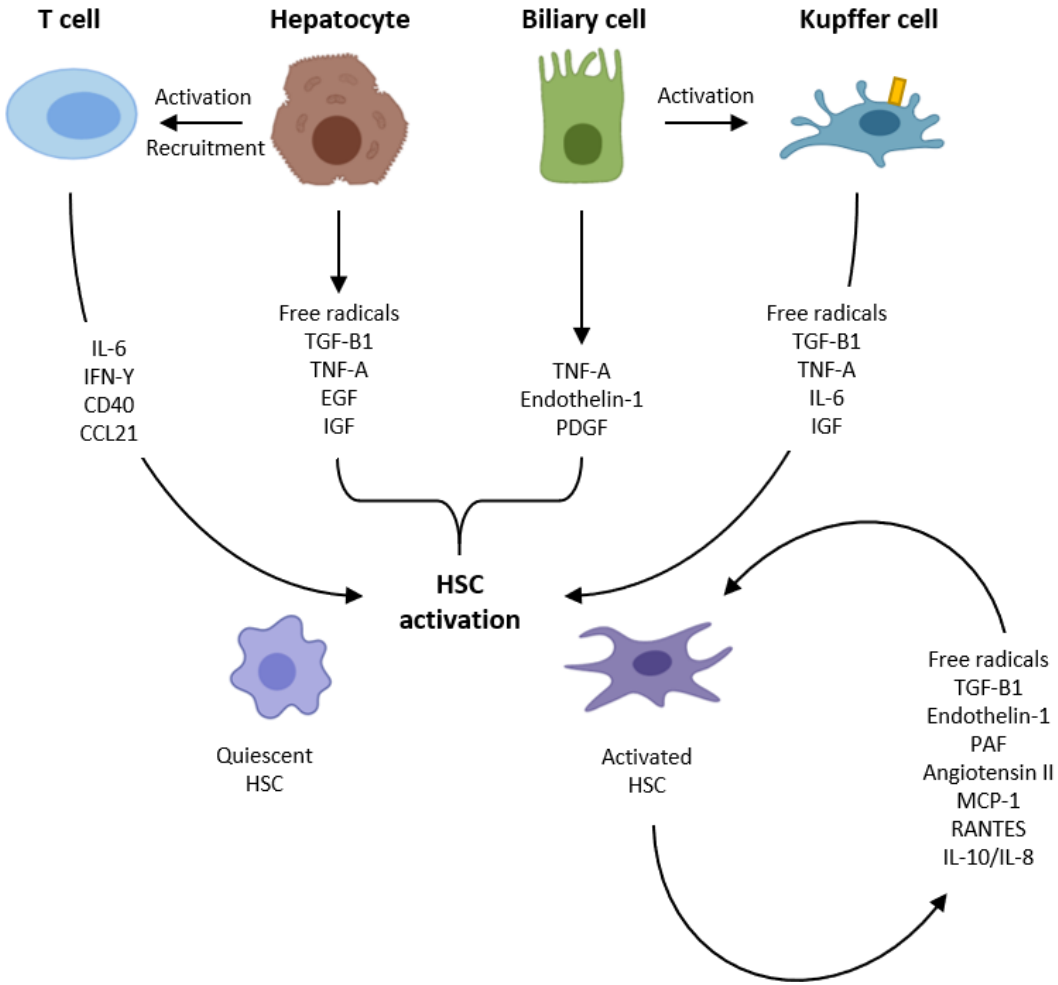

Figure 7.4: Mechanisms of the inflammatory phase of liver fibrosis. After liver injury factors released by hepatocytes or biliary cells activate the macrophages and hepatic stellate cells. Activated hepatic stellate cells express a myofibroblast morphology release further proinflammatory factors to maintain the inflammatory state. Adapted from Bataller and Brenner, 2005.

If the liver injury is stopped then the liver can undergo regeneration and eventually return to the healthy phenotype, assuming the damage is not too severe (Figure 7.5). Increases in the levels of MMPs due to inhibition of TIMPs allows the ECM to be degraded and begin the process of removing the fibrotic scarring (Duarte *et al.*, 2015). Apoptosis of the activated HSCs aids this process by reducing collagen production and levels of TIMP-1 and TIMP-3 being produced. At the end stage of fibrosis resolution the healthy hepatocytes can replicate and reconstruct the damaged areas of tissue (Ramachandran and Iredale, 2012).

This plasticity of many cells in the liver is one reason why *in vitro* models struggle to recapitulate the development of fibrosis with their limited subsets of liver cells and improper architecture and patterning. While research is ongoing to create more physiologically relevant *in vitro* models for fibrosis modelling, *ex vivo* tissue slices remain a technique with more potential due to the presence of the full array of hepatic cells coupled with undisturbed tissue architecture.

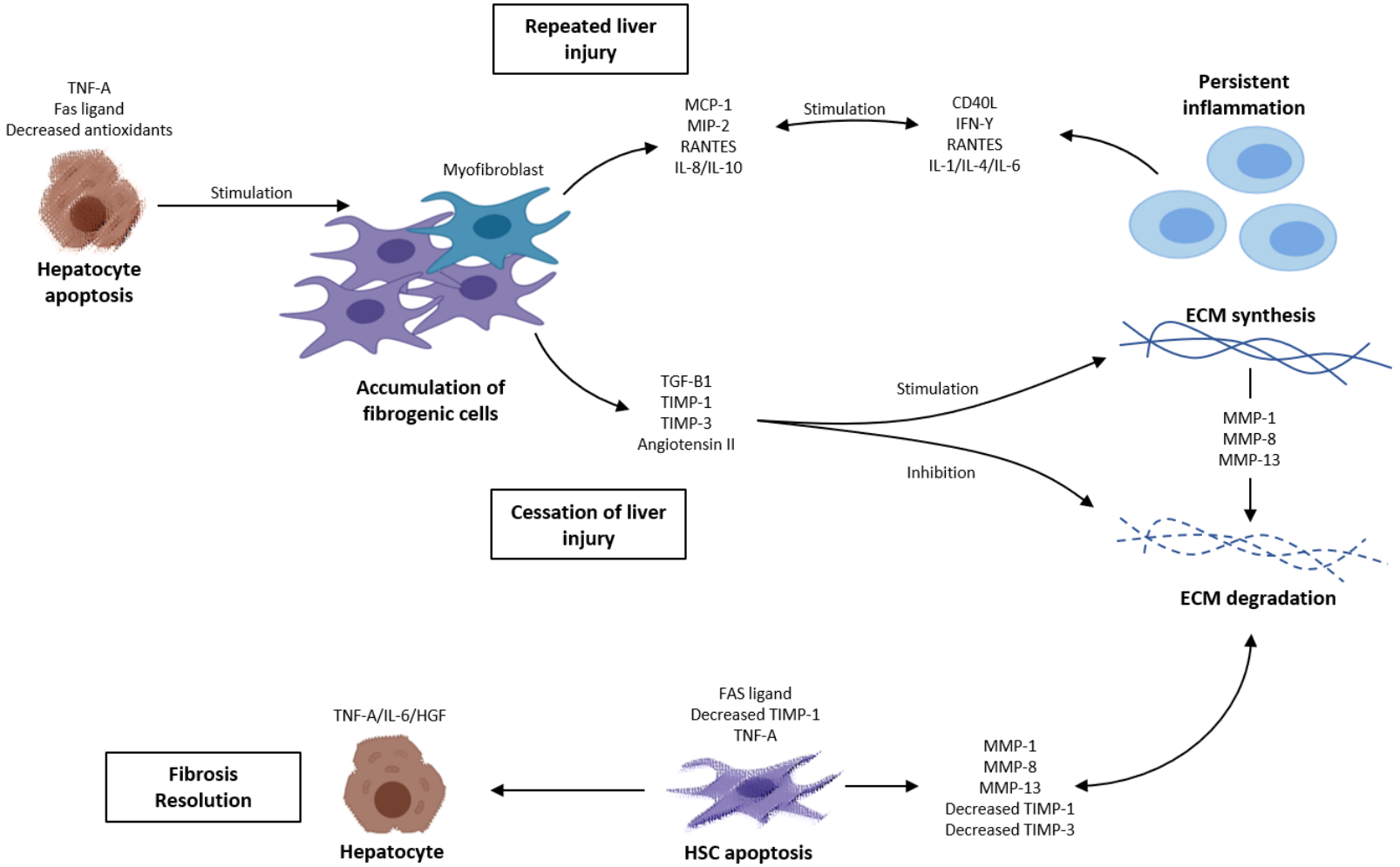

Figure 7.5: Mechanisms of fibrogenesis and resolution phases of liver fibrosis. Liver injury causes release of proinflammatory stimuli which lead to the activation of hepatic stellate cells. Activated stellate cells promote ECM synthesis and release factors which maintain the inflammatory state. At the end of injury inhibitory factors break down ECM, lead to apoptosis of stellate cells and resolution of injury. Adapted from Bataller and Brenner, 2005.

7.1.5. Methods to study liver fibrosis in PCLS

The intact cellular microenvironment present in PCLS makes them excellent potential candidates for models of liver fibrosis and many studies have investigated this application (Westra *et al.*, 2013; Inge M. Westra *et al.*, 2014; Paish *et al.*, 2019a).

Due to the key role of HSCs in liver fibrosis, these tend to be the primary target for studies of fibrotic induction and activation of HSCs is often used as a marker for fibrosis onset, though methods used to identify activated HSCs typically also detect myofibroblasts from other activated cell populations such as portal fibroblasts (Guyot *et al.*, 2006; Bovenkamp *et al.*, 2007). In PCLS fibrosis occurs spontaneously due to the reduced viability of the tissue slices and issues such as necrotic tissue cores leading to release of inflammatory factors (Vickers *et al.*, 2004). Induction of fibrosis, via the activation of HSCs, is often also carried out by treatment of PCLS with compounds such as carbon tetrachloride (van de Bovenkamp *et al.*, 2005, 2006), ethanol (Schaffert *et al.*, 2010; Duryee *et al.*, 2014) and cocktails of proinflammatory cytokines like TGF-β and platelet-derived growth factor (PDGF) (Sadasivan *et al.*, 2015; Paish *et al.*, 2019a).

Measures such as α-SMA expression and collagen deposition are used as simple methods to examine onset of fibrosis in these models and test anti-fibrotic compounds. Through measurement of these the efficacy of different antifibrotic drugs can be investigated (Elferink *et al.*, 2011). Studies have looked at different TGF-β and PDGF inhibitors in PCLS and successfully shown that these can be effective to reduction of fibrosis, though some markers can give varying results. For example collagen 1 protein expression was found to be decreased with addition of antifibrotic compounds whilst hydroxyproline content and deposited collagen were unchanged (Inge M. Westra *et al.*, 2014). On the other hand a modest decrease was seen in *Pcol1A1* expression compared with an almost 50 % decrease in collagen 1 protein expression when treated with the TGF-β inhibitors perindopril and tetrandrine (Inge M Westra *et al.*, 2014).

One of the major limitations of these studies in general is the short time points used for fibrosis measurements. Typically, studies culture the slices for up to 48 hours due to limitations with viability and spontaneous fibrosis at later timepoints, limiting the effectiveness for the study of chronic fibrosis (Inge M. Westra *et al.*, 2014; Westra *et al.*, 2016; Luangmonkong *et al.*, 2017). Whilst more recent studies have used later time points, culture of slices for more than 7 days without significant loss of function or viability has yet to be demonstrated (Wu *et al.*, 2018; Paish *et al.*, 2019a).

7.1.6. Conclusion

Precision-cut liver slices represent a promising avenue of research for the modelling of diseases and toxicology. The intact *in vivo* structure of the tissue is a property that has yet to be properly reconstructed *in vitro* and therefore the successful culture of PCLS would be very valuable for research both in academia and industry. Whilst many systems are used for the culture of *ex vivo* PCLS, these struggle to maintain viable and functional tissue for periods of over one week. Due to the improved oxygenation properties exhibited by our bioreactor system we hypothesise that application of this for the culture of rat PCLS could lead to improved maintenance of tissue over time.

7.2. Hypothesis, Aims and Objectives

7.2.1. Hypothesis

The high oxygen and nutrient requirements of *ex vivo* PCLS limits their viability and prevents long-term maintenance of these tissues. We hypothesise that the enhanced oxygen transport in our bioreactor system, due to convective mixing of medium, will be able to overcome this to some extent and therefore allow us to maintain the viability of PCLS over prolonged periods. Further to this, the addition of an oxygenation system to our bioreactor could allow even further performance benefits, potentially creating a model which can be of use for chronic studies of liver disease.

7.2.2. Aims

Precision-cut liver slices offer an alternative platform to *in vitro* cell-based cultured techniques for modelling of disease. The presence of all the cells found *in vivo* alongside an undisrupted tissue morphology means that this system bears far more physiological relevance to *in vivo* conditions. It also allows complex pathways and cell behaviours to be examined, with the interactions of different cells in fibrosis pathways one potential application of this system.

In this chapter the use of the bioreactor system for the maintenance of rat precision-cut liver slices will be investigated. The slices typically suffer from very limited viability in culture, no more than a couple of weeks at most, therefore making them mainly useful for acute studies. By increasing the functional lifespan of these slices their utility for modelling chronic disease will be significantly enhanced. Alongside culture in the bioreactor system, a novel oxygenation system will also be developed to allow a high-oxygen environment for tissue growth, as is often carried out in literature.

7.2.3. Objectives

1. Optimise a protocol for viable culture of rat PCLS in the novel bioreactor system.
2. Investigate the growth characteristics of the tissue slices and their response to profibrotic compounds.
3. Develop an oxygenation system to complement the bioreactor system which can aid with the maintenance of PCLS.

7.3. Results

7.3.1. Optimising the growth of rat PCLS on Alvetex membranes

To produce an effective PCLS model the first step was to ensure that acceptable PCLS could be developed. This requires the PCLS to conform closely to the predicted measurements as well as exhibiting a high level of reproducibility. Figure 7.6 shows the properties of the slices developed using a Leica VT1000 S vibratome (Leica) and a sapphire cutting blade (Agar Scientific, Stansted, UK). The slice area is almost exactly as expected if the slice were perfectly circular, with very minimal variation (Figure 7.6A). This is supported by the circularity also being very close to perfect, suggesting that the slices are not getting severely damaged during the processing and slicing procedure. The thickness is noticeable less than the desired value of 250 µm, but not problematically so and this reduction is seen in all slices, so reproducibility is acceptable.

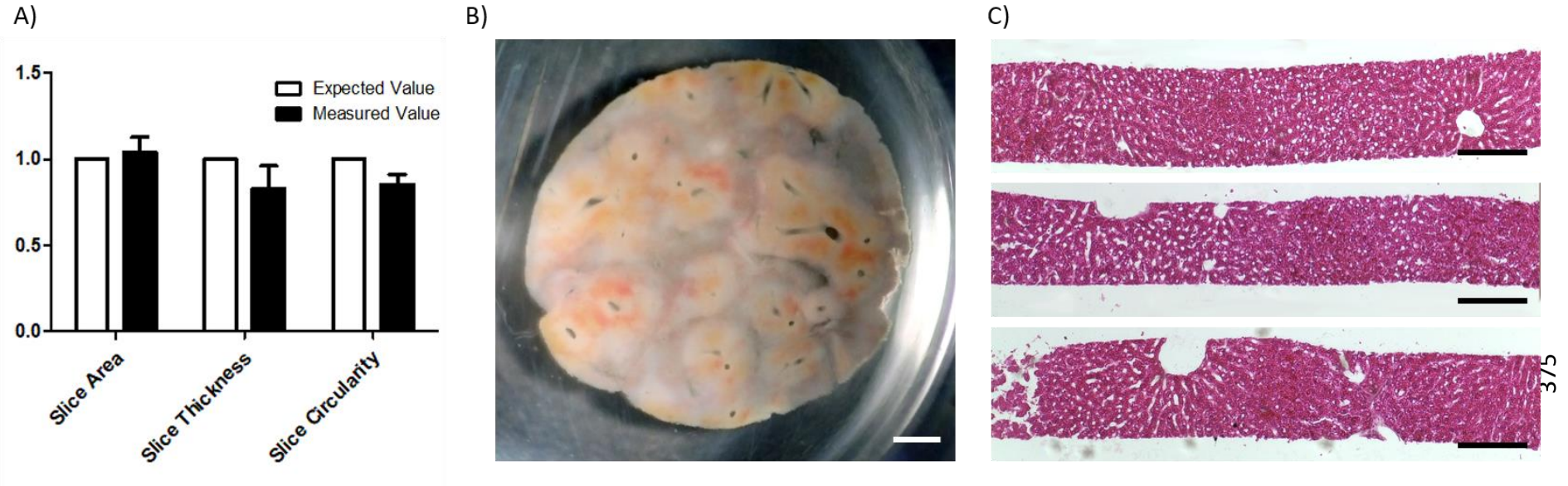

Figure 7.6: Properties of precision-cut liver slices produced using the protocol developed. A) Characterisation of properties of the processed liver slices. Slice area, thickness and circularity were all close to the values predicted mathematically. Values are mean ± SD, n = 12. B) Photograph of an 8 mm diameter, 250 µm thick liver slice sectioned with a Leica VT1000 S vibratome to show the tissue structure. Holes in the tissue correspond with larger blood vessels. Scale bar is 1 mm. C) H&E stains of several PCLS which were fixed with PFA and embedded in wax. These cross sections of the three PCLS show the high reproducibility between slices. Scale bars are 200 µm.

As can be seen by Figure 7.6B, the slices exhibit a uniform morphology across the surface. The holes visible in the surface are due to the vasculature, with the lobular localisation of these apparent in higher magnification images and the H&E stains. The H&E stains also demonstrate the reproducibility of the slices, with the three slices displayed showing a very similar morphology, as is desired.

Initial culture of these slices was investigated using Alvetex Scaffold due to its high porosity maximising nutrient transfer. With this Scaffold it was noticed with the MTT assay that the dark staining, representing regions of viable cells, was not constrained to the PCLS and was instead also in the surrounding Alvetex (Figure 7.7A). Further examination with a H&E analysis (Figure 7.7C) shows that the cells from the tissue slice were invading into the Alvetex Scaffold and fully populating the regions around the PCLS. These cells were viable for up to 28 days of culture, though the morphology became more compact over time. Meanwhile the PCLS itself became drawn up into a compact, tall structure with significant cell death throughout, likely representing the death of the sensitive hepatocytes (Figure 7.7B). It was also observed that an MTT assay performed on older, less viable, PCLS showed dark staining in networks resembling the vasculature whilst minimal production of the dark MTT product was seen elsewhere. This further suggests that the non-parenchymal cells are more robust against tissue damage and supports the observation of these cells appearing to migrate away from the tissue slice while the hepatocytes rapidly lose viability.

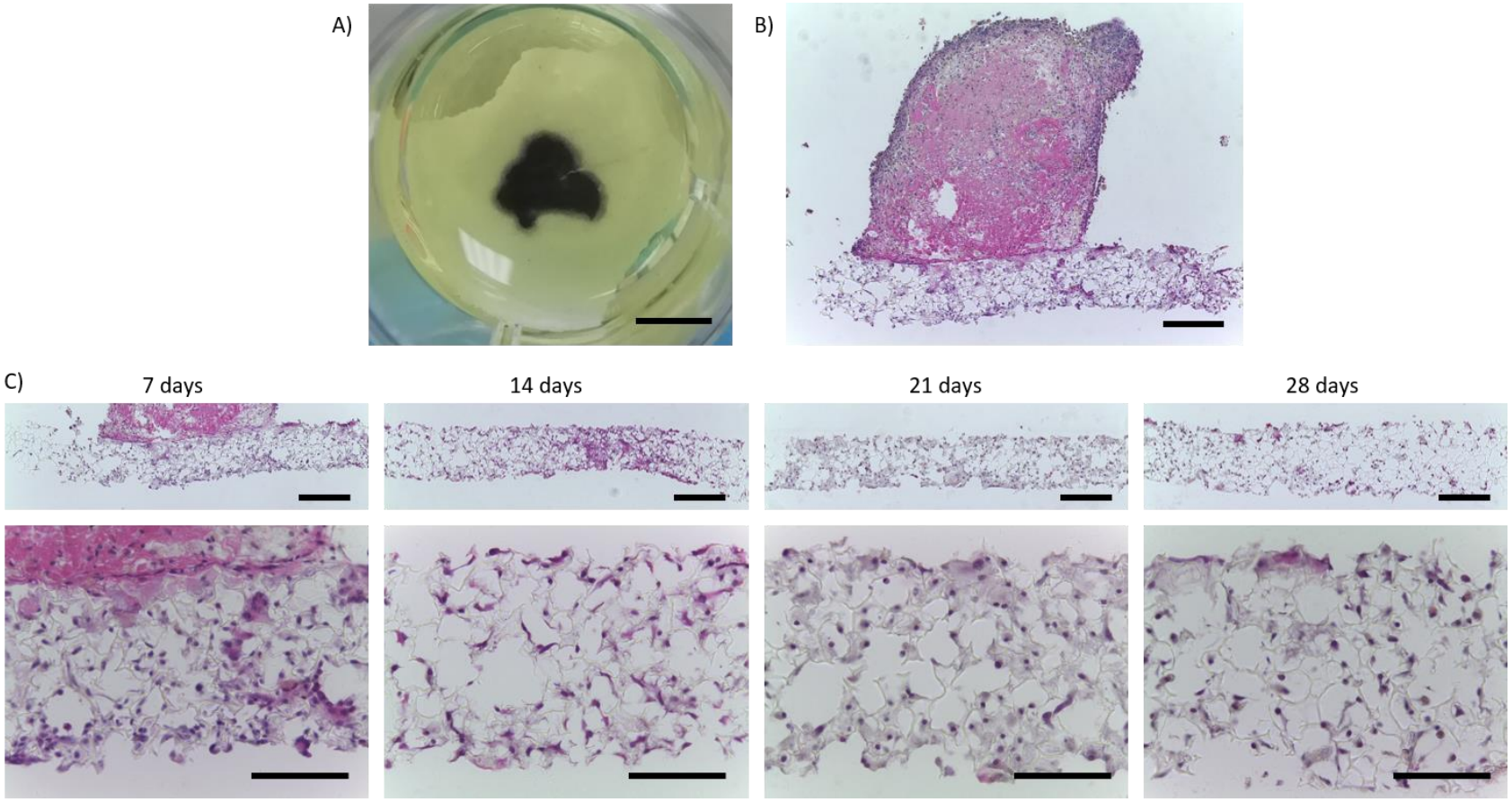

Figure 7.7: Rat PCLS grown for up to 28 days on Alvetex Scaffold. A) Photograph of an MTT assay carried out on a PCLS cultured on Alvetex Scaffold to show the extension of MTT positive regions (dark colour) outwards from the slice. Scale bar is 5 mm. B) The large, compacted structure of the liver slice after invasion into of NPCs into the Alvetex Scaffold. A large quantity of cells has migrated out of the slice and into the supporting Scaffold. Scale bar is 200 µm C) PCLS cultured on Alvetex Scaffold from 7 to 28 days showing invasion of cells into the membrane. The morphology appears to be relatively unchanged between 14 days and 28 days. Scale bars are 200 µm (top) and 100 µm (bottom).

The implications of the cell invasion into the Scaffold are interesting for a variety of reasons, such as the potential for forming repopulated stromal compartments without the 2D culture step between removal of cells and culture in 3D. For the purposes of this investigation, however, it was not desirable as the aim was to support an intact tissue slice. To culture a healthy, functional PCLS the hepatocytes are required to be present and healthy, which doesn't appear to be the case with Alvetex Scaffold.

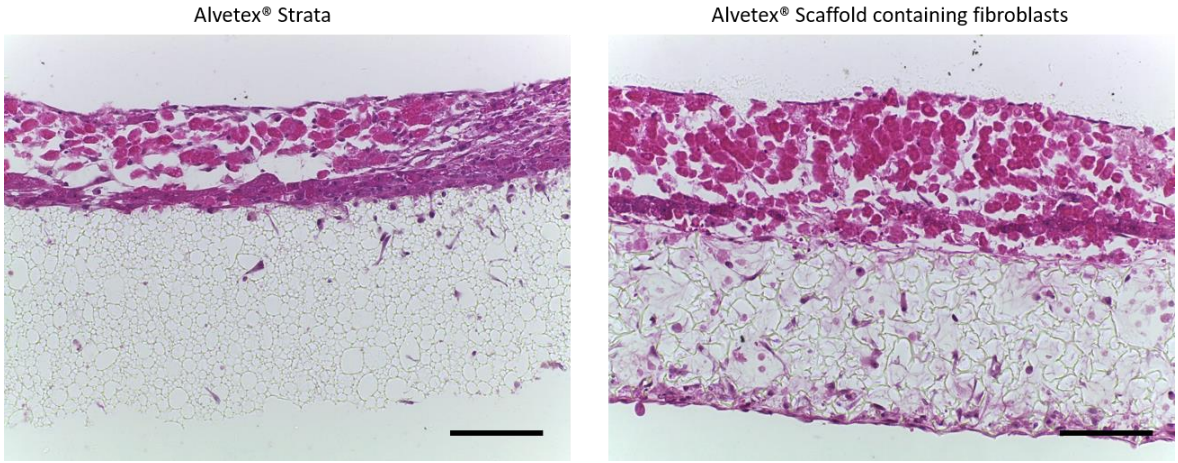

Figure 7.8: Rat PCLS grown on Alvetex Scaffold, Strata and HDFn-seeded Scaffold. A) Rat PCLS cultured for 7 days on Alvetex Strata. Minimal invasion into the membrane is seen however a large quantity of cellular death is also apparent. B) Rat PCLS cultured for 7 days on Alvetex Scaffold seeded with HDFn cells for 21 days prior to addition of PCLS. This method leads to an almost complete loss of viability within the tissue slice, with a lot of pink cytoplasmic staining and loss of nuclei. Scale bars are 100 µm.

Two techniques were investigated to work around this invasion problem. The use of a form of Alvetex with less pores, in this case Alvetex Strata, was one way which was investigated whilst the other potential option was to use Alvetex Scaffold seeded with dermal fibroblasts, as had been carried out for HepG2 previously in this work.

Culture on Alvetex Strata for 7 days maintained the morphology of the PCLS far more effectively than Alvetex Scaffold, with a uniform layer visible on the surface and very minimal cell invasion (Figure 7.8). The tissue itself also appears to be maintaining reasonable level of viability, with minimal pink cytoplasmic staining or loss of nuclei as seen on Alvetex Scaffold after 7 days. Growth on Alvetex Polaris was also investigated as an option, however PCLS grown in this way suffered a complete loss of viability with no cells remaining at the end of the culture period (data not shown).

The alternative method used was to grow PCLS on HDFn-seeded Alvetex Scaffold. This maintained the shape of the PCLS however almost complete cell death can be seen within the PCLS with only small numbers of cells around the periphery remaining. It was therefore decided to continue this work using Alvetex Strata as the substrate for the tissue slices.

7.3.2. Supporting thicker tissue slices using through-membrane fluid flow

One of the issues with tissue slices around 250 µm or thinner, as used here, is that the number of damaged cells where the slices were cut is at quite a high ratio to the undamaged interior cells. This could lead to detrimental effects due to cytotoxic compounds released by the dead cells. The use of thicker tissue slices, therefore, is generally preferable, but supporting them at greater thicknesses is difficult due to the diffusion limit of oxygen in tissue. It was hypothesised that the direction of fluid flow through the membrane in this system could help to maintain thicker slices and overcome the diffusion limitations.

As seen in Figure 7.9, production of thicker slices with the protocol used here was possible. Slices at 400 µm thick and 500 µm thick were used as alternatives to the 250 µm control slices. These slices showed greater reproducibility than the thinner slices and were easier to handle due to being less delicate.

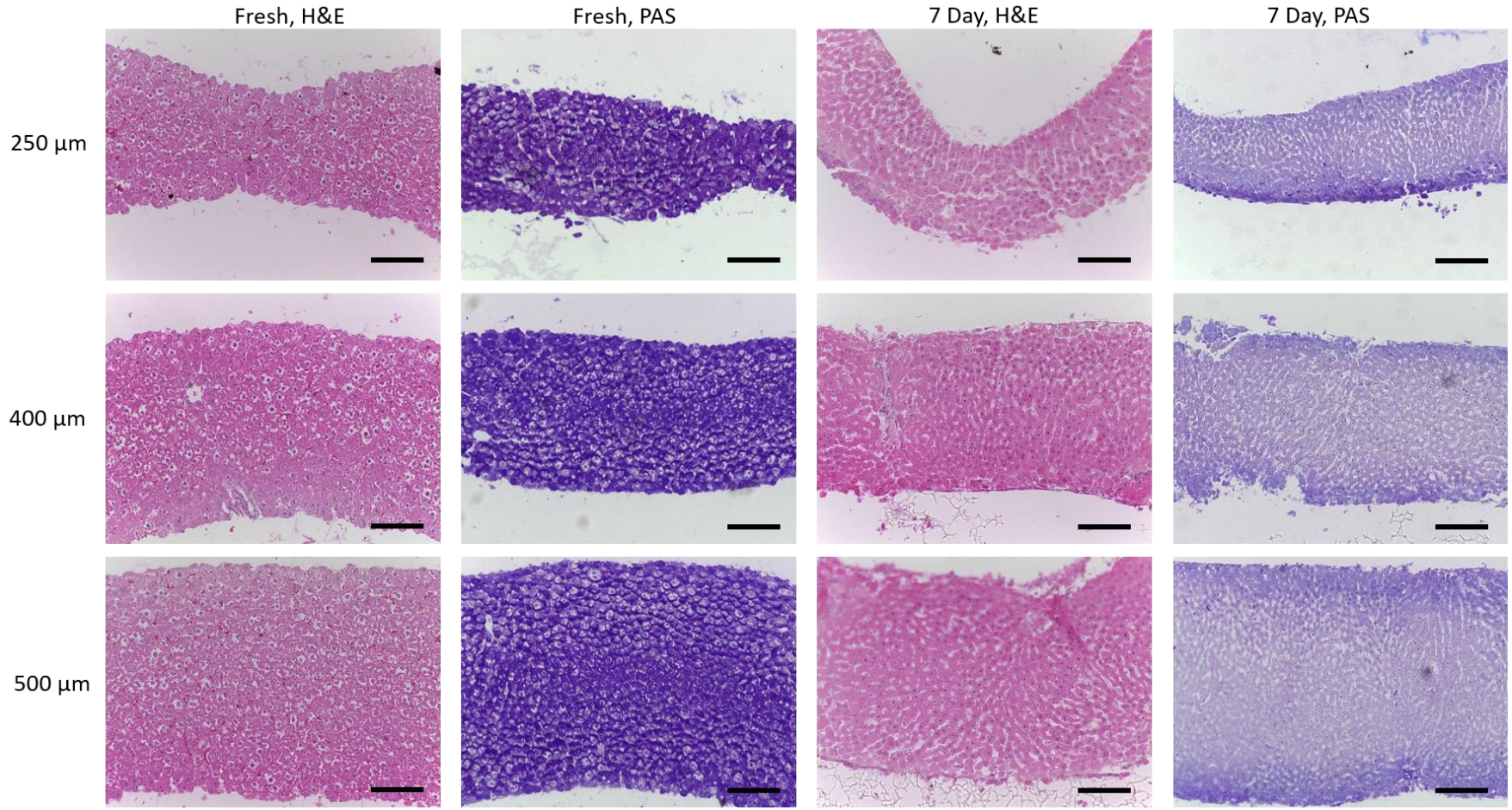

Figure 7.9: Histology of rat PCLS cut at different thicknesses. H&E and PAS stains of rat PCLS show the changes in morphology between fresh tissue slices and after 7 days in stirred culture on an Alvetex® Strata membrane. The purple staining of the PAS stain is for glycogen, which is stored by healthy hepatocytes leading to the deep purple colour seen in the fresh slices. Different thickness slices exhibit similar viability towards the edges, but a large necrotic core is formed with larger slices, seen by loss of nuclei and minimal purple staining. Scale bars are 100 µm.

When cultured for 7 days the slices showed negligible benefits over the thinner, 250 µm, slices. From the H&E stain it is clear that the centre of the slices is non-viable in both thicker slices, with a reduction in nuclear staining. Meanwhile, when using the PAS stain the same gradient of purple glycogen staining can be seen inwards from the edges for all the slice thicknesses. Due to this the 250 µm slice appears to be the most viable, with both thicker slices lacking any significant glycogen staining in their cores. Due to this a thickness of 250 µm will continue to be used going forwards in this work.

7.3.3. Culture properties of rat PCLS in the bioreactor system

Upon developing the protocol for growth of the rat PCLS in the bioreactor system, the viability of the slices over prolonged periods was investigated. As can be seen in Figure 7.10, the viability of slices in static 2D and 3D culture drops significantly after 24 hours, with almost complete loss of viability. By comparison, the slices cultured on Alvetex® Strata in dynamic conditions maintained a consistent level of viability, albeit at a lower level than fresh slices. This viability was maintained over the entire 7-day culture period, suggesting that the bioreactor system had the potential to support these slices.

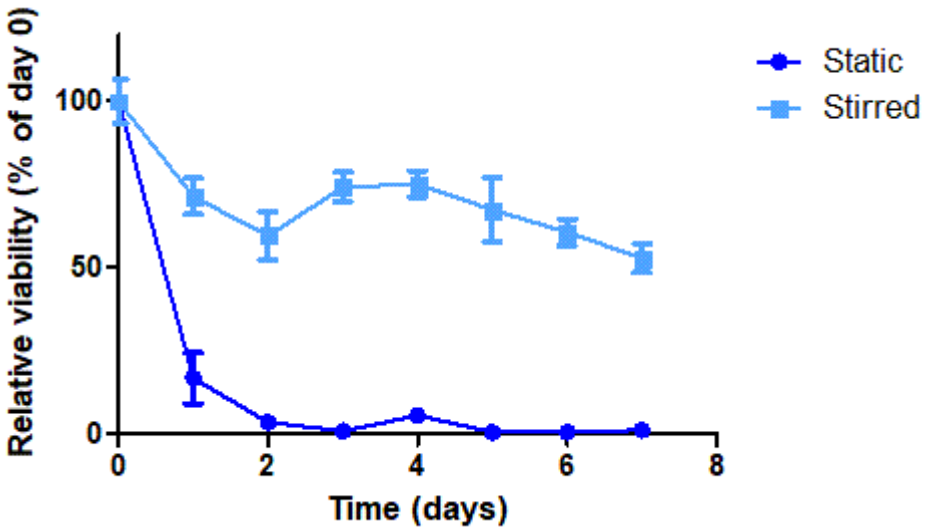

Figure 7.10: MTT Assay of PCLS cultured on Alvetex® Strata over 7 days. After the initial drop in viability dynamic culture maintains rat PCLS with a stable viability. In static an almost complete loss of viability is seen after one day in culture with no recovery at later time points. Values are mean ± SEM, n = 3.

Another area of interest for the slices was the ability to culture them with profibrotic compounds to study the onset of fibrosis in the slices. TGF-β and ethanol were chosen for this purpose. TGF-β

is an important inflammatory molecule which activates the fibrotic response in hepatic stellate cells and therefore promotes fibrosis. Ethanol causes damage to the liver which also leads to a fibrotic response and this is often used for disease modelling in literature due to its low cost and availability in biological laboratories.

These compounds were added to fresh cultures of precision-cut liver slices and incubated for three days before fixation and histological analysis. As can be seen by Figure 7.11, all three samples maintained high levels of cell viability over this period, with minimal pink cytoplasm and very few condensed or absent nuclei. The picrosirius red stain was also used to analyse these samples. This stain shows collagen and has the benefit over other methods such as trichrome in that the collagen stain does not get obscured by the other components of the staining in dense tissues.

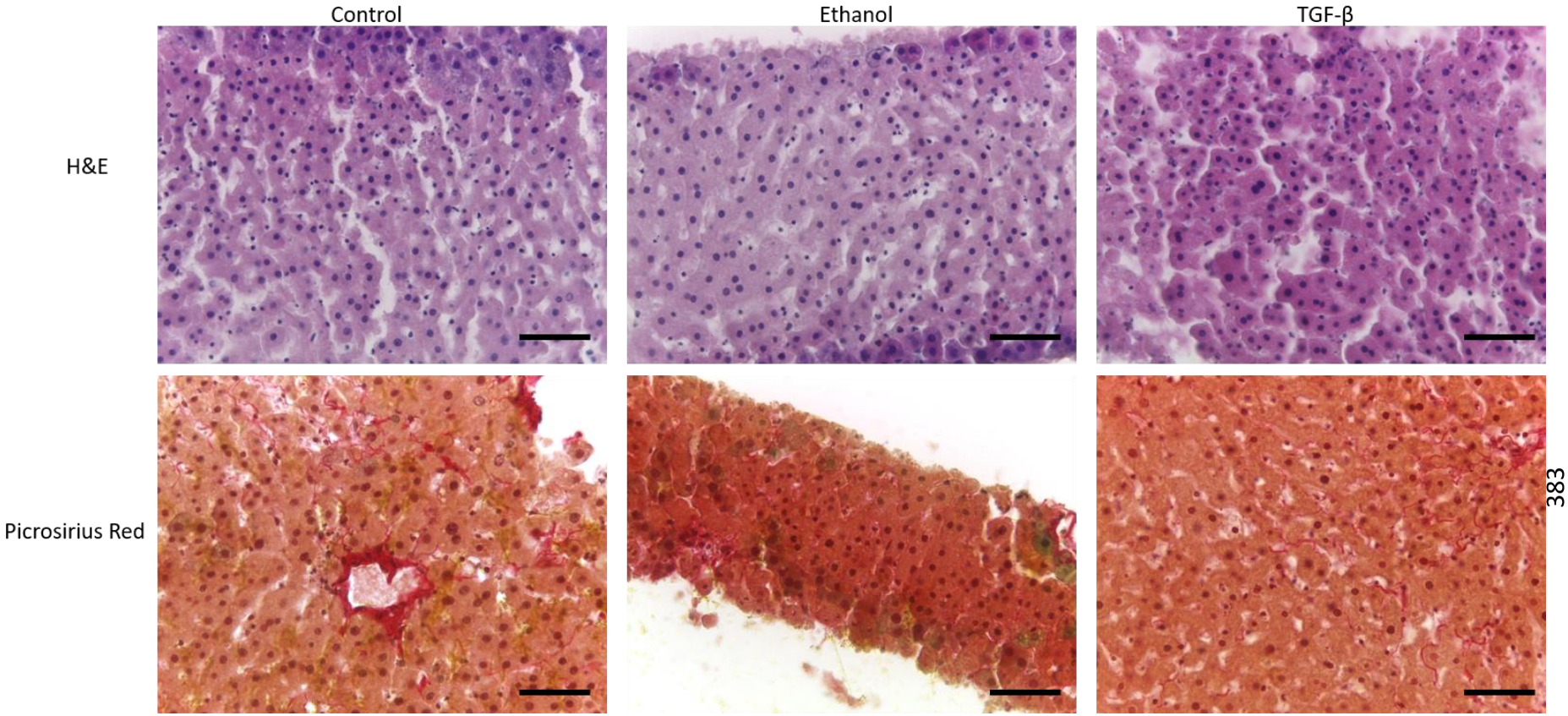

Figure 7.11: Histology of rat PCLS cultured for 7 days in the bioreactor system. Slices were either culture under normal conditions or with the addition of ethanol or TGF-β. H&E Stain shows changes to tissue health and morphology whilst picrosirius red shows collagen deposition. Similar levels of health can be seen across the conditions with minimal loss of nuclei. Due to low contrast of staining and structural variation of the tissue slices it is difficult to make direct comparisons between the picrosirius red stains. Scale bars are 100 µm.

From the picrosirius red stain there is limited difference that can be seen, with high levels of collagen present around vasculature, as seen in the control sample, and lesser levels around regions such as the sinusoids. It is possible that the levels of sinusoidal collagen are higher in the samples treated with TGF-β, however due to the low number of slices used for this experiment and the high variability between regions of the slices it is difficult to make a firm conclusion.

7.3.4. Incorporation of oxygenation into the bioreactor cultures

Including an oxygenation system as part of the bioreactor apparatus was investigated as many PCLS models in literature utilise a high oxygen environment to maintain the slices. A series of criteria for the system needed to be created, as shown by Table 7.2, before development could begin. These include values from literature, such as the use of carbogen with a 95 % O2 / 5 % CO2 mixture, whilst minimising usage to enable the cultures to run for prolonged periods without requiring large volumes of gas. Specific properties were also required to ensure maximum compatibility with the bioreactor system. This includes ease of placement on the multi-point stirrer systems, the ability to be easily sterilised. A method to maintain high levels of humidity was also necessary as dry gases cause a large amount of evaporation in cell culture systems.

Table 7.2: Criteria to be used for the oxygenation system. Different properties such as the reusability, ability to scale up easily and provision of correct gas composition can affect the ultimate success of the oxygenation system. These criteria form the minimum requirements that the system must achieve however further beneficial features can also be factored in during the development process.

Parameter	Criteria
Oxygenation levels	95 % O2 / 5 % CO2
Humidity	95 % RH
Format	Compatible with multi-point stirrer
Sterility	Reuseable and easy to sterilize
Corrosion resistance	Suitable for humidified incubator at 37 °C
Other features	User friendly Minimal gas usage Easy to add and remove cultures

Several potential systems were explored for the oxygenation of the bioreactors, from individually oxygenated bioreactor lids to an entire oxygenated incubator. The final system decided upon balanced a low size with the ease of use with multiple bioreactor vessels, as shown in Figure 7.12.

This system uses a sealed container to hold the cultures, with the capacity for 6 bioreactors on the stirrer. A barbed gas connection on one end allows the container to be connected to an external gas supply. The gas, upon entering the container, is fed into a beaker containing sterile water. By bubbling the gas through this to oxygenate the container a high level of humidity can be maintained and therefore evaporation levels will be minimised. An outlet is located on the upper surface at the opposite end of the container to the inlet. The placement at the top of the container means that air will be purged before the incoming carbogen, due to the higher density of both oxygen and carbon dioxide to nitrogen which causes them to sink to the bottom of the container while it is being filled.

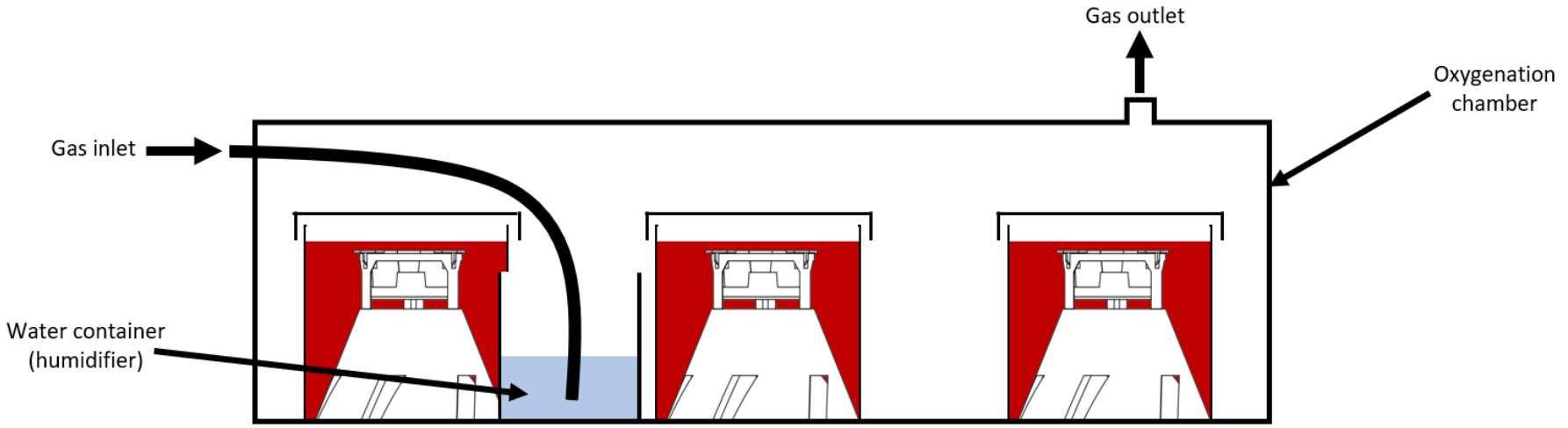

Figure 7.12: Schematic of the oxygenation system. The system consists of a central chamber which holds up to six bioreactors. This has a gas inlet to provide the oxygenation and a gas outlet to release excess pressure. Gas is bubbled through a beaker of water on entry to the chamber, maintaining a suitable level of humidity. This container is the minimum size required to fit the bioreactors with ease, therefore reducing unnecessary wastage of oxygen. A further access port is mounted on one side of the container (not shown) to allow access for electronics such as temperature and dissolved oxygen probes.

The final system was designed using a sealable container which was commercially available, therefore minimising costs. Images of the system can be seen in Figure 7.13. This container has a removable lid which allows easy access to the cultures. A 0.2 µm filter was placed on the gas outlet attached to the lid to ensure the chamber remained sterile. A sterile biopsy container was used to hold the sterile water for humidification. Locations for the six bioreactors were marked on the chamber to allow easy positioning and alignment with the stirrer unit. For further functionality a capped access port was placed at the side of the vessel which allowed the entry of wires into the system. This access port was used for temperature and oxygen probes which were used to measure the effectiveness of the system.

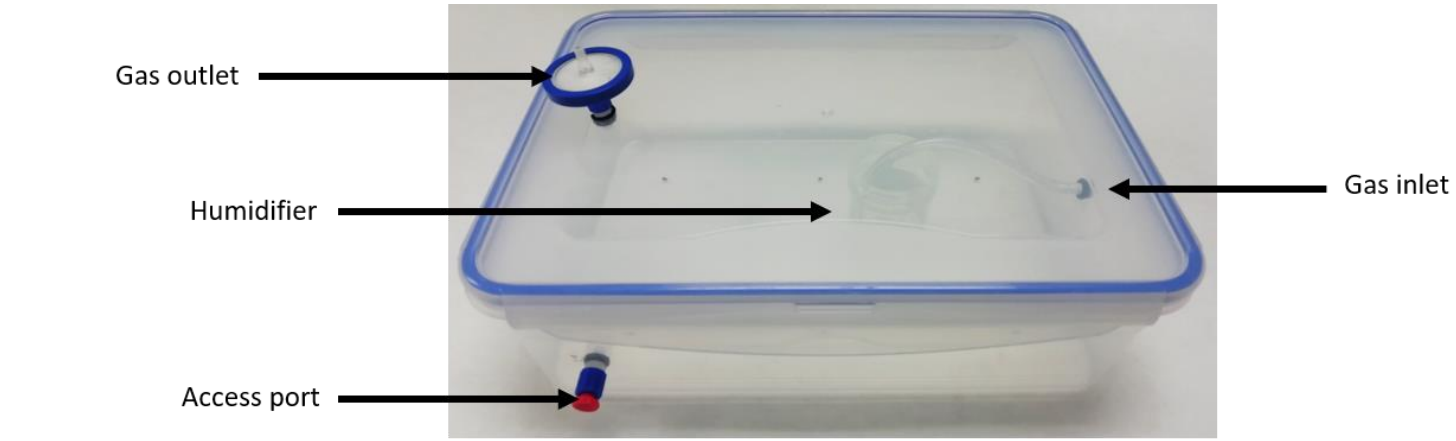

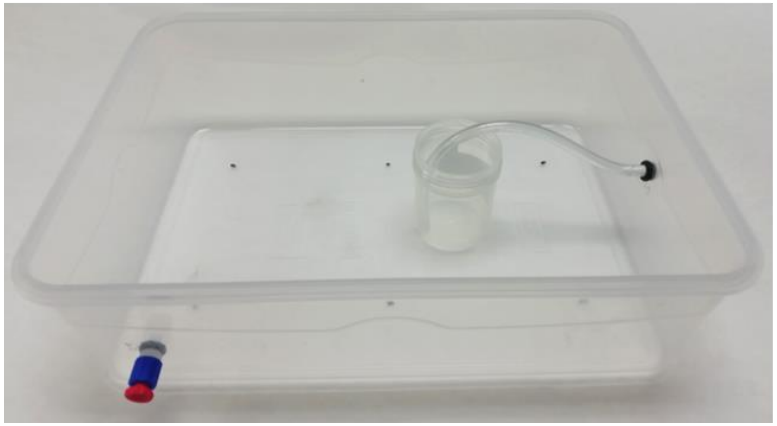

Dimensions

Width	195 mm
Depth	275 mm
Height	80 mm
Total Volume	4.3 l

Figure 7.13: Photos of the oxygenation chamber. The system consists of a central chamber which holds up to six bioreactors. This has a gas inlet to provide the oxygenation and a gas outlet to release excess pressure. Gas is bubbled through a beaker of water on entry to the chamber, maintaining a suitable level of humidity. The lid can be easily removed by unclipping the plastic sides. The internal dimensions and total volume of the chamber are shown in the bottom right.

The refilling rate of the oxygenation chamber was calculated mathematically, with an input flow rate of 100 ml/minute leading to a full container after 43 minutes, assuming 100 % efficiency of air replacement and no reduction due to dissolution of oxygen into the water and culture media. This is a reasonable flow rate to use as a maximum value as the oxygen turnover at equilibrium should be significantly less than this value. A Bronkhorst EL-Flow mass flow controller (Bronkhorst, Suffolk, UK) was purchased to provide a flow rate of up to 100 ml/minute to suit this need.

To confirm that this would work successfully for the system, a direct measurement of the dissolved oxygen levels in the cell culture medium was carried out. The level of dissolved oxygen was around 30 mg/l in the oxygenation system, compared with around 7 mg/ml in dynamic culture without oxygenation (Figure 7.14A). This clearly shows a major impact on medium oxygen levels and is close to the theoretical maximum value of around 35 mg/ml if the oxygenation was 100 % efficient at transferring oxygen to the medium.

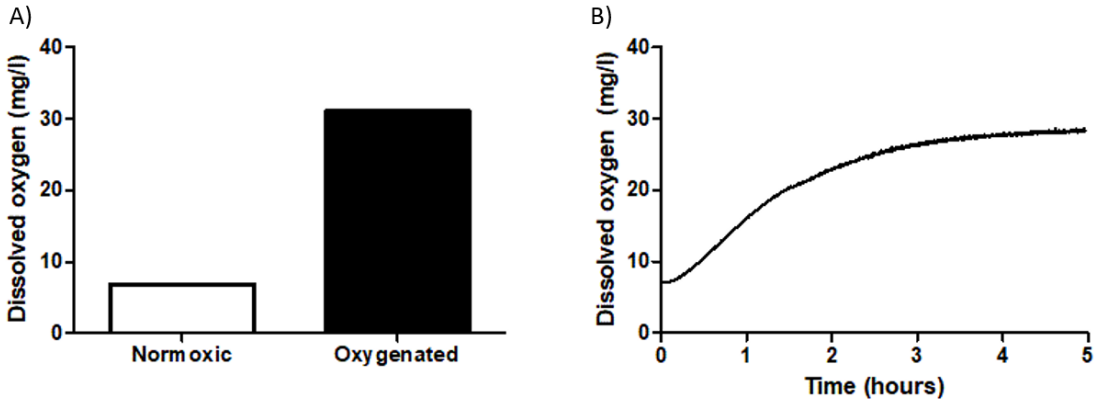

Figure 7.14: Measurements of dissolved oxygen levels in the oxygenated bioreactor system. A) At equilibrium the dissolved oxygen levels in the oxygenated bioreactor are roughly three to four times higher than those in standard incubator conditions. This is in line with what was expected from predicted values. Values were calculated after one day of incubation at the respective conditions. The values are an average of 720 data points equally spaced across one hour. n = 1. B) When unconditioned cell culture medium is added to the oxygenation system it takes three to four hours to reach the maximum levels. For the slices cultured in the system the medium is pre-oxygenated, removing this initial lower oxygen period. Values are raw data points collected ever 5 seconds over the time explored. n = 1.

Figure 7.14B shows that it takes approximately three to four hours for the oxygen levels to reach their maximum in the bioreactor with this system using unconditioned medium. For experiments using this system the medium was preoxygenated to eliminate this initial lower oxygen level.

As can be seen in Figure 7.15, the addition of oxygenation has a significant effect on the culture of PCLS in the bioreactor. Over the shorter time points the standard and oxygenated bioreactor setups

appear to show similar levels of viability (Figure 7.15A). When looking at the longer time points of up to two weeks the oxygenation system has a noticeable advantage with higher viability at these longer time points (Figure 7.15B). Each of these MTT assays represents a pilot study in which only one sample was used for each time point in the oxygenation system due to the limited throughput of only six samples, therefore a larger data set is required to be able to make any robust conclusions about the impacts of oxygenation.

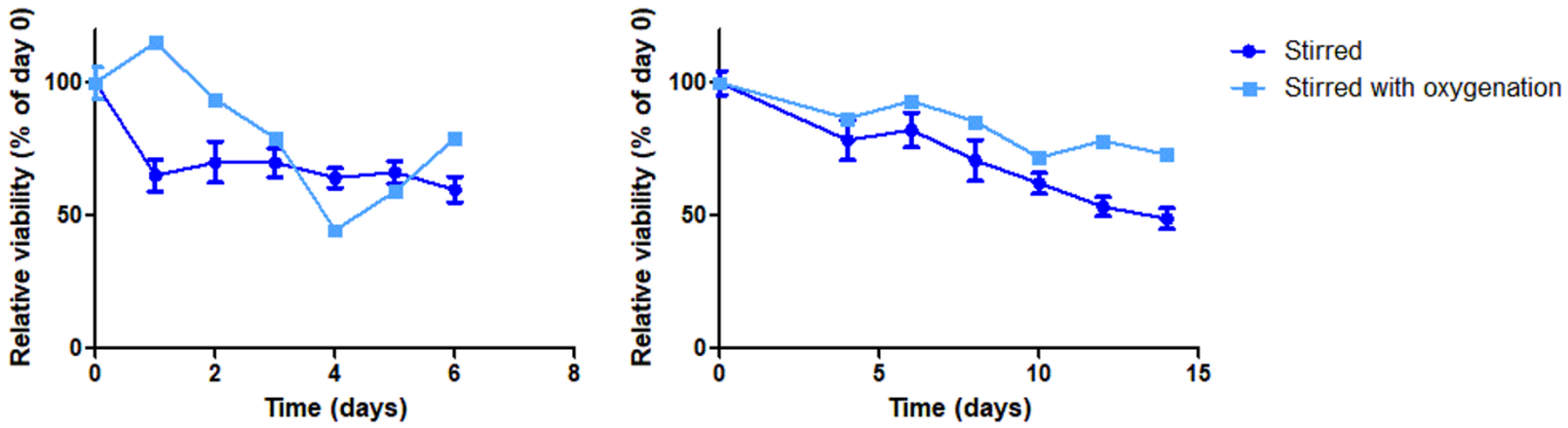

Figure 7.15: MTT Assays of rat PCLS culture in the bioreactor system in normal conditions and with oxygenation. Due to the low throughput of the prototype oxygenation system, this experiment was carried out twice with one shorter experiment up to six days and a longer experiment of up to 14 days. This also means that only a single repeat was carried out for the oxygenation samples, therefore no error bars are shown for these. n = 3 for stirred control samples, values are mean ± SEM. For oxygenated samples n = 1, values are mean.

7.4. Discussion

In this chapter the use of the bioreactor system for the culture of *ex vivo* precision cut liver slices was investigated. Such a system has numerous benefits over typical *in vitro* models due to having the entire cellular microenvironment intact, including a full complement of cell types and an ECM composition and structure that is the same as that *in vivo.* Due to this, these models have a lot of potential for the study of diseases such as liver fibrosis. The difficulty maintaining the viability of these models over periods of more than a week is the major problem preventing them from being more routinely used and it was hypothesised that the novel bioreactor system could overcome this due to the fluid turnover and increased dissolved oxygen levels.

7.5.1. Liver slices can be maintained for up to a week in the bioreactor system

Due to the increase in fluid flow in this system one hypothesis was that a thicker slice could be maintained in the system than the 250 µm thick slices commonly used in literature (Wu *et al.*, 2018; Paish *et al.*, 2019b). This would have significant benefits due to the damage cells at the edges of the tissue slices being a larger proportion of the total tissue in small slices, therefore having a greater negative impact on tissue health.

When this was examined with the bioreactor system it was found that 250 µm remained the optimum thickness for viability, supporting the reason for this thickness being the most commonly used in literature (Dewyse, Reynaert and van Grunsven, 2021). Both the 400 µm and 500 µm slices showed significant loss of viability towards the centre of the tissue, both with loss of nuclei seen in the H&E stain and reduced glycogen storage seen with that PAS stain. This agrees with results in literature for PCLS of this thickness in roller bottle systems in which a significant loss of glycogen storage is also seen in the cores of thicker slices (Fisher *et al.*, 2001). On the other hand, the 250 µm tissue slice maintained consistent glycogen storage levels across the tissue therefore suggesting a greater tissue viability and limited cell death at the centre. This suggests that, although the bioreactor system can provide more nutrients to the cell surface, the transport of nutrients through a tissue continues to be limited by the diffusion rate through tissue (Rouwkema *et al.*, 2009).

Maintenance of PCLS for time periods of over one week is rarely reported in literature, with a recent study showing that of 107 papers on PCLS, only 7% of these used time points greater than 72 hours(Dewyse, Reynaert and van Grunsven, 2021). Culture of slices for longer than one week would be of great research value for studying chronic toxicity pathways, however such time points are

used by few groups (Wu *et al.*, 2018; Paish *et al.*, 2019a; Barcena-Varela *et al.*, 2020; Kartasheva-Ebertz *et al.*, 2021). It is of note that these studies all used human PCLS, with the culture of animal PCLS having not yet been reported for such time periods. Whilst the data presented here suggest that slices are viable for up to 7 days in the bioreactor system, a more detailed analysis would have to be performed to fully investigate the function of the slices over this time and accurately compare the outcomes to those reported in literature.

7.5.2. Migration and proliferation of non-parenchymal cells could limit the utility of PCLS over longer time periods

In this work the migration of cells out of the tissue slices and into the substrate was observed when using the highly porous Alvetex Scaffold. Such a result, to the best of the author's knowledge, has not previously been reported with 3D scaffolds for PCLS, though a study found a similar result when culturing precision-cut tumour slices on Alvetex Strata (Davies *et al.*, 2015). This, coupled with the loss of viability within the slice itself, suggests that basic measures of viability may not be useful due to being skewed by the increasing ratio of non-parenchymal cells to hepatocytes.

One study has quantified the levels of different cell types in the tissues visually through immunohistochemistry with relative success, showing how the number of hepatocytes declines over multiple days in culture whilst A-SMA activity increases (Verrill *et al.*, 2002). This is supported by further gene expression data showing large increases in genes for A-SMA and procollagens whilst genes such as the CYPs are hugely downregulated (Vickers *et al.*, 2004). This is in opposition to studies which have suggested drug metabolising genes are maintained in liver slices, however this is reported over 24 hours, compared with 48 - 72 hours in studies showing downregulation (Elferink *et al.*, 2011). Many studies, however, use simplistic measures such as viability assays to measure health of the liver slices (Koch *et al.*, 2014) or use a range of genes which give an unclear picture of cell health (Wu *et al.*, 2018). This could lead to a false assumption that the slice is maintained in the same state as *in vivo* whilst the reality is a tissue with significantly disproportionate levels of different cells.

The invasion of cells out of the tissue slice is not necessarily problematic in all circumstances. Whilst for studying the function of the tissue slice it can lead to misleading results, the capacity to infiltrate a 3D scaffold with cells which have not previously been cultured in 2D flasks could be an interesting avenue of study for creation of physiologically relevant stromal equivalents. Such '3D to 3D' techniques have previously been used successfully for the culture of mesenchymal stem cells,

helping to maintain their viability and multipotency (Papadimitropoulos *et al.*, 2014; Egger *et al.*, 2019). The presence of different cell types in this infiltrated scaffold such as macrophages and endothelial cells, something which was not investigated here, would further its potential for use as a stromal equivalent. These stromal equivalents could then be used as a support for epidermal cells with potential applications for other tissue types such as skin and intestine. Further characterisation would be required to investigate the lineages of the cells within the scaffold to determine the optimum applications for such models.

7.5.3. Further refinements of the protocol are required for accurate testing of profibrotic agents.

Whilst this chapter demonstrated the potential for culturing rat PCLS in the bioreactor system the ability to do this reproducibly was a limiting factor. One of these limitations came from the choice of vibratome used, which has a significantly lower blade oscillation amplitude than those used in literature (Wu *et al.*, 2018; Paish *et al.*, 2019b). This reduces the cutting ability and leads to many slices being discarded due to tissue damage or variable morphology, therefore limiting the throughput of the system beyond the limitations of the scale of the bioreactor system. If this could be overcome, much higher throughput could be achieved and therefore higher numbers of repeats and consequent robustness of data would be possible.

In this study the use of different culture media was not investigated, instead using a simple formulation chosen from a review of the literature. However, studies have investigated the applications of proprietary medium formulations such as supplementation with RegeneMed® and Cellartis® additives (Starokozhko *et al.*, 2015; Starokozhko, Greupink, *et al.*, 2017) whilst others have incorporated low-serum formulations (Paish *et al.*, 2019b; Barcena-Varela *et al.*, 2020). Optimisation of this parameter for the bioreactor system could be beneficial for supporting long-term tissue viability.

7.5.4. Incorporating oxygenation into the biore system further improves the viability of cultured PCLS.

Creating an oxygenation system for the bioreactor apparatus was a relatively straightforward process and allowed the inclusion of oxygenation as is commonly used in studies of PCLS in literature. Minimised volumes for this using a relatively small chamber allow the system to be running for prolonged periods without using up the gas supply, something which can be an issue

for systems which involve large, oxygenated chambers or incubators. Measurement of the oxygen levels in the cell culture medium showed that the oxygenation was significantly increased, as determined from previous calculations. This demonstrated the success of the oxygenation system, which could also have applications for other tissue and cell cultures with high oxygen requirements or inversely could also be used for the study of hypoxia. With the convective mixing of the medium leading to uniform dissolved oxygen concentration, research using alternative oxygen levels can be carried out more accurately due to the absence of variation with depth of medium, something which makes the actual value of the dissolved oxygen at the cell surface incredibly difficult to measure.

When cultured with the addition of oxygenation the tissue slices showed an improved viability in the MTT assay over a period of up to 14 days. As discussed previously, while oxygenation may have increased hepatocyte viability there is still a possibility that this maintained MTT value is due to proliferation of non-parenchymal cells disguising the loss of hepatocyte viability and further research needs to be performed to investigate this.

7.5. Conclusion

In this chapter the use of the novel bioreactor system for the culture of *ex vivo* liver tissue slices was explored, in contrast to the previous work using *in vitro* cell models. This would allow a more physiologically relevant tissue model to be created which could be very useful for studies into diseases such as fibrosis.

Initial investigations into slice properties showed that it was possible to maintain the slices within the bioreactor system with reasonable viability over 7 days. Optimisation was required to ensure reproducibility of slices and to overcome issues such as invasion of cells into the substrate. Experiments also showed that despite the fluid flow through the membrane, tissue slices thicker than 250 µm could not easily be supported without loss of viability towards the centre of the slice.

Experiments were performed to investigate the effects of two fibrotic inducers, ethanol and TGF-β, on the slices. Over the 3 days that the slices were cultured to investigate this, limited changes could be seen in the slices both histologically and using the picrosirius red stain for collagen. It is likely this is due to the high variability in outcome of the slices in culture, with effects over 3 days which are not obviously any greater than variation seen naturally.

Further development of the bioreactor apparatus to include an oxygenation chamber showed that addition of extra components such as this was easily achievable, and the system designed allowed a high level of oxygenation of cell culture medium whilst using a relatively low volume of gas. Use of this system for the culture of PCLS showed enhanced viability over dynamic culture conditions without oxygenation, with maintenance of this over 14 days, however further work is needed to confirm that this is due to increased viability of hepatocytes and not due to other effects such as proliferation of non-parenchymal cells.

Overall, this chapter served as an effective proof of concept for the use of precision-cut liver slices within the culture system. Further optimisation of culture properties to improve reproducibility by the end-stage of the culture is required to ensure measurable results can be readily distinguished from culture variability. A greater analysis of the cultures would also be required for future work to confirm whether the increased viability in the system is due to improved hepatocyte viability or proliferation of other cells whilst work could also investigate possible uses for scaffolds seeded with cells directly from tissue slices, foregoing the usual 2D culture steps.

Chapter 8: General Discussion, Future Directions and Conclusion

8.1. Summary of Key Findings

In this project the development of a novel system to create *in vitro* tissue equivalents with a high physiological relevance, overcoming some of the limitations of more basic models, was carried out. Initially the worked aimed to build a system with properties such as a 3D cell microenvironment and fluid flow, and further work developed this to contain a variety of cell types with endogenous ECM deposition. The hepatocellular carcinoma cell line HepG2 was used to create a model of the liver and determine whether a highly complex microenvironment could overcome inherent limitations of immortal cell lines such as this. The system was also examined for use with rat precision-cut liver slices to investigate its utility to maintain the tissue slices over prolonged periods. The key findings in this work are as follows:

- Using magnetic stirrers as a basis for fluid flow, it is possible to create a simple but highly controllable bioreactor system for cell culture.
- Stirrer-based fluid flow has great potential for scalability and mass adoption due to its low cost and user friendliness.
- Bioreactor systems can influence cell culture conditions through a variety of different mechanisms which may not always be desirable, such through additional heat generated by the equipment and generation of magnetic fields. Thorough characterisation of a system is therefore of great value to ensure observed results can be accurately interpreted.
- HepG2 cells can be successfully incorporated into a bioreactor system utilising Alvetex® Strata as a support. Cells cultured in this way exhibit improvements to key aspects of hepatic function such as CYP expression and transporter localisation.
- The drug response of stirred HepG2 models differs from the response in static conditions, however the exact benefit of this is unclear due to the small number of drugs tested and lack of consensus in literature.
- Further cell lineages, such as fibroblasts and endothelial cells, can be incorporated into the model, providing heterogeneous cell-cell contact, endogenous ECM production and creating a more physiologically relevant microenvironment.
- The bioreactor system has potential for supporting the viability of *ex vivo* liver slices, providing an alternative platform to the few that are currently routinely used.
- Modifications to the system to increase functionality can be readily performed, as demonstrated by the creation of an oxygen chamber and the incorporation of probes to monitor oxygen levels.

8.2. Discussion

8.2.1. Development of a d cell culture system

Conventional cell culture techniques are inherently limited due to the incredibly simple microenvironment, typically containing a single cell type, no ECM and with the cells simply placed onto plastic immersed in a static medium. This is significantly different from the complex microenvironment in the body, with cells experiencing a 3D environment, interactions with other cell types and surrounding ECM and convective flow of fluids providing a turnover of nutrients and disruption of unstirred layers as well as mechanical shear stresses(Yamada and Cukierman, 2007). This work aimed to overcome these limitations by creating a physiologically relevant culture system which maintained desirable characteristics such as technical simplicity and low cost. One of the main aims of this system is to incorporate fluid flow into the culture, mimicking the flow of fluids present *in vivo,* alongside other techniques such as 3D scaffolds and co-culture with multiple cell types. To test this the liver was used as a model organ due to the high levels of fluid flow that it experiences *in vivo*, with a dual blood supply as well as a counter current flow of bile, suggesting that it may benefit greatly from recapitulation of these properties *in vitro*.

Cell culture bioreactors in literature are often complex, expensive and take up large quantities of laboratory space(Bale *et al.*, 2014; de Bournonville *et al.*, 2019). In this work a system was developed to try and overcome some of these issues using a magnetic stirrer-based fluid flow system, as shown in Figure 8.1. This keeps costs low due to the simplicity of the parts involved whilst only requiring very basic equipment for functionality, specifically the bioreactor itself and a magnetic stirrer unit to place it on. The development of multi-point magnetic stirrers allows the throughput of this system to be easily increased, whilst custom stirrer systems such as the one also developed herein allows maximum use of the available laboratory space through the bespoke specification.

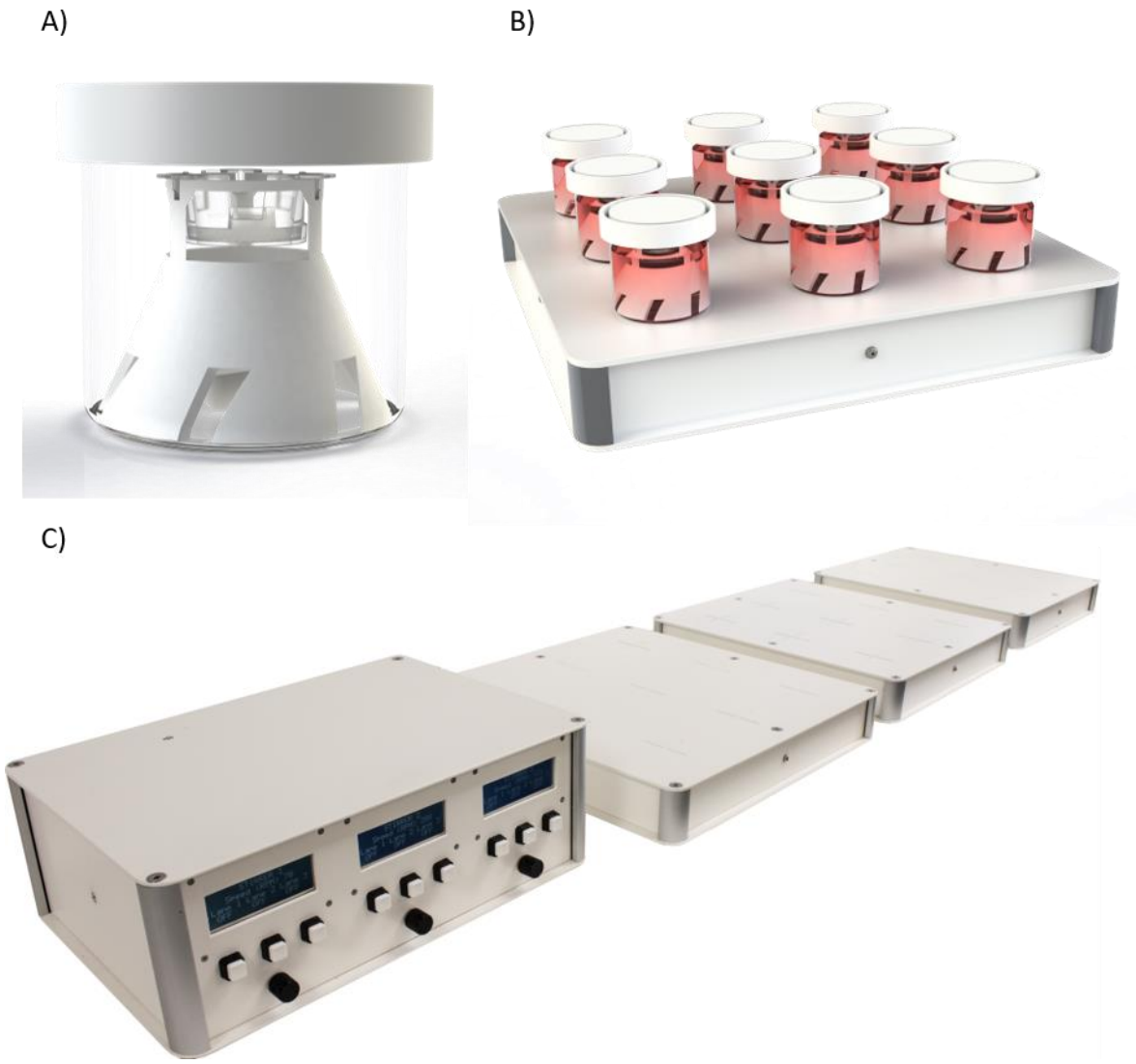

Figure 8.1: Overview of the finalised bioreactor apparatus developed in this thesis. A) The bioreactor vessel contains a vented, conical stand to hold a 6-well Alvetex® insert within the bioreactor system. A stir bar at the base of the vessel provides the convective mixing and recirculation. B) A total of nine bioreactors can be run simultaneously on one of the multi-point stirrer units developed in this work. C) The whole stirrer system consists of a control unit (left) and three stirrer units, each able to run nine bioreactors simultaneously.

One of the key limitations of many bioreactor systems used in literature is the minimal characterisation of the properties of the system. Whilst some properties such as flow parameters and shear stress are regularly reported(Leo *et al.*, 2009; Hidalgo-Bastida *et al.*, 2012; Rathore, Kanwar Shekhawat and Loomba, 2016), often as part of the system development process, other properties are disregarded. These include implications of a system in factors such as temperature fluctuations, media evaporation and magnetic fields. In this work one of the aims was to characterise the system as fully as possible, therefore leading to a greater understanding of the exact environment experienced by the contained cells.

One of the other aspects of cultures that is rarely reported in literature are the properties of the membrane on which the cells are grown. With increased use of 3D substrates, greater variability is introduced to the system, making comparisons between studies difficult. Whilst the gross morphology of these membranes is typically reported, less often are properties such as the porosity or permeability discussed, meanwhile the use of a wide range of different materials further increases variation(Domansky *et al.*, 2010; Tripathi and Melo, 2015; Schmid *et al.*, 2018). In this work polystyrene Alvetex® membranes were used, matching the material used in conventional cell culture plates, as well as having a large amount of information already available about the structure and porosity of these scaffolds(Carnachan *et al.*, 2006; Bokhari, Carnachan, Przyborski, *et al.*, 2007; Knight *et al.*, 2011). Further characterisation of these membranes was also carried out, generating data which could be used for the CFD models, leading to the final system having very well-defined properties. This highlights the fact that such thorough characterisation is readily achievable with standard laboratory equipment and should form the basis for the development of any such system to allow maximum reproducibility between experiments and laboratories.

Using this culture system, a series of liver models were developed with increasing levels of complexity to test whether the application of fluid flow in a 3D cellular microenvironment would enhance the cell function. The hepatocellular carcinoma cell line HepG2 was used as an alternative to primary hepatocytes due to its ease of culture and low cost, with the aim to see if it could acquire a phenotype more closely related to primary hepatocytes when cultured in the bioreactor. This would not only increase the research value of this cell line significantly, but also present researchers with an alternative to primary cells which could provide far more flexibility due to the simplicity of culturing this cell line coupled with its availability in high quantities.

8.2.1. Summary of models developed in this work

In this work the potential for creating a series of liver models using the novel bioreactor system was investigated. Four models were explored for this purpose with varying levels of complexity. The basic HepG2-only model was characterised in-depth with analysis of protein expression and localisation, basic metabolic function, and gene expression carried out. Further investigation of the toxicological response of this model was also carried out to explore whether the performance of HepG2 could be enhanced in these through the addition of fluid flow.

The co-culture model incorporating a supporting layer of fibroblasts was developed, building on previous work with similar models for other tissues(Roger *et al.*, 2019; Darling *et al.*, 2020), and the structural characteristics and basic metabolic function were characterised. A proof-of-concept was carried out to see if the hepatic endothelial cell line SK-Hep-1 could be incorporated into these models. This model showed potential for enhancing the function of HepG2 cells however the characterisation carried out on this model was limited.

The most technically challenging model involved the culture of *ex vivo* precision-cut liver slices. The use of these was also performed as a proof-of-concept to investigate whether the bioreactor system could improve the viability and longevity of these slices, which suffer from poor viability in current culture systems(Wu *et al.*, 2018; Paish *et al.*, 2019b). The tissue slices showed promising results with maintained viability up to 7 days and potential for further extending this with the addition of an oxygenation system. Further work is needed, however, to further optimise this technique and to ensure reproducible results to maximise the utility of this model for the study of liver disease.

8.2.3. A more physiological microenvironment enhances cell structure and function

The most significant finding in this work is the enhancement of hepatocyte structure and function caused by using a highly physiologically relevant microenvironment, particularly on the expression of key metabolic genes. All the models experienced improved function, measured through a variety of techniques, when cultured in the bioreactor system. This was the major hypothesis for this work, as much of the literature demonstrates the improvements to both primary hepatocytes and cell lines such as HepG2 from the inclusion of techniques such as 3D culture and fluid flow (Xia *et al.*, 2009, 2012; Sassi *et al.*, 2021).

It is also notable that the combination of these techniques overcomes some of the issues that are found when using one alone. One example of this is the limited induction of some genes, such as the CYP enzymes, seen when culturing HepG2 in 3D(Luckert *et al.*, 2016). This was seen in this work, with no difference in CYP expression of any of the eight investigated genes when moving from 2D to 3D culture. Contrary to this, the inclusion of fluid flow had a major impact on the gene expression, in some cases leading to over tenfold higher CYP expression than in the equivalent static cultures. Generally, CYP expression is reported in literature to increase with the addition of fluid flow, though the vast range of different bioreactor systems used makes direct comparison difficult(Deng *et al.*, 2019; Sassi *et al.*, 2021).

Likewise, 3D culture using a scaffold helps to overcome some of the issues seen in dynamic cultures. Limited attachment to substrates is an issue reported in some 2D studies of fluid flow systems(Sun *et al.*, 2012), and can also be problematic for 3D based systems using spheroid technologies(Tong *et al.*, 2016). The large attachment area provided by porous scaffolds such as Alvetex® allows cells to adhere effectively to the membrane as is the case *in vivo*, firmly anchoring them in place and allowing for their anchorage-dependant polarisation(Selden, Khalil and Hodgson, 1999).

Further to the addition of 3D culture and fluid flow, the apparatus also allows the addition of ECM to the system, either through endogenous secretion of ECM from incorporated cells, as demonstrated herein and elsewhere (Roger *et al.*, 2019), or through coating of the Alvetex® membrane with proteins such as collagen as is carried out for many growth substrates in literature (Michalopoulos *et al.*, 1999; Berginc and Kristl, 2011; Zheng *et al.*, 2017). The flexibility to customise the system in this way increases the wide range of applications whilst allowing variations to study complex pathways such as diseases like liver fibrosis, in which the ECM dynamics play an important role in the outcome of the disease (Karsdal *et al.*, 2015, 2017).

8.2.4. Applications of the stirred *in vitro* liver models

The application of the simple HepG2 monoculture bioreactor model was investigated in this work for predicting drug hepatoxicity. Typical models used at present are limited by loss of viability and polarisation over time, as is the case for primary hepatocytes (Mizoi *et al.*, 2020), or limited expression of key drug transporters and metabolic enzymes, as is the case for many cell lines (Gerets *et al.*, 2012; Yun *et al.*, 2019). Many new methods are being developed with the aim to overcome these limitations through more physiologically relevant models (Kang *et al.*, 2013) and use of more functional cell lines (Guillouzo and Guguen-Guillouzo, 2008). Despite this, experiments

to look into hepatotoxicity of drugs often fail to accurately predict toxicity, both due to limitations of the models alongside inadequate techniques to measure toxicity (Chan and Benet, 2018; Kuna *et al.*, 2018).

Use of the bioreactor system developed herein showed that fluid flow had a major impact on the function of cells which is hypothesised to correlate to changes in drug hepatotoxicity. The improved expression of phase I metabolic enzymes in particular suggests more physiologically relevant results would be found due to the major involvement of phase I metabolism in the formation of reactive metabolites and consequent toxicity of many drugs (Attia, 2010). The results using the bioreactor system showed the decreased sensitivity for many drugs, as seen in static 3D experiments, was often maintained in stirred conditions. For tamoxifen and flutamide, both known hepatoxic drugs with the highest level of severity according to the DILIrank database (Chen *et al.*, 2016), an increase in sensitivity was seen in the stirred models. This suggests that, although some drugs appear to have limited differences, there are changes occurring which can improve predictive capacity for certain drugs. With a wider range of endpoint assays and longer-term drug exposure it is possible this system could lead to improved results across the board; however, this was not explored in this work.

The more complex *in vitro* models have potential applications for disease modelling, with the pathways between different cell types present in these systems. Endothelial cells have frequently been included in hepatocyte cultures, often alongside further NPCs (Kang *et al.*, 2013; Liu *et al.*, 2014; Sundhar Bale *et al.*, 2015; Ahmed *et al.*, 2017; Wang *et al.*, 2018; Ware *et al.*, 2018). Substantial paracrine signalling occurs between the these cells and this can play an important role in disease such as liver fibrosis and viral infections (Shetty, Lalor and Adams, 2018). In cirrhosis the endothelial cells lose their fenestrae and gain a basement membrane, leading to further activation of HSCs and promotion of the inflammatory phenotype (Poisson *et al.*, 2017). Bioreactor cultures of these with hepatocytes can lead to mechanistic studies investigating the changes in shear stress on the morphology and function of the endothelial cells and further downstream impacts this may have (Ballermann *et al.*, 1998; Soydemir *et al.*, 2020). Whilst in this study cultures were generated using a single level of shear stress, the highly tuneable nature of the novel bioreactor allows it to be readily adjusted to perform such investigations.

8.2.5. The limitations of the HepG2 cell line

In this work the limitations of the HepG2 cell line as an alternative to primary hepatocytes can be readily visible. Under fluid flow, a substantial upregulation of many key genes was seen with increased localisation of proteins, as discussed previously. While this shows the effectiveness of bioreactor models for inducing this function, some limitations could not be overcome.

Lack of expression of key hepatocyte transporters such as BSEP and NTCP in HepG2 cells has been known to be a major limitation for their use as *in vitro* models of hepatocytes (Yan *et al.*, 2012; Donato, Tolosa, Laia and Gomez-Lechon, 2015). This limitation is of increasing importance due to the build-up of literature suggesting the use of BSEP inhibition as an effective predictor of DILI whilst NTCP is required for maintenance of physiological levels of intracellular bile salts. In this work it was found that the addition of 3D culture, fluid flow and additional cell types were not able to overcome this lack of expression in HepG2 cells. Whilst this limitation could be avoided through transfection of cells with functional transporter expression, as has been carried out successfully in some studies (Yan *et al.*, 2012), the availability of more effective hepatic cell lines without this limitation such as HepaRG makes this undertaking less desirable.

Other key proteins in HepG2 also suffer due to genetic defects. β-catenin, a highly important protein in hepatocytes due to its role in adherens junction formation on top of its function as a transcription factor in key pathways such as canonical Wnt signalling (Valenta, Hausmann and Basler, 2012), is one such protein. The CTNNB1 gene suffers from a deletion of over 500 base pairs in HepG2 (Zhou *et al.*, 2019). It has been shown that this prevents inhibitor function on the protein, leading to high levels of activity and aberrant localisation in HepG2 cells as seen herein (Dar *et al.*, 2016). Whilst this is just one gene, HepG2 have been found to have over 5,000 mutant genes, alongside possessing between 49 and 52 chromosomes, suggesting that there are many other, less heavily studied, problems with the cells which cannot be overcome through use of advanced cell culture techniques (Zhou *et al.*, 2019).

8.2.6. Use of *ex vivo* tissue slices in the bioreactor system for *in vitro* disease modelling

Precision-cut liver slices offer an alternative platform to *in vitro* culture models. These have major advantages due to intact ECM with the structural organisation matching that *in vivo* whilst also containing the full complement of different cell types and polarised structures (van de Bovenkamp

et al., 2008). The major issue with *ex vivo* PCLS is that they suffer from a very short functional lifespan of typically only a few days, whilst at most some studies have maintained them for up to 2 weeks (Wu *et al.*, 2018; Paish *et al.*, 2019). Due to the increased oxygen levels measured within the novel bioreactor system it was hypothesised that this may be beneficial for maintenance of PCLS.

Characterisation of PCLS cultured in the bioreactor system on Alvetex® Strata showed the ability to maintain the slices with a reasonable level of viability over 7 days. This is comparable with other models developed in literature however some potential issues with these were also highlighted. Using the highly porous Alvetex® Scaffold membranes, a high level of invasion of non-parenchymal cells out of the tissue slice and into the membrane was apparent, an effect which does not appear to have been previously reported. Even when using Alvetex® Strata this was not completely prevented and the proliferation of NPCs has been reported elsewhere to continue within the slices when in culture (Verrill *et al.*, 2002; Vickers *et al.*, 2004). This limits the effectiveness of using viability as a measure of tissue slice health due to the potential loss of viability of parenchymal cells being masked by the increasing levels of non-parenchymal cells. Using an oxygenation system in tandem with the bioreactor further improved slice viability however, due to low throughput of the oxygenation system, no further measures of slice health were taken to examine any beneficial effects on the hepatocytes.

Models investigating the use of antifibrotic agents have shown that the spontaneous activation of hepatic stellate cells can be slowed with the use of these compounds (van de Bovenkamp *et al.*, 2008). Similarly, profibrotic drugs can be used to speed up the fibrotic process, allowing these slices to be used as a platform for studying fibrotic pathways and further testing antifibrotic drugs (van de Bovenkamp *et al.*, 2006; Luangmonkong *et al.*, 2017).

In the system developed in this work a high level of variability was found between slices which made any comparison between slices treated with profibrotic compounds and untreated slices difficult. The limited apparatus to produce slices is likely to be one of the causes of this variability, with studies in literature typically using a Krumdieck slicer (Gore *et al.*, 2019) or vibratomes with significantly higher blade oscillation amplitudes and consequently much more effective cutting ability (Wu *et al.*, 2018; Paish *et al.*, 2019). If this high variability could be overcome, then the bioreactor could prove to be a very effective system for disease modelling and drug testing.

8.3. Future Directions

The experiments carried out in this work demonstrate the potential for such a system to improve the physiological relevance of *in vitro* and *ex vivo* tissue models and make cell culture a step closer to accurate recapitulation of the *in vivo* microenvironment. The work presented here leads to a range of further studies which could be performed to increase the utility of the system and lead to even more effective tissue models.

8.3.1. Recreating the model with alternative hepatocyte sources

The HepG2 cell line has been very effective in this work for investigating the potential applications of the novel bioreactor system for recapitulating the liver microenvironment. The limitations with HepG2 cell lines discussed previously mean that their phenotype can only be improved to a certain extent before reaching a point at which the remaining shortcomings cannot be overcome through increasingly complex culture techniques.

Two major sources of hepatocytes could be investigated for further use with this system to lead to a more effective liver model. The first of these are primary hepatocytes. For a system of this scale, primary hepatocytes can be problematic due to the high cost and low yield of the cells however the benefits of these cells would be immense. Primary hepatocytes express the full complement of proteins as are present *in vivo* and can be tailored to individual patients. This would further allow investigations into aspects of hepatotoxicity caused by factors such as genetic variations in phase I and II enzyme expression. Culture these cells in the bioreactor system as a monolayer, supported by ECM or fibroblasts, could be a possibility to overcome the large quantities of cells typically needed for 3D culture methods which would be a limiting factor for primary hepatocytes in tissue equivalents of this scale.

A second alternative would be the HepaRG cell line. These are generally regarded as being the cell line which bears the most similarity to primary hepatocytes (Gerets *et al.*, 2012), whilst maintaining the ease of subculturing and proliferative capacity of immortalised cell lines (Gripon *et al.*, 2002). These cells exist as bipotent hepatic progenitor cells and can be differentiation into either hepatocyte-like or biliary-like cells (Cerec *et al.*, 2007). This allows the more complex liver microenvironment to be studied with these, representing parenchyma of both the biliary and hepatocyte regions as would be found *in vivo* in the liver. The high levels of expression of a wide range of phase I and II enzymes (Aninat *et al.*, 2006; Guillouzo *et al.*, 2007), a full complement of

apical and basolateral transporters (Le Vee *et al.*, 2006) and improved urea cycle function (Moedas *et al.*, 2017) are all advantages that these cells have over HepG2 and would therefore make them ideal as a replacement for these models.

8.3.2. Including the full range of liver cell types

Two cell types were tested in the models alongside the HepG2 cells in this work: dermal fibroblasts and liver sinusoidal endothelial cells. These demonstrated the potential for creating co-cultures with complex patterning and high viability using the bioreactor system however can be of limited physiological relevance. Fibroblasts are heavily used in literature to support the growth of hepatocytes *in vitro* (Fry and Bridges, 1977; Cho *et al.*, 2010; Novik *et al.*, 2017; Sakai *et al.*, 2018), however are present in only limited numbers in regions of the liver such as the portal tract (Lavoie *et al.*, 2005). Although endothelial cells account for a large proportion of cells in the liver, they would typically be separated from direct contact with hepatocytes by the space of Disse and its component ECM and stellate cells (Sörensen *et al.*, 2015). As such there are several additional options for cells which could be incorporated into future models in this system to further increase the functionality and create more physiologically relevant tissue architecture.

8.3.2.1. Stellate cells

Stellate cells play an important role in liver homeostasis and are a major component of the response to livery injury (Fujita and Narumiya, 2016). Incorporating them into the *in vitro* liver models could have a significant impact on the applications of the models and greatly increase physiological relevance of the models. Whilst stellate cells have been shown to be beneficial for hepatocytes in culture (Thomas *et al.*, 2005), their role in disease pathways is also an advantage of their use. Diseases such as fibrosis could be modelled *in vitro* with functional stellate cells incorporated into the models, something which is not easily possibly with many models containing hepatocytes alone whilst such co-culture models have rarely been successfully created (van Grunsven, 2017).

To maintain the use of simple and readily available cell lines there are currently available immortalised stellate cell lines which could be used for this purpose. The LX-2 cell line shows the most promise for this function, being readily grown in a variety of media and displaying many functional markers of primary hepatic stellate cells (Castilho-Fernandes *et al.*, 2011). Whilst few studies have incorporated these cells into co-culture with hepatocytes, one study has found promising results in a co-culture model when exposed to viruses (Akil *et al.*, 2019). Such cells could

be incorporated into the dynamic models in this work as an alternative to the dermal fibroblasts used at present, creating endogenous liver-specific ECM, and providing a supporting structure for hepatocytes to be cultured on.

8.3.2.2. Kupffer cells

As with stellate cells, incorporation of Kupffer cells would allow for a broader range of disease models to be created. Many diseases are immune-mediated and Kupffer cells play a role in many inflammatory pathways in the liver (Kolios, Valatas and Kouroumalis, 2006; Dixon *et al.*, 2016). Further to this, diseases such as hepatitis B virus could be probed with such a model, allowing an effective platform for the study of a disease which, at present, has very limited treatment options (Rajbhandari and Chung, 2016).

Potential cell lines for use in cell culture are limited with no immortalised human cell lines of Kupffer cells current available, though work has been carried out to successfully immortalise mouse Kupffer cells (Kitani *et al.*, 2014). Primary Kupffer cells are readily available, though limited in number due to minimal proliferative capacity *in vitro*. These are often used in literature and several models have successfully shown benefits to DILI predictivity and disease modelling when using such co-culture models (Nguyen *et al.*, 2015; Sarkar *et al.*, 2015; Li *et al.*, 2020).

8.3.2.3. Patterned co-cultures containing all major NPCs

While many improvements have been seen with co-culture of hepatocytes and other NPCs, to truly maximise the physiological relevance of a model all these NPCs should be incorporated into the same model. Models incorporating a range of cell types have typically used isolated NPCs added to hepatocytes, which limits the control over both the proportions of different NPCs and the patterning of the cells (Drucker *et al.*, 2006; Baze *et al.*, 2018). A couple of models incorporating these cells at defined ratios on 3D membranes have been created which show high levels of cellular organisation and suggest that this could be used in a more complex bioreactor model (Bale *et al.*, 2016; Ahmed *et al.*, 2017). The Alvetex-based system developed in this work would allow for such organisation to be developed in dynamic culture, creating distinct layers for stellate cells, hepatocytes, endothelial cells and Kupffer cells, and would be of significant interest for future research.

8.3.3 Utility of the bioreactor system for recreation of other tissues

Whilst the research carried out herein has focused on the applications of the bioreactor system for modelling the liver, the limitations of conventional *in vitro* culture methods apply to all tissues. Further research could investigate the use of the bioreactor system in other tissues to investigate whether the application of fluid flow can enhance the structure and function of these.

Research has already been carried out with fluid flow for a range of tissue models. For epidermal and full-thickness models of the skin, many papers have shown beneficial impacts of fluid flow such as an increase in epidermal thickness and barrier function (Lee *et al.*, 2017; Sriram *et al.*, 2018) as well as an upregulation in tight junction proteins such as claudin 1 and occludin (Strüver, Friess and Hedtrich, 2017). Studies have also investigated dynamic models of the intestine. With the addition of fluid flow, the Caco-2 cell line was found to have an improved morphology more closely related to primary enterocytes than in static culture whilst the active transport across the monolayer was also increased (Pusch *et al.*, 2011; Deng *et al.*, 2013). Similarly, bioreactors have also been shown to improve CYP3A4 and MDR1 levels in models using primary enterocytes (Schweinlin *et al.*, 2016). For renal organoids, fluid flow has been shown to accelerate the organisation of epithelial cells, whilst models of the proximal tubule have demonstrated the utility of such systems for the study of renal reabsorption of solutes (Homan *et al.*, 2016; Lin *et al.*, 2019).

These examples demonstrate some of the many potential applications that the novel bioreactor system could have for improvement of *in vitro* models of other organs. It could therefore play a major role as a low-cost, simple, and effective platform for reproducible production of physiologically relevant tissue equivalents.

8.4. Conclusion

In this thesis, the development of a novel stirred, 3D culture bioreactor was performed with an aim to overcome some of the limitations of conventional static culture. Using magnetic stirrer-based technology it was possible to create a low cost, easy to use and small-scale bioreactor which could effectively create a dynamic environment for 3D cell culture. This system was testing using a liver model based around the HepG2 hepatocellular carcinoma cell line. Initial characterisation showed some beneficial impacts of the bioreactor, such as increased localisation of some transporter proteins and enhanced expression of a range of drug metabolism genes. Testing this system with toxicological challenge demonstrated similar levels of sensitivity to 3D cell culture for a lot of drugs, with some showing increased sensitivity. The flexibility of this system allowed further cell lines to be incorporated to create a more physiologically relevant system. Finally, the system was tested for its ability to support precision-cut liver slices, which it appeared to be capable of over short time periods. Future work with this bioreactor system will aim to further improve liver models with use of cell lines with greater functionality whilst models for other organs could also be created within the bioreactor syste

Chapter 9: Bibliography

Chapter 9: Bibliography

3D Biotek Bioreactor System (2021). Available at: https://www.sigmaaldrich.com/labware/labware-products.html?TablePage=106837632 (Accessed: 26 March 2021).

3DKUBE by Kiyatec (2021). Available at: https://www.sigmaaldrich.com/labware/labware-products.html?TablePage=9572935 (Accessed: 26 March 2021).

Abdel-Misih, S. R. Z. and Bloomston, M. (2014) 'Liver Anatomy', *Surgical Clinics of North America*, 90(4), pp. 643–653. doi: 10.1016/j.suc.2010.04.017.Liver.

Abu-Absi, S. F. *et al.* (2002) 'Structural polarity and functional bile canaliculi in rat hepatocyte spheroids.', *Experimental cell research*, 274(1), pp. 56–67. doi: 10.1006/excr.2001.5467.

Abu-Absi, S. F., Hansen, L. K. and Hu, W. S. (2004) 'Three-dimensional co-culture of hepatocytes and stellate cells', *Cytotechnology*, 45(3), pp. 125–140. doi: 10.1007/s10616-004-7996-6.

Adam, A. A. A. *et al.* (2018) 'A practice-changing culture method relying on shaking substantially increases mitochondrial energy metabolism and functionality of human liver cell lines', *PLoS ONE*, 13(4), pp. 1–19. doi: 10.1371/journal.pone.0193664.

Aden, D. P. *et al.* (1979) 'Controlled synthesis of HBsAg in a differentiated human liver carcinoma-derived cell line', *Nature*, 282(5739), pp. 615–616. doi: 10.1038/282615a0.

Ahmed, H. M. M. *et al.* (2017a) '3D liver membrane system by co-culturing human hepatocytes, sinusoidal endothelial and stellate cells', *Biofabrication*, 9(2). doi: 10.1088/1758-5090/aa70c7.

Ahmed, H. M. M. *et al.* (2017b) '3D liver membrane system by co-culturing human hepatocytes, sinusoidal endothelial and stellate cells', *Biofabrication*, 9(2). doi: 10.1088/1758-5090/aa70c7.

Ahmed, S. *et al.* (2019) 'New generation of bioreactors that advance extracellular matrix modelling and tissue engineering', *Biotechnology Letters*, 41(1), pp. 1–25. doi: 10.1007/s10529-018-2611-7.

Ahn, J. *et al.* (2019) 'Human three-dimensional in vitro model of hepatic zonation to predict zonal hepatotoxicity', *Journal of Biological Engineering*, 13(1), pp. 1–15. doi: 10.1186/s13036-019-0148-5.

Akil, A. *et al.* (2019) 'Fibrogenic Gene Expression in Hepatic Stellate Cells Induced by HCV and HIV Replication in a Three Cell Co-Culture Model System', *Scientific Reports*, 9(1), pp. 1–12. doi: 10.1038/s41598-018-37071-y.

Akram, K. M. *et al.* (2019) 'Live imaging of alveologenesis in precision-cut lung slices reveals dynamic epithelial cell behaviour', *Nature Communications*, 10(1). doi: 10.1038/s41467-019-09067-3.

Albrecht, W. *et al.* (2019) 'Prediction of human drug-induced liver injury (DILI) in relation to oral doses and blood concentrations', *Archives of Toxicology*, 93(6), pp. 1609–1637. doi: 10.1007/s00204-019-02492-9.

Allen, C. B., Schneider, B. K. and White, C. W. (2001) 'Limitations to oxygen diffusion and equilibration in in vitro cell exposure systems in hyperoxia and hypoxia', *American Journal of Physiology-Lung Cellular and Molecular Physiology*, 281, pp. 1021–1027.

Allen, J. W. and Bhatia, S. N. (2003) 'Formation of steady-state oxygen gradients in vitro: Application to liver zonation', *Biotechnology and Bioengineering*, 82(3), pp. 253–262. doi: 10.1002/bit.10569.

Allen, J. W., Khetani, S. R. and Bhatia, S. N. (2005) 'In vitro zonation and toxicity in a hepatocyte bioreactor', *Toxicological Sciences*, 84(1), pp. 110–119. doi: 10.1093/toxsci/kfi052.

Altmann, B. *et al.* (2008) 'The three-dimensional cultivation of the carcinoma cell line HepG2 in a perfused chip system leads to a more differentiated phenotype of the cells compared to monolayer culture.', *Biomedical materials*, 3(3), p. 034120. doi: 10.1088/1748-6041/3/3/034120.

Amann, T. *et al.* (2009) 'Activated hepatic stellate cells promote tumorigenicity of hepatocellular carcinoma', *Cancer Science*, 100(4), pp. 646–653. doi: 10.1111/j.1349-7006.2009.01087.x.

Ammar, A., Lagenaur, C. and Jannetta, P. (1990) 'Neural tissue compatibility of Teflon as an implant material for microvascular decompression', *Neurosurgical Review*, 13(4), pp. 299–303. doi: 10.1007/BF00346368.

Chapter 9: Bibliography

Aninat, C. *et al.* (2006) 'EXPRESSION OF CYTOCHROMES P450, CONJUGATING ENZYMES AND NUCLEAR RECEPTORS IN HUMAN HEPATOMA HepaRG CELLS', *Drug Metabolism and Disposition*, 34(1), pp. 75–83. doi: 10.1124/dmd.105.006759.

Annamalai, R. T. and Matthew, H. W. T. (2019) 'Transport Analysis of Engineered Liver Tissue Fabricated Using a Capsule-Based, Modular Approach', *Annals of Biomedical Engineering*, 47(5), pp. 1223–1236. doi: 10.1007/s10439-018-02192-y.

Arias, I. M. *et al.* (1993) 'The biology of the bile canaliculus', *Hepatology (Baltimore, Md.)*, 17(2), pp. 318–29. doi: 10.1002/hep.1840170225.

Arterburn, L. M. *et al.* (1995) 'A morphological study of differentiated hepatocytes in vitro', *Hepatology*, 22(1), pp. 175–187. doi: 10.1016/0270-9139(95)90371-2.

Assunção, M. *et al.* (2020) 'Cell-Derived Extracellular Matrix for Tissue Engineering and Regenerative Medicine', *Frontiers in Bioengineering and Biotechnology*, 8(December), pp. 1–10. doi: 10.3389/fbioe.2020.602009.

Astashkina, A., Mann, B. and Grainger, D. W. (2012) 'A critical evaluation of in vitro cell culture models for high-throughput drug screening and toxicity', *Pharmacology and Therapeutics*, 134(1), pp. 82–106. doi: 10.1016/j.pharmthera.2012.01.001.

Atienzar, F. A. *et al.* (2016) 'Key Challenges and Opportunities Associated with the Use of in Vitro Models to Detect Human Dili: Integrated Risk Assessment and Mitigation Plans', *BioMed Research International*, 2016. doi: 10.1155/2016/9737920.

Attia, S. M. (2010) 'Deleterious effects of reactive metabolites', *Oxidative Medicine and Cellular Longevity*, 3(4), pp. 238–253. doi: 10.4161/oxim.3.4.13246.

Bae, Y. J. *et al.* (2017) 'Enhanced differentiation of mesenchymal stromal cells by three-dimensional culture and azacitidine', *Blood Research*, 52(1), pp. 18–24. doi: 10.5045/br.2017.52.1.18.

Bailey, K. E. *et al.* (2020) 'Embedding of precision-cut lung slices in engineered hydrogel biomaterials supports extended ex vivo culture', *American Journal of Respiratory Cell and Molecular Biology*, 62(1), pp. 14–22. doi: 10.1165/rcmb.2019-0232MA.

Baker, B. M. and Chen, C. S. (2012) 'Deconstructing the third dimension-how 3D culture microenvironments alter cellular cues', *Journal of Cell Science*, 125(13), pp. 3015–3024. doi: 10.1242/jcs.079509.

Bakos, É. and Homolya, L. (2007) 'Portrait of multifaceted transporter, the multidrug resistance-associated protein 1 (MRP1/ABCC1)', *Pflugers Archiv European Journal of Physiology*, 453(5), pp. 621–641. doi: 10.1007/s00424-006-0160-8.

Balakrishnan, S. *et al.* (2015) 'A Scalable Perfusion Culture System with Miniature Peristaltic Pumps for Live-Cell Imaging Assays with Provision for Microfabricated Scaffolds', *BioResearch Open Access*, 4(1), pp. 343–357. doi: 10.1089/biores.2015.0024.

Bale, S. S. *et al.* (2014) 'In Vitro Platforms for Evaluating Liver Toxicity', *Exp Biol Med*, 239(9), pp. 1180–1191. doi: 10.1177/1535370214531872.

Bale, S. S. *et al.* (2016) 'Isolation and co-culture of rat parenchymal and non-parenchymal liver cells to evaluate cellular interactions and response', *Scientific Reports*, 6(January), pp. 1–10. doi: 10.1038/srep25329.

Ball, A. L. *et al.* (2016) 'Identification of the additional mitochondrial liabilities of 2-hydroxyflutamide when compared with its parent compound, flutamide in HepG2 cells', *Toxicological Sciences*, 153(2), pp. 341–351. doi: 10.1093/toxsci/kfw126.

Ballermann, B. J. *et al.* (1998) 'Shear stress and the endothelium', *Kidney International, Supplement*, 54(67), pp. 100–108. doi: 10.1046/j.1523-1755.1998.06720.x.

Ballet, F. (1997) 'Hepatotoxicity in drug development: detection, significance and solutions.', *Journal of*

hepatology, 26 Suppl 2(6), pp. 26–36. doi: 10.1016/S0168-8278(97)80494-1.

Barbetta, A. *et al.* (2005) 'Porous polymers by emulsion templating', *Macromolecular Symposia*, 226, pp. 203–211. doi: 10.1002/masy.200550819.

Barcena-Varela, M. *et al.* (2020) 'Epigenetic mechanisms and metabolic reprogramming in fibrogenesis: Dual targeting of G9a and DNMT1 for the inhibition of liver fibrosis', *Gut*, pp. 1–13. doi: 10.1136/gutjnl-2019-320205.

Barry, P. H. and Diamond, J. M. (1984) 'Effects of unstirred layers on membrane phenomena', *Physiological Reviews*, 64(3), pp. 763–872. Available at: http://physrev.physiology.org/content/64/3/763.abstract.

De Bartolo, L. *et al.* (2009) 'Human hepatocyte functions in a crossed hollow fiber membrane bioreactor', *Biomaterials*, 30(13), pp. 2531–2543. doi: 10.1016/j.biomaterials.2009.01.011.

Bartolo, L. De (2015) 'Hollow Fiber Membrane Bioreactor for Cell Growth', in *Encyclopedia of Membranes*. doi: 10.1007/978-3-642-40872-4.

Bataller, R. and Brenner, D. (2005) 'Liver fibrosis', *The journal of clinical investigation*, 115(2), pp. 209–218. doi: 10.1172/JCI200524282.The.

Baudoin, R. *et al.* (2007) 'Trends in the development of microfluidic cell biochips for in vitro hepatotoxicity', *Toxicology in Vitro*, 21(4), pp. 535–544. doi: 10.1016/j.tiv.2006.11.004.

Baudoin, R. *et al.* (2011) 'Behavior of HepG2/C3A cell cultures in a microfluidic bioreactor', *Biochemical Engineering Journal*, 53(2), pp. 172–181. doi: 10.1016/j.bej.2010.10.007.

Baudoin, R. *et al.* (2012) 'Parallelized microfluidic biochips in multi well plate applied to liver tissue engineering', *Sensors and Actuators, B: Chemical*, 173, pp. 919–926. doi: 10.1016/j.snb.2012.06.050.

Baze, A. *et al.* (2018) 'Three-Dimensional Spheroid Primary Human Hepatocytes in Monoculture and Coculture with Nonparenchymal Cells', *Tissue Engineering - Part C: Methods*, 24(9), pp. 534–545. doi: 10.1089/ten.tec.2018.0134.

Bell, C. C. *et al.* (2018) 'Comparison of hepatic 2D sandwich cultures and 3d spheroids for long-term toxicity applications: A multicenter study', *Toxicological Sciences*, 162(2), pp. 655–666. doi: 10.1093/toxsci/kfx289.

Bender, V., Büschlen, S. and Cassio, D. (1998) 'Expression and localization of hepatocyte domain-specific plasma membrane proteins in hepatoma x fibroblast hybrids and in hepatoma dedifferentiated variants.', *Journal of cell science*, 111 (Pt 2, pp. 3437–3450.

Bergemann, C. *et al.* (2015) 'Cellular Nutrition in Complex Three-Dimensional Scaffolds: A Comparison between Experiments and Computer Simulations', *International Journal of Biomaterials*, 2015. doi: 10.1155/2015/584362.

Berginc, K. and Kristl, A. (2011) 'Transwell-Grown HepG2 Cell Monolayers as *In Vitro* Permeability Model to Study Drug–Drug or Drug–Food Interactions', *Journal of Medicinal Food*, 14(1–2), pp. 135–139. doi: 10.1089/jmf.2010.0041.

Berthiaume, F. *et al.* (1996) 'Effect of extracellular matrix topology on cell structure, function, and physiological responsiveness: hepatocytes cultured in a sandwich configuration.', *FASEB journal*, 10(13), pp. 1471–84. Available at: http://www.ncbi.nlm.nih.gov/pubmed/8940293.

Berthier, E. *et al.* (2008) 'Managing evaporation for more robust microscale assays: Part 1. Volume loss in high throughput assays', *Lab on a Chip*, 8(6), pp. 852–859. doi: 10.1039/b717422e.

Bessems, M. *et al.* (2006) 'The isolated perfused rat liver: Standardization of a time-honoured model', *Laboratory Animals*, 40(3), pp. 236–246. doi: 10.1258/002367706777611460.

Bethesda (MD): National Institute of Diabetes and Digestive and Kidney Diseases (2021a) *Indomethacin*, *LiverTox: Clinical and Research Information on Drug-Induced Liver Injury*.

Bethesda (MD): National Institute of Diabetes and Digestive and Kidney Diseases (2021b) *Tamoxifen*, *LiverTox: Clinical and Research Information on Drug-Induced Liver Injury*. Available at: https://www.ncbi.nlm.nih.gov/books/NBK548902/ (Accessed: 9 March 2021).

Bhandari, R. N. B. *et al.* (2001) 'Liver Tissue Engineering: A Role for Co-culture Systems in Modifying Hepatocyte Function and Viability', *Tissue Engineering*, 7(3), pp. 345–357. doi: 10.1089/10763270152044206.

Bhardwaj, N., Singh, Y. P. and Mandal, B. B. (2019) 'Silk Fibroin Scaffold-Based 3D Co-Culture Model for Modulation of Chondrogenesis without Hypertrophy via Reciprocal Cross-talk and Paracrine Signaling', *ACS Biomaterials Science and Engineering*, 5(10), pp. 5240–5254. doi: 10.1021/acsbiomaterials.9b00573.

Bhatia, S. N. *et al.* (1999) 'Effect of cell-cell interactions in preservation of cellular phenotype: Cocultivation of hepatocytes and nonparenchymal cells', *FASEB Journal*, 13(14), pp. 1883–1900. doi: 10.1096/fasebj.13.14.1883.

Bhushan, A. *et al.* (2013) 'Towards a three-dimensional microfluidic liver platform for predicting drug efficacy and toxicity in humans', *Stem Cell Research and Therapy*, 4(SUPPL.1), pp. 2–7. doi: 10.1186/scrt377.

Bibi, Z. (2008) 'Role of cytochrome P450 in drug interactions', *Nutrition and Metabolism*, 5(1), pp. 1–10. doi: 10.1186/1743-7075-5-27.

Bicer, M., Cottrell, G. S. and Widera, D. (2021) 'Impact of 3D cell culture on bone regeneration potential of mesenchymal stromal cells', *Stem Cell Research and Therapy*, 12(1), pp. 1–13. doi: 10.1186/s13287-020-02094-8.

Bigaeva, E. *et al.* (2019) *Transcriptomic characterization of culture-associated changes in murine and human precision-cut tissue slices*, *Archives of Toxicology*. Springer Berlin Heidelberg. doi: 10.1007/s00204-019-02611-6.

Biles, J. E. *et al.* (1997) 'Determination of Bisphenol-A in Reusable Polycarbonate Food-Contact Plastics and Migration to Food-Simulating Liquids', *Journal of Agricultural and Food Chemistry*, 45(9), pp. 3541–3544. doi: 10.1021/jf970072i.

Billiar, T. R. *et al.* (1989) 'Kupffer Cell Cytotoxicity to Hepatocytes in Coculture Requires L-Arginine', *The Archives of Surgery*, 124(12), pp. 1416–1421.

Bilzer, M., Roggel, F. and Gerbes, A. L. (2006) 'Role of Kupffer cells in host defense and liver disease', *Liver International*, 26(10), pp. 1175–1186. doi: 10.1111/j.1478-3231.2006.01342.x.

BioIVT (2021) *HEPATOPAC Technology*. Available at: https://bioivt.com/about/technologies/hepatopactechnology (Accessed: 31 March 2021).

Bircsak, K. M. *et al.* (2021) 'A 3D microfluidic liver model for high throughput compound toxicity screening in the OrganoPlate®', *Toxicology*, 450(January), p. 152667. doi: 10.1016/j.tox.2020.152667.

Bissell, D. M., Arenson, D. M., *et al.* (1987) 'Support of cultured hepatocytes by a laminin-rich gel. Evidence for a functionally significant subendothelial matrix in normal rat liver', *Journal of Clinical Investigation*, 79(3), pp. 801–812. doi: 10.1172/JCI112887.

Bissell, D. M., Arenson, D M, *et al.* (1987) 'Support of cultured hepatocytes by a laminin-rich gel', *The Journal of clinical investigation*, 79(3), pp. 801–12. Available at: http://www.pubmedcentral.nih.gov/articlerender.fcgi?artid=424203&tool=pmcentrez&rendertype=abstract.

Bojesen, I. N. and Hansen, H. S. (2006) 'Effect of an unstirred layer on the membrane permeability of anandamide', *Journal of Lipid Research*, 47, pp. 561–570. doi: 10.1016/S0376-7388(00)82169-9.

Bokhari, M., Carnachan, R. J., Cameron, N. R., *et al.* (2007a) 'Culture of HepG2 liver cells on three dimensional polystyrene scaffolds enhances cell structure and function during toxicological challenge', *Journal of Anatomy*, 211(4), pp. 567–576. doi: 10.1111/j.1469-7580.2007.00778.x.

Bokhari, M., Carnachan, R. J., Przyborski, S. A., *et al.* (2007) 'Emulsion-templated porous polymers as scaffolds

for three dimensional cell culture: Effect of synthesis parameters on scaffold formation and homogeneity', *Journal of Materials Chemistry*, 17(38), pp. 4088–4094. doi: 10.1039/b707499a.

Bokhari, M., Carnachan, R. J., Cameron, N. R., *et al.* (2007b) 'Novel cell culture device enabling three-dimensional cell growth and improved cell function', *Biochemical and Biophysical Research Communications*, 354(4), pp. 1095–1100. doi: 10.1016/j.bbrc.2007.01.105.

Borst, P. *et al.* (2000) 'A family of drug transporters: The multidrug resistance-associated proteins', *Journal of the National Cancer Institute*, 92(16), pp. 1295–1302. doi: 10.1093/jnci/92.16.1295.

Bouchagier, K. A. *et al.* (2014) 'Expression of claudins-1, -4, -5, -7 and occludin in hepatocellular carcinoma and their relation with classic clinicopathological features and patients' survival', *In Vivo*, 28(3), pp. 315–326.

de Bournonville, S. *et al.* (2019) 'Towards Self-Regulated Bioprocessing: A Compact Benchtop Bioreactor System for Monitored and Controlled 3D Cell and Tissue Culture', *Biotechnology Journal*, 14(7). doi: 10.1002/biot.201800545.

Bouwens, L. *et al.* (1992) 'Liver Cell Heterogeneity: Functions of Non-Parenchymal Cells', *Enzyme*, 46, pp. 155–168.

van de Bovenkamp, M. *et al.* (2005) 'Precision-cut liver slices as a new model to study toxicity-induced hepatic stellate cell activation in a physiologic milieu', *Toxicological Sciences*, 85(1), pp. 632–638. doi: 10.1093/toxsci/kfi127.

van de Bovenkamp, M. *et al.* (2006) 'Precision-cut fibrotic rat liver slices as a new model to test the effects of anti-fibrotic drugs in vitro', *Journal of Hepatology*, 45(5), pp. 696–703. doi: 10.1016/j.jhep.2006.04.009.

van de Bovenkamp, M. *et al.* (2008) 'Liver slices as a model to study fibrogenesis and test the effects of anti-fibrotic drugs on fibrogenic cells in human liver', *Toxicology in Vitro*, 22(3), pp. 771–778. doi: 10.1016/j.tiv.2007.11.019.

Bovenkamp, M. Van De *et al.* (2007) 'Liver fibrosis in vitro : Cell culture models and precision-cut liver slices', *Toxicology in Vitro*, 21, pp. 545–557. doi: 10.1016/j.tiv.2006.12.009.

Boyer, J. L. (2013) 'Bile Formation and Secretion', *Compr Physiol.*, 3(3), pp. 1035–1078. doi: 10.1002/cphy.c120027.Bile.

Brauer, R. W. (1963) 'Liver Circulation and Function', *Physiological Reviews*, 43, pp. 115–213.

Breslin, S. and O'Driscoll, L. (2016) 'The relevance of using 3D cell cultures, in addition to 2D monolayer cultures, when evaluating breast cancer drug sensitivity and resistance', *Oncotarget*, 7(29), pp. 45745–45756. doi: 10.18632/oncotarget.9935.

Brill, S. *et al.* (2002) 'The role of fetal and adult hepatocyte extracellular matrix in the regulation of tissue-specific gene expression in fetal and adult hepatocytes', *European Journal of Cell Biology*, 81(1), pp. 43–50. doi: 10.1078/0171-9335-00200.

Brophy, C. M. *et al.* (2009) 'Rat hepatocyte spheroids formed by rocked technique maintain differentiated hepatocyte gene expression and function', *Hepatology*, 49(2), pp. 578–586. doi: 10.1002/hep.22674.Rat.

De Bruyn, T. *et al.* (2013) 'Sandwich-cultured hepatocytes: utility for *in vitro* exploration of hepatobiliary drug disposition and drug-induced hepatotoxicity', *Expert Opinion on Drug Metabolism & Toxicology*, 9(5), pp. 589–616. doi: 10.1517/17425255.2013.773973.

Bryson, K. J. *et al.* (2020) 'Precision cut lung slices: A novel versatile tool to examine host-pathogen interaction in the chicken lung', *Veterinary Research*, 51(1), pp. 1–16. doi: 10.1186/s13567-019-0733-0.

Bual, R. P. and Ijima, H. (2019) 'Intact extracellular matrix component promotes maintenance of liver-specific functions and larger aggregates formation of primary rat hepatocytes', *Regenerative Therapy*, 11, pp. 258–268. doi: 10.1016/j.reth.2019.08.006.

Buggey, J. *et al.* (2015) 'Amiodarone-induced liver injury and cirrhosis', *ACG Case Reports Journal*, 2(2), pp.

116–118. doi: 10.14309/crj.2015.23.

Burkard, A. *et al.* (2012) 'Generation of proliferating human hepatocytes using upcyte® technology: characterisation and applications in induction and cytotoxicity assays', *Xenobiotica*, 42(10), pp. 939–956. doi: 10.3109/00498254.2012.675093.

Burt, A. D. and Day, C. P. (2002) 'Pathophysiology of the Liver', in MacSween, R. N. M. et al. (eds) *Pathology of the Liver*. New York: Churchill Livingstone, pp. 67–105.

Burt, A. D., Ferrell, L. D. and Hubscher, S. G. (2017) *MacSween's Pathology of the Liver*. 7th edn, *Journal of Chemical Information and Modeling*. 7th edn. Edited by A. D. Burt, L. D. Ferrell, and S. G. Hubscher. Philadelphia, PA: Elsevier. doi: 10.1017/CBO9781107415324.004.

Busche, M. *et al.* (2020) 'HepaChip-MP-a twenty-four chamber microplate for a continuously perfused liver coculture model', *Lab on a Chip*, 20(16), pp. 2911–2926. doi: 10.1039/d0lc00357c.

Caliari, S. R. and Burdick, J. A. (2016) 'A Practical Guide to Hydrogels for Cell Culture', *Nature Methods*, 13(5), pp. 404–414. doi: 10.25260/ea.16.26.1.0.106.

Cambria, E. *et al.* (2020) 'Cell-Laden Agarose-Collagen Composite Hydrogels for Mechanotransduction Studies', *Frontiers in Bioengineering and Biotechnology*, 8(April), pp. 1–14. doi: 10.3389/fbioe.2020.00346.

Caneparo, C. *et al.* (2020) 'Conditioned medium produced by fibroblasts cultured in low oxygen pressure allows the formation of highly structured capillary-like networks in fibrin gels', *Scientific Reports*, 10(1), pp. 1–11. doi: 10.1038/s41598-020-66145-z.

Carmeliet, P. and Jain, R. K. (2000) 'Angiogenesis in cancer and other diseases.', *Nature*, 407, pp. 249–257. doi: 10.1038/35025220.

Carnachan, R. J. *et al.* (2006) 'Tailoring the morphology of emulsion-templated porous polymers.', *Soft Matter*, pp. 608–616. doi: 10.1039/b603211g.

Carrel, A. and Burrows, M. T. (1911) 'An addition to the technique of the cultivation of tissues in vitro', *Journal of Experimental Medicine*, 14(3), pp. 244–247.

Casteleijn, E. *et al.* (1988) 'Conditioned media of Kupffer and endothelial liver cells influence protein phosphorylation in parenchymal liver cells. Involvement of prostaglandins', *Biochemical Journal*, 252(2), pp. 601–605. doi: 10.1042/bj2520601.

Castell, J. V *et al.* (2006) 'Hepatocyte cell lines: their use, scope and limitations in drug metabolism studies', *Expert Opinion on Drug Metabolism & Toxicology*, 2(2), pp. 183–212. doi: 10.1517/17425255.2.2.183.

Castilho-Fernandes, A. *et al.* (2011) 'Human hepatic stellate cell line (LX-2) exhibits characteristics of bone marrow-derived mesenchymal stem cells', *Experimental and Molecular Pathology*, 91(3), pp. 664–672. doi: 10.1016/j.yexmp.2011.09.002.

Centeno, E. G. Z., Cimarosti, H. and Bithell, A. (2018) '2D versus 3D human induced pluripotent stem cell-derived cultures for neurodegenerative disease modelling', *Molecular Neurodegeneration*, 13(1), pp. 1–15. doi: 10.1186/s13024-018-0258-4.

Cerec, V. *et al.* (2007) 'Transdifferentiation of hepatocyte-like cells from the human hepatoma hepaRG cell line through bipotent progenitor', *Hepatology*, 45(4), pp. 957–967. doi: 10.1002/hep.21536.

Chan, R. and Benet, L. Z. (2018a) 'Evaluation of the relevance of DILI predictive hypotheses in early drug development: Review of: In vitro methodologies vs. BDDCS classification', *Toxicology Research*, 7(3), pp. 358–370. doi: 10.1039/c8tx00016f.

Chan, R. and Benet, L. Z. (2018b) 'Measures of BSEP inhibition in vitro are not useful predictors of DILI', *Toxicological Sciences*, 162(2), pp. 499–508. doi: 10.1093/toxsci/kfx284.

Chanet, S. and Martin, A. C. (2014) 'Mechanical force sensing in tissues', *Progress in Molecular Biology and Translational Science*, 126, pp. 317–352. doi: 10.1016/B978-0-12-394624-9.00013-0.

Chang, T. T. and Hughes-Fulford, M. (2009) 'Monolayer and spheroid culture of human liver hepatocellular carcinoma cell line cells demonstrate distinct global gene expression patterns and functional phenotypes.', *Tissue engineering. Part A*, 15(3), pp. 559–567. doi: 10.1089/ten.tea.2007.0434.

Chapman, K. A. *et al.* (2016) 'Recapitulation of metabolic defects in a model of propionic acidemia using patient-derived primary hepatocytes', *Molecular Genetics and Metabolism*, 117(3), pp. 355–362. doi: 10.1016/j.ymgme.2015.12.008.

Charni-Natan, M. *et al.* (2019) 'Liver and steroid hormones-can a touch of p53 make a difference?', *Frontiers in Endocrinology*, 10(JUN), pp. 1–9. doi: 10.3389/fendo.2019.00374.

Chen, H. L. *et al.* (1998) 'Long-term culture of hepatocytes from human adults', *Journal of Biomedical Science*, 5(6), pp. 435–440. doi: 10.1007/BF02255932.

Chen, L. *et al.* (2014) 'OCT1 is a high-capacity thiamine transporter that regulates hepatic steatosis and is a target of metformin', *Proceedings of the National Academy of Sciences of the United States of America*, 111(27), pp. 9983–9988. doi: 10.1073/pnas.1314939111.

Chen, Minjun *et al.* (2014) 'A testing strategy to predict risk for drug-induced liver injury in humans using high-content screen assays and the "rule-of-two" model', *Archives of Toxicology*, 88(7), pp. 1439–1449. doi: 10.1007/s00204-014-1276-9.

Chen, M *et al.* (2014) 'Toward predictive models for drug-induced liver injury in humans : are we there yet ?', *Biomarkers Med*, 8(2), pp. 201–213. doi: 10.2217/bmm.13.146.

Chen, M. *et al.* (2016) 'DILIrank: the largest reference drug list ranked by the risk for devleoping drug-induced liver injury in humans', *Drug Discovery Today*, 21(4), pp. 648–653.

Chen, M., Borlak, J. and Tong, W. (2016) 'A Model to predict severity of drug-induced liver injury in humans', *Hepatology*, 64(3), pp. 931–940. doi: 10.1002/hep.28678.

Chen, X. *et al.* (2018) 'Mechanical stretch-induced osteogenic differentiation of human jaw bone marrow mesenchymal stem cells (hJBMMSCs) via inhibition of the NF-κB pathway', *Cell Death and Disease*, 9(2). doi: 10.1038/s41419-018-0279-5.

Chen, Y. T. *et al.* (2019) 'The superiority of conditioned medium derived from rapidly expanded mesenchymal stem cells for neural repair', *Stem Cell Research and Therapy*, 10(1), pp. 1–15. doi: 10.1186/s13287-019-1491-7.

Chiang, J. Y. L. (2002) 'Bile acid regulation of gene expression: roles of nuclear hormone receptors.', *Endocrine reviews*, 23(4), pp. 443–463. doi: 10.1210/er.2000-0035.

Chiang, J. Y. L. (2013) 'Bile acid metabolism and signaling', *Comprehensive Physiology*, 3(3), pp. 1191–1212. doi: 10.1002/cphy.c120023.

Cho, C. H. *et al.* (2006) 'Oxygen Uptake Rates and Liver-Specific Functions of Hepatocyte and 3T3 Fibroblast Co-Cultures', *Biotechnology and Bioengineering*, 97, pp. 188–199. doi: 10.1002/bit.

Cho, C. H. *et al.* (2008) 'A new technique for primary hepatocyte expansion in vitro', *Biotechnology and Bioengineering*, 101(2), pp. 345–356. doi: 10.1016/j.physbeh.2017.03.040.

Cho, C. H. *et al.* (2010) 'Layered patterning of hepatocytes in co-culture systems using microfabricated stencils', *Biotechniques*, 48(1), pp. 47–52. doi: 10.2144/000113317.Layered.

Cho, S., Wood, A. and Bowlby, M. (2007) 'Brain Slices as Models for Neurodegenerative Disease and Screening Platforms to Identify Novel Therapeutics', *Current Neuropharmacology*, 5(1), pp. 19–33. doi: 10.2174/157015907780077105.

Choi, J. H. *et al.* (2020) 'Microfluidic confinement enhances phenotype and function of hepatocyte spheroids', *American Journal of Physiology - Cell Physiology*, 319(3), pp. C552–C560. doi: 10.1152/ajpcell.00094.2020.

Choi, J. M. *et al.* (2015) 'HepG2 cells as an in vitro model for evaluation of cytochrome P450 induction by

xenobiotics', *Archives of Pharmacal Research*, 38(5), pp. 691–704. doi: 10.1007/s12272-014-0502-6.

Chung, C. and Iwakiri, Y. (2013) 'The lymphatic vascular system in liver diseases: its role in ascites formation.', *Clinical and molecular hepatology*, 19(2), pp. 99–104. doi: 10.3350/cmh.2013.19.2.99.

Chung, T. W. *et al.* (2002) 'Preparation of alginate/galactosylated chitosan scaffold for hepatocyte attachment', *Biomaterials*, 23(14), pp. 2827–2834. doi: 10.1016/S0142-9612(01)00399-4.

Clement, B. *et al.* (1986) 'Cell types involved in collagen and fibronectin production in normal and fibrotic human liver', *Hepatology*, 6(2), pp. 225–234. doi: 10.1002/hep.1840060212.

Collins, P. C., Miller, W. M. and Papoutsakis, E. T. (1998) 'Stirred culture of peripheral and cord blood hematopoietic cells offers advantages over traditional static systems for clinically relevant applications', *Biotechnology and Bioengineering*, 59(5), pp. 534–543. doi: 10.1002/(SICI)1097-0290(19980905)59:5<534::AID-BIT2>3.0.CO;2-B.

Colombo, F. *et al.* (2014) 'Giant lysosomes as a chemotherapy resistance mechanism in hepatocellular carcinoma cells', *PLoS ONE*, 9(12), pp. 1–20. doi: 10.1371/journal.pone.0114787.

Coluccio, M. L. *et al.* (2019) 'Microfluidic platforms for cell cultures and investigations', *Microelectronic Engineering*, 208(November 2018), pp. 14–28. doi: 10.1016/j.mee.2019.01.004.

Cooper, A. J. L. and Hanigan, M. H. (2018) 'Metabolism of Glutathione S -Conjugates : Multiple Pathways', *Comprehensive Toxicology*, pp. 363–406.

Corbett, J. L. and Duncan, S. A. (2019) 'iPSC-Derived Hepatocytes as a Platform for Disease Modeling and Drug Discovery', *Frontiers in Medicine*, 6(November), pp. 1–12. doi: 10.3389/fmed.2019.00265.

Cordero-Espinoza, L. and Huch, M. (2018) 'The balancing act of the liver: tissue regeneration versus fibrosis', *Journal of Clinical Investigation*, 128(1), pp. 85–96. doi: 10.1172/JCI93562.

Coronado, R. E. *et al.* (2017) 'Decellularization and Solubilization of Porcine Liver for Use as a Substrate for Porcine Hepatocyte Culture: Method Optimization and Comparison', *Cell Transplantation*, 26(12), pp. 1840–1854. doi: 10.1177/0963689717742157.

Costantini, D. *et al.* (2019) 'Simulated microgravity promotes the formation of tridimensional cultures and stimulates pluripotency and a glycolytic metabolism in human hepatic and biliary tree stem/progenitor cells', *Scientific Reports*, 9(1), pp. 1–10. doi: 10.1038/s41598-019-41908-5.

Court, M. H. and Greenblatt, D. J. (2000) 'Molecular genetic basis for deficient acetaminophen glucuronidation by cats: UGT1A6 is a pseudogene, and evidence for reduced diversity of expressed hepatic UGT1A isoforms', *Pharmacogenetics*, 10(4), pp. 355–369.

Coward, S. M. *et al.* (2005) 'Proliferation rates of HepG2 cells encapsulated in alginate are increased in a microgravity environment compared with static cultures', *Artificial Organs*, 29(2), pp. 152–158. doi: 10.1111/j.1525-1594.2005.29026.x.

Cox, C. R. *et al.* (2020) 'Current Perspective: 3D Spheroid Models Utilizing Human-Based Cells for Investigating Metabolism-Dependent Drug-Induced Liver Injury', *Frontiers in Medical Technology*, 2(November), pp. 1–22. doi: 10.3389/fmedt.2020.611913.

Crawford, J. M., Bioulac-Sage, P. and Hytiroglou, P. (2018) 'Structure, Function and Responses to Injury', in *MacSween's Pathology of the Liver*, pp. 1–87.

Croce, S. *et al.* (2019) 'A hepatic scaffold from decellularized liver tissue: Food for thought', *Biomolecules*, 9(12), pp. 1–25. doi: 10.3390/biom9120813.

Croft, C. L. *et al.* (2019) 'Organotypic brain slice cultures to model neurodegenerative proteinopathies', *Molecular Neurodegeneration*, 14(1), pp. 1–11. doi: 10.1186/s13024-019-0346-0.

Cukierman, E. *et al.* (2001) 'Taking Cell-Matrix Adhesions to the Third Dimension', *Science*, 294(5547), pp. 1708–1712. doi: 10.1126/science.1064829.

Dambach, D. M., Andrews, B. A. and Moulin, F. (2005) 'New Technologies and Screening Strategies for Hepatotoxicity: UsE of In Vitro Models', *Toxicologic Pathology*, 33(1), pp. 17–26. doi: 10.1080/01926230590522284.

Dao Thi, V. L. *et al.* (2020) 'Stem cell-derived polarized hepatocytes', *Nature Communications*, 11(1). doi: 10.1038/s41467-020-15337-2.

Dar, M. S. *et al.* (2016) 'Terminal regions of β-catenin are critical for regulating its adhesion and transcription functions', *Biochimica et Biophysica Acta - Molecular Cell Research*, 1863(9), pp. 2345–2357. doi: 10.1016/j.bbamcr.2016.06.010.

Darling, N. J. *et al.* (2020) 'Bioengineering Novel in vitro Co-culture Models That Represent the Human Intestinal Mucosa With Improved Caco-2 Structure and Barrier Function', *Frontiers in Bioengineering and Biotechnology*, 8(August), pp. 1–15. doi: 10.3389/fbioe.2020.00992.

Darnell, M. *et al.* (2011) 'Cytochrome P450-Dependent Metabolism in HepaRG Cells Cultured in a Dynamic Three-Dimensional Bioreactor', *Drug Metabolism and Disposition*, 39(7), pp. 1131–1138.

Dash, A. *et al.* (2009) 'Liver tissue engineering in the evaluation of drug safety.', *Expert opinion on drug metabolism & toxicology*, 5(10), pp. 1159–74. doi: 10.1517/17425250903160664.

Dash, A. *et al.* (2013) 'Hemodynamic flow improves rat hepatocyte morphology, function, and metabolic activity in vitro.', *American Journal of Physiology - Cell Physiology*, 304(11), pp. 1053–1063. doi: 10.1152/ajpcell.00331.2012.

Dash, M. *et al.* (2011) 'Chitosan - A versatile semi-synthetic polymer in biomedical applications', *Progress in Polymer Science (Oxford)*, 36(8), pp. 981–1014. doi: 10.1016/j.progpolymsci.2011.02.001.

Davies, E. J. *et al.* (2015) 'Capturing complex tumour biology in vitro: Histological and molecular characterisation of precision cut slices', *Scientific Reports*, 5(December), pp. 1–17. doi: 10.1038/srep17187.

Davis, B. M. *et al.* (2018) 'Automated Closed-System Expansion of Pluripotent Stem Cell Aggregates in a Rocking-Motion Bioreactor', *SLAS Technology*, 23(4), pp. 364–373. doi: 10.1177/2472630318760745.

Dekant, W. (2009) 'The role of biotransformation and bioactivation in toxicity', in Luch, A. (ed.) *Molecular, Clinical and Environmental Toxicology: Volume 1: Molecular Toxicology*. Basel: Birkhäuser Basel, pp. 57–86. doi: 10.1007/978-3-7643-8336-7_3.

Delaine-Smith, R. M., MacNeil, S. and Reilly, G. C. (2012) 'Matrix production and collagen structure are enhanced in two types of osteogenic progenitor cells by a simple fluid shear stress stimulus', *European Cells and Materials*, 24(0), pp. 162–174. doi: 10.22203/eCM.v024a12.

Deng, J. *et al.* (2019) 'A cell lines derived microfluidic liver model for investigation of hepatotoxicity induced by drug-drug interaction', *Biomicrofluidics*, 13(2). doi: 10.1063/1.5070088.

Deng, X. *et al.* (2009) 'Inflammatory stress and idiosyncratic hepatotoxicity: Hints from animal models', *Pharmacological Reviews*, 61(3), pp. 262–282. doi: 10.1124/pr.109.001727.

Deng, X. *et al.* (2013) 'Hollow fiber culture accelerates differentiation of Caco-2 cells', *Applied Microbiology and Biotechnology*, 97(15), pp. 6943–6955. doi: 10.1007/s00253-013-4975-x.

Deng, X. *et al.* (2015) 'Enhanced liver functions of HepG2 cells in the alginate/xyloglucan scaffold', *Biotechnology Letters*, 37(1), pp. 235–240. doi: 10.1007/s10529-014-1663-6.

DeQuach, J. A. *et al.* (2010) 'Simple and high yielding method for preparing tissue specific extracellular matrix coatings for cell culture', *PLoS ONE*, 5(9), pp. 1–11. doi: 10.1371/journal.pone.0013039.

Dewyse, L., Reynaert, H. and van Grunsven, L. A. (2021) 'Best practices and progress in precision-cut liver slice cultures', *International Journal of Molecular Sciences*, 22(13), pp. 1–18. doi: 10.3390/ijms22137137.

Dich, J. and Grunnet, N. (1992) 'A perifusion system for cultured hepatocytes', *Analytical Biochemistry*, 206(1), pp. 68–72. doi: 10.1016/S0003-2697(05)80012-0.

DiMasi, J. A., Grabowski, H. G. and Hansen, R. W. (2016) 'Innovation in the pharmaceutical industry: New estimates of R&D costs', *Journal of Health Economics*, 47, pp. 20–33. doi: 10.1016/j.jhealeco.2016.01.012.

DiMasi, J. a (2002) 'The value of improving the productivity of the drug development process: faster times and better decisions.', *PharmacoEconomics*, 20 Suppl 3, pp. 1–10. doi: 10.2165/00019053-200220003-00001.

Dini, L. and Abbro, L. (2005) 'Bioeffects of moderate-intensity static magnetic fields on cell cultures', *Micron*, 36(3), pp. 195–217. doi: 10.1016/j.micron.2004.12.009.

Dionne, K. R. and Tyler, K. L. (2013) 'Slice Culture Modeling of Central Nervous System (CNS) Viral Infection', *Methods in Molecular Biology*, 1078, pp. 97–117. doi: 10.1007/978-1-62703-640-5.

DiPersio, C. M., Jackson, D. a and Zaret, K. S. (1991) 'The extracellular matrix coordinately modulates liver transcription factors and hepatocyte morphology.', *Molecular and cellular biology*, 11(9), pp. 4405–4414. doi: 10.1128/MCB.11.9.4405.Updated.

Dixon, A. R. *et al.* (2014) 'Microfluidic device capable of medium recirculation for non-adherent cell culture', *Biomicrofluidics*, 8(1), pp. 1–14. doi: 10.1063/1.4865855.

Dixon, L. J. *et al.* (2016) 'Kupffer Cells in the Liver', *Compr Physiology*, 3(2), pp. 785–797. doi: 10.1002/cphy.c120026.Kupffer.

Doi, Y. *et al.* (2007) 'Development of complementary expression patterns of E- and N-cadherin in the mouse liver', *Hepatology Research*, 37(3), pp. 230–237. doi: 10.1111/j.1872-034X.2007.00028.x.

Domansky, K. *et al.* (2010) 'Perfused multiwell plate for 3D liver tissue engineering.', *Lab on a chip*, 10(1), pp. 51–58. doi: 10.1039/b913221j.

Donato, M. T. *et al.* (2008) 'Functional assessment of the quality of human hepatocyte preparations for cell transplantation', *Cell Transplantation*, 17(10–11), pp. 1211–1219. doi: 10.3727/096368908787236620.

Donato, M. T., Tolosa, Laia and Gomez-Lechon, M. (2015) 'Culture and Functional Characterization of Human Hepatoma HepG2 Cells', in *Protocols in In Vitro Hepatocyte Research*. New York, NY: Humana Press, pp. 77–93. Available at: https://link.springer.com/protocol/10.1007%2F978-1-4939-2074-7_5.

Döring, B. and Petzinger, E. (2014) 'Phase 0 and phase III transport in various organs: Combined concept of phases in xenobiotic transport and metabolism', *Drug Metabolism Reviews*, 46(3), pp. 261–282. doi: 10.3109/03602532.2014.882353.

Dotson, R. J. *et al.* (2017) 'Influence of Cholesterol on the Oxygen Permeability of Membranes: Insight from Atomistic Simulations', *Biophysical Journal*, 112(11), pp. 2336–2347. doi: 10.1016/j.bpj.2017.04.046.

Dowling, P. and Clynes, M. (2011) 'Conditioned media from cell lines: A complementary model to clinical specimens for the discovery of disease-specific biomarkers', *Proteomics*, 11(4), pp. 794–804. doi: 10.1002/pmic.201000530.

Dranoff, J. A. and Wells, R. G. (2010) 'Portal fibroblasts : Underappreciated mediators of biliary fibrosis', *Hepatology*, 51(4), pp. 1438–1444. doi: 10.1002/hep.23405.Portal.

Drobner, C., Glöckner, R. and Müller, D. (2000) 'Optimal oxygen tension conditions for viability and functioning of precision-cut liver slices.', *Experimental and toxicologic pathology : official journal of the Gesellschaft für Toxikologische Pathologie*, 52(4), pp. 335–8. doi: 10.1016/S0940-2993(00)80059-7.

Drucker, C. *et al.* (2006) 'Non-parenchymal liver cells support the growth advantage in the first stages of hepatocarcinogenesis', *Carcinogenesis*, 27(1), pp. 152–161. doi: 10.1093/carcin/bgi202.

Duarte, S. *et al.* (2015) 'Matrix metalloproteinases in liver injury, repair and fibrosis', *Matrix Biology*, 0, pp. 147–156. doi: 10.1016/j.matbio.2015.01.004.Matrix.

Dunn, J. C. *et al.* (1989) 'Hepatocyte function and extracellular matrix geometry: long-term culture in a sandwich configuration.', *FASEB journal : official publication of the Federation of American Societies for Experimental Biology*, 3(2), pp. 174–7. doi: 10.1093/nar/gks1337.

Duryee, M. J. *et al.* (2014) 'Precision-cut liver slices from diet-induced obese rats exposed to ethanol are susceptible to oxidative stress and increased fatty acid synthesis.', *American journal of physiology. Gastrointestinal and liver physiology*, 306(3), pp. G208-17. doi: 10.1152/ajpgi.00124.2013.

Duval, K. *et al.* (2017) 'Modeling physiological events in 2D vs. 3D cell culture', *Physiology*, 32(4), pp. 266–277. doi: 10.1152/physiol.00036.2016.

Eagle, H. (1959) 'Amino acid metabolism in human cell cultures.', *Science*, 130(3373), pp. 432–437.

Eastman, A. (2017) 'Improving anticancer drug development begins with cell culture: misinformation perpetrated by the misuse of cytotoxicity assays', *Oncotarget*, 8(5), pp. 8854–8866. doi: 10.18632/oncotarget.12673.

Egger, D. *et al.* (2019) 'From 3D to 3D: Isolation of mesenchymal stem/stromal cells into a three-dimensional human platelet lysate matrix', *bioRxiv*, 2, pp. 1–10. doi: 10.1101/617738.

Elferink, M. G. L. *et al.* (2011) 'Gene expression analysis of precision-cut human liver slices indicates stable expression of ADME-Tox related genes', *Toxicology and Applied Pharmacology*, 253(1), pp. 57–69. doi: 10.1016/j.taap.2011.03.010.

Elliott, N. T. and Yuan, F. (2011) 'A review of three-dimensional in vitro tissue models for drug discovery and transport studies', *Journal of Pharmaceutical Sciences*, 100(1), pp. 59–74. doi: 10.1002/jps.22257.

Eniwumide, J. O., Lee, D. A. and Bader, D. L. (2009) 'The development of a bioreactor to perfuse radially-confined hydrogel constructs: Design and characterization of mass transport properties', *Biorheology*, 46(5), pp. 417–437. doi: 10.3233/BIR-2009-0552.

Estes, C. *et al.* (2018) 'Modeling the epidemic of nonalcoholic fatty liver disease demonstrates an exponential increase in burden of disease', *Hepatology*, 67(1), pp. 123–133. doi: 10.1002/hep.29466.

Evenou, F. *et al.* (2011) 'Gas-permeable membranes and co-culture with fibroblasts enable high-density hepatocyte culture as multilayered liver tissues', *Biotechnology Progress*, 27(4), pp. 1146–1153. doi: 10.1002/btpr.626.

Faber, K. N., Müller, M. and Jansen, P. L. M. (2003) 'Drug transport proteins in the liver', *Advanced Drug Delivery Reviews*, 55(1), pp. 107–124. doi: 10.1016/S0169-409X(02)00173-4.

Feaver, R. E. *et al.* (2016) 'Development of an in vitro human liver system for interrogating nonalcoholic steatohepatitis', *JCI Insight*, 1(20), pp. 0–18. doi: 10.1172/jci.insight.90954.

Feng, W. *et al.* (2018) 'HIF-1α promotes the migration and invasion of hepatocellular carcinoma cells via the IL-8–NF-κB axis', *Cellular and Molecular Biology Letters*, 23(1), pp. 1–8. doi: 10.1186/s11658-018-0077-1.

Fey, S. J., Korzeniowska, B. and Wrzesinski, K. (2020) 'Response to and recovery from treatment in human liver-mimetic clinostat spheroids: A model for assessing repeated-dose drug toxicity', *Toxicology Research*, 9(4), pp. 379–389. doi: 10.1093/TOXRES/TFAA033.

Fey, S. J. and Wrzesinski, K. (2012) 'Determination of drug toxicity using 3D spheroids constructed from an immortal human hepatocyte cell line', *Toxicological Sciences*, 127(2), pp. 403–411. doi: 10.1093/toxsci/kfs122.

Fisher, R. L., Hasal, S. J., *et al.* (1995) 'Determination of optimal incubation media and suitable slice diameters in precision-cut liver slices: Optimization of tissue slice culture, part 2', *Toxicology Mechanisms and Methods*, 5(2), pp. 115–130. doi: 10.3109/15376519509045906.

Fisher, R. L., Shaughnessy, R. P., *et al.* (1995) 'Dynamic organ culture is superior to multiwell plate culture for maintaining precision-cut tissue slices: Optimization of tissue slice culture, part 1', *Toxicology Mechanisms and Methods*, 5(2), pp. 99–113. doi: 10.3109/15376519509045905.

Fisher, R. L. *et al.* (2001) 'Histological and Biochemical Evaluation of Precision-Cut Liver Slices', *Toxicology Methods*, 11, pp. 59–79.

Fleischaker, R. J. and Sinskey, A. J. (1981) 'Oxygen demand and supply in cell culture', *European Journal of*

Applied Microbiology and Biotechnology, 12(4), pp. 193–197. doi: 10.1007/BF00499486.

Fonsato, V. *et al.* (2009) 'Use of a Rotary Bioartificial Liver in the Differentiation of Human Liver Stem Cells', *Tissue Engineering Part C: Methods*, 16(1), pp. 123–132.

Fontana, R. J. (2014) 'Pathogenesis of Idiosyncratic Drug-Induced Liver Injury and Clinical Perspectives', *Gastroenterology*, 146(4), pp. 914–928. doi: 10.1053/j.gastro.2013.12.032.Pathogenesis.

Fotakis, G. and Timbrell, J. A. (2006) 'In vitro cytotoxicity assays: Comparison of LDH, neutral red, MTT and protein assay in hepatoma cell lines following exposure to cadmium chloride', *Toxicology Letters*, 160(2), pp. 171–177. doi: 10.1016/j.toxlet.2005.07.001.

Foty, R. (2011) 'A simple hanging drop cell culture protocol for generation of 3D spheroids.', *Journal of visualized experiments : JoVE*, 20(51), pp. 4–7. doi: 10.3791/2720.

Fox, B. C. *et al.* (2010) 'Validation of reference gene stability for APAP hepatotoxicity studies in different in vitro systems and identification of novel potential toxicity biomarkers', *Toxicology in Vitro*, 24(7), pp. 1962–1970. doi: 10.1016/j.tiv.2010.08.007.

Fred Peter, G. (2008) 'Cytochrome p450 and chemical toxicology', *Chemical Research in Toxicology*, 21(Table 1), pp. 70–83.

Freyberg, M. A. and Friedl, P. (1998) 'The use of a conventional tissue culture plate as an optically accessible perfusion chamber for in situ assays and for long-term cultivation of mammalian cells', *Cytotechnology*, 26(1), pp. 49–58. doi: 10.1023/A:1007989802251.

Freyer, N. *et al.* (2018) 'Microscale 3D liver bioreactor for in vitro hepatotoxicity testing under perfusion conditions', *Bioengineering*, 5(1), pp. 1–18. doi: 10.3390/bioengineering5010024.

Freyer, N. *et al.* (2019) 'Metabolism of remimazolam in primary human hepatocytes during continuous long-term infusion in a 3-D bioreactor system', *Drug Design, Development and Therapy*, 13, pp. 1033–1047. doi: 10.2147/DDDT.S186759.

Freyria, A. M. *et al.* (2004) 'Influence of medium composition, static and stirred conditions on the proliferation of and matrix protein expression of bovine articular chondrocytes cultured in a 3-D collagen scaffold', *Biomaterials*, 25(4), pp. 687–697. doi: 10.1016/S0142-9612(03)00568-4.

Friedman, S. L. (2008) 'Hepatic Stellate Cells : Protean , Multifunctional , and Enigmatic Cells of the Liver', pp. 125–172. doi: 10.1152/physrev.00013.2007.

Fry, J. R. and Bridges, J. W. (1977) 'A NOVEL MIXED HEPATOCYTE-FIBROBLAST CULTURE SYSTEM AND ITS USE AS A TEST FOR METABOLISM-MEDIATED CYTOTOXICITY', *Biochemical Pharmacology*, 26, pp. 969–973.

Fujita, T. and Narumiya, S. (2016) 'Roles of hepatic stellate cells in liver inflammation: a new perspective', *Inflammation and Regeneration*, 36(1), pp. 1–6. doi: 10.1186/s41232-016-0005-6.

Funk, C. and Roth, A. (2017) 'Current limitations and future opportunities for prediction of DILI from in vitro', *Archives of Toxicology*, 91(1), pp. 131–142. doi: 10.1007/s00204-016-1874-9.

García Cruz, D. M., Salmerón-Sánchez, M. and Gómez-Ribelles, J. L. (2012) 'Stirred flow bioreactor modulates chondrocyte growth and extracellular matrix biosynthesis in chitosan scaffolds', *Journal of Biomedical Materials Research - Part A*, 100 A(9), pp. 2330–2341. doi: 10.1002/jbm.a.34174.

Garg, K. and Bowlin, G. L. (2011) 'Electrospinning jets and nanofibrous structures', *Biomicrofluidics*, 5(1), pp. 1–19. doi: 10.1063/1.3567097.

Garnier, D. *et al.* (2018) 'Expansion of human primary hepatocytes in vitro through their amplification as liver progenitors in a 3D organoid system', *Scientific Reports*, 8(1), pp. 1–10. doi: 10.1038/s41598-018-26584-1.

Garzel, B. *et al.* (2014) 'The role of bile salt export pump gene repression in drug-induced cholestatic liver toxicity s', *Drug Metabolism and Disposition*, 42(3), pp. 318–322. doi: 10.1124/dmd.113.054189.

Gaskell, H. *et al.* (2016) 'Characterization of a functional C3A liver spheroid model', *Toxicology research*, 5, pp. 1053–1065. doi: 10.1039/c6tx00101g.

Gebhardt, R. *et al.* (2003) 'New Hepatocyte In Vitro Systems for Drug Metabolism: Metabolic Capacity and Recommendations for Application in Basic Research and Drug Development, Standard Operation Procedures', *Drug Metabolism Reviews*, 35(2–3), pp. 145–213. doi: 10.1081/DMR-120023684.

Gebhardt, R. and Mecke, D. (1979) 'Perifused monolayer cultures of rat hepatocytes as an improved in vitro system for studies on ureogenesis', *Experimental Cell Research*, 124(2), pp. 349–359. doi: 10.1016/0014-4827(79)90210-6.

Geier, A. *et al.* (2007) 'Principles of hepatic organic anion transporter regulation during cholestasis, inflammation and liver regeneration', *Biochimica et Biophysica Acta - Molecular Cell Research*, 1773(3), pp. 283–308. doi: 10.1016/j.bbamcr.2006.04.014.

Gelinsky, M., Bernhardt, A. and Milan, F. (2015) 'Bioreactors in tissue engineering: Advances in stem cell culture and three-dimensional tissue constructs', *Engineering in Life Sciences*, 15(7), pp. 670–677. doi: 10.1002/elsc.201400216.

Genovese, F. *et al.* (2016) 'Precision-Cut Kidney Slices as a Tool to Understand the Dynamics of Extracellular Matrix Remodeling in Renal Fibrosis', *Biomarker Insights*, 11, pp. 77–84. doi: 10.4137/BMI.S38439.

Gerets, H. H. J. *et al.* (2012) 'Characterization of primary human hepatocytes, HepG2 cells, and HepaRG cells at the mRNA level and CYP activity in response to inducers and their predictivity for the detection of human hepatotoxins', *Cell Biology and Toxicology*, 28(2), pp. 69–87. doi: 10.1007/s10565-011-9208-4.

Ghibellini, G., Leslie, E. M. and Brouwer, K. L. R. (2006) 'Methods to Evaluate Biliary Excretion of Drugs in Humans: an Updated Review', *Molecular Pharmaceutics*, 3(3), pp. 198–211. doi: 10.1021/mp060011k.Methods.

Ghorbel, M. T. *et al.* (2019) 'Reconstruction of the pulmonary artery by a novel biodegradable conduit engineered with perinatal stem cell-derived vascular smooth muscle cells enables physiological vascular growth in a large animal model of congenital heart disease', *Biomaterials*, 217, p. 119284. doi: 10.1016/j.biomaterials.2019.119284.

Gibson, G. G. and Skett, P. (1994) 'Enzymology and molecular mechanisms of drug metabolism reactions', in *Introduction to Drug Metabolism*. Boston, MA: Springer US, pp. 35–76. doi: 10.1007/978-1-4899-6844-9_2.

Gilbert, E. *et al.* (2014) 'A novel through-thickness perfusion bioreactor for the generation of scaffold-free tissue engineered cartilage', *Processes*, 2(3), pp. 658–674. doi: 10.3390/pr2030658.

Gilglioni, E. H. *et al.* (2018) 'Improved oxygenation dramatically alters metabolism and gene expression in cultured primary mouse hepatocytes', *Hepatology Communications*, 2(3), pp. 299–312. doi: 10.1002/hep4.1140.

Gissen, P. and Arias, I. M. (2015) 'Structural and functional hepatocyte polarity and liver disease', *Journal of Hepatology*, 63(4), pp. 1023–1037. doi: 10.1016/j.jhep.2015.06.015.

Glicklis, R. *et al.* (2000) 'Hepatocyte behavior within three-dimensional porous alginate scaffolds', *Biotechnology and Bioengineering*, 67(3), pp. 344–353. doi: 10.1002/(SICI)1097-0290(20000205)67:3<344::AID-BIT11>3.0.CO;2-2.

Goda, R. *et al.* (2006) 'Detection of a new N-oxidized metabolite of flutamide, N-[4-nitro-3-(trifluoromethyl)phenyl]hydroxylamine, in human liver microsomes and urine of prostate cancer patients', *Drug Metabolism and Disposition*, 34(5), pp. 828–835. doi: 10.1124/dmd.105.008623.

Godoy, P. *et al.* (2009) 'Extracellular matrix modulates sensitivity of hepatocytes to fibroblastoid dedifferentiation and transforming growth factor β-induced apoptosis', *Hepatology*, 49(6), pp. 2031–2043. doi: 10.1002/hep.22880.

Godoy, P. *et al.* (2013) *Recent advances in 2D and 3D in vitro systems using primary hepatocytes, alternative*

hepatocyte sources and non-parenchymal liver cells and their use in investigating mechanisms of hepatotoxicity, cell signaling and ADME, *Archives of Toxicology*. doi: 10.1007/s00204-013-1078-5.

Golubitskii, G. B. *et al.* (2007) 'Stability of ascorbic acid in aqueous and aqueous-organic solutions for quantitative determination', *Journal of Analytical Chemistry*, 62(8), pp. 742–747. doi: 10.1134/S1061934807080096.

Gomez-Lechon, M. *et al.* (2008) 'Cell Lines: A Tool for In Vitro Drug Metabolism Studies', *Current Drug Metabolism*, 9(1), pp. 1–11. doi: 10.2174/138920008783331086.

Gomez-Lechon, M. J. *et al.* (2014) 'Competency of different cell models to predict human hepatotoxic drugs', *Expert opinion on drug metabolism & toxicology*, 10(11), pp. 1553–1568. doi: 10.1517/17425255.2014.967680 [doi].

Gonzalez-Sanchez, E. *et al.* (2015) 'E-cadherin, guardian of liver physiology', *Clinics and Research in Hepatology and Gastroenterology*, 39(1), pp. 3–6. doi: 10.1016/j.clinre.2014.09.008.

Gonzalez, F. J. (2005) 'Role of cytochromes P450 in chemical toxicity and oxidative stress: Studies with CYP2E1', *Mutation Research - Fundamental and Molecular Mechanisms of Mutagenesis*, 569(1–2), pp. 101–110. doi: 10.1016/j.mrfmmm.2004.04.021.

González, H. E. *et al.* (2002) 'Regulation of hepatic connexins in cholestasis: Possible involvement of Kupffer cells and inflammatory mediators', *American Journal of Physiology - Gastrointestinal and Liver Physiology*, 282(6 45-6), pp. 991–1001. doi: 10.1152/ajpgi.00298.2001.

Goral, V. N. and Yuen, P. K. (2012) 'Microfluidic platforms for hepatocyte cell culture: New technologies and applications', *Annals of Biomedical Engineering*, 40(6), pp. 1244–1254. doi: 10.1007/s10439-011-0453-8.

Gore, E. *et al.* (2019) 'PI3K inhibition reduces murine and human liver fibrogenesis in precision-cut liver slices', *Biochemical Pharmacology*, 169(June), p. 113633. doi: 10.1016/j.bcp.2019.113633.

Gorelik, J. V. *et al.* (2000) 'Matrigel increases the rate of split wound healing and promotes keratinocyte "take" in deep wounds in rats', *Cytotechnology*, 32(2), pp. 79–86. doi: 10.1023/A:1008192111856.

Gouws, C. *et al.* (2021) 'Anticancer Potential of Sutherlandia frutescens and Xysmalobium undulatum in LS180 Colorectal Cancer Mini-Tumors', *Molecules (Basel, Switzerland)*, 26(3). doi: 10.3390/molecules26030605.

de Graaf, I. A. M. *et al.* (2010) 'Preparation and incubation of precision-cut liver and intestinal slices for application in drug metabolism and toxicity studies', *Nature Protocols*, 5(9), pp. 1540–1551. doi: 10.1038/nprot.2010.111.

De Graaf, I. A. M. *et al.* (2006) 'Empirical validation of a rat in vitro organ slice model as a tool for in vivo clearance prediction', *Drug Metabolism and Disposition*, 34(4), pp. 591–599. doi: 10.1124/dmd.105.006726.

Granitzny, A. *et al.* (2017) 'Maintenance of high quality rat precision cut liver slices during culture to study hepatotoxic responses: Acetaminophen as a model compound', *Toxicology in Vitro*, 42(March), pp. 200–213. doi: 10.1016/j.tiv.2017.05.001.

Green, K. and Otori, T. (1970) 'Direct Measurements of Membrane Unstirred Layers.', *The Journal of Physiology*, 207(1), pp. 93–102. doi: 10.1113/jphysiol.1970.sp009050.

Griffiths, J. B. (1971) 'The effect of medium changes on the growth and metabolism of the human diploid cell, W1-38.', *Journal of Cell Science*, 8(1), pp. 43–52.

Gripon, P. *et al.* (2002) 'Infection of a human hepatoma cell line by hepatitis B virus', *Proceedings of the National Academy of Sciences of the United States of America*, 99(24), pp. 15655–15660. doi: 10.1073/pnas.232137699.

Groothuis, G. M. M. and de Graaf, I. a M. (2013) 'Precision-cut intestinal slices as in vitro tool for studies on drug metabolism.', *Current drug metabolism*, 14(1), pp. 112–9. doi: 10.2174/138920013804545197.

Gross-Steinmeyer, K. *et al.* (2005) 'Influence of Matrigel-overlay on constitutive and inducible expression of

nine genes encoding drug-metabolizing enzymes in primary human hepatocytes', *Xenobiotica*, 35(5), pp. 419–438.

Grün, C., Altmann, B. and Gottwald, E. (2020) 'Advanced 3D Cell Culture Techniques in Micro-Bioreactors, Part I: A Systematic Analysis of the Literature Published between 2000 and 2020', *Processes*, 8, pp. 1656–1680.

van Grunsven, L. A. (2017) '3D in vitro models of liver fibrosis', *Advanced Drug Delivery Reviews*, 121, pp. 133–146. doi: 10.1016/j.addr.2017.07.004.

Guillouzo, A. (1998) 'Liver Cell Models in in Vitro Toxicology', *Environmental Health Perspectives*, 106(SUPPL. 2), pp. 511–532. doi: 10.2307/3433803.

Guillouzo, A. *et al.* (2007) 'The human hepatoma HepaRG cells: A highly differentiated model for studies of liver metabolism and toxicity of xenobiotics', *Chemico-Biological Interactions*, 168(1), pp. 66–73. doi: 10.1016/j.cbi.2006.12.003.

Guillouzo, A. and Guguen-Guillouzo, C. (2008) 'Evolving concepts in liver tissue modeling and implications for *in vitro* toxicology', *Expert Opinion on Drug Metabolism & Toxicology*, 4(10), pp. 1279–1294. doi: 10.1517/17425255.4.10.1279.

Gunness, P. *et al.* (2013) '3D organotypic cultures of human heparg cells: A tool for in vitro toxicity studies', *Toxicological Sciences*, 133(1), pp. 67–78. doi: 10.1093/toxsci/kft021.

Guo, L. *et al.* (2011) 'Similarities and differences in the expression of drug-metabolizing enzymes between human hepatic cell lines and primary human hepatocytes', *Drug Metabolism and …*, 39(3), pp. 528–538. doi: 10.1124/dmd.110.035873.

Gupta, G., Khadem, F. and Uzonna, J. E. (2019) 'Role of hepatic stellate cell (HSC)-derived cytokines in hepatic inflammation and immunity', *Cytokine*, 124(September 2018), p. 154542. doi: 10.1016/j.cyto.2018.09.004.

Guyot, C. *et al.* (2006) 'Hepatic fibrosis and cirrhosis: The (myo)fibroblastic cell subpopulations involved', *International Journal of Biochemistry and Cell Biology*, 38(2), pp. 135–151. doi: 10.1016/j.biocel.2005.08.021.

Guzzardi, M. A., Vozzi, F. and Ahluwalia, A. D. (2009) 'Study of the Crosstalk Between Hepatocytes and Endothelial Cells Using a Novel Multicompartmental Bioreactor: A Comparison Between Connected Cultures and Cocultures', *Tissue Engineering - Part A*, 15(11), pp. 3635–3644.

Hadi, M. *et al.* (2012) 'Mouse precision-cut liver slices as an ex vivo model to study idiosyncratic drug-induced liver injury', *Chemical Research in Toxicology*, 25(9), pp. 1938–1947. doi: 10.1021/tx300248j.

Hahn, E. *et al.* (1980) 'Distribution of basement membrane proteins in normal and fibrotic human liver: Collagen type IV, laminin, and fibronectin', *Gut*, 21(1), pp. 63–71. doi: 10.1136/gut.21.1.63.

Haider, A., Haider, S. and Kang, I. K. (2018) 'A comprehensive review summarizing the effect of electrospinning parameters and potential applications of nanofibers in biomedical and biotechnology', *Arabian Journal of Chemistry*, 11(8), pp. 1165–1188. doi: 10.1016/j.arabjc.2015.11.015.

Halldorsson, S. *et al.* (2015) 'Advantages and challenges of microfluidic cell culture in polydimethylsiloxane devices', *Biosensors and Bioelectronics*, 63, pp. 218–231. doi: 10.1016/j.bios.2014.07.029.

Hamilton, G. A. *et al.* (2001) 'Regulation of cell morphology and cytochrome P450 expression in human hepatocytes by extracellular matrix and cell-cell interactions', *Cell and Tissue Research*, 306(1), pp. 85–99. doi: 10.1007/s004410100429.

Hammer, H. *et al.* (2021) 'Cross-species analysis of hepatic cytochrome P450 and transport protein expression', *Archives of Toxicology*, 95(1), pp. 117–133. doi: 10.1007/s00204-020-02939-4.

Hammond, T., Allen, P. and Birdsall, H. (2016) 'Is There a Space-Based Technology Solution to Problems with Preclinical Drug Toxicity Testing?', *Pharmaceutical Research*, 33(7), pp. 1545–1551. doi: 10.1007/s11095-016-1942-0.

Hansen, L. K. and Albrecht, J. H. (1999) 'Regulation of the hepatocyte cell cycle by type I collagen matrix: Role

of cyclin D1', *Journal of Cell Science*, 112(17), pp. 2971–2981.

Hansmann, J. *et al.* (2013) 'Bioreactors in tissue engineering-principles, applications and commercial constraints', *Biotechnology Journal*, 8(3), pp. 298–307. doi: 10.1002/biot.201200162.

Haque, A., Gheibi, P., Gao, Y., *et al.* (2016) 'Cell biology is different in small volumes: Endogenous signals shape phenotype of primary hepatocytes cultured in microfluidic channels', *Scientific Reports*, 6(June), pp. 1–15. doi: 10.1038/srep33980.

Haque, A., Gheibi, P., Stybayeva, G., *et al.* (2016) 'Ductular reaction-on-a-chip: Microfluidic co-cultures to study stem cell fate selection during liver injury', *Scientific Reports*, 6(June), pp. 1–13. doi: 10.1038/srep36077.

Harris, G. M., Raitman, I. and Schwarzbauer, J. E. (2018) 'Cell-derived decellularized extracellular matrices', *Methods in Cell Biology*, 143, pp. 97–114. doi: 10.1016/bs.mcb.2017.08.007.

Harrison, R. G. (1907) 'Observations of the living developing nerve fiber', *The Anatomical Record*, 1(5), pp. 116–128. doi: 10.1002/ar.1090010503.

Hartsock, A. and Nelson, W. J. (2008) 'Adherens and tight junctions: Structure, function and connections to the actin cytoskeleton', *Biochimica et Biophysica Acta - Biomembranes*, 1778(3), pp. 660–669. doi: 10.1016/j.bbamem.2007.07.012.

Häussinger, D., Sies, H. and Gerok, W. (1985) 'Functional hepatocyte heterogeneity in ammonia metabolism. The intercellular glutamine cycle', *Journal of Hepatology*, 1(1), pp. 3–14. doi: 10.1016/S0168-8278(85)80063-5.

Hayman, M. W. *et al.* (2004) 'Enhanced neurite outgrowth by human neurons grown on solid three-dimensional scaffolds', *Biochemical and Biophysical Research Communications*, 314(2), pp. 483–488. doi: 10.1016/j.bbrc.2003.12.135.

He, Q. *et al.* (2018) 'Origami-based self-folding of co-cultured NIH/3T3 and HepG2 cells into 3D microstructures', *Scientific Reports*, 8(1), pp. 2–8. doi: 10.1038/s41598-018-22598-x.

He, X. *et al.* (2004) 'Safe time to warm ischemia and posttransplant survival of liver graft from non-heart-beating donors', 10(21), pp. 3157–3160.

Heffelfinger, S. U. E. C. *et al.* (1992) 'Sk hep-i: a human cell line of endothelial origin', 1(February), pp. 136–142.

Hemmann, S. *et al.* (2007) 'Expression of MMPs and TIMPs in liver fibrosis - a systematic review with special emphasis on anti-fibrotic strategies', *Journal of Hepatology*, 46(5), pp. 955–975. doi: 10.1016/j.jhep.2007.02.003.

Hernandez-gea, V. and Friedman, S. L. (2011) 'Pathogenesis of Liver Fibrosis'. doi: 10.1146/annurev-pathol-011110-130246.

Herrema, H. *et al.* (2006) 'Rho Kinase, Myosin-II, and p42/44 MAPK Control Extracellular Matrix-mediated Apical Bile Canalicular Lumen Morphogenesis in HepG2 Cells', *Molecular biology of the cell*, 17, pp. 3291–3303. doi: 10.1091/mbc.E06.

Hewitt, N. J. *et al.* (2007) 'Primary Hepatocytes: Current Understanding of the Regulation of Metabolic Enzymes and Transporter Proteins, and Pharmaceutical Practice for the Use of Hepatocytes in Metabolism, Enzyme Induction, Transporter, Clearance, and Hepatotoxicity Studies', *Drug Metabolism Reviews*, 39(1), pp. 159–234. doi: 10.1080/03602530601093489.

Hewitt, N. J. and Hewitt, P. (2004) 'Phase I and II enzyme characterization of two sources of HepG2 cell lines.', *Xenobiotica; the fate of foreign compounds in biological systems*, 34(3), pp. 243–256. doi: 10.1080/00498250310001657568.

Hidalgo-Bastida, L. A. *et al.* (2012) 'Modeling and design of optimal flow perfusion bioreactors for tissue engineering applications', *Biotechnology and Bioengineering*, 109(4), pp. 1095–1099. doi: 10.1002/bit.24368.

Hiemstra, S. *et al.* (2019) 'High-throughput confocal imaging of differentiated 3D liver-like spheroid cellular stress response reporters for identification of drug-induced liver injury liability', *Archives of Toxicology*, 93(10),

pp. 2895–2911. doi: 10.1007/s00204-019-02552-0.

Hirsch, C. and Schildknecht, S. (2019) 'In vitro research reproducibility: Keeping up high standards', *Frontiers in Pharmacology*, 10(December), pp. 1–9. doi: 10.3389/fphar.2019.01484.

Hoffmann, S. A. *et al.* (2012) 'Analysis of drug metabolism activities in a miniaturized liver cell bioreactor for use in pharmacological studies', *Biotechnology and Bioengineering*, 109(12), pp. 3172–3181. doi: 10.1002/bit.24573.

Hohenester, E. *et al.* (2017) 'Laminins in basement membrane assembly Laminins in basement membrane assembly', 6918(February), pp. 56–63.

Holownia, A. and Braszko, J. J. (2004) 'Tamoxifen cytotoxicity in hepatoblastoma cells stably transfected with human CYP3A4', *Biochemical Pharmacology*, 67(6), pp. 1057–1064. doi: 10.1016/j.bcp.2003.10.027.

Homan, K. A. *et al.* (2016) 'Bioprinting of 3D Convoluted Renal Proximal Tubules on Perfusable Chips', *Scientific Reports*, 6, pp. 1–13. doi: 10.1038/srep34845.

Homolya, L., Váradi, A. and Sarkadi, B. (2003) 'Multidrug resistance-associated proteins: Export pumps for conjugates with glutathione, glucuronate or sulfate.', *BioFactors*, 17(1–4), pp. 103–114. doi: 10.1002/biof.5520170111.

Hosoya, S. *et al.* (2014) 'Hepatocyte morphology by culturing them in 3D collagen gels', *Kitasato Med J*, 44(December 2013), pp. 139–147.

Hu, J. *et al.* (2014) 'Endothelial Cell-Derived Angiopoietin-2', 343(January), pp. 416–420.

Huch, M. *et al.* (2015) 'Long-term culture of genome-stable bipotent stem cells from adult human liver', *Cell*, 160(1–2), pp. 299–312. doi: 10.1016/j.cell.2014.11.050.

Huebert, R. C. *et al.* (2010) 'Immortalized liver endothelial cells: A cell culture model for studies of motility and angiogenesis', *Laboratory Investigation*, 90(12), pp. 1770–1781. doi: 10.1038/labinvest.2010.132.

Hughes, D. J., Kostrzewski, T. and Sceats, E. L. (2017) 'Opportunities and challenges in the wider adoption of liver and interconnected microphysiological systems', *Experimental Biology and Medicine*, 242(16), pp. 1593–1604. doi: 10.1177/1535370217708976.

Hurrell, T. *et al.* (2018) 'Characterization and reproducibility of HepG2 hanging drop spheroids toxicology in vitro', *Toxicology in Vitro*, 50(87880), pp. 86–94. doi: 10.1016/j.tiv.2018.02.013.

Hussein, K. H. *et al.* (2016) 'Three dimensional culture of HepG2 liver cells on a rat decellularized liver matrix for pharmacological studies', *Journal of Biomedical Materials Research - Part B Applied Biomaterials*, 104(2), pp. 263–273. doi: 10.1002/jbm.b.33384.

Hwa, A. J. *et al.* (2007) 'Rat liver sinusoidal endothelial cells survive without exogenous VEGF in 3D perfused co-cultures with hepatocytes', *The FASEB Journal*, 21(10), pp. 2564–2579. doi: 10.1096/fj.06-7473com.

Idkaidek, N. M. (2017) 'Comparative assessment of saliva and plasma for drug bioavailability and bioequivalence studies in humans', *Saudi Pharmaceutical Journal*, 25(5), pp. 671–675. doi: 10.1016/j.jsps.2016.10.002.

Inamori, M., Mizumoto, H. and Kajiwara, T. (2009) 'An Approach for Formation of Vascularized Liver Tissue by Endothelial Cell-Covered Hepatocyte Spheroid Integration', *Tissue Engineering - Part A*, 15(8), pp. 2029–2037.

Ingram, M. *et al.* (1997) 'Three-Dimensional Growth Patterns of Various Human Tumor Cell Lines in Simulated Microgravity of a NASA Bioreactor', *In Vitro Cellular & Developmental Biology*, 33, pp. 459–466.

Ionescu, C. and Caira, M. R. (eds) (2005) 'Pathways of Biotransformation --- Phase II Reactions', in *Drug Metabolism: Current Concepts*. Dordrecht: Springer Netherlands, pp. 129–170. doi: 10.1007/1-4020-4142-X_3.

Ishibashi, H. *et al.* (2009) 'Liver architecture, cell function, and disease', *Seminars in Immunopathology*, 31(3), pp. 399–409. doi: 10.1007/s00281-009-0155-6.

Ito, A. *et al.* (2007) 'Construction of Heterotypic Cell Sheets by Magnetic Force-Based 3-D Coculture of HepG2 and NIH3T3 Cells', *Journal of Bioscience and Bioengineering*, 104(5), pp. 371–378. doi: 10.1263/jbb.104.371.

Iulianella, A. (2017) 'Cutting Thick Sections Using a Vibratome', *Cold Spring Harbor Protocols*, 2017(6), p. pdb.prot094011. doi: 10.1101/pdb.prot094011.

Iwahasi, S. *et al.* (2020) 'Hepatic Stellate Cells Contribute to the Tumor Malignancy of Hepatocellular Carcinoma Through the IL-6 Pathway', *Anticancer Research*, 40(2), pp. 743–749.

Izzo, L. *et al.* (2019) 'Influence of the static magnetic field on cell response in a miniaturized optically accessible bioreactor for 3D cell culture', *Biomedical Microdevices*, 21(1), pp. 1–12. doi: 10.1007/s10544-019-0387-8.

J. Richardson, S. *et al.* (2016) 'Efficiency in Drug Discovery: Liver S9 Fraction Assay As a Screen for Metabolic Stability', *Drug Metabolism Letters*, 10(2), pp. 83–90. doi: 10.2174/1872312810666160223121836.

Jagušić, M. *et al.* (2016) 'Stability of Minimum Essential Medium functionality despite l-glutamine decomposition', *Cytotechnology*, 68(4), pp. 1171–1183. doi: 10.1007/s10616-015-9875-8.

Jancova, P., Anzenbacher, P. and Anzenbacherova, E. (2010) 'Phase II drug metabolizing enzymes', *Biomedical Papers*, 154(2), pp. 103–116. doi: 10.5507/bp.2010.017.

Jančová, P. and Šiller, M. (2012) 'Phase II Drug Metabolism', in Paxton, J. (ed.) *Topics on Drug Metabolism*. Rijeka: IntechOpen. doi: 10.5772/29996.

Jang, K. J. *et al.* (2019) 'Reproducing human and cross-species drug toxicities using a Liver-Chip', *Science Translational Medicine*, 11(eaax5516). doi: 10.1101/631002.

Jang, M. *et al.* (2015) 'On-chip three-dimensional cell culture in phaseguides improves hepatocyte functions in vitro', *Biomicrofluidics*, 9(3). doi: 10.1063/1.4922863.

Jauregui, H. O. *et al.* (1994) 'Primary cultures of rat hepatocytes in hollow fiber chambers', *In Vitro Cellular & Developmental Biology - Animal*, 30(1), pp. 23–29. doi: 10.1007/BF02631414.

Jedlitschky, G., Hoffmann, U. and Kroemer, H. K. (2006) 'Structure and function of the MRP2 (ABCC2) protein and its role in drug disposition', *Expert Opinion on Drug Metabolism and Toxicology*, 2(3), pp. 351–366. doi: 10.1517/17425255.2.3.351.

Jeffries, R. E. *et al.* (2013) 'Effect of oxygen concentration on viability and metabolism in a fluidized-bed bioartificial liver using ^{31}P and ^{13}C NMR spectroscopy.', *Tissue engineering. Part C, Methods*, 19(2), pp. 93–100. doi: 10.1089/ten.TEC.2011.0629.

Jemal, A. *et al.* (2017) 'Annual Report to the Nation on the Status of Cancer, 1975-2014, Featuring Survival', *Journal of the National Cancer Institute*, 109(9), pp. 1–22. doi: 10.1093/jnci/djx030.

Jennen, D. G. J. *et al.* (2010) 'Comparison of HepG2 and HepaRG by whole-genome gene expression analysis for the purpose of chemical hazard identification', *Toxicological Sciences*, 115(1), pp. 66–79. doi: 10.1093/toxsci/kfq026.

Jensen, C. and Teng, Y. (2020) 'Is It Time to Start Transitioning From 2D to 3D Cell Culture?', *Frontiers in Molecular Biosciences*, 7(March), pp. 1–15. doi: 10.3389/fmolb.2020.00033.

Jeong, D. *et al.* (2016) 'Effect of concentrated fibroblast-conditioned media on in vitro maintenance of rat primary hepatocyte', *PLoS ONE*, 11(2), pp. 1–14. doi: 10.1371/journal.pone.0148846.

Jian, J. *et al.* (2015) 'Development of novel tools for the in vitro investigation of drug-induced liver injury', *Expert Opinion on Drug Metabolism and Toxicology*, 11(10), pp. 1523–1537.

Jiankang, H. *et al.* (2009) 'Preparation of chitosan-gelatin hybrid scaffolds with well-organized microstructures for hepatic tissue engineering', *Acta Biomaterialia*, 5(1), pp. 453–461. doi: 10.1016/j.actbio.2008.07.002.

Jigorel, E. *et al.* (2006) 'Differential regulation of sinusoidal and canalicular hepatic drug transporter expression by xenobiotics activating drug-sensing receptors in primary human hepatocytes', *Drug Metabolism and*

Disposition, 34(10), pp. 1756–1763. doi: 10.1124/dmd.106.010033.

Johnson, H. L. and Maibach, H. I. (1971) 'Drug excretion in human eccrine sweat.', *The Journal of investigative dermatology*, 56(3), pp. 182–188. doi: 10.1111/1523-1747.ep12260784.

Justice, B. A., Badr, N. A. and Felder, R. A. (2009) '3D cell culture opens new dimensions in cell-based assays', *Drug Discovery Today*, 14(1–2), pp. 102–107. doi: 10.1016/j.drudis.2008.11.006.

Kaarj, K. and Yoon, J. Y. (2019) 'Methods of delivering mechanical stimuli to Organ-on-a-Chip', *Micromachines*, 10(10). doi: 10.3390/mi10100700.

Kaiser, S. C. *et al.* (2014) 'Single-Use Bioreactors for Animal and Human Cells', in *Animal Cell Culture*, pp. 445–500.

Kalgutkar, A. S. and Soglia, J. R. (2005) 'Minimising the potential for metabolic activation in drug discovery', *Expert Opinion on Drug Metabolism \& Toxicology*, 1(1), pp. 91–142. doi: 10.1517/17425255.1.1.91.

Kang, Y. B. A. *et al.* (2013) 'Layered long-term co-culture of hepatocytes and endothelial cells on a transwell membrane: toward engineering the liver sinusoid.', *Biofabrication*, 5(4), p. 045008. doi: 10.1088/1758-5082/5/4/045008.

Kang, Y. B. A. *et al.* (2015) 'Liver sinusoid on a chip: Long-term layered co-culture of primary rat hepatocytes and endothelial cells in microfluidic platforms', *Biotechnology and Bioengineering*, 112(12), pp. 2571–2582. doi: 10.1002/bit.25659.

Kanta, J. (2015) 'Collagen matrix as a tool in studying fibroblastic cell behavior', *Cell Adhesion and Migration*, 9(4), pp. 308–316. doi: 10.1080/19336918.2015.1005469.

de Kanter, R. and Koster, H. J. (1995) 'Cryopreservation of Rat and Monkey Liver Slices', *Alternatives to Laboratory Animals*, 23(5), pp. 653–665. doi: 10.1177/026119299502300519.

Kapałczyńska, M. *et al.* (2018) '2D and 3D cell cultures – a comparison of different types of cancer cell cultures', *Archives of Medical Science*, 14(4), pp. 910–919. doi: 10.5114/aoms.2016.63743.

Karin, D. *et al.* (2016) 'The Characteristics of Activated Portal Fibroblasts / Myofibroblasts in Liver Fibrosis', *Physiology & behavior*, 176(12), pp. 139–148. doi: 10.1016/j.diff.2016.07.001.The.

Karsdal, M. A. *et al.* (2015) 'Novel insights into the function and dynamics of extracellular matrix in liver fibrosis', *American Journal of Physiology - Gastrointestinal and Liver Physiology*, 308(10), pp. G807–G830. doi: 10.1152/ajpgi.00447.2014.

Karsdal, M. A. *et al.* (2017) 'The good and the bad collagens of fibrosis – Their role in signaling and organ function', *Advanced Drug Delivery Reviews*. doi: 10.1016/j.addr.2017.07.014.

Kartasheva-Ebertz, D. *et al.* (2021) *Adult human liver slice cultures: Modelling of liver fibrosis and evaluation of new anti-fibrotic drugs*, *World Journal of Hepatology*. doi: 10.4254/wjh.v13.i2.187.

Kasuya, J. *et al.* (2010) 'Hepatic Stellate Cell-Mediated Three-Dimensional Hepatocyte and Endothelial Cell Triculture Model', *Tissue Engineering - Part A*, 17(3–4), pp. 361–370.

Kazemnejad, S. (2009) 'Hepatic tissue engineering using scaffolds: state of the art.', *Avicenna journal of medical biotechnology*, 1(3), pp. 135–45. Available at: http://www.ncbi.nlm.nih.gov/pubmed/23408654%0Ahttp://www.pubmedcentral.nih.gov/articlerender.fcgi?artid=PMC3558138.

Kehtari, M. *et al.* (2018) 'Fabrication of a co-culture micro-bioreactor device for efficient hepatic differentiation of human induced pluripotent stem cells (hiPSCs)', *Artificial Cells, Nanomedicine and Biotechnology*, 46(sup2), pp. 161–170. doi: 10.1080/21691401.2018.1452753.

Kenna, J. G. *et al.* (2015) 'Multiple Compound-Related Adverse Properties Contribute to Liver Injury Caused by Endothelin Receptor Antagonists', *Journal of Pharmacology and Experimental Therapeutics*, 352(2), pp. 281–290. doi: 10.1124/jpet.114.220491.

Kenna, J. G. *et al.* (2018) 'Can Bile Salt Export Pump Inhibition Testing in Drug Discovery and Development Reduce Liver Injury Risk? An International Transporter Consortium Perspective', *Clinical Pharmacology and Therapeutics*, 104(5), pp. 916–932. doi: 10.1002/cpt.1222.

Kenna, J. G. and Uetrecht, J. (2018) 'Do In Vitro assays predict drug candidate idiosyncratic drug-induced liver injury risk?', *Drug Metabolism and Disposition*, 46(11), pp. 1658–1669. doi: 10.1124/dmd.118.082719.

Kervancioglu, M. E. *et al.* (1994) 'A simple technique for the long-term non-polarised and polarised culture of human fallopian tube epithelial cells', *Biology of the Cell*, 82(2–3), pp. 103–107. doi: 10.1016/S0248-4900(94)80012-X.

Khan, K. and Elia, M. (1991) 'Factors affecting the stability of L-glutamine in solution', *Clinical Nutrition*, 10(4), pp. 186–192. doi: 10.1016/0261-5614(91)90037-D.

Khaoustov, V. I. *et al.* (1999) 'Induction of Three-Dimensional Assembly of Human Liver Cells by Simulated Microgravity', *In Vitro Cellular and Developmental Biology - Animal*, 35(9), pp. 3–12.

Khodabakhshaghdam, S., Khoshfetrat, A. B. and Rahbarghazi, R. (2021) 'Alginate-chitosan core-shell microcapsule cultures of hepatic cells in a small scale stirred bioreactor: impact of shear forces and microcapsule core composition', *Journal of Biological Engineering*, 15(1), pp. 1–12. doi: 10.1186/s13036-021-00265-6.

Kia, R. *et al.* (2013) 'Stem cell-derived hepatocytes as a predictive model for drug-induced liver injury: Are we there yet?', *British Journal of Clinical Pharmacology*, 75(4), pp. 885–896. doi: 10.1111/j.1365-2125.2012.04360.x.

Kietzmann, T. (2017) 'Metabolic zonation of the liver: The oxygen gradient revisited', *Redox Biology*, 11(December 2016), pp. 622–630. doi: 10.1016/j.redox.2017.01.012.

Kim, D., Seo, Y. and Kwon, S. (2015) 'Role of gap junction communication in hepatocyte/fibroblast co-cultures: Implications for hepatic tissue engineering', *Biotechnology and Bioprocess Engineering*, 20(2), pp. 358–365. doi: 10.1007/s12257-014-0595-2.

Kim, M. *et al.* (2010) 'Heparin-based hydrogel as a matrix for encapsulation and cultivation of primary hepatocytes', *Biomaterials*, 31(13), pp. 3596–3603. doi: 10.1016/j.biomaterials.2010.01.068.

Kim, M. S., Yeon, J. H. and Park, J. K. (2007) 'A microfluidic platform for 3-dimensional cell culture and cell-based assays', *Biomedical Microdevices*, 9(1), pp. 25–34. doi: 10.1007/s10544-006-9016-4.

Kim, S. C. *et al.* (2016) 'Static magnetic field controls cell cycle in cultured human glioblastoma cells', *Cytotechnology*, 68(6), pp. 2745–2751. doi: 10.1007/s10616-016-9973-2.

Kim, Y. *et al.* (2018) 'Prolongation of liver-specific function for primary hepatocytes maintenance in 3D printed architectures', *Organogenesis*, 14(1), pp. 1–12. doi: 10.1080/15476278.2018.1423931.

Kim, Y. *et al.* (2019) 'Small molecule-mediated reprogramming of human hepatocytes into bipotent progenitor cells', *Journal of Hepatology*, 70(1), pp. 97–107. doi: 10.1016/j.jhep.2018.09.007.

Kim, Y. and Rajagopalan, P. (2010) '3D hepatic cultures simultaneously maintain primary hepatocyte and liver sinusoidal endothelial cell phenotypes', *PLoS ONE*, 5(11), pp. 1–10. doi: 10.1371/journal.pone.0015456.

Kimura, A. *et al.* (2008) 'Characterization of heparan sulfate on hepatocytes in regenerating rat liver', *Journal of Hepato-Biliary-Pancreatic Surgery*, 15(6), pp. 608–614. doi: 10.1007/s00534-007-1321-7.

Kirchheiner, J. *et al.* (2007) 'Pharmacokinetics of codeine and its metabolite morphine in ultra-rapid metabolizers due to CYP2D6 duplication', *Pharmacogenomics Journal*, 7(4), pp. 257–265. doi: 10.1038/sj.tpj.6500406.

Kitani, H. *et al.* (2014) 'Establishment of c-myc-immortalized Kupffer cell line from a C57BL/6 mouse strain', *Results in Immunology*, 4(1), pp. 68–74. doi: 10.1016/j.rinim.2014.08.001.

Kmiec, Z. (2001) 'Cooperation of Liver Cells in Health and Disease', *Advances in Anatomy Embryology and Cell*

Biology, 161, p. 1. doi: 10.1007/978-3-642-55977-8.

Knight, E. *et al.* (2011) 'Alvetex® : Polystyrene Scaffold Technology for Routine Three Dimensional Cell Culture', in *3D Cell Culture Methods and Protocols*, pp. 323–340. doi: 10.1007/978-1-60761-984-0_1.

Knöspel, F. *et al.* (2016) 'In vitro model for hepatotoxicity studies based on primary human hepatocyte cultivation in a perfused 3D bioreactor system', *International Journal of Molecular Sciences*, 17(4), pp. 1–21. doi: 10.3390/ijms17040584.

Koch, A. *et al.* (2014) 'Murine precision-cut liver slices (PCLS): A new toolfor studying tumor microenvironments and cell signaling ex vivo', *Cell Communication and Signaling*, 12(1), pp. 1–13. doi: 10.1186/s12964-014-0073-7.

Kock, K. and Brouwer, K. L. R. (2012) 'A Perspective on Efflux Transport Proteins in the Liver', *Clinical Pharmacology and Therapeutics*, 92(5), pp. 599–612. doi: 10.1016/B978-0-12-801238-3.99186-4.

Kojima, T. *et al.* (2003) 'Regulation of the blood-biliary barrier: Interaction between gap and tight junctions in hepatocytes', *Medical Electron Microscopy*, 36(3), pp. 157–164. doi: 10.1007/s00795-003-0220-5.

Kolios, G., Valatas, V. and Kouroumalis, E. (2006) 'Role of Kupffer cells in the pathogenesis of liver disease', *World Journal of Gastroenterology*, 12(46), pp. 7413–7420. doi: 10.3748/wjg.v12.i46.7413.

Kono, Y. and Roberts, E. A. (1996) 'Modulation of the expression of liver-specific functions in novel human hepatocyte lines cultured in a collagen gel sandwich configuration', *Biochemical and Biophysical Research Communications*, 220(3), pp. 628–632. doi: 10.1006/bbrc.1996.0454.

Konopka, G. *et al.* (2007) 'Junctional adhesion molecule-A is critical for the formation of pseudocanaliculi and modulates E-cadherin expression in hepatic cells', *Journal of Biological Chemistry*, 282(38), pp. 28137–28148. doi: 10.1074/jbc.M703592200.

Kook, Y. M. *et al.* (2017) 'Design of biomimetic cellular scaffolds for co-culture system and their application', *Journal of Tissue Engineering*, 8. doi: 10.1177/2041731417724640.

Kool, Marcel *et al.* (1999) 'Expression of human MRP6, a homologue of the multidrug resistance protein gene MRP1, in tissues and cancer cells', *Cancer Research*, 59(1), pp. 175–182.

Kool, M *et al.* (1999) 'MRP3, an organic anion transporter able to transport anti-cancer drugs.', *Proceedings of the National Academy of Sciences of the United States of America*, 96(12), pp. 6914–9. doi: 10.1073/pnas.96.12.6914.

Korjamo, T., Heikkinen, A. and Monkkonen, J. (2009) 'Analysis of Unstirred Water Layer in In Vitro Permeability Experiments', *Journal of pharmaceutical sciences*, 98, pp. 4469–4479. doi: 10.1002/jps.

Kostadinova, R. *et al.* (2013) 'A long-term three dimensional liver co-culture system for improved prediction of clinically relevant drug-induced hepatotoxicity', *Toxicology and Applied Pharmacology*, 268(1), pp. 1–16. doi: 10.1016/j.taap.2013.01.012.

Krause, P. *et al.* (2009) 'Maintaining hepatocyte differentiation in vitro through co-culture with hepatic stellate cells', *In Vitro Cellular & Developmental Biology - Animal*, 45, pp. 205–212. doi: 10.1007/s11626-008-9166-1.

Krishnan, V., Permuth, F. and Alto, P. (1993) 'Bisphenol-A: An Estrogenic Substance Is Released from Polycarbonate Flasks during Autoclaving', *Endocrinology*, 132(6), pp. 2279–2286.

Krumdieck, C. L., dos Santos, J. and Ho, K. J. (1980) 'A new instrument for the rapid preparation of tissue slices', *Analytical Biochemistry*, 104(1), pp. 118–123. doi: 10.1016/0003-2697(80)90284-5.

Kubitz, R. *et al.* (2001) 'Protein kinase C-dependent distribution of the multidrug resistance protein 2 from the canalicular to the basolateral membrane in human HepG2 cells', *Hepatology*, 34(2), pp. 340–350. doi: 10.1053/jhep.2001.25959.

Kubitz, R. *et al.* (2012) 'The bile salt export pump (BSEP) in health and disease', *Clinics and Research in Hepatology and Gastroenterology*, 36(6), pp. 536–553. doi: 10.1016/j.clinre.2012.06.006.

Kuna, L. *et al.* (2018) 'Models of Drug Induced Liver Injury (DILI) – Current Issues and Future Perspectives', *Current Drug Metabolism*, 19(10), pp. 830–838. doi: 10.2174/1389200219666180523095355.

De La Coste, A. *et al.* (1998) 'Somatic mutations of the β-catenin gene are frequent in mouse and human hepatocellular carcinomas', *Proceedings of the National Academy of Sciences of the United States of America*, 95(15), pp. 8847–8851. doi: 10.1073/pnas.95.15.8847.

Lagaye, S. *et al.* (2012) 'Efficient replication of primary or culture hepatitis C virus isolates in human liver slices: A relevant ex vivo model of liver infection', *Hepatology*, 56(3), pp. 861–872. doi: 10.1002/hep.25738.

Laing, R. W. *et al.* (2017) 'The Use of an Acellular Oxygen Carrier in a Human Liver Model of Normothermic Machine Perfusion', *Transplantation*, 101(11), pp. 2746–2756. doi: 10.1097/TP.0000000000001821.

Lalor, P. F. and Adams, D. H. (1999) 'Adhesion of lymphocytes to hepatic endothelium', *Journal of Clinical Pathology - Molecular Pathology*, 52(4), pp. 214–219. doi: 10.1136/mp.52.4.214.

Lam, D. *et al.* (2019) 'Tissue-specific extracellular matrix accelerates the formation of neural networks and communities in a neuron-glia co-culture on a multi-electrode array', *Scientific Reports*, 9(1), pp. 1–15. doi: 10.1038/s41598-019-40128-1.

Langer, M. and Chiandussi, L. (1987) 'Hormones and Liver: Some Aspects of the Problem', in Okolicsányi, L., Csomós, G., and Crepaldi, G. (eds) *Assessment and Management of Hepatobiliary Disease*. Berlin, Heidelberg: Springer Berlin Heidelberg, pp. 217–225.

Lasli, S. *et al.* (2019) 'A Human Liver-on-a-Chip Platform for Modeling Nonalcoholic Fatty Liver Disease', *Advanced Biosystems*, 3(8), pp. 1–12. doi: 10.1002/adbi.201900104.

Lasprilla-Botero, J., Álvarez-Láinez, M. and Lagaron, J. M. (2018) 'The influence of electrospinning parameters and solvent selection on the morphology and diameter of polyimide nanofibers', *Materials Today Communications*, 14(December 2017), pp. 1–9. doi: 10.1016/j.mtcomm.2017.12.003.

Lau, E. Y. T. *et al.* (2016) 'Cancer-Associated Fibroblasts Regulate Tumor-Initiating Cell Plasticity in Hepatocellular Carcinoma through c-Met/FRA1/HEY1 Signaling', *Cell Reports*, 15(6), pp. 1175–1189. doi: 10.1016/j.celrep.2016.04.019.

Laura, D. (2018) 'Codeine Therapy and CYP2D6 Genotype', *Medical Genetics Summaries*, (Md), pp. 1–3.

Lavoie, G. *et al.* (2005) 'Portal Fibroblasts Regulate the Proliferation of Bile Duct Epithelia via Expression of NTPDase2 *', *The Journal of Biological Chemistry*, 280(24), pp. 22986–22992. doi: 10.1074/jbc.M412371200.

Law, J. X. *et al.* (2017) 'Electrospun Collagen Nanofibers and Their Applications in Skin Tissue Engineering', *Tissue Engineering and Regenerative Medicine*, 14(6), pp. 699–718. doi: 10.1007/s13770-017-0075-9.

LeCluyse, E. L. *et al.* (2012) 'Organotypic liver culture models: meeting current challenges in toxicity testing.', *Critical reviews in toxicology*, 42(6), pp. 501–48. doi: 10.3109/10408444.2012.682115.

LeCluyse, E. L., Audus, K. L. and Hochman, J. H. (1994) 'Formation of extensive canalicular networks by rat hepatocytes cultured in collagen-sandwich configuration.', *The American journal of physiology*, 266(6 Pt 1), pp. C1764-74. Available at: http://www.ncbi.nlm.nih.gov/pubmed/8023906.

Lee, A. *et al.* (2019) '3D bioprinting of collagen to rebuild components of the human heart', *Science*, 365(6452), pp. 482–487. doi: 10.1126/science.aav9051.

Lee, H. W. *et al.* (2014) 'A three-dimensional co-culture of HepG2 spheroids and fibroblasts using double-layered fibrous scaffolds incorporated with hydrogel micropatterns', *RSC Advances*, 4, pp. 61005–61011. doi: 10.1039/c4ra12269k.

Lee, H. W. H. J. *et al.* (2014) 'A three-dimensional co-culture of HepG2 spheroids and fibroblasts using double-layered fibrous scaffolds incorporated with hydrogel micropatterns', *RSC Adv.*, 4(105), pp. 61005–61011. doi: 10.1039/C4RA12269K.

Lee, J. and Liu, X. (2007) 'The conduct of drug metabolism studies considered good practice (II): in vitro

experiments', *Curr Drug Metab. 2007*, 8(8), pp. 822–829. doi: 10.2174/138920007782798207.

Lee, J. Y. *et al.* (2020) 'Use of 3D human liver organoids to predict drug-induced phospholipidosis', *International Journal of Molecular Sciences*, 21(8). doi: 10.3390/ijms21082982.

Lee, N. P. and Luk, J. M. (2010) 'Hepatic tight junctions: From viral entry to cancer metastasis', *World Journal of Gastroenterology*, 16(3), pp. 289–295. doi: 10.3748/wjg.v16.i3.289.

Lee, S. *et al.* (2017) 'Construction of 3D multicellular microfluidic chip for an in vitro skin model', *Biomedical Microdevices*, 19(2). doi: 10.1007/s10544-017-0156-5.

Lee, S. W. *et al.* (2015) 'Optimization of Matrigel-based culture for expansion of neural stem cells', *Animal Cells and Systems*, 19(3), pp. 175–180. doi: 10.1080/19768354.2015.1035750.

Leeman, W. R., van de Gevel, I. A. and Rutten, A. A. J. J. L. (1995) 'Cytotoxicity of retinoic acid, menadione and aflatoxin B1 in rat liver slices using Netwell inserts as a new culture system', *Toxicology in Vitro*, 9(3). doi: 10.1016/0887-2333(95)00008-V.

Lefebvre, P. *et al.* (2009) 'Role of bile acids and bile acid receptors in metabolic regulation', *Physiological Reviews*, 89(1), pp. 147–191. doi: 10.1152/physrev.00010.2008.

Lei, X. hua *et al.* (2011) 'Nasa-approved rotary bioreactor enhances proliferation of human epidermal stem cells and supports formation of 3d epidermis-like structure', *PLoS ONE*, 6(11), pp. 1–8. doi: 10.1371/journal.pone.0026603.

Leite, S. B. *et al.* (2012) 'Three-dimensional HepaRG model as an attractive tool for toxicity testing', *Toxicological Sciences*, 130(1), pp. 106–116. doi: 10.1093/toxsci/kfs232.

Leo, H. L. *et al.* (2009) 'Computational Fluid Dynamics Investigation of the Effect of the Fluid-Induced Shear Stress on Hepatocyte Sandwich Perfusion Culture', *13th International Conference on Biomedical Engineering, Vols 1-3*, 23(1–3), pp. 1405–1408.

Lerche-langrand, C. and Toutain, H. J. (2000) 'Precision-cut liver slices : characteristics and use for in vitro pharmaco-toxicology', *Toxicology*, 153, pp. 221–253.

Levitt, D. G. and Levitt, M. D. (2016) 'Human serum albumin homeostasis: A new look at the roles of synthesis, catabolism, renal and gastrointestinal excretion, and the clinical value of serum albumin measurements', *International Journal of General Medicine*, 9, pp. 229–255. doi: 10.2147/IJGM.S102819.

Li, F. *et al.* (2020) 'Three-Dimensional Spheroids With Primary Human Liver Cells and Differential Roles of Kupffer Cells in Drug-Induced Liver Injury', *Journal of Pharmaceutical Sciences*, 109(6), pp. 1912–1923. doi: 10.1016/j.xphs.2020.02.021.

Li, M., De Graaf, I. A. M. and Groothuis, G. M. M. (2016) 'Precision-cut intestinal slices: Alternative model for drug transport, metabolism, and toxicology research', *Expert Opinion on Drug Metabolism and Toxicology*, 12(2), pp. 175–190. doi: 10.1517/17425255.2016.1125882.

Li, N. *et al.* (2019) 'Vessel graft fabricated by the on-site differentiation of human mesenchymal stem cells towards vascular cells on vascular extracellular matrix scaffold under mechanical stimulation in a rotary bioreactor', *Journal of Materials Chemistry B*, 7(16), pp. 2703–2713. doi: 10.1039/c8tb03348j.

Li, S. *et al.* (2011) 'Role of organic cation transporter 1, OCT1 in the pharmacokinetics and toxicity of cis-diammine(pyridine)chloroplatinum(II) and oxaliplatin in mice', *Pharmaceutical Research*, 28(3), pp. 610–625. doi: 10.1007/s11095-010-0312-6.

Lichtenberg, A. *et al.* (2005) 'A multifunctional bioreactor for three-dimensional cell (co)-culture', *Biomaterials*, 26(5), pp. 555–562. doi: 10.1016/j.biomaterials.2004.02.063.

Lin, N. Y. C. *et al.* (2019) 'Renal reabsorption in 3D vascularized proximal tubule models', *Proceedings of the National Academy of Sciences of the United States of America*, 116(12), pp. 5399–5404. doi: 10.1073/pnas.1815208116.

Lindblad, W. J. *et al.* (1991) 'Hepatocellular phenotype in Vitro is influenced by biophysical features of the collagenous substratum', *Hepatology*, 13(2), pp. 282–288. doi: 10.1002/hep.1840130213.

Lindros, K. O. (1997) 'Zonation of cytochrome P450 expression, drug metabolism and toxicity in liver', *General Pharmacology*, 28(2), pp. 191–196. doi: 10.1016/S0306-3623(96)00183-8.

Liu, G. *et al.* (2019) 'Use of precision cut lung slices as a translational model for the study of lung biology', *Respiratory Research*, 20(1), pp. 1–14. doi: 10.1186/s12931-019-1131-x.

Liu, J. *et al.* (2007) 'Functional three-dimensional HepG2 aggregate cultures generated from an ultrasound trap: Comparison with HepG2 spheroids', *Journal of Cellular Biochemistry*, 102(5), pp. 1180–1189. doi: 10.1002/jcb.21345.

Liu, J. *et al.* (2018) 'Liver Extracellular Matrices Bioactivated Hepatic Spheroids as a Model System for Drug Hepatotoxicity Evaluations', *Advanced Biosystems*, 2(10), pp. 1–14. doi: 10.1002/adbi.201800110.

Liu, M., Li, Y. and Yang, S. T. (2014) 'Expansion of human amniotic fluid stem cells in 3-dimensional fibrous scaffolds in a stirred bioreactor', *Biochemical Engineering Journal*, 82, pp. 71–80. doi: 10.1016/j.bej.2013.11.001.

Liu, X. *et al.* (1998) 'Partial maintenance of taurocholate uptake by adult rat hepatocytes cultured in a collagen sandwich configuration', *Pharmaceutical Research*, pp. 1533–1539. doi: 10.1023/A:1011994831139.

Liu, X. *et al.* (1999) 'Biliary excretion in primary rat hepatocytes cultured in a collagen-sandwich configuration.', *The American journal of physiology*, 277(1 Pt 1), pp. G12–G21. doi: 10.1007/s10616-008-9168-6.

Liu, Y., Li, H., *et al.* (2014) 'Hepatocyte cocultures with endothelial cells and fibroblasts on micropatterned fibrous mats to promote liver-specific functions and capillary formation capabilities', *Biomacromolecules*, 15(3), pp. 1044–1054. doi: 10.1021/bm401926k.

Liu, Y., Zhang, L., *et al.* (2014) 'Promoting hepatocyte spheroid formation and functions by coculture with fibroblasts on micropatterned electrospun fibrous scaffolds', *Journal of Materials Chemistry B*, 2(20), p. 3029. doi: 10.1039/c3tb21779e.

Liu, Y. A. *et al.* (2015) 'Loss of N-cadherin is associated with loss of E-cadherin expression and poor outcomes of liver resection in hepatocellular carcinoma', *Journal of Surgical Research*, 194(1), pp. 167–176. doi: 10.1016/j.jss.2014.09.031.

Loessner, D. *et al.* (2010) 'Bioengineered 3D platform to explore cell-ECM interactions and drug resistance of epithelial ovarian cancer cells', *Biomaterials*, 31(32), pp. 8494–8506. doi: 10.1016/j.biomaterials.2010.07.064.

Loh, C. Y. *et al.* (2019) *The E-Cadherin and N-Cadherin Switch in Epithelial-to-Mesenchymal Transition: Signaling, Therapeutic Implications, and Challenges*, *Cells*. doi: 10.3390/cells8101118.

Long, K. *et al.* (2015) 'Improving the mechanical properties of collagen-based membranes using silk fibroin for corneal tissue engineering', *Journal of Biomedical Materials Research - Part A*, 103(3), pp. 1159–1168. doi: 10.1002/jbm.a.35268.

Long, T. J. *et al.* (2016) 'Modeling therapeutic antibody-small molecule drug-drug interactions using a 3D perfusable human liver co-culture platform', *Drug Metabolism and Disposition*, 44(12), pp. 1940–1948. doi: 10.1124/dmd.116.071456.

Loomba, R. and Sanyal, A. J. (2013) 'The global NAFLD epidemic', *Nature Reviews Gastroenterology and Hepatology*, 10(11), pp. 686–690. doi: 10.1038/nrgastro.2013.171.

Loryan, I., Fridén, M. and Hammarlund-Udenaes, M. (2013) 'The brain slice method for studying drug distribution in the CNS', *Fluids and Barriers of the CNS*, 10(1), pp. 1–9. doi: 10.1186/2045-8118-10-6.

Louisa, M. *et al.* (2016) 'Differential expression of several drug transporter genes in HepG2 and Huh-7 cell lines', *Advanced Biomedical Research*, 5(1), p. 104. doi: 10.4103/2277-9175.183664.

Lovett, M. *et al.* (2009) 'Vascularization Strategies for Tissue Engineering', *Tissue Engineering Part B: Reviews*,

15(3), pp. 353–370. doi: 10.1089/ten.TEB.2009.0085.

Lowe, K. C. (2002) 'Perfluorochemical respiratory gas carriers: Benefits to cell culture systems', *Journal of Fluorine Chemistry*, 118(1–2), pp. 19–26. doi: 10.1016/S0022-1139(02)00200-2.

Luangmonkong, T. *et al.* (2017) 'Evaluating the antifibrotic potency of galunisertib in a human ex vivo model of liver fibrosis', *British Journal of Pharmacology*, 174(18), pp. 3107–3117. doi: 10.1111/bph.13945.

Luckert, C. *et al.* (2016) 'Comparative analysis of 3D culture methods on human HepG2 cells', *Archives of Toxicology*, pp. 1–14. doi: 10.1007/s00204-016-1677-z.

Luo, D. *et al.* (2014) 'The role of hypoxia inducible factor-1 in hepatocellular carcinoma', *BioMed Research International*, 2014. doi: 10.1155/2014/409272.

Lv, Q. *et al.* (2007) 'Preparation and characterization of PLA/fibroin composite and culture of HepG2 (human hepatocellular liver carcinoma cell line) cells', *Composites Science and Technology*, 67(14), pp. 3023–3030. doi: 10.1016/j.compscitech.2007.05.003.

Ma, X. *et al.* (2016) 'Deterministically patterned biomimetic human iPSC-derived hepatic model via rapid 3D bioprinting', *Proceedings of the National Academy of Sciences of the United States of America*, 113(8), pp. 2206–2211. doi: 10.1073/pnas.1524510113.

Madon, J. *et al.* (2000) 'Transport function and hepatocellular localization of mrp6 in rat liver', *Molecular Pharmacology*, 57(3), pp. 634–641. doi: 10.1124/mol.57.3.634.

Mak, K. M. and Mei, R. (2017) 'Basement Membrane Type IV Collagen and Laminin: An Overview of Their Biology and Value as Fibrosis Biomarkers of Liver Disease', *Anatomical Record*, 300(8), pp. 1371–1390. doi: 10.1002/ar.23567.

Malakian, A. *et al.* (2019) 'Synthesis and in situ functionalization of microfiltration membranes via high internal phase emulsion templating', *Polymer International*, 68(7), pp. 1378–1386. doi: 10.1002/pi.5828.

Malarkey, D. E. *et al.* (2005) 'New Insights into Functional Aspects of Liver Morphology', *Toxicologic Pathology*, 33(1), pp. 27–34. doi: 10.1080/01926230590881826.

Malda, J. *et al.* (2008) 'Cell Nutrition', in Blitterswijk, C. van et al. (eds) *Tissue Engineering*. Academic Press, pp. 327–362. doi: 10.1016/B978-0-12-370869-4.00012-4.

Mall, F. P. (1906) 'A study of the structural unit of the liver', *American Journal of Anatomy*, 5(3), pp. 227–308. doi: 10.1002/aja.1000050302.

Manka, P., Zeller, A. and Syn, W. K. (2019) 'Fibrosis in Chronic Liver Disease: An Update on Diagnostic and Treatment Modalities', *Drugs*, 79(9), pp. 903–927. doi: 10.1007/s40265-019-01126-9.

March, S. *et al.* (2009) 'Microenvironmental regulation of the sinusoidal endothelial cell phenotype in vitro', *Hepatology*, 50(3), pp. 920–928. doi: 10.1002/hep.23085.

Martín-Saavedra, F. *et al.* (2017) 'Substrate Microarchitecture Shapes the Paracrine Crosstalk of Stem Cells with Endothelial Cells and Osteoblasts', *Scientific Reports*, 7(1), pp. 1–13. doi: 10.1038/s41598-017-15036-x.

Martin, Y. and Vermette, P. (2005) 'Bioreactors for tissue mass culture: Design, characterization, and recent advances', *Biomaterials*, 26(35), pp. 7481–7503. doi: 10.1016/j.biomaterials.2005.05.057.

Martinez-Hernandez, A. and Amenta, Peter S (1993) 'The hepatic extracellular matrix. I. Components and distribution in normal liver', *Virchows Archiv A Pathol Anat*, 423, pp. 1–11. doi: 10.1007/BF01606425.

Martinez-Hernandez, A. and Amenta, Peter S. (1993) 'The hepatic extracellular matrix - II. Ontogenesis, regeneration and cirrhosis', *Virchows Archiv A Pathological Anatomy and Histopathology*, 423(2), pp. 77–84. doi: 10.1007/BF01606580.

Massai, D. *et al.* (2016) 'A versatile bioreactor for dynamic suspension cell culture. Application to the culture of cancer cell spheroids', *PLoS ONE*, 11(5), pp. 1–16. doi: 10.1371/journal.pone.0154610.

Matsuda, M. and Seki, E. (2020) 'The liver fibrosis niche: Novel insights into the interplay between fibrosis-composing mesenchymal cells, immune cells, endothelial cells, and extracellular matrix', *Food and Chemical Toxicology*, p. 111556. doi: 10.1016/j.fct.2020.111556.

Matsumoto, T. and Kawakami, M. (1982) 'The unit-concept of hepatic parenchyma-a re-examination based on angioarchitectural studies.', *Acta Pathologica Japonica*, 32(2), pp. 285–314.

Mattei, G., Giusti, S. and Ahluwalia, A. (2014) 'Design criteria for generating physiologically relevant in vitro models in bioreactors', *Processes*, 2(3), pp. 548–569. doi: 10.3390/pr2030548.

Mavri-Damelin, D. *et al.* (2007) 'Ornithine transcarbamylase and arginase I deficiency are responsible for diminished urea cycle function in the human hepatoblastoma cell line HepG2', *International Journal of Biochemistry and Cell Biology*, 39(3), pp. 555–564. doi: 10.1016/j.biocel.2006.10.007.

Mazaleuskaya, L. L. *et al.* (2015) 'PharmGKB summary: Pathways of acetaminophen metabolism at the therapeutic versus toxic doses', *Pharmacogenetics and Genomics*, 25(8), pp. 416–426. doi: 10.1097/fpc.0000000000000170.

Mazza, G. *et al.* (2015) 'Decellularized human liver as a natural 3D-scaffold for liver bioengineering and transplantation', *Scientific Reports*, 5, pp. 1–15. doi: 10.1038/srep13079.

McConkey, C. A. *et al.* (2016) 'A three-dimensional culture system recapitulates placental syncytiotrophoblast development and microbial resistance', *Science Advances*, 2(3), pp. 1–9. doi: 10.1126/sciadv.1501462.

McGill, M. R. and Jaeschke, H. (2019) 'Animal models of drug-induced liver injury', *Biochimica et Biophysica Acta - Molecular Basis of Disease*, 1865(5), pp. 1031–1039. doi: 10.1016/j.bbadis.2018.08.037.

McMurtrey, R. J. (2014) 'Analytic Models of Oxygen and Nutrient Diffusion, Metabolism Dynamics, and Architecture Optimization in 3D tissue Constructs with Applications and Insights in Cerebral Organoids', *Igarss 2014*, 22(1), pp. 1–5. doi: 10.1007/s13398-014-0173-7.2.

Melton, A. C. and Yee, H. F. (2007) 'Hepatic stellate cell protrusions couple platelet-derived growth factor-BB to chemotaxis', *Hepatology*, 45(6), pp. 1446–1453. doi: 10.1002/hep.21606.

Memon, N. *et al.* (2016) 'Inherited Disorders of Bilirubin Clearance', *Pediatric Research*, 79(3), pp. 378–386. doi: 10.1016/j.physbeh.2017.03.040.

Meng, F. *et al.* (2015) 'Dynamic virus-bacterium interactions in a porcine precision-cut lung slice coinfection model: Swine influenza virus paves the way for Streptococcus suis infection in a two-step process', *Infection and Immunity*, 83(7), pp. 2806–2815. doi: 10.1128/IAI.00171-15.

Messina, A. *et al.* (2020) 'Pluripotent-Stem-Cell-Derived Hepatic Cells : and Regeneration', *Cells*, 9(2), p. 420.

Messner, S. *et al.* (2013) 'Multi-cell type human liver microtissues for hepatotoxicity testing', *Archives of Toxicology*. doi: 10.1007/s00204-012-0968-2.

Metzen, E. *et al.* (1995) 'Pericellular PO2 and O2 consumption in monolayer cell cultures', *Respiration Physiology*, 100(2), pp. 101–106. doi: 10.1016/0034-5687(94)00125-J.

Mewes, A., Franke, H. and Singer, D. (2012) 'Organotypic Brain Slice Cultures of Adult Transgenic P301S Mice-A Model for Tauopathy Studies', *PLoS ONE*, 7(9). doi: 10.1371/journal.pone.0045017.

Mi, S. *et al.* (2018) 'Construction of a liver sinusoid based on the laminar flow on chip and self-assembly of endothelial cells', *Biofabrication*, 10(2). doi: 10.1088/1758-5090/aaa97e.

Michalopoulos, G. K. *et al.* (1999) 'Morphogenetic events in mixed cultures of rat hepatocytes and nonparenchymal cells maintained in biological matrices in the presence of hepatocyte growth factor and epidermal growth factor', *Hepatology*, 29(1), pp. 90–100. doi: 10.1002/hep.510290149.

Miessen, K. *et al.* (2011) 'Modelling the porcine oviduct epithelium: A polarized in vitro system suitable for long-term cultivation', *Theriogenology*, 76(5), pp. 900–910. doi: 10.1016/j.theriogenology.2011.04.021.

Miranda, J. P. *et al.* (2009) 'Towards an extended functional hepatocyte in vitro culture', *Tissue engineering: Part C*, 15(2), pp. 157–167. doi: 10.1089/ten.tec.2008.0352.

Miranda, J. P. *et al.* (2010) 'Extending Hepatocyte Functionality for Drug-Testing Applications Using High-Viscosity Alginate–Encapsulated Three-Dimensional Cultures in Bioreactors', *Tissue Engineering Part C: Methods*, 16(6), pp. 1223–1232. doi: 10.1089/ten.tec.2009.0784.

Mirbagheri, M. *et al.* (2019) 'Advanced cell culture platforms: a growing quest for emulating natural tissues', *Materials Horizons*, 6(1), pp. 45–71. doi: 10.1039/c8mh00803e.

Missner, A. *et al.* (2008) 'Carbon dioxide transport through membranes', *Journal of Biological Chemistry*, 283(37), pp. 25340–25347. doi: 10.1074/jbc.M800096200.

Mittal, N. *et al.* (2018) 'Complex interplay between serum and fibroblasts in 3D hepatocyte co-culture', *bioRxiv*. doi: 10.1101/286088.

Mitteregger, R. *et al.* (1999) 'Rotary cell culture system (RCCS): A new method for cultivating hepatocytes on microcarriers', *International Journal of Artificial Organs*, 22(12), pp. 816–822. doi: 10.1177/039139889902201207.

Miyakoshi, J. (2005) 'Effects of static magnetic fields at the cellular level', *Progress in Biophysics and Molecular Biology*, 87(2-3 SPEC. ISS.), pp. 213–223. doi: 10.1016/j.pbiomolbio.2004.08.008.

Miyoshi, N. *et al.* (2011) 'Reprogramming of mouse and human cells to pluripotency using mature microRNAs', *Cell Stem Cell*, 8(6), pp. 633–638. doi: 10.1016/j.stem.2011.05.001.

Mizoi, K. *et al.* (2020) 'Utility of three-dimensional cultures of primary human hepatocytes (spheroids) as pharmacokinetic models', *Biomedicines*, 8(10). doi: 10.3390/BIOMEDICINES8100374.

Moedas, M. F. *et al.* (2017) 'Advances in methods for characterization of hepatic urea cycle enzymatic activity in HepaRG cells using UPLC-MS/MS', *Analytical Biochemistry*, 535, pp. 47–55. doi: 10.1016/j.ab.2017.07.025.

Moghe, P. V. *et al.* (1996) 'Culture matrix configuration and composition in the maintenance of hepatocyte polarity and function', *Biomaterials*, 17(3), pp. 373–385. doi: 10.1016/0142-9612(96)85576-1.

Mohyeldin, A., Garzón-Muvdi, T. and Quiñones-Hinojosa, A. (2010) 'Oxygen in stem cell biology: A critical component of the stem cell niche', *Cell Stem Cell*, 7(2), pp. 150–161. doi: 10.1016/j.stem.2010.07.007.

Monga, S. P. S. *et al.* (2001) 'Changes in wnt/β-catenin pathway during regulated growth in rat liver regeneration', *Hepatology*, 33(5), pp. 1098–1109. doi: 10.1053/jhep.2001.23786.

Mosedale, M. and Watkins, P. B. (2017) 'Drug-Induced Liver Injury: Advances in Mechanistic Understanding that will Inform Risk Management', *Clinical Pharmacology and Therapeutics*, 101(4), pp. 469–480. doi: 10.1002/cpt.564.Drug-Induced.

Mravljak, R. *et al.* (2021) 'Effect of polyHIPE porosity on its hydrodynamic properties', *Polymer Testing*, 93(February 2020). doi: 10.1016/j.polymertesting.2020.106590.

Mueller, D. *et al.* (2013) 'Real-time in situ viability assessment in a 3D bioreactor with liver cells using resazurin assay', *Cytotechnology*, 65(2), pp. 297–305. doi: 10.1007/s10616-012-9486-6.

Mueller, D. *et al.* (2014) '3D organotypic HepaRG cultures as in vitro model for acute and repeated dose toxicity studies', *Toxicology in Vitro*, 28(1), pp. 104–112. doi: 10.1016/j.tiv.2013.06.024.

Mueller, D., Koetemann, A. and Noor, F. (2011) 'Organotypic Cultures of Hepg2 Cells for In Vitro Toxicity Studies', *Journal of Bioengineering and Biomedical Sciences*, 01(S2), p. 9538. doi: 10.4172/2155-9538.S2-002.

Murphy, S. V. and Atala, A. (2014) '3D bioprinting of tissues and organs', *Nature Biotechnology*, 32(8), pp. 773–785. doi: 10.1038/nbt.2958.

Müsch, A. (2014) 'The unique polarity phenotype of hepatocytes', *Experimental Cell Research*, 328(2), pp. 276–283. doi: 10.1016/j.yexcr.2014.06.006.

Nagata, S. (2000) 'Apoptotic DNA fragmentation', *Experimental Cell Research*, 256(1), pp. 12–18. doi: 10.1006/excr.2000.4834.

Nakamura, M. *et al.* (2010) 'Biomatrices and biomaterials for future developments of bioprinting and biofabrication', *Biofabrication*, 2(1), pp. 0–6. doi: 10.1088/1758-5082/2/1/014110.

Nakayama, S. *et al.* (2009) 'A Zone Classification System for Risk Assessment of Idiosyncratic Drug Toxicity Using Daily Dose and Covalent Binding', *Drug Metabolism and Disposition*, 37(9), pp. 1970–1977. doi: 10.1124/dmd.109.027797.

Nathanson, M. H. *et al.* (1999) 'Communication via gap junctions modulates bile secretion in the isolated perfused rat liver', *Gastroenterology*, 116(5), pp. 1176–1183. doi: 10.1016/S0016-5085(99)70021-1.

National Centre for the Replacement, R. & R. of A. in R. (2020) *The 3Rs*. Available at: https://www.nc3rs.org.uk/the-3rs (Accessed: 7 April 2020).

Neiman, J. A. S. S. *et al.* (2015) 'Photopatterning of hydrogel scaffolds coupled to filter materials using stereolithography for perfused 3D culture of hepatocytes', *Biotechnology and Bioengineering*, 112(4), pp. 777–787. doi: 10.1002/bit.25494.

Németh, Z. *et al.* (2009) 'Zonula occludens-1, occludin, and E-cadherin protein expression in biliary tract cancers', *Pathology and Oncology Research*, 15(3), pp. 533–539. doi: 10.1007/s12253-009-9150-4.

Neupert, G., Glockner, R. and Muller, D. (1998) 'Immunohistochemical localization of cytochrome P450 1A1 in precision- cut rat liver slices after in vitro exposure to β-naphthoflavone', *Experimental and Toxicologic Pathology*, 50(4–6), pp. 514–518. doi: 10.1016/S0940-2993(98)80043-2.

Neveu, M. J. *et al.* (1995) 'Proliferation-associated differences in the spatial and temporal expression of gap junction genes in rat liver', *Hepatology*, 22(1), pp. 202–212. doi: 10.1016/0270-9139(95)90374-7.

Nguyen, D. G. *et al.* (2016) 'Bioprinted 3D primary liver tissues allow assessment of organ-level response to clinical drug induced toxicity in vitro', *PLoS ONE*, 11(7), pp. 1–17. doi: 10.1371/journal.pone.0158674.

Nguyen, T. V. *et al.* (2015) 'Establishment of a hepatocyte-kupffer cell coculture model for assessment of proinflammatory cytokine effects on metabolizing enzymes and drug transporters', *Drug Metabolism and Disposition*, 43(5), pp. 774–785. doi: 10.1124/dmd.114.061317.

Nicholson, B. J., Babcock, K. L. and Pitot, H. C. (1994) 'Colocalized Alterations in Connexin32 and Cytochrome P450IIB1/2 by Phenobarbital and Related Liver Tumor Promoters', *Cancer Research*, 54(12), pp. 3145–3152.

Nii, T. *et al.* (2020) 'A Co-Culture System of Three-Dimensional Tumor-Associated Macrophages and Three-Dimensional Cancer-Associated Fibroblasts Combined with Biomolecule Release for Cancer Cell Migration', *Tissue Engineering - Part A*, 26(23=24), pp. 1272–1282.

Niles, A. L., Moravec, R. A. and Riss, T. L. (2009) 'In vitro viability and cytotoxicity testing and same-well multi-parametric combinations for high throughput screening', *Current Chemical Genomics*, 3(1), pp. 33–41. doi: 10.2174/1875397300903010033.

Nishida, Y. and Taniguchi, A. (2016) 'A three-dimensional collagen-sponge-based culture system coated with simplified recombinant fibronectin improves the function of a hepatocyte cell line', *In Vitro Cellular and Developmental Biology - Animal*, 52(3), pp. 271–277. doi: 10.1007/s11626-015-9973-0.

Nomura, S. and Takano-Yamamoto, T. (2000) 'Molecular events caused by mechanical stress in bone', *Matrix Biology*, 19(2), pp. 91–96. doi: 10.1016/S0945-053X(00)00050-0.

Norona, L. M. *et al.* (2016) 'Modeling compound-induced fibrogenesis in vitro using three-dimensional bioprinted human liver tissues', *Toxicological Sciences*, 154(2), pp. 354–367. doi: 10.1093/TOXSCI/KFW169.

Novik, E. I. *et al.* (2017) 'Long-enduring primary hepatocyte-based co-cultures improve prediction of hepatotoxicity', *Toxicology and Applied Pharmacology*, 336(September), pp. 20–30. doi: 10.1016/j.taap.2017.09.013.

Nudischer, R. *et al.* (2020) 'Characterization of a long-term mouse primary liver 3D tissue model recapitulating innate-immune responses and drug-induced liver toxicity', *PLoS ONE*, 15(7 July), pp. 1–22. doi: 10.1371/journal.pone.0235745.

Nwosu, Z. C. *et al.* (2018) 'Liver cancer cell lines distinctly mimic the metabolic gene expression pattern of the corresponding human tumours', *Journal of Experimental and Clinical Cancer Research*, 37(1), pp. 1–15. doi: 10.1186/s13046-018-0939-4.

Nyberg, S. L. *et al.* (1993) 'Evaluation of a hepatocyte-entrapment hollow fiber bioreactor: A potential bioartificial liver', *Biotechnology and Bioengineering*, 41(2), pp. 194–203.

O'Brien, P. J. *et al.* (2006) 'High concordance of drug-induced human hepatotoxicity with in vitro cytotoxicity measured in a novel cell-based model using high content screening', *Archives of Toxicology*, 80(9), pp. 580–604. doi: 10.1007/s00204-006-0091-3.

Ogu, C. C. and Maxa, J. L. (2000) 'Drug interactions due to cytochrome P450.', *Proceedings (Baylor University. Medical Center)*, 13(4), pp. 421–3. doi: 10.1016/0090-6980(92)90063-Y.

Ohtani, N. and Kawada, N. (2019) 'Role of the Gut-Liver Axis in Liver Inflammation, Fibrosis, and Cancer: A Special Focus on the Gut Microbiota Relationship', *Hepatology Communications*, 3(4), pp. 456–470. doi: 10.1002/hep4.1331.

Oleaga, C. *et al.* (2016) 'Multi-Organ toxicity demonstration in a functional human in vitro system composed of four organs', *Scientific Reports*, 6(February), pp. 1–17. doi: 10.1038/srep20030.

Olinga, Peter *et al.* (1997) 'Comparison of Five Incubation Systems for Rat Liver Slices Using Functional and Viability Parameters', *Journal of Pharmocological and Toxicological Methods*, 8719(97).

Olinga, P. *et al.* (1997) 'Liver slices in in vitro pharmacotoxicology with special reference to the use of human liver tissue', *Toxicology in Vitro*, 12(1). doi: 10.1016/S0887-2333(97)00097-0.

Olinga, P. *et al.* (1998) 'Effect of cold and warm ischaemia on drug metabolism in isolated hepatocytes and slices from human and monkey liver', *Xenobiotica*, 28(4), pp. 349–360.

Olinga, P. and Schuppan, D. (2013) 'Precision-cut liver slices : A tool to model the liver ex vivo', *Journal of Hepatology*, 58(6), pp. 1252–1253. doi: 10.1016/j.jhep.2013.01.009.

Ortega-Ribera, M. *et al.* (2018) 'Resemblance of the human liver sinusoid in a fluidic device with biomedical and pharmaceutical applications', *Biotechnology and Bioengineering*, 115(10), pp. 2585–2594. doi: 10.1002/bit.26776.

Oshikata-Miyazaki, A. and Takezawa, T. (2015) 'Development of an oxygenation culture method for activating the liver-specific functions of HepG2 cells utilizing a collagen vitrigel membrane chamber', *Cytotechnology*, 68(5), pp. 1–11. doi: 10.1007/s10616-015-9934-1.

Ostrowski, M. A. *et al.* (2014) 'Microvascular endothelial cells migrate upstream and align against the shear stress field created by impinging flow', *Biophysical Journal*, 106(2), pp. 366–374. doi: 10.1016/j.bpj.2013.11.4502.

Otsuka, H. *et al.* (2013) 'Micropatterned co-culture of hepatocyte spheroids layered on non-parenchymal cells to understand heterotypic cellular interactions', *Science and Technology of Advanced Materials*, 14(6). doi: 10.1088/1468-6996/14/6/065003.

Owens, G. K. (1995) 'Regulation of differentiation of vascular smooth muscle cells', *Physiological Reviews*, 75(3), pp. 487–517. doi: 10.1152/physrev.1995.75.3.487.

Paim, A. *et al.* (2018) 'Human dental pulp stem cell adhesion and detachment in polycaprolactone electrospun scaffolds under direct perfusion', *Brazilian Journal of Medical and Biological Research*, 51(5), pp. 1–10. doi: 10.1590/1414-431x20186754.

Paish, H. L. *et al.* (2019a) 'A Bioreactor Technology for Modeling Fibrosis in Human and Rodent Precision-Cut

Liver Slices', *Hepatology*, 70(4), pp. 1377–1391. doi: 10.1002/hep.30651.

Paish, H. L. *et al.* (2019b) 'A Bioreactor Technology for Modeling Fibrosis in Human and Rodent Precision-Cut Liver Slices', *Hepatology*, 0(0), pp. 1–15. doi: 10.1002/hep.30651.

Palakkan, A. A., Nanda, J. and Ross, J. A. (2017) 'Pluripotent stem cells to hepatocytes, the journey so far', *Biomedical Reports*, 6(4), pp. 367–373. doi: 10.3892/br.2017.867.

Palma, E., Doornebal, E. J. and Chokshi, S. (2019) 'Precision-cut liver slices: a versatile tool to advance liver research', *Hepatology International*, 13(1), pp. 51–57. doi: 10.1007/s12072-018-9913-7.

Papadimitropoulos, A. *et al.* (2014) 'Expansion of human mesenchymal stromal cells from fresh bone marrow in a 3D scaffold-based system under direct perfusion', *PLoS ONE*, 9(7), pp. 1–12. doi: 10.1371/journal.pone.0102359.

Parent, R. *et al.* (2004) 'Origin and Characterization of a Human Bipotent Liver Progenitor Cell Line', *Gastroenterology*, 126(4), pp. 1147–1156. doi: 10.1053/j.gastro.2004.01.002.

Park, J. *et al.* (2007) 'Radial Flow Hepatocyte Bioreactor Using Stacked Microfabricated Grooved Substrates', *Biotechnology and Bioengineering*, 99(2), pp. 455–467. doi: 10.1002/bit.

Parmaksiz, M., Elçin, A. E. and Elçin, Y. M. (2020) 'Decellularized Cell Culture ECMs Act as Cell Differentiation Inducers', *Stem Cell Reviews and Reports*, 16(3), pp. 569–584. doi: 10.1007/s12015-020-09963-y.

Parrish, A. R., Gandolfi, A. J. and Brendel, K. (1995) 'Precision-Cut Tissue Slices: Applications in Pharmacology and Toxicology', *Life Sciences*, 57(21), pp. 1887–1901.

Pastor, C. M. (2018) 'Isolated Perfused Rat Livers to Quantify the Pharmacokinetics and Concentrations of Gd-BOPTA', *Contrast Media and Molecular Imaging*, 2018. doi: 10.1155/2018/3839108.

Patel, H., Bonde, M. and Srinivasan, G. (2011) 'Biodegradable polymer scaffolds for tissue engineering', *Trends Biomater. Artif. Organs*, 25(1), pp. 20–29. doi: 10.1038/nbt0794-689.

Paul, S. M. *et al.* (2010) 'How to improve R&D productivity: The pharmaceutical industry's grand challenge', *Nature Reviews Drug Discovery*, 9(3), pp. 203–214. doi: 10.1038/nrd3078.

Pavlacky, J. and Polak, J. (2020) 'Technical Feasibility and Physiological Relevance of Hypoxic Cell Culture Models', *Frontiers in Endocrinology*, 11(February), pp. 1–15. doi: 10.3389/fendo.2020.00057.

Pelkonen, O. *et al.* (1998) 'Inhibition and induction of human cytochrome P450 (CYP) enzymes', *Xenobiotica*, 28(12), pp. 1203–1253.

Penz-Österreicher, M., Österreicher, C. H. and Trauner, M. (2011) 'Fibrosis in autoimmune and cholestatic liver disease', *Best Practice and Research: Clinical Gastroenterology*, 25(2), pp. 245–258. doi: 10.1016/j.bpg.2011.02.001.

Persson, M. *et al.* (2013) 'A high content screening assay to predict human drug-induced liver injury during drug discovery', *Journal of Pharmacological and Toxicological Methods*, 68(3), pp. 302–313. doi: 10.1016/j.vascn.2013.08.001.

Peterson, T. C. and Renton, K. W. (1986) 'Kupffer cell factor mediated depression of hepatic parenchymal cell cytochrome P-450', *Biochemical Pharmacology1*, 35(9), pp. 1491–1497.

Pettersen, E. O. *et al.* (2005) 'Pericellular oxygen depletion during ordinary tissue culturing, measured with oxygen microsensors', *Cell Proliferation*, 38(4), pp. 257–267. doi: 10.1111/j.1365-2184.2005.00345.x.

Pham, B. T. *et al.* (2015) 'Precision-cut rat, mouse, and human intestinal slices as novel models for the early-onset of intestinal fibrosis', *Physiological Reports*, 3(4), p. e12323. doi: 10.14814/phy2.12323.

Piard, C. *et al.* (2019) '3D printed HUVECs/MSCs cocultures impact cellular interactions and angiogenesis depending on cell-cell distance.', *Biomaterials*, 222, p. 119423. doi: 10.1016/j.biomaterials.2019.119423.3D.

Place, T. L., Domann, F. E. and Case, A. J. (2017) 'Limitations of oxygen delivery to cells in culture: An underappreciated problem in basic and translational research', *Free Radical Biology and Medicine*, 113(May), pp. 311–322. doi: 10.1016/j.freeradbiomed.2017.10.003.

Plant, N. (2004) 'Strategies for using in vitro screens in drug metabolism', *Drug Discovery Today*, 9(7), pp. 328–336. doi: 10.1016/S1359-6446(03)03019-8.

Plunkett, N. and O'Brien, F. J. (2011) 'Bioreactors in tissue engineering', *Technology and Health Care*, 19(1), pp. 55–69. doi: 10.3233/THC-2011-0605.

Poisson, J. *et al.* (2017) 'Liver sinusoidal endothelial cells: Physiology and role in liver diseases', *Journal of Hepatology*, 66(1), pp. 212–227. doi: 10.1016/j.jhep.2016.07.009.

Poosti, F. *et al.* (2015) 'Precision-cut kidney slices (PCKS) to study development of renal fibrosis and efficacy of drug targeting ex vivo', *DMM Disease Models and Mechanisms*, 8(10), pp. 1227–1236. doi: 10.1242/dmm.020172.

Porceddu, M. *et al.* (2012) 'Prediction of liver injury induced by chemicals in human with a multiparametric assay on isolated mouse liver mitochondria', *Toxicological Sciences*, 129(2), pp. 332–345. doi: 10.1093/toxsci/kfs197.

Powers, M. J. *et al.* (2002) 'A microfabricated array bioreactor for perfused 3D liver culture', *Biotechnology and Bioengineering*, 78(3), pp. 257–269. doi: 10.1002/bit.10143.

Pradhan-sundd, T. and Monga, S. P. (2019) 'Blood–Bile Barrier: Morphology, Regulation, and Pathophysiology', *Gene Expression*, 19, pp. 69–87.

Price, R J *et al.* (1998) 'Influence of Slice Thickness and Culture Conditions on the Metabolism of 7-Ethoxycoumarin in Precision-cut Rat Liver Slices.', *Alternatives to laboratory animals : ATLA*, 26(4), pp. 541–548.

Price, R. J. *et al.* (1998) 'Use of precision-cut rat liver slices for studies of xenobiotic metabolism and toxicity: Comparison of the Krumdieck and Brendel tissue slicers', *Xenobiotica*, 28(4), pp. 361–371. doi: 10.1080/004982598239470.

Prior, N., Inacio, P. and Huch, M. (2019) 'Liver organoids: From basic research to therapeutic applications', *Gut*, 68(12), pp. 2228–2237. doi: 10.1136/gutjnl-2019-319256.

Proctor, W. R. *et al.* (2017) 'Utility of spherical human liver microtissues for prediction of clinical drug-induced liver injury', *Archives of Toxicology*, 91(8), pp. 2849–2863. doi: 10.1007/s00204-017-2002-1.

Protzer, U., Maini, M. K. and Knolle, P. A. (2012) 'Living in the liver: Hepatic infections', *Nature Reviews Immunology*, 12(3), pp. 201–213. doi: 10.1038/nri3169.

Punyadarsaniya, D. *et al.* (2015) 'Precision-cut intestinal slices as a culture system to analyze the infection of differentiated intestinal epithelial cells by avian influenza viruses', *Journal of Virological Methods*, 212, pp. 71–75. doi: 10.1016/j.jviromet.2014.10.015.

Pusch, J. *et al.* (2011) 'The physiological performance of a three-dimensional model that mimics the microenvironment of the small intestine', *Biomaterials*, 32(30), pp. 7469–7478. doi: 10.1016/j.biomaterials.2011.06.035.

R. Burt, A. Portmann, Ferrell, L. D. (2017) *MacSween's Pathology of the Liver*. 7th edn. Elsevier.

Rad, A. T. *et al.* (2014) 'Conducting scaffolds for liver tissue engineering', *Journal of Biomedical Materials Research - Part A*, 102(11), pp. 4169–4181. doi: 10.1002/jbm.a.35080.

Rajbhandari, R. and Chung, R. T. (2016) 'Treatment of Hepatitis B: A Concise Review', *Clinical and Translational Gastroenterology*, 7(9), p. e190. doi: 10.1038/ctg.2016.46.

Ramachandran, P. and Iredale, J. P. (2012) 'Liver fibrosis: A bidirectional model of fibrogenesis and resolution', *Qjm*, 105(9), pp. 813–817. doi: 10.1093/qjmed/hcs069.

Ramaiahgari, Sreenivasa C. *et al.* (2014) 'A 3D in vitro model of differentiated HepG2 cell spheroids with improved liver-like properties for repeated dose high-throughput toxicity studies', *Archives of Toxicology*, 88(5), pp. 1083–1095. doi: 10.1007/s00204-014-1215-9.

Ramaiahgari, Sreenivasa C *et al.* (2014) 'A 3D in vitro model of differentiated HepG2 cell spheroids with improved liver-like properties for repeated dose high-throughput toxicity studies', *Arch Toxicol*, 88, pp. 1083–1095. doi: 10.1007/s00204-014-1215-9.

Ramaiahgari, S. C. *et al.* (2017) 'Three-dimensional (3D) HepaRG spheroid model with physiologically relevant xenobiotic metabolism competence and hepatocyte functionality for liver toxicity screening', *Toxicological Sciences*, 159(1), pp. 124–136. doi: 10.1093/toxsci/kfx122.

Ramond, M. J., Martinot-Peignoux, M. and Erlinger, S. (1985) 'Dome formation in the human colon carcinoma cell line Caco-2 in culture. Influence of ouabain and permeable supports', *Biology of the Cell*, 54(1), pp. 89–92.

Rappaport, A. M. *et al.* (1952) 'Subdivisions of Hexagonal Liver Lobules into a Structural and Functional Unit', *Role in hepatic physiology and pathology*, pp. 11–33. doi: 10.1002/ar.1091190103.

Rappel, W. J. and Edelstein-Keshet, L. (2017) 'Mechanisms of cell polarization', *Current Opinion in Systems Biology*, 3, pp. 43–53. doi: 10.1016/j.coisb.2017.03.005.

Rashidi, H. *et al.* (2016) 'Fluid shear stress modulation of hepatocyte-like cell function', *Archives of Toxicology*, 90(7), pp. 1757–1761. doi: 10.1007/s00204-016-1689-8.

Rathore, A. S., Kanwar Shekhawat, L. and Loomba, V. (2016) 'Computational Fluid Dynamics for Bioreactor Design', *Bioreactors*, pp. 295–322. doi: 10.1002/9783527683369.ch10.

Rebelo, P. *et al.* (2015) 'Three-dimensional co-culture of human hepatocytes and mesenchymal stem cells : improved functionality in long-term bioreactor cultures', *Journal of tissue engineering and regenerative medicine*. doi: 10.1002/term.

Reid, L. M. *et al.* (1980) 'Long-Term Cultures of Normal Rat Hepatocytes on Liver Biomatrix', *Annals of the New York Academy of Sciences*, 349(1), pp. 70–76. doi: 10.1111/j.1749-6632.1980.tb29516.x.

Reprocell Europe (2021) *Retrieval of Cells from Alvetex™ Strata*, *Reprocell Europe*. Available at: https://info.reprocell.com/hubfs/website/resources/protocols-alvetex/PR-ALVETEX-STRATA-D002002-US-1.pdf?hsLang=en (Accessed: 16 March 2021).

Reshetnyak, V. I. (2013) 'Physiological and molecular biochemical mechanisms of bile formation', *World Journal of Gastroenterology*, 19(42), pp. 7341–7360. doi: 10.3748/wjg.v19.i42.7341.

Rijal, G. and Li, W. (2018) 'Native-mimicking in vitro microenvironment: An elusive and seductive future for tumor modeling and tissue engineering', *Journal of Biological Engineering*, 12(1), pp. 1–22. doi: 10.1186/s13036-018-0114-7.

Rimann, M. and Graf-hausner, U. (2012) 'Synthetic 3D multicellular systems for drug development', *Current Opinion in Biotechnology*, 23, pp. 803–809. doi: 10.1016/j.copbio.2012.01.011.

Riss, T. L. *et al.* (2013) 'Cell Viability Assays', *Assay Guidance Manual [Internet]*, 114(8), pp. 785–796. doi: 10.1016/j.acthis.2012.01.006.

Rius, M. *et al.* (2003) 'Cotransport of reduced glutathione with bile salts by MRP4 (ABCC4) localized to the basolateral hepatocyte membrane', *Hepatology*, 38(2), pp. 374–384. doi: 10.1053/jhep.2003.50331.

Roehlen, N., Crouchet, E. and Baumen, T. E. (2020) *Liver Fibrosis : Mechanistic Concepts and Therapeutic Perspectives*, *Cells*. doi: doi:10.3390/cells9040875.

Roger, M. *et al.* (2019) 'Bioengineering the microanatomy of human skin', *Journal of Anatomy*, 234(4), pp. 438–455. doi: 10.1111/joa.12942.

Rojkind, M., Giambrone, M. A. and Biempica, L. (1979) 'Collagen Types in Normal and Cirrhotic Liver', *Gastroenterology*, 76(4), pp. 710–719. doi: 10.1016/S0016-5085(79)80170-5.

Rollins, D. E. and Klaassen, C. D. (1979) 'Biliary excretion of drugs in man.', *Clinical pharmacokinetics*, 4(5), pp. 368–379. doi: 10.2165/00003088-197904050-00003.

Rosales Gerpe, M. C. *et al.* (2018) 'Use of Precision-Cut Lung Slices as an Ex Vivo Tool for Evaluating Viruses and Viral Vectors for Gene and Oncolytic Therapy', *Molecular Therapy - Methods and Clinical Development*, 10(September), pp. 245–256. doi: 10.1016/j.omtm.2018.07.010.

Rose, Kelly A. *et al.* (2016) 'Co-culture of Hepatocytes and Kupffer Cells as an in Vitro Model of Inflammation and Drug-Induced Hepatotoxicity', *Journal of Pharmaceutical Sciences*, 105(2), pp. 950–964. doi: 10.1016/S0022-3549(15)00192-6.

Rose, K. A. *et al.* (2016) 'Co-culture of Hepatocytes and Kupffer Cells as an In Vitro Model of Inflammation and Drug-Induced Hepatotoxicity', *Journal of Pharmaceutical Sciences*, 105(2), pp. 950–964. doi: 10.1016/S0022-3549(15)00192-6.Co-culture.

Roth, A. D. and Lee, M. Y. (2017) 'Idiosyncratic Drug-Induced Liver Injury (IDILI): Potential Mechanisms and Predictive Assays', *BioMed Research International*, 2017. doi: 10.1155/2017/9176937.

Roth, R. A. and Ganey, P. E. (2011) 'Animal models of idiosyncratic drug-induced liver injury—Current status', *Critical Reviews in Toxicology*, 41(9), pp. 723–739. doi: 10.3109/10408444.2011.575765.

Rouwkema, J. *et al.* (2009) 'Supply of nutrients to cells in engineered tissues', *Biotechnology and Genetic Engineering Reviews*, 26(1), pp. 163–178. doi: 10.5661/bger-26-163.

Rowe, C. *et al.* (2018) 'Perfused human hepatocyte microtissues identify reactive metabolite-forming and mitochondria-perturbing hepatotoxins', *Toxicology in Vitro*, 46(June 2017), pp. 29–38. doi: 10.1016/j.tiv.2017.09.012.

Rozga, J. *et al.* (1993) 'Development of a bioartificial liver: Properties and function of a hollow-fiber module inoculated with liver cells', *Hepatology*, 17(2), pp. 258–265. doi: 10.1002/hep.1840170216.

Ruoß, M. *et al.* (2019) 'Epigenetic modifications of the liver tumor cell line HepG2 increase their drug metabolic capacity', *International Journal of Molecular Sciences*, 20(2). doi: 10.3390/ijms20020347.

Sadasivan, S. K. *et al.* (2015) 'Developing an in vitro screening assay platform for evaluation of antifibrotic drugs using precision-cut liver slices', *Fibrogenesis and Tissue Repair*, 8(1), pp. 1–9. doi: 10.1186/s13069-014-0017-2.

Saddiq, Z. A., Barbenel, J. C. and Grant, M. H. (2009) 'The mechanical strength of collagen gels containing glycosaminoglycans and populated with fibroblasts', *Journal of Biomedical Materials Research - Part A*, 89(3), pp. 697–706. doi: 10.1002/jbm.a.32007.

Sainz, B., Tencate, V. and Uprichard, S. L. (2009) 'Three-dimensional Huh7 cell culture system for the study of Hepatitis C virus infection', *Virology Journal*, 6, pp. 1–8. doi: 10.1186/1743-422X-6-103.

Sakai, Y. *et al.* (1996) 'Large-Scale Preparation and Function of Porcine Hepatocyte Spheroids', *The International Journal of Artificial Organs*, 19(5), pp. 294–301. doi: 10.1177/039139889601900507.

Sakai, Y. *et al.* (2013) 'Rapid Fabricating Technique for Multi-Layered Human Hepatic Cell Sheets by Forceful Contraction of the Fibroblast Monolayer', *PLoS ONE*, 8(7). doi: 10.1371/journal.pone.0070970.

Sakai, Y. *et al.* (2018) 'Controlled cell morphology and liver-specific function of engineered primary hepatocytes by fibroblast layer cell densities', *Journal of Bioscience and Bioengineering*, 126(2), pp. 249–257. doi: 10.1016/j.jbiosc.2018.02.006.

Saldaña, L. *et al.* (2017) 'Paracrine interactions between mesenchymal stem cells and macrophages are regulated by 1,25-dihydroxyvitamin D3', *Scientific Reports*, 7(1), pp. 1–15. doi: 10.1038/s41598-017-15217-8.

Salehi-Nik, N. *et al.* (2013) 'Engineering parameters in bioreactor's design: A critical aspect in tissue engineering', *BioMed Research International*, 2013(3). doi: 10.1155/2013/762132.

Sánchez, A. *et al.* (2000) 'Fibronectin regulates morphology, cell organization and gene expression of rat fetal

hepatocytes in primary culture', *Journal of Hepatology2*, 32(2), pp. 242–250.

dos Santos, V. N. *et al.* (2005) 'Serum laminin, type IV collagen and hyaluronan as fibrosis markers in non-alcoholic fatty liver disease', *Brazilian Journal of Medical and Biological Research*, 38(5), pp. 747–753. doi: 10.1590/s0100-879x2005000500012.

Sarika, P. R. *et al.* (2015) 'A non-adhesive hybrid scaffold from gelatin and gum Arabic as packed bed matrix for hepatocyte perfusion culture', *Materials Science and Engineering C*, 46, pp. 341–347. doi: 10.1016/j.msec.2014.10.044.

Sarika, P. R. *et al.* (2016) 'Microgravity as a means to incorporate HepG2 aggregates in polysaccharide–protein hybrid scaffold', *Journal of Materials Science: Materials in Medicine*, 27(2), pp. 1–10. doi: 10.1007/s10856-015-5638-5.

Sarkar, U. *et al.* (2015) 'Metabolite profiling and pharmacokinetic evaluation of hydrocortisone in a perfused three-dimensional human liver bioreactor', *Drug Metabolism and Disposition*, 43(7), pp. 1091–1099. doi: 10.1124/dmd.115.063495.

Sassi, L. *et al.* (2021) 'A perfusion bioreactor for longitudinal monitoring of bioengineered liver constructs', *Nanomaterials*, 11(2), pp. 1–18. doi: 10.3390/nano11020275.

Schadt, S. *et al.* (2015) 'Minimizing DILI risk in drug discovery - A screening tool for drug candidates', *Toxicology in Vitro*, 30(1), pp. 429–437. doi: 10.1016/j.tiv.2015.09.019.

Schaffert, C. S. *et al.* (2010) 'Exposure of precision-cut rat liver slices to ethanol accelerates fibrogenesis.', *American journal of physiology. Gastrointestinal and liver physiology*, 299(3), pp. G661-8. doi: 10.1152/ajpgi.00287.2009.

Schlaermann, P. *et al.* (2016) 'A novel human gastric primary cell culture system for modelling Helicobacter pylori infection in vitro', *Gut*, 65(2), pp. 202–213. doi: 10.1136/gutjnl-2014-307949.

Schmid, J. *et al.* (2018) 'A perfusion bioreactor system for cell seeding and oxygen-controlled cultivation of three-dimensional cell cultures', *Tissue Engineering - Part C: Methods*, 24(10), pp. 585–595. doi: 10.1089/ten.tec.2018.0204.

Schulze, R. J. *et al.* (2019) 'The cell biology of the hepatocyte: A membrane trafficking machine', *Journal of Cell Biology*, 218(7), pp. 2096–2112. doi: 10.1083/jcb.201903090.

Schupp, A.-K. *et al.* (2016) 'Bile Acids Act as Soluble Host Restriction Factors Limiting Cytomegalovirus Replication in Hepatocytes', *Journal of Virology*, 90(15), pp. 6686–6698. doi: 10.1128/jvi.00299-16.

Schwarz, N. *et al.* (2019) 'Long-term adult human brain slice cultures as a model system to study human CNS circuitry and disease', *eLife*, 8, pp. 1–26. doi: 10.7554/eLife.48417.

Schweinlin, M. *et al.* (2016) 'Development of an Advanced Primary Human In Vitro Model of the Small Intestine', *Tissue Engineering Part C: Methods*, 22(9), pp. 873–883. doi: 10.1089/ten.tec.2016.0101.

Sekine, S. *et al.* (2009) 'Dicer is required for proper liver zonation', *Journal of Pathology*, 219, pp. 365–372. doi: 10.1002/path.

Selden, C., Khalil, M. and Hodgson, H. J. F. (1999) 'What keeps hepatocytes on the straight and narrow? Maintaining differentiated function in the liver', *Gut*, 44(4), pp. 443–446. doi: 10.1136/gut.44.4.443.

Sellaro, T. L. *et al.* (2010) 'Maintenance of Human Hepatocyte Function In Vitro by Liver-Derived Extracellular Matrix Gels', *Tissue Engineering: Part A*, 16(3).

Semenza, G. L. (2000) 'Expression of hypoxia-inducible factor 1: Mechanisms and consequences', *Biochemical Pharmacology*, 59(1), pp. 47–53. doi: 10.1016/S0006-2952(99)00292-0.

Sevior, D. K., Pelkonen, O. and Ahokas, J. T. (2012) 'Hepatocytes: The powerhouse of biotransformation', *International Journal of Biochemistry and Cell Biology*, 44(2), pp. 257–261. doi: 10.1016/j.biocel.2011.11.011.

Sewald, K. and Braun, A. (2013) 'Assessment of immunotoxicity using precision-cut tissue slices', *Xenobiotica*, 43(1), pp. 84–97. doi: 10.3109/00498254.2012.731543.

Sharifi, F., Firoozabadi, B. and Firoozbakhsh, K. (2019) 'Numerical Investigations of Hepatic Spheroids Metabolic Reactions in a Perfusion Bioreactor', *Frontiers in Bioengineering and Biotechnology*, 7(September), pp. 1–17. doi: 10.3389/fbioe.2019.00221.

Shetty, S., Lalor, P. F. and Adams, D. H. (2018) 'Liver sinusoidal endothelial cells — gatekeepers of hepatic immunity', *Nature Reviews Gastroenterology and Hepatology*, 15(9), pp. 555–567. doi: 10.1038/s41575-018-0020-y.

Shoemaker, J. T. *et al.* (2020) 'A 3D Cell Culture Organ-on-a-Chip Platform With a Breathable Hemoglobin Analogue Augments and Extends Primary Human Hepatocyte Functions in vitro', *Frontiers in Molecular Biosciences*, 7(October), pp. 1–21. doi: 10.3389/fmolb.2020.568777.

Shvartsman, I. *et al.* (2009) 'Perfusion cell seeding and cultivation induce the assembly of thick and functional hepatocellular tissue-like construct', *Tissue Engineering - Part A*, 15(4), pp. 751–760. doi: 10.1089/ten.tea.2008.0024.

Simmers, M. B., Pryor, A. W. and Blackman, B. R. (2007) 'Arterial shear stress regulates endothelial cell-directed migration, polarity, and morphology in confluent monolayers', *American Journal of Physiology - Heart and Circulatory Physiology*, 293(3), pp. 1937–1946. doi: 10.1152/ajpheart.00534.2007.

Simunovic, M. and Brivanlou, A. H. (2017) 'Embryoids, organoids and gastruloids: New approaches to understanding embryogenesis', *Development (Cambridge)*, 144(6), pp. 976–985. doi: 10.1242/dev.143529.

Sirenko, O. *et al.* (2016) 'Phenotypic characterization of toxic compound effects on liver spheroids derived from ipsc using confocal imaging and three-dimensional image analysis', *Assay and Drug Development Technologies*, 14(7), pp. 381–394. doi: 10.1089/adt.2016.729.

Sison-Young, R. L. *et al.* (2017) 'A multicenter assessment of single-cell models aligned to standard measures of cell health for prediction of acute hepatotoxicity', *Archives of Toxicology*, 91(3), pp. 1385–1400. doi: 10.1007/s00204-016-1745-4.

Smith, P. F. *et al.* (1985) 'Dynamic organ culture of precision liver slices for in vitro toxicology', *Life Sciences*, 36(14), pp. 1367–1375. doi: https://doi.org/10.1016/0024-3205(85)90042-6.

Smith, P. F. *et al.* (1987) 'In vitro cytotoxicity of allyl alcohol and bromobenzene in a novel organ culture system', *Toxicology and Applied Pharmacology*, 87(3), pp. 509–522. doi: 10.1016/0041-008X(87)90257-2.

Sneader, W. (1996) *Drug Prototypes and their Exploitation*. Chichester: John Wiley & Sons, Ltd.

Sobral, C. S. *et al.* (2007) 'Human keratinocytes cultured on collagen matrix used as an experimental burn model.', *Journal of burns and wounds*, 7, p. e6. Available at: http://www.ncbi.nlm.nih.gov/pubmed/18091983%0Ahttp://www.pubmedcentral.nih.gov/articlerender.fcgi?artid=PMC2064970.

Song, Y. *et al.* (2016) 'Activated hepatic stellate cells play pivotal roles in hepatocellular carcinoma cell chemoresistance and migration in multicellular tumor spheroids', *Scientific Reports*, 6(June), pp. 1–14. doi: 10.1038/srep36750.

Sörensen, K. K. *et al.* (2015) 'Liver sinusoidal endothelial cells', *Comprehensive Physiology*, 5(4), pp. 1751–1774. doi: 10.1002/cphy.c140078.

Soydemir, S. *et al.* (2020) 'Does Mechanocrine Signaling by Liver Sinusoidal Endothelial Cells Offer New Opportunities for the Development of Anti-fibrotics?', *Frontiers in Medicine*, 6(January), pp. 1–7. doi: 10.3389/fmed.2019.00312.

Spicer, C. D. (2020) 'Hydrogel scaffolds for tissue engineering: The importance of polymer choice', *Polymer Chemistry*, 11(2), pp. 184–219. doi: 10.1039/c9py01021a.

Spivak, C. E. *et al.* (2006) 'Diffusion delays and unstirred layer effects at monolayer cultures of Chinese hamster ovary cells: radioligand binding, confocal microscopy, and mathematical simulations.', *Cell biochemistry and biophysics*, 45(1), pp. 43–58. doi: 10.1385/CBB:45:1:43.

Sriram, G. *et al.* (2018) 'Full-thickness human skin-on-chip with enhanced epidermal morphogenesis and barrier function', *Materials Today*, 21(4), pp. 326–340. doi: 10.1016/j.mattod.2017.11.002.

Štampar, M. *et al.* (2020) 'Characterization of In Vitro 3D Cell Model Developed from Human Hepatocellular Carcinoma (HepG2) Cell Line', *Cells*, 9(12). doi: 10.3390/cells9122557.

Stanca, C. *et al.* (2001) 'Hepatocellular transport proteins and their role in liver disease', *World Journal of Gastroenterology*, 7(2), pp. 157–169. doi: 10.3748/wjg.v7.i2.157.

Stangar, B. Z. and Greenbaum, L. (2012) 'The Role of Paracrine Signals During Liver Regeneration Ben', *Hepatology*, 56(4), pp. 1577–1579. doi: 10.1002/hep.25911.The.

Starokozhko, V. *et al.* (2015) 'Viability, function and morphological integrity of precision-cut liver slices during prolonged incubation: Effects of culture medium', *Toxicology in Vitro*, 30(1), pp. 288–299. doi: 10.1016/j.tiv.2015.10.008.

Starokozhko, V., Vatakuti, S., *et al.* (2017) 'Maintenance of drug metabolism and transport functions in human precision-cut liver slices during prolonged incubation for 5 days (Arch Toxicol, 10.1007/s00204-016-1865-x)', *Archives of Toxicology*, 91(7), p. 2711. doi: 10.1007/s00204-016-1895-4.

Starokozhko, V., Greupink, R., *et al.* (2017) 'Rat precision-cut liver slices predict drug-induced cholestatic injury', *Archives of Toxicology*, 91(10), pp. 3403–3413. doi: 10.1007/s00204-017-1960-7.

Storm, M. P. *et al.* (2016) 'Hollow fiber bioreactors for In Vivo-like mammalian tissue culture', *Journal of Visualized Experiments*, 111, p. e53431. doi: 10.3791/53431.

Stowe, C. M. (1968) 'Extrarenal Excretion of Drugs and Chemicals', *Annual Review of Pharmacology*, 8, pp. 337–356.

Strazzabosco, M. and Fabris, L. (2008) 'Functional Anatomy of Normal Bile Ducts', *Anatomical Record*, 291(6), pp. 653–660. doi: 10.1038/jid.2014.371.

Stribos, E. G. D. *et al.* (2017) 'Murine precision-cut kidney slices as an ex vivo model to evaluate the role of transforming growth factor-β1 signaling in the onset of renal fibrosis', *Frontiers in Physiology*, 8(DEC), pp. 1–9. doi: 10.3389/fphys.2017.01026.

Strüver, K., Friess, W. and Hedtrich, S. (2017) 'Development of a Perfusion Platform for Dynamic Cultivation of in vitro Skin Models', *Skin Pharmacology and Physiology*, 30(4), pp. 180–189. doi: 10.1159/000476071.

Stücker, M. *et al.* (2002) 'The cutaneous uptake of atmospheric oxygen contributes significantly to the oxygen supply of human dermis and epidermis', *Journal of Physiology*, 538(3), pp. 985–994. doi: 10.1113/jphysiol.2001.013067.

Stümpel, F. *et al.* (1998) 'Connexin 32 Gap junctions enhance stimulation of glucose output by glucagon and noradrenaline in mouse liver', *Hepatology*, 28(6), pp. 1616–1620. doi: 10.1002/hep.510280622.

Sun, T. *et al.* (2006) 'Culture of skin cells in 3D rather than 2D improves their ability to survive exposure to cytotoxic agents', *Journal of Biotechnology*, 122(3), pp. 372–381. doi: 10.1016/j.jbiotec.2005.12.021.

Sun, T. *et al.* (2012) 'A miniaturized bioreactor system for the evaluation of cell interaction with designed substrates in perfusion culture', *Journal of Tissue Engineering and Regenerative Medicine*, 6, pp. 4–14. doi: 10.1002/term.

Sundhar Bale, S. *et al.* (2015) 'Long-Term Coculture Strategies for Primary Hepatocytes and Liver Sinusoidal Endothelial Cells', *Tissue Engineering*, 21(4), pp. 413–422. doi: 10.1089/ten.tec.2014.0152.

Sung, J. H., Kam, C. and Shuler, M. L. (2010) 'A microfluidic device for a pharmacokinetic-pharmacodynamic (PK-PD) model on a chip', *Lab on a Chip*, 10(4), pp. 446–455. doi: 10.1039/b917763a.

Swift, B., Pfeifer, N. D. . and Brouwer, K. L. R. (2011) 'Sandwich-Cultured Hepatocytes: An In Vitro Model to Evaluate Hepatobiliary Transporter-Based Drug Interatctions and Hepatotoxicity', *Drug Metabolism Reviews*, 42(3), pp. 446–471. doi: 10.3109/03602530903491881.Sandwich-Cultured.

Tai, Y. *et al.* (2018) 'SK-Hep1 : not hepatocellular carcinoma cells but a cell model for liver sinusoidal endothelial cells', 11(5), pp. 2931–2938.

Tan, G. D. S. *et al.* (2013) 'A thin-walled polydimethylsiloxane bioreactor for high-density hepatocyte sandwich culture', *Biotechnology and Bioengineering*, 110(6), pp. 1663–1673. doi: 10.1002/bit.24822.

Tan, K. *et al.* (2019) 'A high-throughput microfluidic microphysiological system (PREDICT-96) to recapitulate hepatocyte function in dynamic, re-circulating flow conditions', *Lab on a Chip*, 19(9), pp. 1556–1566. doi: 10.1039/c8lc01262h.

Tanaka, M. and Iwakiri, Y. (2016) 'The Hepatic Lymphatic Vascular System: Structure, Function, Markers, and Lymphangiogenesis', *Cellular and Molecular Gastroenterology and Hepatology*, 2(6), pp. 733–749. doi: 10.1016/j.jcmgh.2016.09.002.

Tanaka, Y. *et al.* (2006) 'Evaluation of effects of shear stress on hepatocytes by a microchip-based system', *Measurement Science and Technology*, 17(12), pp. 3167–3170. doi: 10.1088/0957-0233/17/12/S08.

Tang, A. *et al.* (2018) 'Epidemiology of hepatocellular carcinoma: target population for surveillance and diagnosis', *Abdominal Radiology*, 43(1), pp. 13–25. doi: 10.1007/s00261-017-1209-1.

Tang, N. *et al.* (2012) 'Stable overexpression of arginase I and ornithine transcarbamylase in HepG2 cells improves its ammonia detoxification', *Journal of Cellular Biochemistry*, 113(2), pp. 518–527. doi: 10.1002/jcb.23375.

Tarbell, J. M. and Shi, Z. (2013) 'Effect of the glycocalyx layer on transmission of interstitial flow shear stress to embedded cells', *Biomech Model Mechanobiol*, 12(1), pp. 111–121. doi: 10.1007/s10237-012-0385-8.Effect.

Tarng, Y. W., Huang, B. F. and Su, F. C. (2012) 'A novel recirculating flow-perfusion bioreactor for periosteal chondrogenesis', *International Orthopaedics*, 36(4), pp. 863–868. doi: 10.1007/s00264-011-1291-x.

Tavill, A. S. (1972) 'The synthesis and degradation of liver-produced proteins.', *Gut*, 13(3), pp. 225–241. doi: 10.1136/gut.13.3.225.

Taylor, M. W. (2014) 'A History of Cell Culture', in *Viruses and Man: A History of Interactions*. Springer, Cham, pp. 41–52. doi: 10.1093/cid/civ222.

Tehranirokh, M. *et al.* (2013) 'Microfluidic devices for cell cultivation and proliferation', *Biomicrofluidics*, 7(5). doi: 10.1063/1.4826935.

Temnov, A. *et al.* (2019) 'The effect of a mesenchymal stem cell conditioned medium fraction on morphological characteristics of hepatocytes in acetaminophen-induced acute liver failure: a preliminary study', *Hepatic Medicine: Evidence and Research*, Volume 11, pp. 89–96. doi: 10.2147/hmer.s196354.

Teschke, R. and Danan, G. (2018) 'Drug-induced liver toxicity.', in Chen, M. and Will, Y. (eds) *Drug Induced Liver Toxicity*. 1st edn. Berlin, Germany: Springer Protocols, Springer Nature, pp. 555–594. doi: 10.1007/978-1-4939-7677-5_27.

Thakkar, S. *et al.* (2018) 'The Liver Toxicity Knowledge Base (LKTB) and drug-induced liver injury (DILI) classification for assessment of human liver injury', *Expert Review of Gastroenterology \& Hepatology*, 12(1), pp. 31–38. doi: 10.1080/17474124.2018.1383154.

Theard, D. *et al.* (2007) 'Cell Polarity Development and Protein Trafficking in Hepatocytes Lacking E-Cadherin/beta-Catenin–based Adherens Junctions', *Molecular biology of the cell*, 18, pp. 2313–2321. doi: 10.1091/mbc.E06.

Theos, A. C. *et al.* (2005) 'Functions of adaptor protein (AP)-3 and AP-1 in tyrosinase sorting from endosomes to melanosomes', *Molecular Biology of the Cell*, 16(November), pp. 5356–5372. doi: 10.1091/mbc.E05.

Thomas, R. J. *et al.* (2005) 'The Effect of Three-Dimensional Co-Culture of Hepatocytes and Hepatic Stellate Cells on Key Hepatocyte Functions in vitro', *Cells Tissues Organs*, 181(2), pp. 67–79.

Thomas, R. J. *et al.* (2006) 'The effect of three-dimensional co-culture of hepatocytes and hepatic stellate cells on key hepatocyte functions in vitro', *Cells Tissues Organs*, 181(2), pp. 67–79. doi: 10.1159/000091096.

Thompson, R. A. *et al.* (2012) 'In vitro approach to assess the potential for risk of idiosyncratic adverse reactions caused by candidate drugs', *Chemical Research in Toxicology*, 25(8), pp. 1616–1632. doi: 10.1021/tx300091x.

Tilles, A. W. *et al.* (2001) 'Effects of oxygenation and flow on the viability and function of rat hepatocytes cocultured in a microchannel flat-plate bioreactor', *Biotechnology and Bioengineering*, 73(5), pp. 379–389. doi: 10.1002/bit.1071.

Todaro, G. J. and Green, H. (1963) 'Quantitative Studies of the Growth of Mouse Embryo Cells in culture and their Development into Established Lines', *The Journal of Cell Biology*, 17(6), pp. 299–313.

Toh, Y. C. *et al.* (2007) 'A novel 3D mammalian cell perfusion-culture system in microfluidic channels', *Lab on a Chip*, 7(3), pp. 302–309. doi: 10.1039/b614872g.

Toh, Y. C. *et al.* (2009) 'A microfluidic 3D hepatocyte chip for drug toxicity testing', *Lab on a Chip*, 9(14), pp. 2026–2035. doi: 10.1039/b900912d.

Tolosa, L. *et al.* (2018) 'Customised in vitro model to detect human metabolism-dependent idiosyncratic drug-induced liver injury', *Archives of Toxicology*, 92(1), pp. 383–399. doi: 10.1007/s00204-017-2036-4.

Tolosa, L. *et al.* (2019) 'Long-term and mechanistic evaluation of drug-induced liver injury in Upcyte human hepatocytes', *Archives of Toxicology*, 93(2), pp. 519–532. doi: 10.1007/s00204-018-2349-y.

Tomlinson, L. *et al.* (2019) 'In vitro Liver Zonation of Primary Rat Hepatocytes', *Frontiers in Bioengineering and Biotechnology*, 7(February), pp. 1–8. doi: 10.3389/fbioe.2019.00017.

Van Tonder, A., Joubert, A. M. and Cromarty, A. D. (2015) 'Limitations of the 3-(4,5-dimethylthiazol-2-yl)-2,5-diphenyl-2H-tetrazolium bromide (MTT) assay when compared to three commonly used cell enumeration assays', *BMC Research Notes*, 8(1), pp. 1–10. doi: 10.1186/s13104-015-1000-8.

Tong, W. H. *et al.* (2016) 'Constrained spheroids for prolonged hepatocyte culture', *Biomaterials*, 80, pp. 106–120. doi: 10.1016/j.biomaterials.2015.11.036.

Tostões, R. M. *et al.* (2012) 'Human liver cell spheroids in extended perfusion bioreactor culture for repeated-dose drug testing', *Hepatology*, 55(4), pp. 1227–1236. doi: 10.1002/hep.24760.

Toutain, H. J. *et al.* (1998) 'Morphological and functional integrity of precision-cut rat liver slices in rotating organ culture and multiwell plate culture: Effects of oxygen tension', *Cell Biology and Toxicology*, 14(3), pp. 175–190. doi: 10.1023/A:1007458408863.

Tracy, L. E., Minasian, R. A. and Caterson, E. J. (2016) 'Extracellular Matrix and Dermal Fibroblast Function in the Healing Wound', *Advances in Wound Care*, 5(3), pp. 119–136. doi: 10.1089/wound.2014.0561.

Tramper, J. (1995) 'Oxygen gradients in animal-cell bioreactors', *Cytotechnology*, 18(1–2), pp. 27–34. doi: 10.1007/BF00744317.

Trepanier, L. A. (2004) 'Idiosyncratic toxicity associated with potentiated sulfonamides in the dog', *Journal of Veterinary Pharmacology and Therapeutics*, 27(3), pp. 129–138. doi: 10.1111/j.1365-2885.2004.00576.x.

Treyer, Aleksandr; Müsch, A. (2013) 'Hepatocyte Polarity', *Compr Physiol.*, 3, pp. 243–287. doi: 10.1002/cphy.c120009.Hepatocyte.

Tripathi, A. and Melo, J. S. (2015) 'Preparation of a sponge-like biocomposite agarose–chitosan scaffold with primary hepatocytes for establishing an in vitro 3D liver tissue model', *RSC Adv.*, 5(39), pp. 30701–30710. doi: 10.1039/C5RA04153H.

Tuan, T. L. *et al.* (1994) 'Dermal fibroblasts activate keratinocyte outgrowth on collagen gels', *Journal of Cell Science*, 107(8), pp. 2285–2289.

Turksen, K. and Troy, T. C. (2011) 'Junctions gone bad: Claudins and loss of the barrier in cancer', *Biochimica et Biophysica Acta - Reviews on Cancer*, 1816(1), pp. 73–79. doi: 10.1016/j.bbcan.2011.04.001.

Turpeinen, M. *et al.* (2007) 'Predictive value of animal models for human cytochrome P450 (CYP)-mediated metabolism: A comparative study in vitro', *Xenobiotica*, 37(12), pp. 1367–1377.

Uetrecht, J. (2006) 'Evaluation of Which Reactive Metabolite, If Any, Is Responsible for a Specific Idiosyncratic Reaction', *Drug Metabolism Reviews*, 38(4), pp. 745–753. doi: 10.1080/03602530600959615.

Uetrecht, J. (2019) 'Mechanistic studies of idiosyncratic DILI: Clinical implications', *Frontiers in Pharmacology*, 10(JULY), pp. 1–9. doi: 10.3389/fphar.2019.00837.

Underhill, G. H. and Khetani, S. R. (2019) ' Emerging trends in modeling human liver disease in vitro ', *APL Bioengineering*, 3(4), p. 040902. doi: 10.1063/1.5119090.

US Food & Drug Administration (2019) *Liver Toxicity Knowledge Base (LTKB)*. Available at: https://www.fda.gov/science-research/bioinformatics-tools/liver-toxicity-knowledge-base-ltkb (Accessed: 31 March 2021).

Valenta, T., Hausmann, G. and Basler, K. (2012) 'The many faces and functions of β-catenin', *EMBO Journal*, 31(12), pp. 2714–2736. doi: 10.1038/emboj.2012.150.

van der Valk, J. *et al.* (2010) 'Optimization of chemically defined cell culture media - Replacing fetal bovine serum in mammalian in vitro methods', *Toxicology in Vitro*, 24(4), pp. 1053–1063. doi: 10.1016/j.tiv.2010.03.016.

Varkhede, N. R. *et al.* (2014) 'Metabolite identification studies on amiodarone in in vitro (rat liver microsomes, rat and human liver S9 fractions) and in vivo (rat feces, urine, plasma) matrices by using liquid chromatography with high-resolution mass spectrometry and multiple-stage m', *Rapid Communications in Mass Spectrometry*, 28(4), pp. 311–331. doi: 10.1002/rcm.6787.

Le Vee, M. *et al.* (2006) 'Functional expression of sinusoidal and canalicular hepatic drug transporters in the differentiated human hepatoma HepaRG cell line', *European Journal of Pharmaceutical Sciences*, 28(1–2), pp. 109–117. doi: 10.1016/j.ejps.2006.01.004.

Verkman, A. S. and Dix, J. A. (1984) 'Effect of unstirred layers on binding and reaction kinetics at a membrane surface', *Analytical Biochemistry*, 142(1), pp. 109–116. doi: 10.1016/0003-2697(84)90524-4.

Verrill, C. *et al.* (2002) 'Organotypic liver culture in a fluid-air interface using slices of neonatal rat and adult human tissue - A model of fibrosis in vitro', *Journal of Pharmacological and Toxicological Methods*, 48(2), pp. 103–110. doi: 10.1016/S1056-8719(03)00042-X.

Vickers, A. E. M. *et al.* (2004) 'Organ slice viability extended for pathway characterization: An in vitro model to investigate fibrosis', *Toxicological Sciences*, 82(2), pp. 534–544. doi: 10.1093/toxsci/kfh285.

Vickers, A. E. M., Ulyanov, A. V. and Fisher, R. L. (2018) 'Progression of repair and injury in human liver slices', *International Journal of Molecular Sciences*, 19(12), pp. 1–19. doi: 10.3390/ijms19124130.

Vildhede, A. *et al.* (2018) 'Quantification of Hepatic Organic Anion Transport Proteins OAT2 and OAT7 in Human Liver Tissue and Primary Hepatocytes', *Molecular Pharmaceutics*, 15(8), pp. 3227–3235. doi: 10.1021/acs.molpharmaceut.8b00320.

Villesen, I. F. *et al.* (2020) 'Review article: the signalling and functional role of the extracellular matrix in the development of liver fibrosis', *Alimentary Pharmacology & Therapeutics*, (January), pp. 1–13. doi: 10.1111/apt.15773.

Vinci, B. *et al.* (2011) 'Modular bioreactor for primary human hepatocyte culture: Medium flow stimulates expression and activity of detoxification genes', *Biotechnology Journal*, 6(5), pp. 554–564. doi:

10.1002/biot.201000326.

Vinken, M. *et al.* (2006) 'Involvement of cell junctions in hepatocyte culture functionality', *Critical Reviews in Toxicology*, 36(4), pp. 299–318. doi: 10.1080/10408440600599273.

Vinken, M. (2012) 'Gap junctions and non-neoplastic liver disease', *Journal of Hepatology*, 57(3), pp. 655–662. doi: 10.1016/j.jhep.2012.02.036.

Vis, M. A. M., Ito, K. and Hofmann, S. (2020) 'Impact of Culture Medium on Cellular Interactions in in vitro Co-culture Systems', *Frontiers in Bioengineering and Biotechnology*, 8(August), pp. 1–8. doi: 10.3389/fbioe.2020.00911.

Visikol (2021) *OpenLiver HepaRG NP 3D*. Available at: https://visikol.com/services/3d-cell-culture-models/openliver-heparg-np-3d/ (Accessed: 31 March 2021).

Vogel, M. *et al.* (2007) 'Flow in the well: Computational fluid dynamics is essential in flow chamber construction', *Cytotechnology*, 55(1), pp. 41–54. doi: 10.1007/s10616-007-9101-4.

Vorrink, S. U. *et al.* (2018) 'Prediction of drug-induced hepatotoxicity using long-term stable primary hepatic 3D spheroid cultures in chemically defined conditions', *Toxicological Sciences*, 163(2), pp. 655–665. doi: 10.1093/toxsci/kfy058.

Walker, P. A. *et al.* (2020) 'The evolution of strategies to minimise the risk of human drug-induced liver injury (DILI) in drug discovery and development', *Archives of Toxicology*, 94(8), pp. 2559–2585. doi: 10.1007/s00204-020-02763-w.

Wang, G. *et al.* (2018) 'Co-culture system of hepatocytes and endothelial cells: two in vitro approaches for enhancing liver-specific functions of hepatocytes', *Cytotechnology*, 70(4), pp. 1279–1290. doi: 10.1007/s10616-018-0219-3.

Wang, L. *et al.* (1998) 'Comparison of porcine hepatocytes with human hepatoma (C3A) cells for use in a bioartificial liver support system', *Cell Transplantation*, 7(5), pp. 459–468.

Wang, S. *et al.* (2008) 'Three-dimensional primary hepatocyte culture in synthetic self-assembling peptide hydrogel.', *Tissue engineering. Part A*, 14(2), pp. 227–236. doi: 10.1089/ten.2007.0143.

Wang, Y. *et al.* (2012) 'Rotating Microgravity-Bioreactor Cultivation Enhances the Hepatic Differentiation of Mouse Embryonic Stem Cells on Biodegradable Polymer Scaffolds', *Tissue Engineering Part A*, 18(21–22), pp. 2376–2385.

Wang, Y. J. *et al.* (2004) 'Primary hepatocyte culture in collagen gel mixture and collagen sandwich', *World Journal of Gastroenterology*, 10(5), pp. 699–702. doi: 10.3748/wjg.v10.i5.699.

Warburg, O. and Minami, S. (1923) 'Versuche an Überlebendem Carcinom-gewebe', *Klinische Wochenschrift*, 2(17), pp. 776–777. doi: 10.1007/BF01712130.

Ware, B. R. *et al.* (2018) 'A Cell Culture Platform to Maintain Long-term Phenotype of Primary Human Hepatocytes and Endothelial Cells', *Cmgh*, 5(3), pp. 187–207. doi: 10.1016/j.jcmgh.2017.11.007.

Ware, B. R. *et al.* (2021) 'Micropatterned Coculture with 3T3-J2 Fibroblasts Enhances Hepatic Functions and Drug Screening Utility of HepaRG Cells', *Toxicological Sciences*. doi: 10.1093/toxsci/kfab018.

Warren, A. *et al.* (2006) 'T lymphocytes interact with hepatocytes through fenestrations in murine liver sinusoidal endothelial cells', *Hepatology*, 44(5), pp. 1182–1190. doi: 10.1002/hep.21378.

Warren, S. M. *et al.* (2009) 'A novel flow-perfusion bioreactor supports 3D dynamic cell culture', *Journal of Biomedicine and Biotechnology*, 2009. doi: 10.1155/2009/873816.

Watkins, P. B. (2019) 'The DILI-sim Initiative: Insights into Hepatotoxicity Mechanisms and Biomarker Interpretation', *Clinical and Translational Science*, 12(2), pp. 122–129. doi: 10.1111/cts.12629.

Wattanapokayakit, S. *et al.* (2016) 'NAT2 slow acetylator associated with anti-tuberculosis drug-induced liver

injury in Thai patients', *International Journal of Tuberculosis and Lung Disease*, 20(10), pp. 1364–1369. doi: 10.5588/ijtld.15.0310.

Wei, G. and Ma, P. X. (2004) 'Structure and properties of nano-hydroxyapatite/polymer composite scaffolds for bone tissue engineering', *Biomaterials*, 25(19), pp. 4749–4757. doi: 10.1016/j.biomaterials.2003.12.005.

Weiss, W. M. *et al.* (2017) 'Coculture of meniscus cells and mesenchymal stem cells in simulated microgravity', *npj Microgravity*, 3(1), pp. 1–13. doi: 10.1038/s41526-017-0032-x.

Wells, R. G. (2015) 'The Portal Fibroblast-Not just a poor man's stellate cell', *Gastroenterology*, 147(1), pp. 41–47. doi: 10.1053/j.gastro.2014.05.001.The.

Werner, S. *et al.* (2014) 'Computational fluid dynamics as a modern tool for engineering characterization of bioreactors', *Pharmaceutical Bioprocessing*, 2(1), pp. 85–99. doi: 10.4155/pbp.13.60.

Westerink, W. M. A. and Schoonen, W. G. E. J. (2007a) 'Cytochrome P450 enzyme levels in HepG2 cells and cryopreserved primary human hepatocytes and their induction in HepG2 cells', *Toxicology in Vitro*, 21(8), pp. 1581–1591. doi: 10.1016/j.tiv.2007.05.014.

Westerink, W. M. A. and Schoonen, W. G. E. J. (2007b) 'Phase II enzyme levels in HepG2 cells and cryopreserved primary human hepatocytes and their induction in HepG2 cells', *Toxicology in Vitro*, 21(8), pp. 1592–1602. doi: 10.1016/j.tiv.2007.06.017.

Westra, I. M. *et al.* (2013) 'Evaluation of fibrosis in precision-cut tissue slices', *Xenobiotica*, 43(1), pp. 98–112. doi: 10.3109/00498254.2012.723151.

Westra, Inge M *et al.* (2014) 'Precision-cut liver slices as a model for the early onset of liver fibrosis to test anti fibrotic drugs', *Toxicology and Applied Pharmacology*, 274(2), pp. 328–338. doi: 10.1016/j.taap.2013.11.017.

Westra, Inge M. *et al.* (2014) 'The effect of antifibrotic drugs in rat precision-cut fibrotic liver slices', *PLoS ONE*, 9(4), pp. 1–10. doi: 10.1371/journal.pone.0095462.

Westra, I. M. *et al.* (2016) 'Human precision-cut liver slices as a model to test anti fibrotic drugs in the early onset of liver fibrosis', *TIV*, 35, pp. 77–85. doi: 10.1016/j.tiv.2016.05.012.

Williams, D. P. *et al.* (2020) 'Predicting Drug-Induced Liver Injury with Bayesian Machine Learning', *Chemical Research in Toxicology*, 33(1), pp. 239–248. doi: 10.1021/acs.chemrestox.9b00264.

Wiśniewski, J. R. *et al.* (2016) 'In-depth quantitative analysis and comparison of the human hepatocyte and hepatoma cell line HepG2 proteomes', *Journal of Proteomics*, 136, pp. 234–247. doi: 10.1016/j.jprot.2016.01.016.

Wiszniewski, L. *et al.* (2006) 'Long-term cultures of polarized airway epithelial cells from patients with cystic fibrosis', *American Journal of Respiratory Cell and Molecular Biology*, 34(1), pp. 39–48. doi: 10.1165/rcmb.2005-0161OC.

Wittkowske, C. *et al.* (2016) 'In Vitro Bone Cell Models: Impact of Fluid Shear Stress on Bone Formation', *Frontiers in Bioengineering and Biotechnology*, 4(NOV). doi: 10.3389/fbioe.2016.00087.

Wojdyla, K. *et al.* (2016) 'Acetaminophen-induced: S -nitrosylation and S -sulfenylation signalling in 3D cultured hepatocarcinoma cell spheroids', *Toxicology Research*, 5(3), pp. 905–920. doi: 10.1039/c5tx00469a.

Woodhead, J. L. *et al.* (2014) 'Exploring BSEP inhibition-mediated toxicity with a mechanistic model of drug-induced liver injury', *Frontiers in Pharmacology*, 5(NOV). doi: 10.3389/fphar.2014.00240.

Wu, F. J. *et al.* (1996) 'Efficient assembly of rat hepatocyte spheroids for tissue engineering applications', *Biotechnology and Bioengineering*, 50(4), pp. 404–415. doi: 10.1002/(SICI)1097-0290(19960520)50:4<404::AID-BIT7>3.0.CO;2-P.

Wu, X. *et al.* (2018) 'Precision-cut human liver slice cultures as an immunological platform', *Journal of Immunological Methods*, 455(October 2017), pp. 71–79. doi: 10.1016/j.jim.2018.01.012.

Wu, Y. *et al.* (2020) '3D bioprinting of bicellular liver lobule-mimetic structures via microextrusion of cellulose nanocrystal-incorporated shear-thinning bioink', *Scientific Reports*, 10(1), pp. 1–12. doi: 10.1038/s41598-020-77146-3.

Wung, N. *et al.* (2014) 'Hollow fibre membrane bioreactors for tissue engineering applications', *Biotechnology Letters*, 36(12), pp. 2357–2366. doi: 10.1007/s10529-014-1619-x.

Xia, L. *et al.* (2009) 'Laminar-flow immediate-overlay hepatocyte sandwich perfusion system for drug hepatotoxicity testing', *Biomaterials*, 30(30), pp. 5927–5936. doi: 10.1016/j.biomaterials.2009.07.022.

Xia, L. *et al.* (2012) 'Hepatocyte function within a stacked double sandwich culture plate cylindrical bioreactor for bioartificial liver system', *Biomaterials*, 33(32), pp. 7925–7932. doi: 10.1016/j.biomaterials.2012.06.078.

Ximénez, C. *et al.* (2017) 'Differential expression of pathogenic genes of Entamoeba histolytica vs E. dispar in a model of infection using human liver tissue explants', *PLoS ONE*, 12(8), pp. 1–22. doi: 10.1371/journal.pone.0181962.

Xin, X. *et al.* (2019) '3D cell coculture tumor model: A promising approach for future cancer drug discovery', *Process Biochemistry*, 78(December 2018), pp. 148–160. doi: 10.1016/j.procbio.2018.12.028.

Xu, J. J. *et al.* (2008) 'Cellular imaging predictions of clinical drug-induced liver injury', *Toxicological Sciences*, 105(1), pp. 97–105. doi: 10.1093/toxsci/kfn109.

Xu, J. J., Diaz, D. and O'Brien, P. J. (2004) 'Applications of cytotoxicity assays and pre-lethal mechanistic assays for assessment of human hepatotoxicity potential', *Chemico-Biological Interactions*, 150(1), pp. 115–128. doi: 10.1016/j.cbi.2004.09.011.

Yajima, Y. *et al.* (2018) 'Development of a perfusable 3D liver cell cultivation system via bundling-up assembly of cell-laden microfibers', *Journal of Bioscience and Bioengineering*, 126(1), pp. 111–118. doi: 10.1016/j.jbiosc.2018.01.022.

Yamada, K. *et al.* (1998) 'Efficient induction of hepatocyte spheroids in a suspension culture using a water-soluble synthetic polymer as an artificial matrix.', *Journal of biochemistry*, 123(6), pp. 1017–1023.

Yamada, K. M. and Cukierman, E. (2007) 'Modeling Tissue Morphogenesis and Cancer in 3D', *Cell*, 130(4), pp. 601–610. doi: 10.1016/j.cell.2007.08.006.

Yamashita, T. *et al.* (2007) 'Activation of hepatic stem cell marker EpCAM by Wnt-β-catenin signaling in hepatocellular carcinoma', *Cancer Research*, 67(22), pp. 10831–10839. doi: 10.1158/0008-5472.CAN-07-0908.

Yan, H. *et al.* (2012) 'Sodium taurocholate cotransporting polypeptide is a functional receptor for human hepatitis B and D virus', *eLife*, 2012(1), pp. 1–28. doi: 10.7554/eLife.00049.

Yang, J., Ichikawa, A. and Tsuchiya, T. (2003) 'A novel function of connexin 32: Marked enhancement of liver function in a hepatoma cell line', *Biochemical and Biophysical Research Communications*, 307(1), pp. 80–85. doi: 10.1016/S0006-291X(03)01117-3.

Yang, K. *et al.* (2016) 'Sandwich-Cultured Hepatocytes as a Tool to Study Drug Disposition and Drug-Induced Liver Injury', *Journal of Pharmaceutical Sciences*, 105(2), pp. 443–459. doi: 10.1016/j.xphs.2015.11.008.

Yang, X. *et al.* (2017) 'A hybrid co-culture model with endothelial cells designed for the hepatic tissue engineering', *Journal of Materials Science: Materials in Medicine*, 28(9), pp. 1–8. doi: 10.1007/s10856-017-5950-3.

Yao, W., Li, Y. and Ding, G. (2012) 'Interstitial fluid flow: The mechanical environment of cells and foundation of meridians', *Evidence-based Complementary and Alternative Medicine*, 2012. doi: 10.1155/2012/853516.

Yeatts, A. B. and Fisher, J. P. (2011) 'Tubular perfusion system for the long-term dynamic culture of human mesenchymal stem cells.', *Tissue engineering. Part C, Methods*, 17(3), pp. 337–48. doi: 10.1089/ten.TEC.2010.0172.

Yin, C. and Evason, K. (2013) 'Hepatic stellate cells in liver development, regeneration, and cancer', *The Journal*

of Cinical Investigation, 123(5), pp. 1902–1910. doi: 10.1172/JCI66369.1902.

Yoo, W. *et al.* (2014) 'HIF-1α expression as a protective strategy of HepG2 cells against fatty acid-induced toxicity', *Journal of Cellular Biochemistry*, 115(6), pp. 1147–1158. doi: 10.1002/jcb.24757.

Yue, B. (2014) 'Biology of the Extracellular Matrix: An Overview', *J Glaucoma*, 23, pp. 20–23. doi: 10.1097/IJG.0000000000000108.Biology.

Yun, S. Y. *et al.* (2019) 'Comparison of three human liver cell lines for in vitro drug-induced liver injury assessment: Huh7, HepaRG, and stem cell-derived hepatocytes', *Molecular and Cellular Toxicology*, 15(3), pp. 271–285. doi: 10.1007/s13273-019-0031-y.

Zandstra, P. W., Eaves, C. J. and Piret, J. M. (1994) 'Expansion of hematopoietic progenitor cell populations in stirred suspension bioreactors of normal human bone marrow cells.', *Bio/technology (Nature Publishing Company)*, 12(9), pp. 909–914. doi: 10.1038/nbt0994-909.

Zeilinger, K. *et al.* (2011) 'Scaling Down of a Clinical Three-Dimensional Perfusion Multicompartment Hollow Fiber Liver Bioreactor Developed for Extracorporeal Liver Support to an Analytical Scale Device Useful for Hepatic Pharmacological In Vitro Studies', *Tissue Engineering Part C: Methods*, 17(5), pp. 549–556.

Zeilinger, K. *et al.* (2016) 'Cell sources for *in vitro* human liver cell culture models', *Experimental Biology and Medicine*, 241(15), pp. 1684–1698. doi: 10.1177/1535370216657448.

Zeisberg, M. *et al.* (2006) 'De-differentiation of primary human hepatocytes depends on the composition of specialized liver basement membrane', *Molecular and Cellular Biochemistry*, 283(1–2), pp. 181–189. doi: 10.1007/s11010-006-2677-8.

Zhang, D. and Surapaneni, S. (eds) (2012) 'Appendix: Drug Metabolizing Enzymes and Biotransformation Reactions', in *ADME-Enabling Technologies in Drug Design and Development*. John Wiley & Sons, Ltd, pp. 545–565. doi: https://doi.org/10.1002/9781118180778.app1.

Zhang, F. Y. *et al.* (2013) 'Simultaneous recovery of dual pathways for ammonia metabolism do not improve further detoxification of ammonia in HepG2 cells', *Hepatobiliary and Pancreatic Diseases International*, 12(5), pp. 525–532. doi: 10.1016/S1499-3872(13)60083-1.

Zhang, J. *et al.* (2018) 'A decade of progress in liver regenerative medicine', *Biomaterials*, 157, pp. 161–176. doi: 10.1016/j.biomaterials.2017.11.027.

Zhang, P. *et al.* (2005) 'Role of glycosylation in trafficking of Mrp2 in sandwich-cultured rat hepatocytes', *Molecular Pharmacology*, 67(4), pp. 1334–1341. doi: 10.1124/mol.104.004481.

Zhang, S. *et al.* (2011) 'A robust high-throughput sandwich cell-based drug screening platform', *Biomaterials*, 32(4), pp. 1229–1241. doi: 10.1016/j.biomaterials.2010.09.064.

Zhang, S. *et al.* (2013) 'Efficient large-scale generation of functional hepatocytes from mouse embryonic stem cells grown in a rotating bioreactor with exogenous growth factors and hormones', *Stem Cell Research and Therapy*, 4(6). doi: 10.1186/scrt356.

Zhang, Y. *et al.* (2009) 'Tissue-specific extracellular matrix coatings for the promotion of cell proliferation and maintenance of cell phenotype', *Biomaterials*, 30(23–24), pp. 4021–4028. doi: 10.1016/j.biomaterials.2009.04.005.

Zhao, X. *et al.* (2010) 'The 3-D culture and in vivo growth of the human hepatocellular carcinoma cell line HepG2 in a self-assembling peptide nanofiber scaffold', *Journal of Nanomaterials*, 2010, pp. 3–10. doi: 10.1155/2010/437219.

Zhao, Y. *et al.* (2019) 'Multi-organs-on-chips: Towards long-term biomedical investigations', *Molecules*, 24(4). doi: 10.3390/molecules24040675.

Zheng, X. *et al.* (2017) 'Collagen I promotes hepatocellular carcinoma cell proliferation by regulating integrin β1/FAK signaling pathway in nonalcoholic fatty liver', *Oncotarget*, 8(56), pp. 95586–95595. doi:

10.18632/oncotarget.21525.

Zhong, C. *et al.* (2016) 'Human hepatocytes loaded in 3D bioprinting generate mini-liver', *Hepatobiliary and Pancreatic Diseases International*, 15(5), pp. 512–518. doi: 10.1016/S1499-3872(16)60119-4.

Zhou, B. *et al.* (2019) 'Haplotype-resolved and integrated genome analysis of the cancer cell line HepG2', *Nucleic Acids Research*, 47(8), pp. 3846–3861. doi: 10.1093/nar/gkz169.

Zhou, W. C., Zhang, Q. B. and Qiao, L. (2014) 'Pathogenesis of liver cirrhosis', *World Journal of Gastroenterology*, 20(23), pp. 7312–7324. doi: 10.3748/wjg.v20.i23.7312.

Zhu, M. *et al.* (2018) 'Development of a new conditionally immortalized human liver sinusoidal endothelial cells', *Biological and Pharmaceutical Bulletin*, 41(3), pp. 440–444. doi: 10.1248/bpb.b17-00661.

Zimmermann, M. *et al.* (2009) 'Improved reproducibility in preparing precision-cut liver tissue slices', (August 2017), pp. 145–152. doi: 10.1007/s10616-009-9246-4.

Zollner, G. *et al.* (2005) 'Hepatobiliary transporter expression in human hepatocellular carcinoma', *Liver International*, 25(2), pp. 367–379. doi: 10.1111/j.1478-3231.2005.01033.x.

Zsembery, A., Thalhammer, T. and Graf, J. (2000) 'Bile formation: A concerted action of membrane transporters in hepatocytes and cholangiocytes', *News in Physiological Sciences*, 15(1), pp. 6–11. doi: 10.1152/physiologyonline.2000.15.1.6.

Chapter 10: Appendices

10.1 Appendix 1 - Abstracts and Posters

10.1.1. Posters

10.1.1.1. Improvement of Three Dimensional Liver Tissue Models through the Deveelopment of a Novel Perfusion Culture System (2017) White Rose Biomaterials and Tissue Engineering Group Conference, Leeds, UK.

IMPROVEMENT OF THREE DIMENSIONAL LIVER TISSUE MODELS THROUGH THE DEVELOPMENT OF A NOVEL PERFUSION CULTURE SYSTEM

H. W. Hoyle[1*], M.F. Roger[1] and S.A. Przyborski[1,2]

*[1] Department of Biosciences, Durham University, UK. [2]ReproCELL Europe, Sedgefield, UK. *Corresponding Author: h.w.hoyle@durham.ac.uk*

Durham University

INTRODUCTION & AIMS:

The growth of cultured cells is governed by factors in the surrounding microenvironment including the physical space in which cells occupy. Three dimensional (3D) culture attempts to mimic *in vivo* conditions to enhance their structure and function[1]. While this can be achieved to some degree, many current 3D models do not address other factors, such as media perfusion to improve gaseous and nutrient diffusion and reduce unstirred layers of medium adjacent to the cells. This is particularly important when attempting to recreate complex highly vascularised tissues such as liver (Figure 1). Pumped perfusion of media has been introduced to overcome this with some success, however many current methods are overly complex and suffer from limitations such as size constraints[2].

Aims:

- To improve current static liver models by creating a more dynamic *in vitro* environment
- To increase the complexity of liver models to more accurately take into account the different factors found in the liver
- To improve the functional lifespan of tissue slices to make them more useful for long term chronic tests

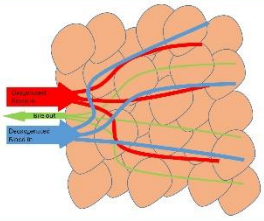

Figure 1: The three main ways in which fluids are transported to and from the liver via veins, arteries and bile ducts.

1. MATERIALS AND METHODS

HepG2 cultures are grown in 3D through the use of Alvetex® Strata as a substrate. This is a porous polystyrene scaffold with an average pore size of 15 µm. This creates a surface which can support cells from many directions as well as allowing some to invade into it therefore allowing more complex tissue cultures to be created[3].

To create perfusion cultures, as shown by figure 3, cells are seeded as a suspension onto Alvetex® Strata in a 6 well insert and cultured for a week to allow adequate adherence and migration. The Alvetex® is then removed from the well insert and placed into the perfusion device (figure 2) and overlaid with a second Alvetex® membrane to create a sandwich culture. This can then be cultured for at least another week to allow the cells to adapt to the perfusion.

Figure 2: The perfusion device which has been developed to hold perfused Alvetex® cultures.

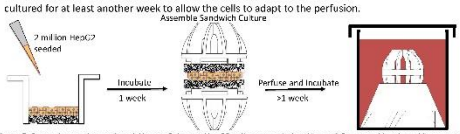

Figure 3: Stages in creating perfused Alvetex Cultures. HepG2 cells are seeded to Alvetex® Strata and incubated for one week. These are then placed in sandwich culture and perfused for another week.

2. DEVELOPMENT OF A NOVEL *IN VITRO* PERFUSION SYSTEM

In order to produce perfused 3D cultures novel apparatus has been developed. A set of criteria was created that the design needed to meet:

- Be autoclavable or easy to sterilise
- Use non-cytotoxic materials
- Use relatively inexpensive equipment
- Have a small footprint to allow scalability
- Create effective media recirculation

For this a design was created which used a magnetic stirrer to move the media (figure 4) . Polytetrafluoroethylene (PTFE), an inert polymer, was used as a stand for the cultures. Custom glass beakers were produced which can easily be fitted into an incubator on a 6-point magnetic stirrer.

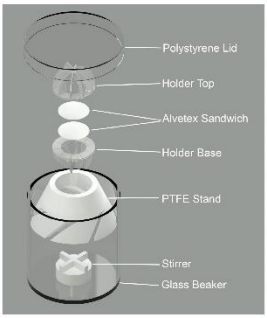

Figure 4: An exploded schematic of the perfusion apparatus developed.

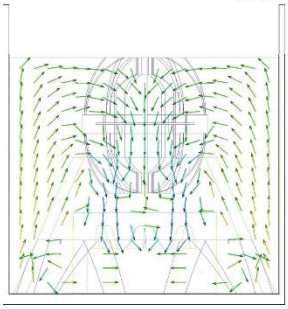

Figure 5: Computational Fluid Dynamics (CFD) simulation of the media recirculation within the apparatus. Arrows represent the direction of media flow at each point.

Simulations of the fluid flow in the system were carried out using the AutoDesk CFD package (figure 5). These show the media to be drawn downwards through the Alvetex® membrane, on which the cells are seeded, and recirculated upwards around the outside of the vessel. This allows both continual flow through the culture as well as complete mixing of the media.

The flow of media through the culture is an improvement over many current perfusion methods in which media is simply moved across the surface of the culture. This allows for more effective removal of waste products from the cell surface and helps to minimise the unstirred layers.

3. CULTURE OF HEPG2 CELLS IN 3D PERFUSION CONDITIONS

Growth of HepG2 cells on Alvetex® in perfusion shows several key improvements over static culture (figure 6);

- Increase in proliferation
- Greater migration across the surface of the substrate
- Formation of a larger surface tissue layer

Issues to overcome with this method mainly revolve around preventing invasion into the Alvetex® in order to form a homogeneous hepatocyte population. Coating the Scaffold in proteins such as collagen can be effective at this.

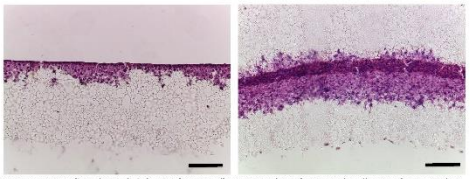

Figure 6: Haemotoxylin and Eosin (H&E) stain of HepG2 cells grown on Alvetex® Strata. Left: Cells grown for two weeks in static conditions. Right: Cells grown for one week in static followed by a further week in perfused sandwich configuration. Scale bars are 100µm.

4. INCREASING THE LIFESPAN OF EX VIVO TISSUE SLICES

Precision-cut liver slices are a method which can be used for functional liver tests. There are several benefits to these cultures over conventional cell culture:

- Increased complexity
- Cells are in their native environment
- High throughput and easy to set up

Typically liver slices have a functional lifespan of a few hours. Methods which have prolonged this typically use culture conditions which differ from physiological conditions such as a 95% oxygen environment. We have tried to use our system to prolong the life of slices whilst maintaining routine culture conditions.

Initial results are promising with the MTT assay showing an increase in metabolism after 24 hours compared to static culture (figure 7).

Further work will look into the effects of culture in this system over a longer period of up to one week.

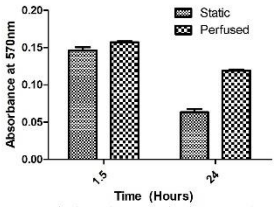

Figure 7: Absorbance values at 570nm for an MTT assay carried out on precision-cut liver tissue cores cultured for times of 1.5 and 24 hours. The two columns for each time point are for static and perfused cultures respectively.

Figure 8: Photograph of an 8mm rabbit liver core embedded in low gelling temperature agarose. Cores are glued to a mounting plate and sectioned at 200 µm using a Leica VT1000S Vibratome.

CONCLUSIONS & FUTURE DIRECTIONS:

Conclusions:

- Addition of media perfusion increases the viability and proliferation of cell cultures.
- Under the right conditions cells can be induced to form a homogeneous tissue disc.
- Precision-cut liver slices can maintain their metabolic function for longer when cultured using this system.

Future Directions:

- Further characterisation of the tissues formed through the perfusion method
- Addition of non-parenchymal hepatic cells to create complex *in-vivo* like tissues
- Optimisation of liver slice cultures to create an effective and reproducible platform for carrying out experiments.

1. The third dimension bridges the gap between cell culture and live tissue. P. Tibbitt et al., P. B. Reynaud, P. H. E. Pienne, Nature Reviews, Molecular Cell Biology (2007) P. 389-395
2. Bioreactors in tissue engineering: Advances in stem cell culture and three-dimensional tissue constructs, M. De Pieckey, A. Bernhard, et al., Milan, Eng. Life Sci. (2015) 15: 675-677
3. Alvetex®: Polystyrene scaffold technology for routine three dimensional cell culture, L. Knight, R. Murray, C. Carnachan and S. Przyborski, Methods V.51, iss., (2011) 383-390

10.1.1.2. Improvement of Three Dimensional Liver Tissue Models through the Deveelopment of a Novel Perfusion Culture System (2018) Durham University Department of Biosciences Research Away Day, Durham, UK.

IMPROVEMENT OF THREE DIMENSIONAL LIVER TISSUE MODELS THROUGH THE DEVELOPMENT OF A NOVEL PERFUSION CULTURE SYSTEM

H. W. Hoyle[1*], M.F. Roger[1] and S.A. Przyborski[1,2]

[1] Department of Biosciences, Durham University, UK. [2]ReproCELL Europe, Sedgefield, UK. *Corresponding Author: h.w.hoyle@durham.ac.uk

Durham University

INTRODUCTION & AIMS:

The growth of cultured cells is governed by factors in the surrounding microenvironment including the physical space in which cells occupy. Three dimensional (3D) culture attempts to mimic *in vivo* conditions to enhance their structure and function[1]. While this can be achieved to some degree, many current 3D models do not address other factors, such as media perfusion to improve gaseous and nutrient diffusion and reduce unstirred layers of medium adjacent to the cells. This is particularly important when attempting to recreate complex highly vascularised tissues such as liver (Figure 1). Pumped perfusion of media has been introduced to overcome this with some success, however many current methods are overly complex and suffer from limitations such as size constraints[2].

Aims:

- To improve current static liver models by creating a more dynamic *in vitro* environment
- To increase the complexity of liver models to more accurately take into account the different factors found in the liver
- To improve the functional lifespan of tissue slices to make them more useful for long term chronic tests

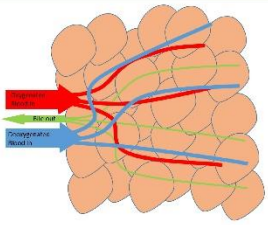

Figure 1: The three main ways in which fluids are transported to and from the liver via veins, arteries and bile ducts.

1. MATERIALS AND METHODS

HepG2 cultures are grown in 3D through the use of Alvetex® Strata as a substrate. This is a porous polystyrene scaffold with an average pore size of 15 µm. This creates a surface which can support cells from many directions as well as allowing some to invade into it therefore allowing more complex tissue cultures to be created[3].

Figure 2: The perfusion device which has been developed to hold perfused Alvetex® cultures.

To create perfusion cultures, as shown by figure 3, cells are seeded as a suspension onto Alvetex® Strata in a 6 well insert and cultured for a week to allow adequate adherence and migration. The Alvetex® is then removed from the well insert and placed into the perfusion device (figure 2) and overlaid with a second Alvetex® membrane to create a sandwich culture. This can then be cultured for at least another week to allow the cells to adapt to the perfusion.

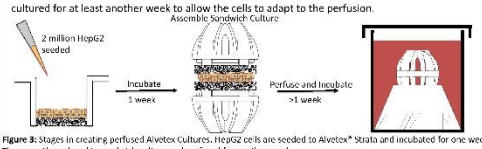

Figure 3: Stages in creating perfused Alvetex Cultures. HepG2 cells are seeded to Alvetex® Strata and incubated for one week. These are then placed in sandwich culture and perfused for another week.

2. DEVELOPMENT OF A NOVEL *IN VITRO* PERFUSION SYSTEM

In order to produce perfused 3D cultures novel apparatus has been developed. A set of criteria was created that the design needed to meet:

- Be autoclavable or easy to sterilise
- Use non-cytotoxic materials
- Use relatively inexpensive equipment
- Have a small footprint to allow scalability
- Create effective media recirculation

For this a design was created which used a magnetic stirrer to move the media (figure 4) . Polytetrafluoroethylene (PTFE), an inert polymer, was used as a stand for the cultures. Custom glass beakers were produced which can easily be fitted into an incubator on a 6-point magnetic stirrer.

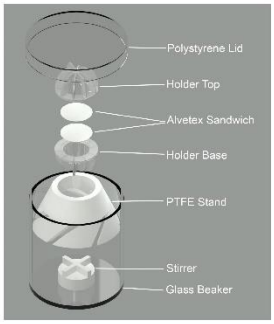

Figure 4: An exploded schematic of the perfusion apparatus developed.

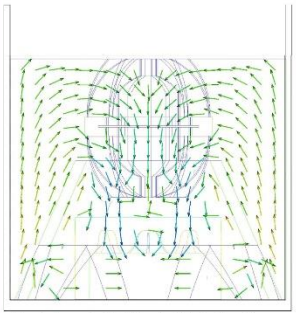

Figure 5: Computational Fluid Dynamics (CFD) simulation of the media recirculation within the apparatus. Arrows represent the direction of media flow at each point.

Simulations of the fluid flow in the system were carried out using the AutoDesk CFD package (figure 5). These show the media to be drawn downwards through the Alvetex® membrane, on which the cells are seeded, and recirculated upwards around the outside of the vessel. This allows both continual flow through the culture as well as complete mixing of the media.

The flow of media through the culture is an improvement over many current perfusion methods in which media is simply moved across the surface of the culture. This allows for more effective removal of waste products from the cell surface and helps to minimise the unstirred layers.

3. CULTURE OF HEPG2 CELLS IN 3D PERFUSION CONDITIONS

Growth of HepG2 cells on Alvetex® in perfusion shows several key improvements over static culture (figure 6);

- Increase in proliferation
- Greater migration across the surface of the substrate
- Formation of a larger surface tissue layer

Issues to overcome with this method mainly revolve around preventing invasion into the Alvetex® in order to form a homogeneous hepatocyte population. Coating the Scaffold in proteins such as collagen can be effective at this.

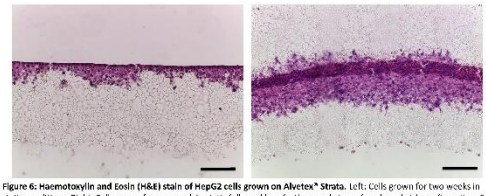

Figure 6: Haemotoxylin and Eosin (H&E) stain of HepG2 cells grown on Alvetex® Strata. Left: Cells grown for two weeks in static conditions. Right: Cells grown for one week in static followed by a further week in perfused sandwich configuration. Scale bars are 100µm.

4. INCREASING THE LIFESPAN OF EX VIVO TISSUE SLICES

Precision-cut liver slices are a method which can be used for functional liver tests. There are several benefits to these cultures over conventional cell culture:

- Increased complexity
- Cells are in their native environment
- High throughput and easy to set up

Typically liver slices have a functional lifespan of a few hours. Methods which have prolonged this typically use culture conditions which differ from physiological conditions such as a 95% oxygen environment. We have tried to use our system to prolong the life of slices whilst maintaining routine culture conditions.

Initial results are promising with the MTT assay showing an increase in metabolism after 24 hours compared to static culture (figure 7).

Further work will look into the effects of culture in this system over a longer period of up to one week.

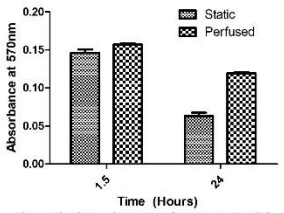

Figure 7: Absorbance values at 570nm for an MTT assay carried out on precision-cut liver tissue cores cultured for times of 1.5 and 24 hours. The two columns for each time point are for static and perfused cultures respectively.

Figure 8: Photograph of an 8mm rabbit liver core embedded in low gelling temperature agarose. Cores are glued to a mounting plate and sectioned at 200 µm using a Leica VT1000S Vibratome.

CONCLUSIONS & FUTURE DIRECTIONS:

Conclusions:

- Addition of media perfusion increases the viability and proliferation of cell cultures.
- Under the right conditions cells can be induced to form a homogeneous tissue disc.
- Precision-cut liver slices can maintain their metabolic function for longer when cultured using this system.

Future Directions:

- Further characterisation of the tissues formed through the perfusion method
- Addition of non-parenchymal hepatic cells to create complex *in-vivo* like tissues
- Optimisation of liver slice cultures to create an effective and reproducible platform for carrying out experiments.

1. The third dimension bridges the gap between cell culture and live tissue. E. Pampaloni, E. G. Reynaud, E. H. K. Stelzer. Nature Reviews. Molecular Cell Biology (2007) 8. 839-845
2. Biomimetics in tissue engineering: Advances in stem cell culture and three dimensional tissue constructs. N. Gribbinsky, A. Bonfield, A. Brennan, J. Chichkov, M. Dalton, E. Hanlon, E. Hoey, C. Inamdar, J. Kelly, L. Kelly, C. Lowery, F. O'Brien, S. O'Connell, S. Prina-Mello, L. Rooney, A. Tofail and V. Wilson. Life Sciences (2005) Vol. 0 (0) 1-7
3. Alvetex®: Polystyrene scaffold technology for routine three dimensional cell culture. C. Knight, B. Murray, I. Carnachan and S. Przyborski. Methods in Cell Biology. (2011) 103: 323-340

10.1.1.3. Improvement of Three Dimensional Liver Tissue Models through the Deveelopment of a Novel Perfusion Culture System (2018) Durham University Department of Biosciences Postgraduate Conference, Durham, UK.

IMPROVEMENT OF THREE DIMENSIONAL LIVER TISSUE MODELS THROUGH THE DEVELOPMENT OF A NOVEL PERFUSION CULTURE SYSTEM

H. W. Hoyle[1*], M.F. Roger[1] and S.A. Przyborski[1,2]
[1] *Department of Biosciences, Durham University, UK.* [2]*ReproCELL Europe, Sedgefield, UK.*
**Corresponding Author: h.w.hoyle@durham.ac.uk*

Durham University

INTRODUCTION & AIMS:

The growth of cultured cells is governed by factors in the surrounding microenvironment including the physical space in which cells occupy. Three dimensional (3D) culture attempts to mimic *in vivo* conditions to enhance their structure and function[1]. While this can be achieved to some degree, many current 3D models do not address other factors, such as media perfusion to improve gaseous and nutrient diffusion and reduce unstirred layers of medium adjacent to the cells. This is particularly important when attempting to recreate complex, highly vascularised tissues such as liver (Figure 1). Numerous bioreactors have been developed to include perfusion however these tend to suffer from limitations such as cost and scalability[2].

Aims:

- To improve current static liver models by creating a more dynamic *in vitro* environment
- To increase the complexity of liver models to more accurately take into account the different factors found in the liver
- To improve the functional lifespan of tissue slices to make them more useful for long term chronic tests

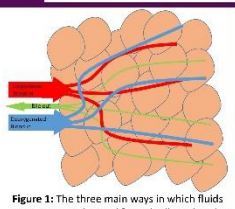

Figure 1: The three main ways in which fluids are transported to and from the liver via veins, arteries and bile ducts.

1. MATERIALS AND METHODS

HepG2 cells can be grown in 3D through the use of Alvetex® Strata. This is a porous polystyrene scaffold with an average pore size of 15 µm. This supports cells from many directions as well as allowing some to invade into it therefore allowing more complex tissue cultures to be created[3].

To create perfusion cultures, as shown by figure 3, cells are seeded as a suspension onto Alvetex® Strata in a 6 well insert and cultured for a week to allow adequate adherence and migration. The Alvetex® is then removed from the well insert and placed into the perfusion device (figure 2). This can then be cultured for at least another week to allow the cells to adapt to the perfusion.

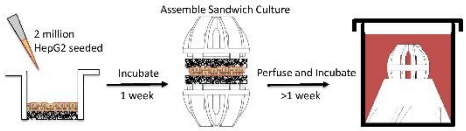

Figure 3: Stages in creating perfused Alvetex Cultures. HepG2 cells are seeded to Alvetex® Strata and incubated for one week. These are then placed in sandwich culture and perfused for another week.

2. DEVELOPMENT OF A NOVEL *IN VITRO* PERFUSION SYSTEM

In order to produce perfused 3D cultures novel apparatus has been developed. A set of criteria was created that the design needed to meet:

- Be **autoclavable** or easy to sterilise
- Use **non-cytotoxic** materials
- Use relatively **inexpensive** equipment
- Have a **small** footprint to allow scalability
- Create effective **media recirculation**

For this a design was created which uses a magnetic stirrer to move the media and a polytetrafluoroethylene (PTFE) shroud to direct fluid flow within the system (figure 4). This system can be easily scaled up through the use of multi-point magnetic stirrers.

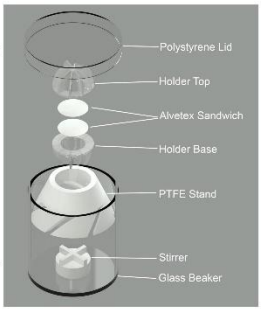

Figure 4: An exploded schematic of the perfusion apparatus developed.

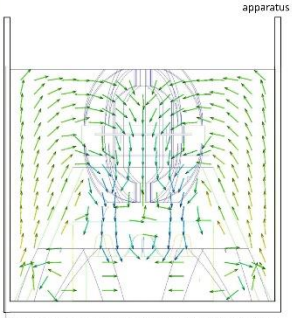

Figure 5: Computational Fluid Dynamics (CFD) simulation of the media recirculation within the apparatus. Arrows represent the direction of media flow at each point.

Simulations of the fluid flow in the system were carried out using the AutoDesk CFD package (figure 5). These show the media to be drawn downwards through the Alvetex® membrane, on which the cells are seeded, and recirculated upwards around the outside of the vessel. This allows both continual flow through the culture as well as complete mixing of the media.

Further work will model the shear stress experienced by the cells due to the perfusion system. This can then be compared and adjusted to create a more physiologically relevant culture environment.

3. CULTURE OF HEPG2 CELLS IN 3D PERFUSION CONDITIONS

Growth of HepG2 cells on Alvetex® in perfusion shows several key improvements over static culture (figure 6):

- Increase in **proliferation**
- Greater **migration** across the surface of the substrate
- Formation of a **larger tissue disk**

Fibroblasts can be incorporated into the Alvetex Scaffold to decrease invasion and promote formation of a more evenly distributed tissue. Further work will also include endothelial cells to mimic the *in vivo* vasculature.

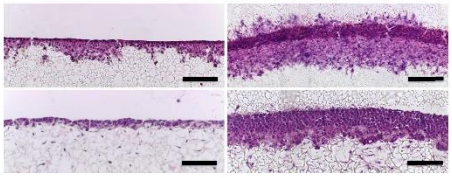

Figure 6: Haemotoxylin and Eosin (H&E) stain of HepG2 cells grown on Alvetex®. Top: Cells grown for one week in static followed by a further week in static or perfusion (left and right respectively). Bottom: HepG2 cells grown on Alvetex® Scaffold seeded with fibroblasts for 3 weeks. Cultures are then carried out either in static or perfusion (left and right). Scale bars are 100 µm.

4. INCREASING THE LIFESPAN OF EX VIVO TISSUE SLICES

Precision-cut liver slices are a method which can be used for functional liver tests. There are several benefits to these cultures over conventional cell culture:

- Increased **complexity**
- Cells are in their **native environment**
- **High throughput** and easy to set up

Typically liver slices have a functional lifespan of a few hours. Methods which have prolonged this typically use culture conditions which differ from physiological conditions such as a 95% oxygen environment. We are using our system to prolong the life of slices whilst maintaining routine culture conditions.

Initial results are promising with the MTT assay showing an increase in metabolism after 24 hours compared to static culture (figure 7). H&E stains of liver slices cultured for 6 days appear to retain their structure more in perfusion culture compared to static.(Figure 8).

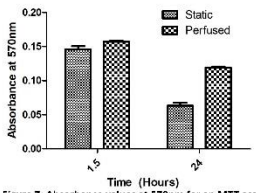

Figure 7: Absorbance values at 570nm for an MTT assay carried out on precision-cut liver tissue cores cultured for times of 1.5 and 24 hours. The two columns for each time point are for static and perfused cultures respectively.

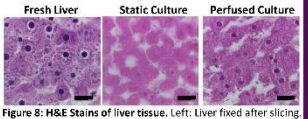

Figure 8: H&E Stains of liver tissue. Left: Liver fixed after slicing. Middle and right: Liver slice cultured for 6 days in a static 6-well plate and perfusion respectively. Scale bars are 20 µm.

CONCLUSIONS & FUTURE DIRECTIONS:

Conclusions:

- Addition of media perfusion increases the viability and proliferation of cell cultures.
- Conditions can be adjusted to control the morphology of the tissue formed.
- Precision-cut liver slices can maintain their metabolic function for longer when cultured using this system.

Future Directions:

- Further characterisation of the tissues formed through the perfusion method.
- Addition of non-parenchymal hepatic cells to create complex *in-vivo* like tissues.
- Optimisation of liver slice cultures to create an effective and reproducible platform for carrying out experiments.

1. *The third dimension bridges the gap between cell culture and live tissue*, E. Pampaloni, E. G. Reynaud, E. H. K. Stelzer, Nature Reviews, Molecular Cell Biology (2007) 8: 839-845
2. *Perfusion in tissue engineering*, Advances in stem cell culture and three-dimensional tissue constructs, N. Gerlinsky, A. Bernhardt and F. Milan, Eng. Life Sc. (2015) 15, 670-677
3. *Alvetex®: Polystyrene scaffold technology for routine three dimensional cell culture*, F. Knight, S. Murray, R. Carnachan and S. Przyborski, Methods Mol. Biol., (2011) 695: 323-340

10.1.1.4. Improvement of Three Dimensional Liver Tissue Models through the Deveelopment of a Novel Perfusion Culture System (2019) Durham University Department of Biosciences Research Away Day, Durham, UK.

IMPROVEMENT OF THREE DIMENSIONAL LIVER TISSUE MODELS THROUGH THE DEVELOPMENT OF A NOVEL PERFUSION CULTURE SYSTEM

H.W. Hoyle[1*] and S.A. Przyborski[1,2]

[1] Department of Biosciences, Durham University, UK. [2]Reprocell Europe, Sedgefield, UK.

**Presenting Author: h.w.hoyle@durham.ac.uk*

Durham University

INTRODUCTION & AIMS:

The growth of cultured cells is governed by factors in the surrounding microenvironment including the physical space in which cells occupy. Three dimensional (3D) culture attempts to mimic *in vivo* conditions to enhance their structure and function[1]. While this can be achieved to some degree, many current 3D models do not address other factors, such as media perfusion to improve gaseous and nutrient diffusion and reduce unstirred layers of medium adjacent to the cells. This is particularly important when attempting to recreate complex highly vascularised tissues such as liver (Figure 1). Pumped perfusion of media has been introduced to overcome this with some success, however many current methods are overly complex and suffer from limitations such as size constraints[2].

Aims:

- To improve current static liver models by creating a more dynamic *in vitro* environment
- To increase the complexity of liver models to more accurately take into account the different factors found in the liver
- To improve the functional lifespan of tissue slices to make them more useful for long term chronic tests

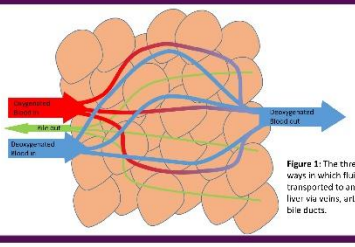

Figure 1: The three main ways in which fluids are transported to and from the liver via veins, arteries and bile ducts.

1. MATERIALS AND METHODS

HepG2 cultures are grown in 3D through the use of Alvetex® Strata as a substrate. This is a porous polystyrene scaffold with an average pore size of 15 µm. This creates a surface which can support cells from many directions as well as allowing some to invade into it therefore allowing more complex tissue cultures to be created[3].

To create perfusion cultures, as shown by figure 3, cells are seeded as a suspension onto Alvetex® Strata in a 6 well insert and cultured for a week to allow adequate adherence and migration. The Alvetex® is then removed from the well insert and placed into the perfusion device (figure 2) and overlaid with a second Alvetex® membrane to create a sandwich culture. This can then be cultured for at least another week to allow the cells to adapt to the perfusion.

Figure 2: The perfusion device which has been developed to hold perfused Alvetex® cultures.

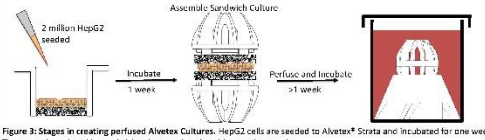

Figure 3: Stages in creating perfused Alvetex Cultures. HepG2 cells are seeded to Alvetex® Strata and incubated for one week. These are then placed in sandwich culture and perfused for another week.

2. DEVELOPMENT OF A NOVEL *IN VITRO* PERFUSION SYSTEM

In order to produce perfused 3D cultures novel apparatus has been developed. A set of criteria was created that the design needed to meet:

- Be **autoclavable** or easy to sterilise
- Use **non-cytotoxic** materials
- Use relatively **inexpensive** equipment
- Have a **small** footprint to allow scalability
- Create effective **media recirculation**

For this a design was created which used a magnetic stirrer to move the media (figure 4) . Polytetrafluoroethylene (PTFE), an inert polymer, was used as a stand for the cultures. Custom glass beakers were produced which can easily be fitted into an incubator on a 6-point magnetic stirrer.

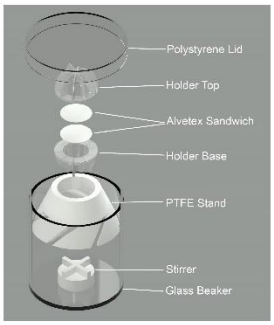

Figure 4: An exploded schematic of the perfusion apparatus.

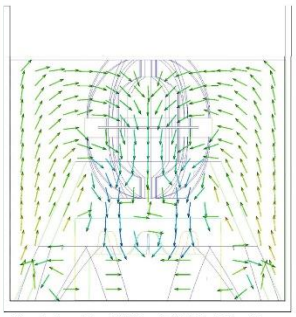

Figure 5: Computational Fluid Dynamics (CFD) simulation of the media recirculation within the apparatus. Arrows represent the direction of media flow at each point.[4]

Simulations of the fluid flow in the system were carried out using the AutoDesk CFD package (figure 5). These show the media to be drawn downwards through the Alvetex® membrane, on which the cells are seeded, and recirculated upwards around the outside of the vessel. This allows both continual flow through the culture as well as complete mixing of the media.

The flow of media through the culture is an improvement over many current perfusion methods in which media is simply moved across the surface of the culture. This allows for more effective removal of waste products from the cell surface and helps to minimise the unstirred layers.

3. CULTURE OF HEPG2 CELLS IN 3D PERFUSION CONDITIONS

Growth of HepG2 cells on Alvetex® in perfusion shows several key improvements over static culture (figure 6);

- Increase in **proliferation**
- **Greater migration** across the surface of the substrate
- Formation of a **larger surface disk**
- Improved localisation of key hepatic markers (Figure 8)

By seeding the Alvetex with fibroblasts a surface can be created which supports the growth of hepatocytes without invasion into the membrane (Figure 7), provides extracellular matrix interactions and still allows perfusion to take place through the culture.

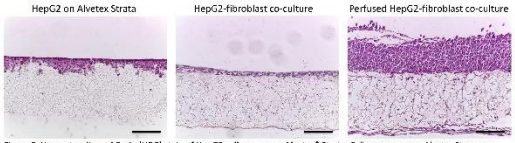

Figure 6: Haemotoxylin and Eosin (H&E) stain of HepG2 cells grown on Alvetex® Strata. Cells are grown on Alvetex Strata as a control (left) compared to static and perfusion on a fibroblast-embedded Alvetex Scaffold. Scale bars are 100 µm.

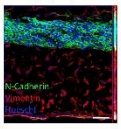

Figure 7: Immunofluorescent stain showing the compartmentalisation of the two cell types. Cells were stained for N-Cadherin (Green) and Vimentin (Red). Nuclei are stained blue.

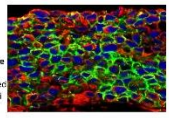

Figure 8: Immunofluorescent stain showing the differential expression of the apical marker MDR1 compared N-Cadherin. Cells were stained for N-Cadherin (Green) and MDR1 (Red). Nuclei are stained blue.

4. INCREASING THE LIFESPAN OF EX VIVO TISSUE SLICES

Precision-cut liver slices are a method which can be used for functional liver tests. There are several benefits to these cultures over conventional cell culture:

- Increased **complexity**
- Cells are in their **native environment**
- **High throughput** and easy to set up

Typically liver slices have a functional lifespan of a few hours. Methods which have prolonged this typically use a 95% oxygen environment leading to high experimental cost. By preoxygenation of the perfusion system this environment can be created without the need for ongoing oxygenation.

Initial results are promising with the MTT assay showing viable tissue still present after 4 days in preoxygenated perfusion culture (figure 9).

Figure 10: H&E Stains of liver tissue. Left: Liver fixed after slicing. Middle and right: Liver slice cultured for 6 days in a static 6-well plate and perfusion respectively. Scale bars are 20 µm.

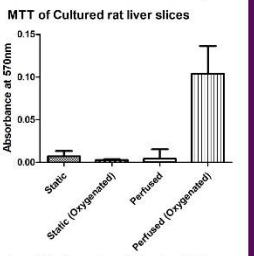

Figure 9: Absorbance values at 570nm for an MTT assay carried out on precision-cut liver tissue cores cultured over 4 days. The slices were cultured on Alvetex in static or perfused configurations both with and without oxygenation

CONCLUSIONS & FUTURE DIRECTIONS:

Conclusions:

- Addition of media perfusion increases the viability and proliferation of cell cultures.
- Under the right conditions cells can be induced to form a homogeneous tissue disc.
- Precision-cut liver slices can maintain their metabolic function for longer when cultured using this system.
- The large volume of media used allows preoxygenation leading to simplified apparatus for culture of liver slices.

Future Directions:

- Further characterisation of the tissues formed through the perfusion method.
- Addition of endothelial cells to mimic vasculature and create complex *in-vivo* like tissues.
- Analysis of cell structure and function compared to real tissue where possible.
- Optimisation of liver slice cultures to create an effective and reproducible platform for carrying out experiments.

1. Use these dynamics bridge the gap between cell culture and live tissue. S. Hanspeter, S. S. Keymer, S. H. S. Stelzer, Yaman Kinaret, Vesicular Cell Biology (2013) 10.1038/nrm3624
2. Bioreactors in tissue engineering: Advances in stem cell culture and three-dimensional tissue constructs, N. Celikkaker, A. Beer Ismail and T. M. ar, Exp. Ur'e Sci. (2015) 15: 570-577
3. Alvetex®, Polystyrene scaffold technology for routine three dimensional cell culture, J. Knight, K. Murray, C. Fitzpatrick and S. Przyborski, Methods Mol. Biol. (2011) Mol. 695 681
4. CFD work carried out with help from Dr Richard Williams, Department of Engineering, Durham University.

10.1.1.5. Increasing the functionality of hepatic cultures through the development of a tissue-specific microenvironment (2020) Durham University Department of Biosciences Research Away Day, Durham, UK.

INCREASING THE FUNCTIONALITY OF HEPATIC CULTURES THROUGH THE DEVELOPMENT OF A TISSUE-SPECIFIC MICROENVIRONMENT

EPSRC Engineering and Physical Sciences Research Council

H.W. Hoyle[1*] and S.A. Przyborski[1,2]

[1] Department of Biosciences, Durham University, UK. [2]Reprocell Europe, Sedgefield, UK.

*Presenting Author: h.w.hoyle@durham.ac.uk

Durham University

1. INTRODUCTION & AIMS:

The growth of cultured cells is governed by factors in the surrounding microenvironment including the physical space in which cells occupy. Three dimensional (3D) culture attempts to mimic *in vivo* conditions to enhance their structure and function[1]. While this can be achieved to some degree, many current 3D models do not address other factors, such as media perfusion to improve gaseous and nutrient diffusion and reduce unstirred layers of medium adjacent to the cells. This is particularly important when attempting to recreate complex highly vascularised tissues such as liver (Figure 1). Pumped perfusion of media has been introduced to overcome this with some success, however many current methods are overly complex and suffer from limitations such as size constraints[2].

Aims:

- To improve current static liver models by creating a more dynamic *in vitro* environment
- To increase the complexity of liver models to more accurately take into account the different factors found in the liver
- To improve the functional lifespan of tissue slices to make them more useful for long term chronic tests

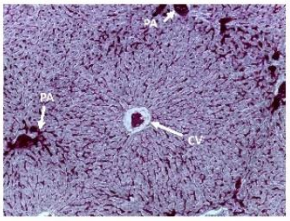

Figure 1: A dye perfused liver section. The hexagonal structure of the liver is apparent with blood flowing through the sinusoids from the portal area (PA) to the central vein (CV).

2. MATERIALS AND METHODS

HepG2 cultures are grown in 3D through the use of Alvetex® Strata as a substrate. This is a porous polystyrene scaffold with an average pore size of 15 µm. This creates a surface which can support cells from many directions as well as allowing some to invade into it therefore allowing more complex tissue cultures to be created[4].

Figure 2: A 6-well Alvetex® insert.

To create perfusion cultures, as shown by figure 3, cells are seeded as a suspension onto Alvetex® Strata in a 6 well insert and cultured overnight to allow the cells to adhere to the substrate. The Alvetex® insert is then removed from the well insert and placed into the perfusion system with 110 ml of media. This can then be cultured for at least another week to allow the cells to adapt to the perfusion.

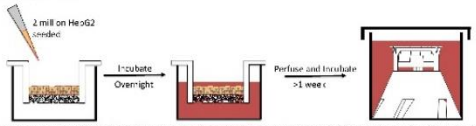

Figure 3: Stages in creating perfused Alvetex Cultures. HepG2 cells are seeded to Alvetex® Strata and incubated for one week. These are then placed in sandwich culture and perfused for another week.

3. DEVELOPMENT OF A NOVEL *IN VITRO* PERFUSION SYSTEM

In order to produce perfused 3D cultures novel apparatus has been developed. A set of criteria was created that the design needed to meet:

- Be **autoclavable** or easy to sterilise
- Use **non-cytotoxic** materials
- Use relatively **inexpensive** equipment
- Have a **small** footprint to allow scalability
- Create effective **media recirculation**

For this a design was created which used a magnetic stirrer to move the media (figure 4). Polytetrafluoroethylene (PTFE), an inert polymer, was used as a stand for the cultures. Custom glass beakers were produced which can easily be fitted into an incubator on a 6-point magnetic stirrer.

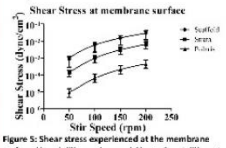

Figure 5: Shear stress experienced at the membrane surface. Use of different forms of Alvetex® and different stirrer speeds a low for control over the shear stress levels.

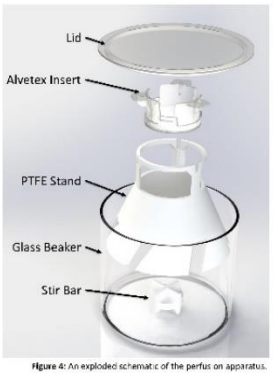

Figure 4: An exploded schematic of the perfusion apparatus.

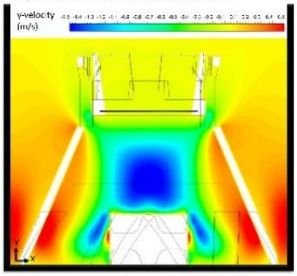

Figure 6: Computational Fluid Dynamics (CFD) simulation of the media recirculation within the apparatus. Arrows represent the direction of media flow at each point.[4]

Simulations of the fluid flow in the system were carried out using ANSYS Fluent. The shear stress can be controlled using the variables of stir speed and membrane porosity to achieve levels which are of physiological relevance to the studied tissue (Figure 5).

The models also show the circulation of media in the system. It is drawn downwards through the Alvetex® membrane, on which the cells are seeded, and recirculated upwards around the outside of the vessel (Figure 6). This allows both continual flow through the culture as well as complete mixing of the media.

The flow of media through the culture allows for more effective removal of waste products from the cell surface and helps to minimise the unstirred layers.

4. CULTURE OF HEPG2 CELLS IN 3D PERFUSION CONDITIONS

Growth of HepG2 cells on Alvetex® in perfusion shows several key improvements over static culture (figure 7);

- Increase in **proliferation**
- **Greater migration** across the surface of the substrate
- Formation of a **larger surface disk**
- Improved localisation of key hepatic markers (Figure 9)

By seeding the Alvetex® with fibroblasts a surface can be created which supports the growth of hepatocytes without invasion into the membrane (Figure 8), provides extracellular matrix interactions and still allows perfusion to take place through the culture.

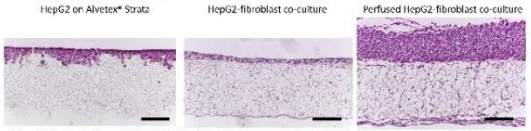

Figure 7: Haemotoxylin and Eosin (H&E) stain of HepG2 cells grown on Alvetex® Strata. Cells are grown on Alvetex® Strata as a control (left) compared to static and perfusion on a fibroblast-embedded Alvetex® Scaffold. Scale bars are 100 µm.

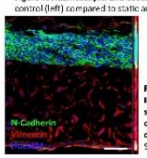

Figure 8: Immunofluorescent stain showing the compartmentalisation of the two cell types. Scale bar is 50 µm.

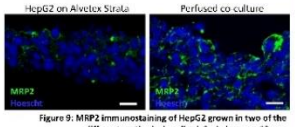

Figure 9: MRP2 immunostaining of HepG2 grown in two of the different methods described. Scale bars are 10 µm.

5. INCREASING THE LIFESPAN OF *EX VIVO* TISSUE SLICES

Precision-cut liver slices are a method which can be used for functional liver tests. There are several benefits to these cultures over conventional cell culture:

- Increased **complexity**
- Cells are in their **native environment**
- **High throughput** and easy to set up

Ex vivo liver slices have a functional lifespan of a few hours. Methods which have prolonged this typically use a 95% oxygen environment leading to high experimental cost. A simple oxygenated chamber can be used to hold the cultures and allow the perfusion system to be oxygenated whilst minimising additional cost.

Initial results are promising with the MTT assay showing viable tissue still present after 3 days in preoxygenated perfusion culture (figure 10).

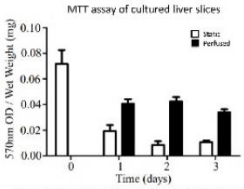

Figure 10: Absorbance values at 570nm for an MTT assay carried out on precision-cut liver tissue cores cultured for up to 3 days. The slices were cultured on Alvetex® in static or perfused configurations.

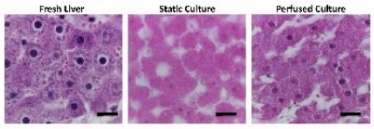

Figure 11: H&E Stains of liver tissue. Left: Liver fixed after slicing. Middle and right: Liver slice cultured for 6 days in a static 6-well plate and perfusion respectively. Scale bars are 20 µm.

CONCLUSIONS & FUTURE DIRECTIONS:

Conclusions:

- Addition of media perfusion increases the viability and proliferation of cell cultures.
- Under the right conditions cells can be induced to form a homogeneous tissue disc.
- Functional hepatocyte proteins such as MRP2 have improved expression in perfusion
- Precision-cut liver slices can maintain their metabolic function for longer when cultured using this system.

Future Directions:

- Addition of endothelial cells to mimic vasculature and create complex *in-vivo* like tissues.
- Functional analysis of cultures to look at effects of perfusion on drug-metabolising enzymes such as the Cytochrome P450 family.
- Optimisation of liver slice cultures to create an effective and reproducible platform for carrying out experiments.

1. The third dimension: bridging the gap between cell culture and live tissue. Pampaloni, E. G. Reynaud, E. H. K. Stelzer, Nature Reviews. Molecular Cell Biology (2007) 8: 839-845.
2. Biomimetic 3D tissue engineering: Advances in stem cell culture and characterisation. Lancaster, M. Dalby, Stem Cell Research & Therapy (2015) 6: 173.
3. Alvetex®: Polystyrene scaffold technology for routine three dimensional cell culture. P. Wright, N. Mallory, S. Gaisford and S. Przyborski, Methods Mol. Biol., (2011) 695: 175-186.
4. CFD simulations to optimise the bioreactor for Stem Cell Culture, Department of Engineering, Durham University.

10.1.2. Oral Presentation Abstracts

10.1.2.1. Improvement of three-dimensional liver tissue models through the development of a novel perfusion culture system (2018) White Rose Biomaterials and Tissue Engineering Group Conference, Sheffield, UK

IMPROVEMENT OF THREE DIMENSIONAL LIVER TISSUE MODELS THROUGH THE DEVELOPMENT OF A NOVEL PERFUSION CULTURE SYSTEM

H W Hoyle[1] & S A Przyborski[1, 2]

[1] Department of Biosciences, Stockton Road, Durham University, Durham, DH1 3LE.
[2] Reprocell Europe, Sedgefield, TS21 3FD

Introduction

The growth of cultured cells is governed by factors in the surrounding microenvironment including the physical space in which cells occupy. We have utilised three-dimensional (3D) and perfusion techniques to create a novel bioreactor system which aims to bring culture conditions closer to those found *in vivo*. The liver has been chosen for testing of the system as it is a complex and highly perfused organ and therefore models of the liver should benefit greatly from this method. The system is used as a platform for hepatic co-culture models using immortalised cell lines with the aim to allow such cells to have more physiological relevance and increase their value in drug development.

Methods

The HepG2 line is a hepatocellular carcinoma cell line which is used extensively for studying liver metabolism and protein trafficking. In an attempt to enhance cell structure and function, we have developed a novel yet simple perfusion system which can be used for 3D culture of HepG2 cells in a more physiologically relevant environment. Further complexity is created through use of a supportive layer of fibroblasts and the addition of non-parenchymal cells such as endothelial cells.

Results

Cultures of HepG2 cells in perfused Alvetex® culture increase in proliferation compared with both 2D and 3D Alvetex® static cultures. An altered morphology is also seen with changes in the levels of cell-cell contacts and hepatocyte polarity. Growth on a fibroblast layer minimises cell invasion into the substrate and helps to minimise effects of shear stress on the hepatocytes, providing a homogeneous 3D tissue disc.

Discussion

Introducing perfusion to 3D Alvetex® based cultures illustrates the potential for more physiologically relevant *in vitro* cell culture. Through this methodology we aim to create models which have improved structure and enhanced function compared with current assays, increasing the accuracy and predictive capacity of such models in drug testing.

10.1.2.2. Enhancing the structure and function of liver tissue models using advanced cell technologies (2019) Durham University Department of Biosciences Postgraduate Conference, Durham, UK

Name: Henry Hoyle

Title of Presentation: Enhancing the Structure and Function of Liver Tissue Models Using Advanced Cell Technologies

Supervisor: Prof. Stefan Przyborski

Abstract :
Liver models used in field such as drug discovery and cancer research suffer from limitations due to the lack of physiological relevance. We have developed a novel perfusion culture system which allows for three dimensional growth of liver tissue in a dynamic environment. This has been used both for culture of immortal liver cell lines to recreate the tissue microenvironment as well as to maintain the viability of precision-cut liver slices over long term periods to increase their usefulness in the drug discovery process. Results suggest an improvement in the structure of the tissues formed and research is ongoing to investigate the impact on functionality.

10.1.2.3. Improvement of three-dimensional liver tissue models through the development of a novel perfusion culture system (2019) Tissue Engineering and Regenerative Medicine International Society (TERMIS) EU Chapter Meeting, Rhodes, Greece.

Abstract Submission Form: TERMIS EU 2019, 27th to 31st of May 2019, Rhodes, Greece

Improvement of Three-Dimensional Liver Tissue Models through the Development of a Novel Perfusion Culture System

H. Hoyle[1], S. Przyborski[1,2]
Presenting Author: Henry Hoyle, h.w.hoyle@durham.ac.uk
[1] *Department of Biosciences, Stockton Road, Durham University, Durham, UK,*
[2] *Reprocell Europe, Sedgefield, UK*

INTRODUCTION: The growth of cultured cells is governed by factors in the surrounding microenvironment including the physical space in which cells occupy[1]. We have utilised three-dimensional (3D) and perfusion techniques to create a novel bioreactor system which aims to bring culture conditions closer to those found *in vivo*. The liver has been chosen for testing of the system as it is a complex and highly perfused organ and therefore models of the liver should benefit greatly from this method[2, 3]. The system is used as a platform for hepatic co-culture models using immortalised cell lines with the aim to allow such cells to have more physiological relevance and increase their value in drug development.

METHODS: The HepG2 line is a hepatocellular carcinoma cell line which is used extensively for studying liver metabolism and protein trafficking. In an attempt to enhance cell structure and function, we have developed a novel yet simple perfusion system which can be used for 3D culture of HepG2 cells in a more physiologically relevant environment. Further complexity is created through use of a supportive layer of fibroblasts and the addition of non-parenchymal cells such as endothelial cells.

RESULTS: Cultures of HepG2 cells in perfused Alvetex® culture show enhanced proliferation and viability compared to both 2D and 3D Alvetex® static cultures. An altered morphology is also seen with changes in the levels of cell-cell contacts and hepatocyte polarity. Growth on a fibroblast layer minimises cell invasion into the substrate and helps to minimise effects of shear stress on the hepatocytes, providing a homogeneous 3D tissue disc. This system was also found to be successful for maintaining the viability of precision-cut liver slices over prolonged periods, another technique which can be used for the modelling of the liver.

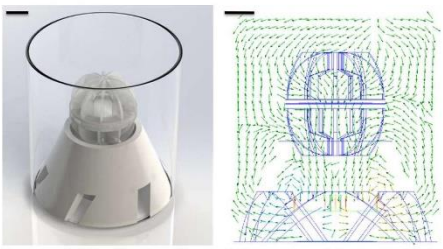

Figure 1: Left: Render of the assembled perfusion system. Right: Computational fluid dynamics to show medium recirculation within the system. Scale bars are 1 cm.

DISCUSSION & CONCLUSIONS: Introducing perfusion to 3D Alvetex® based cultures illustrates the potential for more physiologically relevant *in vitro* cell culture. Through this methodology we aim to create models which have improved structure and enhanced function compared to current assays, increasing the accuracy and predictive capacity of such models in drug testing.

ACKNOWLEDGEMENTS: Financial support was received from the EPSRC and the Faculty of Science, Durham University.

REFERENCES

[1] Cukierman E. et al. Science 2001; 294(5547):1708-12
[2] V. Soldatow et al. Toxicol. Res. 2013 2(1): 23-39
[3] C. Lin and S. Khetani, Biomed. Res. Int. 2016 (14): 1-20

10.2. Appendix 2: Schematics of custom apparatus

Unless otherwise stated, all dimensions are in millimetres.

10.2.1. PTFE Components

10.2.1.1. Vented Table

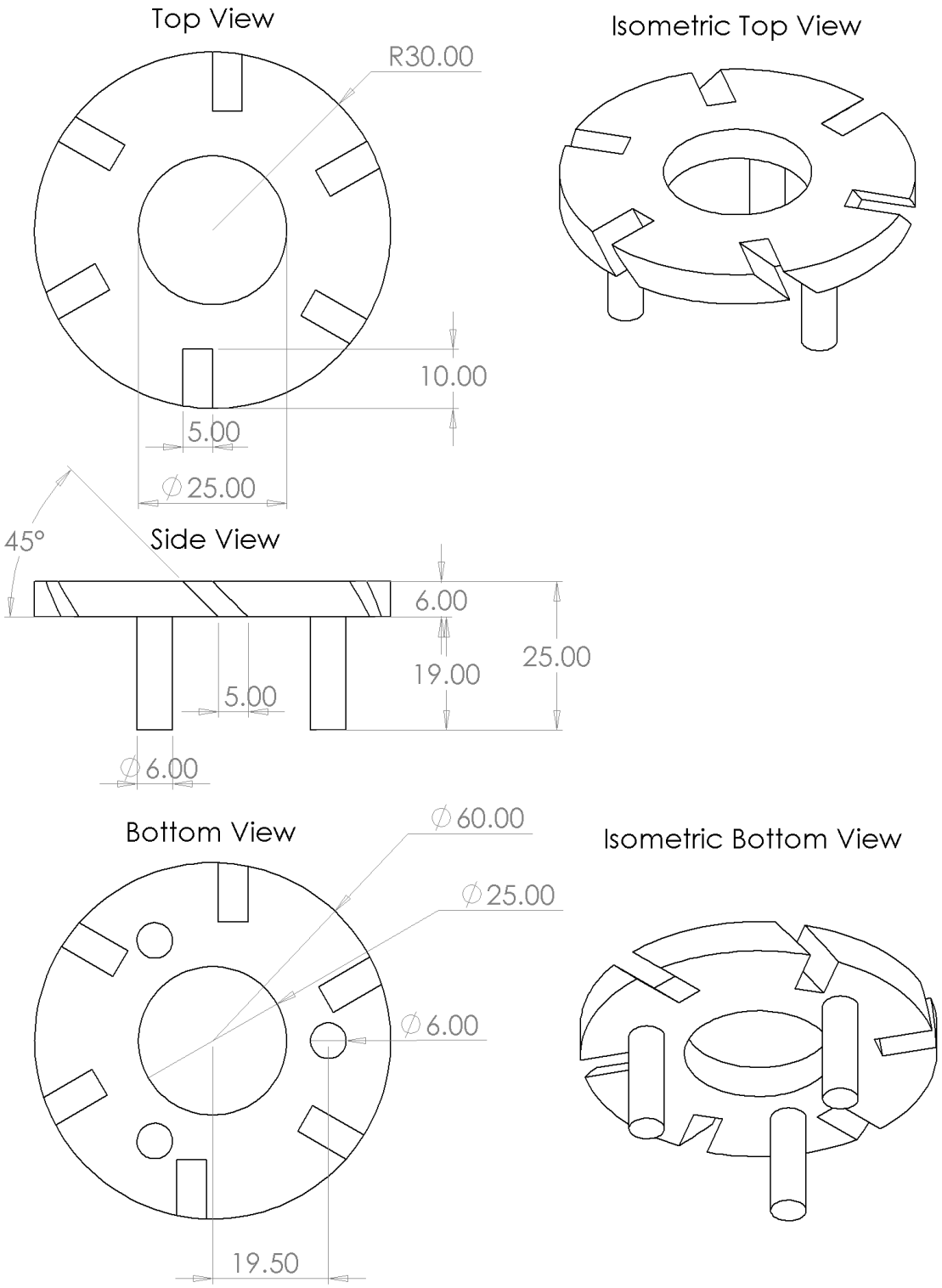

10.2.1.2. Clockwise Vented Cone

Note: Anticlockwise vented cone is identical to this design but mirrored in the XY plane.

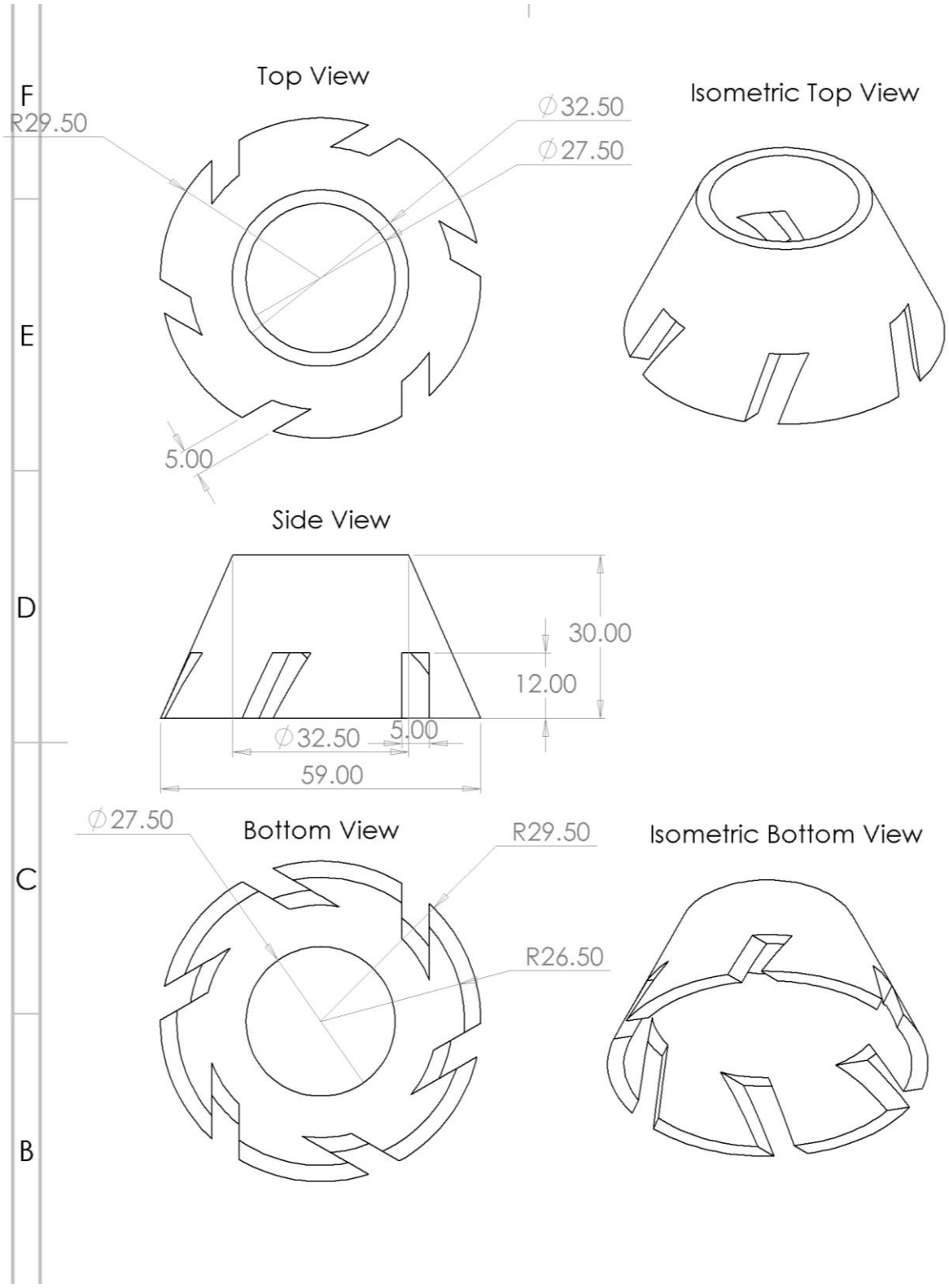

10.2.1.3. 6-Well insert holder

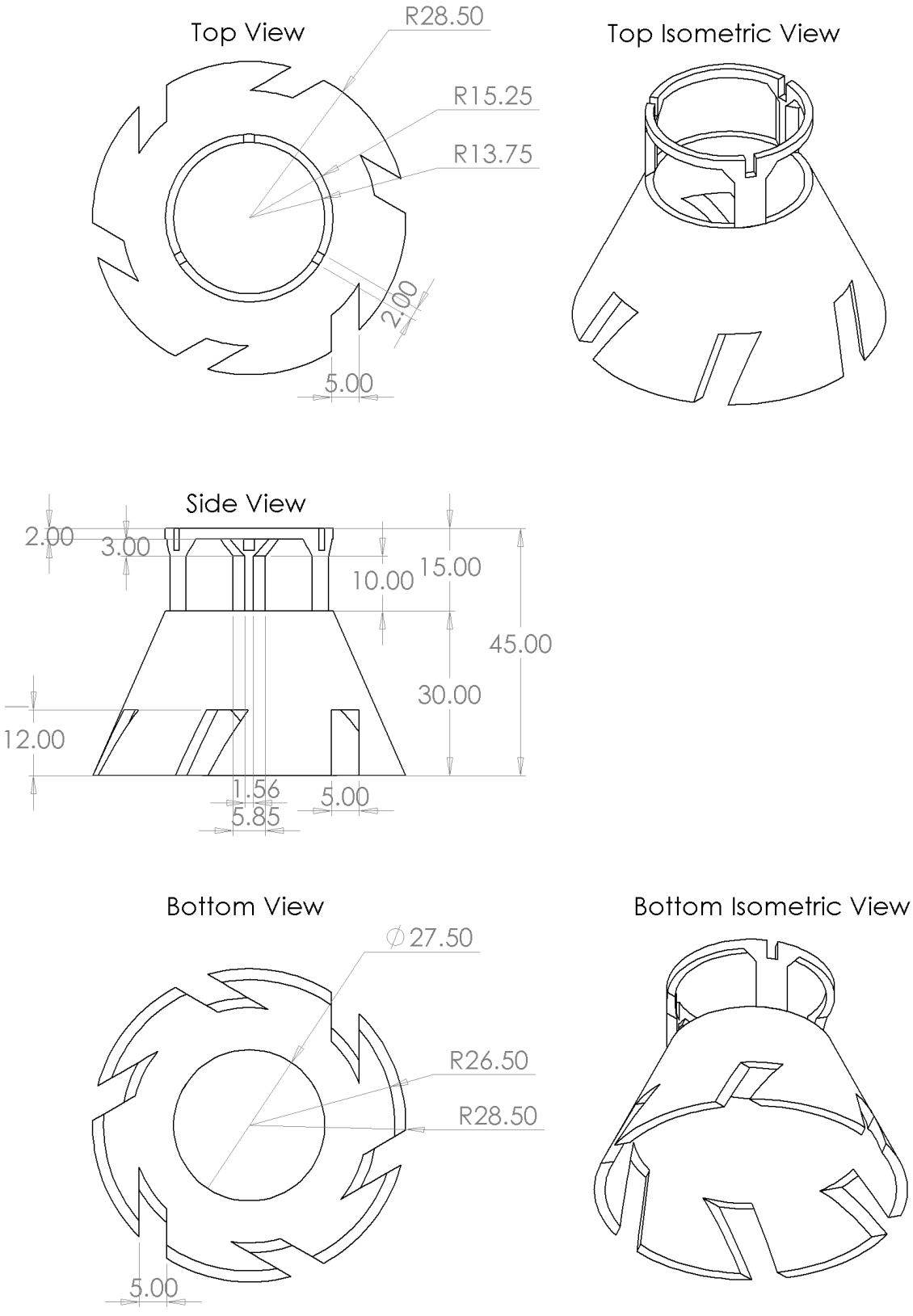

10.2.1.4. Reversible Lid

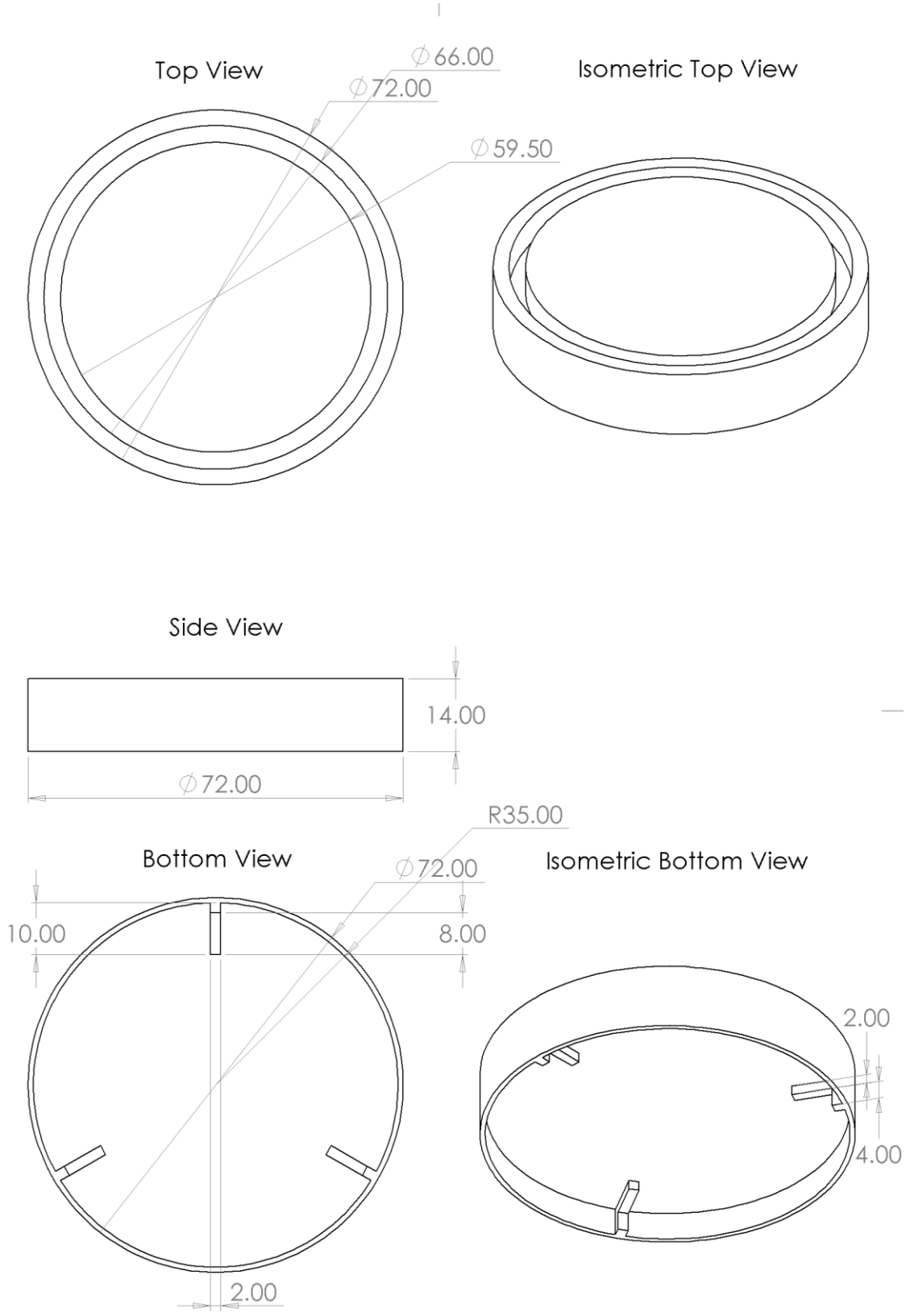

10.2.2. Glass Beakers

10.2.2.1. Initial Beaker design

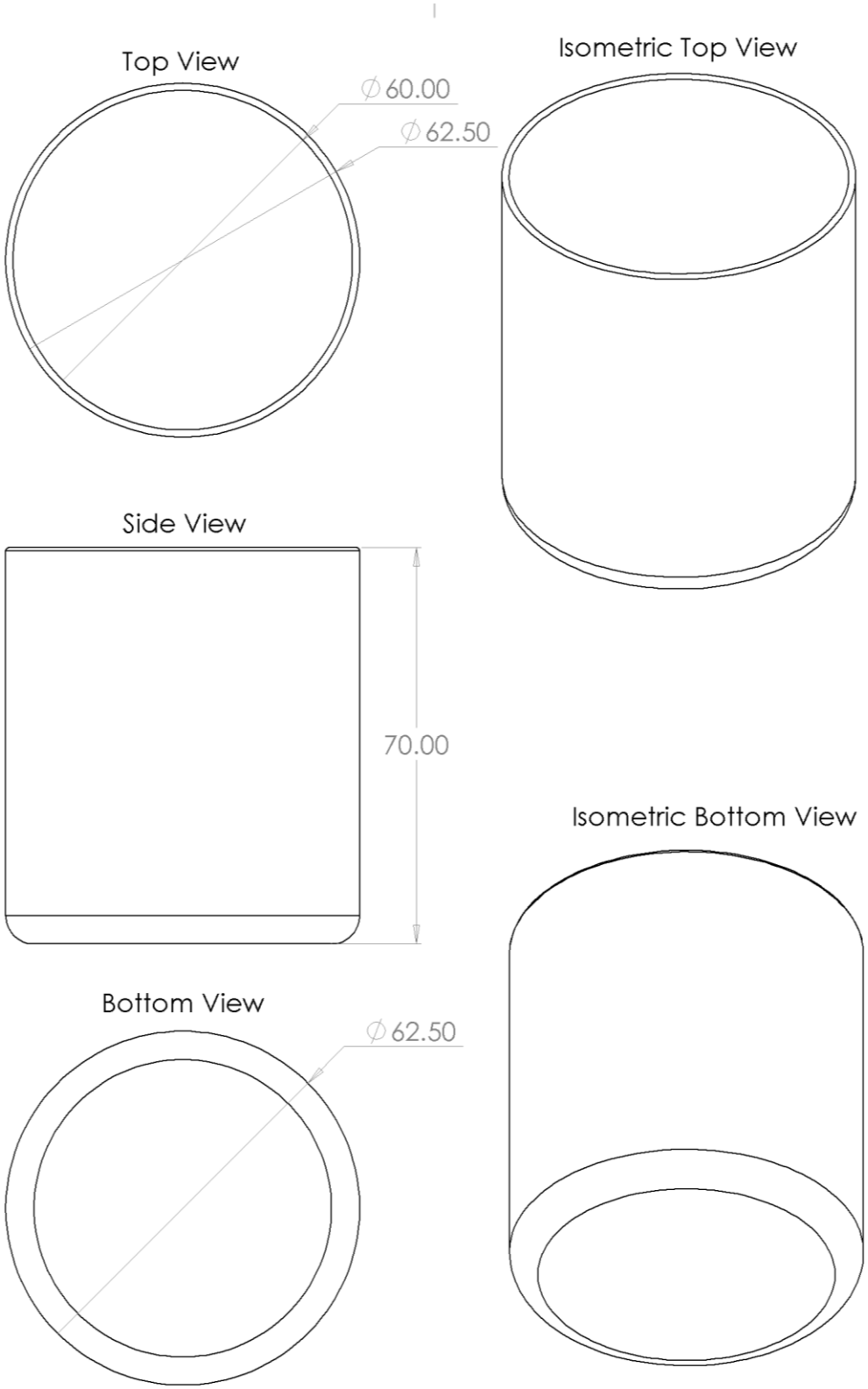

10.2.2.2. Final Beaker Design

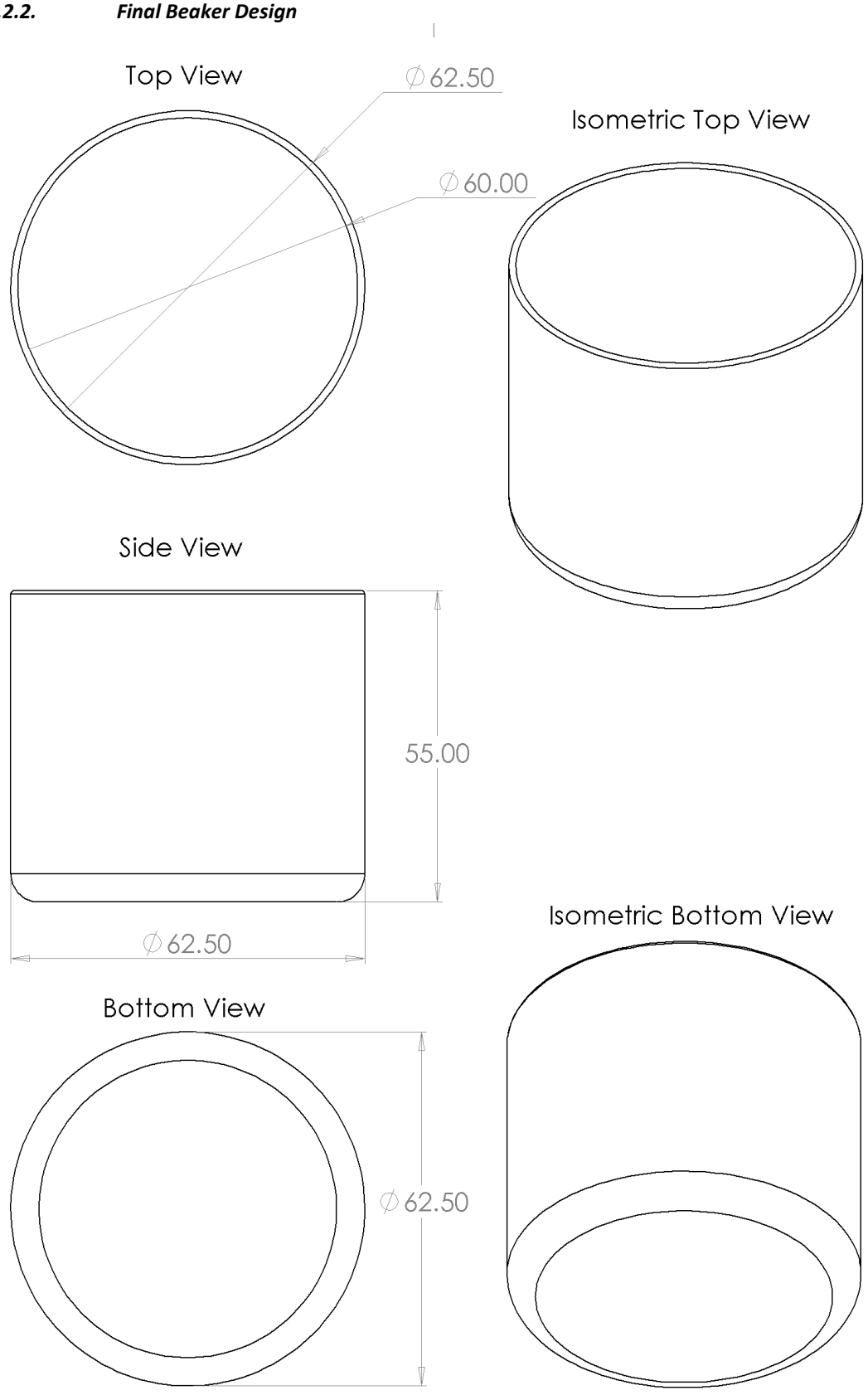

10.2.3. Magnetic Stirrer units

10.2.3.1. Control Unit

10.2.3.1.1. Case schematics

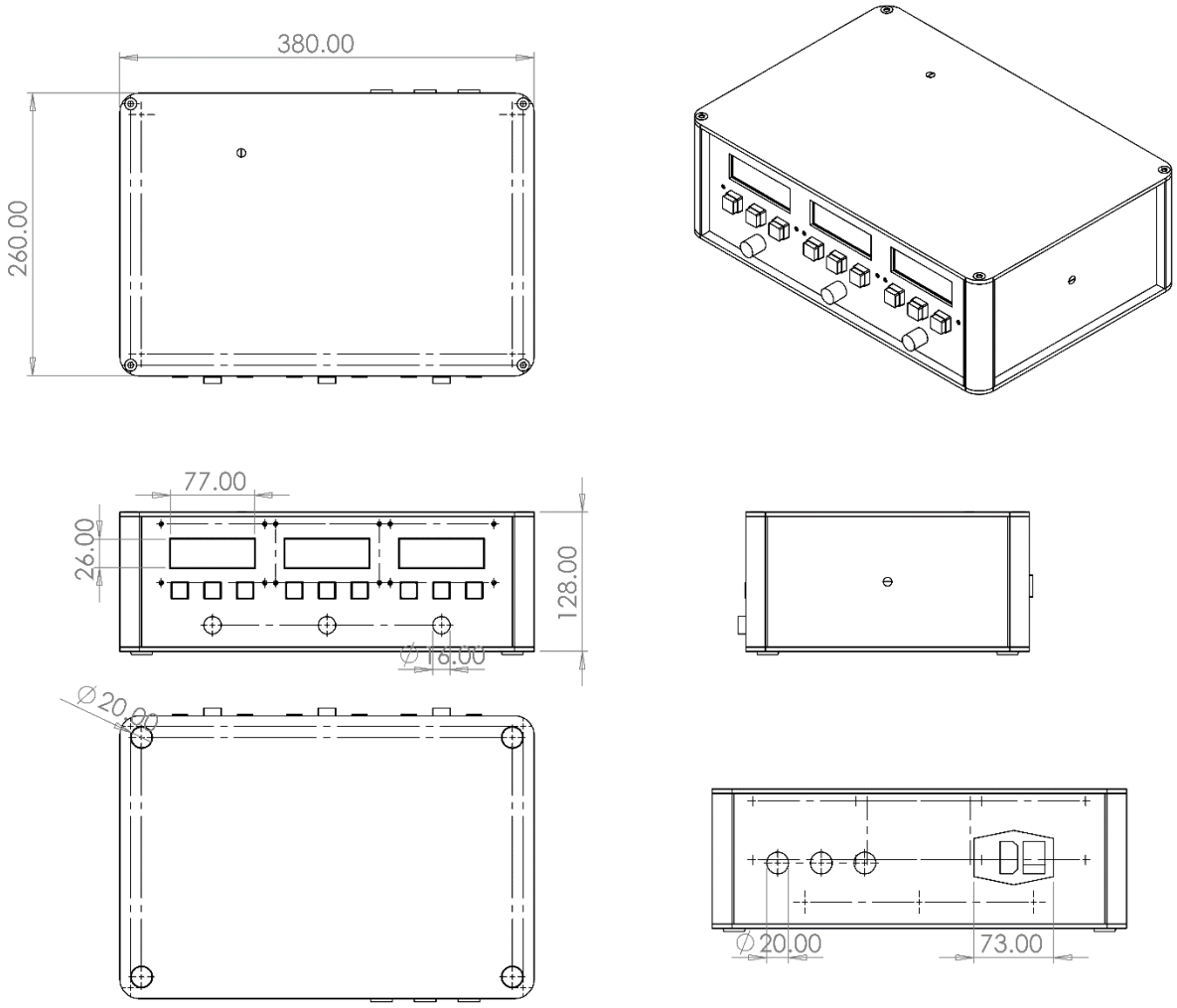

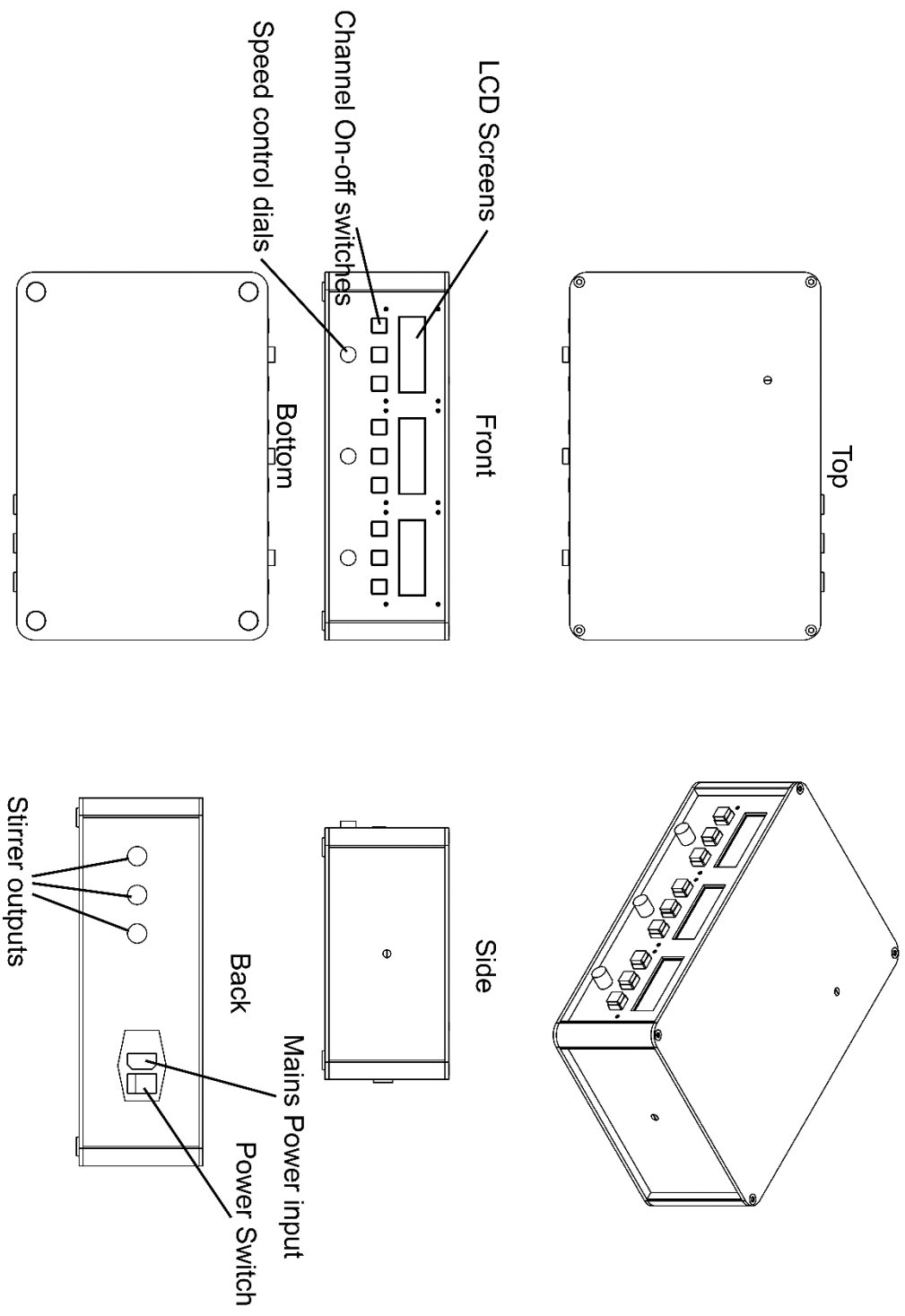
Top
LCD Screens
Channel On-off switches
Speed control dials
Front
Bottom
Side
Stirrer outputs
Back
Mains Power input
Power Switch

10.2.3.1.2. Photographs

STIRRER 1
Speed (RPM) 250
Lane 1 Lane 2 Lane 3
OFF OFF OFF
STIRRER 2
Speed (RPM) 123
Lane 1 Lane 2 Lane 3
OFF OFF OFF
STIRRER 3
Speed (RPM) 98
Lane 1 Lane 2 Lane 3
OFF OFF OFF

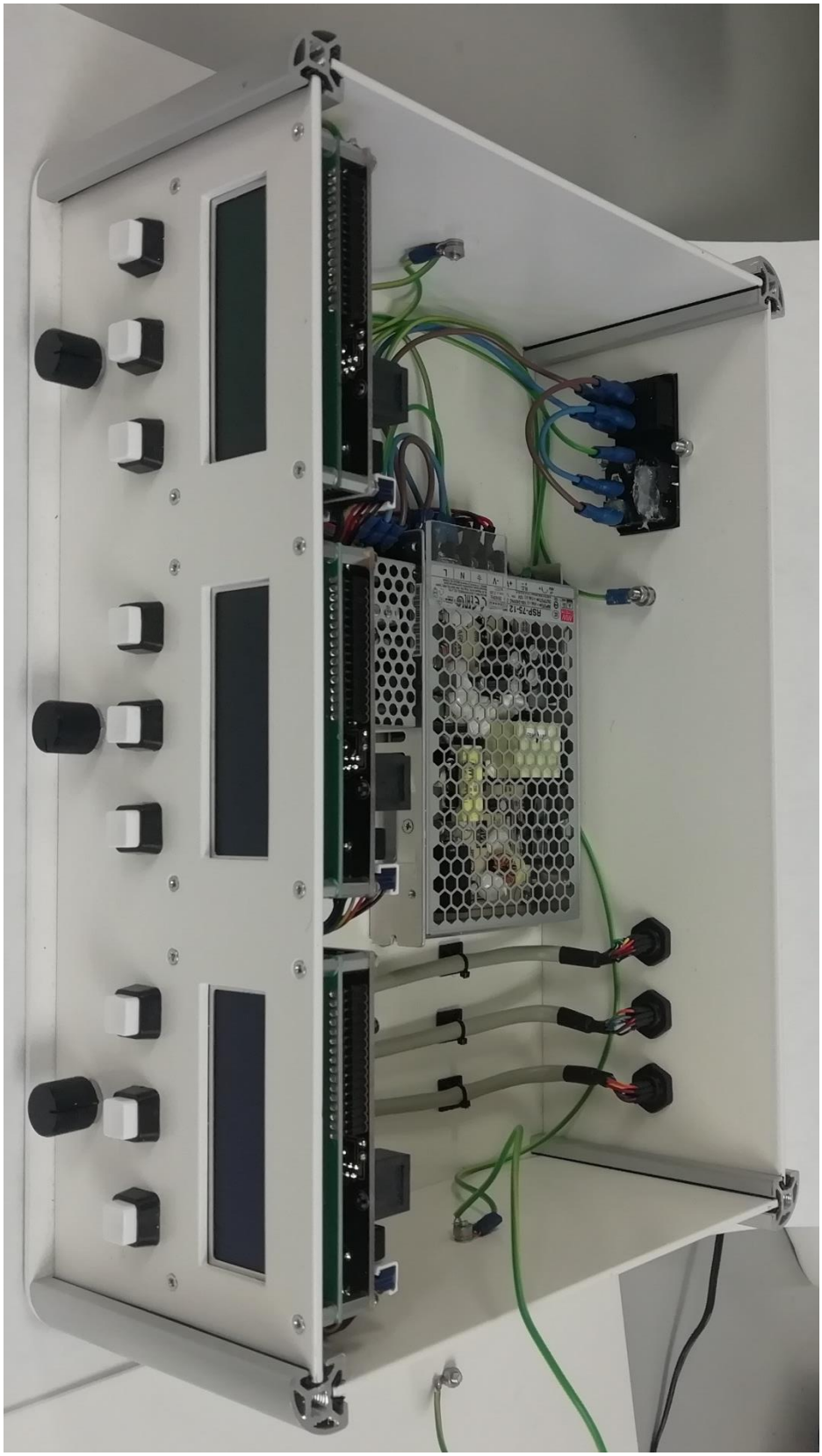

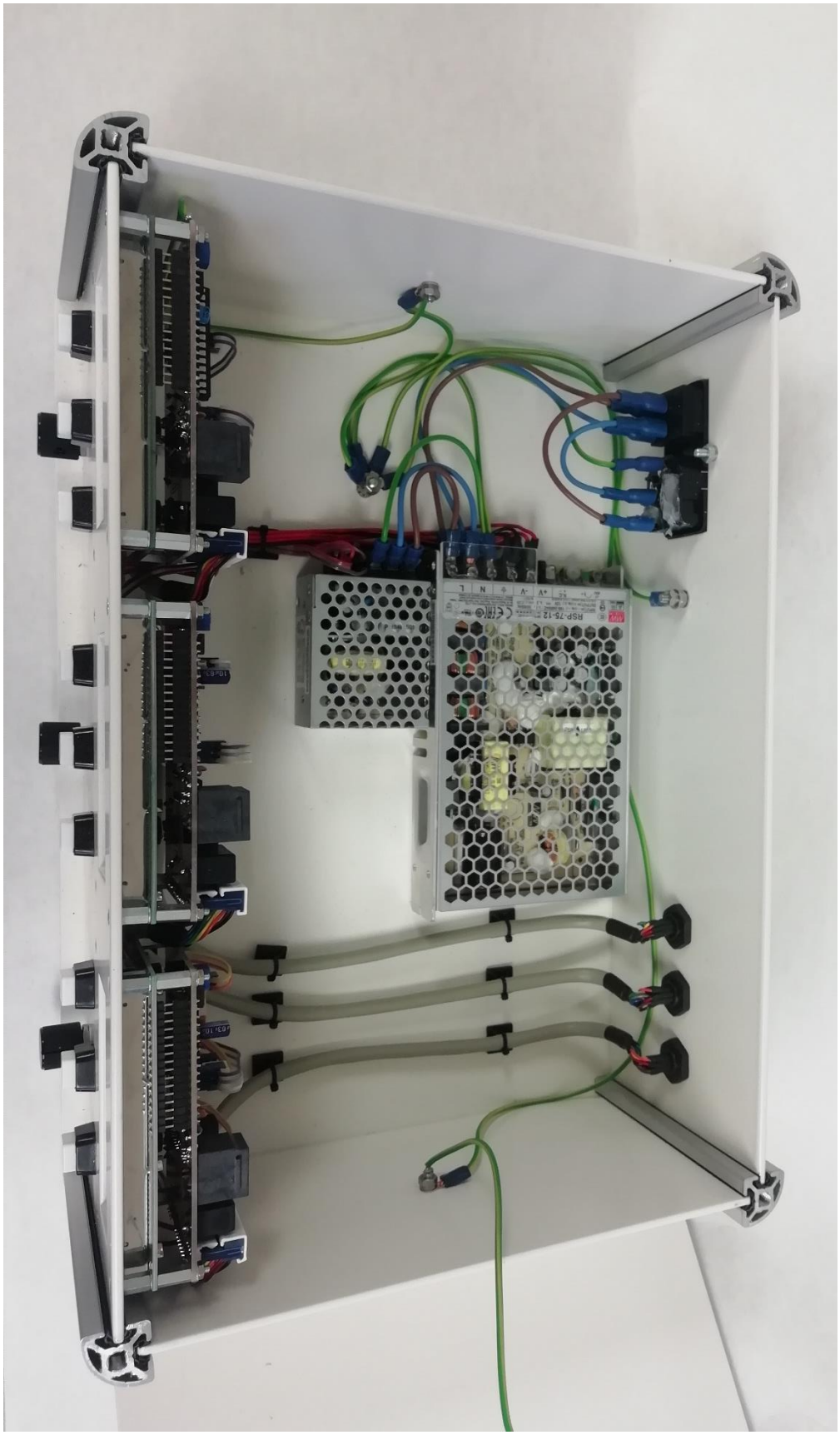
RSP-75-12

STIRRER 3
STIRRER 2
STIRRER 1

STIRRER 3
STIRRER 2
STIRRER 1
REPLACE FUSE WITH SAME TYPE AND RATING
DO NOT DO A PAT LOAD TEST!

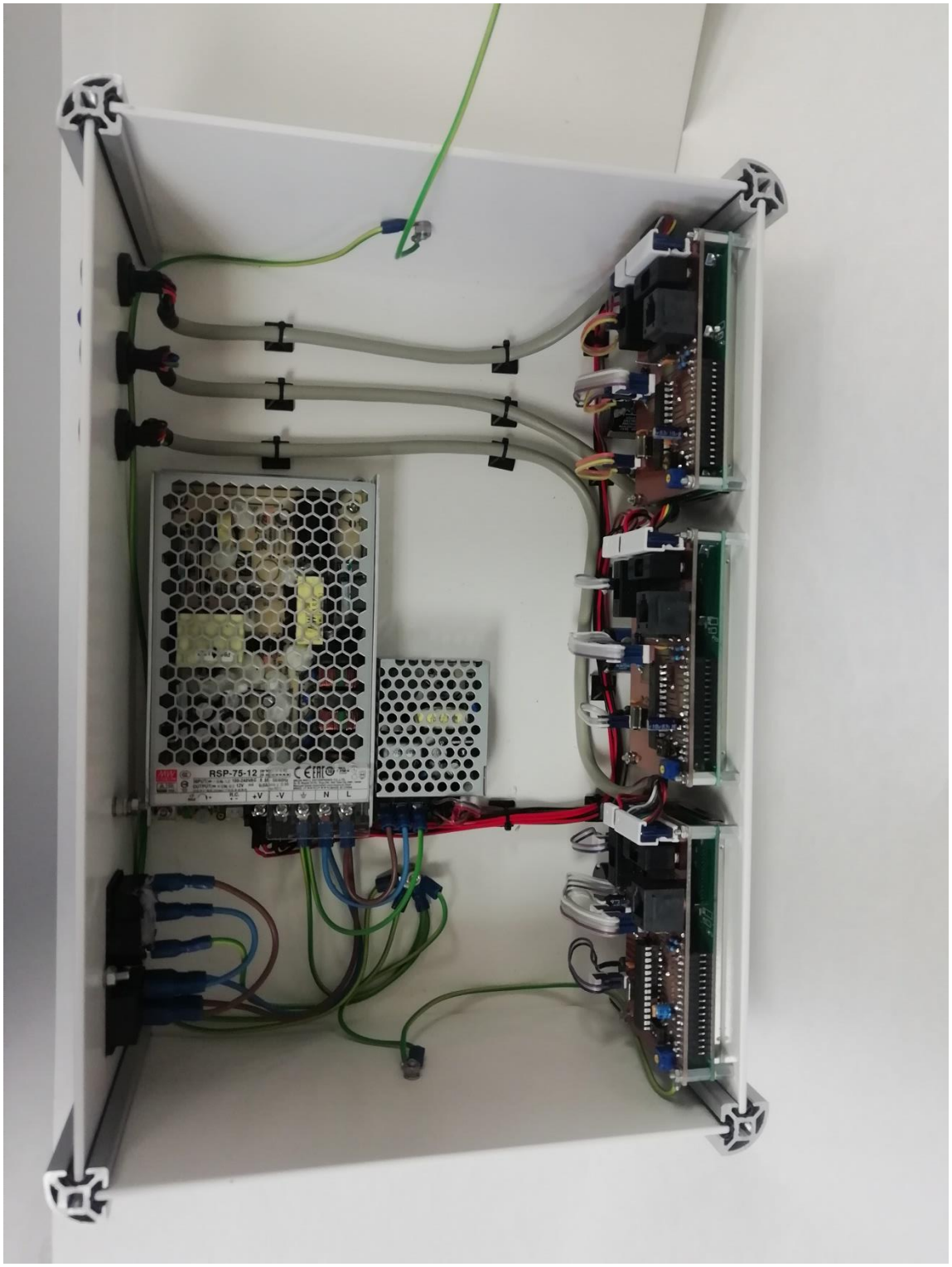
RSP-75-12
+V
-V
N
L

10.2.3.1.3. Circuit Diagrams

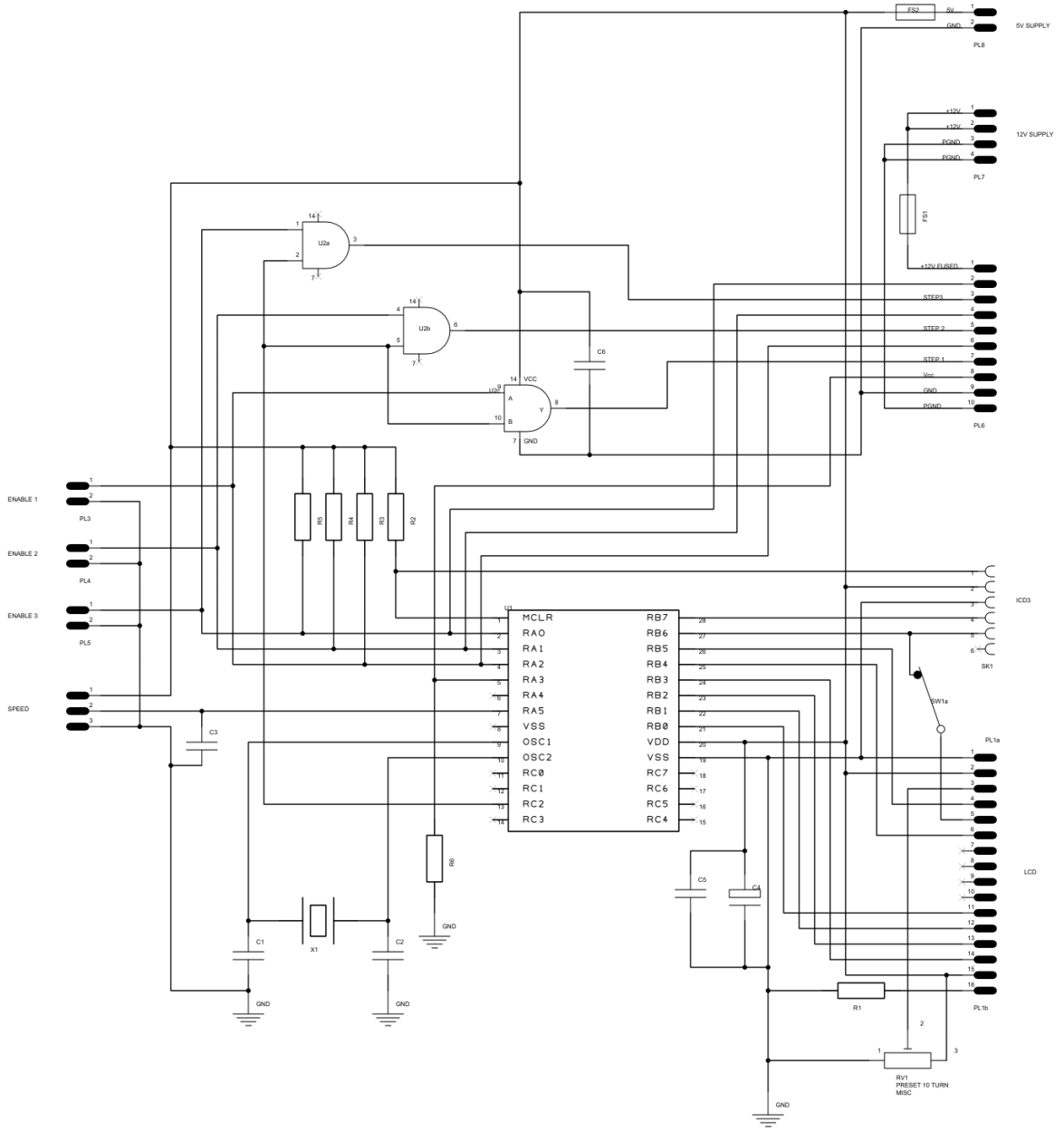

10.2.3.1.4. PCB schematics

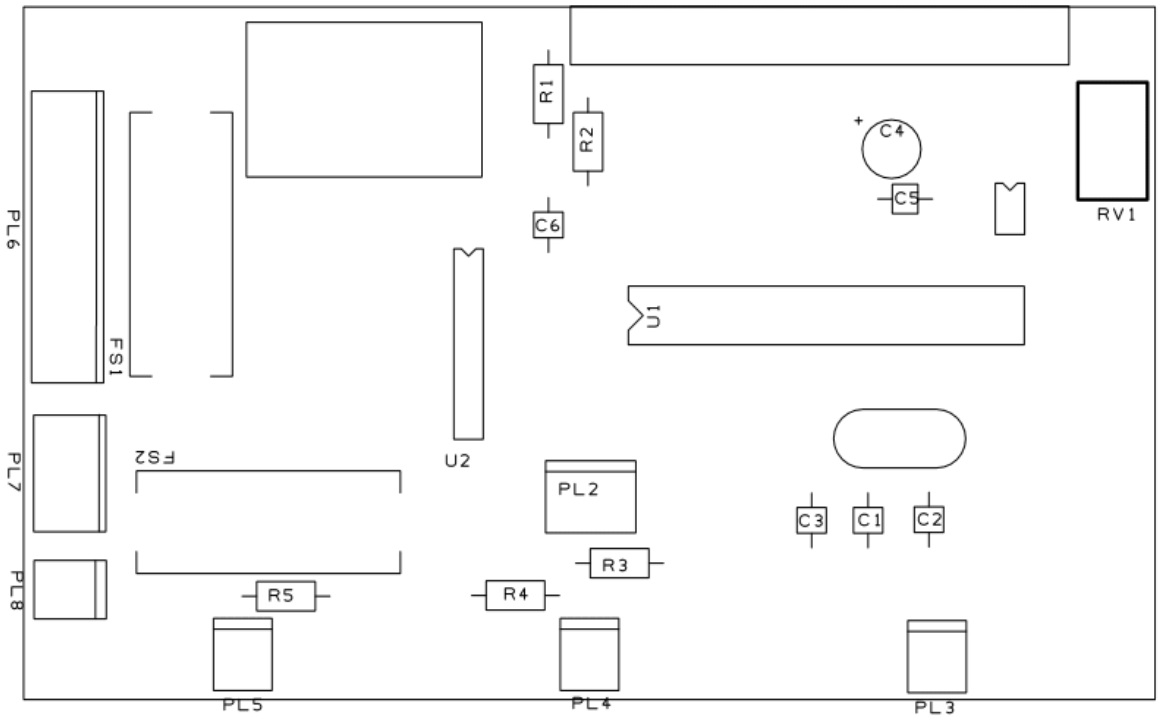

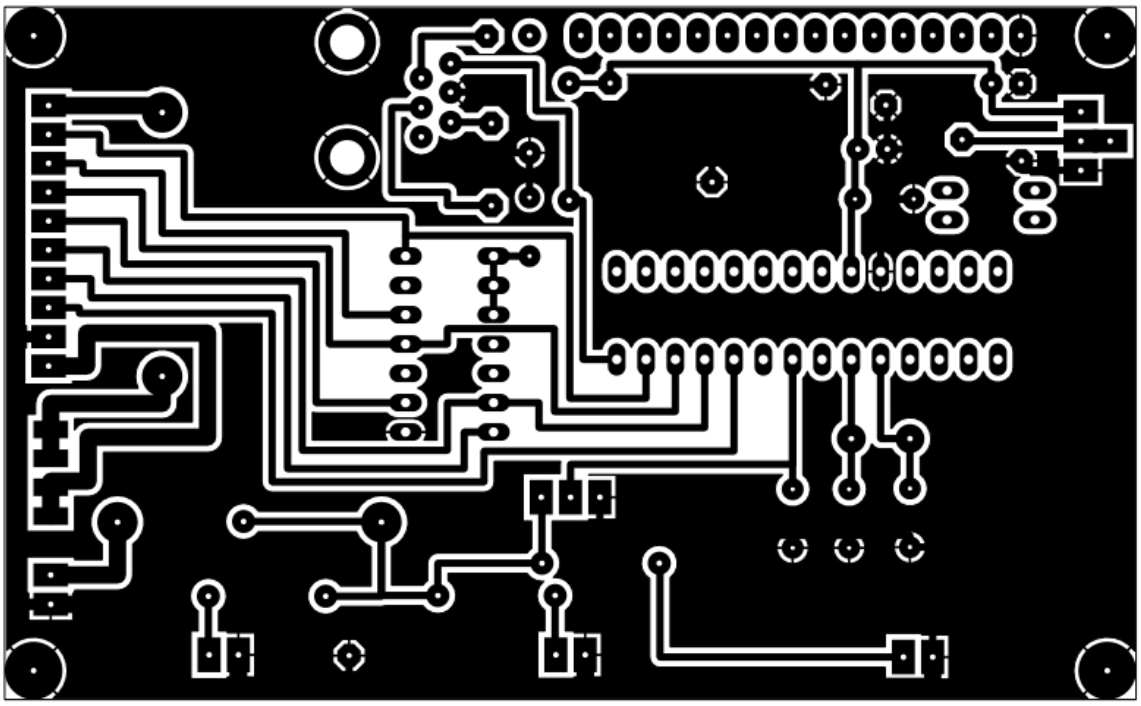

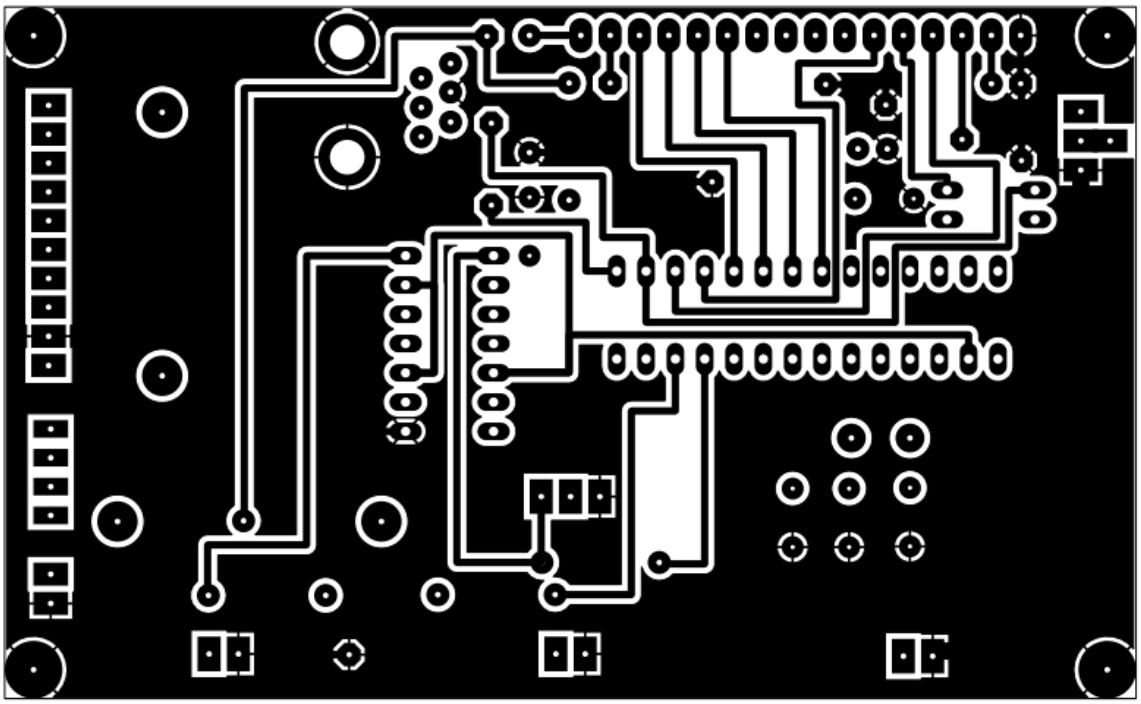

10.2.3.2. Stirrer units

10.2.3.2.1. Case Schematics

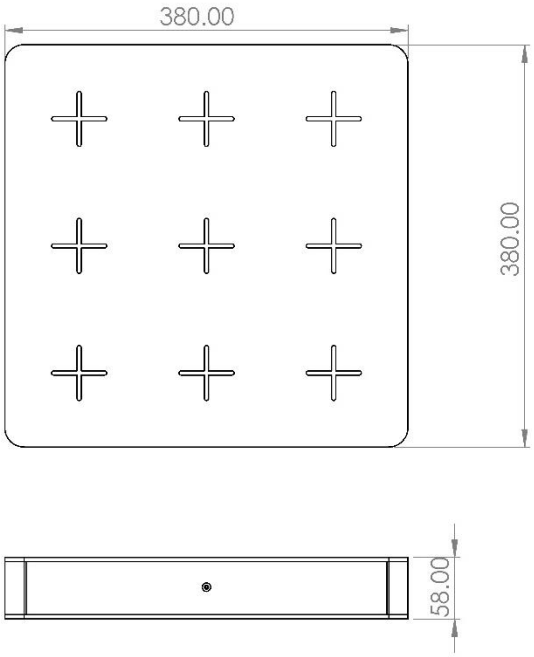

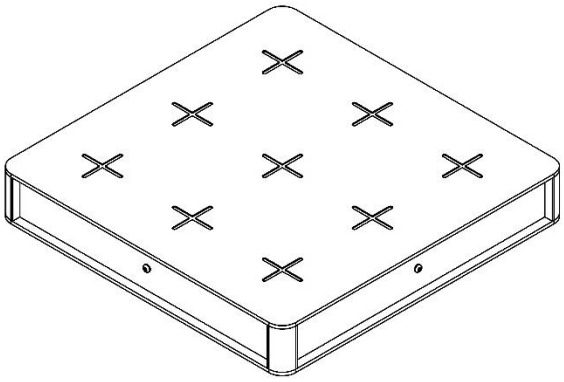

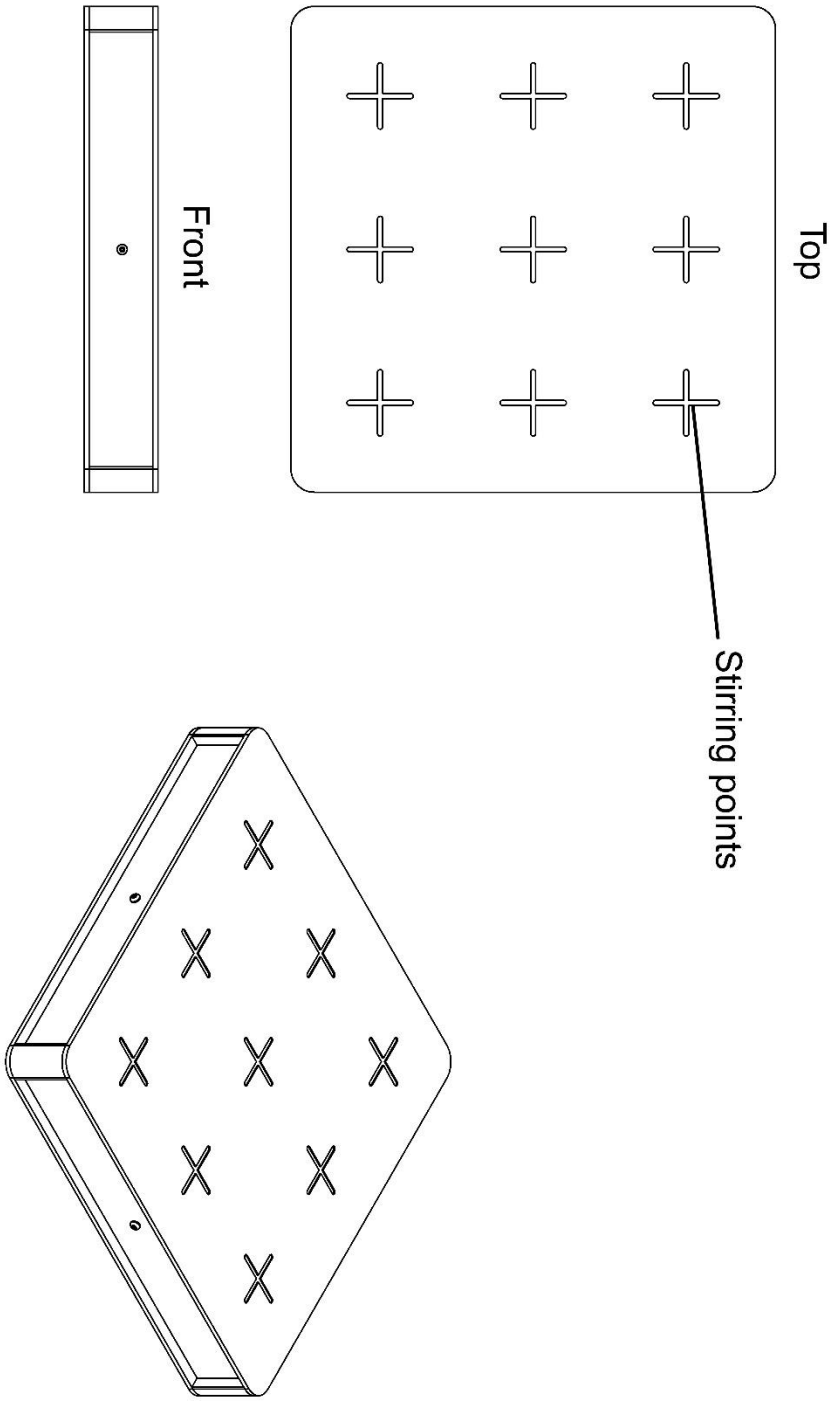
Front
Top
Stirring points

10.2.3.2.2. Photographs

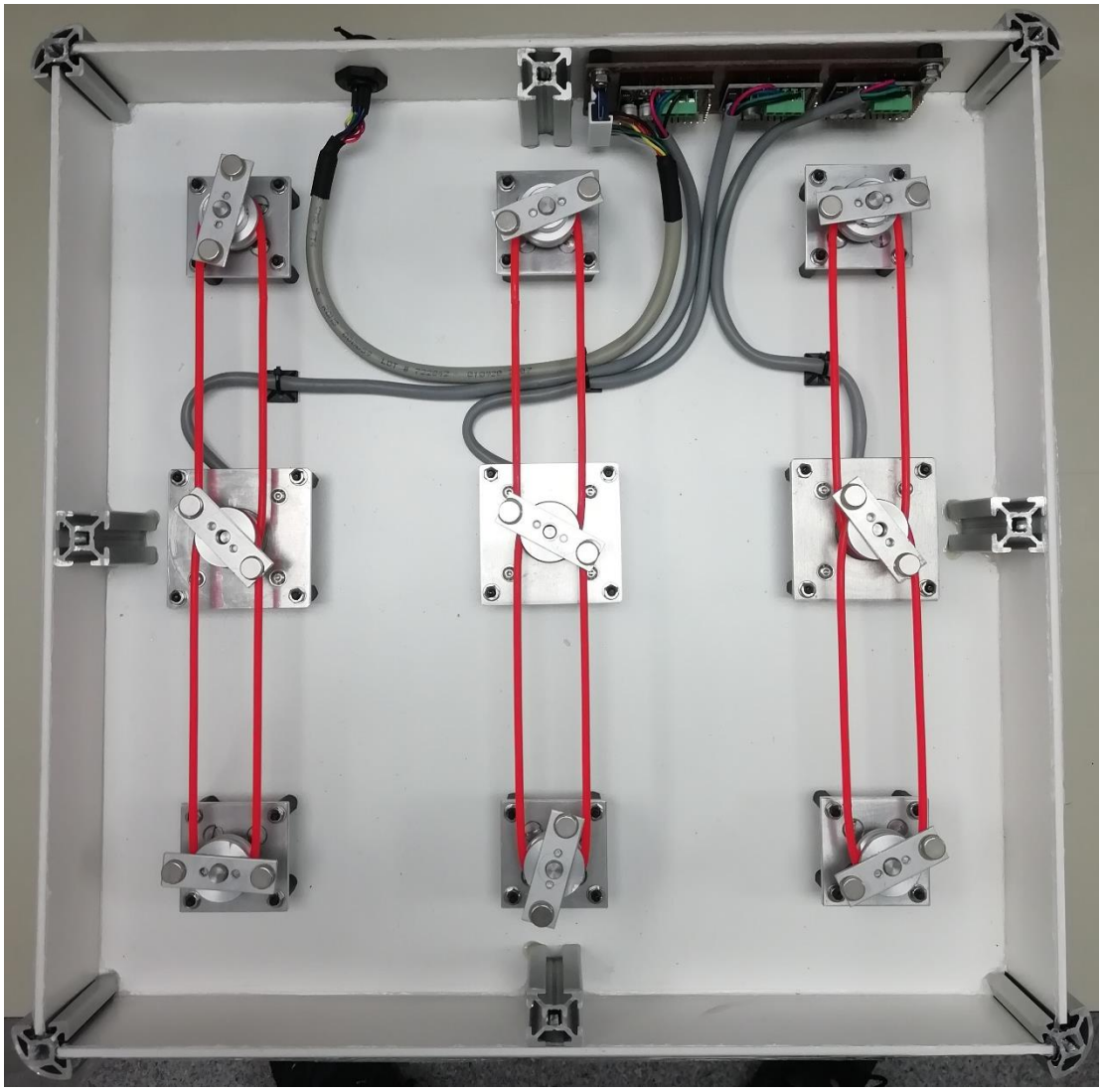

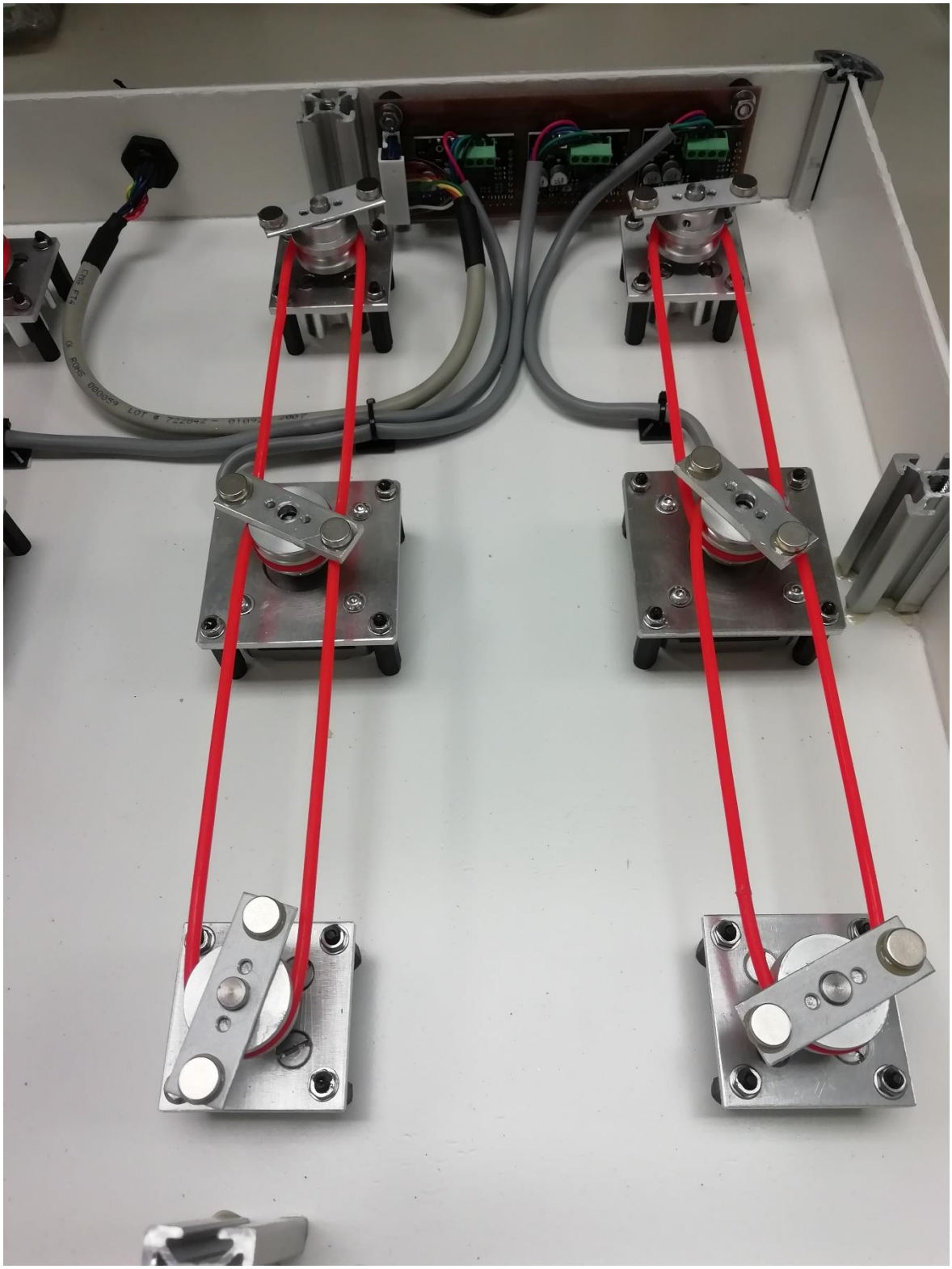

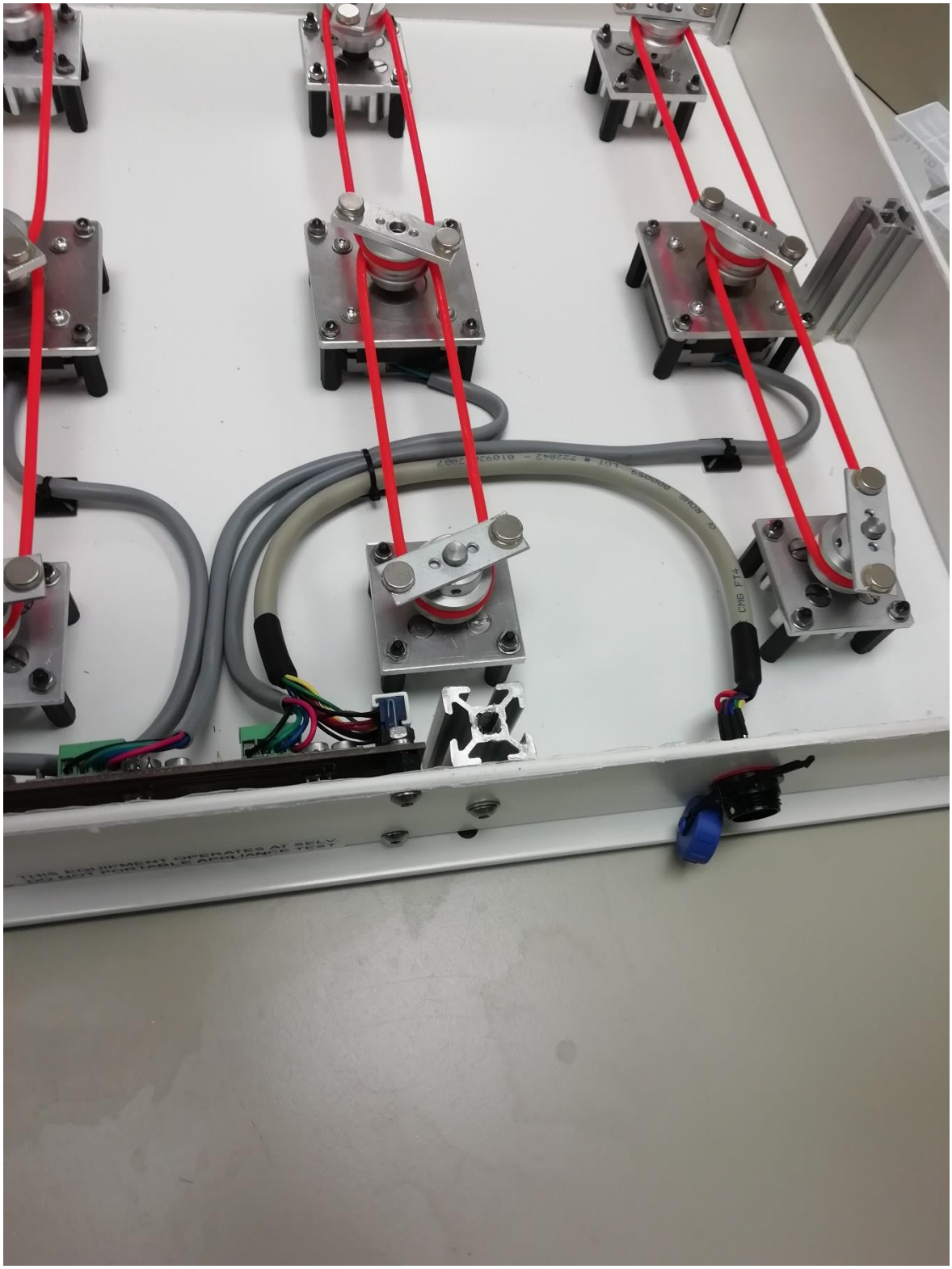

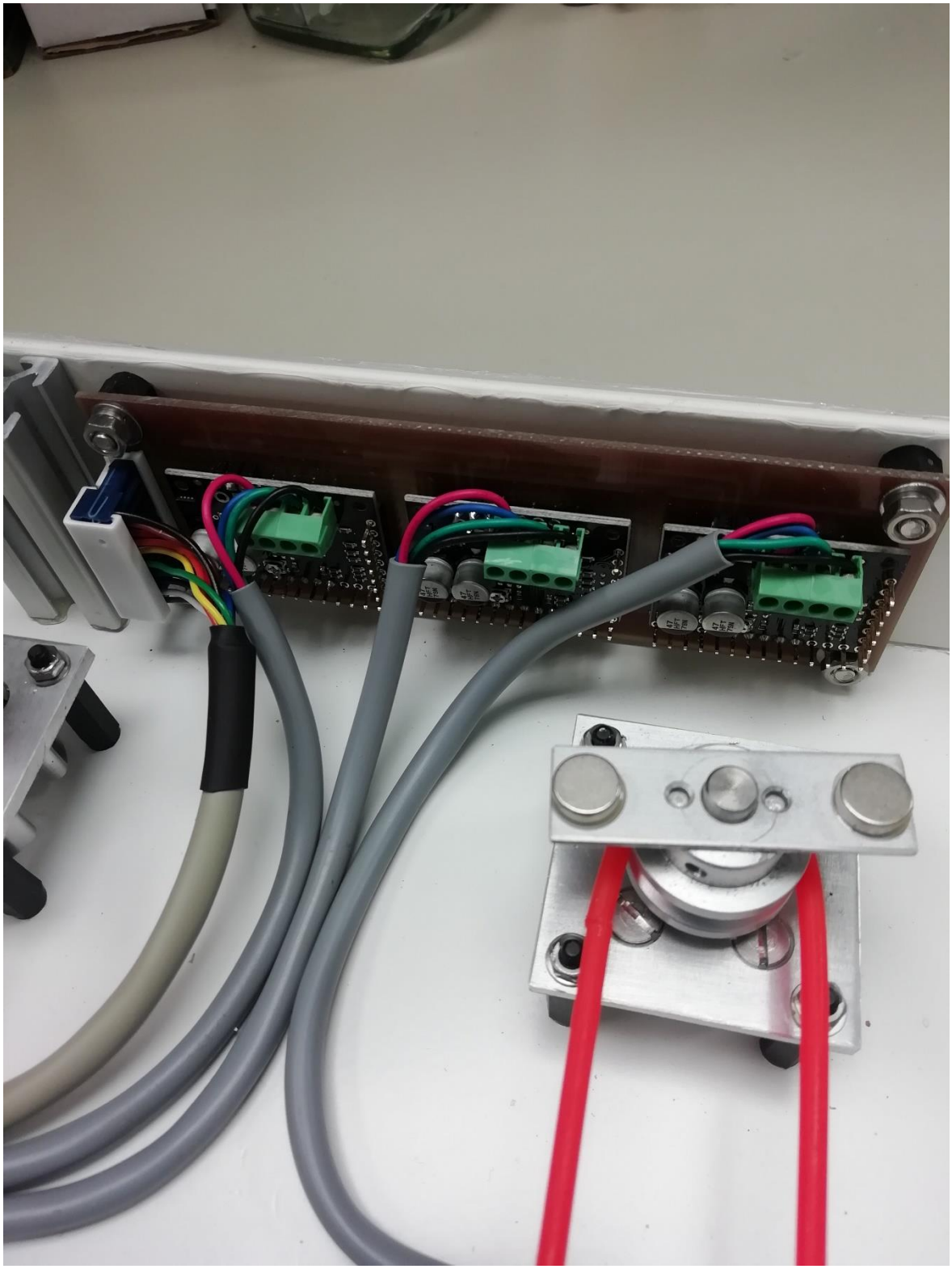

10.2.3.2.3. Circuit Diagrams

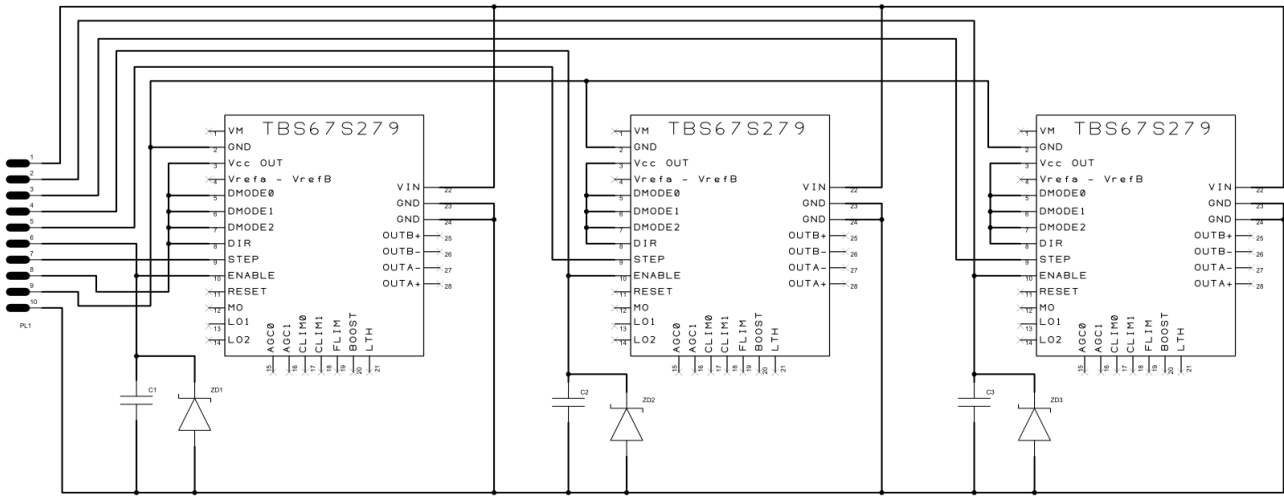

10.2.3.2.4. PCB Schematics

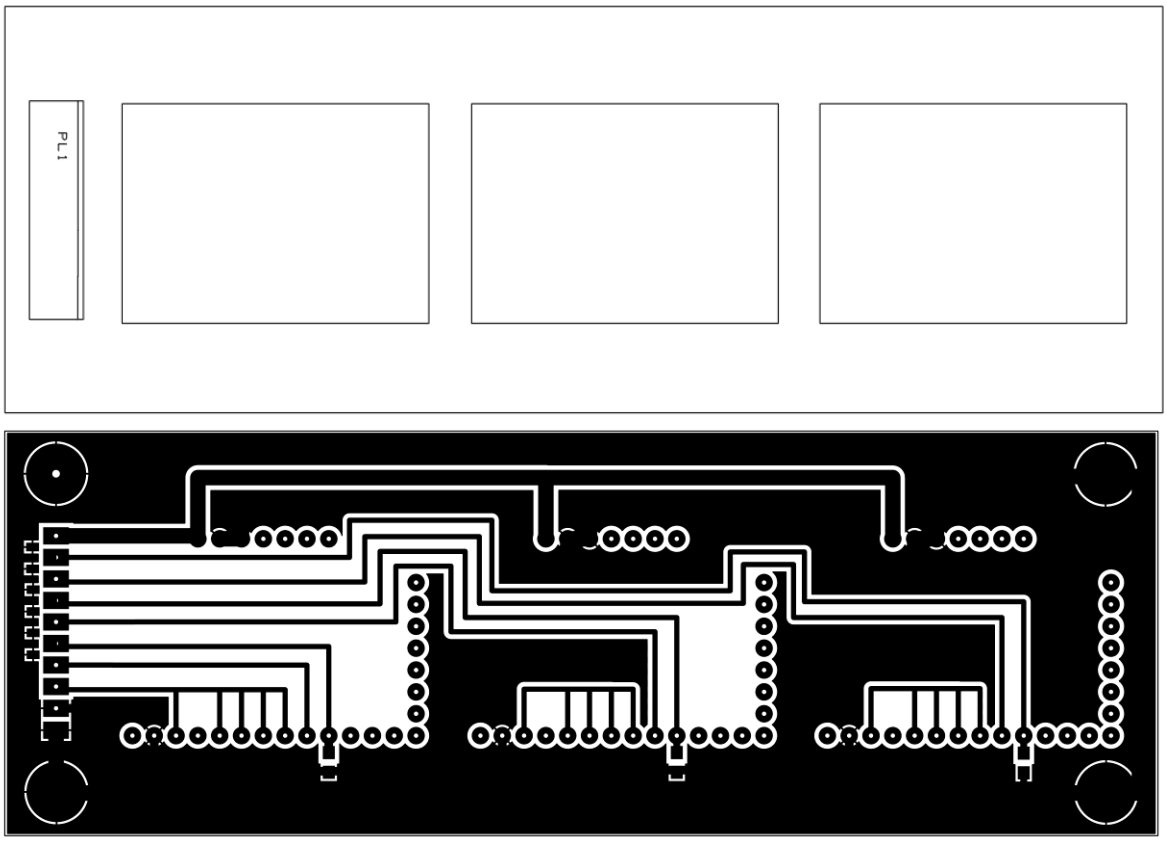

10.3. Appendix 3: Recipes

10.3.1. Phosphate Buffered Saline (PBS)

One litre of 10X solution of PBS was made up according to the below recipe and pH balanced to pH 7.4. To use, this was diluted 1:10 in distilled water.

NaCl	-	80 g
KCl	-	2 g
Na_2HPO_4	-	11.5 g
KH_2PO_4 -	-	2 g

10.3.2. Citrate Buffer

A 10X stock solution of citrate buffer was made up and pH balanced to pH 6. This was diluted 1:10 in distilled water upon use and 0.5 % Tween-20 added.

Citric acid	-	19.2 g
dH_2O	-	1 L

10.3.3. Krebs – Henseleit Buffer (KHB)

Krebs – Henseleit buffer was made fresh when required. This was supplemented with higher glucose to a final concentration of 25 mM as well as 10 mM HEPES. Calcium chloride was first dissolved in distilled water before adding it to the mixture. Once fully dissolved the KHB was filtered through a 0.2 µm sterile filter. One litre of KHB was made up as follows:

NaCl	-	6.9 g
KCl	-	0.35 g
$MgSO_4$	-	0.1 g
$CaCl_2$	-	0.14 g
KH_2PO_4	-	0.16 g
$NaHCO_3$	-	2.1 g
Glucose	-	4.5 g
HEPES	-	2.4 g

10.3.4. Haemotoxyin and Eosin (H&E) stain

10.3.4.1. Mayer's Haematoxylin

Mayer's Haematoxylin was bought premade from Sigma Aldrich, Dorset, UK.

10.3.4.2. Eosin

One litre of eosin was made up as follows:

Eosin Y	-	2g
95 % ethanol	-	1 l

Eosin solution was left overnight on a magnetic stirrer to fully dissolve into the ethanol.

10.3.5. Periodic Acid Schiff (PAS) stain

10.3.5.1. Acid Alcohol

Acid alcohol was made up in small quantities when needed. 50 ml of acid alcohol was made up as follows:

HCl	-	0.5 mL
100 % Ethanol	-	50 mL

10.3.6. Picrosirius Red Stain

10.3.6.1. Picrosirius Red

Picrosirius red solution was made up and stored in a glass container in an separate explosives cupboard away from other chemicals. 100 ml of picrosirius red was made up as follows:

Direct red 80	-	0.1 g
Saturated picric acid solution	-	100 mL

10.3.6.2. Weighert's Iron Haematoxylin

Weighert's iron haematoxylin was made fresh from a two-part solution on the day of use. The two solutions were made up as follows:

Solution A:

Haematoxylin	-	1 g
95 % ethanol	-	100 mL

Solution B:

29 % Ferric Chloride in dH_2O	-	4 mL
dH_2O	-	95 mL
Concentrated HCl	-	1 mL

10.3.6.3. Acidified Water

Distilled water	-	1 L
Glacial acetic acid	-	5 mL

10.4. Appendix 4: Calculation of Alvetex Permeability

The darcy permeability of a material using a head which drains over time can be calculated from the initial height of liquid above the membrane, final height of the liquid above the membrane and the time taken between these two points. The relationship between these two variables can be derived as follows:

Darcy's law:

$$Q = \frac{\kappa A_{membrane}}{\mu L} \Delta p \quad \text{(A4.1)}$$

Where Q is the flow rate, κ is the permeability coefficient $A_{membrane}$ is the surface area of the membrane, L is the thickness of the membrane, μ is the viscosity of the liquid and Δp is the pressure difference across the membrane. Using a head of water to provide the pressure, Δp can be substituted for the height of fluid above the membrane using the equation for a head of pressure. With the origin set such that $h_{membrane} = 0$, the equation for head pressure can be simplified to Equation A4.2

$$\Delta p = \rho g(h_{head} - h_{membrane}) = \rho g h \quad \text{(A4.2)}$$

Equation A4.2 contains g, the acceleration due to gravity, ρ, the density of the fluid and h which is the height of the head above the membrane. To integrate Darcy's law the Bernoulli principle, shown in Equation A4.3, can be used.

$$v_{head} A_{head} = v_{membrane} A_{membrane} \quad \text{(A4.3)}$$

Ahead is the surface area of the fluid head, whilst the fluid velocity in the header tank can be defined as shown in Equation A4.4.

$$v_{head} = \frac{dh}{dt} \quad \text{(A4.4)}$$

For the membrane the velocity can be calculated using Darcy's law:

$$v_{membrane} = \frac{Q}{A_{membrane}} = -\frac{\kappa \rho g}{L\mu} h \quad \text{(A4.5)}$$

Combining equations A4.4 and A4.5 together using the Bernoulli principle leads to the following equation:

$$A_{head} \frac{dh}{dt} = -A_{membrane} \frac{\kappa \rho g}{L\mu} h \quad \text{(A4.6)}$$

This can be rearranged and integrated to give:

$$ln\left(\frac{h_1}{h_2}\right) = -\frac{A_{membrane}}{A_{head}} \frac{\kappa \rho g}{L\mu} t \quad \text{(A4.7)}$$

Permeability can therefore be presented as:

$$\kappa = -\frac{A_{head} L\mu}{A_{membrane} \rho g t} ln\left(\frac{h_1}{h_2}\right) \quad \text{(A4.8)}$$

By measuring the time taken for the head to move between two points, the results can be plotted on a graph of t against $\ln\left(\frac{h1}{h2}\right)$ where h_1 and h_2 are the initial and final heights of the fluid head, and t is the time taken for the fluid to drain the height from h_1 to h_2. This produces a linear graph for a material which obeys Darcy's law, with the inverse of the gradient equal Equation A4.9. All variables are either known constants or can be readily measured.

$$\frac{ln\left(\frac{h_1}{h_2}\right)}{t} = -\frac{A_{membrane}\rho g}{A_{head}L\mu}\kappa. \qquad \text{(A4.9)}$$